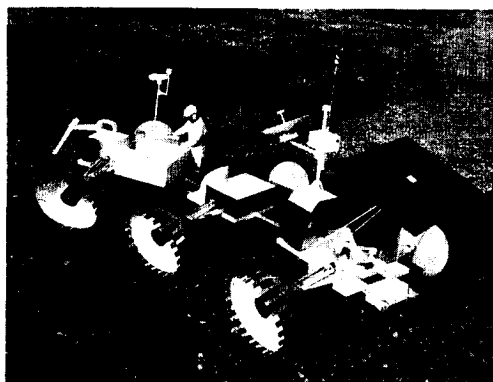


# DUAL MODE LUNAR ROVING VEHICLE

## Preliminary Design Study



KSS-10 HEADQUARTERS LIBRARY

### Volume II

### Vehicle Design & System Integration

#### Book I

#### DLRV System Design and Analysis

#### Book II

#### DLRV Tie-Down, Off-Loading, and Checkout

#### Book III

#### Ground Support Equipment

#### Book IV

#### System Safety Analysis

(NAS8-OR-113455) DUAL MODE LUNAR ROVING  
VEHICLE PRELIMINARY DESIGN STUDY. VOLUME II:  
VEHICLE DESIGN AND SYSTEM INTEGRATION. BOOK  
1: DLRV SYSTEM DESIGN AND ANALYSIS. BOOK  
2: DLRV TIE-DOWN, OFF-LOADING, AND

George C. Marshall Space Flight Center  
Huntsville, Alabama 35812  
Contract No. NAS8-24529



Volume I      Summary Report

Volume II     Vehicle Design & System Integration

- Book I      DLRV System Design and Analysis
- Book II     DLRV Tie-Down, Off-Loading, and Checkout
- Book III    Ground Support Equipment
- Book IV    System Safety Analysis

Volume III    Astrionics Systems

- Book I      Navigation Subsystem Design and Analysis
- Book II     Communications Subsystem Design and Analysis
- Book III    Hazard Detection Subsystem Design and Analysis
- Book IV    Control Subsystem Design and Analysis
- Book V     Power Subsystem Design and Analysis

Volume IV    Scientific Systems

- Book I      Scientific Equipment Interface Design
- Book II     Techniques for Determining Engineering Properties of the Lunar Surface

Volume V     Mission Operations

Volume VI    DLRV Systems Specifications

- Book I      Vehicle CEI Specification
- Book II     Ground Support Specification

Volume VII   Resources Analysis

- Book I      Development and Functional Plans
- Book II     Cost and Resources Plan

# DLRV System Design and Analysis

## **DLRV Tie-Down, Off-Loading, and Checkout**



# Ground Support Equipment

# System Safety Analysis

# DUAL MODE LUNAR ROVING VEHICLE

## Preliminary Design Study

### Volume II Vehicle Design & System Integration

Book I  
DLRV System Design and Analysis

Book II  
DLRV Tie-Down, Off-Loading, and Checkout

Book III  
Ground Support Equipment

Book IV  
System Safety Analysis

Prepared for  
George C. Marshall Space Flight Center  
Huntsville, Alabama 35812  
Contract No. NAS8-24529

## FOREWORD

This document is one of seven volumes which present the results of an eight-month, Phase-B preliminary design study of the Dual-Mode Lunar Roving Vehicle (DLRV). This study was performed for the National Aeronautics and Space Administration, Marshall Space Flight Center, Huntsville, Alabama, under Contract NAS 8-24529, Modification Number 1, by the Grumman Aerospace Corporation, Bethpage, New York.

### BACKGROUND

With two lunar landings successfully behind us, it is becoming increasingly important to justify future lunar flights on the basis of scientific yield rather than on the accomplishment of the lunar landing alone. Lunar surface mobility is the key toward achieving this goal. The DLRV will not only provide this mobility for astronauts on the moon, but will also provide the capability for performing long-range geological and geophysical traverses by remote control from earth for a period of one year, thus enabling scientific activities to continue even during times when lunar flights are infrequent.

The scientific value of the DLRV is its area of coverage and its duration of operations. It will also provide a continuum of lunar activity, with real time command capability, while promoting scientific and popular interest in the lunar program between the lunar landings.

### OBJECTIVE

The primary objective of the DLRV is to provide the first step in a combined manned/automated capability for lunar exploration. A continuing requirement of the scientific community is long traverses of the lunar surface to allow collection of data over wide areas and identification of areas of geological, mineralogical, seismic, magnetic, and gravitational interest.

An automated or remotely controlled roving vehicle is not constrained in stay-time because it is not dependent on a life support system when it is operated in the unmanned mode. It also can be essentially a "one-way" vehicle in the remote mode since it need not return an astronaut or the samples it has collected to the initial landing site; it can be remotely driven to a future landing site for return to earth of its samples. It can also be operated again in the manned mode, permitting the landing craft's payload to be used for something other than a rover. These

features enable the dual-mode vehicle to cover much greater ranges and distances on the lunar surface. By collecting lunar samples from widely separated areas of the moon, making scientific measurements with on-board instrumentation, and deploying small self-contained packages of geophysical instruments, a continuum of scientific data can be obtained which will hopefully cast new insight into the physical nature and origin of the moon.

#### CONFIGURATION

As currently configured, the DLRV is compatible with all IM and IM-derived delivery systems, although this study has focused attention primarily on the Extended Lunar Module (ELM).

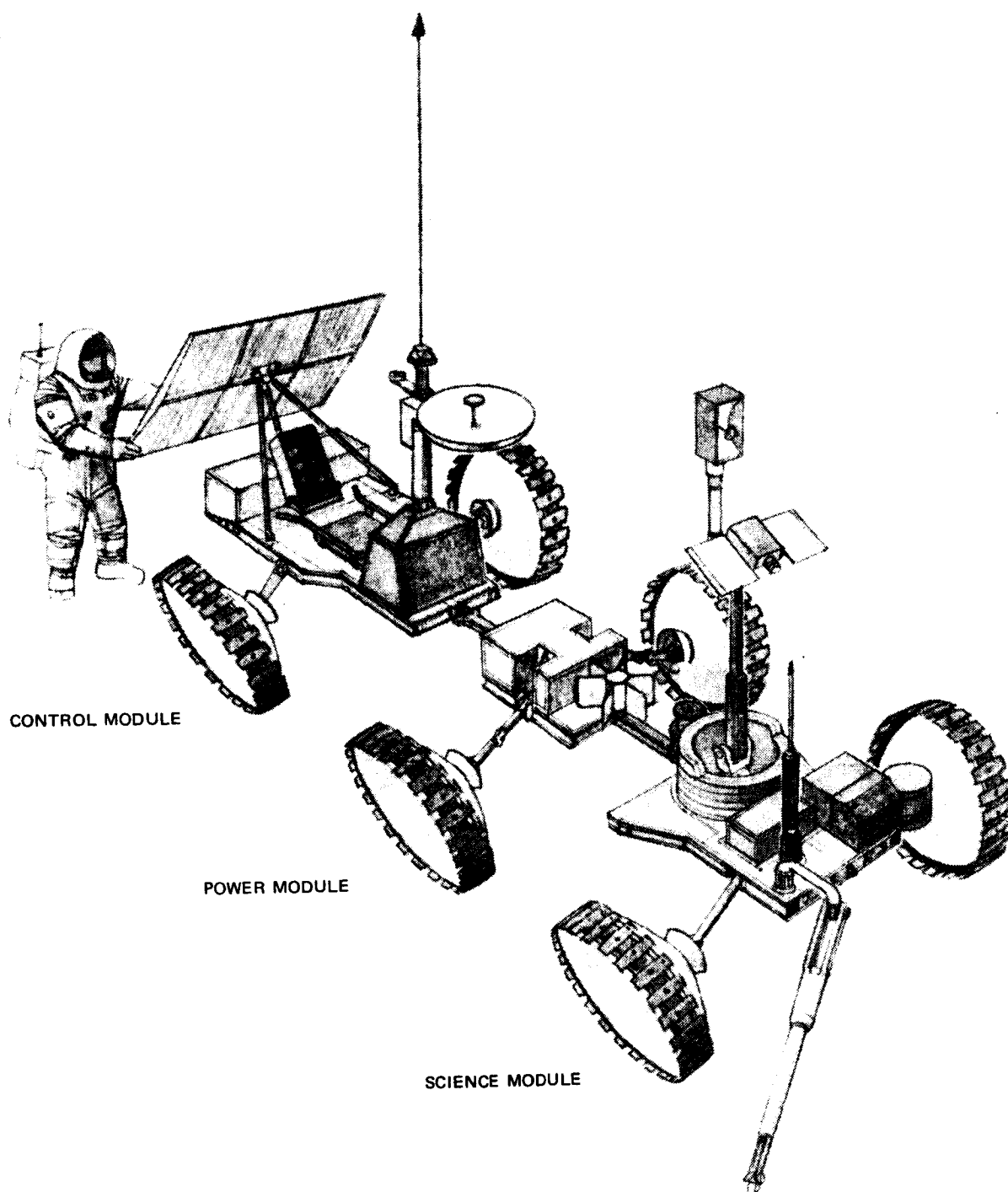
The DLRV configuration consists of three two-wheeled modules, designated the Control Module, the Power Module, and the Science Module, arranged left to right in the view shown in the accompanying illustration. The Control and Power Modules are stowed as one folded assembly in Quadrant I of the ELM's descent stage.

Deployed on the lunar surface by the astronauts using either automatic or manual means, this four-wheeled rover is operated in the manned mode with its driver seated on the Control Module together with the manned science payload.

Following the manned sorties, the astronauts deploy the science module, which is saddle-bag mounted to Quadrant IV of the ELM. The unmanned science payload is integral to the Science Module, having been installed before launch. The Science module is manually connected to the power module, and the solar array which was manually erected on the lunar surface to charge batteries between sorties is transferred to the control module. This is the DLRV configuration shown here. The six-wheeled, remotely controlled configuration has the science module, carrying the television camera and the sample collection arm, up front. Electronic equipment and batteries are mounted in insulated bays for thermal protection. The equipment mounts on heat sinks which are thermally connected by heat pipes to radiators mounted on the top of the bays. The heat sinks contain a phase-change material which absorbs heat when the radiators are not operating. The radiators may be covered when driving to protect the surfaces from dust.

#### REQUIREMENTS

The DLRV described in this report meets or exceeds NASA's requirements and guidelines. Installed in the ELM the DLRV weighs 650 pounds, exclusive of science payload. In the manned mode the rover must accomplish the two 30-km sorties per



DLRV UNMANNED CONFIGURATION

day, and in the unmanned mode it can traverse 1000 km with numerous science stops in a year's time. The full complement of 100 pounds of manned science equipment and 250 pounds of unmanned scientific payload can be accommodated in addition to samples.

The DLRV must perform manned traverses over smooth mare at peak speeds of 15 km/hr and unmanned traverses at a maximum speed of 2 km/hr limited primarily by the ground control capability. Furthermore, the manned vehicle can easily negotiate a 30-cm step obstacle, cross a 70-cm crevasse, or climb a 35° slope. In the unmanned mode the obstacle-climbing and crevasse-crossing capability increases to 100 cm.

Although the DLRV is not primarily designed for lunar night operations its subsystems have some limited capability to perform at dusk. The basic DLRV can traverse for approximately 2 hours during lunar night while growth versions of the power subsystem will permit equal day/night roving capability.

#### SUBSYSTEM

The system is divided into the following subsystems:

##### Mobility

Each cone wheel is individually powered by a brushless dc motor and gear train. An actuator at the joint between the modules provides the power for articulated steering. The rear joint in the six-wheeled configuration is not powered, the joint being free in yaw. An electronics assembly receives signals from either the astronaut's hand controller or the earth-based driver by way of remote commands and provides the logic and amplification for control of the steering and wheel drive motors. The suspension is the swing-arm type with torsion bars.

##### Crew Systems

The driver's adjustable seat is positioned safely between the front wheels. He ingresses from the front and his feet are protected from hazards. An emergency passenger station is provided on the control module for rescue of an astronaut. The astronaut's instrument panel contains the hand controller, navigation displays, a warning light, and essential subsystem controls.

##### Navigation

The navigation subsystem provides a heading reference in the form of a sun sensor

on the control module during the manned mode and a directional gyro on the science module during the unmanned mode. Distance traveled is determined from odometers on all wheels. All computations are done on the ground including those necessary for the astronaut's navigation display. Unmanned updating of position is accomplished by using the TV camera for landmark sightings and star field patterns.

#### Communications/Instrumentation (including Remote Control)

Communications with earth is accomplished by S-band transmitters and receivers through the 85-foot antennas of the MSFN/NASCOM. A high-gain, steerable antenna capable of tracking its received signal and an omnidirectional antenna are located on the rover. The astronauts are linked to the S-band equipment via a VHF link through the PLSS. Data handling equipment digitally formats data from the vehicle and the scientific equipment. The DLRV's S-band transmitter can simultaneously transmit voice and biomedical data from the astronaut, digital data and a video signal. The video may come from the lunar survey system in the manned mode or either the facsimile camera or the rover's television camera in the unmanned mode. Commands, voice and data for the astronaut's display are received by the S-band equipment, decoded and distributed.

#### Hazard Detection

A pulsed radar detects the size and location of hazards that can immobilize the DLRV. An electronic processor analyzes the radar's output and certain vehicle parameters and compares these to preset criteria. Slow or stop signals are generated to prevent damage to the rover.

#### Power

Electrical power is provided by a combination of three sources: batteries, solar array, and a radiosotope thermoelectric generator (RTG). The array is not carried on the manned configuration but is used for battery recharge between sorties. It is manually installed on the control module during conversion to the unmanned configuration and self-tracks the sun. The RTG is the primary source for standby power during the lunar night. Conditioning and distribution equipment control the potential of ac and dc busses and protect the power subsystem from faults.

#### Space Support

Space support equipment in the form of tie-down fittings, struts, release mechanisms, and unloading devices allows stowage of the vehicle in the ELM and deployment on the lunar surface. Some equipment remains with the ELM; other is



integral with the vehicle chassis.

#### Science

The DLRV provides tie-down and deployment for a variety of vehicle-mounted scientific equipment. Typical of this equipment for the manned mission is the lunar survey system and the Apollo lunar hand tools (geology tools). For unmanned (remote control) mode, typical experiment packages include the sample collection arm, facsimile camera, X-ray diffractometer/spectrometer, gravimeter, magnetometer and remote geophysical monitor. Electric power, command reception and data transmission are provided for the science payload.

## CONTENTS

<u>Section</u>		<u>Page</u>
1	INTRODUCTION . . . . .	1-1
2	MISSION ANALYSIS . . . . .	2-1
	2.1 MISSION RULES AND CONSTRAINTS . . . . .	2-1
	2.1.1 Manned . . . . .	2-1
	2.1.2 Unmanned . . . . .	2-2
	2.2 REFERENCE MISSIONS . . . . .	2-3
	2.2.1 Manned Mission . . . . .	2-3
	2.2.2 Unmanned Mission . . . . .	2-9
	2.2.3 Prelaunch Operations . . . . .	2-18
	2.3 DESIGN MISSIONS . . . . .	2-20
	2.3.1 Electrical Power . . . . .	2-20
	2.3.2 Temperature Control . . . . .	2-21
	2.4 METEORIDS AND RADIATION . . . . .	2-21
	2.4.1 Micrometeoroids . . . . .	2-21
	2.4.2 Radiation . . . . .	2-24
3	SYSTEM DESIGN . . . . .	3-1
	3.1 CONFIGURATION DESIGN RATIONALE . . . . .	3-1
	3.1.1 Delivery Vehicle Accommodation . . . . .	3-1
	3.1.2 Mobility Requirements . . . . .	3-6
	3.1.3 Science Accommodation . . . . .	3-9
	3.1.4 Crew Accommodation . . . . .	3-13
	3.1.5 Subsystem Equipment Requirements . . . . .	3-13
	3.1.6 Arrangement Alternatives . . . . .	3-14
	3.2 SELECTED CONFIGURATION . . . . .	3-16
	3.2.1 General Arrangements . . . . .	3-16
	3.2.2 Mass Properties . . . . .	3-27
	3.2.3 Equipment Integration . . . . .	3-37
4	SYSTEMS ANALYSIS . . . . .	4-1
	4.1 MOBILITY . . . . .	4-1

~~PRECEDING PAGE BLANK NOT FILMED~~

## CONTENTS CON'T

<u>Section</u>		<u>Page</u>
	4.1.1 Locomotion Performance . . . . .	4-1
	4.1.2 Obstacle Negotiation . . . . .	4-31
	4.1.3 Probability of Traverse Success . . . . .	4-38
	4.1.4 References for Section 4.1 . . . . .	4-52
4.2	DYNAMICS . . . . .	4-53
	4.2.1 Response to Random Terrain . . . . .	4-53
	4.2.2 Loads due to Obstacle Encounter . . . . .	4-61
	4.2.3 Selection of Wheel and Suspension Characteristics . . . . .	4-66
	4.2.4 Turning Stability . . . . .	4-67
	4.2.5 References for Section 4.2 . . . . .	4-68
4.3	LOADS AND STRUCTURAL DESIGN CRITERIA . . . . .	4-68
	4.3.1 Stowed Condition Loads . . . . .	4-68
	4.3.2 Lunar Operation Loads . . . . .	4-70
	4.3.3 Design Criteria . . . . .	4-73
4.4	THERMAL CONTROL . . . . .	4-76
	4.4.1 Rationale . . . . .	4-76
	4.4.2 Thermal System Approaches . . . . .	4-78
	4.4.3 System Concept . . . . .	4-90
	4.4.4 Operations Concept . . . . .	4-95
	4.4.5 Thermal Loads . . . . .	4-96
	4.4.6 Thermal Performance . . . . .	4-103
4.5	RELIABILITY . . . . .	4-116
	4.5.1 Failure Mode Effects and Criticality Analysis . . . . .	4-117
	4.5.2 Reliability Prediction . . . . .	4-149
	4.5.3 Parts Environmental Requirements . . . . .	4-161
	4.5.4 Hardware Test Requirements . . . . .	4-166
5	MOBILITY SUBSYSTEM DESIGN . . . . .	5-1
5.1	CHASSIS . . . . .	5-1
	5.1.1 Design Requirements . . . . .	5-1
	5.1.2 Chassis Preliminary Design . . . . .	5-2
	5.1.3 Thermal Considerations . . . . .	5-11

CONTENTS CON'T

<u>Section</u>		<u>Page</u>
5.2	WHEELS . . . . .	5-12
5.2.1	Candidate Evaluation . . . . .	5-12
5.2.2	Material Selection . . . . .	5-17
5.2.3	Wheel Preliminary Design . . . . .	5-19
5.2.4	Structural Analysis and Test . . . . .	5-23
5.2.5	Thermal Analysis . . . . .	5-25
5.3	SUSPENSION . . . . .	5-25
5.3.1	Candidate Evaluation . . . . .	5-25
5.3.2	Suspension Preliminary Design . . . . .	5-35
5.4	STEERING MECHANISM . . . . .	5-44
5.4.1	Candidate Evaluation . . . . .	5-44
5.4.2	Steering Mechanism Preliminary Design . . . . .	5-52
5.4.3	Conversion from Manned to Unmanned Mode . . . . .	5-61
5.4.4	Thermal Analysis . . . . .	5-62
5.4.5	References for Section 5.4 . . . . .	5-62
5.5	WHEEL DRIVE MECHANISM . . . . .	5-63
5.5.1	Design Requirements . . . . .	5-63
5.5.2	Candidate Evaluation . . . . .	5-63
5.5.3	Wheel Drive Mechanism Preliminary Design . . . . .	5-66
5.5.4	Thermal Analysis . . . . .	5-74
6	CREW SYSTEMS/HUMAN FACTORS . . . . .	6-1
6.1	RATIONALE FOR CREW STATION SELECTION . . . . .	6-1
6.1.1	Driver Station Studies . . . . .	6-1
6.1.2	Passenger Station Studies . . . . .	6-3
6.1.3	Displays and Controls Studies . . . . .	6-3
6.1.4	Areas Requiring Further Study . . . . .	6-7
6.2	CREW STATION CONFIGURATION . . . . .	6-7
6.2.1	Driver Station . . . . .	6-7
6.2.2	Controls and Displays . . . . .	6-12
6.2.3	Passenger Station . . . . .	6-16

CONTENTS CON'T

<u>Section</u>		<u>Page</u>
7	SYSTEM TRADEOFFS AND ALTERNATIVES . . . . .	7-1
	7.1 PENALTY FOR MANNED CAPABILITY . . . . .	7-1
	7.2 NIGHT OPERATIONS . . . . .	7-1
	7.3 REDUCED SIZE VEHICLE . . . . .	7-3

## ILLUSTRATIONS

<u>Fig.</u>		<u>Page</u>
2.2-1	Continuous Science Load .....	2-15
2.2-2	Power Profile Increments for Routine Science Stop .....	2-16
2.2-3	Increment in Power for Routine Science Stop .....	2-17
2.2-4	Prelaunch Flow Timeline .....	2-19
3.1-1	ELM Payload Arrangements .....	3-3
3.1-2	ELM Payload Envelopes Quadrants I and IV .....	3-5
3.1-3	Comparison Diagram Ackerman/Articulated With Equal Platform .....	3-7
3.1-4	Stability and Acceleration Trends With Vehicle Size .....	3-8
3.1-5	Selected Mobility Geometry .....	3-11
3.1-6	DLRV Arrangements .....	3-15
3.2-1	DLRV Manned Mission Arrangement .....	3-17
3.2-2	DLRV Unmanned Mission Arrangement .....	3-19
3.2-3	Stowed Arrangement .....	3-23
3.2-4	Stowed Configuration Control and Power Modules .....	3-25
3.2-5	Stowed Configuration Science Module .....	3-27
3.2-6	Coordinate System Defination .....	3-31
3.2-7	System Schematic Diagram .....	3-39
3.2-8	Level 1 Vehicle-Ground Functional Schematic .....	3-41
3.2-9	Hardware Tree .....	3-45
4.1-1	Footprint Length vs. Sinkage .....	4-4
4.1-2	Test Apparatus for Rolling Resistance .....	4-5
4.1-3	Tests of 38-in. 1/6-g Wheel .....	4-6
4.1-4	Estimated Wheel Pressure vs. Sinkage .....	4-7
4.1-5	Wheel Torque Required vs. Slope .....	4-10
4.1-6	Soft Soil Wheel Performance, 10-Inch Cleats .....	4-12
4.1-7	Soft Soil Wheel Performance, Angle Cleats .....	4-13
4.1-8	Firm Soil Wheel Performance, 10-Inch Cleats .....	4-14
4.1-9	Firm Soil Wheel Performance, Angle Cleats .....	4-15

# ILLUSTRATIONS CON'T

<u>Fig.</u>		<u>Page</u>
4.1-10	Maximum Slope Climbing Ability, 42" Wheel, 12" Angle Cleats .....	4-18
4.1-11	Motor Efficiency-Series Mode, Low Speed .....	4-20
4.1-12	Motor Efficiency-Series Mode, Medium Speed .....	4-21
4.1-13	Motor Efficiency-Manned .....	4-22
4.1-14	Power Requirements-Manned Mode .....	4-23
4.1-15	Manned Mode Specific Energy .....	4-24
4.1-16	Manned Mode Distance for 1000 Watt-hr .....	4-25
4.1-17	Mobility Power Requirements-Unmanned Vehicle .....	4-26
4.1-18	Unmanned Distance Before Recharge vs. Slope .....	4-29
4.1-19	Unmanned Distance for Equal Up and Down Slopes .....	4-30
4.1-20	1/6 Scale Obstacle Negotiation Model .....	4-32
4.1-21	1/6 Scale Model Crossing Step Obstacle .....	4-34
4.1-22	1/6 Scale Model Crossing Crevasse .....	4-35
4.1-23	Mission Success Analysis .....	4-39
4.1-24	Relationship of G to $K\phi$ .....	4-47
4.1-25	Effect of Wheel Diameter on Probability .....	4-49
4.1-26	Effect of Wheel Width on Probability .....	4-50
4.1-27	Effect of Vehicle Weight on Probability .....	4-51
4.2-1	Math Model for Analog Study .....	4-54
4.2-2	Idealized Suspension Stiffnesses .....	4-55
4.2-3	Idealized Wheel Stiffness .....	4-55
4.2-4	Response to Random Terrain, 2 Wheel Model .....	4-57
4.2-5	Peak Probability Distributions .....	4-59
4.2-6	Effect of Auxiliary Suspension Damping .....	4-60
4.2-7	Comparison of Random Terrain Response for 2 and 4 Wheel Math Models .....	4-62
4.2-8	Math Model for Bump Encounter Analyses .....	4-63
4.2-9	Time Histories of Bump Response .....	4-64
4.2-10	Loads Due to 4, 8, and 12 in. Spike Bump Encounters .....	4-65

## ILLUSTRATIONS CON'T

<u>Fig.</u>		<u>Page</u>
4.2-11	Effect of Wheel Stiffness on Bump Encounter Loads .....	4-65
4.2-12	Turning Stability .....	4-65
4.4-1	Surveyor Thermal Switch .....	4-80
4.4-2	Heat Pipe Schematic and Steam Analogy .....	4-81
4.4-3	Conductance Comparison Of Pipe and Bar .....	4-82
4.4-4	Maximum Height Of Dust .....	4-85
4.4-5	Variation Of Total Solar Absorptance With Dust Coverage .....	4-87
4.4-6	Lunar Dust Thermal Resistance .....	4-88
4.4-7	Dust Shield and Cleaning Mechanism .....	4-89
4.4-8	Thermal System Block Diagram .....	4-91
4.4-9	Sizing Load Vs. Drive Cycle .....	4-101
4.4-10	Radiator Capacity .....	4-112
4.4-11	Variable Heat Pipe Design Performance .....	4-115
4.5-1	Electrical Power Subsystem Block Diagram .....	4-121
4.5-2	Navigation Subsystem-Manned Mode .....	4-123
4.5-3	Navigation Subsystem-Unmanned Mode .....	4-124
4.5-4	Mobility And Steering Block Diagram .....	4-125
4.5-5	Communication/Instrumentation Block Diagram .....	4-127
4.5-6	Hazard Detection Block Diagram .....	4-129
4.5-7	Equipment Failures With/Without Development Program .....	4-168
4.5-8	Qualification Endurance Test Alternatives .....	4-170
5.1-1	Structural Arrangement-Control and Power Module Chassis Stowed .....	5-3
5.1-2	Chassis Structural Arrangement-Control and Power Modules .....	5-5
5.1-3	Structural Arrangement-Science Module Chassis Stowed .....	5-7
5.1-4	Chassis Structural Arrangement-Science Module .....	5-9
5.2-1	Candidate Wheels .....	5-14
5.2-2	DLRV Wheel Assembly .....	5-21



# ILLUSTRATIONS CON'T

<u>Fig.</u>		<u>Page</u>
5.2-3	Instrumented DLRV Wheel Undergoing Tests .....	5-24
5.2-4	Load Deflection Curve for Cone Wheel .....	5-26
5.2-5	Circumferential Stress Distribution .....	5-27
5.2-6	Meridional Stress Distribution .....	5-27
5.2-7	Worst Case Total Incident Radiation .....	5-29
5.2-8	Wheel/Drive Thermal Diagram .....	5-30
5.3-1	Candidate Suspensions .....	5-32
5.3-2	Control Module Suspension .....	5-37
5.3-3	Power Module Suspension .....	5-39
5.3-4	Suspension Load/Deflection Characteristics .....	5-43
5.4-1	Candidate Steering Concepts (6 x 6) .....	5-45
5.4-2	Measuring Steering Forces for Candidate Ackerman System .....	5-48
5.4-3	Steering Comparison .....	5-49
5.4-4	Steering Reliability Block Diagrams .....	5-51
5.4-5	DLRV Steering Actuator Assembly .....	5-55
5.4-6	Bellows Design .....	5-59
5.5-1	DLRV Wheel Drive Assembly .....	5-67
5.5-2	Wheel Drive Assembly Performance Curve .....	5-69
6.1-1	Candidate Driver Positions .....	6-2
6.1-2	Alternate Passenger Positions .....	6-4
6.2-1	DLRV Crew Station Arrangement .....	6-8
6.2-2	Crew Station Stowage .....	6-11
6.2-3	Display And Control Panel .....	6-13
7.3-1	Minimum Planform DLRV .....	7-5
7.3-2	Minimum Size Vehicle Vs. Selected Configuration .....	7-7

## TABLES

<u>Table</u>		<u>Page</u>
2.1-1	Ground Velocity (km/hr) for Terrain and Lighting .....	2-2
2.2-1	Major Phases-Manned Reference Mission .....	2-4
2.2-2	Initial Sortie (2nd EVA) .....	2-6
2.2-3	Typical Manned Reference Sorties (3rd, 4th and 5th EVA) .....	2-7
2.2-4	Conversion to Unmanned Mode (6th EVA) .....	2-8
2.2-5	Major Science Sites-Unmanned Mission .....	2-11
2.2-6	Science Equipment Operations for Unmanned Mode .....	2-13
2.2-7	Unmanned Reference Mission Summary .....	2-14
2.3-1	Thermal Design Mission Timeline-Manned .....	2-22
3.2-1	Weight Statement .....	3-33
3.2-2	Roving Mass Properties and Wheel Loadings .....	3-35
3.2-3	Sprung Mass Properties .....	3-36
3.2-4	Stowed DLRV Mass Properties .....	3-30
4.1-1	Tests of 1-g Flexible Wheel at Stevens Institute .....	4-2
4.1-2	Calculation of Required Wheel Torque .....	4-9
4.1-3	Soil Bin Test Conditions .....	4-11
4.1-4	Stevens Soil Bin Test Results .....	4-16
4.1-5	Obstacle Negotiation Tests .....	4-36
4.1-6	Obstacle Negotiation With Single Wheel Drive Failure, One Meter Step .....	4-37
4.1-7	Vehicle Models Studied .....	4-42
4.1-8	Pothole Model Inputs .....	4-43
4.1-9	Predicted Distribution of One Meter Slope .....	4-45
4.1-10	Slope Histogram .....	4-46
4.3-1	Mission Vibration Loads .....	4-69
4.3-2	Equipment Vibration Levels .....	4-70
4.3-3	Wheel Ground Loads Criteria .....	4-71
4.4-1	Thermal System Mission Capability Subsolar Conditions .....	4-77

# TABLES CON'T

<u>Table</u>		<u>Page</u>
4.4-2	Max. Incident Thermal Radiation .....	4-95
4.4-3	Thermal Dissipation Rates .....	4-97
4.4-4	Heat Storage Required .....	4-104
4.4-5	Allowable Equipment Temperatures .....	4-105
4.4-6	Thermal Compartment Control System Characteristics .....	4-107
4.5-1	Summary Of Critical Equipment Failure Modes .....	4-118
4.5-2	DLRV Failure Mode and Criticality Analysis .....	4-131
4.5-3	Reliability Predictions .....	4-150
4.5-4	Reliability Goals .....	4-151
4.5-5	Equipment Failure Rates .....	4-153
4.5-6	Solar Flare Proton Environment .....	4-162
4.5-7	Parts Vulnerability Assessment .....	4-164
4.5-8	Hardware Test Environments Summary .....	4-167
5.2-1	Wheel Evaluation Study .....	5-15
5.2-2	Cone Wheel Material Evaluation .....	5-18
5.2-3	Wheel Design Criteria .....	5-20
5.2-4	Traction Drive Thermal Load .....	5-28
5.3-1	Suspension System Evaluation .....	5-33
5.3-2	Suspension Design Criteria .....	5-36
5.4-1	Steering System Evaluation Criteria (6 x 6) .....	5-47
5.4-2	Steering Energy Comparison .....	5-47
5.4-3	Steering Design Criteria .....	5-53
5.5-1	Wheel Drive Assembly Design Criteria .....	5-64
6.1-1	Passenger Station Evaluation .....	6-5
7.3-1	Size Tradeoff .....	7-9
7.3-2	Performance Comparison Small Vs. Large Vehicle .....	7-10

## SECTION 1

### INTRODUCTION

The system design and analysis results reported in this book involve the derivation of requirements for, and the design and analysis of, the entire system as opposed to similar work at the subsystem level. Requirements from Vol. IV, Scientific Equipment Interface Design, are a major input to this book.

The categories of study effort that correspond to the subsections of this book are briefly identified. Mission analysis establishes mission/operations requirements and defines mission capability. System design arranges the subsystems into a vehicle configuration and assures physical compatibility among the subsystems and complementary systems. Systems analysis assesses and optimizes the system from the view of each design discipline: thermodynamics, reliability, etc. Human factors analysis and crew station design optimize the integration of the crew. The design of the mobility subsystem is also considered because of the inseparable relation to the configuration and arrangement of a lunar mobility vehicle.

## SECTION 2

### MISSION ANALYSIS

#### 2.1 MISSION RULES AND CONSTRAINTS

In order to construct the sequence of events and operations, it is first necessary to set down the variety of assumptions and constraints to which the mission must conform. These represent the starting point for the generation of the Reference Missions and in some instances are also operational and design requirements.

The primary source of information for the rules and constraints is the Statement of Work, Nov. 1, 1968, Exhibit "A" of the Procurement Request. This has been supplemented and amended by informal discussions with MSFC and directions received at splinter group meetings following the regular monthly progress reports. An additional principal source is the U. S. Geological Survey Report, "Lunar Terrain and Traverse Data for Lunar Roving Vehicle Design Study", by Moore, Pike and Ulrich, March 19, 1969.

##### 2.1.1 Manned

- o Manned mode operations consist of three types of EVA:
  - A checkout sortie
  - A typical sortie
  - Conversion to the unmanned mode
- o The vehicle will traverse 30 km during each typical sortie
- o The traverse distance is within a radius of 10 km of the ELM
- o The vehicle is capable of a continuous speed of 15 km/hr
- o The total time of all crew transfers is 30 minutes
- o The lunar sample payload is 70 lb
- o Data and voice links are on continuously
- o The following science equipment is used:
  - Apollo Lunar Hand Tools
  - Lunar Survey System
- o A typical sortie includes four 20 minute science stops and four 5-minute science stops
- o Nominal astronaut walk range from the DLRV during the 20-minute science stop is 700 meters, the range limit of the Survey Staff

### 2.1.2 Unmanned

- o The map distance to be traversed is 1000 km
- o The maximum duration of the mission is one year
- o There are 21 major science stops, each 50-hours long:
  - Twenty hours are used for local maneuvering
  - Thirty hours are used for science stops
- o The distances between sites are 50 km except for two sites which are 100 km apart
- o There are science stops every 0.5 km
- o The velocity of the vehicle is determined by the sun angle and the terrain as shown below. The speed variations at 20° - 70° sun angles are from the U. S. Geological Survey study

TABLE 2.1-1 GROUND VELOCITY (km/hr) FOR TERRAIN AND LIGHTING

Terrain	Sun 0° to 5° 85° to 90°	Sun 5° to 20° 70° to 85°	Sun 20° to 70°
Smooth Mare	0	1.00	2.0
Rough Mare	0	.90	1.8
Hummocky Upland	0	.60	1.2
Rough Upland	0	.60	.6
Large Crater	0	.40	.4

- o The vehicle is to avoid areas covered by shadows
- o The vehicle is to avoid craters larger than two meters across
- o All subsystems will be deactivated during lunar nights with the exception of the command receiver and required heaters
- o All subsystems, except communications, will be deactivated during battery recharge
- o The lunar sample payload is 250 pounds
- o The following science equipment is used
  - Sample Collection Arm
  - Sample Storage Device
  - Facsimile Camera
  - X-ray Diffractometer/Spectrometer
  - Gravimeter
  - Magnetometer
  - Remote Geophysical Monitor
- o No samples are retained unless analyzed by the X-ray device

## 2.2 REFERENCE MISSIONS

The Reference Mission is a normal sequence of events and operations which illustrates how the equipment is used to achieve the objectives. It is used as a baseline or point of departure for various project purposes, equipment operations, crew task analysis, weight reporting, and reliability modeling. Since other operations, as emergencies, may be more critical for subsystem design, the related Reference Mission requirements should be considered only as minimums.

### 2.2.1 Manned Mission

The manned DLRV mission starts with the deployment of the vehicle. This is followed sequentially by an initial checkout sortie and three regular sorties which include eight science stops per sortie. A conversion to the unmanned mode concludes the manned mode of operations. One EVA is scheduled during a twenty-four-hour period.

See Table 2.2-1 for a summary of the major phases.

#### 2.2.1.1. Deployment

Deployment consists of the structural disconnecting of the DLRV and the fold-out and separation from the ELM.

Structural disconnect is a solenoid-operated unlatching of primary structural tiedown members. Fold-out consists of the spring-assisted deployment of the vehicle using a slave mechanism to sequentially stage wheel struts and chassis lockout during fold-out sequence. Separation occurs via the astronauts' signal from the ascent stage which powers the aft wheels to drive the DLRV out of the deployment rack.

The science module is remotely deployed in a similar kinematic fashion to the control and power modules. The final off-loading stages are accomplished by the astronaut. Details of the deployment are explained in Book II of this volume.

TABLE 2.2-1 MAJOR PHASES - MANNED REFERENCE MISSION

EVENTS		Duration Hr : Min	Elapsed Time Hr : Min
1	Prelaunch, Earth Ascent thru ELM Touchdown, LM Post-Landing Checkout, and First EVA	103:10	
2	Post EVA activities, Personal Maintenance, Sleep, Preparation for the next EVA, Egress and Ingress	12:30	103:10
3	Second EVA Initial Checkout Sortie. See Table 2.2-2	04:06	115:40
4	Post EVA activities, Personal Maintenance Sleep, Preparation for the next EVA, Egress and Ingress	19:54	119:46
5	Third EVA Typical Sortie. See Table 2.2-3	04:34	139:40
6	Post EVA activities, Personal Maintenance Sleep, Preparation for the next EVA, Egress and Ingress	19:26	144:14
7	Fourth and Fifth EVA, Repeat Steps 5 and 6 twice.	48:00	163:40
8	Sixth EVA, Conversion to Unmanned Mode. See Table 2.2-4	02:20	211:40
9	Begin unmanned operations		214:00



#### 2.2.1.2 Initial Sortie (2nd EVA)

The events of the initial sortie are delineated in Table 2.2-2 and include the following features:

- o One astronaut
- o Checkout procedures as described in Volume II, Book II
- o A test drive which takes 29 minutes and is restricted to a radius of 0.5 km. The velocity is varied to the maximum of 15 km/hr
- o Two five-minute science stops during which geological tools are used to gather samples which are photographed and stored
- o Two twenty-minute science stops. The astronaut dismounts from the vehicle and walks up to 700 meters from the vehicle

#### 2.2.1.3 Typical Reference Sorties

The second, third and fourth sorties are the third, fourth and fifth EVA's and are referred to as Typical Reference Sorties. The events are delineated in Table 2.2-3 and include the following features:

- o Checkout procedures as described in Volume II, Book II
- o Four five-minute science stops previously described
- o Four twenty-minute science stops as previously described
- o The driving velocity of the vehicle is 15 km/hr
- o The total distance travelled is 30 km within a radius of 10 km from the ELM

#### 2.2.1.4 Conversion to Unmanned Mode

The activities that occur during the conversion to the unmanned mode are delineated in Table 2.2-4

The following are removed:

- o Apollo Lunar Hand Tools
- o Lunar Survey System

The following are installed:

- o Science Module
- o RGM unit
- o Solar array

TABLE 2.2-2 INITIAL SORTIE (2nd EVA)

	Distance in km.		Time in Hr: Min	
	Increment	Cumulative	Duration	Elapsed Time
1 Crew transfer from ELM to DLRV			00:15	
2 Set-up tasks (See Book II)			00:10	00:15
3 Checkout (See Book II, Paragraph 4.1)			01:16	00:25
4 Drive to science module, deploy science module			00:20	01:41
5 Remove manned science from ELM and install on DLRV			00:30	02:01
6 Drive to First Science Stop at 5km/hr	.5		00:06	02:31
7 Pick up samples and store, use geological tools, photograph geological features			00:05	02:37
8 Drive to second stop at 10km/hr staying within 0.5 km of ELM	1.0	.5	00:06	02:42
9 Dismount, pick up and store samples, use geological tools and Survey Staff, photograph features, remount			00:20	02:48
10 Drive to third science stop at 12km/hr staying within 0.5 km of ELM	.4	1.5	00:02	03:08
11 Same as 7			00:05	03:10
12 Drive to Fourth science stop at 15km/hr, staying within .5 km of ELM.	.5	1.9	00:02	03:15
13 Same as 9			00:20	03:17
14 Return to ELM at 7.5 km/hr	.5	2.4	00:04	03:37
15 Post-sortie check (See Book II Paragraph 4.1 )		2.9	00:10	03:41
16 Transfer to ELM			00:08	03:51
				04:06

TABLE 2.2-3 TYPICAL MANNED REFERENCE SORTIES (3rd, 4th and 5th EVA)

	Distance in km		Time in Hours:Min	
	Increment	Cumulative	Duration	Elapsed
1 Egress ELM Ingress DLRV			0:15	
2 Perform C/O (See Book II Para.4.1)			0:14	00:15
3 Drive to First Stop at 15 km/hr	3.5	0	0:14	00:29
4 Dismount, pick up and store samples, use geological tools, photograph geological features, use Survey Staff, remount vehicle.			0:20	00:43
5 Drive to Second Stop	3.0	3.5	0:12	01:03
6 Pick up and store samples, use geological tools, photograph geological features.			0:05	01:15
7 Drive to 3rd Site at 15 km/hr	3.5	6.5	0:14	01:20
8 Repeat Step #4			0:20	01:34
9 Drive to 4th Site at 15 km/hr	3.0	10.0	0:12	01:54
10 Repeat Step #6			0:05	02:06
11 Drive to 5th Site at 15km/hr	3.5	13.0	0:14	02:11
12 Repeat Step #4			0:20	02:25
13 Drive to 6th Site at 15 km/hr	3.0	16.5	0:12	02:45
14 Repeat Step #6			0:05	02:57
15 Drive to 7th Site at 15 km/hr	3.5	19.5	0:14	03:02
16 Repeat Step #4			0:20	03:16
17 Drive to 8th Site at 15 km/hr	3.0	23.0	0:12	03:36
18 Repeat Step #6			0:05	03:48
19 Return to ELM at 15 km/hr	4.0	26.0	0:16	03:53
20 Post-Sortie Checkout (See Book II, paragraph 4.1)		30.0	0:10	04:09
21 Ingress ELM			0:15	04:19
				04:34

TABLE 2.2-4 CONVERSION TO UNMANNED MODE (6TH EVA)

	<u>Duration</u> <u>Hr: Min</u>	<u>Elapsed Time</u> <u>Hr: Min</u>
1 Egress EIM	00:15	0
2 Remove equipment not required for unmanned mode	00:15	00:15
3 Clean and inspect vehicle	00:10	00:30
4 Configure crew station for unmanned mode	00:05	00:40
5 Cover instrument panel with thermal insulating bag	00:15	00:45
6 Connect science module mechanically and electrically to the power module	00:20	01:00
7 Remove steering actuator from manned configuration position and place between science and power module	00:03	01:02
8 Mount solar array	00:05	01:05
9 Elevate suspension system of power and control modules	00:02	01:10
10 Load RGM	00:05	01:12
11 Install magnetometer on control module	00:05	01:17
12 Observe ground checkout. See Book II, Par. 4.1	01:41	01:22
13 Enter ELM	00:15	03:03
14 Begin unmanned operations		03:18

### 2.2.2 Unmanned Mission

The distances traveled, stops and speeds are well defined in the U. S. Geological Survey report previously mentioned. Speeds have been additionally amended for lighting as mentioned under Constraints. A list of the terrain and the major science sites from the same report is given in Table 2.2-5. The percent increment in ground-to-map distance is also indicated.

The mission briefly consists of a series of phases which are repeated until the specified 1000-km map distance (1155 km ground) is completed. The phases are:

- o Driving between and at major sites
- o Science stops at major sites
- o Routine science stops every  $\frac{1}{2}$  km while traversing between major sites
- o Quiescent periods during lunar night and poor lighting conditions.

Other repetitive phases result from the operation of science and vehicle equipment. Loading of the X-ray device requires a 3-minute stop every 12 minutes. Stops are also required when the batteries are recharged.

The unmanned science equipment operations as determined from the Science Interface Book of Volume VI, are listed in Table 2.2-6. They are briefly described as follows:

- o The magnetometer is on continuously except during battery recharge and lunar night
- o The X-ray device is on continuously except during battery recharge and lunar night. It operates in active and standby modes for 7 minutes and 8 minutes respectively
- o No samples are retained unless analyzed by the X-ray device.
- o The sampler is fully active for 10 minutes at every science stop and on standby for 8 minutes. It also operates 3 minutes of every 15 minutes to load the X-ray device, except during battery recharge and lunar night
- o The facsimile camera operates for 28 minutes at every routine science stop along the traverse. It operates for 34 minutes at major science stops and 3 minutes of every 15 minutes to load the X-ray device, except during battery recharge and lunar nights
- o The gravimeter operates in place on the surface for 8 minutes at every science stop. Deployment and retrieval require 2 minutes. It is kept on standby at all other times except during battery recharge and lunar night
- o The sample storage operates for 2 minutes at every science stop and one minute of every 15 minutes except during battery recharge and lunar night

TABLE 2.2-5 MAJOR SCIENCE SITES - UNMANNED MISSIONS

	Terrain Type		Percent Increment Ground To Map Distance	Ground Distance At Each Site km	Driving Time At Each Site hr
	Site-To-Site	At Site			
T-1	Smooth Mare	Smooth Mare	16	20	15
V-1	Smooth Mare	Rough Mare	16	15	20
I-1	Rough Mare	Rough Mare	18	10	20
I-2	Rough Mare	Rough Mare	18	15	20
V-2	Hummocky	Rough Mare	18	15	20
T-2	Rough Mare	Rough Uplands	24	15	20
T-3	Hummocky	Hummocky	16	10	20
I-3	Large Crater	Rough Upland	18	5	20
I-4		Large Crater	31	5	20
I-5	Large Crater	Rough Mare	31	12	20
I-6		Large Crater	31	13	20
I-7	Hummocky	Large Crater	31	7	20
T-4	Large Crater	Large Crater	24	13	20
V-3	Rough Upland	Rough Mare	31	10	20
T-5	Rough Mare	Rough Mare	18	15	20
V-4	Rough Mare	Rough Mare	18	15	20
V-5	Smooth Mare	Hummocky	18	10	20
V-6	Smooth Mare	Rough Upland	24	5	20
T-6	Rough Upland	Rough Mare	16	10	20
V-7	Smooth Mare	Hummocky	13	10	20
V-8	Rough Mare	Rough Mare	18	15	15

- T-1
- Smooth regolith at traverse origin
- V-1
- Lava flow front and top with linear depressions
- I-1
- Crater with secondary impacts and blocks
- I-2
- Secondary field of small blocky craters and concentric craters in regional ray-covered area.
- V-2
- Mare ridge with terrace
- T-2
- Mare-upland contact and talus slopes
- T-3
- Straight rille with fault scarps
- I-3
- Large fresh crater rim
- I-4
- Normal and inverted stratigraphic
- I-5
- "Ponded" plains on crater rim or wall
- I-6
- Floor-wall contact near concentric rilles
- I-7
- Central peak in large crater floor
- T-4
- Debris flow
- V-3
- Caldera or pit crater
- T-5
- Mare rilles concentric with basin rim
- V-4
- Low lava dome
- V-5
- Crater-top dome (or steep-sided dome)
- V-6
- Maar or chain crater
- T-6
- Sinuuous rille with levees
- V-7
- Dark halo craters and associated rille
- V-8
- Transient phenomenon/thermal anomaly

FOLDOUT FRAME

FOLDOUT FRAME II/I.2-11/12

2

TABLE 2.2-6 SCIENCE EQUIPMENT OPERATIONS FOR UNMANNED MISSION

EQUIPMENT	DRIVING (Min.)	STOPPED (Min.)	POWER (Watts)
1. TV Camera Scan of Site Includes 2 Landmark Sightings		2	15
2. Magnetometer	Continuous *		5
3. Gravimeter		(10)	
Deploy Gravimeter		1	15
Stabilization		5	10
Measurements		3	100
Retrieve Gravimeter		1	9
Standby	Continuous *		4
4. Sample Arm		(18)**	
Concurrent With Gravimeter Operations		10	15
Standby		8	5
During X-Ray Diffractometer/Spectrometer Load Cycle	Three minutes per 15 min. throughout mission		
5. Sample Storage Container (Run Concurrently with Sampler Arm)	One minute during three minute interval of 15 min. cycle		
	2		5
6. Facsimile Camera		(28)	15
Two panoramic views		10	
Observe Sample Arm and Samples		8**	
Observe Deployment of Gravimeter		2	
Status Check of Magnetometer		1	
Photograph Terrain		4	
Mode Transition		3	
During loading of X-ray Device	Three minutes during 15 minute cycle		
7. X-ray Diffractometer/Spectrometer	Continuous throughout Mission in 15-minute cycle		
Standby & Prepare	7		11
Active	8		55

\* Except during night and battery recharge

\*\* Increase by 6 minutes at Major Science Stops

The resulting electrical power profile is shown in Figure 2.2-1 for the continuous science load (X-ray analysis cycle, magnetometer and gravimeter) and is equivalent to a 50W continuous load. The electrical power profile for the additional intermittent science load at each routine science stop is shown in Figure 2.2-2 and 2.2-3 and is equivalent to an additional 33.7 watts. The profile is the same for major science stops except that the sample arm and facsimile camera are operated 6 min. longer for a more careful scrutiny of samples.

The terrain types from Table 2.2-5 are distributed as follows:

Smooth mare 25%  
 Rough mare 25%  
 Hummocky upland 20%  
 Rough upland 15%  
 Large craters 15%

This distribution plus the reduction in velocity due to sun angle (see Table 2.1-1) was used to determine a weighted velocity of 1.1 km/hr for the entire year. From the science operations, other constraints, and average driving speed of 1.1 km/hr, the times required to accomplish the mission were derived and are shown below:

TABLE 2.2-7 UNMANNED REFERENCE MISSION SUMMARY

1 year		8760 hr
Less Unusable Time		
12 Lunar Nights	4248	
Poor Lighting	482	<u>4730</u>
Available for Operations		4030
Less time at Major Sites (21 sites at 50 hr. each)		<u>1050</u>
Available for 1000 km Traverse Operations		2980
Less Driving: 1155 km at 1.1 km/hr	1050	
Less Science:		
- 30 min. stops, every $\frac{1}{2}$ km (2000 stops)	1000	
- 3 min. stops every 12 min. driving	263	<u>2313</u>
Surplus time		667 hr

The surplus time of 667 hr. is the maximum allowable for battery recharge or possible thermal cool-down stops.



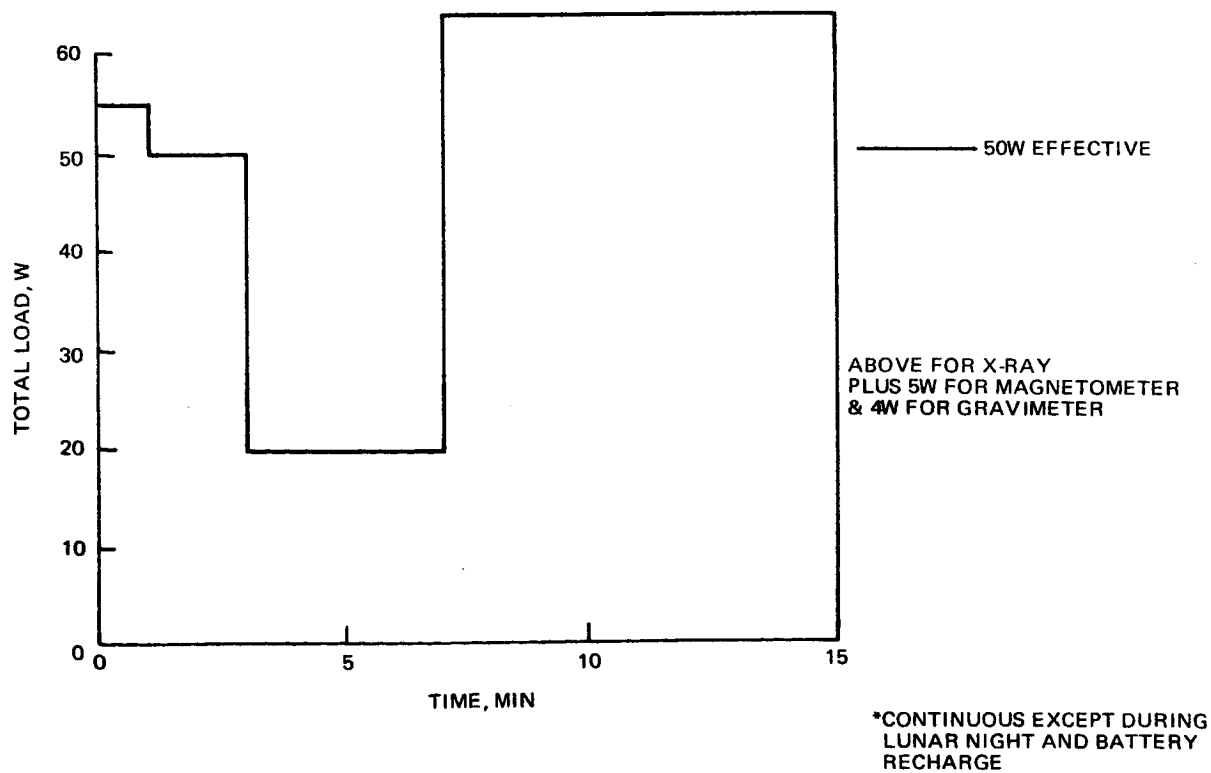
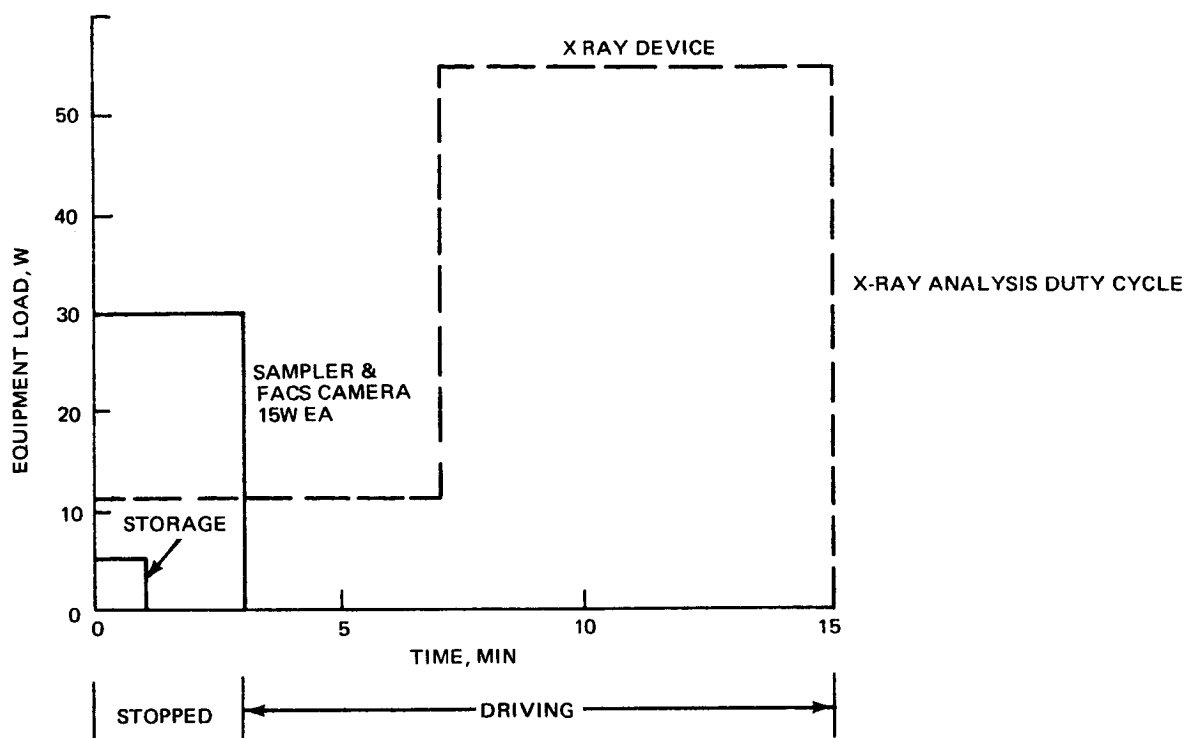


FIG. 2.2-1 CONTINUOUS\* SCIENCE LOAD

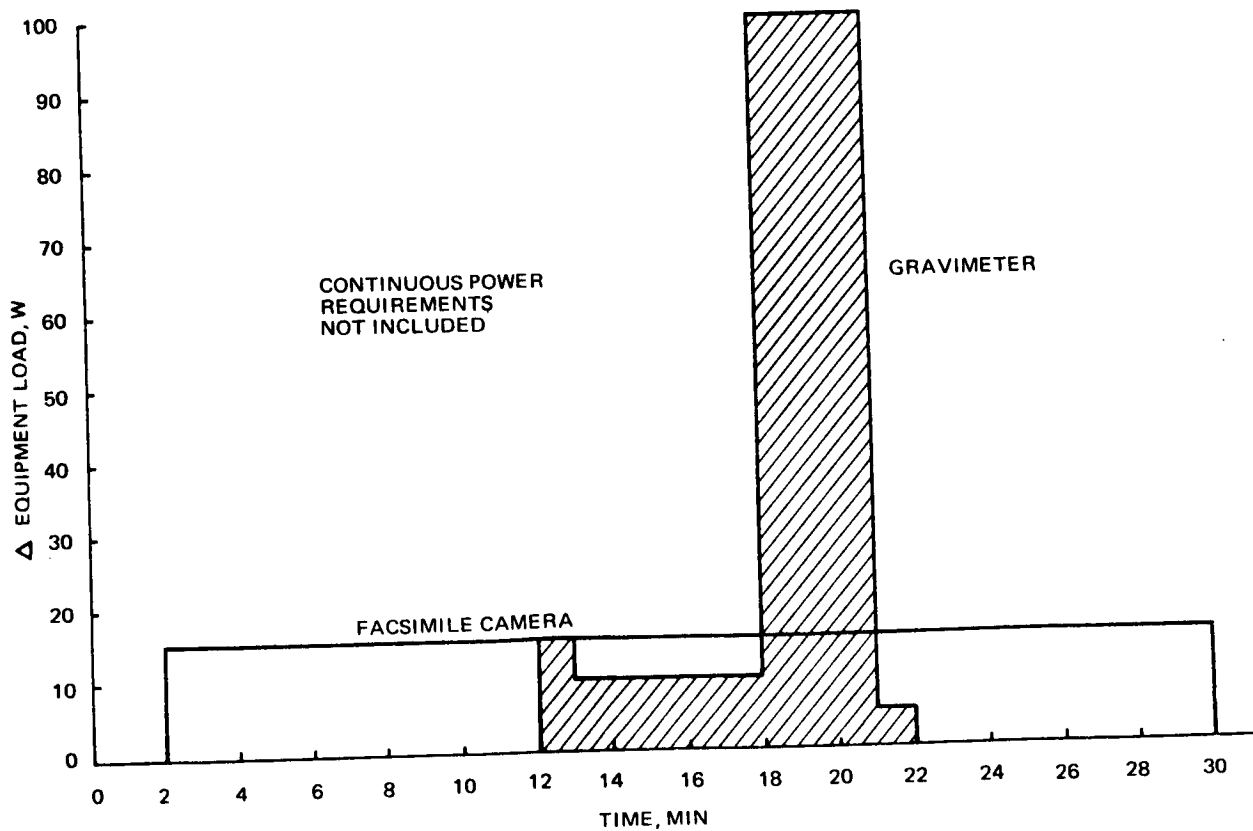
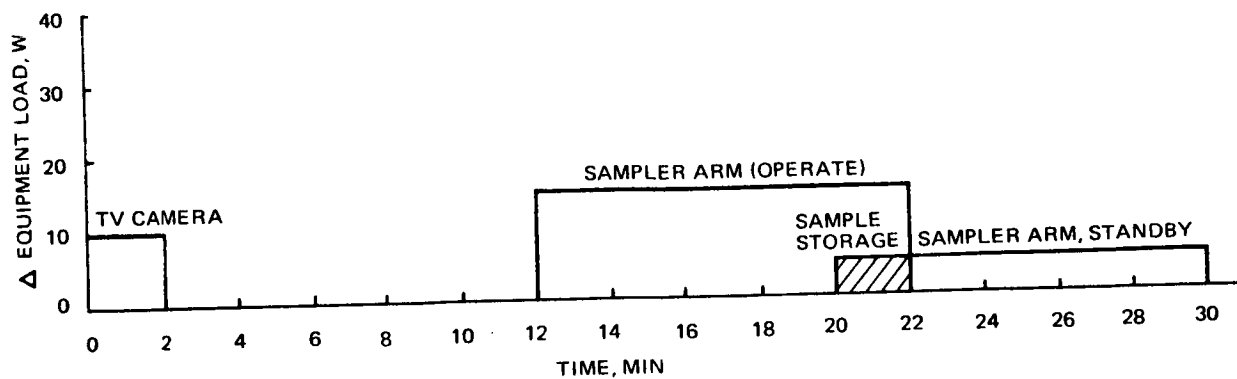


FIG. 2.2-2 POWER PROFILE INCREMENTS FOR ROUTINE SCIENCE STOP

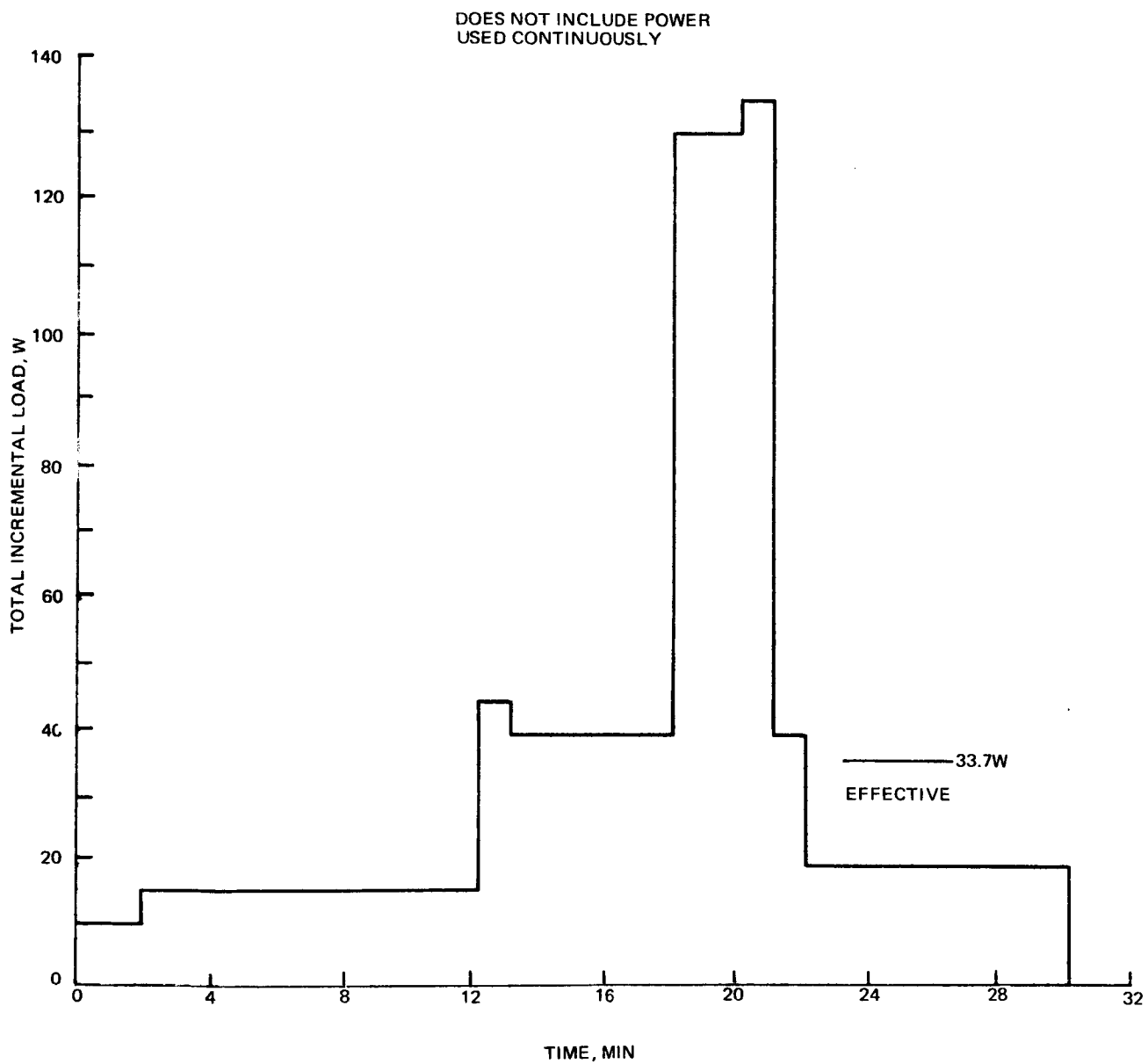


FIG. 2.2-3 INCREMENT IN POWER FOR ROUTINE SCIENCE STOP

### 2.2.3 Prelaunch Operations

The KSC prelaunch checkout phase completes the DLRV flight article test program. This phase of the test program includes the verification of the complete flight system (DLRV with the ground station) and the final launch pad activities.

The KSC prelaunch activities include system level checkout in the MSOB utilizing the MCC located at MSC and final stowage of scientific equipment, prior to SIA mate. The launch pad activities include calibration of scientific equipment approximately three (3) weeks prior to launch, battery installation seventy two (72) hours prior to launch and RTG installation twenty four (24) hours prior to launch. With the exception of verifying bus voltage at the time of battery and RTG installation, the DLRV system will not be monitored from SIA mate to launch. Figure 2.2-4 shows the complete DLRV prelaunch flow timeline. A more detailed description of the prelaunch checkout activities may be found in the Test Plan contained in Volume VIII, Book I.

#### 2.2.3.1 Final Checkout (T-15.5 weeks)

The DLRV is installed on its checkout stand in the MSOB. A mission simulation utilizing the Mission Control Center (MCC) is then performed. At the completion of this simulation, the DLRV is mated with its spacecraft and the deployment mechanism is checked.

#### 2.2.3.2 SIA Mate (T-13 weeks)

The DLRV with its spacecraft is mated with the SIA. After the SIA work platforms are installed, a fit check of DLRV flight batteries and the RTG is made. Mock-ups are used for the fit checks.

#### 2.2.3.3 Launch Complex Operations (T-11 weeks)

The SIA/Spacecraft/DLRV is transported to the VAB where it is stacked on the booster.

#### 2.2.3.4 Launch Pad (T-10 weeks)

After transporting the complete space vehicle to the pad, a series of launch vehicle and spacecraft checks are performed. The DLRV does not participate in this testing.

Significant events for the DLRV at the launch pad include:

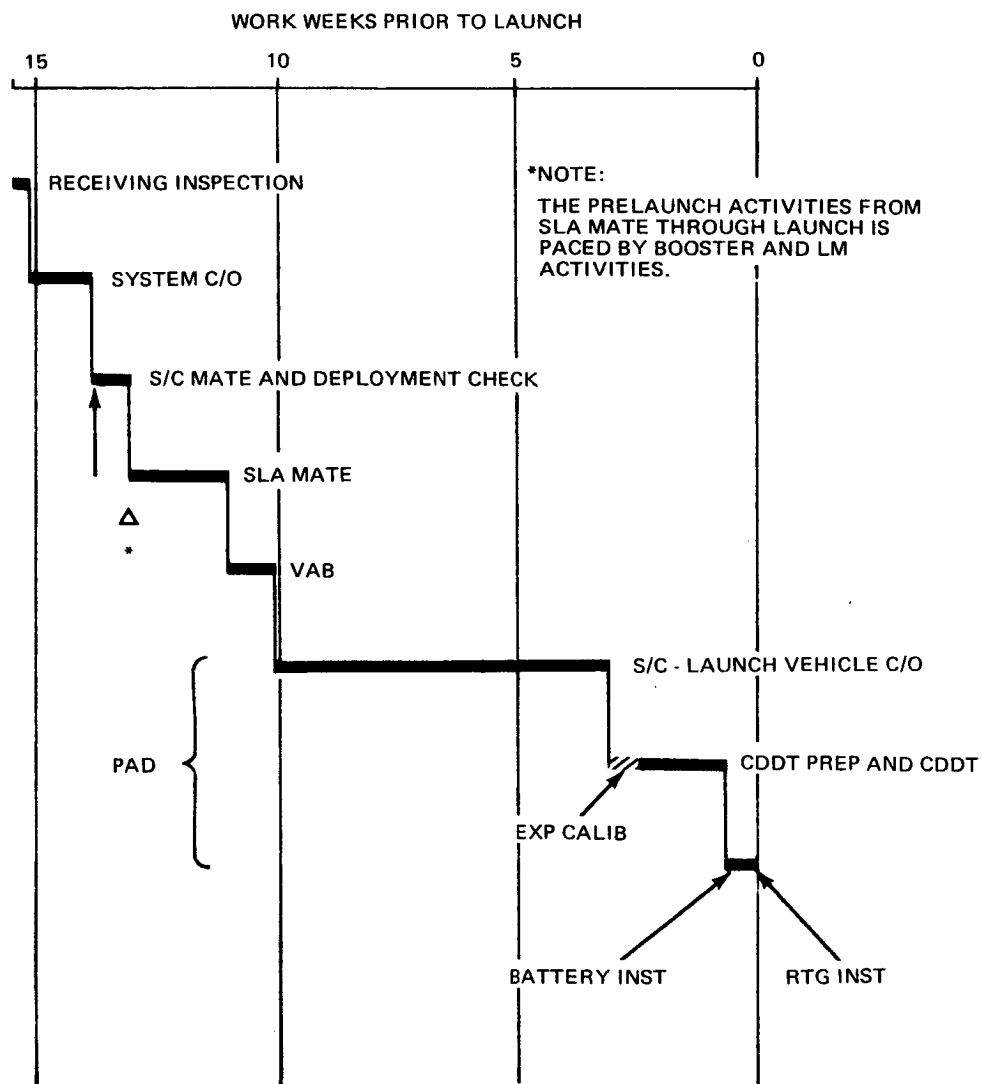


**FIG. 2.2-4 PRELAUNCH FLOW TIMELINE**

- o Final Scientific Equipment Calibration (T-3 weeks)  
Experiment equipment located on the science module that requires calibration prior to launch is calibrated during this period. Calibrations are expected for the accelerometers, gravimeter, magnetometer, alignment of X-ray device, and light level of the facsimile camera. The magnetometer sensor should not be exposed to fields greater than 25 gauss either before or after calibration. Specific requirements and procedures are still to be determined.
- o Flight Battery Installation (T-72 hours)  
At the beginning of the space vehicle countdown, the DLRV flight batteries are installed. After the mechanical installation and the electrical connection is made, the flight connection is verified by reading out bus voltage. Battery temperature is monitored until SLA closeout at T-10 hours
- o RTG Installation (T-24 hours)  
The RTG is the last piece of equipment to be installed on the DLRV. After the mechanical installation and the electrical connection is made, the flight connection is verified by reading out bus voltage

## 2.3 DESIGN MISSIONS

Some subsystems and/or components are dependent not only on time durations but on the sequence in which functions are performed. The missions and objectives are then considered in combination with some prior knowledge of the subsystem components to derive appropriate requirements for subsystem design. Maximum growth and flexibility are obviously desired but must be compromised for practicality.

The critical subsystems/components usually involve expendables and/or heat transfer. For the case of the DLRV the principal functions considered are:

- o Electrical power
- o Temperature control

### 2.3.1 Electrical Power

Battery energy and load, solar cell array size, and RTG size are the parameters affected by the mission. The Reference Missions of Subsections 2.1 and 2.2 include the range, radius, time and science requirements of the SOW and are considered applicable without further modification. One deviation is the minimum time between manned sorties which has been increased from 3 hours in the SOW (Annex A) to 8 hours as per discussion with MSFC at the 4th Monthly Progress Report.

### 2.3.2 Temperature Control

Except for batteries and traction motors, the Reference Missions, at the worst sun angles, are applicable. Battery and traction motor heat outputs, however, are related to wheel power, i.e., sustained slope climbing. The criteria given by MSFC for the LRV were:

- o Climb a 6° slope at 10 km/hr for 15 km
- o Climb a 25° slope at any speed for 0.5 km

The DLRV should have comparable capability and therefore the above are incorporated in the manned thermal design mission timeline, Table 2.3-1. The manned case is considered more power-critical than the unmanned case where all speeds are less than 2 km/hr.

The unmanned case, however, is more critical from a time duration viewpoint since thermal surfaces may be covered while driving and also may be degraded by dust and repetitive cleaning. If heat storage devices are used, they would be sensitive to equipment duty cycles. The most critical parameter is sustained driving time between science stops. Equipment loads, and therefore thermal cooling requirements, are higher when driving than during the stopped science operations. Considering the lowest driving speed to be  $\frac{1}{2}$  km/hr between science stops which are  $\frac{1}{2}$  km apart, the longest drive time is one (1) hour. Science stop time is  $\frac{1}{2}$  hr. This drive/stop time cycle should be sustainable during a 100-km traverse or for 200 cycles through worst solar lighting conditions.

## 2.4 METEORIDS AND RADIATION

### 2.4.1 Micrometeoroids

Since the DLRV is essentially shielded by the ELM delivery vehicle during the translunar trip, the only concern is for the long duration, one-year, stay on the lunar surface.

Mechanical structure is inherently invulnerable to damage. Electronic parts and solar cells, however, require consideration. Using the data of Annex C of the Statement of Work, and the top and side areas of all electronic compartments, a required aluminum thickness of 0.02 in. is calculated for a 0.95 probability of no penetration. The secondary particles in this case are of greater concern than the primary particles. In general, the electronic packaging should be more than adequate to rule out any concern over survival of the electronics.

TABLE 2.3-1 THERMAL DESIGN MISSION TIMELINE - MANNED

PHASE	TERRAIN	SPEED km/hr	DIST km	PHASE TIME min.
Drive Out up a 6° slope	Smooth Upland	10	15	90
Science Stop at Rim	-----	0	0	20
Descend Crater Wall, 25° slope	Rough Upland	2	0.5	15
Science Stop at Floor	-----	0	0	5
Ascend Crater Wall, 25° slope	Rough Upland	2	0.5	15
Explore Along Crater Rim	Rough Upland	4	2.0	30
Science Stop at Rim	-----	0	0	20
Drive Back	Smooth Upland	15	8	30
TOTAL			24	225



The solar panels present an area of approximately 44 ft<sup>2</sup> but little area is projected to the secondary particle source, the greater concern. Additionally, the parallel-series connections of the solar cells will cause almost negligible power loss in the event of cell disablement.

In summary, particle penetration is unlikely, but even if penetration occurs, mission success will not be seriously impaired.

#### 2.4.2 Radiation

The effects of natural radiation on the crew and scientific equipment have not been considered. It is assumed that both crew and equipment protection for this given environment will have been resolved by prior NASA direction.

Except for solar cells and certain semiconductors, the DLRV is unaffected by radiation environment, natural, or induced by the installation of a radioisotope thermoelectric generator. Mechanical parts are intrinsically hard. Allowance for solar cell degradation has been made in the design of the solar array. Most electronic parts are not affected. Sensitive electronic parts are shielded, (usually by adjacent components) derated or preselected as discussed under Parts Environmental Requirements of Reliability, Section 4.5. Radiation presents no problem to the vehicle or crew operations.

The effect on the scientific equipment is discussed in Book I of Volume IV, Scientific Equipment Interface Design.

#### 3.1.1.1 Delivery Vehicle Payload Arrangement

Annex A of the work statement defined the available locations for stowage of the DLRV in the Extended IM as being quadrants I and IV of the descent stage including some negotiable volume external to the descent stage. However, before the DLRV Study Contract was initiated, it became apparent that any near-term IM derivative vehicle would not have two open quadrants available.

Several EIM payload arrangements, as summarized in Figure 3.1-1 were studied. These were compared on the basis of their effect on DLRV chassis planform, available equipment volume, and deployment complexity.

Figure 3.1-1a shows an arrangement that could be used if both quads were available as per Annex A. It causes the least interface problems with the EIM RCS, and provides 47 sq. ft. of platform area and 25 cu. ft. of equipment/science volume. If only one quadrant is open for payload use, an arrangement in which the total DLRV is stowed as a unit, such as shown in Figure 3.1-1b might be used. A study of this arrangement showed that its advantage of joined-up deployment is more than offset by a 40% reduction in available equipment and science volume, and a requirement for more manual set-up at deployment.

If no internal volume is available, the vehicle can be carried externally as shown in Figure 3.1-1c. This arrangement allows easier deployment, but affords less equipment/science volume, and the necessarily shallow shape will make equipment integration difficult.

This recommended arrangement is shown in Figure 3.1-1d. The forward two modules are stowed internally in Quad I as originally proposed, and the third module is carried external to Quad IV. This arrangement retains nearly as much equipment/science volume as the two quad internal one, but is moderately degraded in shape factor due to the shallow payload volume. DLRV growth of the 3rd module is compatible with the potential availability of portions of Quad IV, a result of subsequent IM modifications.

#### 3.1.1.2 Delivery Vehicle Payload Envelope

Annex A of the work statement and subsequent modifications have defined EIM payload volumes which are usable for DLRV stowage. The protrusion of the envelope beyond the descent stage under the RCS thrusters has been limited to a line representing the projection of the surface of the IM plume deflector. With this limitation no serious thermal impact on the DLRV equipment or adverse effects on the IM attitude control will occur. In the absence of high angle plume impingement, thermal

## SECTION 3

### SYSTEM DESIGN

This section deals with the design of the overall vehicle. It consists of two main subsections. The first of these, "Configuration Design Rationale", discusses the requirements and underlying reasons for the selection of the design. The second subsection, "Selected Configuration", gives details such as stowed and deployed arrangements, mass properties, and schematic diagrams for the selected design.

#### 3.1 CONFIGURATION DESIGN RATIONALE

The objective of the DLRV configuration study was to arrive at a design which best satisfied the manned and unmanned mission requirements. Both this and earlier studies indicated that the configuration best suited for the lunar mission would be the one with the largest planform and wheel diameter; a major configuration guideline was, therefore, to deploy wheels of the largest stowable diameter to a vehicle geometry having the largest practical wheelbase and tread. Emphasis in the area of crew integration was also important in the design philosophy. Minimizing the astronaut's time required for deployment and operational readiness stressed the importance of utilizing EVA time for the scientific mission objectives. Also, since the primary purpose of the DLRV will be lunar exploration through the accumulation of data from a large number of locations, the requirements of the science components played a major role in configuring the vehicle.

##### 3.1.1 Delivery Vehicle Accomodation

A dominant constraint on the DLRV configuration is caused by the delivery vehicle. The wheel size, chassis shape and size, and equipment location are all critically limited by the stowage envelopes available on the IM derivative lunar lander. The method of deployment from these stowage envelopes also greatly affects vehicle configuration.

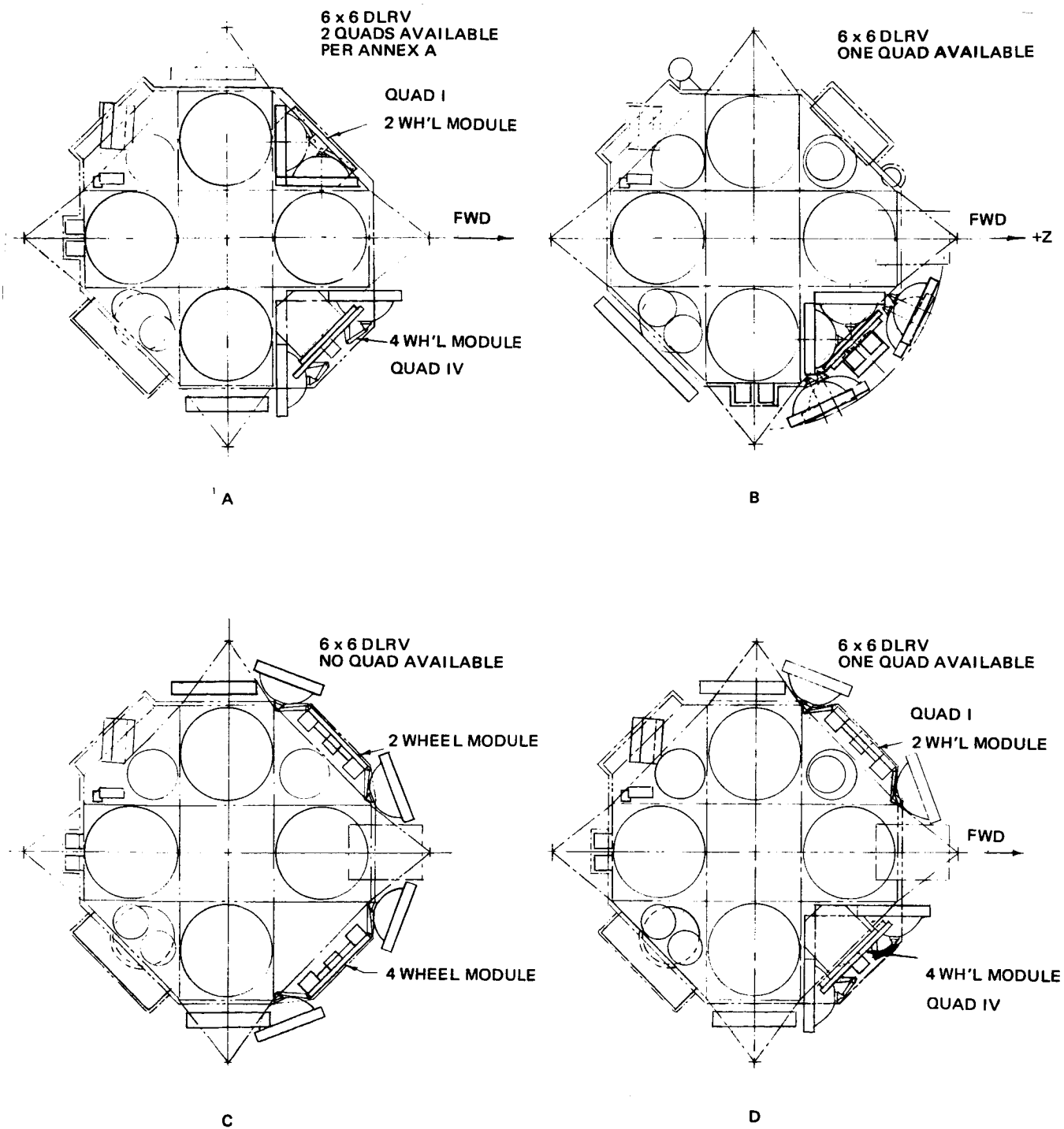


FIG. 3.1-1 ELM PAYLOAD ARRANGEMENTS

shielding weight is minimized. In addition, an 18 inch clearance between the payload envelope and the SLA has been maintained for easy access to pad-installed or replaceable components. The volume that was cut off from the external portion of Quad IV in Annex A has been assumed usable, since the EIM solar array installation that required that space has been eliminated. Definition of this assumed working payload envelope is shown in Figure 3.1-2.

#### 3.1.1.3 Battery and RTG Loading

The DLRV batteries and RTG require installation late in the launch countdown. Therefore they must be in a location on the stowed DLRV where the launch crew can make the installation while within the SLA and out on the launch pad. The installation must be accomplished quickly and easily because of time constraints and limited working conditions.

During installation the two batteries are fastened to a supporting cold plate and electrically connected. Since they are located in a thermally controlled area, a radiator panel must be installed following battery installation.

The Snap-19 RTG is fueled at manufacture. Because of its continuous heat output, it should be installed last. Special handling equipment will be required to move it within the SLA to the DLRV. After installation, thermal control, similar to that used with the Snap-27 fuel cask on the IM, must be used until launch.

#### 3.1.1.4 Science Accessibility

For mission flexibility, the DLRV design provides the possibility of making changes in the science complement at any time between missions, including the four to six months after staging. When staged, the confinement of the stowed DLRV by the spacecraft and the SLA prevents removal. Therefore, the science equipment was located on the stowed configuration such that adjustments, replacements, or substitutions may be accomplished while in the stack.

#### 3.1.1.5 Other Delivery Vehicles

If, in the future, some other delivery vehicle is available for the DLRV, advantage should be taken of the relief of IM imposed constraints. In simplest form, this will result in a DLRV configuration having considerable variation in equipment/science arrangement while retaining the basic mobility subsystem.

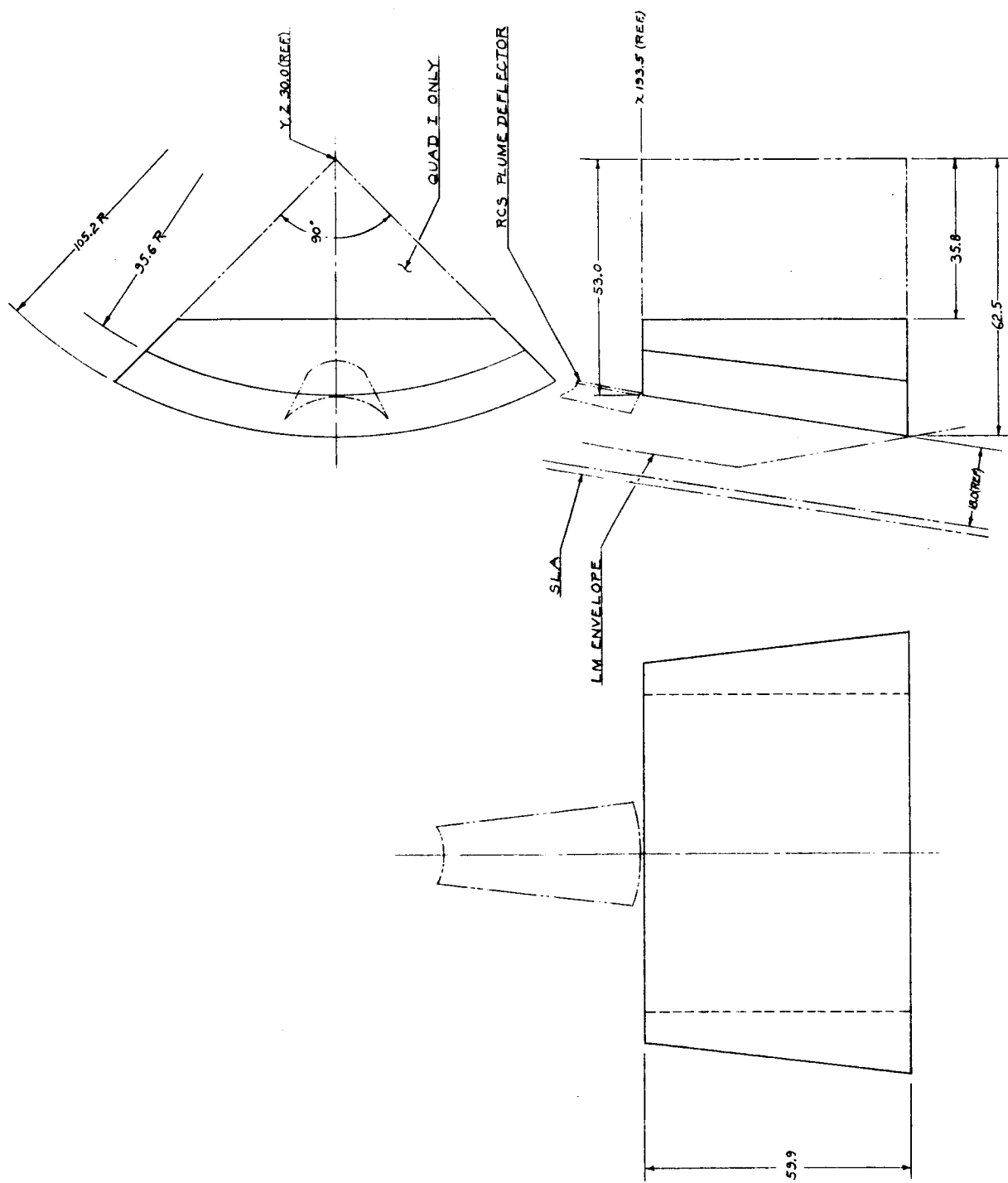


FIG. 3.1-2 ELM PAYLOAD ENVELOPES QUADRANTS I & IV

### 3.1.2 Mobility Requirements

#### 3.1.2.1 Mobility Characteristics

Although a number of steering methods were considered, only the articulated and Ackermann systems remained candidates in the final evaluation. Figure 3.1-3 shows sketches of the two arrangements for equal inside turning radii. The major difference affecting the overall configuration between the two steering systems is in the stowage complexity, for which the articulated system has the advantage. A penalty that is generally associated with the articulated system is a loss in platform area to provide for steering clearance. However, no such penalty occurs with the extendable drawbar design shown, since the clearance between modules is required for stowage; the drawbar extension provides for large wheelbase in the operational condition, but the front two modules slide together for stowage. An evaluation of the two steering candidates, reported in Section 5.3, led to the selection of the articulated system for use on DLRV.

Vehicle turning stability is another important consideration. The potentially serious consequences of overturning, combined with the unlimited combinations of slope and surface roughness, the difficulty in judging inclination without references, and the instinctive reaction of a driver to swerve to avoid obstacles, dictates a low c.g. and a large tread and wheelbase for maximum turning stability. The basic requirement is for a minimum static stability angle of  $45^\circ$ ; but, further stability about the roll axis is desirable if it can be achieved with little weight penalty, because overturning would still be possible within the normal operating range of the vehicle in the low gravity lunar environment (see Section 4.2.4). Figure 3.1-4 shows the minimum stable turn radius as a function of vehicle tread.

A further advantage of a large tread and wheelbase is improved ride quality, due to reduced roll and pitch accelerations. Roll acceleration trends, which are considered the more critical ride quality parameter, are also shown in Figure 3.1-4.

Large wheels provide a number of benefits to mobility performance: They make possible a large footprint which lowers rolling resistance and increases drawbar pull and locomotion efficiency; they enhance obstacle negotiation capability, particularly for crevasse crossing; and finally, the result in increased ground clearance. A primary objective was, therefore, to utilize the largest wheels that could be stowed in the available IM envelope.

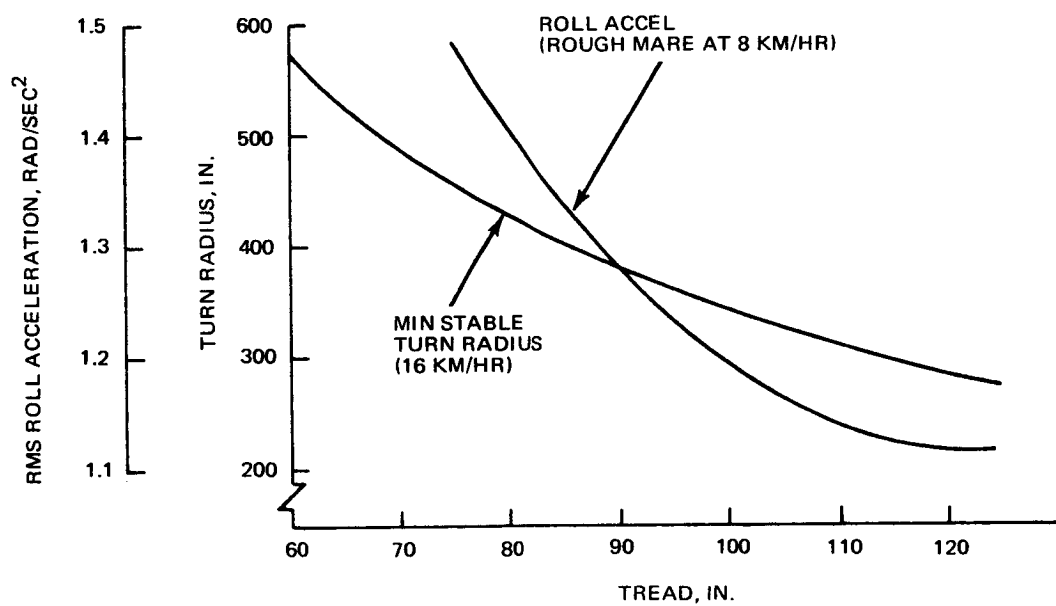


FIG. 3.1-4 STABILITY AND ACCELERATION TRENDS WITH VEHICLE SIZE



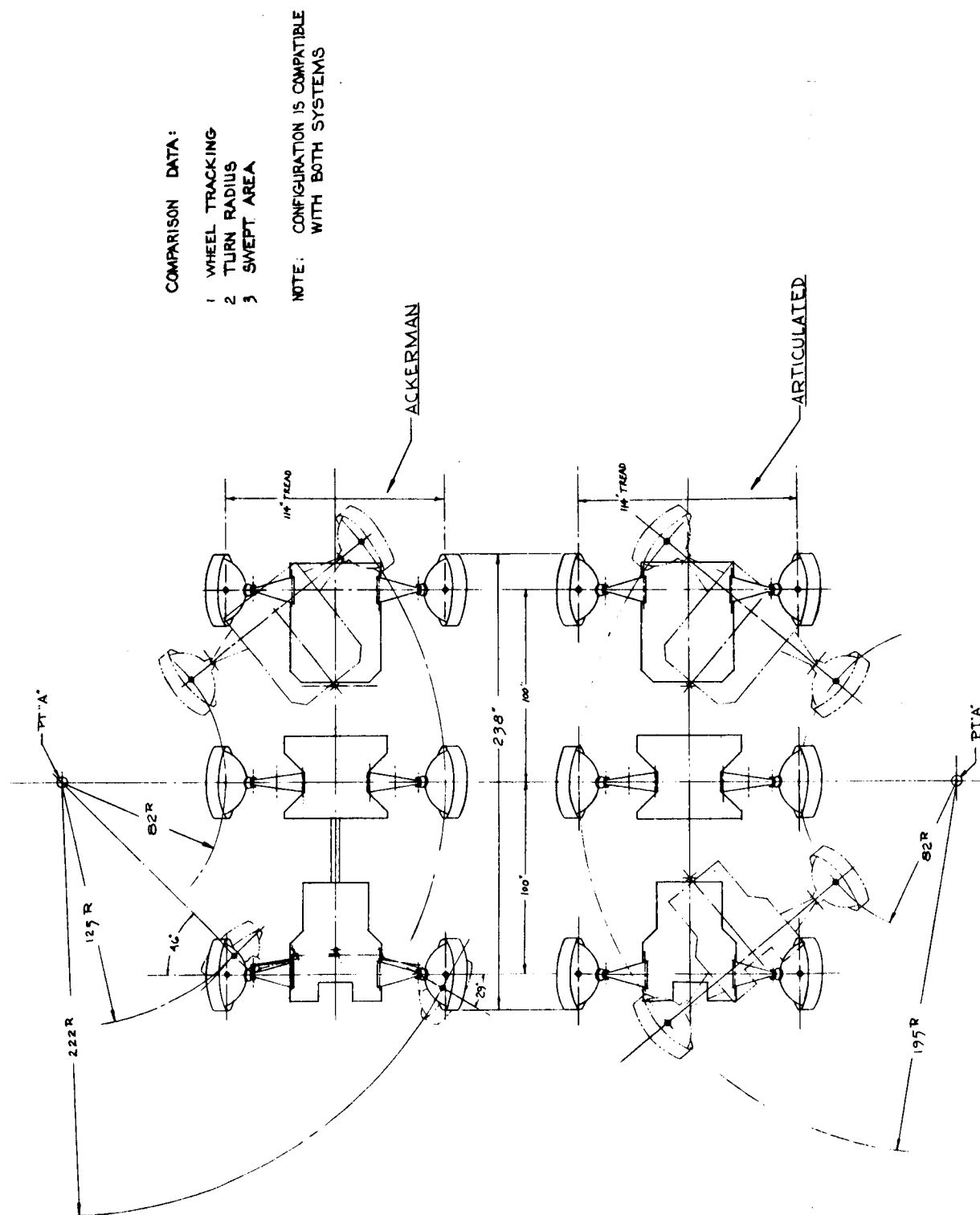


FIG. 3.1-3 COMPARISON DIAGRAM ACKERMAN/ARTICULATED WITH EQUAL PLATFORM

### 3.1.2.2 Best Mobility Geometry Vehicle

Utilization of the above design objectives for mobility led to the configuration having the most favorable vehicle geometry that could be contained in the available stowage volume. Figure 3.1-5 shows the mobility geometry and available platform area and equipment volume of the selected design. The vehicle has a large 114" tread, 96" wheelbase, and 38" diameter wheels. It meets or exceeds the turn radius, ground clearance and obstacle and crevasse crossing requirements. The 45° static roll stability requirement is greatly exceeded for any realistic c.g. height. The intermodular drawbar has high torsional flexibility to allow the individual wheels to follow the ground contour with little restraint, thereby retaining maximum traction even on irregular terrain.

The large platform area is achieved at the expense of little weight. A swing arm suspension naturally provides a wide tread, and a light-weight extendable drawbar is used to achieve a large wheelbase.

The vehicle geometry shown was used as the basis for the detailed crew/equipment/science integration studies that led to the selection of a DLRV configuration design.

### 3.1.3 Science Accommodation

The location of the science equipment plays an important role in its proper operation. A variety of requirements, such as accessibility, deployability, moveability, and stowability, exist for the equipment. In addition, interaction of some science equipment with elements of DLRV subsystems is an important consideration. The three categories of science equipment - vehicle mounted remote science, manned science, and remote deployable science - have differing requirements.

The vehicle mounted remote science must be stowable on the DLRV during delivery to the lunar surface. The sample acquisition device requires ready access to the lunar surface, in view of the TV camera. The sampler arm, sample stowage container, facsimile camera, and X-ray diffractometer spectrometer are interdependent, and must be located near each other in a relationship that allows proper operation. The locations of the magnetometer and gravimeter must allow the deployment and return to the vehicle needed for their operation.

The manned science equipment should be accessible to the astronaut, with the most used items being within easiest reach. Since the manned science is loaded onto the DLRV after deployment, it should be located to facilitate this task.

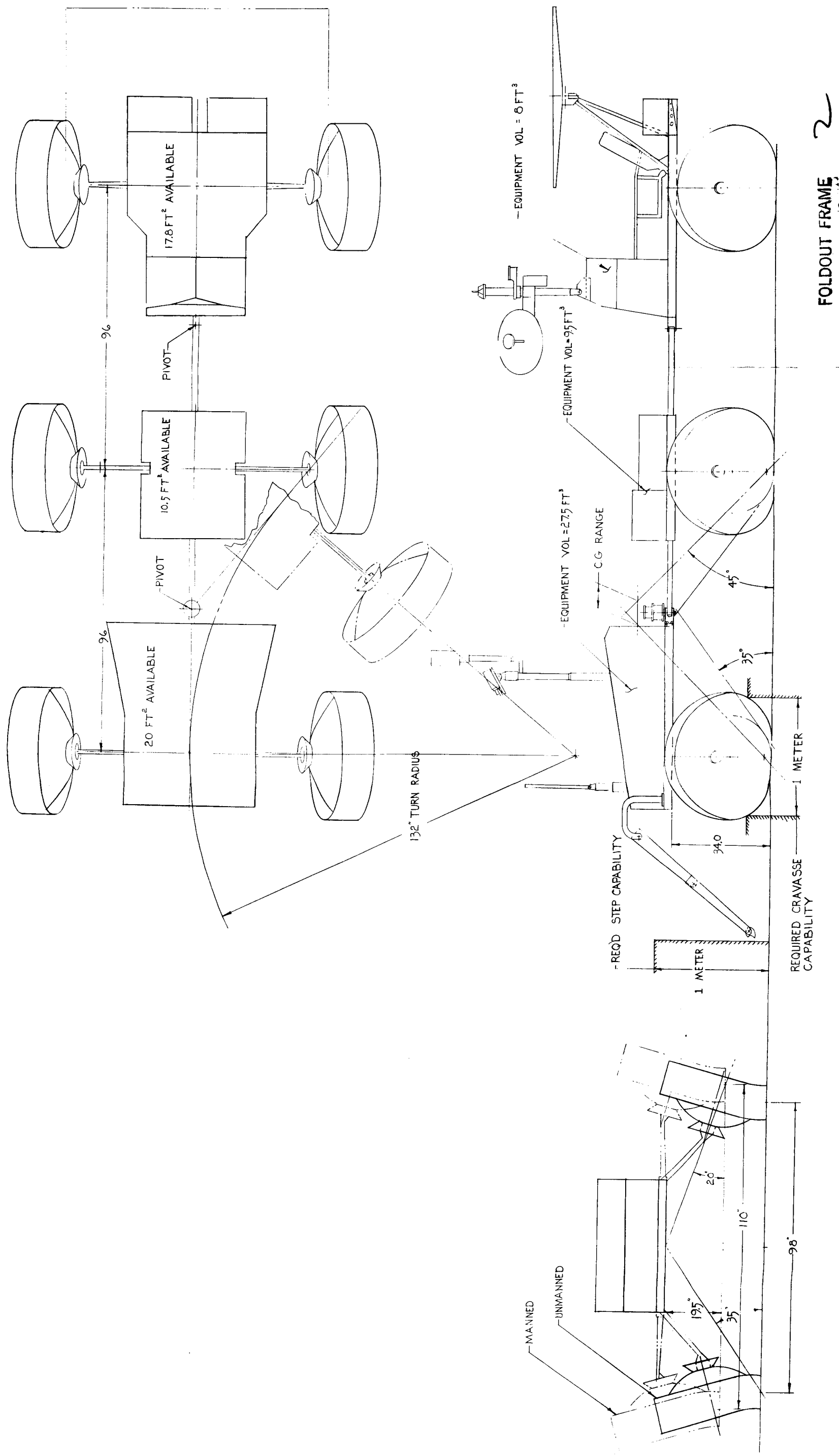


**FIG. 3.15 SELECTED MOBILITY GEOMETRY**

### 3.1.6 Arrangement Alternatives

Although the DLRV must be a six-wheeled vehicle in order to meet the unmanned mobility requirements, a four-wheeled vehicle is adequate for manned sorties, where the obstacle negotiation requirements are less stringent and there is no need for automated science. A substantial power savings results from using a manned 4 x 4 instead of a 6 x 6, and it is the manned mission that sizes the power system. In order to retain manned 4 x 4 capability, all equipment required for manned operation (including manned science) must be placed on two modules, with the remaining automated science placed on the third module. This approach was examined early in the study and found to be quite feasible with little or no identifiable penalty. A number of alternatives exist when adding the 2 x 2 module containing the science to convert from manned 4 x 4 to unmanned 6 x 6 operation:

- o The science module can be added to the rear of the 4 x 4 vehicle as a trailer
- o The science module can be placed in front of the 4 x 4 to become the lead module
- o The science module can be placed in the rear of the 4 x 4 but the forward direction can be reversed for unmanned operation to allow the science module to lead

Some of the arrangements that have been considered are shown in Figure 3.1-6. These are all stowable in the selected two-quad stowage arrangement. All have sufficient volume for the equipment and science, with adequate thermal control area and growth capability. All can be operated as a manned 4 x 4.

The remote deployable science is also loaded on the DLRV after deployment. It requires a location allowing both easy manual loading and remotely controlled off-loading.

#### 3.1.4 Crew Accommodation

The manned portion of the DLRV mission imposes certain constraints on the vehicle configuration. To be effective, the driver must be located where he has good forward visibility and can see the surface immediately ahead of the front wheels. Also, his position must afford easy ingress/egress within the restrictions imposed by the pressurized suit. Safety considerations require that the driver location be out of the path of debris thrown by the wheels. Because the weight of an astronaut is a large portion of the vehicle gross weight, the emergency passenger station should be located where it will not severely unbalance the vehicle. If a degraded mode of operation is assumed for the unlikely rescue condition, a favorable weight distribution will eliminate the need for adding strength to the basic mobility system.

#### 3.1.5 Subsystem Equipment Requirements

Many subsystem components have a great effect on configuration because of their operational requirements:

- o Antennae must be located as high as possible. In addition, the S-Band steerable antenna cannot be obscured at low elevation angles.
- o The TV camera has a position requirement that must satisfy driving, navigation, and science monitoring.
- o The solar sensor does not function if shadowed.
- o The RTG accessibility requirements during stowage have already been noted. Additionally, the RTG must be able to radiate its heat to space to avoid overheating neighboring components.
- o The solar array must be located where it can operate throughout its tilt range, without antenna and camera viewing problems.
- o Equipment items must be arranged in the equipment bays to provide a good thermal balance. Heat loads must be within the capabilities of the radiation areas available on each module.

The simplest of these arrangements is the one in which the science module is added as a trailer; but, this approach is least desirable from the science viewpoint, because of the restricted access of the sampler arm. Either of the arrangements that have the science module leading in the unmanned mode permit relatively independent optimization for the manned and unmanned missions. The leading science module provides the sampler with unrestricted access to virgin soil, and the TV is in a favorable position for viewing sampler operation. The only significant disadvantage is that either the steering actuator must be moved from one joint to another during conversion to unmanned operation, or a second actuator must be provided. The movable actuator approach costs less weight with little demand on the astronaut's time; it is, therefore, the best choice for the critically weight-limited DLRV.

Comparison of the two leading-science-module versions shows that the double-ended vehicle has least difficulty in providing adequate solar array clearance, convenient RGM deployment, and a favorable weight distribution. Because of these advantages the "double-ender" was selected for the DLRV configuration.

### 3.2 SELECTED CONFIGURATION

After selecting the basic vehicle configuration and stowage arrangement, emphasis was shifted to optimization and further development of the selected design. These studies resulted in a more detailed definition of the manned, unmanned, and stowed configurations, and the associated mass properties and equipment integration diagrams.

A self-contained description of the selected configuration is given in this section.

#### 3.2.1 General Arrangements

##### 3.2.1.1 Manned Mode

For the manned mode the DLRV is a four-wheel two-module vehicle having the general arrangement shown in Figure 3.2-1. It has a large platform - 110-in. tread by 96-in. wheelbase - and large 38-in.-diameter cone wheels with 11.6-in. grousers. The suspension is swing arm, which produces the large tread at little expense and provides scuff damping to control the ride. The suspension has two positions: a low one, as shown, for the manned mode to provide high stability, and a higher one for the unmanned mode, for maximum obstacle negotiation capability. Steering is by chassis articulation, using a rotary actuator to power the steering joint. A telescoping drawbar connects the two modules, providing a large wheelbase

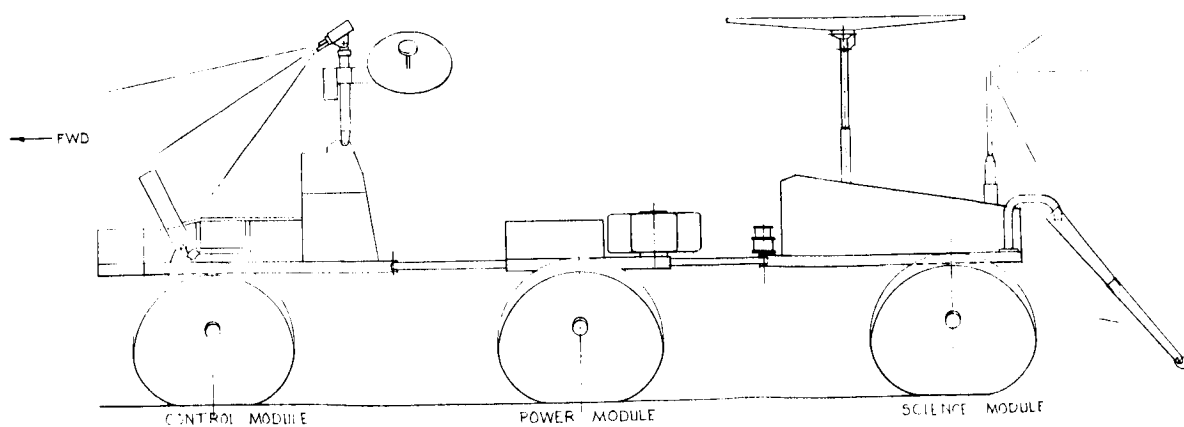
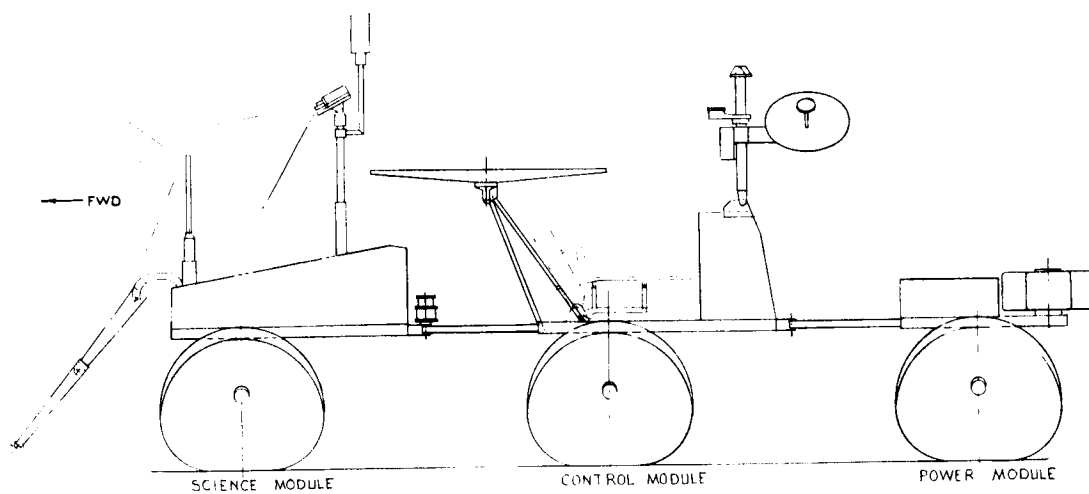
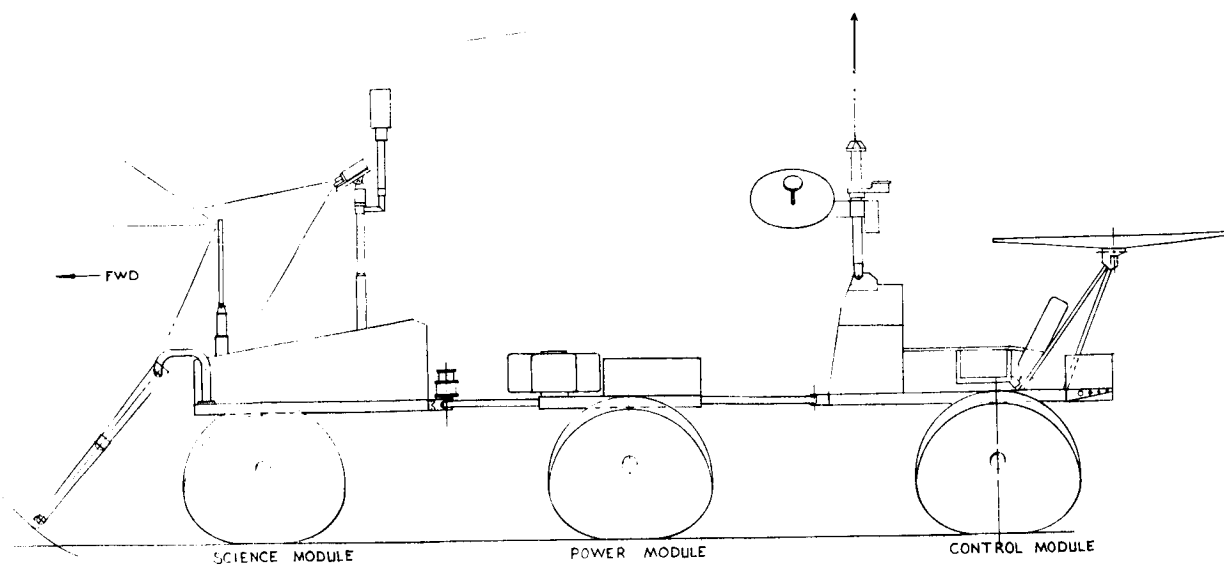
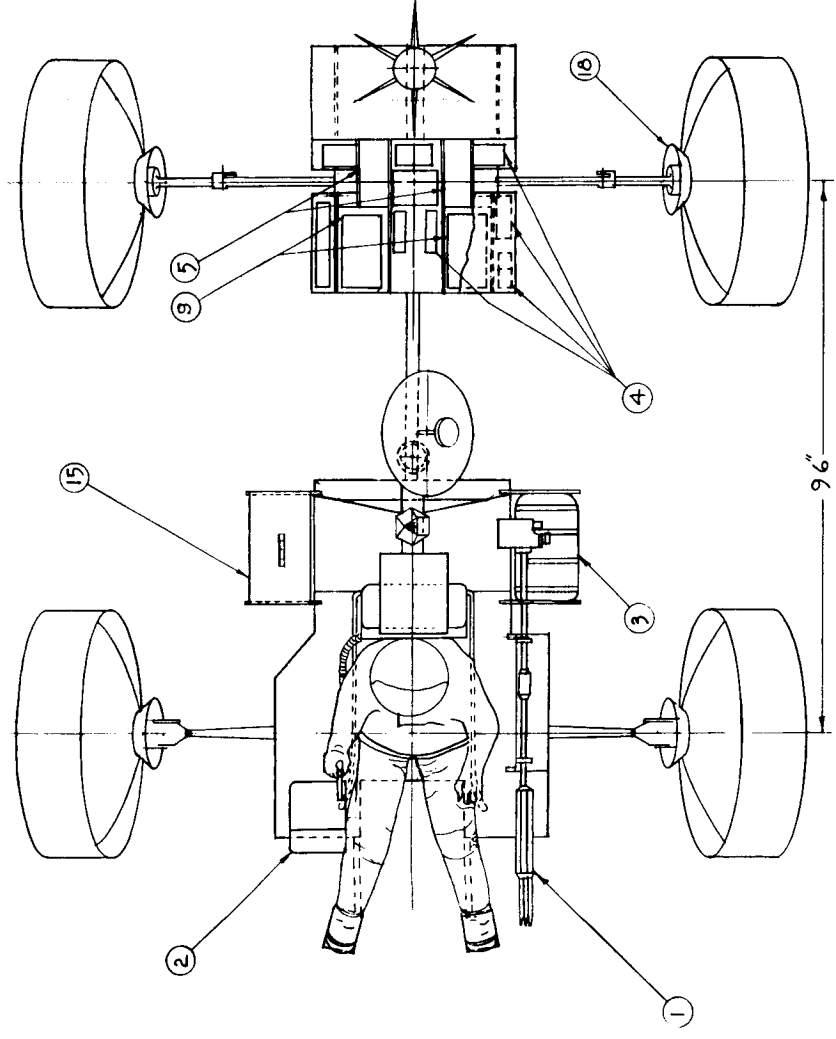


**FIG. 3.1-6 DLRV ARRANGEMENTS**



- LEGEND**
- 1 SURVEY STAFF
  - 2 CONTROLS & DISPLAYS
  - 3 BULK STORAGE
  - 4 EPS
  - 5 BATTERY (2)
  - 6 SOLAR ASPECT SENSOR
  - 7 S-BAND STEERABLE ANTENNA
  - 8 SENSOR ELECTRONICS
  - 9 COMM & INSTR
  - 10 CONTROLLER
  - 11 RTG-SNAP 19 2N-TAGS
  - 12 GEO TOOLS
  - 13 RANGER TRACKER
  - 14 S-BAND OMNI ANTENNA
  - 15 PRU
  - 16 HEATER TUBES
  - 17 DUST PROTECTOR
  - 18 RADIATOR

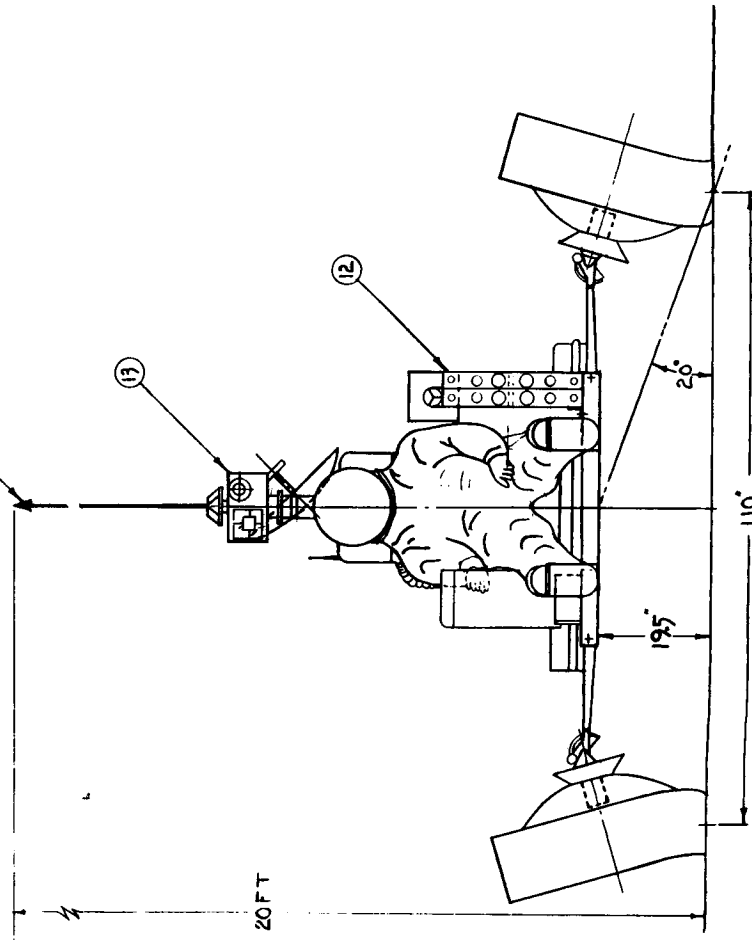
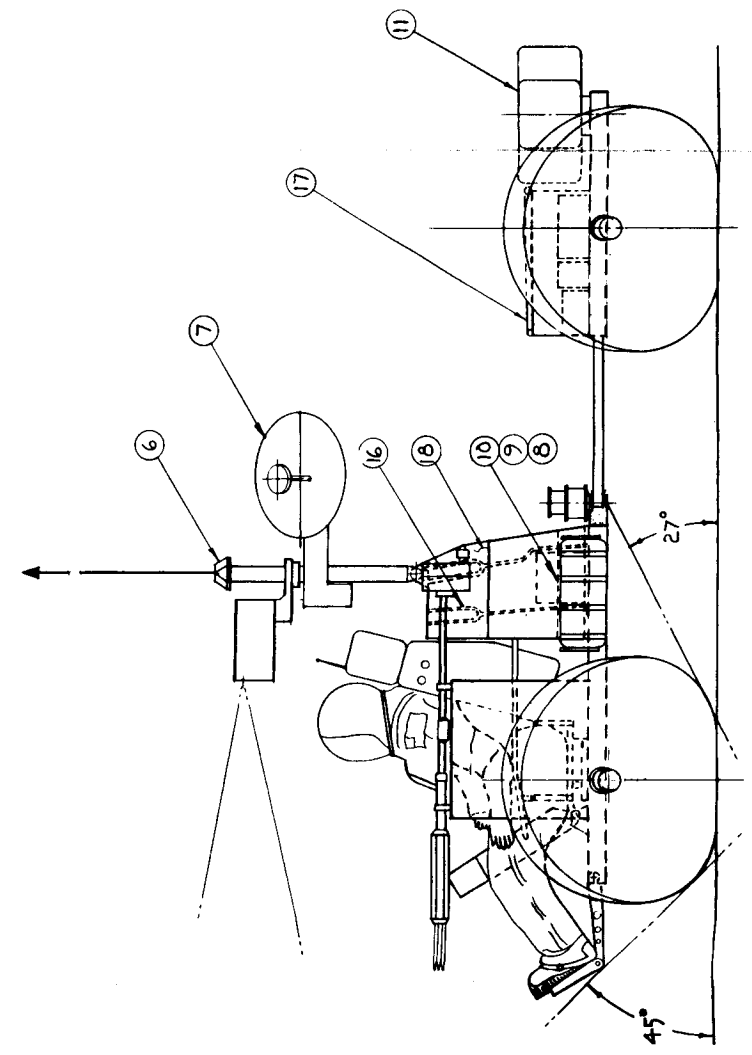


FIG. 3.2.1 DLRV MANNED MISSION ARRANGEMENT



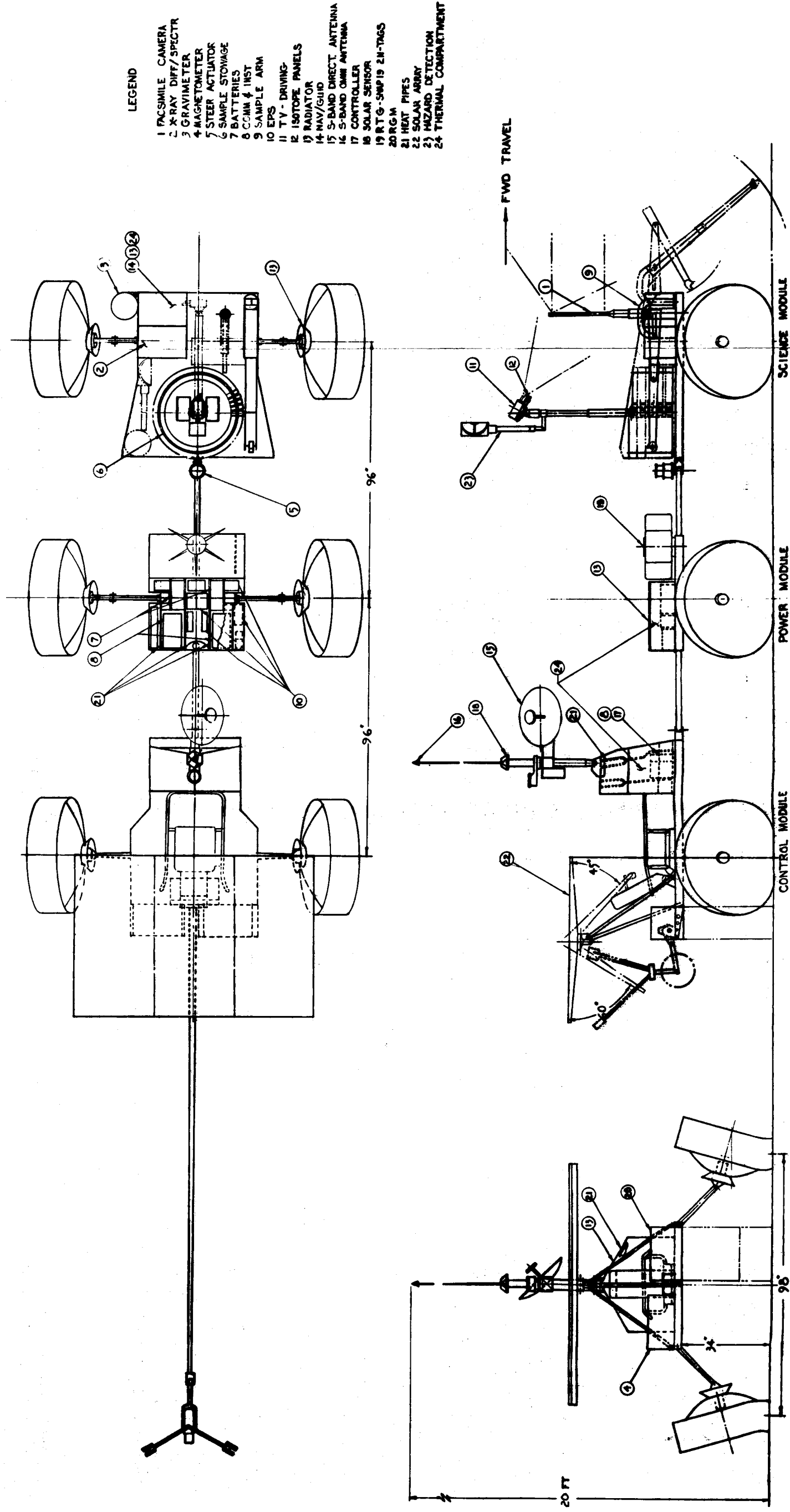


FIG. 3.2-2 UNMANNED MISSION ARRANGEMENT

for operation and a small one for stowage. The drawbar also provides high torsional flexibility between modules, resulting in more uniform wheel-ground contact pressures for better traction in uneven terrain.

The forward module is called the "Control Module". It contains the crew station, control electronics, part of the communications system, and the manned science. Most of the electronics is contained in a thermally controlled equipment compartment located behind the driver. An emergency passenger station can be erected behind this compartment to carry an astronaut in a cantilever sling arrangement. Mounted on top of the equipment compartment is the S-band steerable antenna, the ranger-tracker (which is used with the survey staff), the solar sensor for the navigation system, and the omni-antenna.

The driver sits in the center of the Control Module where he has unrestricted forward visibility. The instrument panel and hand controller are on his right, while the geology tools and survey staff are on his left. His protruding legs are protected by the support structure, which is designed to withstand impact or to ride over a smaller obstacle that might inadvertently be encountered.

The rear module of the four-wheeled vehicle is the "Power Module". It contains the SNAP-19 RTG, the batteries, the EPS, and the heavier and more power consuming portions of the communications system. The latter were located on the power module to provide a more favorable mass and thermal balance. The equipment is housed in a thermally controlled compartment with a protective dust covering and cleaning mechanism.

#### 3.2.1.2 Unmanned Mode

For the unmanned or remotely operated mode, a two-wheeled "Science Module" is added to the four-wheeled vehicle. The general arrangement is shown in Figure 3.2-2. The DLRV is a double-ended vehicle, in that the forward direction for the unmanned mode is opposite to that of the manned. This enables more independent optimization for the two missions: manned requirements governing for the manned mission and science requirements for the unmanned.

With the Science Module leading, the sampler arm has ready access to virgin soil. The facsimile camera and the TV camera both have unrestricted forward visibility, with the capability of serving as back-up for each other. The sample stowage container is within easy reach of the sampler arm and the view of the facsimile camera.

The more sophisticated unmanned gyro navigation system is located on the science module for ease of alignment with the TV camera. (The solar sensor used for the manned mission serves as a backup for the unmanned.) The TV camera, being on the Science Module always points in the direction the vehicle is moving, an advantage which derives from the articulated steering system. The steering actuator has been moved from its manned position between the Power and Control modules to the unmanned position between the Power and Science modules.

The two-position suspension on the Control and Power Modules has been raised to the high position for unmanned operation, providing the required 35° break angle with a ground clearance of 34 inches. The instrument console for the driver station has been returned to the stowed position in the center of the module, and the solar array has been erected above the crew station. Two of the automated science experiments, the magnetometer and the RGM, are located on the Control module to allow for easier deployment behind the vehicle. All the manned science has been removed for the unmanned mode.

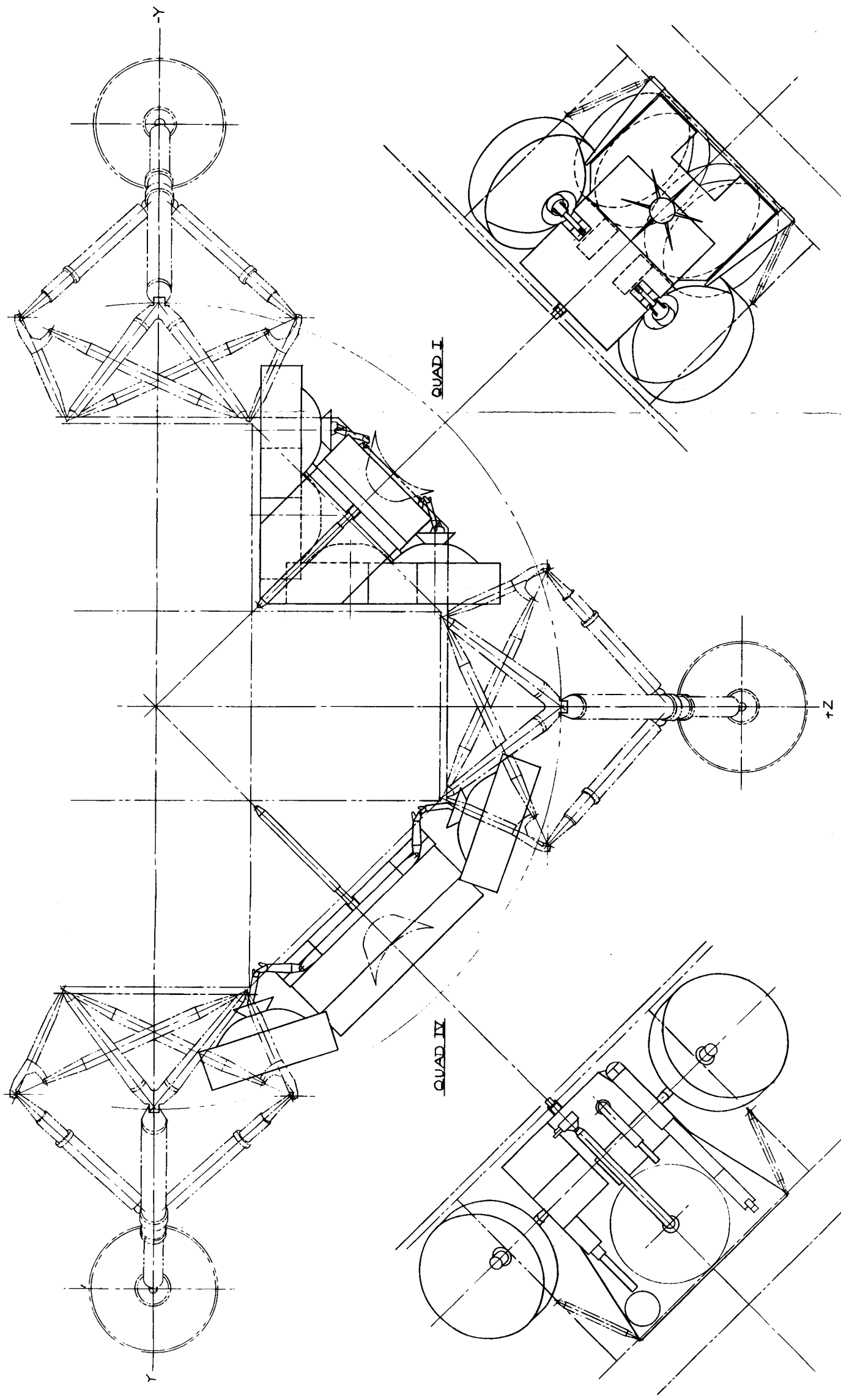
#### 3.2.1.3 Stowed Condition

The DLRV is stowed in two Quads of the Extended LM for delivery to the lunar surface. The arrangement is shown in Figure 3.2-3. The Control and Power Modules lie within Quad I, while the Science Module is stowed in a "saddle bag" fashion outside Quad IV. These two Quadrants are on the front or window side of the ELM. Deployment may take place in view of the astronauts before they go EVA. All modules are held close enough to the LM that they are not exposed to direct plume impingement from the RCS; thus, only limited lightweight thermal protection is required.

With the two-Quad stowage arrangement the 4-wheeled vehicle that is deployed from Quad I is the one required for the initial manned sorties. The Science Module used for the unmanned mission can be conveniently added when needed.

Figures 3.2-4 and 3.2-5 show the stowed configuration in more detail. The Control Module is seen to be closest to the ELM in Quad I. The crew station and the mast and equipment supports stow forward of the main equipment compartment between the wheels. The vehicle is folded at the steering pivot behind the equipment compartment so that the Power Module faces outward. This permits ready access for installation of the batteries, RTG, and radiators after staging.

The Science Module also faces outward, allowing access to the remote science and TV camera. The solar array and other movable equipment are stowed on the stowage

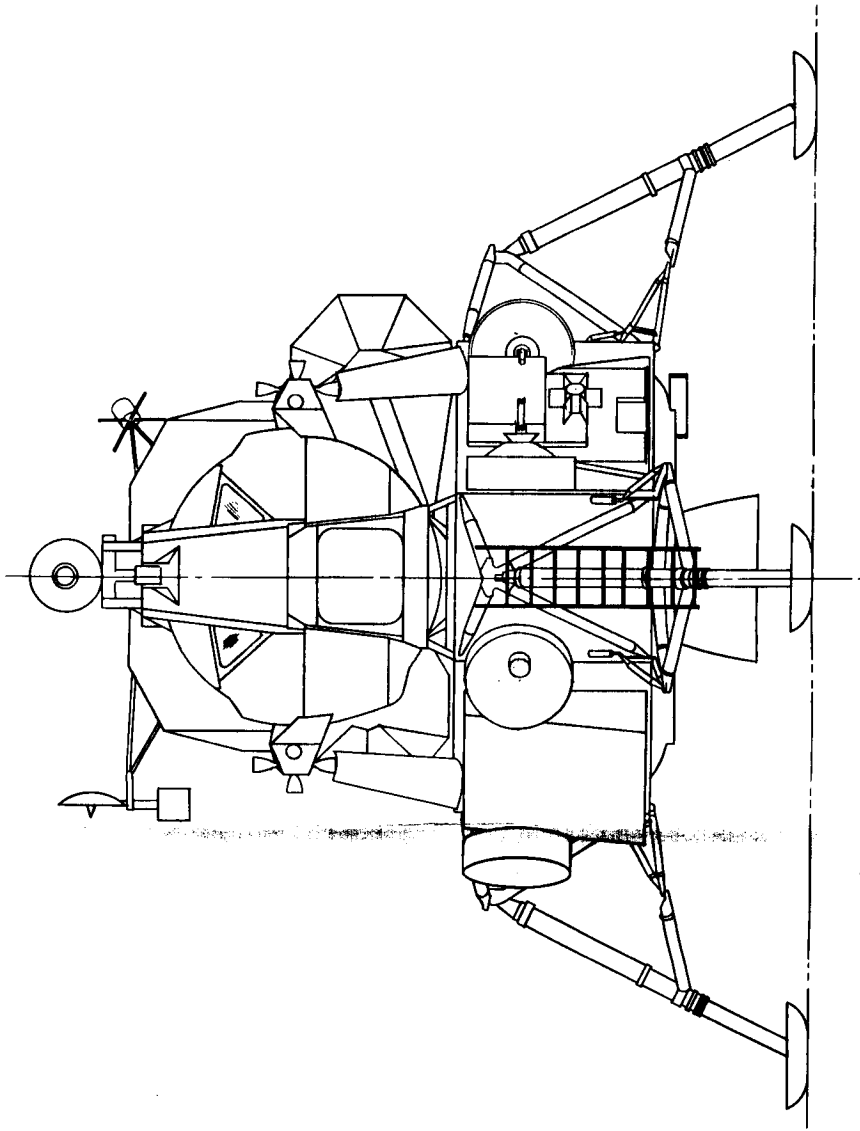


FOLDOUT FRAME 3

FIG. 3.23 STOWED ARRANGEMENT

II/I.3-23/24

FOLDOUT FRAME 2



FOLDOUT FRAME 1

FOLDOUT FRAME

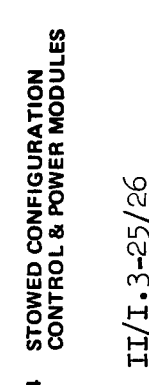
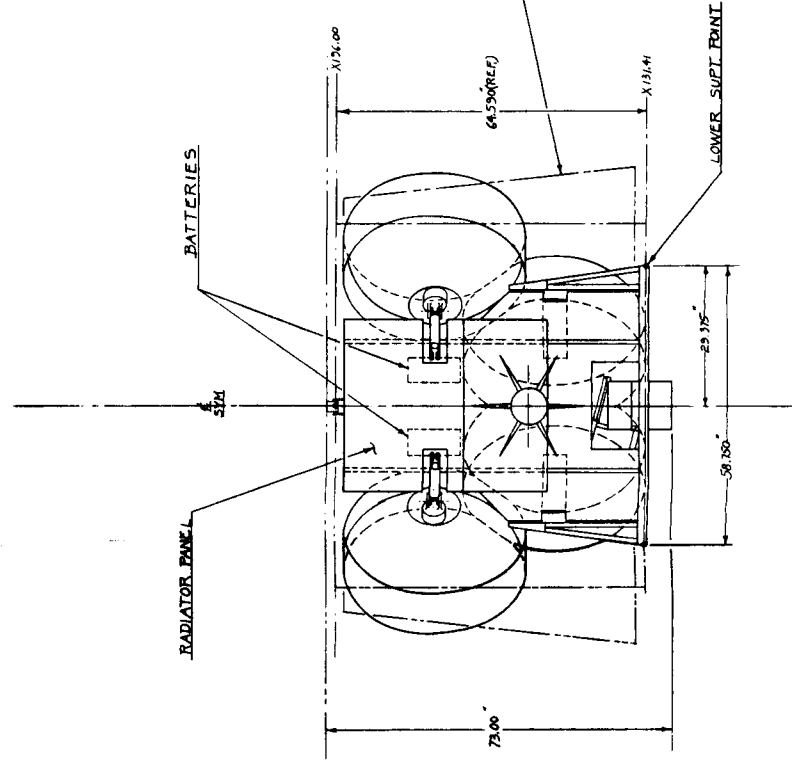
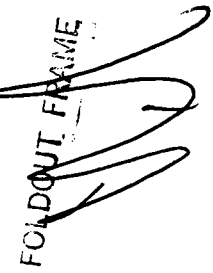
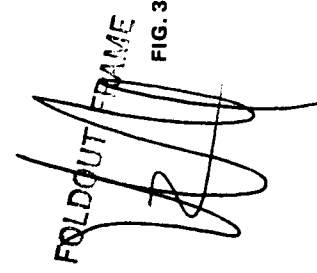
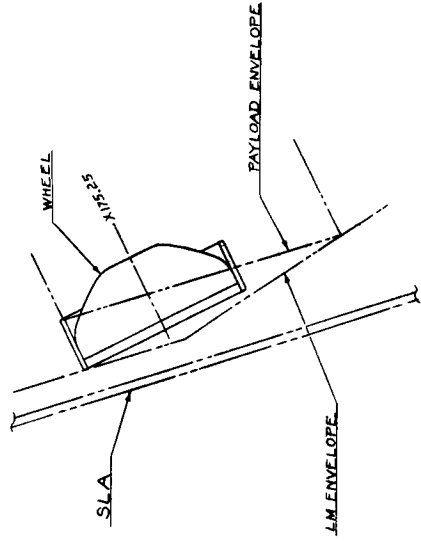
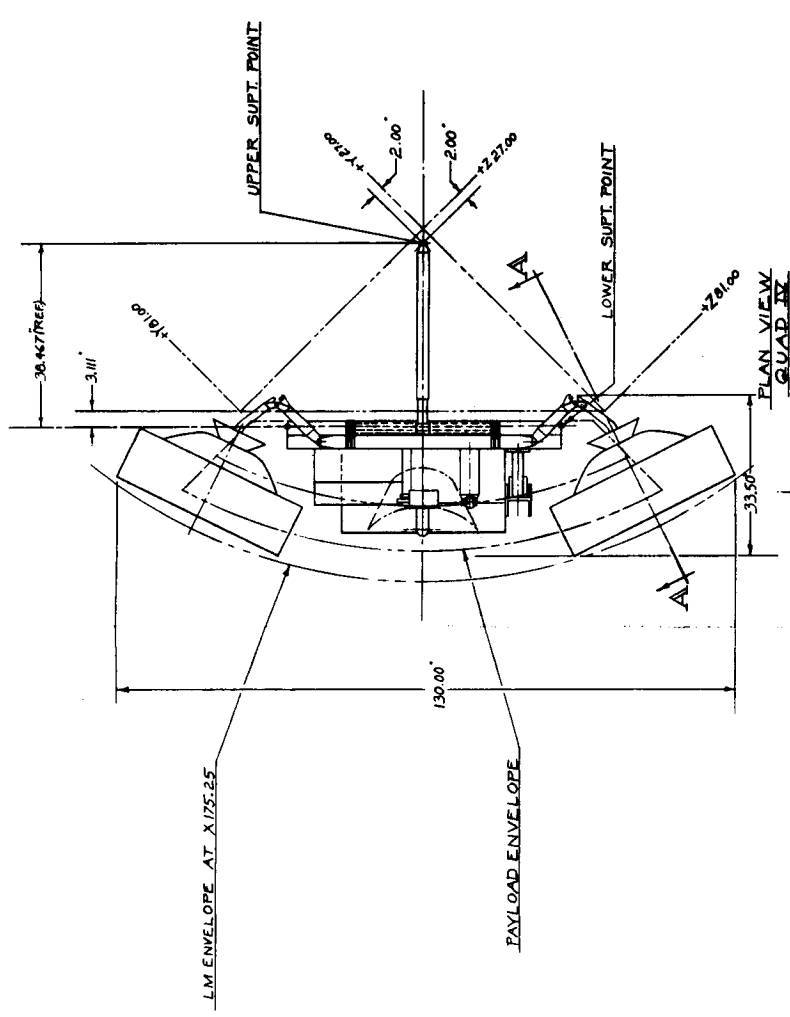
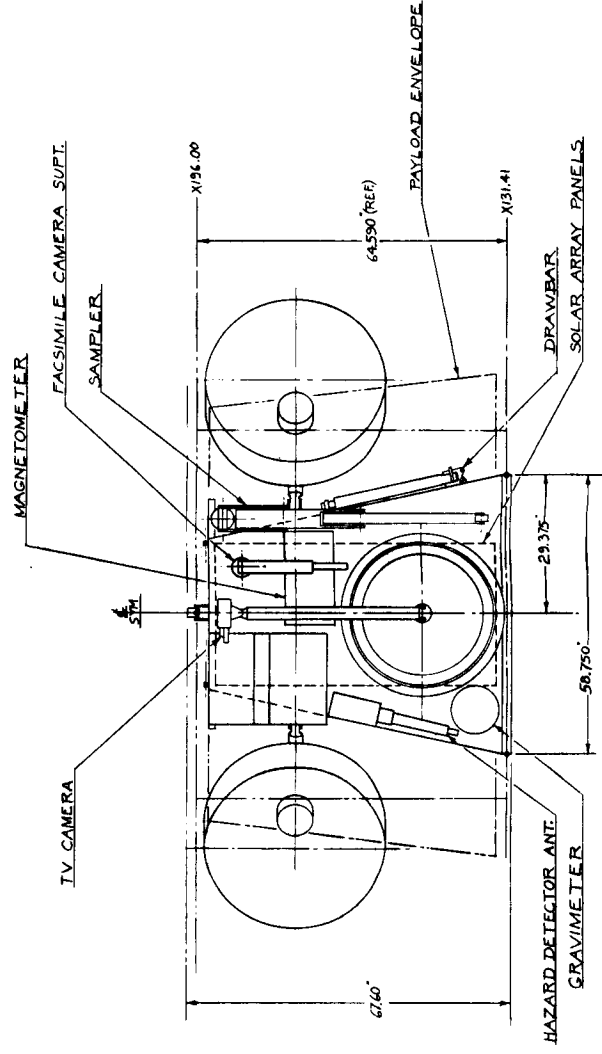


**FIG. 3.2-4 STOWED CONFIGURATION CONTROL & POWER MODULES**

NOTE:  
X, Y, & Z REFERENCES ARE LM STATIONS IN INCHES.



SECTION A-A



STOWED CONFIGURATION  
SCIENCE MODULE

FOLDOUT FRAME

2

FOLDOUT FRAME

FIG. 3.25 STOWED CONFIGURATION  
SCIENCE MODULE

and deployment rack that supports the Science Module. In the later delivery vehicles Quad IV will contain less equipment, permitting the available stowage volume behind the Science Module to grow naturally into the Quad.

The tiedown arrangement and supporting structure for both Quads are quite similar. The differences lie in 1) the use of the deployment and support rack in Quad IV, taking the place of the Control Module, to help sustain delivery loads and to allow sufficient lifting of the Science Module during deployment to clear an adverse ground line, and 2) the use of a deployment yoke assembly to support the Control Module and allow the translation needed during deployment for the trailing wheels to clear the ELM landing gear.

In both Quadrants, the wheels penetrate the ELM payload envelope (Refer to Figure 3.1-2) at the upper corners, as noted on the drawings. However, the high location of these protrusions is such that they will not obstruct access to or by the DLRV payload while in the stack.

### 3.2.2 Mass Properties

Tables 3.2-1 through 3.2-4 contain the mass properties of the DLRV for earth launch and lunar roving conditions. The earth launch weight of the DLRV including its tiedown and unloading equipment is 641.1 lb. The DLRV including the manned (100 lb) and unmanned science (250 lb.) will be 991.1 lb at earth launch. The weight history for the DLRV design weight of 650 lb is as follows:

<u>Manned Mode</u>		Weight - lb
o Earth Launch Design Weight		650
Minus - Science Module		-124
Tiedown and Unloading		- 28
Solar Array and Support		- 33
Plus - Manned Science		+100
Astronaut		+400
1/2 Samples		+ 35
o Mid-Traversal		1000
Plus - Remaining Samples		+ 35
o End Nominal Traversal		1035
Plus - Rescued Astronaut		+400
o Laden/Rescue		
<u>Unmanned Mode</u>		1435
Minus - Rescued Astronaut		-400
Manned Samples		- 70
Astronaut		-400
Manned Science		-100

Plus - Solar Array and Support	+ 33	
Science Module (Less Science)	+124	
Unmanned Science	+250	
o Begin Traverse		872
Plus - Samples (1/2)	+100	
o Mid Traverse		972
Plus - Samples (1/2)	+100	
Minus - RGM	- 75	
o End Traverse		997

The roving mass properties and wheel loadings for the above conditions are given in Table 3.2-2. The coordinate system is defined in Figure 3.2-6. The science and power modules are locked in pitch during the unmanned mode. The mass properties of the sprung mass (module less wheels, drives and suspension) of each module are given in Table 3.2-3. The scientific equipment loadings vary significantly during the mission, particularly during the transition between the manned and unmanned modes. Care has been taken in the placement of these equipments so that the resultant wheel loading variations are minimized during the mission.

The weights of the components in Table 3.2-1 are representative of the latest state of the art designs. There is a high degree of confidence in these estimates but, historically, past aircraft and spacecraft programs have shown that weight growth can be expected after the preliminary design phase, and 8.9 lb has been reserved for growth. If necessary, weight growth can be offset by taking additional weight reductions. For example, a reduction in the current design "g" loading from 5.5 to 4 g would yield a 13-lb weight reduction. Other reductions are possible if necessary by reducing wheel and/or vehicle size. (See Section 7.) Mass properties of the stowed DLRV are shown in Table 3.2-4.

TABLE 3.2-4 - STOWED DLRV MASS PROPERTIES

LOCATION	WEIGHT lb.	CENTER OF GRAVITY - in. (ELM COORDINATES)		
		X	Y	Z
Quad I - Control and Power Modules	483	170.0	-55.2	+55.2
Quad IV - Science Module and Solar Array	302*	165.4	+61.5	+61.5

\* Includes 135 lb of installed science

The stowed DLRV Y and Z coordinates vary from those used to define the payload distribution envelope in Annex A of the Statement of Work. The payload distribution



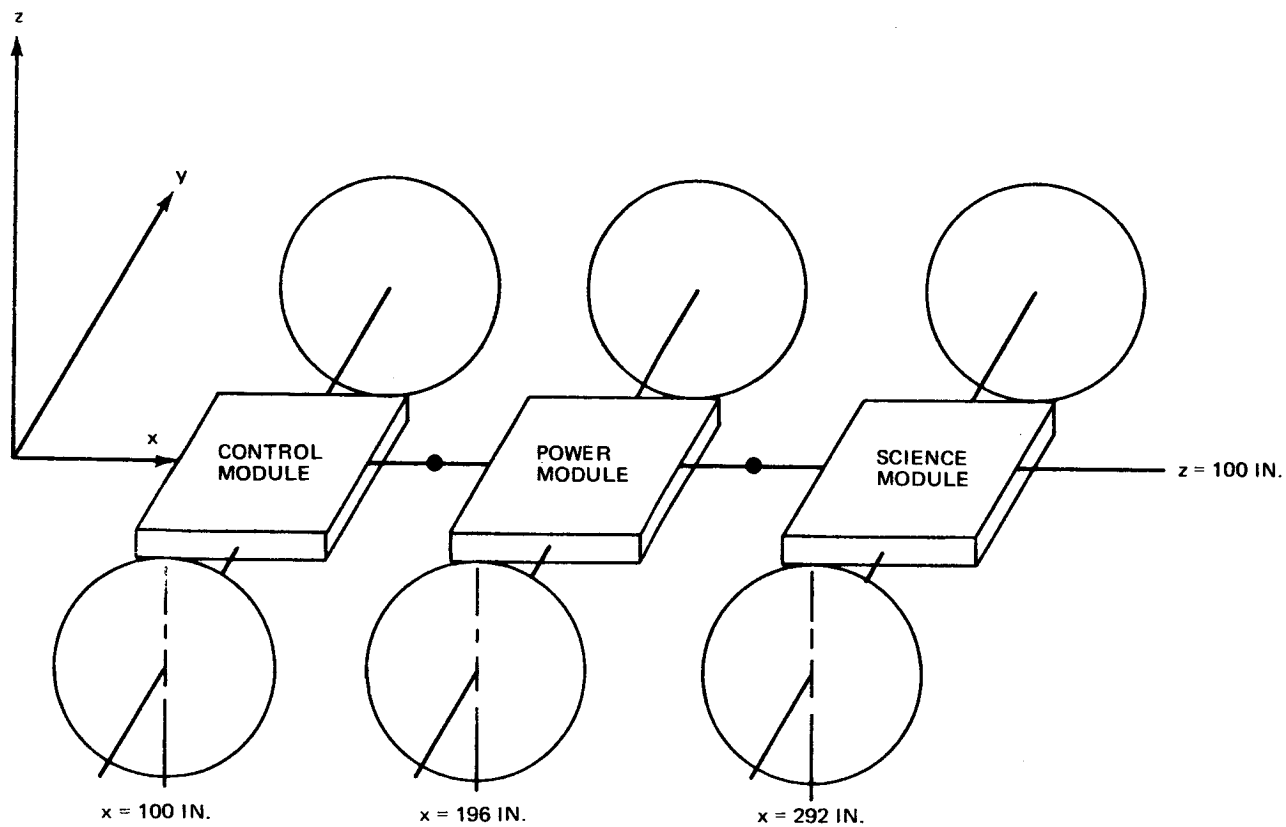


FIG. 3.2.6 COORDINATE SYSTEM DEFINITION

Table 3.2-1  
Weight Statement

ITEM	LB	ITEM	LB	ITEM	LB
<u>Mobility</u>	(288.0)	<u>Navigation</u>	(16.5)	<u>Space Support Equipment</u>	(28.0)
Chassis and Frame	71.0	Solar Aspect Sensors and electronics	4.0	Structures & Mechanisms	20.0
Suspension	28.8	Accelerometers	2.0	Thermal Control - Cmt.	5.0
Steering	13.0	Vertical Sensors	0.5	Controls and Umbilicals	3.0
Wheels	71.2	VHF Homing Assy.	3.0	<u>Thermal Control</u>	(26.4)
Drive Assembly	69.0	Directional Gyro	7.0	Space Radiators Support	6.0
Controller	30.0	<u>Communications</u>	(55.3)	Dust Control	2.7
Equipment supports	5.0	Antennas and R.F.		Heat Pipes	5.8
<u>Crew Systems</u>	(25.2)	S-Band Antenna & Drives	15.3	Phase Change Heat Sink	4.8
Seats and Restraints	12.0	Omni Antenna & Supt	0.5	Isotope Heaters	1.4
Displays and Control		R.F. Switch and Diplexer	1.0	Insulation	0.7
Panel	2.0	Transmitter - Wide Band	2.5	Dust Cleaning Solution	5.0
Fold Mechanisms	1.5	Narrow Band	5.0	DLELV AT EARTH LAUNCH	641.1
EPS Instruments	0.8	S-Band Receiver	5.0	<u>Manned Science</u>	(100)
Mobility Instruments	1.6	Signal Processor	6.0	Hand Tools	25
Navigation Instruments	1.9	Data Handling Assy.	15.0	Survey Staff and Tracker	55
Communications Instruments	0.2	Transducers	5.0	Bulk Storage and Equipment Support	20
Remote Control Instruments	0.2	<u>Remote Control</u>	(27.0)	<u>Unmanned Science</u>	(250)
Hand Controller	3.0	Television System		Facsimile Camera	10
Crew Provisions	2.0	Camera	7.3	Sample Arm	10
<u>Electrical Power Supply</u>	(165.2)	Gimbals, Motors & Electronics	5.0	Sample Storage	31
Batteries	50.0	Lenses	1.0	X-Ray Diffractometer & Spectrometer	20
RTG	30.0	Shaft Encoders	0.7	Magnetometer	19
Solar Array & Drives	27.0	Command Equipment	9.0	Cravimeter	35
Distribution	34.0	Decoder	4.0	Remote Geophysical Monitor	75
Conditioning		Distribution Assy.		Deployment & Misc.	5
Regulator	3.0	<u>Hazard Detection</u>	(9.5)	Isotope Heaters	10
Inverter	4.0	Sensor	6.0	Additional Science Allowance	35
Charger	12.0	Electronics	3.5	TOTAL DLELV WITH SCIENTIFIC EQUIPMENT	991.1
A-H Transducers	2.2			AT EARTH LAUNCH	
DC/DC Converter	3.0				

FOLDOUT FRAME

FOLDOUT FRAME

2

Table 3.2-2  
ROVING MASS PROPERTIES AND WHEEL LOADINGS  
(650-lb DLRV)

	MANNED MODE			UNMANNED MODE		
	Mid Traverse	End Nominal Traverse	Rescue	Begin Traverse	Mid Traverse	End Traverse
	Control and Power Modules (4 x 4)			Power and Science Modules (4 x 4)		
Weight - lb	1000	1035	1435	512	612	712
cg x - in.	132.2	132.3	140.0	246.6	249.6	252.0
y - in.	- 2.8	- 3.6	- 2.6	2.2	1.9	1.6
z - in.	112.7	112.4	118.2	103.5	104.7	105.6
Ixx Slug - ft <sup>2</sup>	120	124	162	88	91	93
Iyy Slug - ft <sup>2</sup>	354	355	445	261	270	277
Izz Slug - ft <sup>2</sup>	401	406	465	288	298	305
				Control Module (2 x 2)		
Weight - lb	Not Applicable			360	360	285
cg x - in.				102.8	102.8	110.2
y - in.				- 1.7	- 1.7	1.5
z - in.				108.5	108.5	109.2
Ixx Slug - ft <sup>2</sup>				104	104	99
Iyy Slug - ft <sup>2</sup>				150	150	134
Izz Slug - ft <sup>2</sup>				140	140	121
TOTAL WEIGHT - lb	1000	1035	1435	872	972	997
WHEEL LOADING PER AXLE - lb						
Control Module	665	687	837	339	339	224
Power Module	335	348	598	274	302	389
Science Module	-	-	-	259	331	384

Table 3.2-3  
SPRUNG MASS PROPERTIES

	MANNED MODE				UNMANNED MODE		
	Mid Traverse	End Nominal Traverse	Rescue	Begin Traverse	Mid Traverse	End Traverse	
Control Module							
Weight - lb	720	755	1155	303	303	228	
cg	114.5	115.4	130.8	103.4	103.4	112.8	
x - in.	- 4.0	- 5.1	- 3.3	- 2.0	- 2.0	1.8	
y - in.	116.9	116.3	122.1	113.2	113.2	115.5	
z - in.	42	47	74	69	69	64	
Slug - ft <sup>2</sup>	67	72	216	139	139	120	
Ixx	63	69	193	115	115	94	
Iyy							
Izz							
Power Module							
Weight - lb	168	168	168	168	168	168	
cg	198	198	198	198	198	198	
x - in.	1	1	1	1	1	1	
y - in.	104.8	104.8	104.8	104.8	104.8	104.8	
z - in.	5	5	5	5	5	5	
Slug - ft <sup>2</sup>	10	10	10	10	10	10	
Ixx	10	10	10	10	10	10	
Iyy							
Izz							
Science Module							
Weight - lb	Not applicable			233	333	433	
cg				282.8	277.5	274.6	
x - in.				4.2	2.9	2.2	
y - in.				112.0	111.7	111.5	
z - in.				22	25	27	
Slug - ft <sup>2</sup>				31	39	43	
Ixx				25	33	39	
Iyy							
Izz							

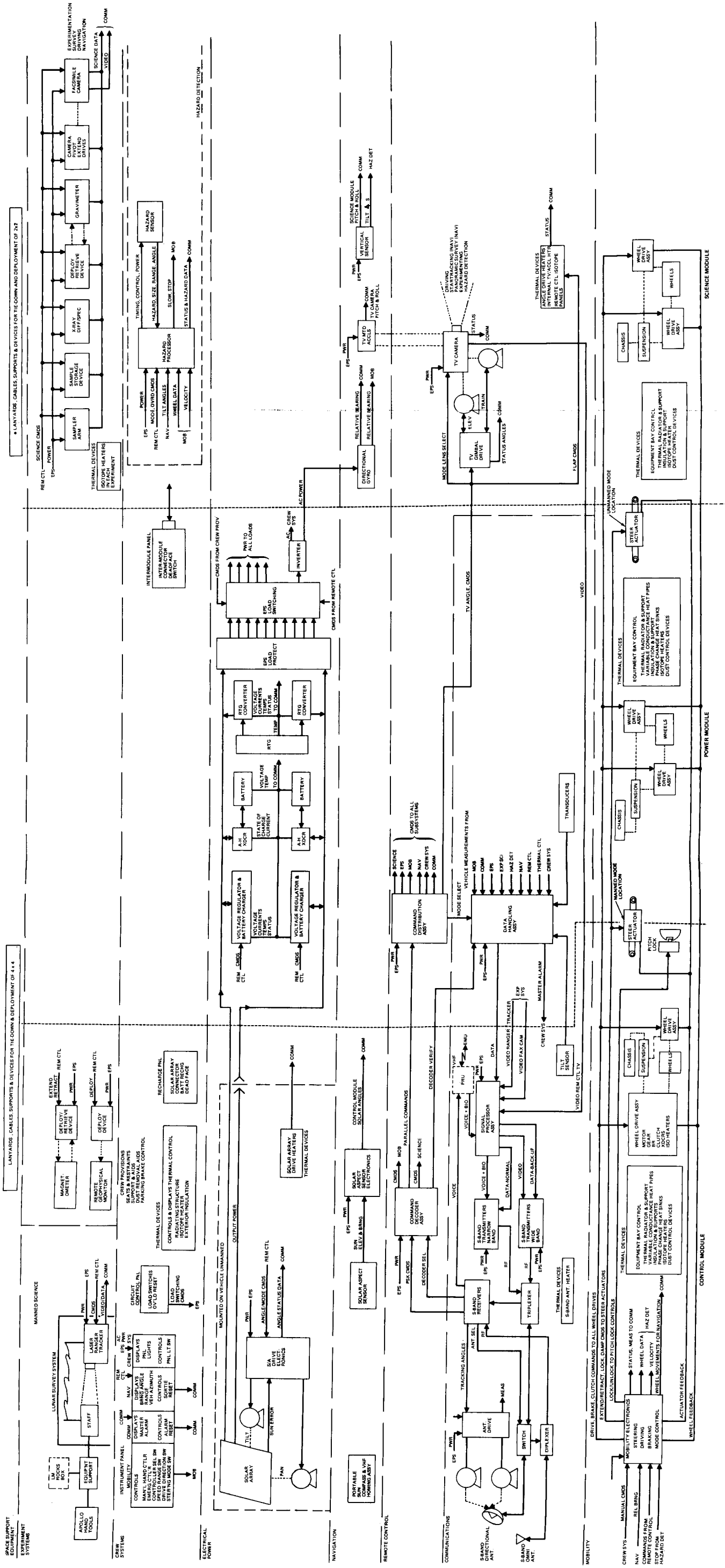
chart shown in Annex A would therefore not be directly applicable. However, for an assumed ELM touchdown weight of 17,000 lb and a center of gravity as given in Annex A, the resultant c.g. of the ELM based on the DLRV'S mass properties is within the  $1^{\circ}$  c.g. boundary.

### 3.2.3 Equipment Integration

The Level 1 schematic diagram is shown in Figure 3.2.-7. Since the manned vehicle is a 4 x 4 consisting of the Control and Power Modules, left and center portions of the figure are used both manned and unmanned. The Science Module, in the right-hand portion of the figure, is only required in the unmanned mode. The mobility subsystem (also called the control subsystem in Volume III) extends to all three modules. The mobility electronics assembly is located in the control module for thermal reasons.

The relationship between vehicle systems and ground support functions is shown in Figure 3.2-8. Typically the remote driving function is accomplished on the ground using data transmitted from the rover including the TV image and angles, (the Facsimile camera is a backup), vehicle steering angle, drive motor currents and speeds, and various subsystem parameters. Other inputs to the driver are ground-computed navigation parameters, hazard parameters and vehicle status parameters. The function is completed by uplink commands for throttle steering and brakes.

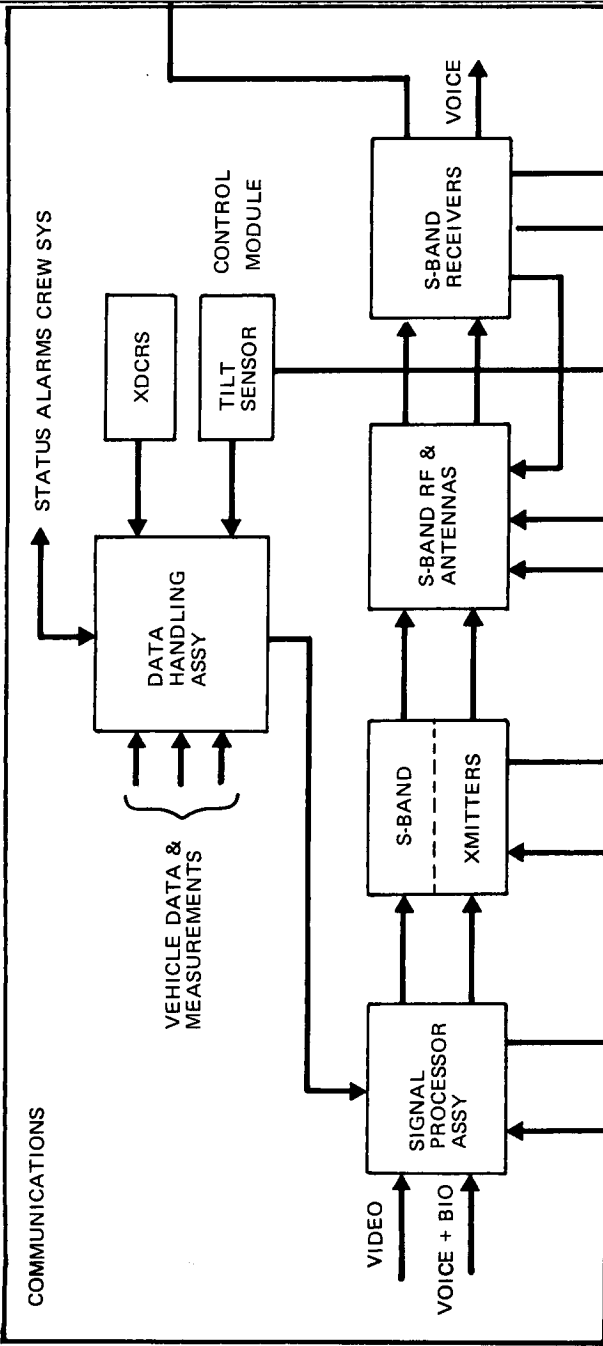
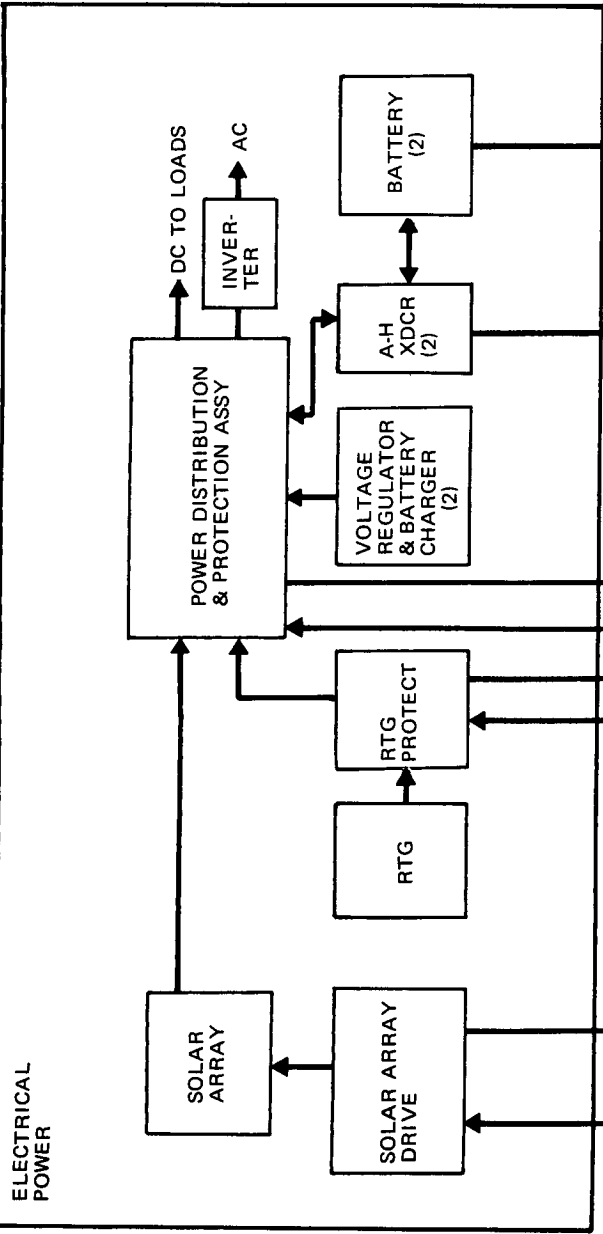
The hardware tree for the vehicle is shown in Figure 3.2-9. The breakdown is consistent with the Work Breakdown Structure received from MSFC.



SCIENCE MODULE

FOLDOUT FRAME

FIG. 3.2-7 SYSTEM SCHEMATIC DIAGRAM



POINTING ANGLES  
ARRAY STATUS POSITION  
CMDS  
STATUS  
SWITCHING CMDS  
STATUS, LOAD CURRENTS  
STATE OF CHARGE  
TEMPERATURES

MODE SELECT  
STATUS  
TX, MODE SELECT  
STATUS DATA  
POINTING ANGLES  
S-BAND DUPLEX LINK  
CONTROL MOD  
TILT ANGLES  
MODE SELECT  
SIGNAL STRENGTH, STATUS

VEHICLE SUPPORT

- COMMUNICATIONS & INSTRUMENTATION
- ELECTRICAL POWER
- THERMAL

- MOBILITY
- NAVIGATION
- REMOTE CONTROL
- HAZARD DETECTION

FOLDOUT FRAME

FOLDOUT FRAME

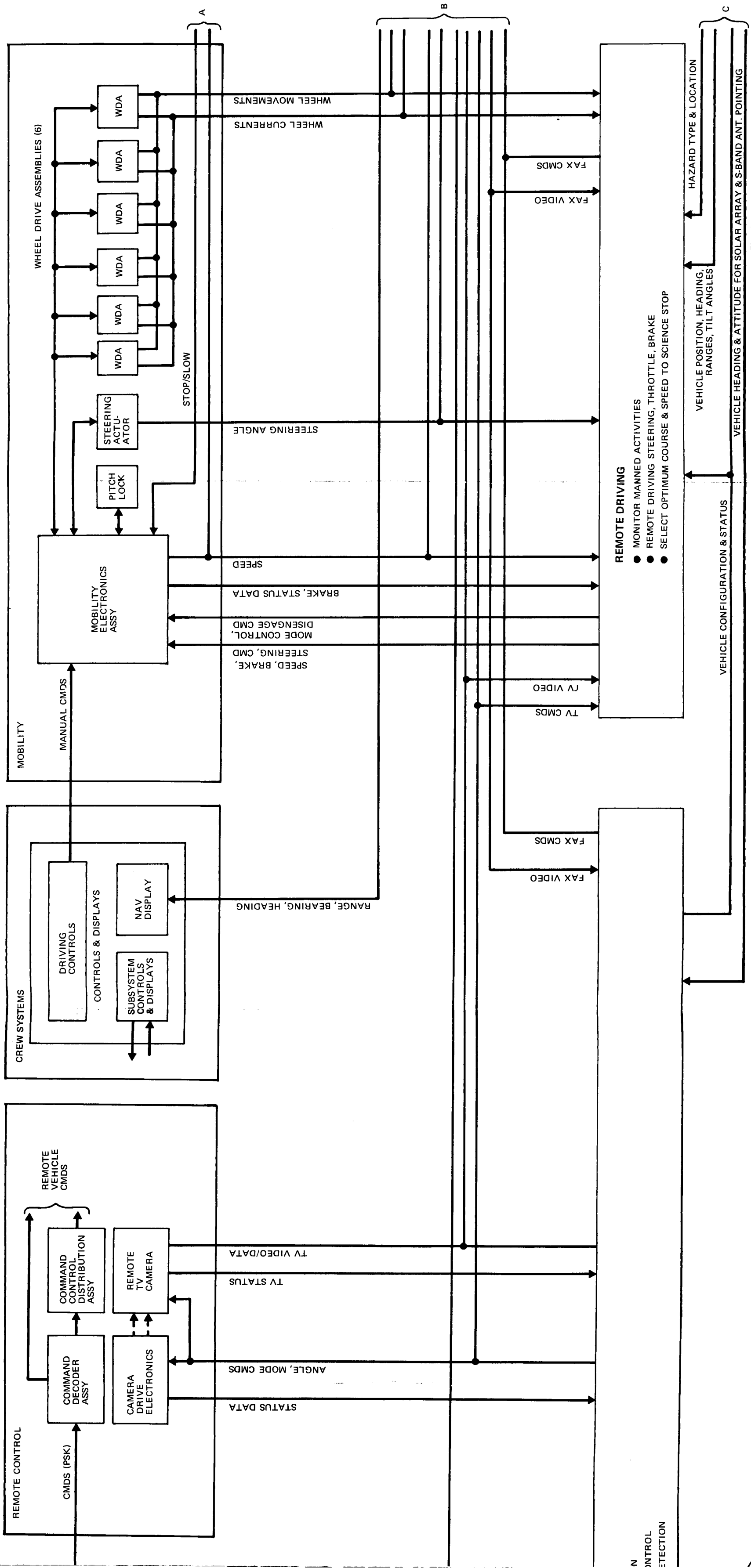
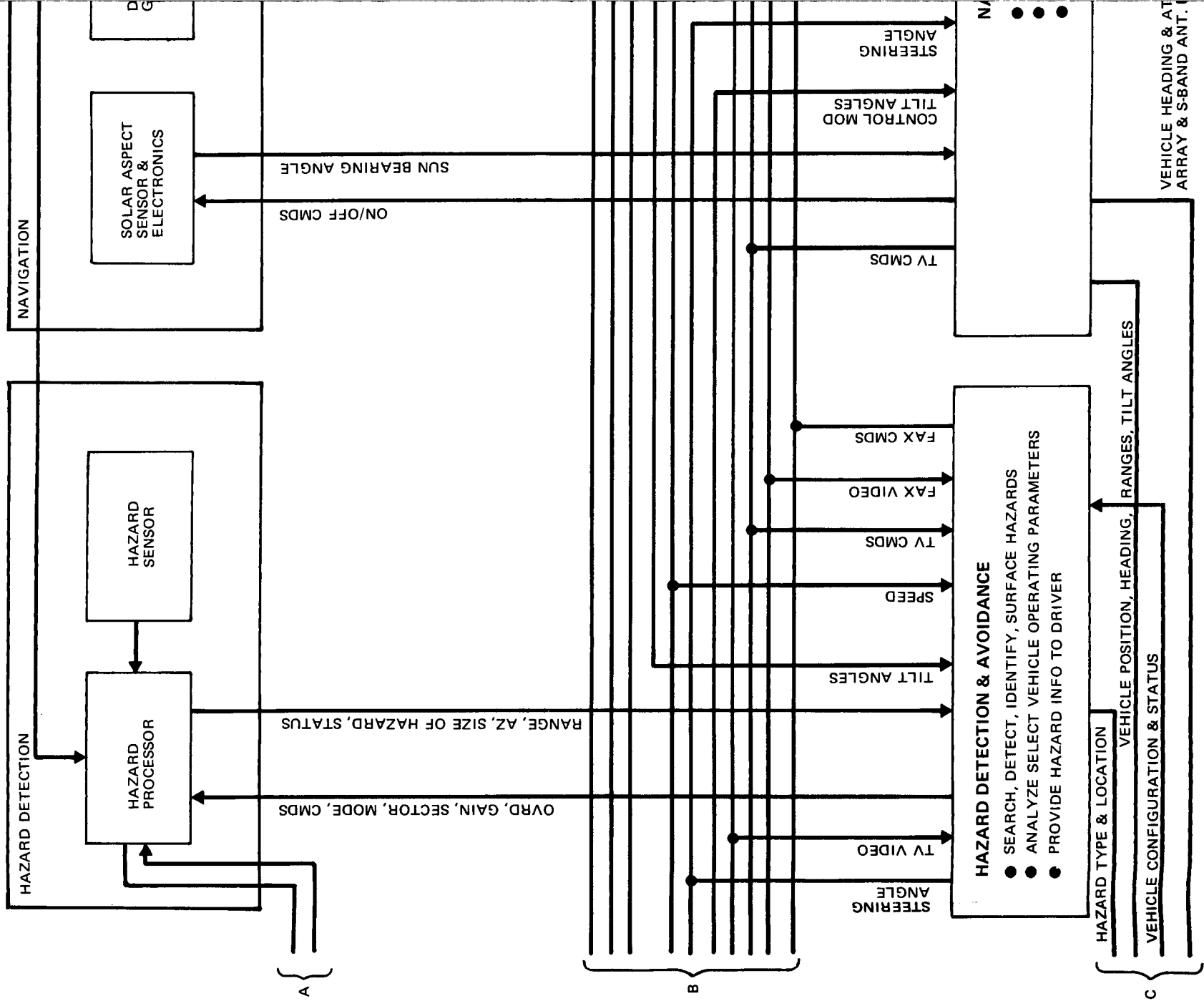


FIG. 3.28 LEVEL 1 VEHICLE-GROUND FUNCTIONAL SCHEMATIC (SHEET 1 OF 2)

FOLDOUT FRAME 3

FOLDOUT FRAME 4  
II/I.3-41/42





HAZARD DETECTION & AVOIDANCE

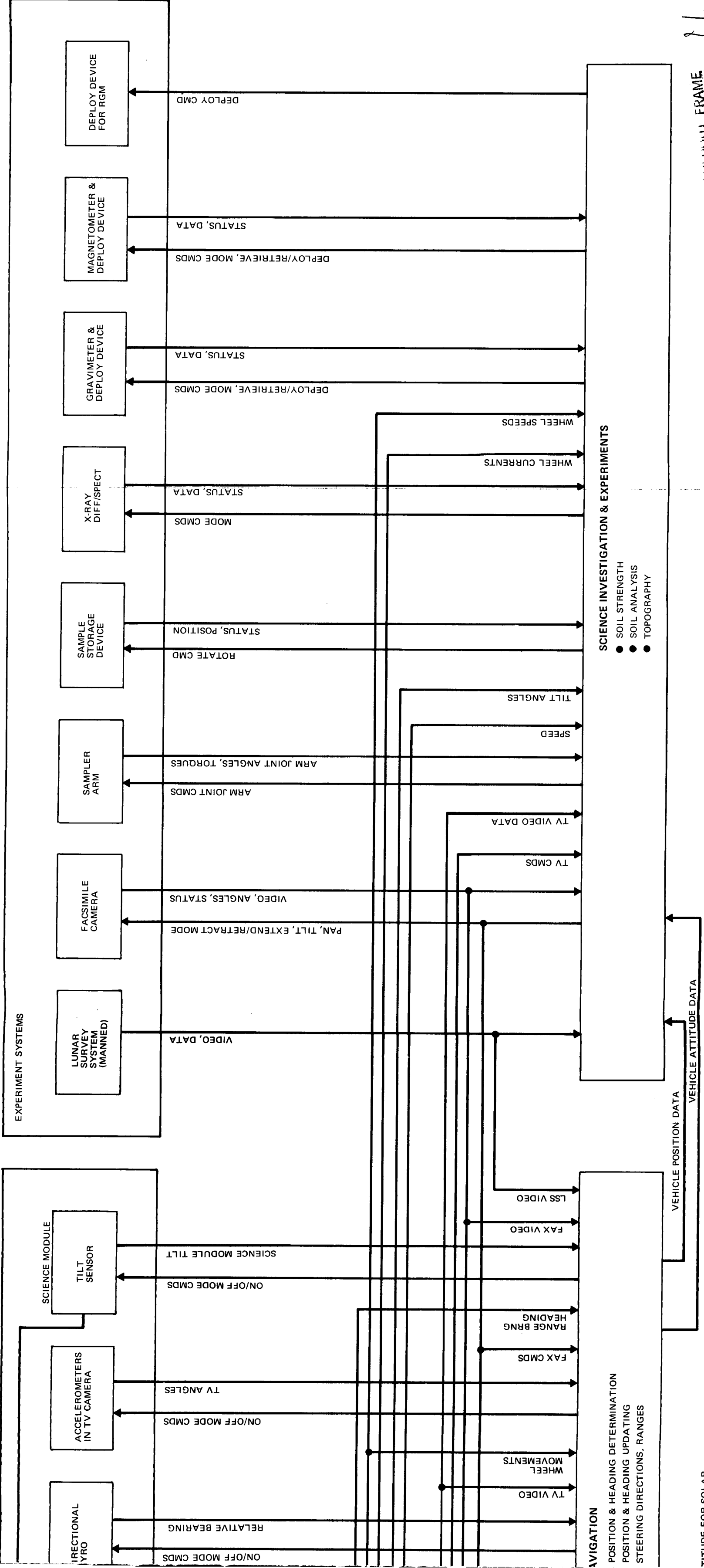
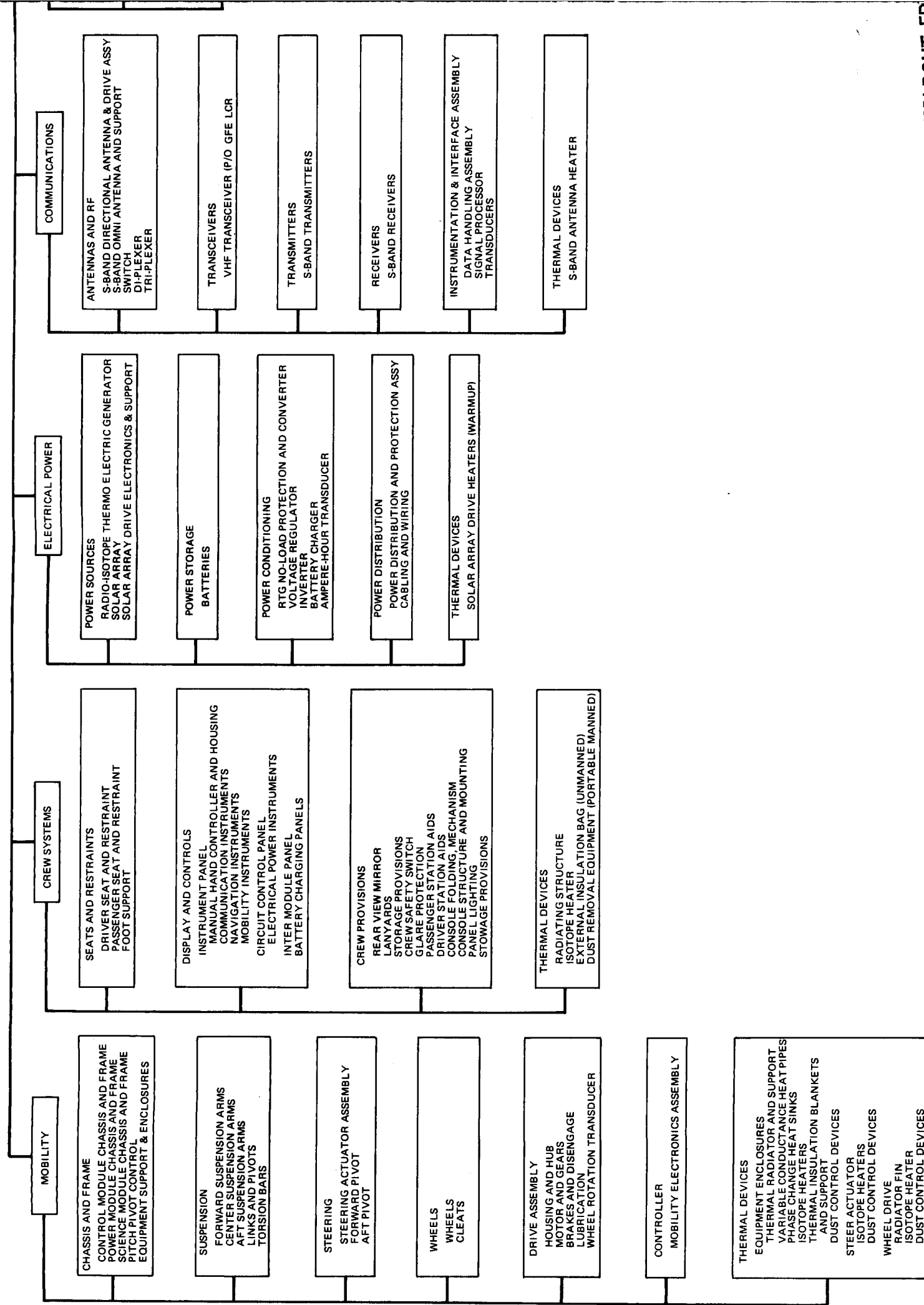
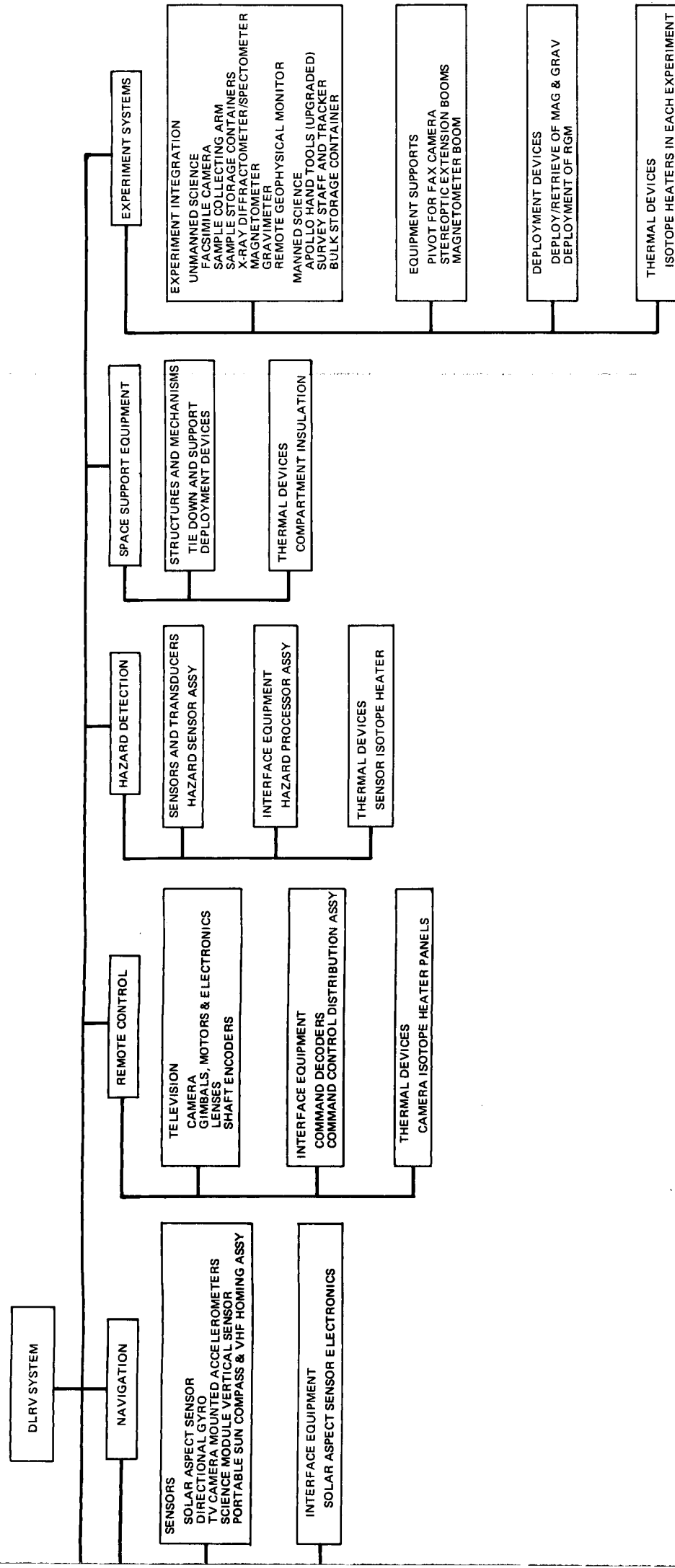


FIG. 3.28 LEVEL 1 VEHICLE-GROUND FUNCTIONAL SCHEMATIC (SHEET 2 OF 2)



FOLDOUT FR

FOLDOUT FRAME



FOI 3017 FRAM 3

AME

FIG. 3.29 HARDWARE TREE

## SECTION 4

### SYSTEMS ANALYSIS

#### 4.1 MOBILITY

##### 4.1.1 Locomotion Performance

##### 4.1.1.1 Rolling Resistance

Total wheel drag  $R$  that must be overcome by the wheel motors consists of three components:

- o Rolling resistance  $R_z$  due to soil compaction and sinkage  $z$
- o Parasitic losses  $R_p$  due to wheel flexure and cleat/soil scuffing
- o The gravity component  $R_g$  when climbing a slope

Hence:  $R = R_z + R_p + R_g$

The latter component,  $R_g$ , is equal to  $W \sin \alpha$  where  $W$  is wheel loading and  $\alpha$  is slope angle.  $R_p$  is proportional to wheel loading and could be expressed as  $qW$ , where  $q$  is generally equal to a few percent. As to the soil compaction resistance,  $R_z$ , it can be shown that

$$R_z = \frac{b p_e^{n+1}}{(n+1)k}$$

or

$$R_z = \frac{b p_e^2}{2k} \quad \text{for } n = 1 \quad (1)$$

where  $b$  is wheel width,  $p_e$  is effective footprint pressure,  $k$  is soil sinkage modulus and  $n$  is the power of the  $p/z$  relations, with  $n = 1$  indicating a linear relation.

A one-g version of a 42" flexible cone wheel was tested at Stevens Institute and the results are reported in Reference 1. A 1/6-g, 38"-diameter wheel was tested at Grumman's Peconic facility at various loadings and with two types of cleats. The latter wheel simulates the actual DLRV wheel design.

The results of the one-g wheel tests are given in Table 4.1-1. The 330-lb wheel loading provides a wheel deflection comparable to that of the 1/6-g wheel at 55 lb. The tests on hard ground show a parasitic loss,  $R_p$ , of 3.8% wheel loading. The

TABLE 4.1-1

## TESTS OF 1g FLEXIBLE WHEEL AT STEVENS INSTITUTE

Rubber Padded Rectangular Cleats Wheel Loading of 330 lb Wheel Diameter 42 inches Cleat Length 10 inches = b			
	Hard Surface	Firm Soil	Soft Soil
k, psi/in		$9 + \frac{1}{2}$	$1\frac{1}{2} + \frac{1}{2}$
Towing force, lb., average of 6 runs	12.4	30.3	56.2
Wheel sinkage, in, average of 6 runs	2.8	2.1	3.7
Measured footprint area, sq. in.		153	246
Footpring pressure using measured area, psi		2.16	1.34
Rolling Resistance, $R_z$ , lb	12.4	17.9	43.8
Effective footprint pressure, $p_e = (2k R_z/b)^{\frac{1}{2}}$		5.68	3.62
Effective area ratio, $p/p_e$		.38	.37

test wheel had rubber padded cleats, however, and the parasitic losses would be less for the rigid cleated DLRV wheel. The effective footprint pressures were calculated in Table 4.1-1 and indicate that about 37% of the measured area is effective in carrying the wheel load. The measured areas were calculated using full footprint lengths, i.e., assuming full bridging between cleats. Two versions of the 1/6-g, 38"-diameter wheel were tested by GAC, one with 7" rectangular wood cleats and the other with 11 5/8" extruded angle cleats. The deflection characteristics and graphical footprint length of the wheel are shown in Figure 4.1-1. The test apparatus consisted of a single wheel canted at  $15^\circ$  and connected to a frictionless pivot by means of a 12-ft rigid member, as shown in Fig. 4.1-2. The wheel was revolved around the pivot by pulling by hand at a point near the hub. A dynamometer and a recorder capable of measuring the turning force to the nearest 1/4 lb was used. The test was performed on asphalt and soft sand. A roto-tiller was used to loosen the sand before each pass. Cone index readings of the uncompacted sand gave a penetration gradient,  $G$ , of 1 to 2 psi/in for the top 4". It is permissible to assume that at these low values, the  $G$  parameter is nearly equal to the soil sinkage modulus  $k$ . Additional measurements of soil constants included the angle of internal friction,  $\phi$ , by means of a "Sheargraph" and the cohesion,  $c$ , by means of a "Torvane". Values of  $\phi = 35^\circ$  and  $c = 0.13$  psi were measured. The 1/6-g wheel test results are plotted in Figure 4.1-3. The parasitic loss with the 7" cleats is 2.1% of wheel loading which is appreciably lower than the 3.8% measured for the one-g wheel.

The estimated values for the 11 5/8" cleat and  $k = 1.5$  are also compared in Figure 4.1-3. These estimates were made using the following procedures:

1. The graphical footprint lengths were determined from Figure 4.1-1
2. The effective areas were calculated using the above lengths, the cleat length of 11 5/8", and the effective area ratio of .37 determined from the Stevens tests
3. The effective footprint pressure,  $p_e$ , and the soil pressure,  $p = kz$  are plotted in Fig. 4.1-4. Curves intersect at the equilibrium point. Equilibrium pressures are tabulated below for  $k = 1.5$

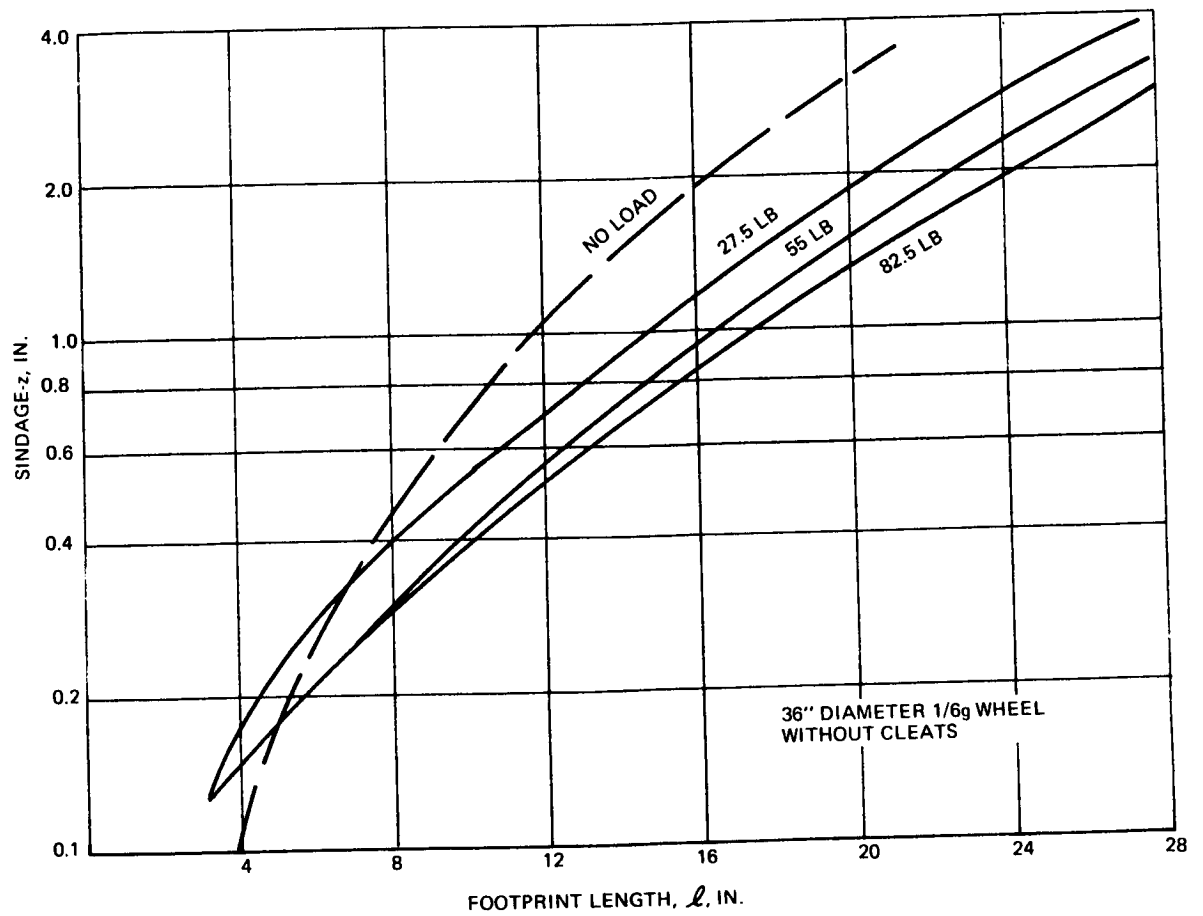
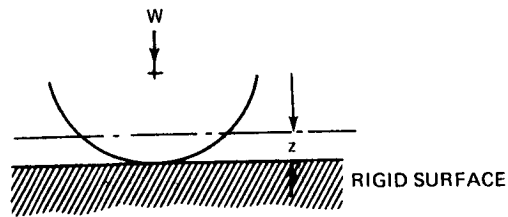


FIG. 4.1-1 FOOTPRINT LENGTH VS SINKAGE



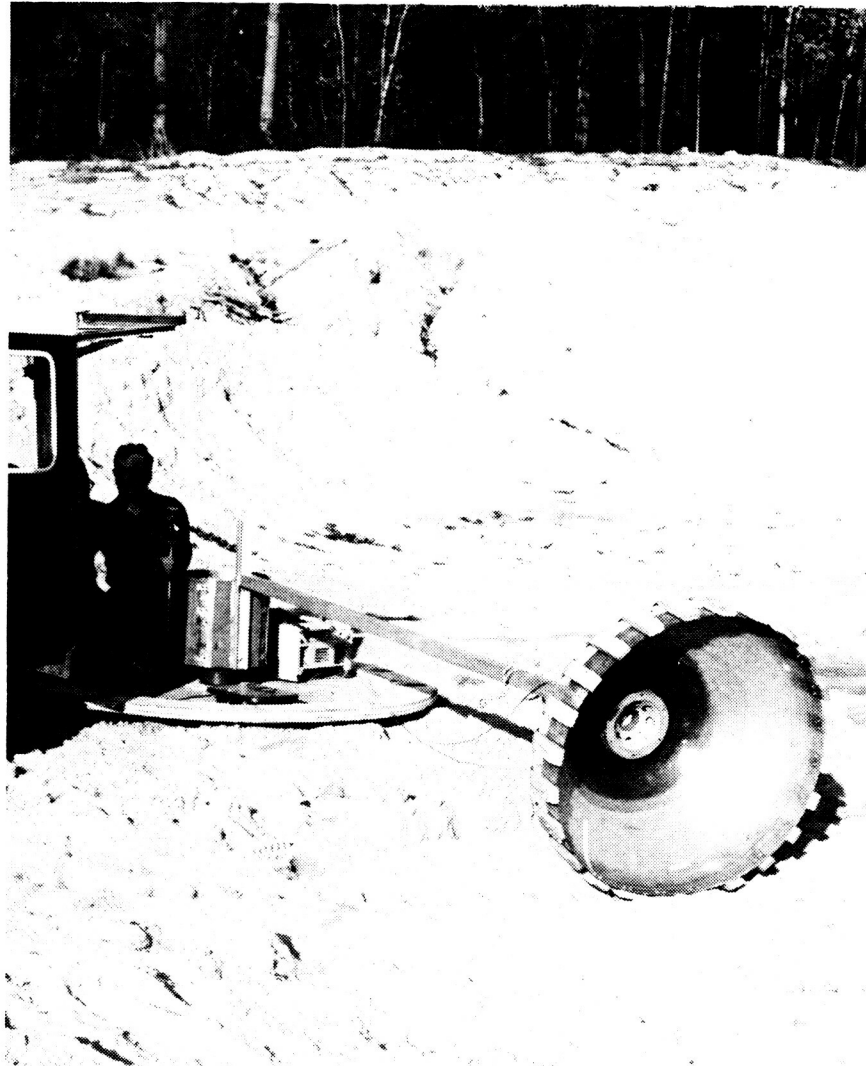


FIG. 4.1-2 TEST APPARATUS FOR ROLLING RESISTANCE

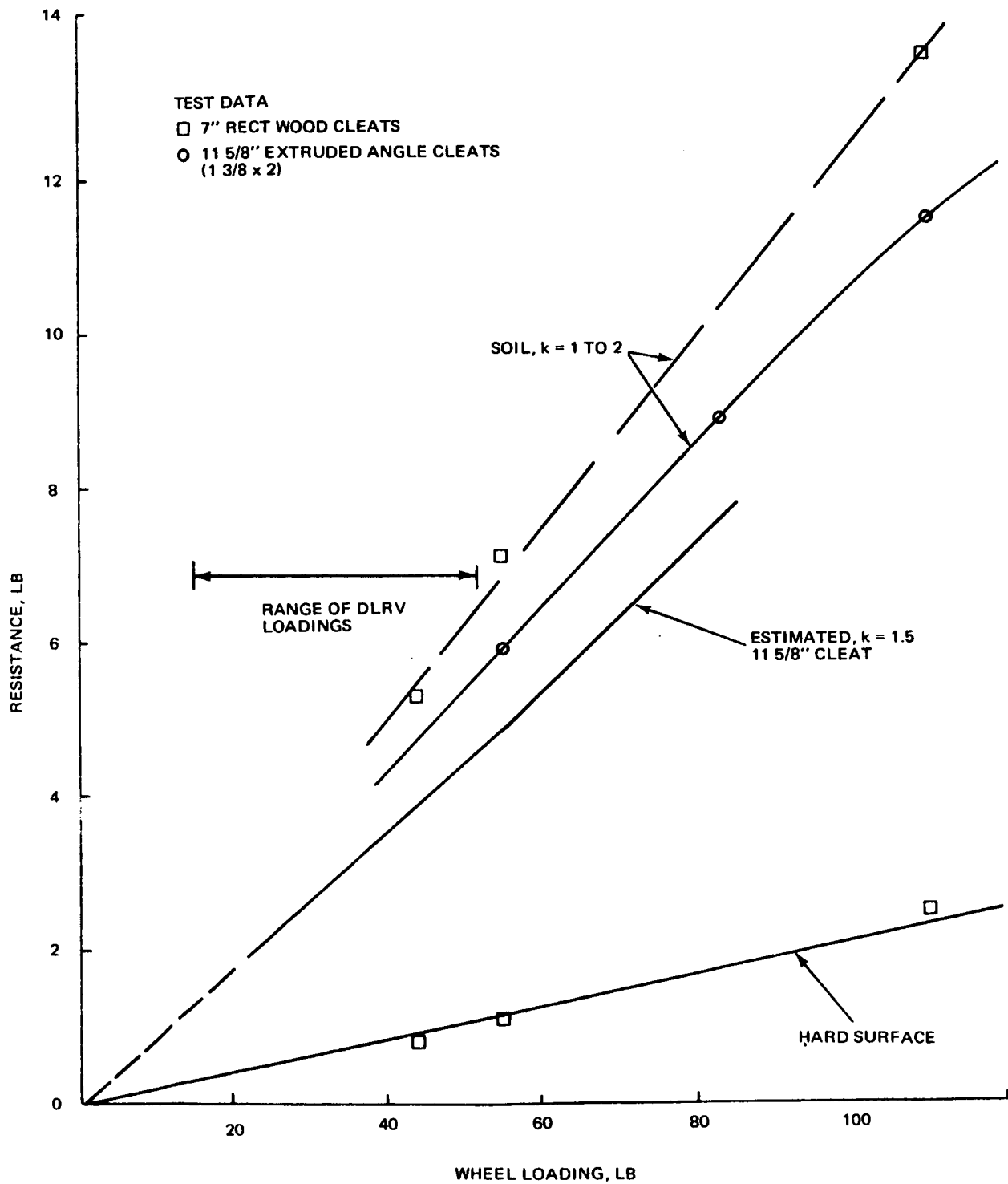


FIG. 4.1-3 TESTS OF 38" 1/8<sub>g</sub> WHEEL

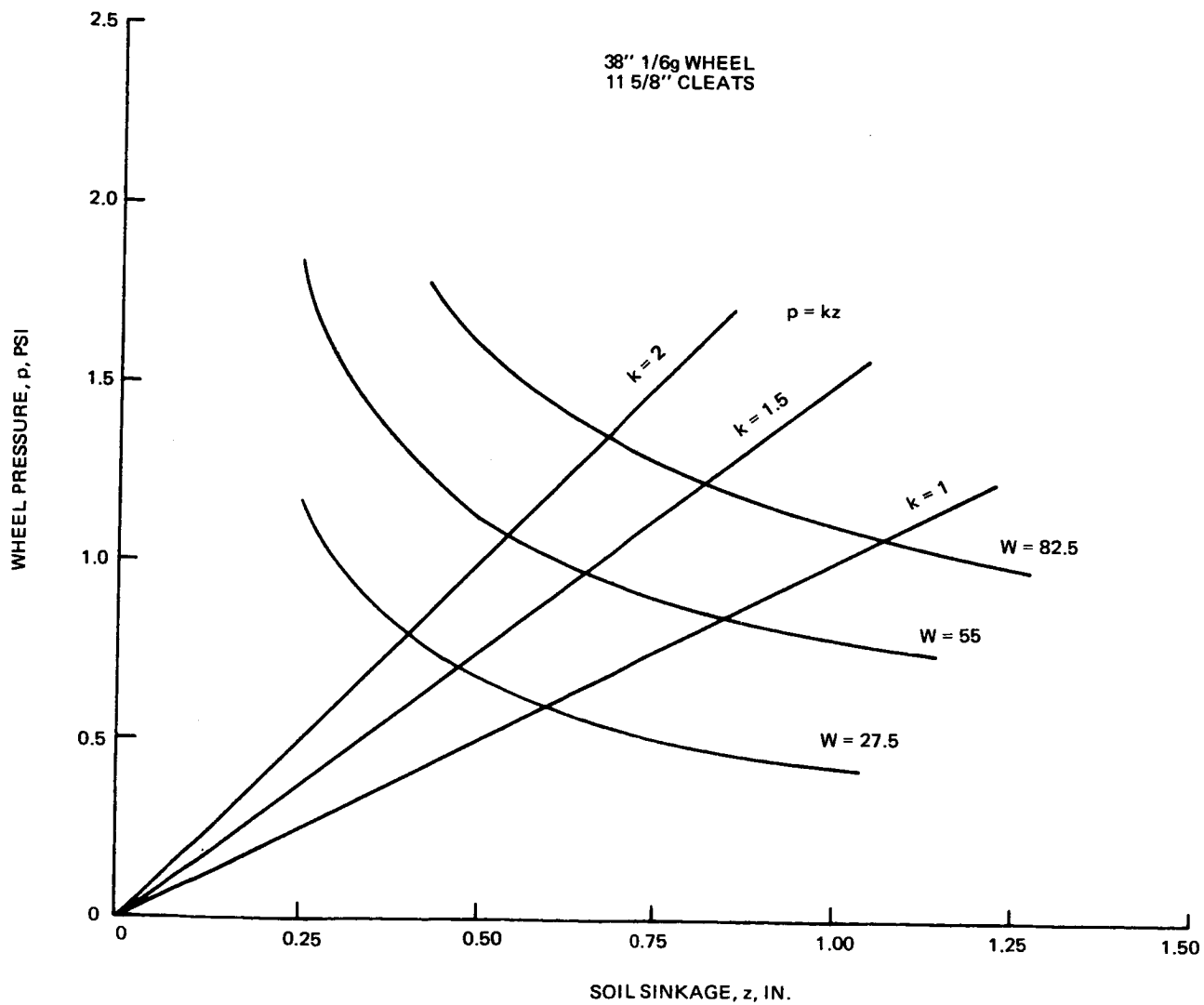


FIG. 4.1-4 ESTIMATED WHEEL PRESSURES VS SINKAGE

W lb	Pe Psi
27.5	0.70
55.0	0.97
82.5	1.22

4. Rolling resistance was calculated from equation (1) using the equilibrium pressures. A parasitic loss of 2.1% was added.

It is seen in Figure 4.1-3 that the estimated resistance value is about 80% of the test value. This is attributed to non-optimum cleat spacing and cleat deflections on the test wheel. It is assumed that the estimate for  $k = 1.5$  is representative of the rolling resistance for all lunar terrain since (1) cleat design will be refined and (2) the reduction in rolling resistance of the tracking wheels has been neglected. Grumman tests of the 38", 1/6-g wheel with the 7" cleats ( $k=1-2$ ) showed a reduction in average resistance to 92% for 2 passes and 87% for 3 passes. Wheel loading, however, was high, 110 lb. Comparable results were obtained from the Steven's tests in soft soil ( $k=1$  to 2) where the average resistance was reduced to 85% for 2 passes.

In order to evaluate required torque for wheel drive motors, it is necessary to determine wheel loading for both level and sloping terrain. The results of these computations are shown in Table 4.1-2 for representative unmanned and manned loadings. The total resistance due to the rolling resistance,  $R_z$ , and the parasitic losses,  $R_p$ , were taken from Figure 4.1-3 using the estimated curve for  $k=1.5$ . Required torques vs slope are plotted in Figure 4.1-5. The average level traverse torque required is 3.9 ft-lb per wheel for unmanned operation and 5.6 ft-lb per wheel for manned operation. These were rounded off conservatively to 4.0 and 6.0 ft-lb respectively for all calculations of level traverse performance.

#### 4.1.1.2 Slope Climbing

The slope-climbing ability of a vehicle and its power consumption on level terrain and on slopes depend on a complex interaction of soil and wheel properties including sinkage and slip. While analytical estimates are possible, they must ultimately be verified or supplemented by full-scale field tests. The pull coefficient, or ratio of draw bar pull to wheel normal load ( $P/W$ ), is essentially equal to the tangent of the slope that the vehicle can climb. The actual climbable slope will be somewhat less than this value due to such factors as redistribution of wheel loading and reductions of soil bearing

TABLE 4.1-2  
CALCULATION OF REQUIRED WHEEL TORQUE

A. Unmanned operation with 100 lb of samples and RGM for a total vehicle weight of 972 lb

Wheel	Slope (deg)	Wheel Loading (lb)	Rolling Resistance & Parasitic Losses (lb)	Gravity Resistance (lb)	Total Resistance (lb)	Required Torque (ft-lb)
Control Module (Rear)	0 20 35	26.4 34.0 37.1	2.4 3.0 3.3	0 12.4 26.0	2.4 15.4 29.3	3.8 24.4 46.4
Power Module (Middle)	0 20 35	24.5 16.7 9.5	2.2 1.5 0.9	0 6.1 6.6	2.2 7.6 7.5	3.5 12.0 11.9
Science Module (Front)	0 20 35	30.1 25.4 19.8	2.7 2.3 1.8	0 9.3 13.9	2.7 11.6 15.7	4.3 18.4 24.8

B. Manned operation with one astronaut and no samples for a total vehicle weight of 946 lb

Control Module (Front)	0 20 35	52.0 39.4 26.7	4.6 3.5 2.4	0 14.3 18.7	4.6 17.8 21.1	7.3 26.2 33.4
Power Module (Rear)	0 20 35	27.0 34.7 37.9	2.45 3.1 3.4	0 12.6 26.6	2.45 15.7 30.0	3.9 24.8 47.5

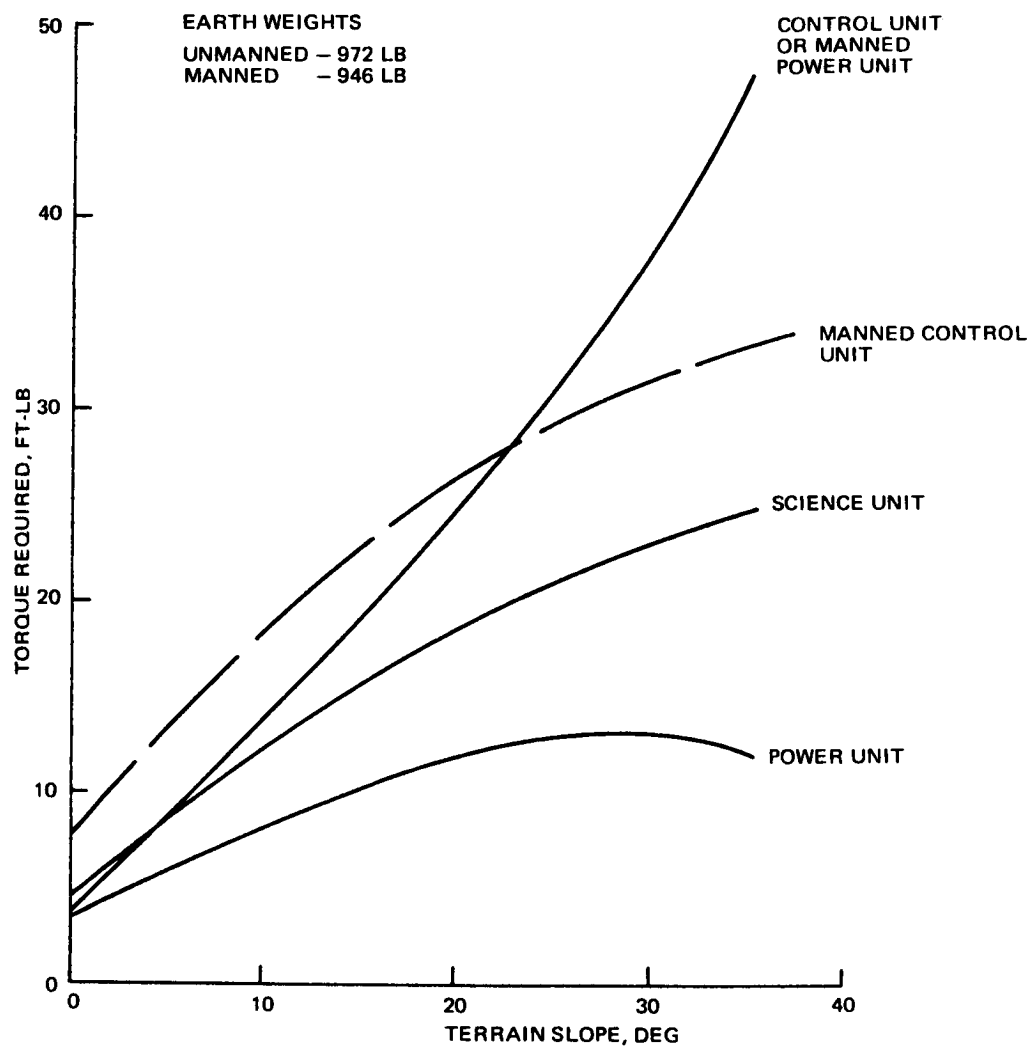


FIG. 4.1-5 WHEEL TORQUE REQUIRED VS SLOPE

strength due to the slope angle.

Two reasons contributed to the selection of wide cleats for the DLRV wheels. One reason was to take advantage of the cohesive nature of lunar soils, and the relatively large contribution of soil cohesion to the total tractive effort in a 1/6-g field. This factor argues for a large footprint, hence, for a wide cleat. The selected size, 11 5/8 inches, is the largest that can be accommodated. The other reason for selecting the wide cleat was to reduce footprint pressure and, hence, rolling resistance, as shown by test data in Figure 4.1-3.

Soil bin tests involving a single prototype wheel are very useful as they permit a better control of the soil and wheel parameters. DLRV type wheels have been tested at Stevens Institute (Reference 1), as previously mentioned, and at Waterways Experiment Station (WES) (Reference 2). Both wheels were 42" diameter. A 1-g version was tested at Stevens, a 1/6-g version was tested at WES.

The test measurements, soil conditions and cleat configurations are listed below for the Stevens tests.

TABLE 4.1-3  
SOIL BIN TEST CONDITIONS Ref. (1)  
(wheel loading = 330 lbs)

<u>Measurements</u>	<u>Soil Conditions</u>	<u>Cleat Configuration</u>
Draw bar pull vs. slip	Cohesionless sand	10-inch flat plate
Torque vs. slip	Soft, k or G=1 to 2	12-inch, 1½ x 1½ in. angle cleat
Sinkage	Firm, k or G=8 to 10	
Footpring length		
Wheel and carriage speed		

The draw bar pull, torque and locomotion efficiencies vs. % slip are shown in Figs. 4.1-6 to 4.1-9 and pertinent results are summarized in Table 4.1-4.

Locomotion efficiency is defined as

$$\eta = \frac{PR}{T} (1-s)$$

where R is nominal wheel radius, T is wheel input torque and s is slip. We may draw the following conclusions from these tests:

- WHEEL LOADING = 330 LB
- SOFT DRY SAND,  $k$  OR  $G = 1$  TO 2 PSI/IN.

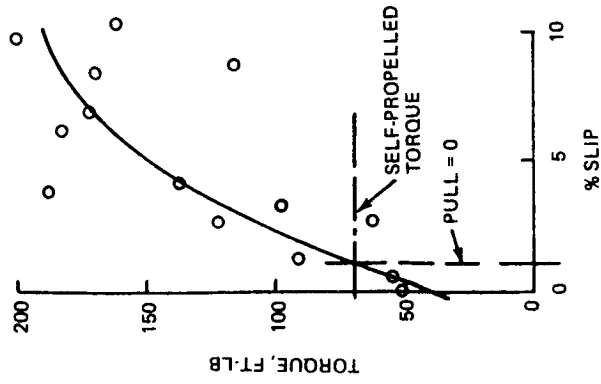
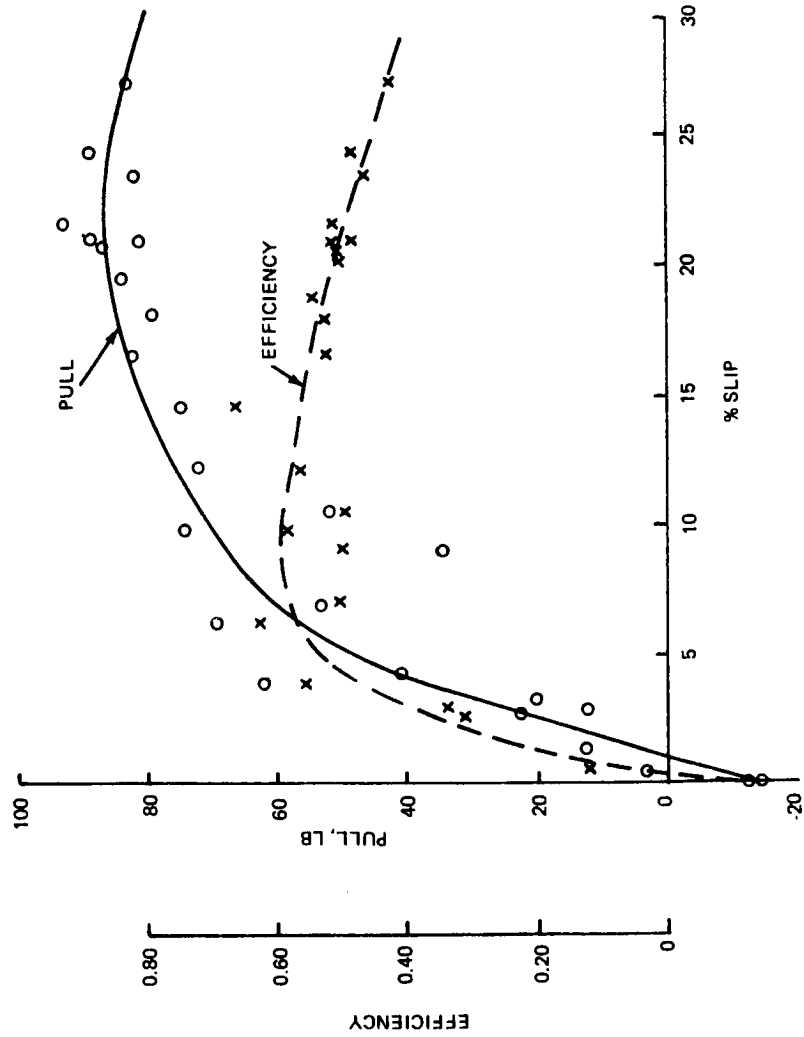


FIG. 4.1-6 SOFT SOIL WHEEL PERFORMANCE, 10-INCH CLEAT



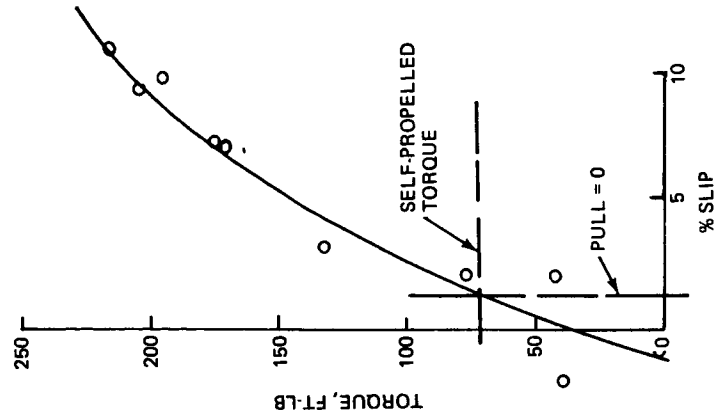
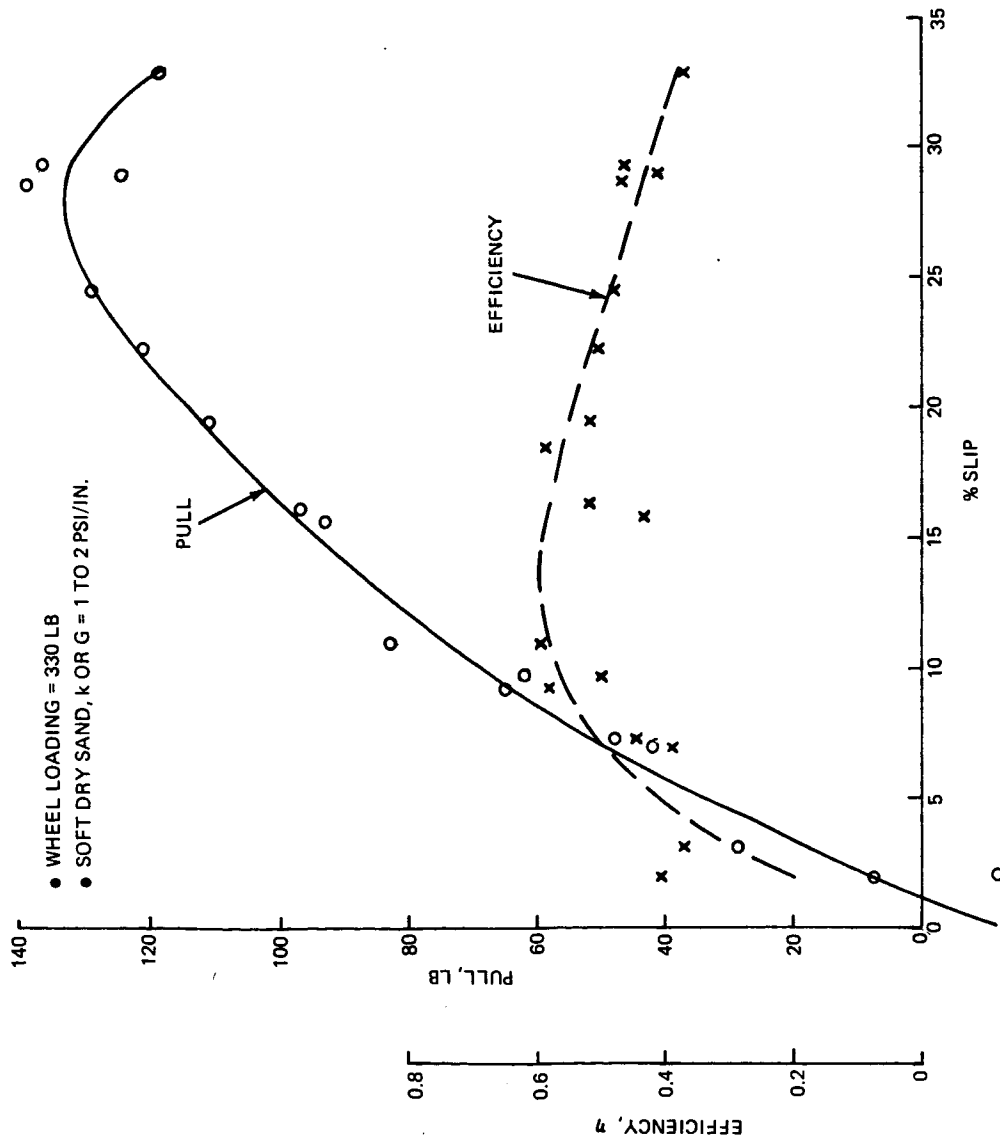


FIG. 4.1.7 SOFT SOIL WHEEL PERFORMANCE, ANGLE CLEATS

- WHEEL LOADING = 330 LB
- FIRM DRY SAND,  $k$  OR  $G = 8$  TO 10 PSI/IN.

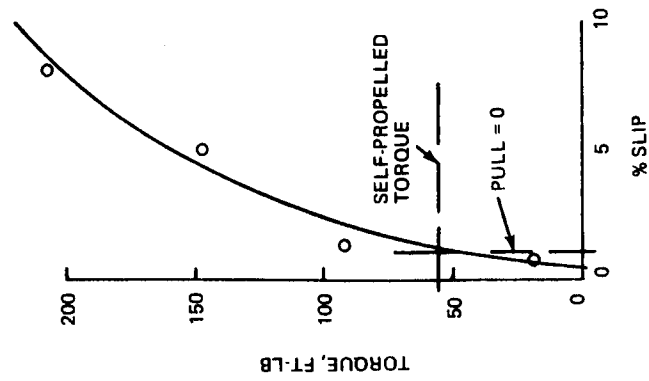
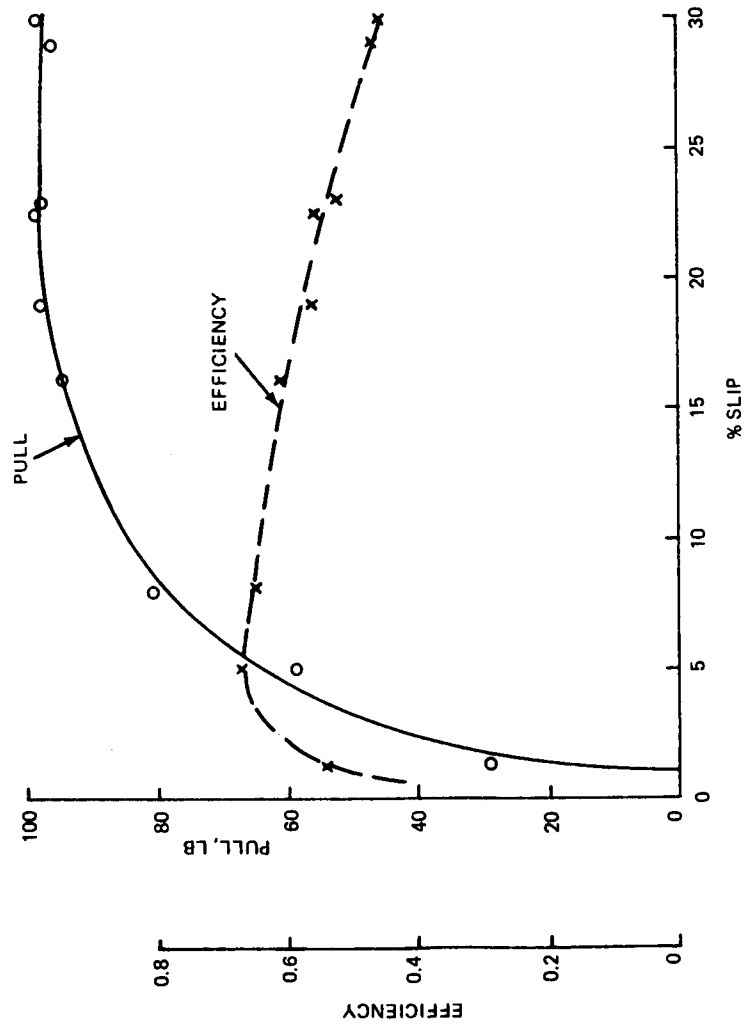


FIG. 4.1-8 FIRM SOIL WHEEL PERFORMANCE, 10-INCH CLEATS

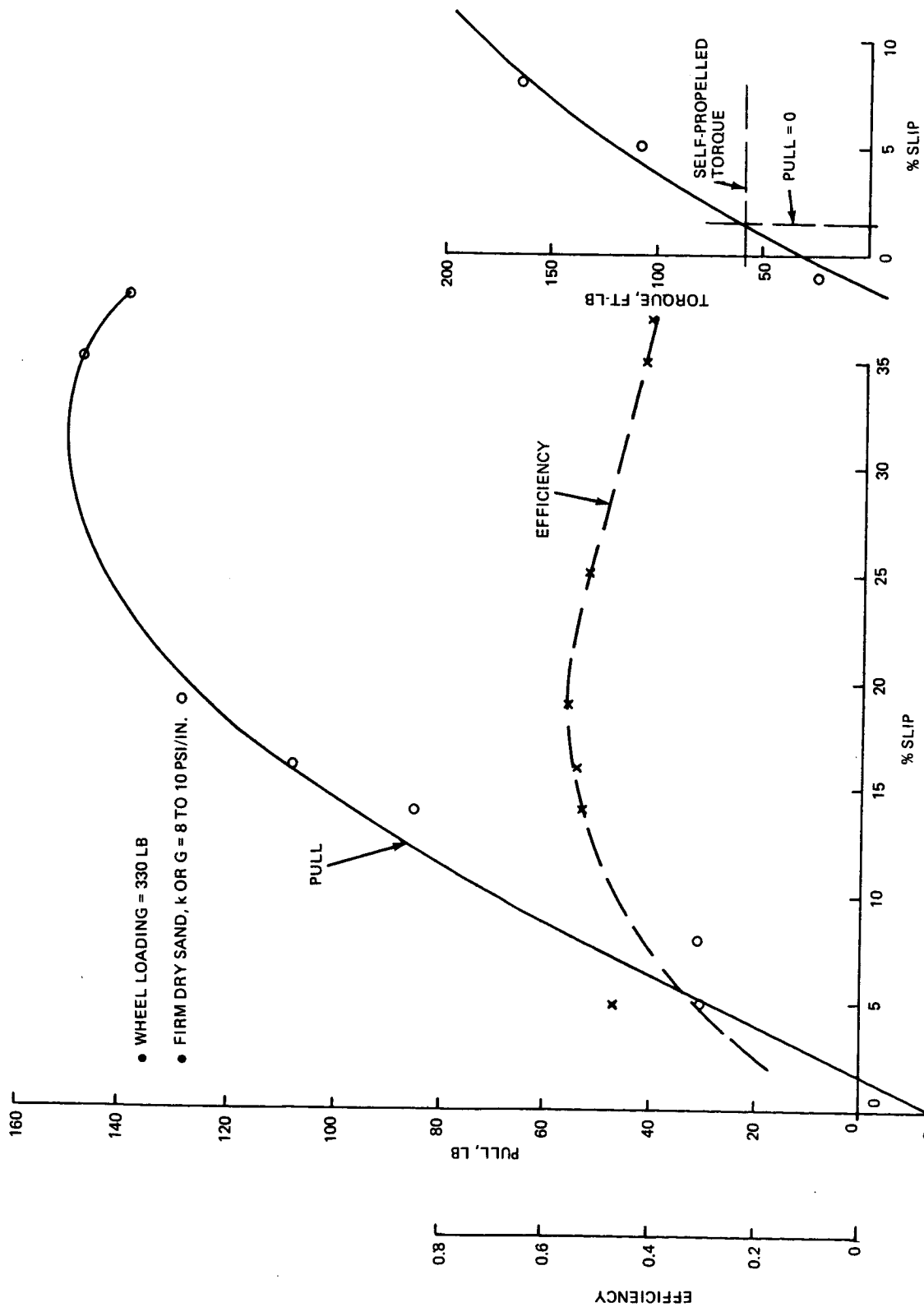


FIG. 4.1-9 FIRM SOIL WHEEL PERFORMANCE, ANGLE CLEATS

TABLE 4.1.1-4

## STEVENS SOIL BIN TEST RESULTS

1-g Wheel, 42-inch diameter, W = 330 lb

SOIL (dry, cohesionless sand)	CLEATS	P = 0 (Level Terrain)			MAX. P/W			MAX. EFFICIENCY		
		% Slip	Torque ft-lb	Rolling Resistance lb	P/W	% Slip	% Eff.	P/W	% Slip	% Eff.
k = 1 to 2	10" flat	1	70	40	.26	22	49	.20	9	60
	12" angle	1.3	73	42	.40	28	45	.27	14	60
k = 8 to 10	10" flat	1	55	31	.30	22	55	.19	5	67
	12" angle	1.5	58	33	.45	32	45	.36	18	56

- o In all four cases, that is regardless of soil or cleat conditions, the slip on level ground in the self-propelled mode (when DBP=0) is 1 to 1.5 percent.
- o The increase in rolling resistance due to the angle cleats is negligible on level ground or at low draw bar pull levels
- o The addition of the angle cleats increases the maximum draw bar pull by 54% in soft soil and by 50% in firm soil. However, a penalty in rolling resistance, hence, in locomotion efficiency, is paid to achieve the higher draw bar pull. This penalty is 9% in soft soil and 22% in firm soil. In conclusion, the angle cleats deliver significantly more draw bar pull in all soil conditions with less cost in efficiency in soft soil than in firm soil

The Grumman wheel achieved a peak pull coefficient of 0.64 in the Waterways Experimental Station soil bin test, Ref. (2), as against a pull coefficient of 0.45 in the Stevens Institute soil bin tests, Ref. (1). These coefficients correspond to maximum climbable slopes of  $33^{\circ}$  and  $24^{\circ}$  respectively. The Cone Index gradient, G, of the soil in both tests was approximately the same; more specifically, it was 9 psi/in. (Stevens tests) and 12 psi/in. (WES tests). The discrepancy between the two test results may be adequately accounted for in terms of the following differences in the test conditions:

- o A 1-g wheel under a loading of 330 lbs was used in the Stevens tests, as against a 1/6-g wheel under a loading of 70 lbs in the WES tests
- o A dry cohesionless sand ( $c=0$ ) was used in the Stevens tests, as against a moist, relatively finer sand with a measured cohesion of 0.16 psi in the WES tests

Figure 4.1-10 shows the resolution of these data and the theoretical relationship between maximum climbable slope (pull coefficient) and wheel loading at various soil cohesions. Steven's P/W of .45 for  $c = 0$  is considered independent of wheel loading. The effective footprint length necessary to account for the WES results at  $c = .16$  was used in conjunction with Figure 4.1-1 to determine the assumed footprint length,  $l_e$ , vs loading. P/W was then computed from

$$\begin{aligned}
 P/W &= (P/W)_{c=0} + \Delta(P/W) \\
 &= (P/W)_{c=0} + l_e bc/W \\
 &= 0.45 + 12 l_e c/W
 \end{aligned}$$

where  $b = 12 \text{ in.} = \text{cleat width.}$

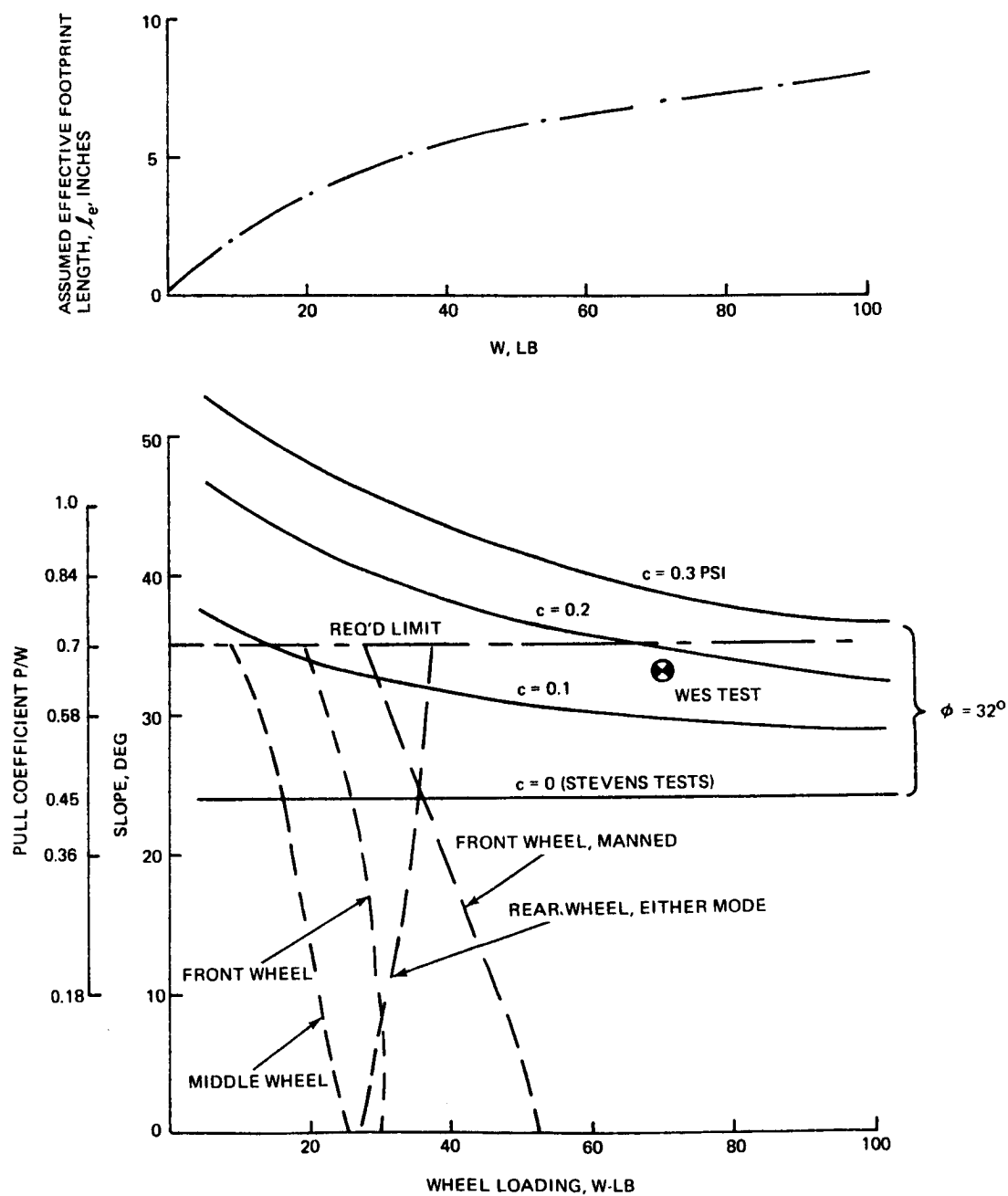


FIG. 4.1-10 MAXIMUM SLOPE CLIMBING ABILITY, 42" WHEEL, 12" ANGLE CLEATS

Cohesion in lunar soils is necessary if the vehicle is to climb a 35° slope in the low gravity of the moon. Notice how, at a given cohesion, climbable slope increases with decreasing wheel loading.

Although the wheels tested are not identical to the DLRV wheels, the results are representative of DLRV slope climbing capability. These results indicate that the DLRV wheel can climb a 35° slope under expected wheel loadings if the soil has a cohesion of the order of 0.1 to 0.2 psi. It is recommended that additional tests be performed to optimize the cleats at wheel loadings from 10 to 50 lb in soils with cohesion from 0.1 to 0.4 psi.

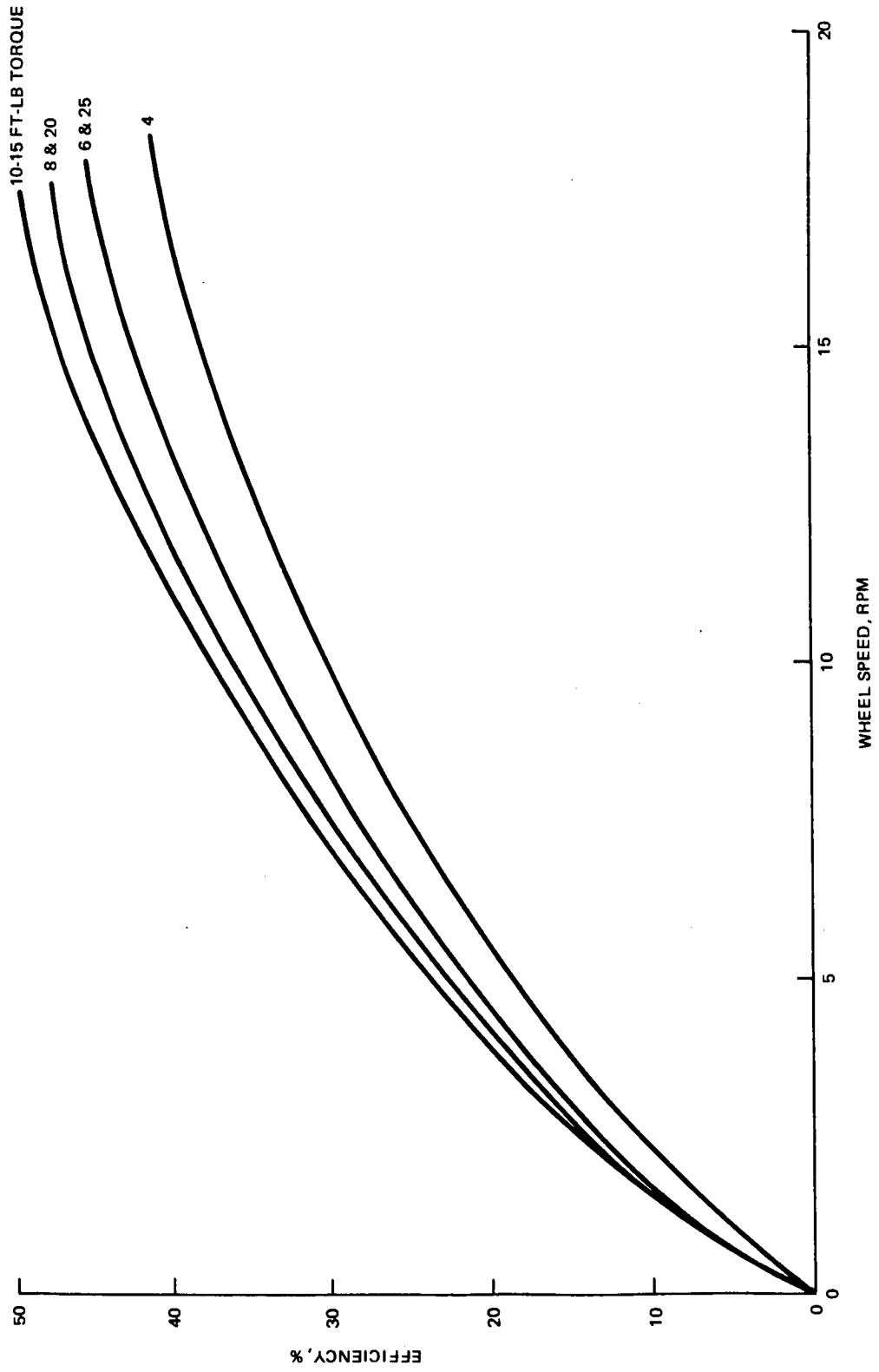
#### 4.1.1.3 Traverse Performance

In order to evaluate the electrical power required at various vehicle speeds over various terrain slopes, the motor performance curves in Volume III Book IV, Control Subsystem Design and Analysis, were used to derive curves showing motor efficiency for various torque loads and wheel speeds. Motor efficiency includes all losses starting at the motor controls but excludes distribution losses prior to that point. These are given in Figure 4.1-11 and 4.1-12 for the series mode. In applying these data the series mode is used at all wheel speeds below 45 RPM (~8 km/hr) and the parallel mode for speeds above this value. The two modes are combined in Figure 4.1-13 for manned operations. The torques are those for the loaded vehicle on level terrain.

The total power requirements for each drive motor excluding distribution losses were computed using the equation:

$$\text{Electrical Power Required} = \frac{\text{Mobility Power}}{\text{Efficiency}}$$

where the Mobility Power is obtained by converting the torque-speed product into watts, and the efficiency for the appropriate values of torque and speed is obtained from the curves previously mentioned. Figures 4.1-14 and 4.1-17 show the total vehicle mobility power requirements, including distribution losses for both the manned and unmanned vehicles, for level terrain and 10° and 20° slopes. For the unmanned vehicle, level terrain and an average of 4 ft-lbs torque was assumed for all six drive motors; in all other cases the torques in Table 4.1-2 and Figure 4.1-5 were used.



II/I.4-20

FIG. 4.1-11 MOTOR EFFICIENCY - SERIES MODE, LOW SPEED



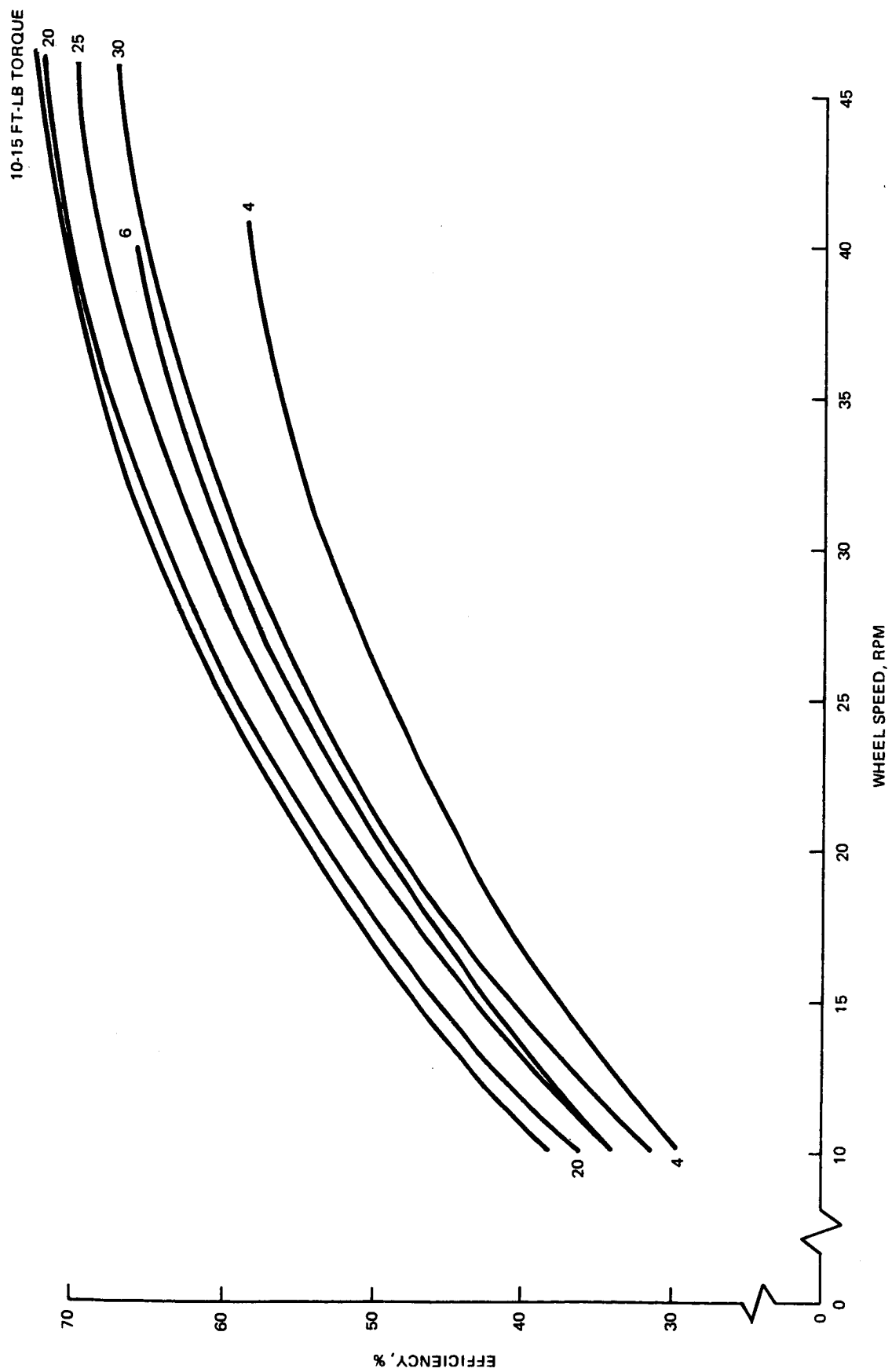


FIG. 4.1-12 MOTOR EFFICIENCY - SERIES MODE, MEDIUM SPEED

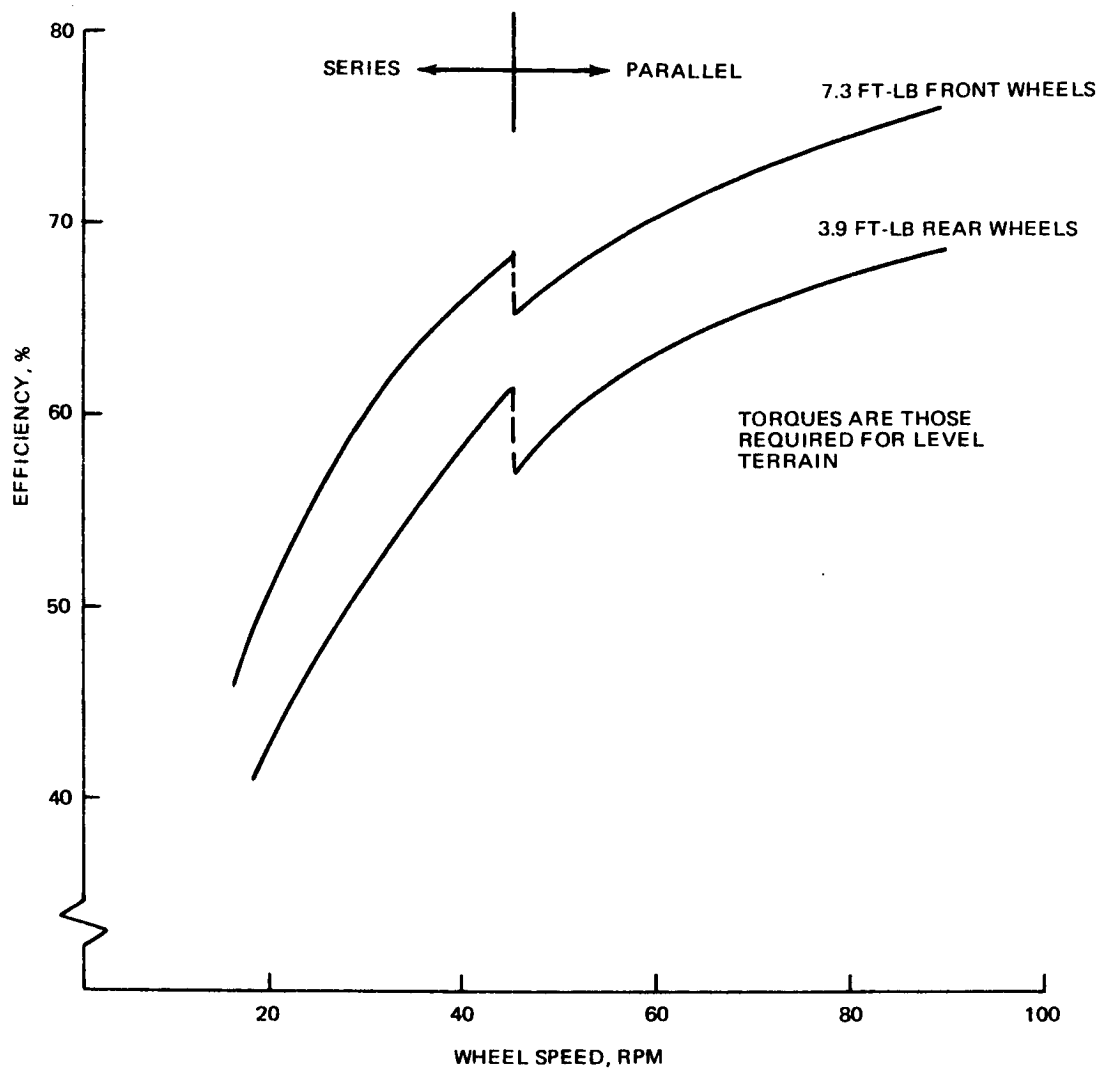


FIG. 4.1-13 MOTOR EFFICIENCY - MANNED

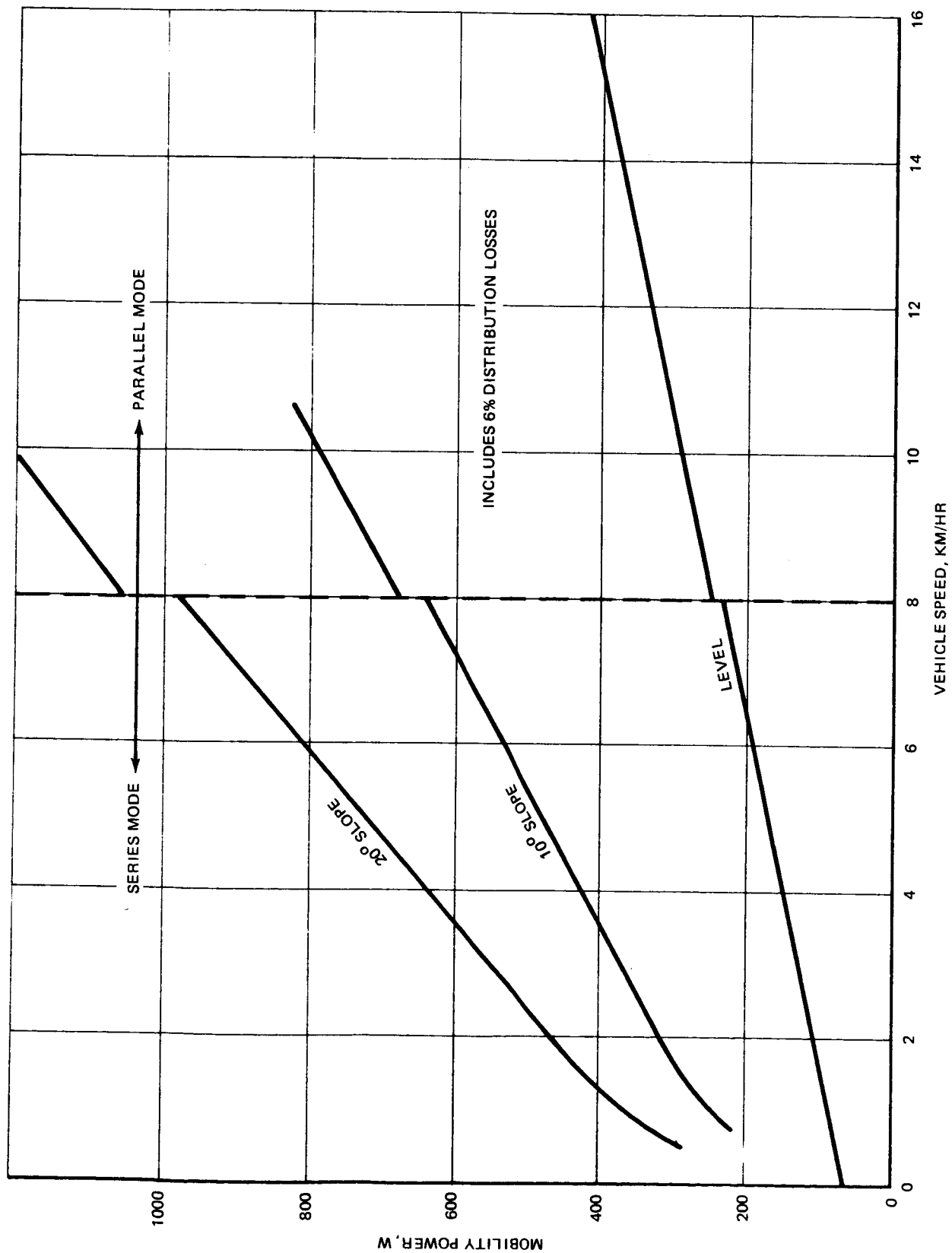


FIG. 4.1-14 POWER REQUIREMENTS - MANNED MODE

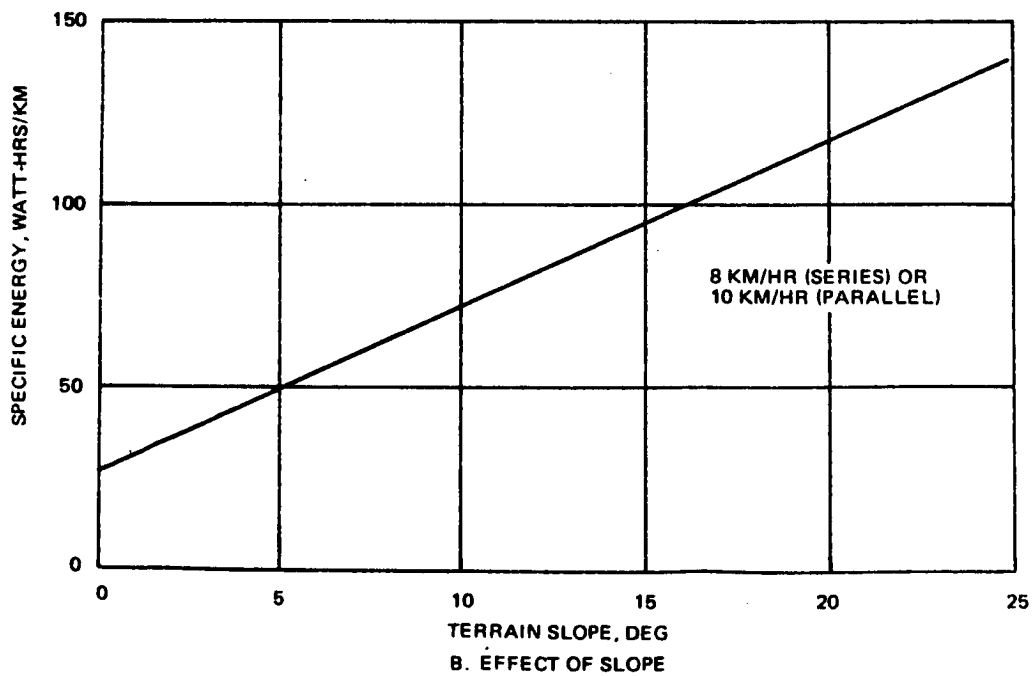
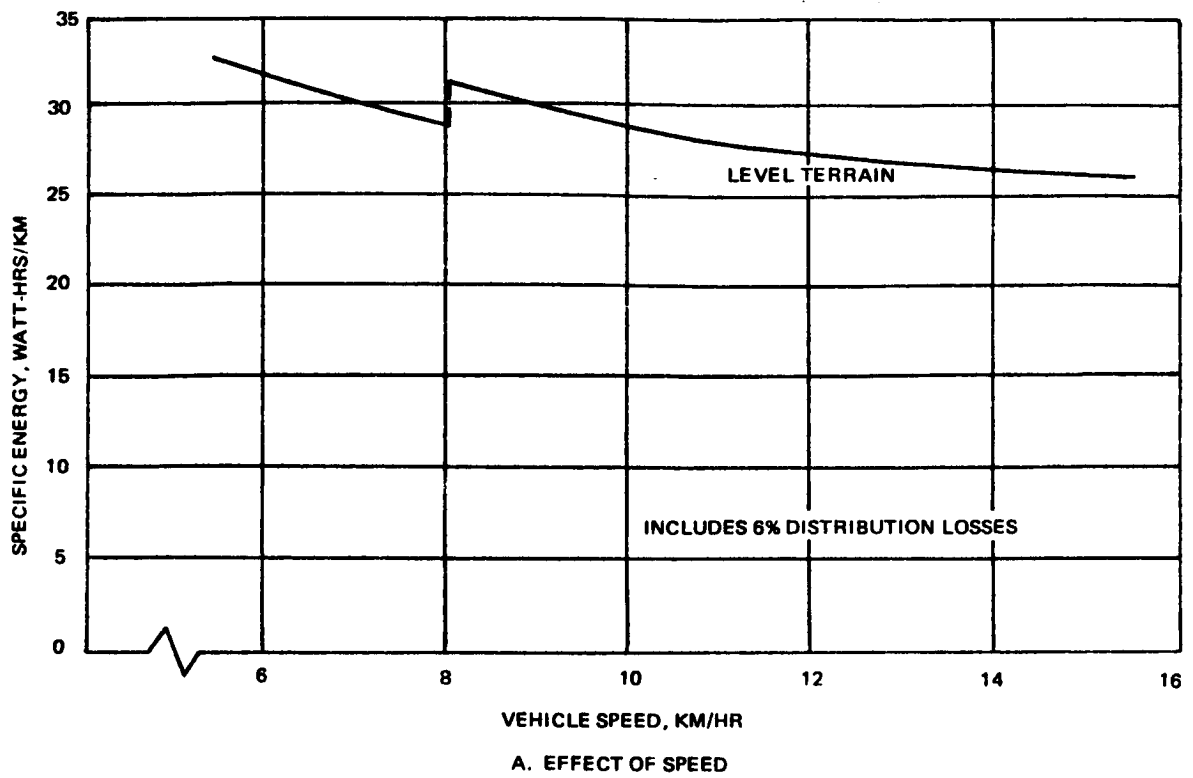


FIG. 4.1-15 MANNED MODE SPECIFIC ENERGY

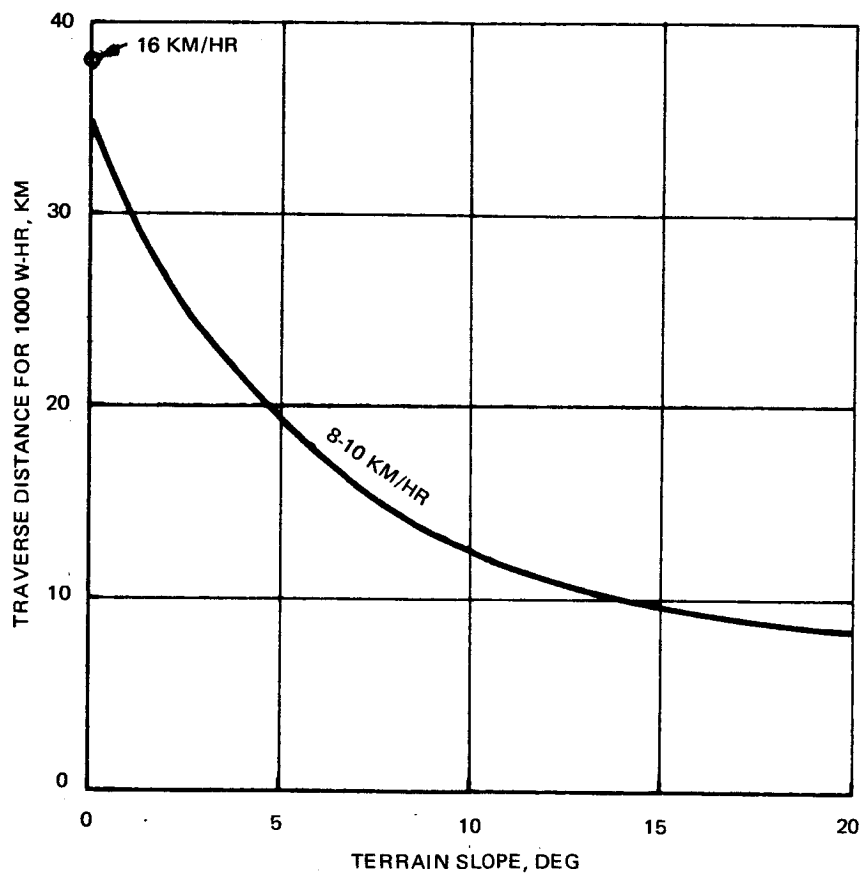


FIG. 4.1-16 MANNED MODE DISTANCE FOR 1000 WATT-HR

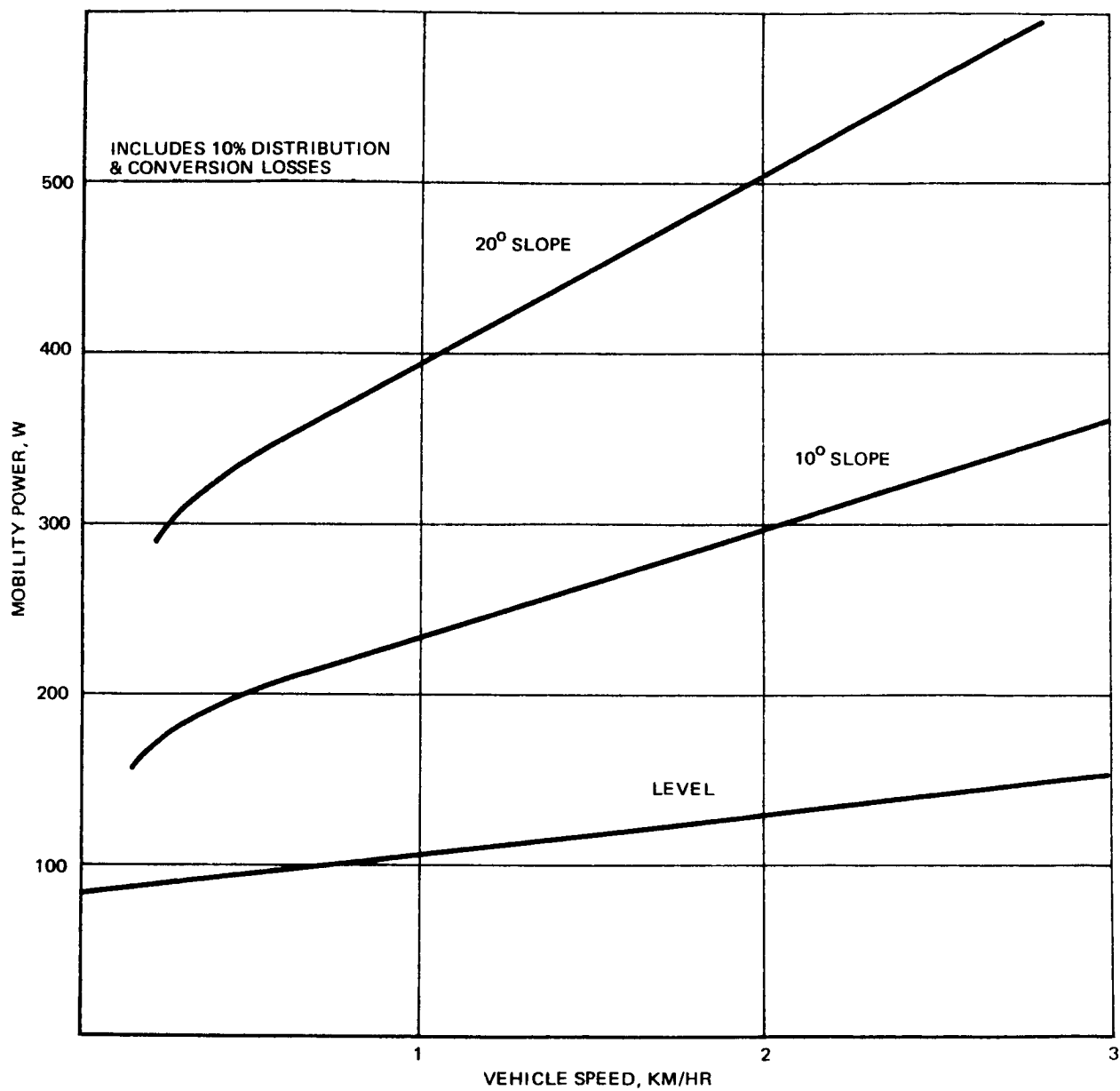


FIG. 4.1-17 MOBILITY POWER REQUIREMENTS - UNMANNED VEHICLE

Analyses were made of mission mobility capability, for both the manned and unmanned modes of operation. These analyses used the Reference Missions in Section 2.2, and especially Table 2.2-3 for the typical manned sortie, and Tables 2.2-5 and 2.2-7 for the unmanned operation. The electrical power for each type of operation is described in Section 2 of Volume III, Book V, which also defines the electrical power requirements for equipment other than the mobility equipment.

During manned operation electrical power is furnished by rechargeable batteries, rated at 1.68 kilowatt-hrs, plus a 32-watt output from the RTG. For this mode of operation 75% depth of discharge of the batteries or 1260 watt-hr is allowed. Another 140 watt-hr are available from the RTG during the  $4\frac{1}{2}$ -hr sortie time. Approximately 8 hours of recharge time are required between sorties. The desired reference sortie described in Table 2.2-3 is 4 hours 35 minutes duration, of which a total of 2 hours are used for a 30-kilometer level traverse at 15 km/hr. Of the 1400 watt-hours allowed for the sortie, 80 watts are required by all other equipment during the 2-hour traverse (160 W-hr). This includes the vehicle subsystems, a steering allowance, and a 6% distribution loss. No energy is assumed to be required for braking. During the non-traverse portions of the sortie, the vehicle and science equipments will require 240 watt-hours. This leaves 1000 watt-hours, which may be allocated to mobility equipment within the 75% depth of discharge capability.

The manned mobility power required for various speeds and slopes is shown in Figure 4.1-14. Approximately 790 watt-hours are required for the 30-km traverse of the Reference Mission. The specific energy vs. speed and slope is shown in Figure 4.1-15 and does not vary appreciably with speed. Traverse distance at 8-10 km/hr is plotted vs. slope in Figure 4.1-16 for the available energy of 1000 watt-hour. Maximum distance at 15 km/hr is 38 km which exceeds the 30-km requirement. Wheel slippage has been neglected in all cases since it is only 4.4% on a 20° slope (See Book I, Volume III).

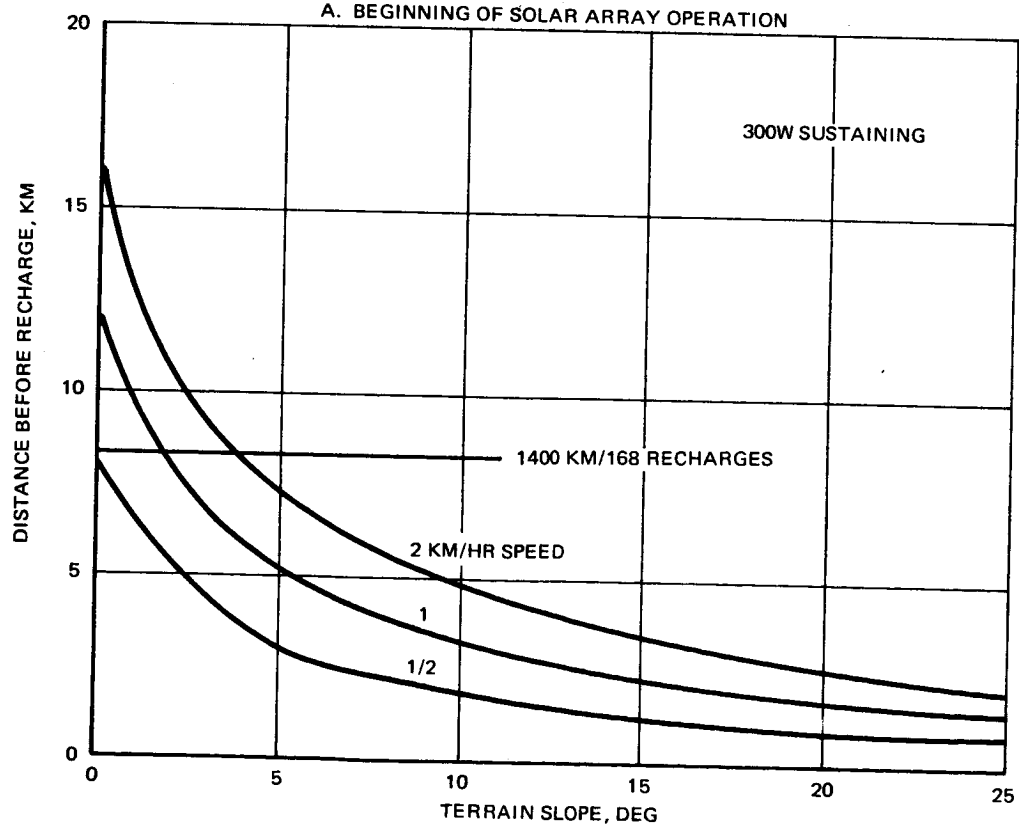
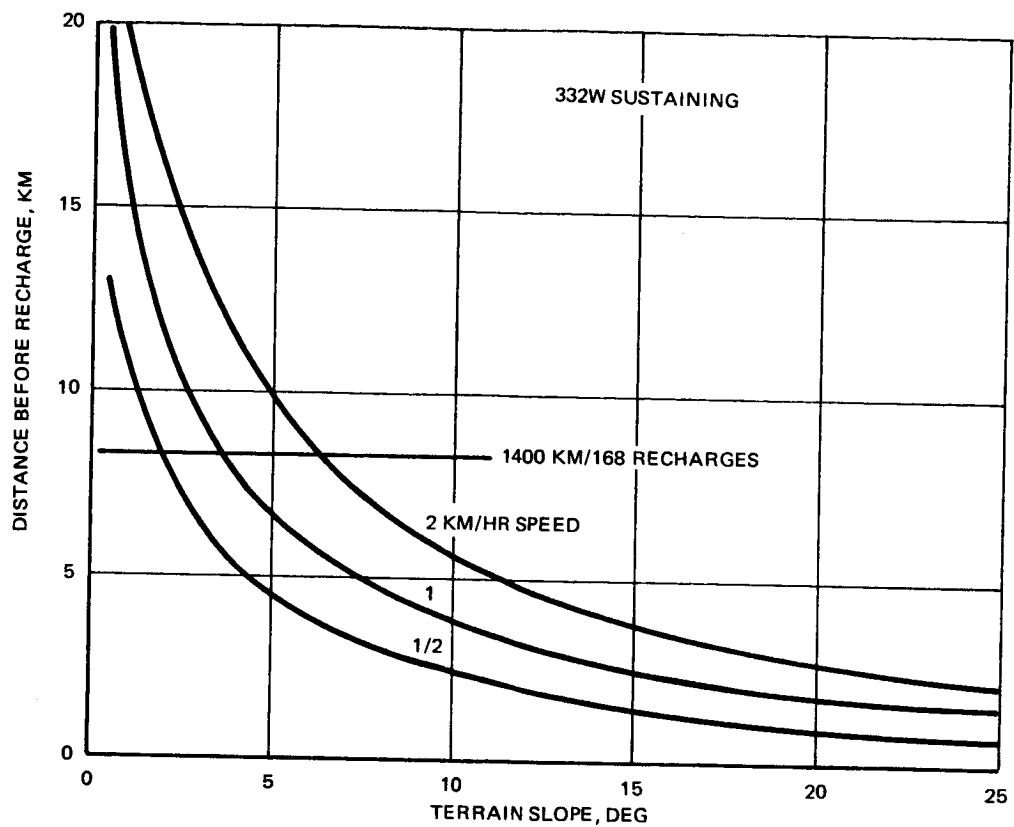
During unmanned operation, electrical power is furnished primarily by a solar array and the RTG. They have a combined capability which is 332 watts at the beginning of the mission, and which degrades to 300 watts at the end of the mission. The power capability also varies slightly over the lunar day as a function of solar elevation and array temperature. Whenever the power requirement exceeds the capability of the solar array and RTG, excess power is supplied from the batteries. When the batteries have reached a 35% depth of discharge (588 watt-hours used), a recharge cycle is required lasting 3.5 hours, during which all equipment is placed in standby. The batteries are not recharged at any other time, and operation periods at power levels below 300 watts may not be used for battery recharge. Batteries are designed for a maximum of 168 recharge cycles.

In evaluating the unmanned mission capability, 242 watts (10% losses included) are required by all equipment other than the mobility subsystem. This includes a steering allowance and an average science load of 50 watts. A total of 667 hr is available for recharge cycles (Table 2.2-7) permitting 190 recharges of  $3\frac{1}{2}$  hours. The traverse distance between recharge cycles for various speeds and slopes is given in Figure 4.1-18 for beginning and end of mission array performance. Total ground distance of the Unmanned Reference Mission is 1400 km (1155 traverse plus 245 at major sites). Average distance required per recharge without exceeding the 168 cycles is then 8.3 km. The vehicle, at the lowest speeds, can satisfactorily complete the mission if the average slope is  $2^\circ$  at the beginning and  $0^\circ$  at the end.

Of more significance is the distance when one assumes a 50% distribution of up and down slopes and up-slope power and down-slope power are averaged. Down-slope power is conservatively estimated the same as level power. The average power is then used to compute distance before recharge and the results are plotted vs. slope angle in Figure 4.1-19. It is seen that the 1400-km distance can be achieved with 168 recharge cycles at an average speed of 1 km/hr if slopes are equivalent to  $8^\circ$  at the beginning and  $3^\circ$  at the end of the mission. Notice the advantage of driving at high speeds, particularly up slopes. Unfortunately, this is contradictory to other criteria which reduce speed with increasing slope or terrain roughness.

0





B. END OF ONE YEAR SOLAR ARRAY OPERATION  
 FIG. 4.1-18 UNMANNED DISTANCE BEFORE RECHARGE VS SLOPE

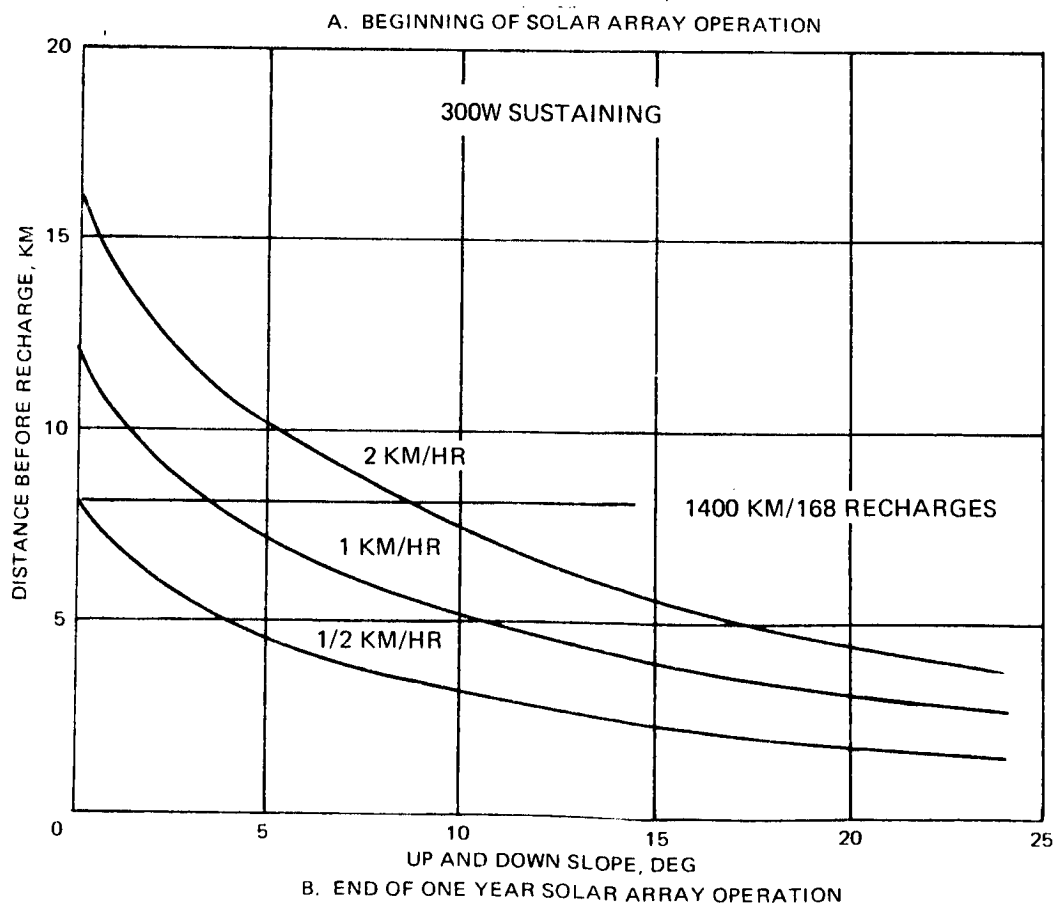
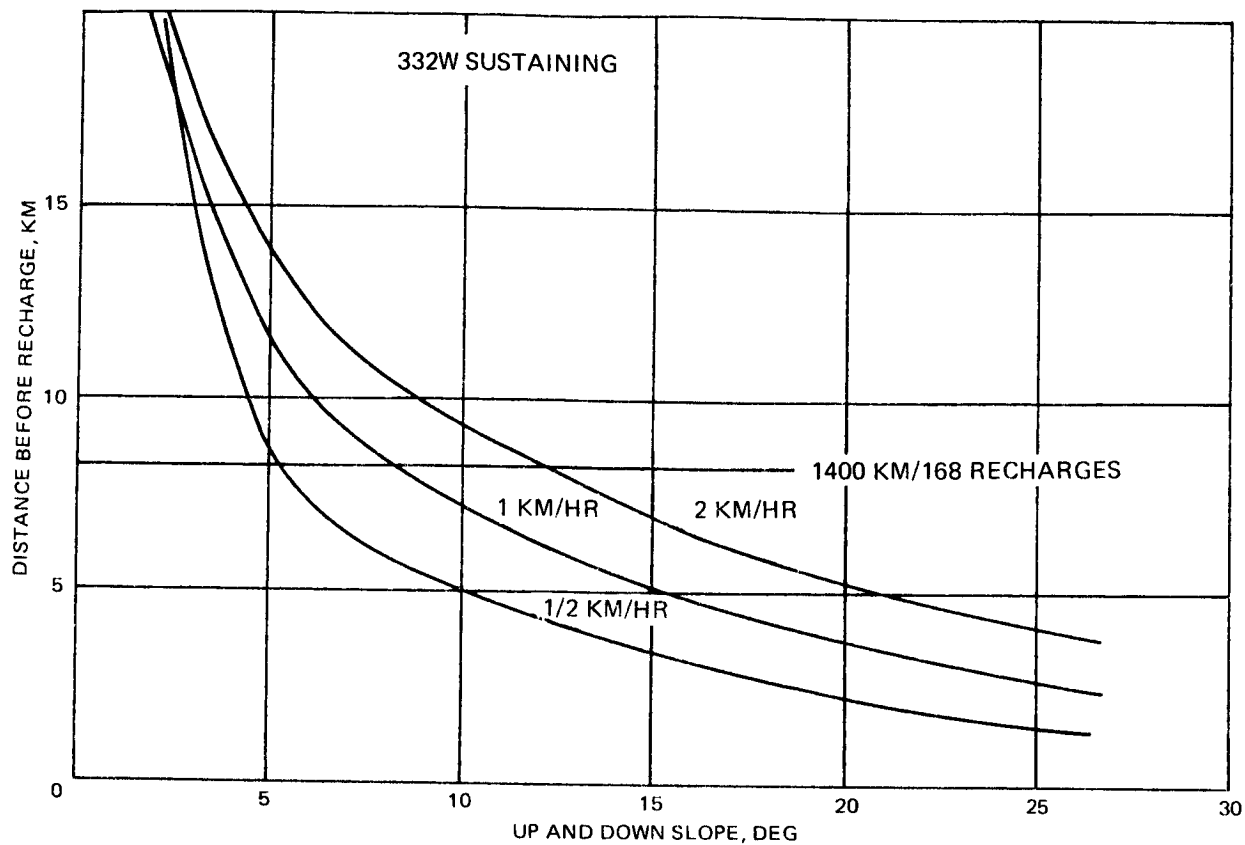


FIG. 4.1-19 UNMANNED DISTANCE FOR EQUAL UP AND DOWN SLOPES

#### 4.1.2 Obstacle Negotiation

##### 4.1.2.1 Approach

Obstacle negotiation capability of a vehicle can best be assessed experimentally. In order to demonstrate capability for the DLRV design, and to study the effects of weight distribution, pitch restraint, vehicle size and failure mode performance, a 1/6-scale model was constructed and exercised over steps and crevasses.

Two distinct sets of design requirements, corresponding to the manned and unmanned modes were specified for the vehicle (Annex C, Part III):

- |            |                |                   |
|------------|----------------|-------------------|
| o Step     | Manned - 30 cm | Unmanned - 100 cm |
| o Crevasse | Manned - 70 cm | Unmanned - 100 cm |

These required obstacles were used as standards for most of the experimental study.

##### 4.1.2.2 Model Characteristics

The one-sixth scale obstacle negotiation model is shown in Figure 4.1-20. The model was built to provide a variable geometry planform to allow for maximum test flexibility consistent with the design configurations under consideration. The model provided wheelbase, tread, percent wheel loadings, and pitch joint freedom. The pitch pivot point was centered between wheel axles. Flexible cone wheels made of ABS plastic closely approximated the required spring rate. Intermodular roll freedom of  $\pm 6^\circ$  was provided to simulate drawbar torsional flexibility. A friction coefficient of 0.6 to 0.8 was maintained at wheel/ground contact. Mass scaling of the model was not attempted; however, weight was kept to a minimum, and was maintained constant for each group of tests. Drive power was provided by an individual motor at each wheel. Motor speeds were generally governed by a single control; however, individual or paired control was available. Steering was locked out for all tests. An intermodular wheelbase of 96 inches and tread of 98 inches, corresponding to the dimensions of the unmanned vehicle, were standard for most tests. Where the effects of reduced vehicle geometry were evaluated, the wheel base and tread used was 88 and 83 inches, respectively, corresponding to the minimum size vehicle discussed in Section 7.1.

##### 4.1.2.3 Test Results

The initial testing with the model was done using a 4 x 4 manned mode configuration. All design requirements were found to be easily satisfied, so only limited testing was done with this configuration.

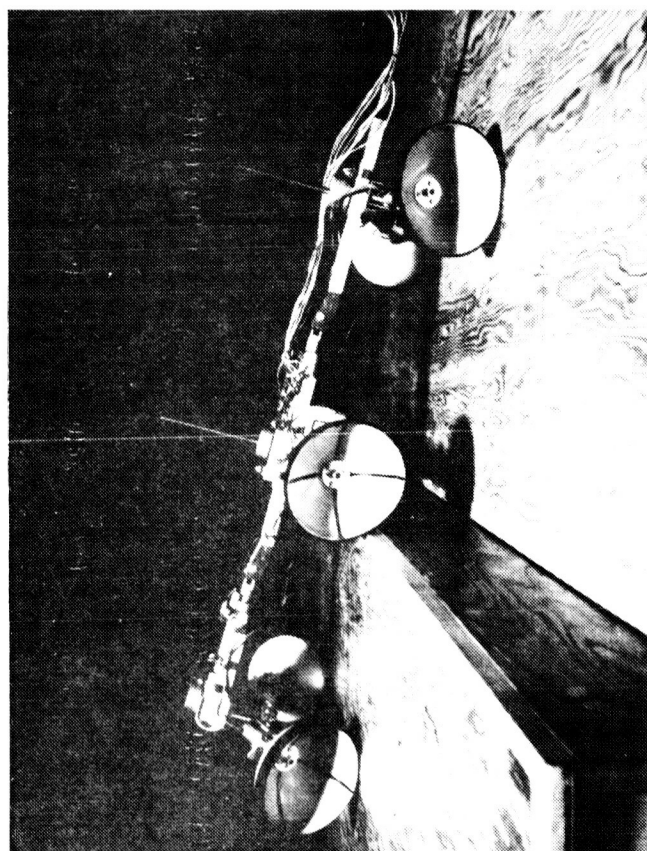
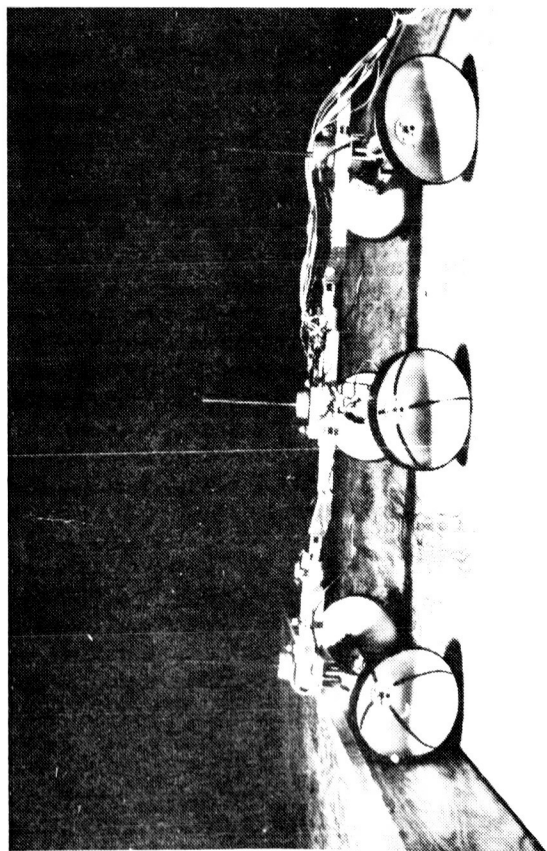
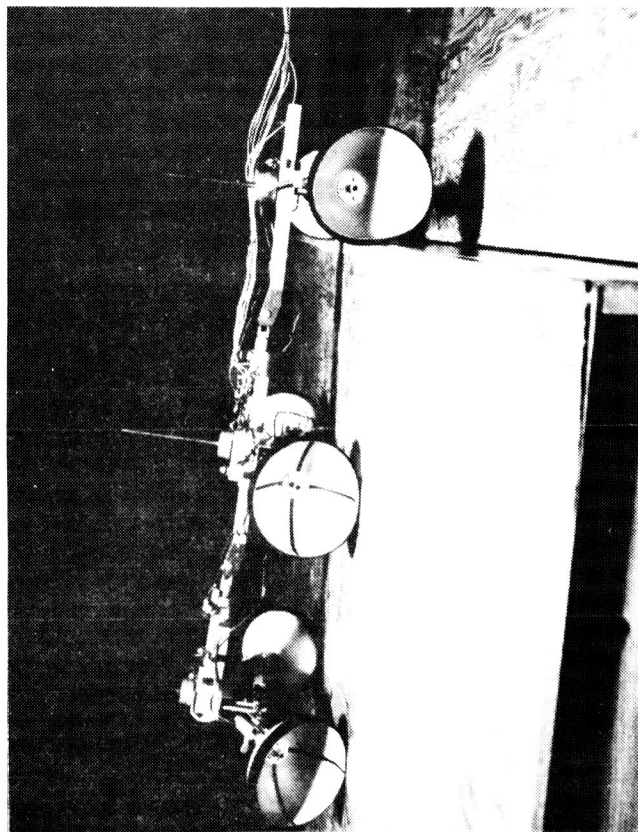
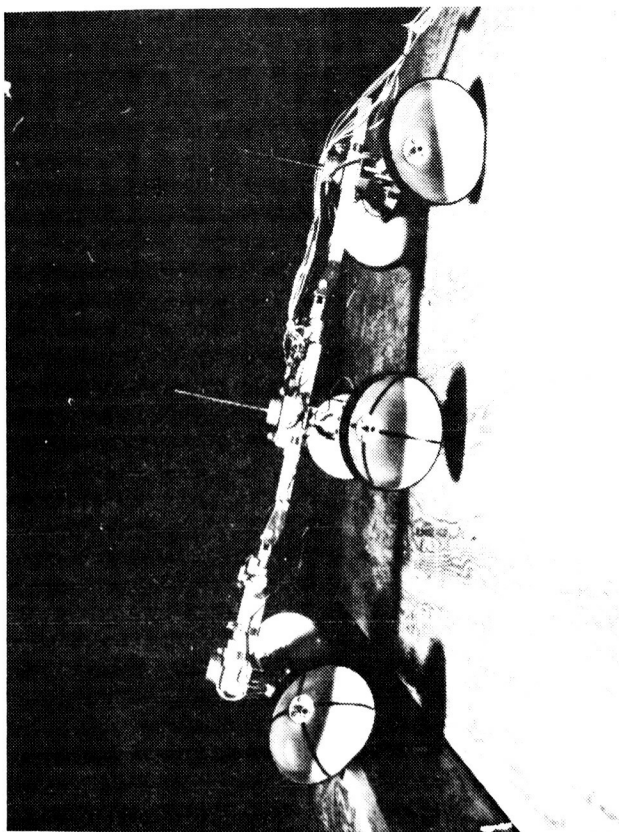


FIG. 4.1-20 1/6 SCALE OBSTACLE NEGOTIATION MODEL

The bulk of the testing was done with the 6 x 6 vehicle. Figure 4.1-21 and 4.1-22 show the vehicle crossing the required step and crevasse. Tables 4.1-5 and 6 define the various test conditions and give the results.

Comparisons were made between the selected 6 x 6 vehicle and a smaller vehicle (88 in. wheelbase and 83 in. tread). No significant difference was observed in obstacle negotiation capability for the one-meter crevasse or step. Although not tested, the larger vehicle should have the capability to cross larger obstacles because of the shallower angles required for step negotiation, and the larger pitch inertia which slows the rate at which the wheels fall into a crevasse. Tests were run to evaluate the effect of weight distribution on obstacle performance. Loading extremes up to 50% on a single module were considered. As shown in Table 4.1-5, an equal weight distribution or one that is biased such that the first module is lighter than the last is more favorable for obstacle negotiation. It becomes difficult to negotiate the obstacles when the leading module weight exceeds one third of the total. In the course of a mission, a critical obstacle could be negotiated in reverse if an adverse weight bias existed.

Obstacle negotiation is affected by the degree of pitch and roll freedom between modules. Roll freedom for the model was established at  $\pm 6$  degrees representing estimated chassis and joint torsional deflection. Pitch freedom was varied for both the front and rear modules. As shown in Table 4.1-5 the best configuration provided no pitch freedom between modules 1 and 2, and a  $+ 20 - 0^\circ$  freedom between modules 2 and 3. No pitch control appeared necessary; the vehicle was allowed to seek its own natural position. This approach provides minimum weight and design complexity.

Obstacle negotiation capability was also tested with respect to a degraded mode in which one wheel was not capable of being powered, but could free-wheel. Only step climbing was evaluated as this was believed to be the more critical obstacle. As shown in Table 4.1-6, all conditions but one were negotiable. The conditions with a failed front motor caused the vehicle to yaw in the direction of the failed wheel until the chassis contacted the obstacle. A combination of individual wheel control and active steering assist would probably resolve this problem.

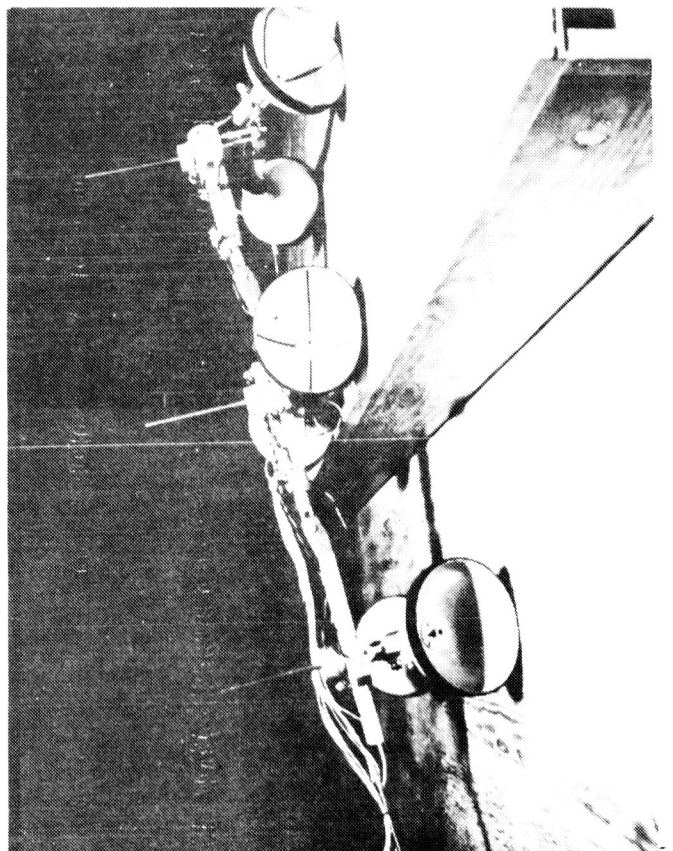
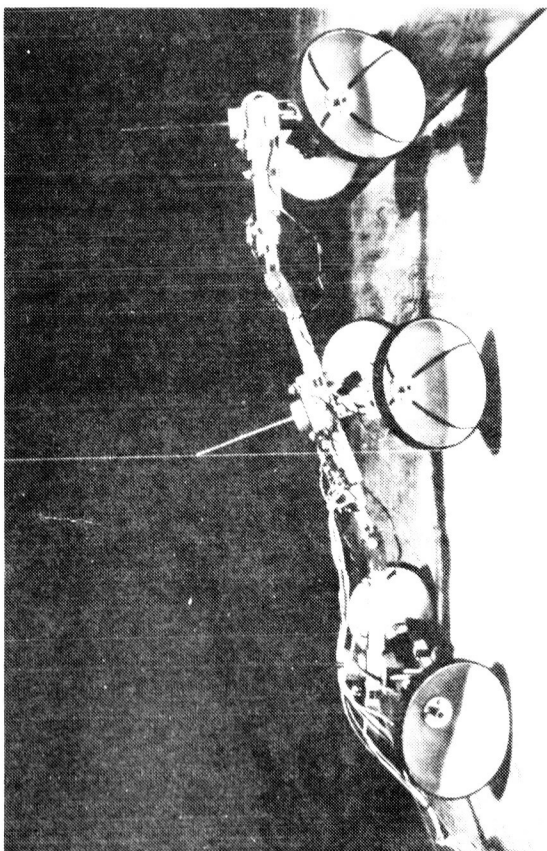
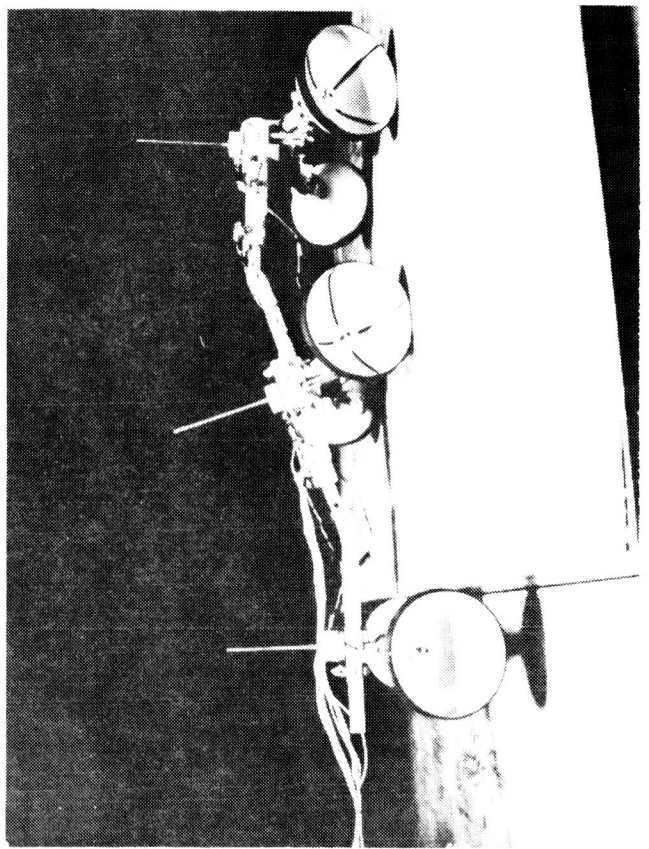
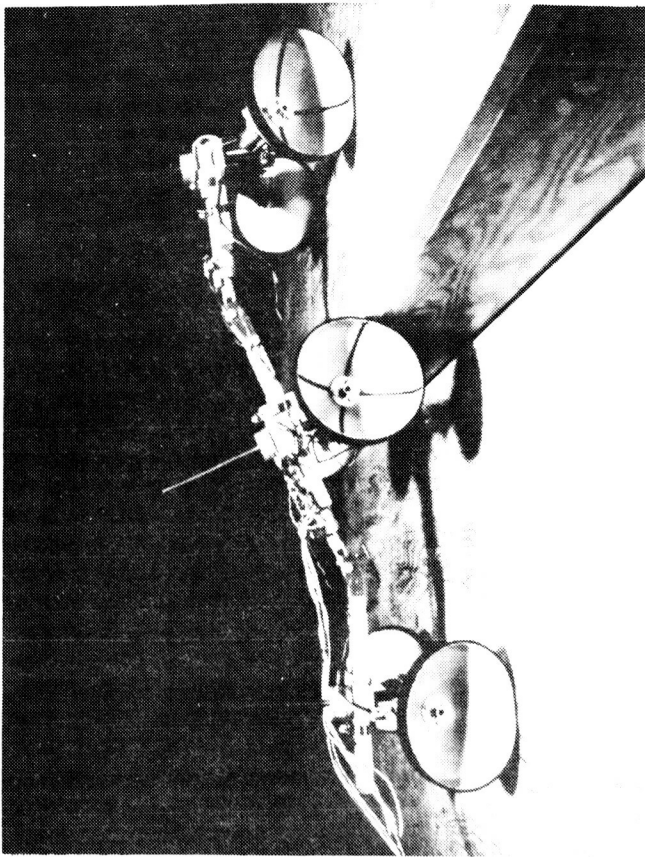


FIG. 4.1-21 1/6 SCALE MODEL CROSSING STEP OBSTACLE



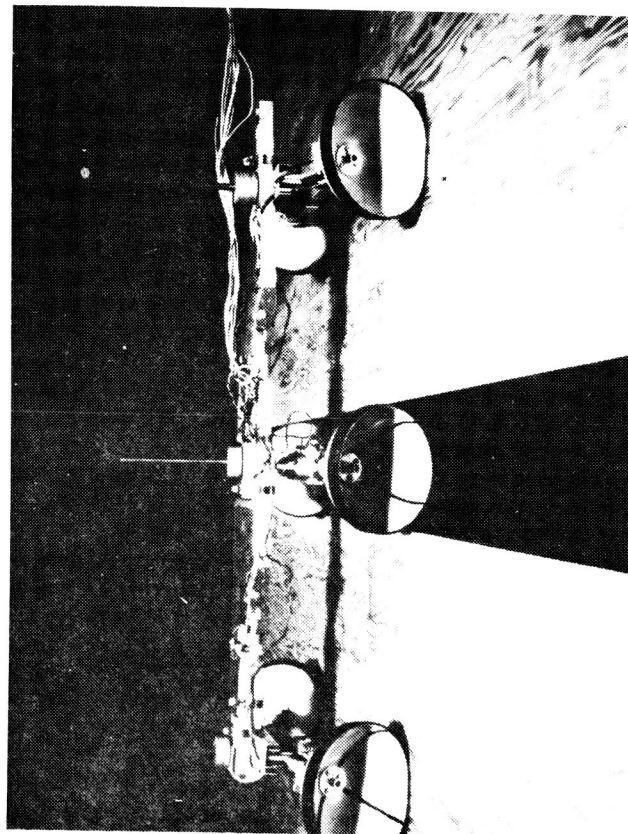
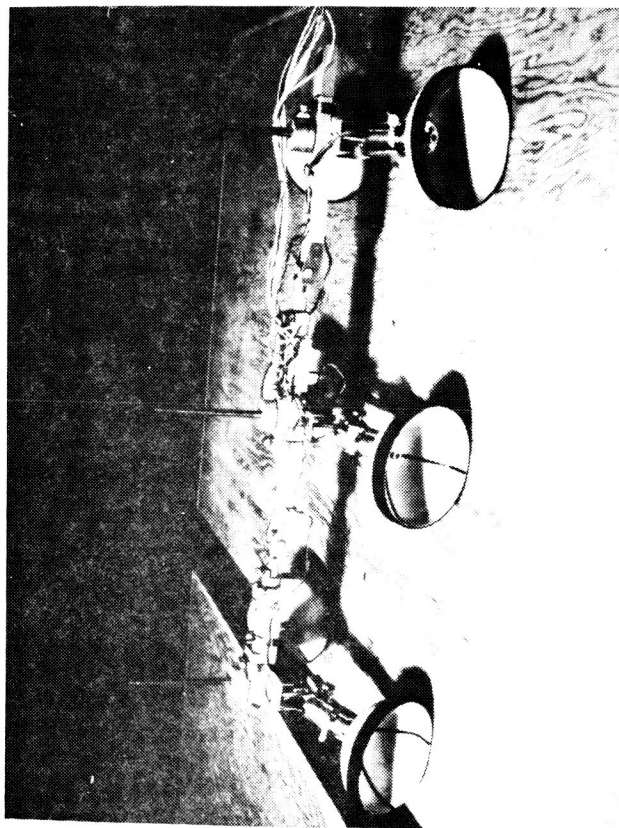
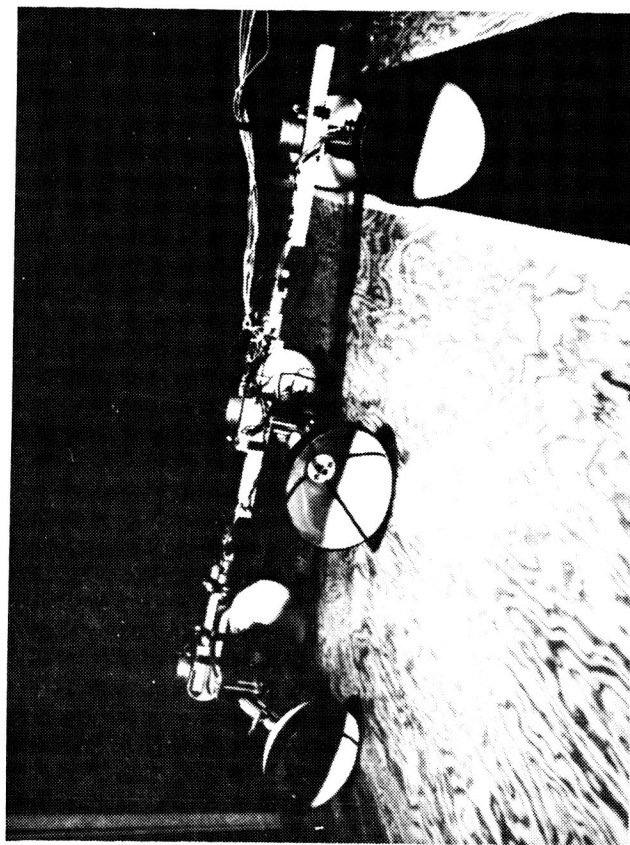
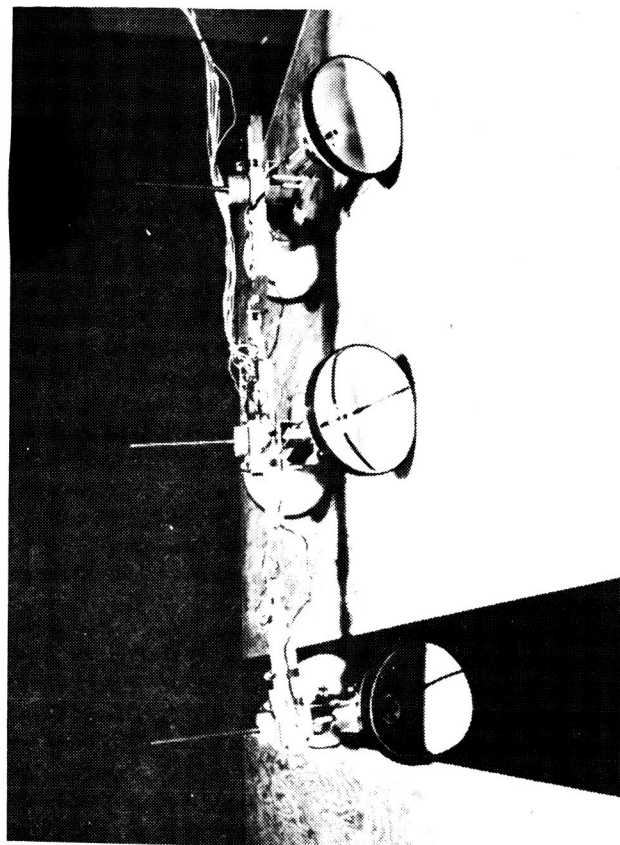


FIG. 4.1-22 1/6 SCALE MODEL CROSSING CREVASSE

TABLE 4.1-5  
OBSTACLE NEGOTIATION TESTS

TREAD/WHEELBASE Inches	WEIGHT DISTRIBUTION			PITCH FREEDOM		NEGOTIATION RATING
	Front	Center	Rear	Front	Rear	
98/96	One Meter Crevasse					
	25	25	50	0°	0°	E
	30	30	40	0°	0°	E
	40	30	30	0°	0°	F
	50	25	25	0°	0°	F
	All of the above distributions			0°	+ 20°	F
				+ 20°	+ 20°	F
				+ 20°	0°	F
				0°	+ 20°, -0°	D
	33	33	33	0°	+20°, -0°	E
	25	33	41	0°	+20°, -0°	F
	41	33	25	0°	+20°, -0°	F
83/88	33	33	33	0°	+20°, -10°	D
	33	33	33	0°	+20°, -20°	F
	33	33	33	0°	+20°, -0°	E
98/96	One Meter Step					
	25	25	50	0°	0°	E
	50	25	25	0°	0°	E
	25	25	50	0°	+ 20°	E
	50	25	25	0°	+ 20°	D
	25	25	50	+ 20°	+ 20°	E
	50	25	25	+ 20°	+ 20°	D
	25	25	50	+ 20°	0°	E
	50	25	25	+ 20°	0°	D
	33	33	33	0°	+20°, 0°	E
	25	33	41	0°	+20°, -0°	E
83/88	33	33	33	0°	+20°, -10°	E
	33	33	33	0°	+ 20°	VD
	33	33	33	0°	+20°, -0°	E

Negotiation Ratings:

E = Easy

D = Difficult

VD = Very difficult (required individual motor control  
and often several attempts)

F = Failed

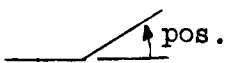
Sign Convention:  pos.



TABLE 4.1-6  
OBSTACLE NEGOTIATION WITH SINGLE WHEEL DRIVE FAILURE  
ONE METER STEP

FREE-WHEELING WHEEL	WEIGHT DISTRIBUTION			PITCH FREEDOM		NEGOTIATION RATING
	Front	Center	Rear	Front	Rear	
right front	25	33	41	0°	+20°, -0°	D
right front	33	33	33	"	"	D
right center	33	33	33	"	"	F
right center	25	33	41	"	"	VD
right rear	33	33	33	"	"	F
right rear	25	33	41	"	"	VD

#### 4.1.3 Probability of Traverse Success

Another means of evaluating DLRV traverse performances is an IBM 360/75 digital computer program which simulates, non-sequentially, the passage of a lunar roving vehicle over assumed lunar terrain. By means of the program, the effects of parametric variation of the vehicle design parameters can be evaluated in terms of the success of the vehicle in completing the traverse over the assumed terrain. Alternate designs may, therefore, be compared. Additionally, a vehicle's performance characteristics may be established for a variety of soils and slope distributions.

The input to the program is based on several models, as follows:

- o Vehicle model (deterministic)
- o Pothole model (statistical)
- o Slope and soil model (statistical)

The program output provides sinkage, slippage, traction, and probability of successfully completing the journey (i.e., probability of negotiating the terrain). In addition, the impassable terrain is specified by identifying the softest soil which the vehicle can traverse. A simplified representation of the success analysis is shown in Figure 4.1-23.

In the above analysis, the overall probability of success is the sum of the products of the probabilities of negotiating various combinations of soil-slope-pothole conditions of the assumed terrain model. True traction is calculated using the following formula which takes the effects of grousers into account:

$$H = (Ac (1 + 2 h/b) + WG) (1 - (1 - \exp(-12s))/12 s)$$

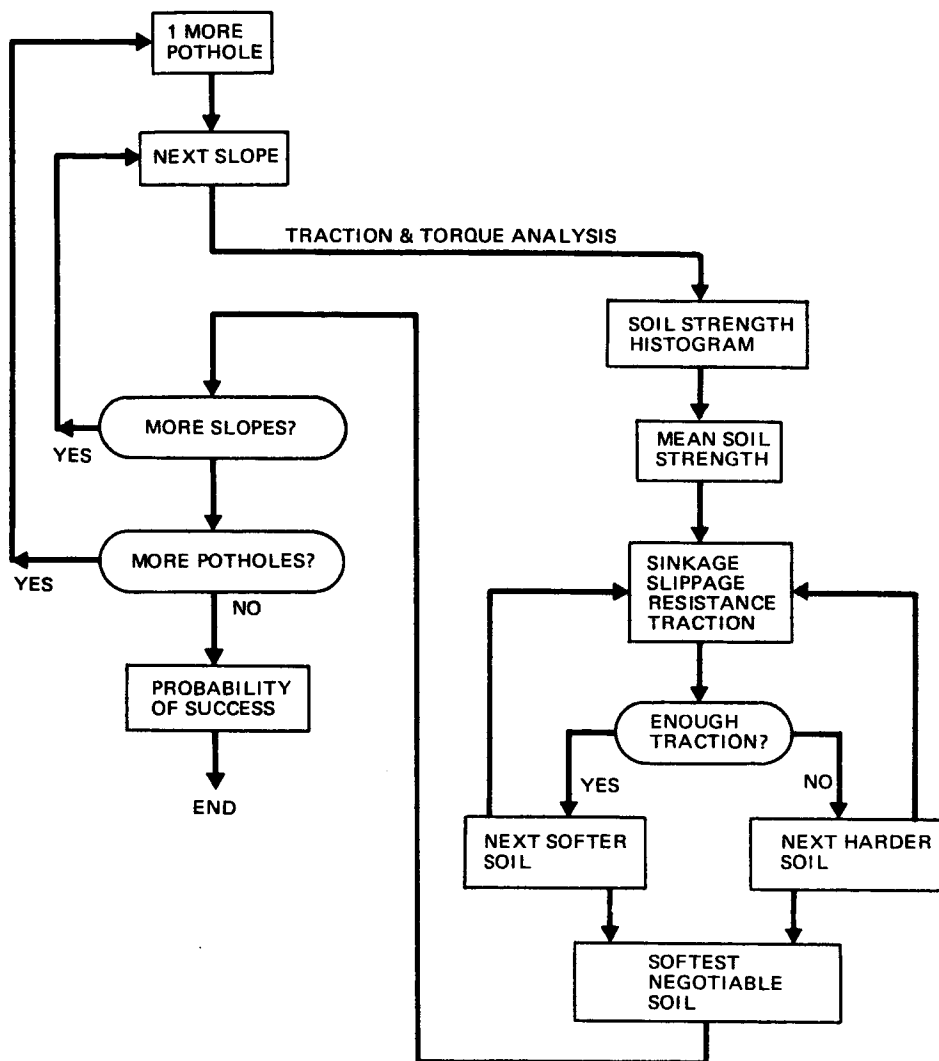


FIG. 4.1-23 MISSION SUCCESS ANALYSIS

where

H = traction, lb

A = footprint area, sq in

c = cohesion, psi

h = grouser height, in

b = wheel (grouser) width, in

W = weight on wheel, lb

s = slippage

$G = (1 + 0.64 (h/b) \arctan (h/b)) \tan \phi$

$\phi$  = angle of friction of the soil

The program accepts up to seven soil strength distributions, each with a corresponding cohesion coefficient assigned to it, and each defined over an explicit range of absolute value of slope. All slopes within this range have the same soil values. Thus, there will be seven mean soil strength values (or less, depending on the number of distributions used) each having a log-normal distribution of soil strength around it. In the soil model used for this study, all mean soil strengths have been assigned the value of 2 psi/in and the -2 sigma soil strength for each mean value was determined using the table of reduction factors found on pg. IV-26 of Annex C of the Statement of Work.

The input to the program can be divided into a number of categories, each relating to a specific type of input. These categories, or models, are:

- o Vehicle
- o Slope
- o Soil
- o Pothole

These models are not independent of each other and, in general, a change of input values for one model results in a related change for another model. Pothole model inputs depend on the vehicle model (chassis geometry) and soil model inputs depend on the slope histogram.

A change in the vehicle's wheelbase and/or width results in a change in the values of the mean diameter of potholes holding a given number of wheels in a pothole. The mathematical structure of the pothole model, however, is independent of the vehicle.

#### 4.1.3.1 Vehicle Models

Vehicle design inputs consist of axle spacing and span, number of vehicle modules, wheel loading, locomotion torque, etc. Two basic types of vehicles were considered: a four-wheeled manned version and a six-wheeled unmanned configuration. Table 4.1-7 details the inputs for the five vehicles studied. Where an input was varied, its maximum plausible range is shown.

#### 4.1.3.2 Pothole Model

Potholes, or rubble-filled craterlets, and soft spots in the lunar terrain exert a detrimental effect on the performance of a lunar roving vehicle. The pothole model is used to quantify this effect by determining the probability that the vehicle will encounter a pothole with any number of its wheels and the expected sizes of the potholes. This information is then reflected in the program's output as a degraded mission success probability and increased energy consumption.

The model is fully described in Grumman memorandum "Construction and Application of a Lunar Pothole Model", PDM-OP-199. The pothole distribution is based on the crater frequency distribution functions contained in "Lunar Terrain and Traverse Data for Lunar Roving Vehicle Design Study" by H. J. Moore, et al.

The cumulative frequency distribution function used is

$$N = \left(\frac{1}{2}\right) 10^{-1} D^{-2} \quad (D \leq 40m)$$

where

N is the cumulative number of craters per square foot

D is the diameter of the craters in feet

The factor one-half, which does not appear in Moore et al., was introduced since, by assumption, one-half of all potholes encountered are detected and avoided. Provision has been made in the program to account for the possibility of overlapping potholes. Table 4.1-8 shows the values of inputs to the pothole model.

#### 4.1.3.3 Slope Model

The slope histogram describes the inclination of the lunar surface relative to the lunar horizon. The probability that the vehicle will encounter a given slope is equal to the percentage of the total terrain having that slope.

TABLE 4.1-7

## VEHICLE MODELS STUDIED

VARIABLES AND UNITS	4 WHEELS			6 WHEELS	
	I	II	III	I	II
Maximum Permitted Velocity of Vehicle (mph)	9.94	9.94	9.94	1.8642	1.8642
Average Velocity of Lunar Vehicle (mph)	6.214	6.214	6.214	.6214	.6214
Vehicle Power Allotted for Locomotion (kw)	0.5	0.5	0.5	0.5	0.5
Nominal Range (statute miles)	18.64 (30 km)	18.64	18.64	621.4	621.4
Number of Axles	2	2	2	3	3
Total Vehicle Weight (Earth) (lbs) *	500,2000, 250	500,2000, 250	500,2000, 250	500,1750, 250	500,1750, 250
Percentage of Wt on each Axle (front to rear)	50/50	50/50	50/50	34/33/33	34/33/33
True Wheel Diameter of Wheels (inches) *	26,44,3	26,44,3	26,44,3	29,41,3	29,41,3
Width of Wheels (inches) *	4.5, 14.5, 2.5	4.5, 14.5, 2.5	4.5, 14.5, 2.5	7, 14.5, 2.5	7, 14.5, 2.5
Height of C.G. above ground over axle (inches) front to rear	39/29	39/29	39/29	49/49/49	49/49/49
Distance between Axles and tread (inches)	114	98	88	114	83

\* Where inputs are varied, they appear in the form:

(From, To, Increment)

TABLE 4.1-8

## POTHOLE MODEL INPUTS

	Chassis Geometry wheelbase (in) tread (in)	Maximum No. of wheels in pothole	Probability of k wheels in a pothole		Corresponding Pothole Diame- ter (ft)
			k	Probability	
Vehicle Type	$\frac{88}{83}$	4	0	0.001	-
			1	0.017	2.571
			2	0.032	8.127
			3	0.475	15.263
			4	0.475	15.263
		4	0	0.001	-
			1	0.022	2.625
			2	0.041	9.103
			3	0.468	16.595
			4	0.468	16.595
		4	0	0.001	-
			1	0.024	2.646
			2	0.057	9.771
			3	0.459	17.923
			4	0.459	17.923
Vehicle Type	$\frac{85}{83}$	6 Smallest accep- table vehicle	0	0.001	-
			1	0.015	2.577
			2	0.026	8.144
			3	0.053	12.163
			4	0.053	12.163
			5	0.426	21.124
			6	0.426	21.124
		6 Largest poss- ible vehicle	0	0.001	-
			1	0.021	2.644
			2	0.052	9.732
			3	0.077	14.897
			4	0.077	14.897
			5	0.386	23.532
			6	0.386	23.532

The slope histogram read into the program is taken from Table 6, pp B-19 of Moore, et al. This table is reproduced in Table 4.1-9 . The terrain profile for the rough upland distribution of one-meter slopes was selected to serve as a reference for comparing different vehicles. This histogram encompasses the widest variation of slopes and, consequently, the most severe conditions to be encountered by the vehicle from the viewpoint of compaction and gravitational resistance. Compaction resistance is a function of the cube root of the modulus of sinkage, and gravitational resistance varies with the sine of the slope angle.

In accordance with Annex C, "Engineering Lunar Model Surface ELMS", all slopes are assumed distributed 50% positive and 50% negative, indicating that there is no overall tendency to consistently move to a higher or lower elevation.

The slope histogram and the division of slopes based upon the soil model are shown in Table 4.1-10. The mean soil strength has a value of  $k_{\phi} = 2$  psi/in for all slopes. Table 4.1-10 combined with the following soil model information, and in particular, the table of reduction factors contained in Annex C, page IV-26, completely specified the relationship between soil strength and slope.

#### 4.1.3.4 Soil Model

The soil model relates the slope of the lunar terrain to such physical characteristics of the soil as mean soil strength,  $\pm 2$  sigma soil strength, cohesion, friction and exponent of sinkage.

The assumptions underlying the present soil model are:

- o Soil strengths for each division of the slope histogram are log-normally distributed; i.e.,  $\log_e (k_{\phi} / k_{\phi} \text{ mean})$  satisfies a normal probability distribution with mean zero and standard deviation  $\sigma = \log_e \sqrt{10}$ . ( $k_{\phi}$  is the modulus of soil deformation due to frictional ingredients)
- o Two-sigma soil strengths are based on the table of reduction factors (Annex C)
- o Sinkage exponent,  $n$ , is identically unity
- o The angle of internal friction,  $\phi$ , is defined in Fig. 9, page 75 of "Vehicle Mission Analysis" by Ehrlich, Markow and Dowd (SAE reprint)
- o  $G$  was initially defined for five values of  $k_{\phi}$  from which a curve was faired and the values of  $G$  taken. This curve is Figure 4.1-24.



TABLE 4.1-9  
PREDICTED DISTRIBUTION OF ONE METER SLOPE

Mean Slope Values		2.9°	5.3°	8.2°	11.0°
% N	Model % of Mean Slope	Smooth Mare	Rough Mare	Hummocky Upland	Rough Upland
100	(450)	(13°)	(24°)	(37°)	(50°)
98	346	10	18	28	38
95	273	8	14	22	30
90	216	6.2	11	18	24
80	152	4.4	8	12	17
70	116	3.4	6.1	10	13
60	96	2.8	5.1	8	10
50	76	2.2	4.0	6.2	8
40	58	1.7	3.1	4.8	6.4
30	44	1.3	2.3	3.6	4.8
20	28	0.8	1.5	2.3	3.1
10	15	0.4	0.8	1.2	1.7

TABLE 4.1-10  
SLOPE HISTOGRAM

Terrain Slope ( $\pm$ degrees)	Probability of Slope	Coefficient of Cohesion
0	.02	.05
1.7	.04	.05
3.1	.05	.05
4.8	.05	.05
6.4	.05	.05
8	.05	.05
10	.05	.05
13	.05	.05
17	.05	.05
24	.05	.10
30	.025	.15
38	.015	.20
50	.01	.20

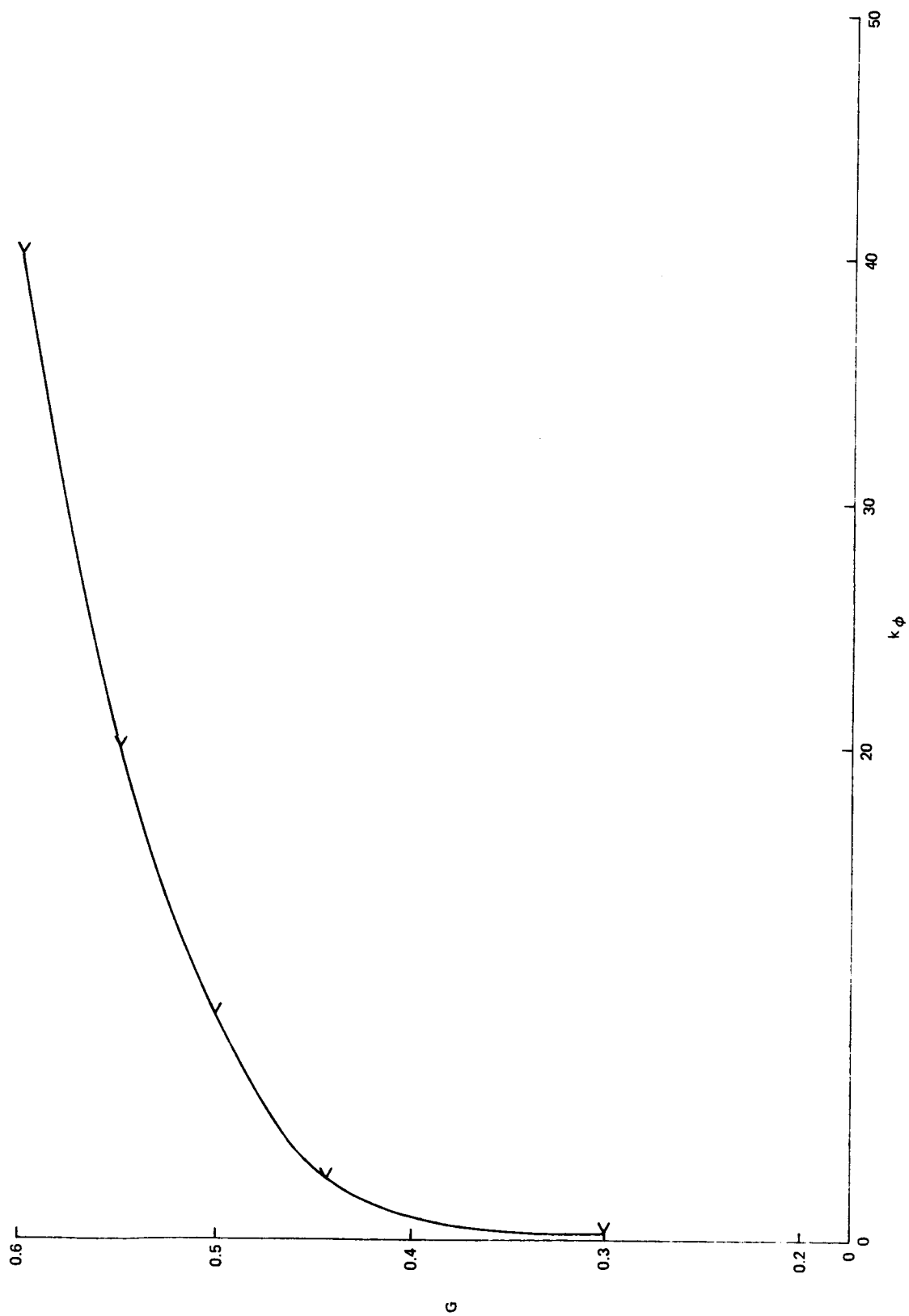


FIG. 4.1-24 RELATIONSHIP OF  $G$  TO  $k\phi$

#### 4.1.3.5 Results and Conclusions

Figures 4.1- 25 through 4.1- 27 show the variation of success probability for variations in wheel size and vehicle weight. It must be understood that the significant measure, success probability, is determined on the basis of the most severe conditions negotiable by the vehicle rather than by assuming that the vehicle travels on level ground and encounters a constant and unchanging  $k_f$ . The program identifies all non-negotiable soil conditions, and probability of success is measured by the portion of the total soil spectrum negotiable by the vehicle.

During the study, it was determined that obstacle distribution would not prove a serious problem from a mobility viewpoint. This conclusion is based upon the distribution data contained in Moore, et al. Generally, 3% of the total area is covered by boulders and this is not sufficient to entrap a vehicle or to cause an inordinate fuel expenditure unless the vehicle lands in a boulder field or encounters a long boulder chain. These conditions are unlikely.

It will be noted that for both four- and six-wheeled vehicles, clearly discernable trends are evident for probability of success versus vehicle characteristics. In all cases, the probability of success varies:

- o Inversely with changes in vehicle weight. An increase in weight implies greater sinkage, greater resistance and more torque necessary for successful negotiation
- o Directly with changes in both true wheel diameter and wheel (grouser) width. Greater footprint area implies smaller sinkage, less resistance and less traction required to negotiate successfully

The program is most useful in defining trends rather than establishing "the best" point design. Changes in the vehicle's weight and wheel geometry exert a major influence on the vehicle's soft soil performance when considered over a relatively large range of variation.

The inclusion of the pothole model did not exert a major influence on the relative performance of vehicle having different chassis dimensions. The probabilities of success are very nearly equal for both small and large vehicles. The probability was very slightly less for the smaller vehicle, indicating at best a marginal difference in performance. This is true because both vehicles develop the same traction regardless of chassis dimensions and, therefore, both can negotiate the same soil strengths in the assumed distributions. The smaller vehicle, however, will expend more energy in negotiating potholes since it will be in potholes

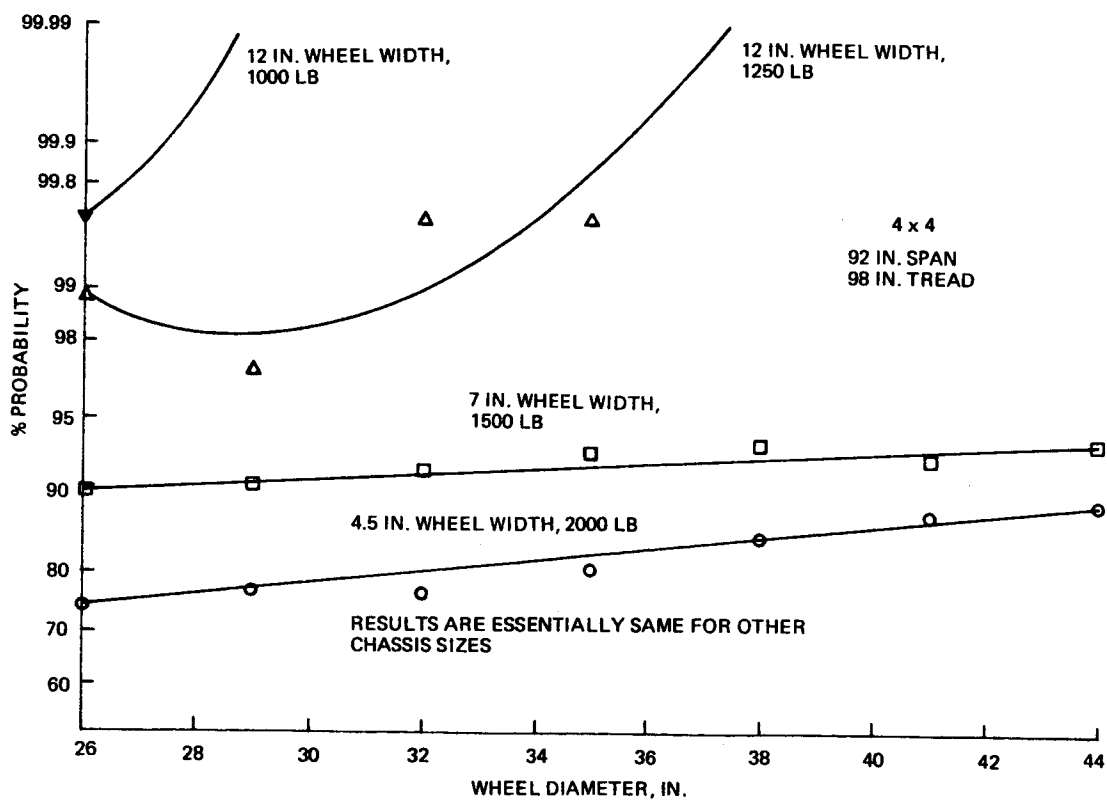
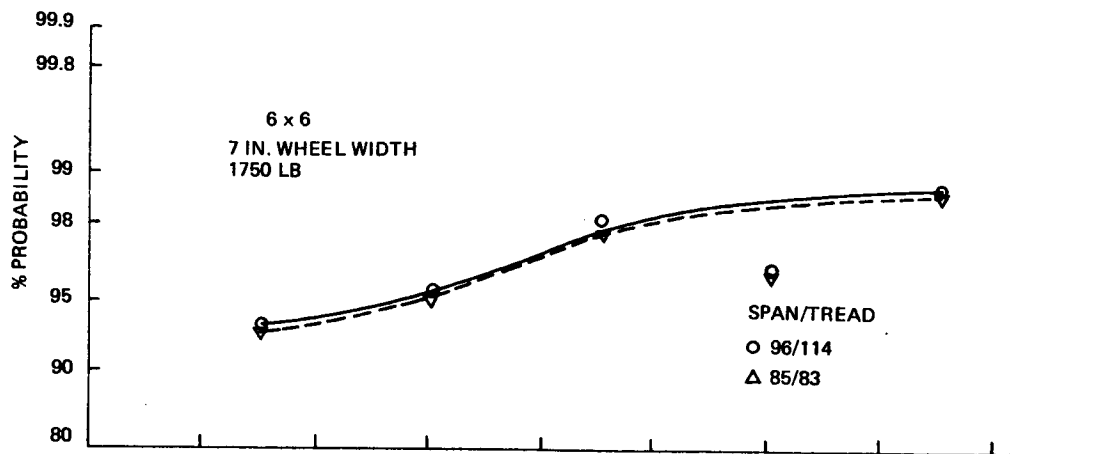


FIG. 4.1-25 EFFECT OF WHEEL DIAMETER ON PROBABILITY

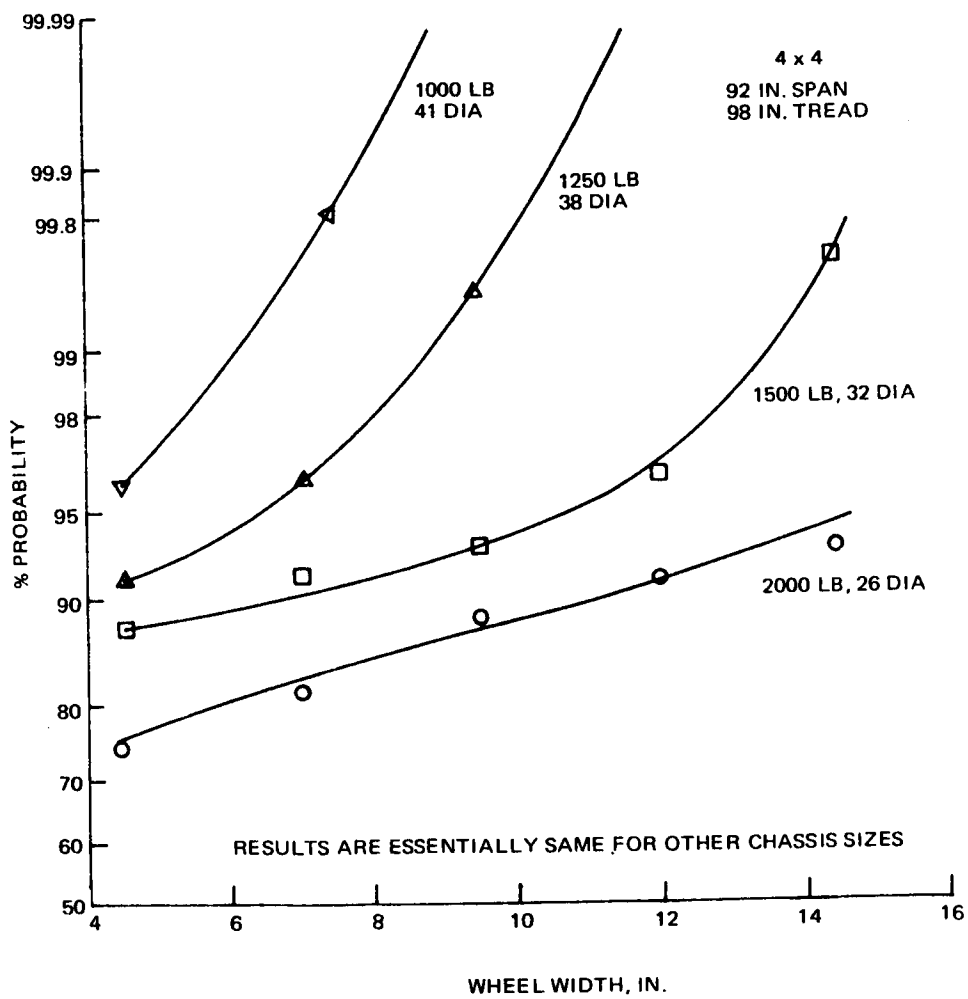
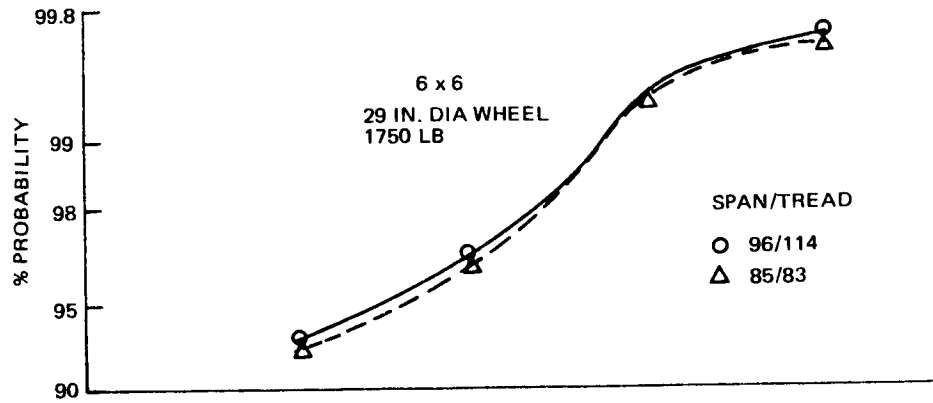


FIG. 4.1-26 EFFECT OF WHEEL WIDTH ON PROBABILITY

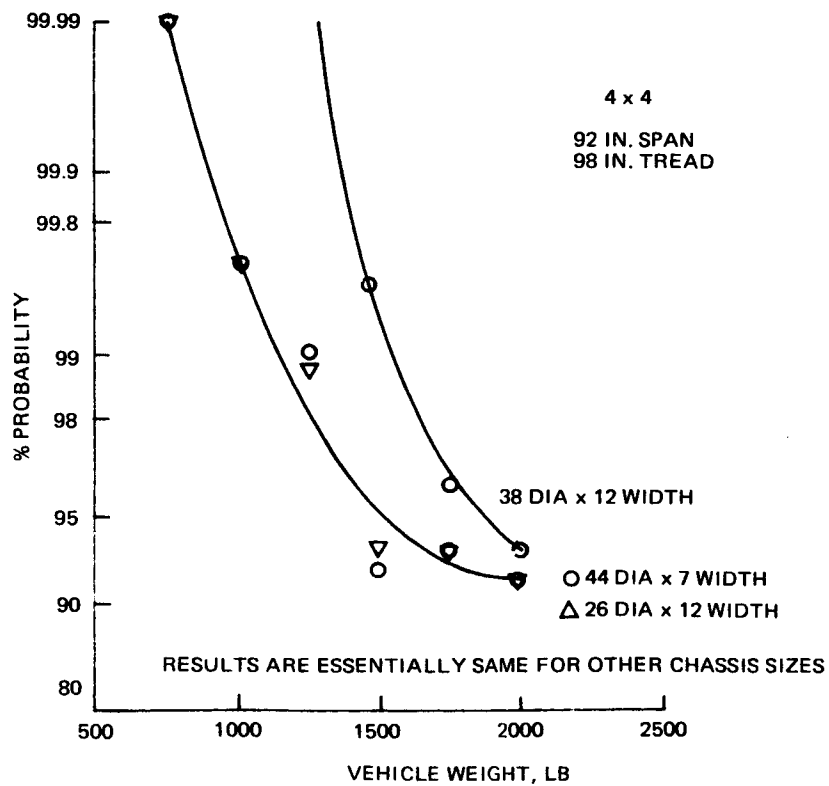
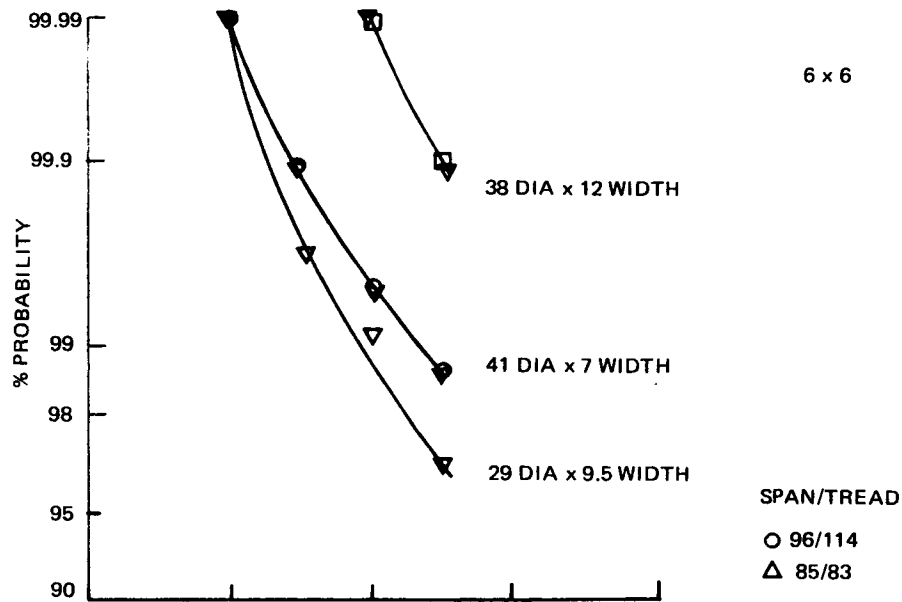


FIG. 4.1-27 EFFECT OF VEHICLE WEIGHT ON PROBABILITY

with all wheels more often than the larger vehicle.

The results support the conclusion that wheel size (width and diameter) is an extremely important parameter to be considered in the improvement of cross-country mobility. Larger wheels imply an improvement in probability of success since a greater portion of the soil spectrum is negotiable. The program described in this section will be particularly useful in route selection during the phases of mission planning when lunar soil-slope-pothole data on alternate routes are available.

#### 4.1.4 References for Section 4.1

1. Stevens Institute of Technology, Davidson Laboratory, "Tests of Lunar Rover Wheel", by L. I. Leviticus and I. R. Ehrlich, Report 1429, November 1969.
2. U. S. Waterways Experiment Station, "Study of Mobility Performance and Slope-Climbing/Traversing Ability of Lightly Loaded Wheeled Vehicle on Soft Soil", Fourth Monthly Progress Report, 1-30 Sept. 1969, Contract DPR H-58504A.



## 4.2 DYNAMICS

The objective of the vehicle dynamics studies was to optimize ride qualities, maximize vehicle controllability (related to the amount of time the wheels are off the ground), and determine damping power dissipation, turning stability boundaries, and dynamic loads during lunar operation. (Dynamic loads in the stowed condition are discussed in subsection 4.3.1.)

The dynamics effort consisted of three main areas: analog computer studies of the response to random terrain (which also made use of a fixed-base simulator), and digital studies of turning stability and the response to obstacle encounters.

### 4.2.1 Response to Random Terrain

The design of the vehicle suspension is determined largely by ride quality and vehicle controllability objectives for constant-speed traverse of random terrain. An analog computer is ideal for studying these characteristics, since it can readily accommodate random excitation, and the outputs of the computer can be connected to a mechanical simulator.

The initial analog modeling consisted of a four-degree-of-freedom roll-plane module with a trilinear suspension and non-linear point-follower wheels with "scuff" damping. Subsequent analog models consisted of two coupled roll-plane modules capable of pitch motion also as shown in Fig. 4.2-1. A modular approach to math modelling was selected for the ease with which it allowed coupling of two or more roll-plane modules for complete vehicle analysis. The major parameters recorded were chassis accelerations, suspension deflection, wheel load, power dissipated, and wheel lift-offs. Wheel and suspension characteristics and intermodular torsional flexibility were varied.

Analog equations which provided inputs for roll and heave motions of a mechanical simulator seat were developed for both the single two-wheel-module and the coupled-modules configurations. The computer was then linked to the Grumman fixed base simulator to check human reaction to vehicle ride characteristics.

The trilinear suspension spring used in the analysis combined a linear spring with a motion-limiting snubber at each end. The three suspensions shown in Fig. 4.2-2 were investigated; these were designated as the 5, 10 and 20 lb/in suspensions after their linear normal-operating-range spring rates. Static deflection positions and deflection before snubber contact are also shown.

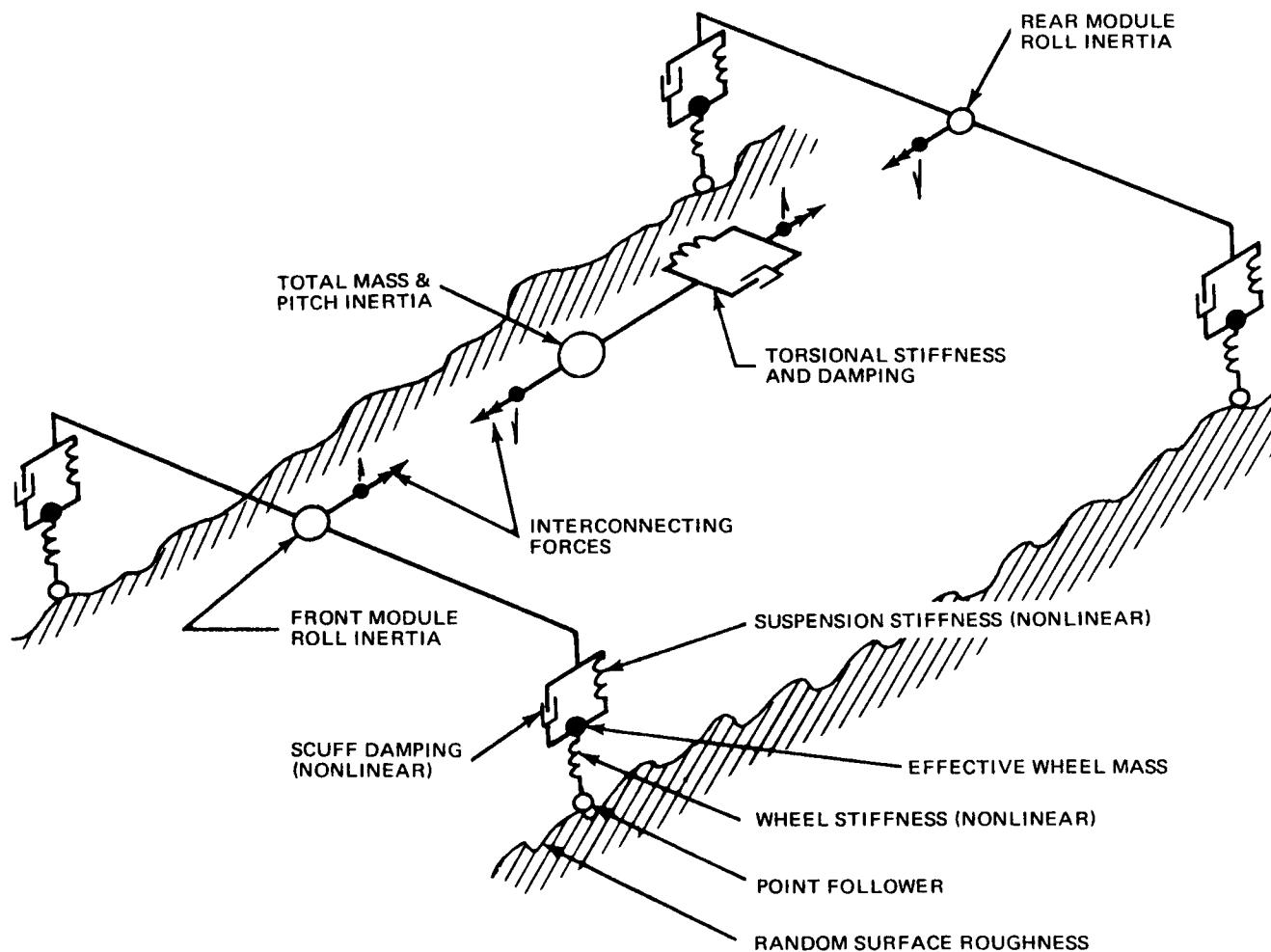


FIG. 4.2-1 MATH MODEL FOR ANALOG STUDY

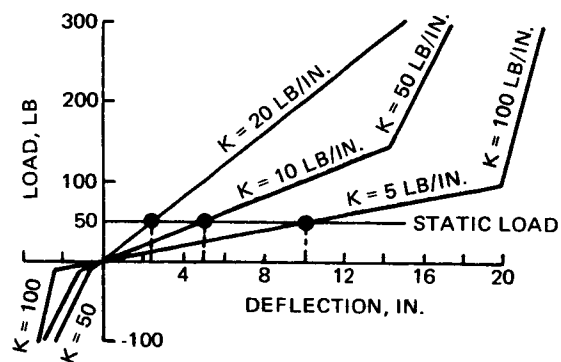


FIG. 4.2-2 IDEALIZED SUSPENSION STIFFNESSES

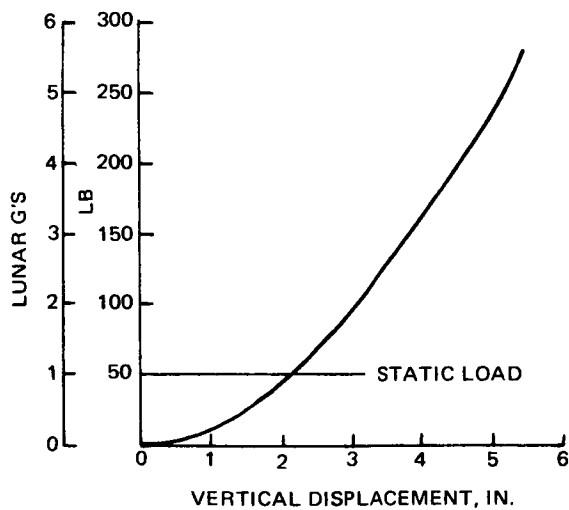


FIG. 4.2-3 IDEALIZED WHEEL STIFFNESS

The nominal stiffness characteristic used for the wheel is shown in Fig. 4.2-3. Wheel stiffness ranging from half to twice that shown were considered. The point follower assumption which was used was reasonable for the analog studies because the detailed wheel/terrain geometry characteristics have small effect on ride qualities. The modelling allowed the wheels to leave the ground when they were unloaded. The "scuff" damping mechanism dissipates energy by means of a lateral scuffing action between the wheel and the lunar surface. This action was modelled as non-linear viscous damping, whose coefficient varied with wheel normal force and vehicle forward velocity. Auxiliary mechanical damping across the suspension was also considered.

Four random terrain roughnesses have been defined for the lunar surface in terms of power spectral densities: smooth mare, rough mare, hummocky upland and rough upland. Upper and lower bounds for these surfaces are given in Ref. 1.

Comparison of the spectra showed that using rough and smooth mare covered the range, and these were actually quite close to the remaining two. Therefore, only these two spectra were used. For each spectrum a straight-line approximation of the average of the upper and lower bounds in the frequency range of interest was used. The analytical spectra increased at 6 db/oct with decreasing frequency down to 0.1 Hz, below which they were made flat to prevent displacement overload of the analog computer, which was scaled for smaller amplitudes on the order of wheel and suspension deflections. This low-frequency deviation would have no significant effect on the dynamic responses since it was well below vehicle resonances. Uncorrelated random excitations were used for the left and right sides; left and right rear wheel excitations were the same as those of the respective front wheels except that a time delay dependent on vehicle velocity was used.

The initial analog computer work was done using a 2 x 2 roll-plane model. Results of the suspension variation study using this model are shown in Fig. 4.2-4. Astronaut roll and heave acceleration responses are lowest for the softest suspension, as would be expected. Both the 5- and 10-lb/in. suspensions provide ride qualities within the human tolerance range for both smooth and rough mare surfaces (Reference 2). RMS suspension deflections increased with speed. The time histories of the runs revealed that snubber contact occurred infrequently; on a rough mare at 12 km/hr, only one contact in a two-minute run occurred with the 5-lb/in. suspension, and no contacts were observed with the 10-lb/in. suspension. (The

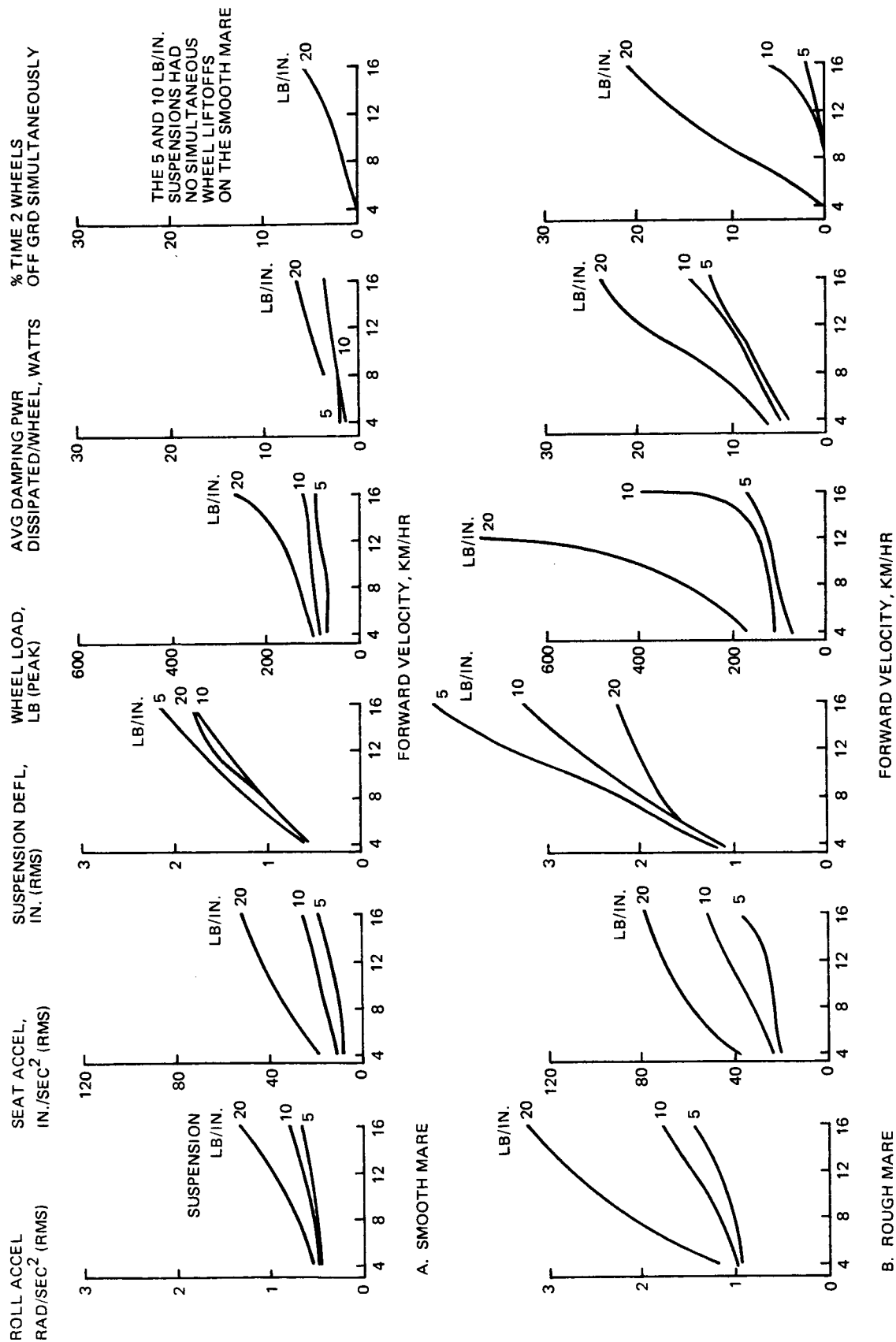
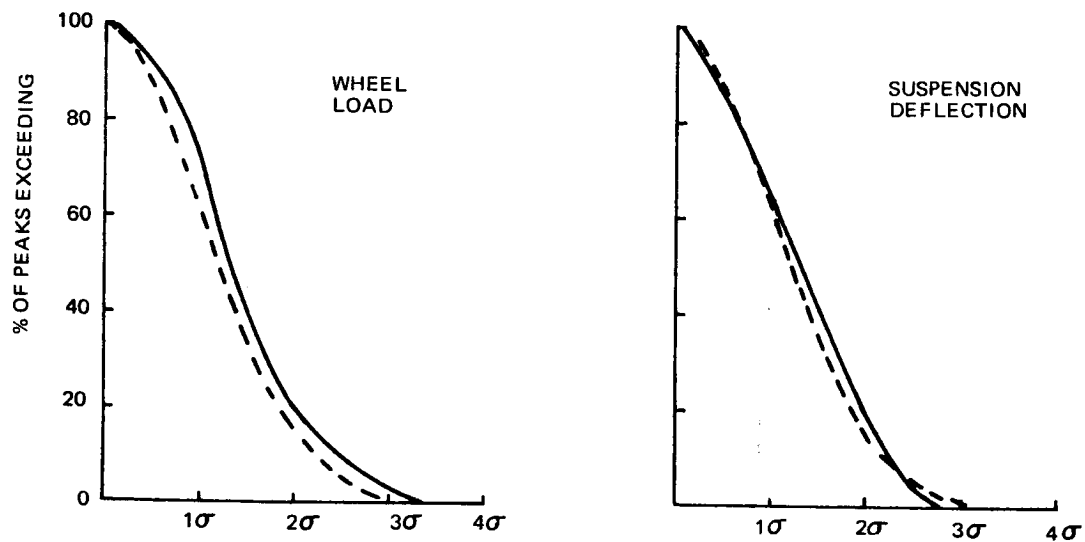


FIG. 4.2.4 RESPONSE TO RANDOM TERRAIN, 2 WHEEL MODEL

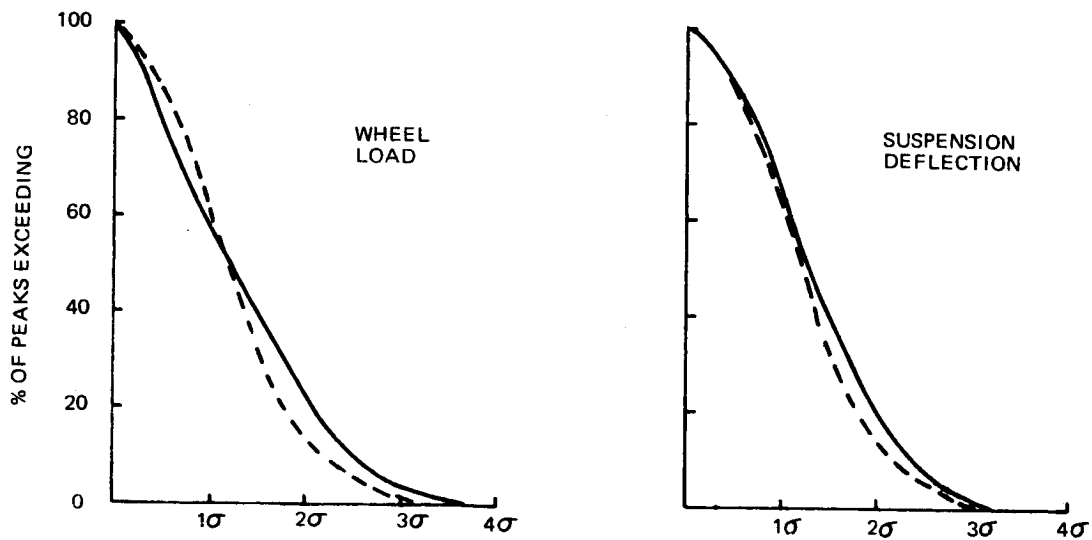
unexpected order of the deflection curves for smooth mare operation is attributable to the abrupt non-linearities of snubber contact.) Also shown are the peak wheel loads that occurred in a two-minute run. Damping power dissipation increased with speed and suspension stiffness; however, a more marked increase occurred for travel on rough surfaces. Thus, the penalty for rough mare operation is a bigger drain on the batteries. It can also be seen that no simultaneous two-wheel lift-offs occurred on smooth mare for the 5-and 10-lb/in. suspension systems. This implies good steering control at all speeds. Analysis was also made of the peak probability distributions associated with the suspension deflections and wheel loads for both rough and smooth mare. The distributions for both parameters were found to be approximately Rayleigh, as shown in Fig. 4.2-5, a result which greatly facilitates determination of fatigue damage due to vehicle traverse on random terrain. (Determination of fatigue damage for the wheel is complicated by the fact that the loading cycles are distributed around the rim rather than applied at a fixed location. This difficulty can be surmounted if damage to the wheel for each complete revolution at a particular load level is estimated and summed for the total number of wheel revolutions at that particular load level.) The rougher the terrain or the greater the vehicle velocity, the more the wheel and suspension peak distributions deviate from a Rayleigh distribution because of the non-linearity of wheel and suspension stiffnesses and wheel lift-off from the ground. The distributions shown in Fig. 4.2-5 represent relatively severe operating conditions; thus, deviations from the Rayleigh distribution significantly larger than those shown would not be expected during normal operation of the DLRV.

Another study was made of the effect of adding an auxiliary damper across the suspension system to supplement the scuff damping which provides the primary dissipation mechanism. The results are shown in Fig. 4.2-6. For the severe condition of 12 km/hr on a rough mare, increasing damping provided substantial reduction in wheel lift-offs; however, this reduction was from an already low value. Wheel loads were reduced, but in either case were well below design values. There was relatively little effect on seat acceleration or suspension deflection, but dissipated power increased significantly. From the overall viewpoint, it appeared that the additional damping provided little benefit to compensate for its adverse effect on weight, power dissipation, and deployment complexity.

— ANALOG RESULT  
 - - - RAYLEIGH DISTRIBUTION



A. SMOOTH MARE, VEL = 18 KM/HR



B. ROUGH MARE, VEL = 9.3 KM/HR

FIG. 4.2.5 PEAK PROBABILITY DISTRIBUTIONS

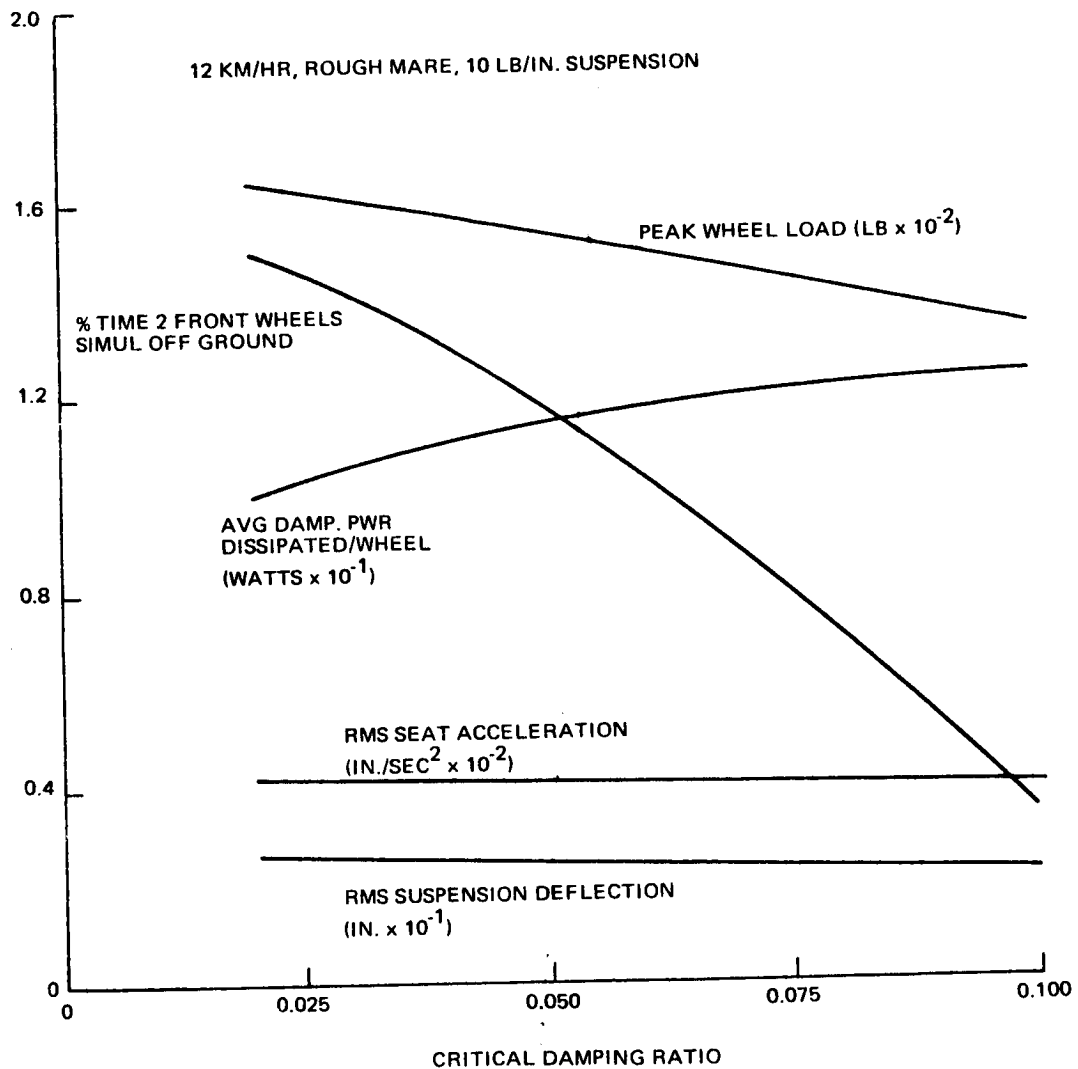


FIG. 4.2-6 EFFECT OF AUXILIARY SUSPENSION DAMPING



Following the initial 2 x 2 work, the program was expanded to accommodate the 4 x 4 vehicle. Results for the 4 x 4 analysis are shown along with comparable 2 x 2 results in Figure 4.2-7. The intermodular torsional stiffness for these runs was 200 in-lb/rad, a value approximating that of the actual structure. A practical range of torsional stiffness was run, but no significant difference in the results was observed.

The responses obtained with the 4 x 4 analysis are seen to be similar to, but generally less than, those of the 2 x 2. The slight conservatism of the simpler analysis is in the right direction. Agreement between the results is close enough to validate the conclusions drawn from the simpler analysis.

#### 4.2.2 Loads Due to Obstacle Encounter

It is evident that loads due to encounter of large-size obstacles would be greater than loads produced by response to rough mare traverse. To accurately evaluate obstacle encounter loads, a more detailed representation of bump/wheel geometry than that provided by the point-follower assumption was required. Because such a representation could not be incorporated into the analog analysis without undue complication, a digital computer analysis was performed. The digital modelling, which is shown in Fig. 4.2-8, consisted of a two-mass, two-degree-of-freedom heave module, with a nonlinear bump-contouring wheel and a trilinear suspension with viscous damping. Wheel radial loads and suspension vertical and drag loads were determined for spike bumps of 4, 8, and 12 inches at velocities ranging from 4 km/hr to 16 km/hr. Results are shown in Figs. 4.2-9 and -10 for the 10 lb/in suspension and the nominal stiffness wheel. The effects of other suspension stiffnesses on the loads were small. The limit load of the nominal stiffness wheel is 300 lbs which corresponds to a 5.5 lunar g loading. It is seen in Fig. 4.2-10 that 4-inch bumps, which probably are so numerous as to be unavoidable, can be negotiated at all speeds. Eight-inch bumps, which would be less numerous and much more visible can be taken at speeds up to 9 km/hr.

The effects of varying wheel stiffness on wheel radial and suspension drag loads are shown in Fig. 4.2-11 for a 10 lb/in. suspension and an 8-in. spike bump. Three wheel stiffnesses were considered. As expected, the loads decreased with decreasing wheel stiffness, but decreasing wheel stiffness implies decreasing load capability.

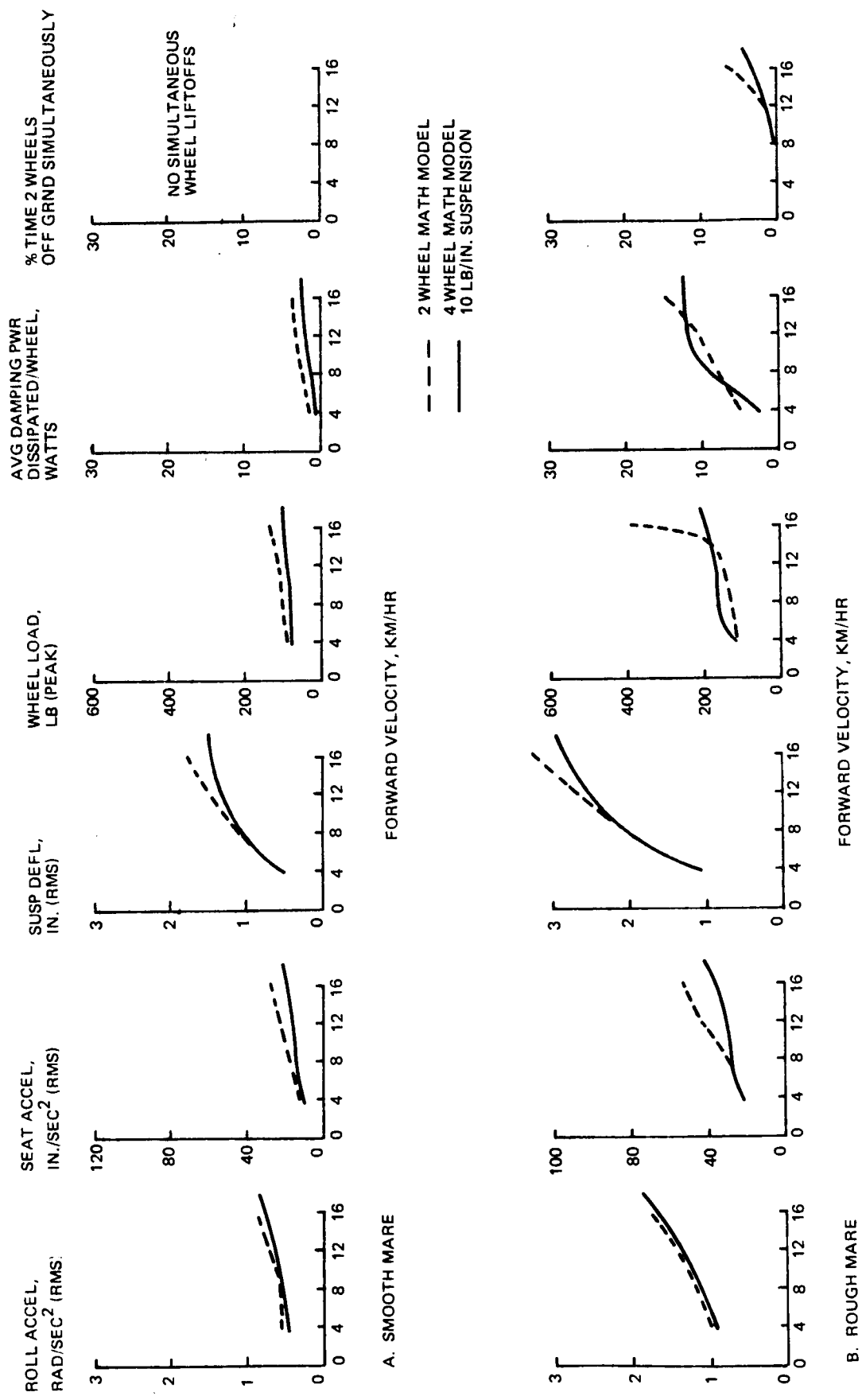


FIG. 4.2.7 COMPARISON OF RANDOM TERRAIN RESPONSE FOR 2 AND 4 WHEEL MATH MODELS

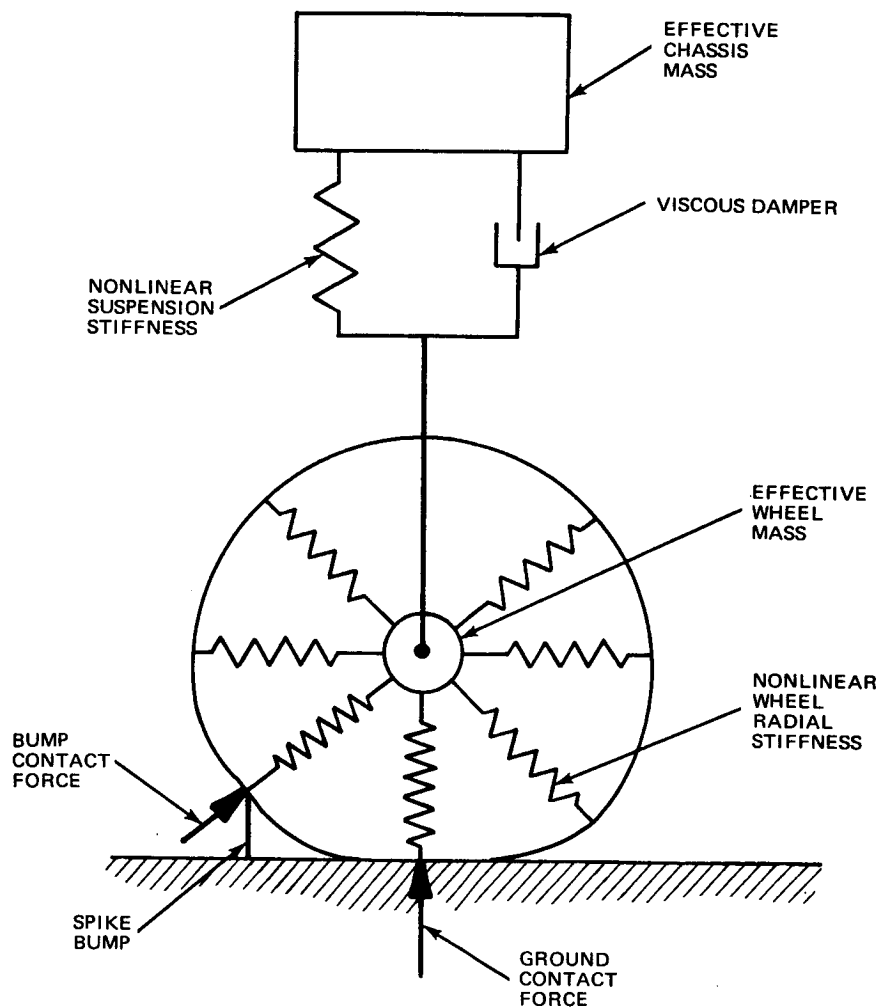


FIG. 4.2-8 MATH MODEL FOR BUMP ENCOUNTER ANALYSIS

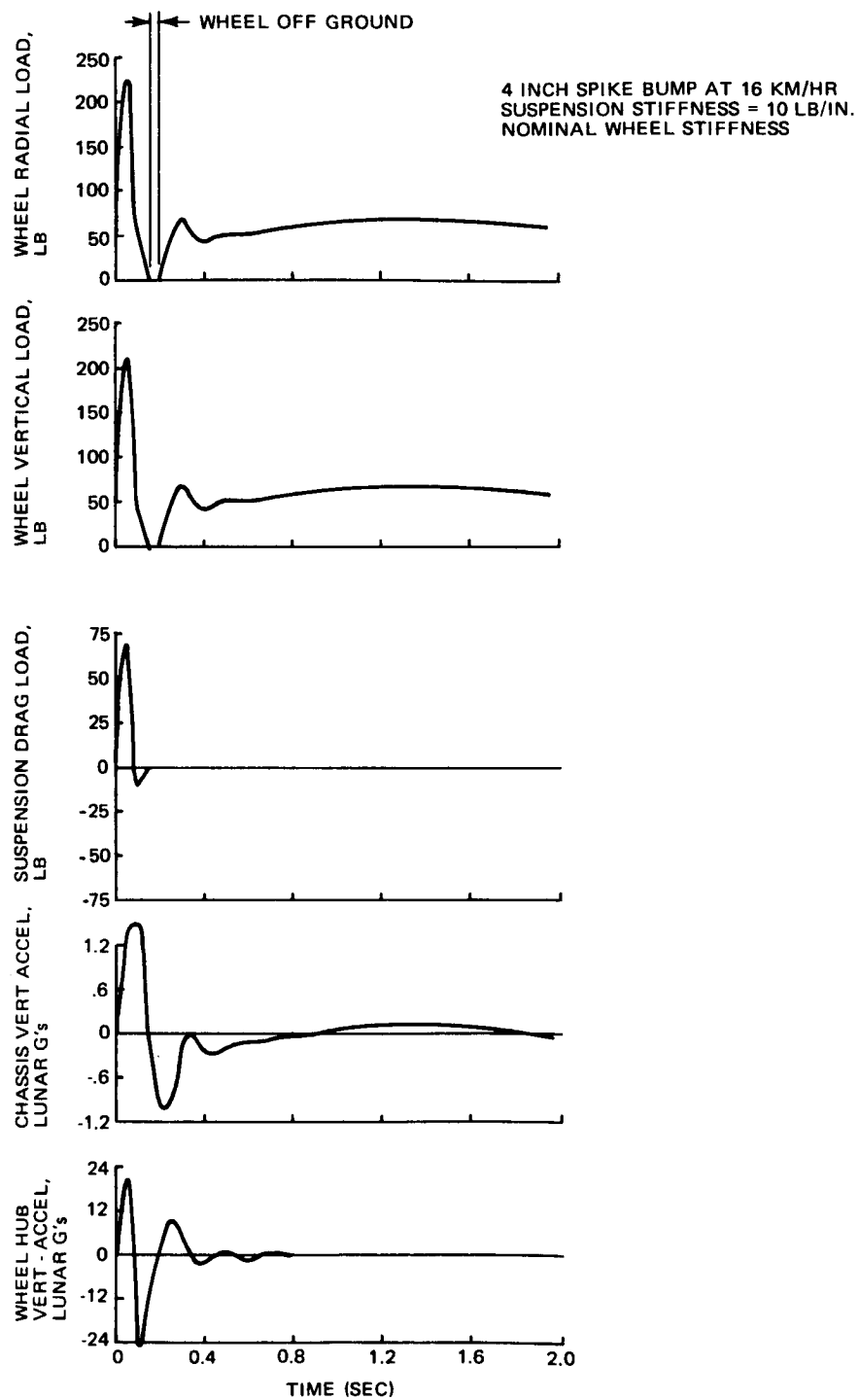


FIG. 4.2-9 TIME HISTORIES OF BUMP RESPONSE

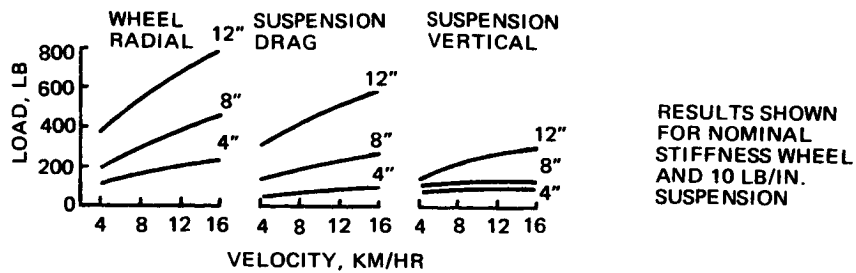


FIG. 4.2-10 LOADS DUE TO 4, 8, AND 12 IN. SPIKE BUMP ENCOUNTERS

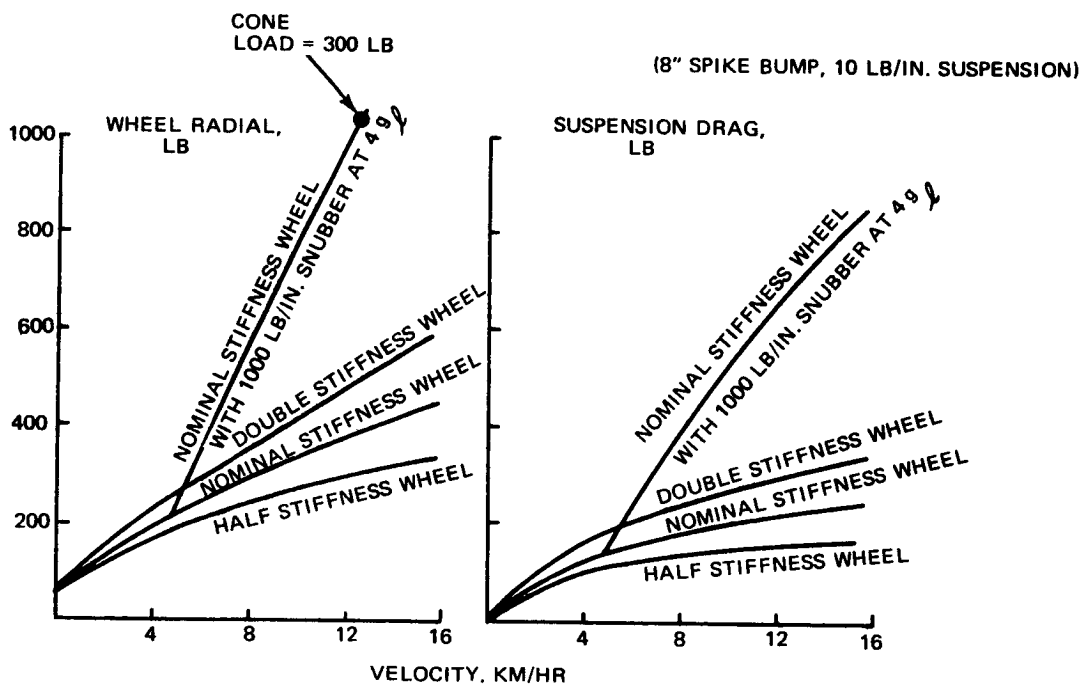


FIG. 4.2-11. EFFECT OF WHEEL STIFFNESS ON BUMP ENCOUNTER LOADS

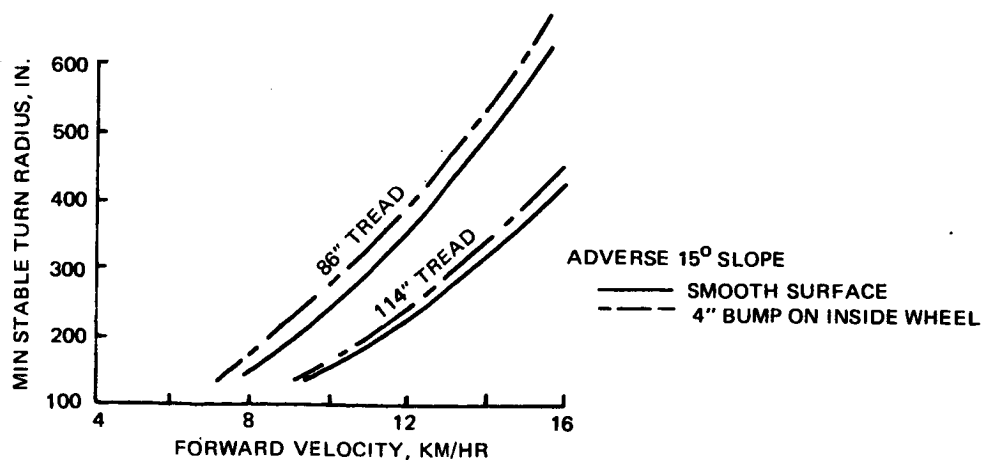


FIG. 4.2-12. TURNING STABILITY

It might appear, intuitively, that bump-encounter capability could be materially increased by the addition of a deflection-limiting snubber to the wheel. To investigate this possibility, a snubber with a spring rate of approximately 1000 lb/in in parallel with the cone wheel was considered. The fourth curve in Fig. 4.2-11 shows the result. Although this snubber increased the wheel load capability from 5.5 to 19 g's, it only increased the allowable velocity over an 8-in. bump from 9 to 12.4 km/hr. Suspension drag loads increased correspondingly from 140 to 690 lb., which would necessitate redesign of the suspension arms and chassis support area. It was concluded that the addition of a wheel snubber could not substantially increase bump encounter velocities without prohibitive weight penalties. It should be noted that there are no specific obstacle encounter requirements for DLRV; however, it is believed that the vehicle should at least be capable of withstanding bumps on the order of 4 in. at maximum speed.

#### 4.2.3 Selection of Wheel and Suspension Characteristics

The information derived from the analog and digital studies was analyzed to determine the "optimum" wheel and suspension system combination. The analog and digital computer results made readily apparent the effect of varying the wheel and suspension system stiffness parameters. The stiffest wheels and suspension springs produced the smallest deflections, but contributed the largest wheel loads and vehicle roll and heave accelerations; the softest wheels and springs produced the smallest loads and accelerations, but the largest static and dynamic deflections.

Allowable deflections are limited by vehicle size and obstacle-clearance considerations. On the basis of dynamic response considerations, optimum suspension system deflection would be the maximum deflection possible without snubber contact. It should, however, be noted that occasional contact, which could be expected with a soft spring, would not have a large effect on rms acceleration levels and, presumably, on crew comfort.

After examination of the computer data, and evaluation of the tradeoffs, the combination considered best for both ride qualities on rough terrain and wheel loads due to bump encounter was the nominal stiffness wheel in combination with a suspension stiffness of between 7.5 and 10 lb/in.

#### 4.2.4 Turning Stability

Stable operation while turning in the low lunar gravitational environment requires vehicle treads that are significantly larger than those on an earth vehicle. This is due to the fact that centrifugal forces tending to overturn the vehicle are the same on the earth and moon; but, the stabilizing gravity force on the moon is only one sixth that on earth.

A complete analysis of the overturning problem would be extremely complex, involving multiple nonlinearities such as those caused by steering and suspension geometry changes, ground friction effects (allowing for side skidding), and large angular motions as the inside wheels lift off the ground or a skidding condition develops. The preliminary studies conducted thus far have used only simple mathematical models to estimate stability boundaries and gain insight. The problem was divided into two parts for initial study: turns with no skidding, as in a rutting soil, and turns which result in a skid.

For the non-skidding case, a two-wheeled roll plane model was used, in which unsprung mass was neglected, but suspension and wheel nonlinearities, and large angle rotations were included. The model was analyzed using numerical integration on a digital computer. Results are shown in Fig. 4.2-12 for turns on an adverse 15-degree slope for the selected 114-in.-tread vehicle and a smaller 86-in. tread vehicle. The solid curves represent smooth surface conditions. At a nominal operating velocity of 10 km/hr., the small tread vehicle requires approximately 50% greater turn radius for stability than the large vehicle. Both vehicles would be capable of turning sharply enough to be in the unstable region.

The dashed set of curves shows the effects of encountering a 4-in. bump on the inside wheel while in the turn. The influence of the bump is, of course, adverse; however, the magnitude of the effect is relatively small. (Improving the math model by including the unsprung mass might increase the effect.)

It is worth noting that crossing the stability boundary does not mean that overturning occurs; only that it initiates. Considerable time passes before overturn is complete. During this period astronaut correction could set the vehicle stable again. The wide-tread vehicle, with its higher moment of inertia about the outside wheel, provides the greatest time to react to an imminent overturning condition. The second overturning condition that was considered is one that is initiated by skidding in a turn. If the front wheels slide first, the rear wheels tend to follow the front and the skid is relatively stable, with small likelihood of

overturn. However, if the rear wheels slide first, the resulting skid is unstable and the vehicle may quickly yaw into an attitude which produces a large lateral velocity component. An obstacle encountered in this uncontrolled side-skidding condition could cause overturning.

To investigate this possibility, a simplified rigid-body analysis which considered minimum frictional losses in the skid and conservation of momentum at impact was conducted. The results showed that the skidding condition could be more critical than the non-skidding condition at speeds above approximately 7 km/hr for the large-tread vehicle and 5.5 km/hr for the small-tread vehicle.

#### 4.2.5 References for Section 4.2

1. "Lunar Terrain and Traverse Data for Lunar Roving Vehicle Design Study", H. Moore, R. Pike, G. Ulrich. NASA Report to be published.
2. "Preliminary Design Study of a Lunar Local Scientific Survey Module (LSSM), Final Technical Report: LSSM Mobility Systems", GM Report D2-83012-1, July 1966, p 5-82.

#### 4.3 LOADS AND STRUCTURAL DESIGN CRITERIA

The DLRV system and subsystem components should be designed to the loads and structural design criteria specified herein. These are based on study and analysis of the mission objectives and requirements, and previous aerospace and lunar roving vehicle engineering and development background. Two primary load environments can be identified:

- o Stowed lunar transport environment including launch and boost through landing and deployment
- o Lunar operation, manned and unmanned

##### 4.3.1 Stowed Condition Loads

The DLRV will be exposed to a variety of static and dynamic loads during its delivery from earth to the lunar surface. The dynamic environment for Quad I payload has been specified in a LM interface document. The Quad IV environment will be similar. LM/Apollo experience has shown that overall design loads for units the size of DLRV are determined more by dynamic considerations than static accelerations.



#### 4.3.1.1 Overall Vehicle Vibration Loads

Random and sinusoidal inputs at the DLRV/IM attachment points are specified in the interface document for launch and boost and lunar descent. The most conservative approach for determining DLRV design loads would be to calculate them using the specified environments as inputs, along with an estimated value of damping. However, for a unit the size of DLRV, loads calculated in this manner would be overly conservative.

An approach used by Grumman to obtain more realistic design loads involved coupling the vibration response of the unit with that of the basic IM structure through the use of impedance methods. This approach has been used to determine preliminary mission vibration design loads for the DLRV. The results are shown in Table 4.3-1.

TABLE 4.3-1		
Mission Vibration Loads, g's		
<u>DLRV Axis</u>	<u>Control/Power Modules</u>	<u>Science Module</u>
x (longitudinal)	9.5	10
y (lateral)	9	10.5
z (normal)	13.5	14.5

Since the above loads are cyclical, account must be taken of low-cycle, high-stress fatigue. In addition, static acceleration loads for the max-q condition must be combined with the vibration loads. These mission static loads are +2.3 g vertically and  $\pm .65$  g laterally, with respect to the launch vehicle axes.

#### 4.3.1.2 Equipment Vibration Loads

The local vibratory input to an item of equipment on DLRV is determined by the transmissibility of the DLRV structure. For large items with low frequency resonances, a vibration analysis must be performed, using a mathematical model of a stowed vehicle to determine loads. For small items, a conservative environment which can be used for preliminary design is an envelope of the secondary structure response measured on IM. Sine and random levels based on this approach are shown in Table 4.3-2.

TABLE 4.3-2  
Equipment Vibration Levels

<u>Random</u>			<u>Sine</u>		
20 to 200 Hz	-	+3db/oct	5 to 25 Hz	-	.2" d.a.
200 to 250 Hz	-	.6g <sup>2</sup> /cps	25 to 100 Hz	-	6.5 g
250 to 2000 Hz	-	3db/oct			

#### 4.3.1.3 Lunar Landing Shock Loads

The most significant information for use in establishing DLRV landing loads is the results of the LM-2 drop tests. Envelopes over the measured data at equipment locations shows mission levels of 10 g for equipment resonant below 91 Hz, 23 g between 91 and 910 Hz, and 38 g between 910 and 2000 Hz. These levels are relatively conservative for large, low-frequency equipment like DLRV; however, there is little penalty in designing to them since the vibration loads are nearly as high. A LM drop test with a roving vehicle in Quad I, which is planned for mid 1970, should provide a better definition of landing loads.

#### 4.3.1.4 Deployment Loads

The static loads due to deployment will not be significant for the basic structure of the DLRV, since the small lunar gravity force will be much less severe than the forces experienced during delivery to the lunar surface. Dynamic deployment loads depend primarily on DLRV translational and rotational velocities at wheel touchdown, and these loads are applied to wheel and suspension structure which is lightly loaded enroute. The deployment rate should, therefore, be limited so that critical design loads do not occur in any basic structural members.

#### 4.3.2 Lunar Operation Loads

During operation on the lunar surface the DLRV will experience a variety of ground loads deriving from many sources, such as random surface roughness, impact with discrete obstacles and braking accelerating, turning, and obstacle negotiating maneuvers. Loads due to the first two of these conditions came out of the dynamics studies reported in Sect. 4.2. Mission design loads for the DLRV mobility system were established based on rational consideration of likely loading conditions, in conjunction with the results of the dynamic analysis. A summary of the principal wheel loading conditions, in terms of lunar g units, is given in Table 4.3-3, while the conditions are discussed in more detail in the following

TABLE 4.3-3  
WHEEL GROUND LOADS CRITERIA

LOAD CONDITIONS	WHEEL DEFLECTION (IN.)	MISSION DESIGN WHEEL LOADS			
		RADIAL FORCE ( $G_L$ ) *	SIDE FORCE ( $G_L$ ) *	TRACTIVE TORQUE (FT-LB)	RADIAL TORQUE (FT-LB)
NOMINAL STATIC	1.8	1.0			
DYNAMIC OPERATING	3.1	3.0	0 TO 2.4		
MAX. BRAKING TORQUE	3.1	3.0	0 TO 2.4	+ 100	
UNSYMMETRIC BRAKING	3.1	3.0	+ 1.44	+ 100	
PIVOTING	3.1	3.0		+ 100	
TURNING	2.5	2.0	3.17		+50
MAXIMUM RADIAL	4.3	5.5	0 TO 2.2		

\* EXPRESSED AS LUNAR GRAVITY UNITS (5.4 FT/SEC/SEC). THE NOMINAL STATIC  $1-G_L$  DESIGN LOAD FOR THE CONTROL MODULE IS 55 LB. FOR THE POWER AND SCIENCE MODULES THE LOAD IS 40 LB.

paragraphs:

- o Nominal static load: This load, which is due to the lunar weight ( $1g_1$ ), is used as the basis or reference for all the ground load conditions. The static load on the wheels varies with the mission (e.g., manned or unmanned, with or without samples) and with the module (power, control, or science), but for practical considerations only two nominal loadings were defined: 55 lb. for the control module and 40 lb. for the power and science modules. These values cover all normal conditions on level ground; however, they are less than the manned rescue mode, where degraded operation is assumed.
- o Dynamic operating load: The dynamic studies on the analog computer utilizing the specified lunar terrain models showed peak loads of approximately 2 and 4  $g_1$  on smooth and rough mares, respectively, at 16 km/hr, during a two-minute run. Allowing for higher  $\sigma$  peaks during the longer-term smooth-mare operation, and selecting a more realistic rough-mare speed of about 8 km/hr, suggests 3  $g_1$  as a reasonable mission load. This radial load has to be combined with loads caused by maneuvering and braking. An inboard-acting side load due to the scuffing action of the swing arm suspension is associated with vertical loading of the wheel. A frictional coefficient of 0.8 was used to establish the side load shown in the table.
- o Maximum braking torque: The braking design torque corresponds to a maximum braking effort of 100 ft-lbs.
- o Unsymmetrical braking: This condition assumes maximum braking on two wheels on the same side of the vehicle; side loads provide the static balance.
- o Pivoting: This condition involves pivoting the vehicle about a single locked wheel. Uniform soil pressure is assumed over the entire footprint length.
- o Turning: This condition corresponds to a sharp turn which puts the vehicle at the point of insipient instability (all load on the outside wheels).
- o Maximum radial load: This high-load requirement provides for a number of radial overload conditions, such as obstacle encounter, longitudinal impact, or a vertical drop.

The dynamic operating loads obtained from the lunar surface spectral densities do not include impacts with discrete short wavelength obstacles. Separate digital computer studies reported in the Dynamics Section (4.2.2) show that a 5.5- $g_1$  capability is required to negotiate 4-in. spike bumps at 16 km/hr., and it is believed that no less capability than this should be provided. The provision of this high load capability for the science module allows it to also be used in the manned mode, if called for by future plans.

During unmanned operation, the probability of encountering a large obstacle is increased, but the driving speeds are much lower. A 5.5  $g_1$  capability allows for longitudinal impact of a vertical wall with a single wheel at a speed of over 2 km/hr.

A large free-fall-height capability is desirable, since it provides for added margin during DLRV deployment, and allows for inadvertently driving into a deep depression. The 5.5  $g_1$  load capability provides for a free-fall height of about 34 inches.

#### 4.3.3 Design Criteria

##### 4.3.3.1 Factors of Safety

The factor of safety, that is, the ratio of allowable load to mission design load, must be selected so that the likelihood of failure under the maximum mission level stress is acceptably remote. The probability of failure, however, depends on a number of factors, such as type of loading, structural configuration, material strength, and constructional variations. Rational factors of safety with proper allowances for stress concentration and repeated thermal and dynamic loadings must therefore be used to achieve adequate strength and maximum design efficiency. The loads given in this section are mission levels. The ultimate factor of safety used for DLRV general structure that is strength-critical is 1.5 on the mission levels. For fatigue-critical structure the factor is 1.3. Higher factors are used for astronaut restraints; factors of 2.5 and 3.0 are applied to the restraints and their attachments, respectively.

##### 4.3.3.2 Fatigue Analysis

Although adequate static strength is assured by the ultimate load stress analysis, adequate service life is not automatically provided for. The latter depends on a number of variables, such as the number and magnitude of load applications during the entire mission, detail and general design configuration of the structure, and properties of the material used.

Fatigue life calculations are based on the cumulative damage method.

The procedure involves determination of maximum allowable stresses for a given spectrum for various stress concentration factors. These stresses are determined and plotted for all fatigue-critical members and desired materials. Equivalent uni-axial tensile stresses, based on the octahedral shearing stress theory are then used for fatigue analysis.

Fatigue spectra, which give frequency of occurrence of various loads, should be derived from a combination of dynamics results showing loads in terms of speeds and terrain characteristics and mission analysis results showing expected time during the vehicle life for various combinations of speed and terrain. Typical, simplified stress and fatigue analyses were performed during the preliminary DLRV design phase. These are discussed under the subsystem sections.

#### 4.3.3.3 Structural Materials

The choice of structural materials for utilization on the DLRV was made on the basis of the following desirable characteristics:

- o High strength-to-weight ratio
- o Good fracture toughness
- o Compatibility with both earth and lunar space environment
- o Ease of fabrication

A number of candidate structural materials were considered for DLRV application, including aluminum, titanium, magnesium, beryllium, and steel alloys, as well as fiberglass reinforced plastics (FRP).

Aluminum has long been the primary aerospace alloy, because it offers a good balance of strength, rigidity, excellent fabricability and good compatibility with space environment. The pre-eminence of aluminum was further enhanced by the development of a) improved stress corrosion resistance of 7075 T73, and b) increased strength of weldable alloys, such as 2219. At elevated temperatures, titanium surpasses aluminum in all structural counts, and its potentially favorable notch sensitivity and fracture toughness make it a contender even at room temperatures. Magnesium is being discarded, despite its potential weight savings, because of its vulnerability to corrosion in earth storage environment, and its poor high-temperature properties, subject to creep. Beryllium was considered, because of its extremely high stiffness and strength-to-weight ratio; its disadvantages are low ductility and formability. The utilization of steels for the DLRV is restricted to isolated applications. This is because

of the inability to utilize its high strength, as limited by minimum gage fabrication and tolerances, and by local buckling considerations. FRP was considered for its excellent corrosion resistance, formability, high strength-to-weight ratio, impact resistance and flexibility. Based on the above considerations, the choice of structural materials for DLRV was narrowed down to the following primary candidates:

- o Aluminum - 7075 T73xxx and 2024-T6xx, T8xx, for the primary unwelded structure; 2219-T6xx, T8xx for welded applications of both primary and secondary structure. An anodic film finish, in accordance with MIL-A-8625 should be considered.
- o Titanium - Ti-6Al-4V or Ti-6Al-6V-2Sn for high temperature primary structure, fasteners, and wherever a weight advantage can be realized.
- o Steels - Stainless steels, and high-strength low-alloy steels for suspension system torsion bars, deployment cabling, pure tension members and other isolated areas.
- o Fiberglass reinforced plastics (FRP) - Applications considered include equipment covers, close out panels, astronaut restraints, foot rests, seats, etc. Temperature-resistant FRP was chosen for the elastic cone wheels, based on the trade-off studies reported in Section 5.4.

#### 4.4 THERMAL CONTROL

All equipments requiring location outside of any enclosure are located as functionally suited and are provided with individual thermal control. The thermal control of these equipments are separately discussed in the respective subsystem sections of this volume and Volume III. All other equipments, generally electric and electronic, are enclosed in compartments to facilitate thermal control. Only the latter are discussed herein.

The subsections of this section are presented in the order of logic leading to the selection and verification of the final selected system. These subsections are:

- o Rationale
- o System Approaches
- o System Concept
- o Operations Concept
- o Thermal Loads
- o Thermal Performance

The mission capability of the selected system is summarized in Table 4.4-1. It should be noted that this capability can be increased appreciably at sun angles less than 60 degrees.

##### 4.4.1 Rationale

The primary thermal requirements are determined by performance characteristics of structural and electronic equipments within the natural and induced environments of lunar surface operation. The designs also are to be compatible with the stowed environment of the ELM during prelaunch, ascent, translunar coast and descent. More critically, all thermal designs must be capable of satisfactory operation under the expected lunar surface dust conditions and be adequate for a one-year mission.

Because of the long life requirements, it becomes highly desirable to design a passive or near passive system minimizing all electrical power requirements, mechanical complexity and avoiding expendables.

Because the vehicle is size and weight constrained, the smallest, lightest thermal control system is obviously a goal. This requires the evaluation of waste heat generation and subsequently, its reduction in the overall operation of the vehicle. The lunar night survival requires careful examination of efficient insulation schemes and low electric power heat sources. Additional insulation vs. extra passive heaters are to be considered.



TABLE 4.4-1

THERMAL SYSTEM MISSION CAPABILITY  
SUBSOLAR CONDITIONS

UNMANNED

Radiator Operations	Drive Speed, km/hr on Slope			
	0 to 1 on Level	1 to 2 on Level	2 to 16 on Level	10 on 6° Slope
All open	continuous drive	continuous drive	NA	NA
Control Module open. Power & Science Module closed during drive, open during stops	—	30 minutes max drive during repetitive 50% drive, 50% stop cycle	NA	NA
		<u>MANNED</u>		
All open (limited degradation assumed)	continuous drive	continuous drive	1.87 hrs (30km) Stop for recycle, 2.1 hr doing science or 1 hr if charging	No limitation for the prescribed thermal design mission time of 90 min
All closed during drive, all open during stops	—	40 min max. drive during repetitive 60% drive 40% stop cycle	9½ min for max drive during repetitive 50% drive 50% stop cycle or 30 min drive & 2.3 hr stop	11 min. max. drive during repetitive 50% drive 50% stop cycle or 28 min. drive and 2.3 hr. stop

Operation in a dust environment requires evaluation of non radiative rejection systems or radiative surface devices with some form of dust abatement and cleanability.

Additionally, mission operations indicate that many equipments need not be on all the time. This philosophy permits time sharing of the final thermal control scheme. Equipment heat loads which can be staggered in time could be satisfactorily cooled by a heat sink sized for the maximum steady state average of the individual loads. This established the design philosophy that all equipment that need not be external or separate for operational purposes should be located in an internal thermally controlled area. It is also desirable to operate the equipments at the highest temperatures allowable commensurate with the desired reliability goals.

#### 4.4.2 Thermal System Approaches

In the course of this study, various candidate approaches for thermal control were examined. The primary effort was in selecting a suitable thermal system capable of contending with the expected dust deposition and low power drain survivability for lunar night. For purposes of analysis, it is convenient to break thermal control into the following sub parts: (1) Heat Transport Devices and (2) Heat Rejection Devices.

##### 4.4.2.1 Heat Transport Devices

Heat transport is defined as the method of transferring heat from the equipment to the ultimate or final heat sink. In evaluating heat transport methods, the following were considered:

- o Direct structural coupling to the final heat sink
- o Variable structural couplings or thermal switches
- o Variable heat pipes
- o Indirect and direct radiation
- o Active coolant loops

Of the five heat transport methods, the direct short structural coupling provides the best thermal conductance and, therefore, the lowest temperature rise from the dissipation source to the final heat sink. However, this method imposes various design limitations as listed below which resulted in its discard:

- o All equipments must be mounted on or within inches of the final heat sink resulting in packaging limitations

- o During low power dissipation phases and cold external environments, i.e., low sun angle, shadows or lunar night exposure, excessive amounts of heater power or a controllable insulation cover would be required to avoid low and/or large fluctuations in equipment temperature
- o If the source and sink are significantly separated, required cross-sectional area and, subsequently, increased weight are serious penalties.

Variable structural couplings or thermal switches such as were applied to the Surveyor program (see Figure 4.4-1) were considered to be more desirable. This type of device senses operational temperatures and provides a high thermal conductance during high thermal load conditions while reducing its conductance to minimize heat flow during cold or lunar night operation. A typical conductance turn down in the ratio of 300:1 is achievable. From evaluation of the data provided by AFML-TR-68-198, Air Force Materials Laboratory report on Surveyor, the following undesirable points were noted:

- o The switches are somewhat heavy and bulky and require close equipment location to the final heat sinks
- o The thermal conductance was somewhat limited by the switch contact surface which must be specially coated to prevent cold welding and to improve thermal contact heat transfer in a vacuum
- o The switch performance appears to decay rapidly with time
- o Reliability of operation for long periods is considered a problem because of bimetallic material fatigue and creep

Variable conductance heat pipes, a relatively new innovation for efficient heat transfer with the variable conductance feature were also examined. These pipes are basically liquid-vapor cycle devices which function in a passive manner providing exceptionally high heat transfer capacity, high thermal conductance and low specific weight. A typical schematic and steam analogy are given in Figure 4.4-2. Figure 4.4-3 shows conductance values for one of several configurations tested under the Grumman Advanced Development Program. The conductance of a solid bar is also shown for comparison. This type of configuration with a non-condensable gas reservoir section could provide conductance turndown ratios in the range of 100:1 at the DLRV low temperature range.

In general, the heat pipes are capable of providing all the features of thermal switches without their undesirable points. The following areas, however, are sensitive and are noted for further consideration

- o The pipe must be designed with a low thermal conductor spacer so as to minimize residual structural heat leak during night operation. This may prevent sealing problems

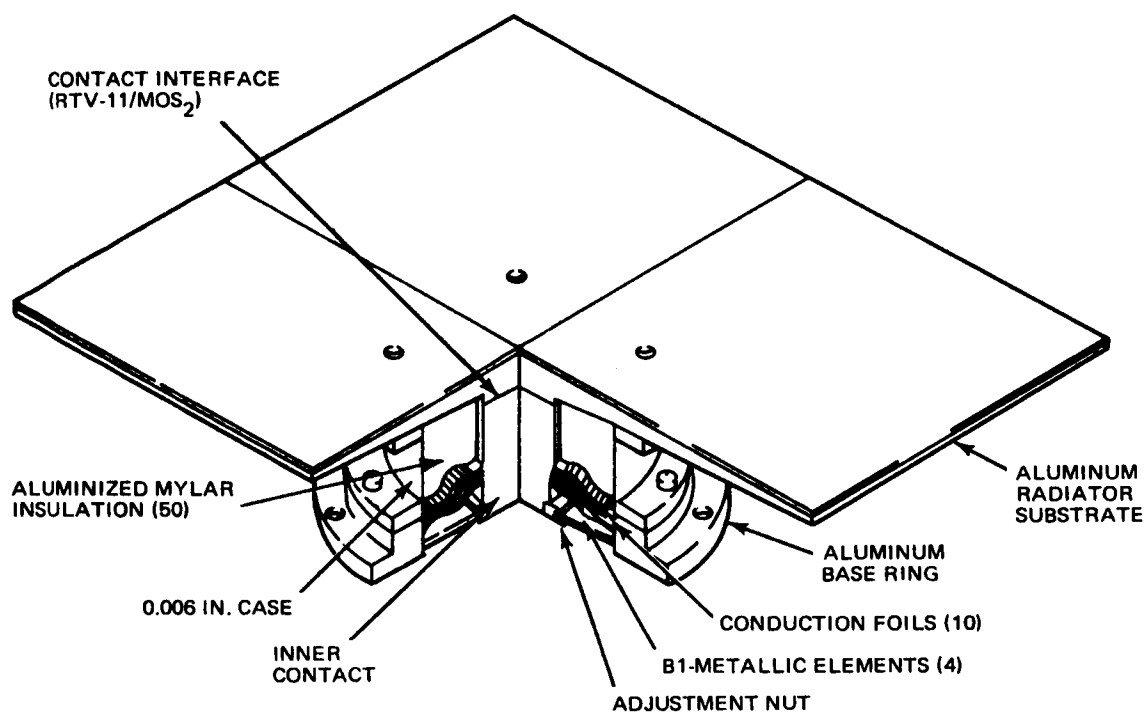


FIG. 4.4-1 SURVEYOR THERMAL SWITCH

# HEAT PIPE

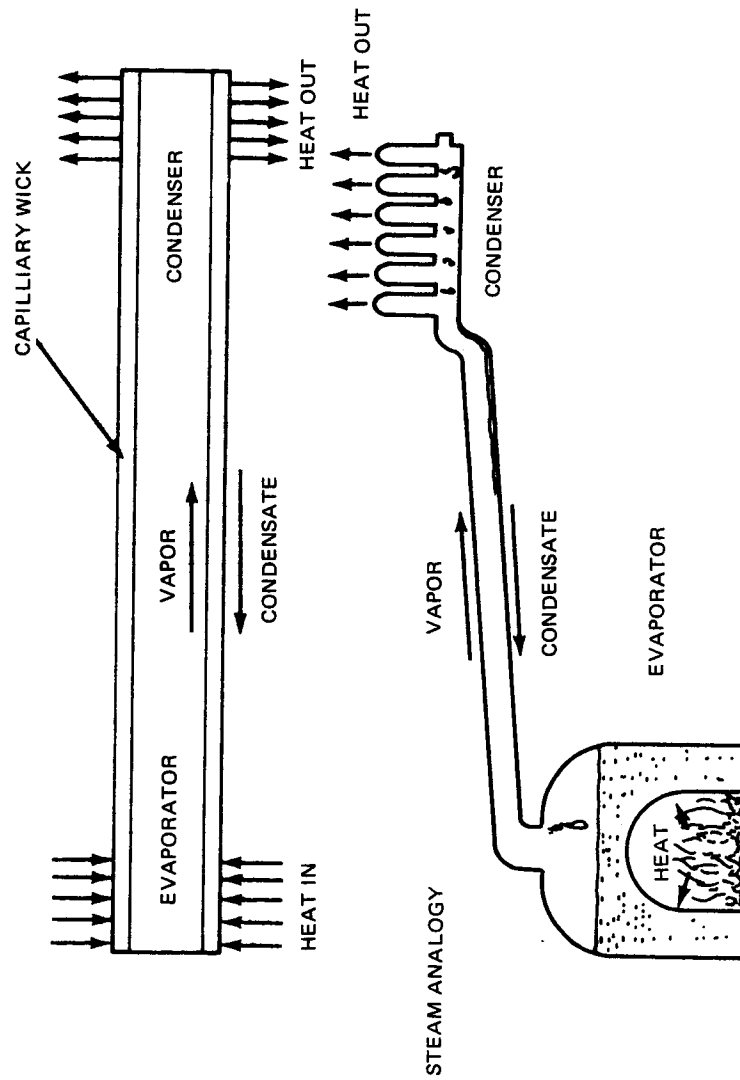


FIG. 4.4-2 HEAT PIPE SCHEMATIC AND STEAM ANALOGY

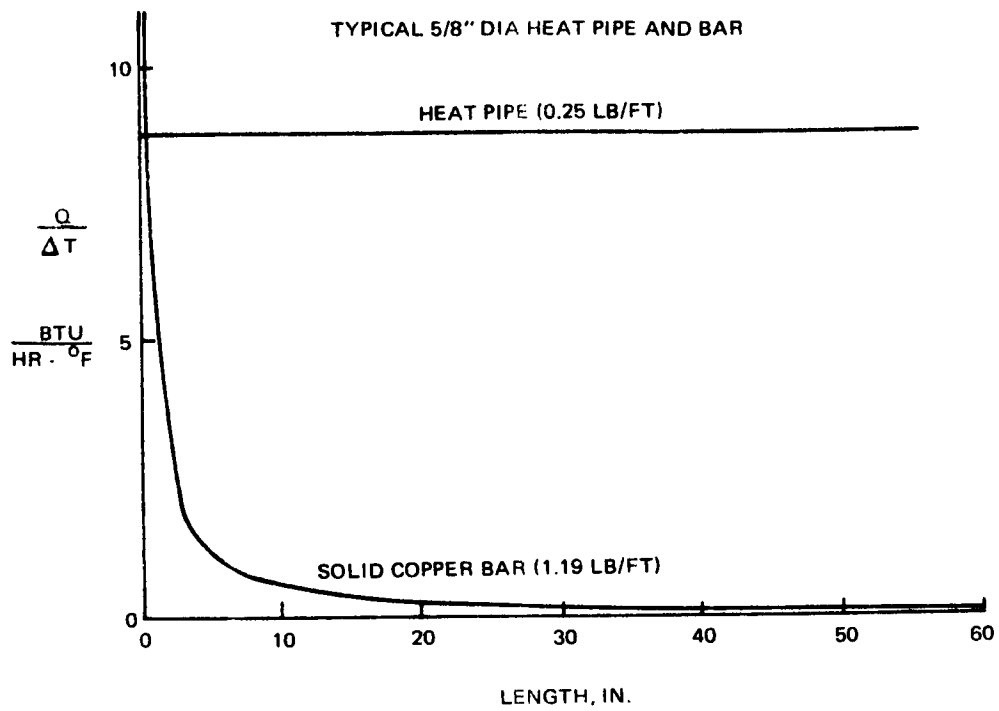


FIG. 4.4.3 CONDUCTANCE COMPARISON OF PIPE AND BAR

- o Since the pipe function requires that the condensate flow from the condensor at the final heat sink to the evaporator at the equipment mount, the tilt of the pipe in a gravity field must be considered

The indirect radiation approach relies on transferring equipment thermal dissipation directly to the final heat sink by radiation. In general, this is a minimal weight approach. However, radiation heat transfer is less effective than conductive transfer, and higher temperature differences between the equipment and the final heat sinks must be tolerated. If a radiator is used as the final heat sink and requires operation with surface property degradation, high thermal coupling and thus low temperature difference between equipment and radiator is even more desirable. This approach is consequently not recommended. Like the heat pipes and thermal switches, this approach can also be implemented by means of insulation shades or movable louvres to provide the variable conductance effect.

Direct radiation of equipments to space was also considered. This scheme would avoid the poor thermal coupling of this indirect approach. A shade or movable shutter could be implemented to provide the desirable variable conductance effect for lunar night. This approach, however, appears to be seriously vulnerable to dust accumulation directly on the equipments and makes the design of any automatic cleaning device quite difficult.

Active coolant loops such as ethylene glycol-water fluid loops, were also studied. A cursory examination showed that achievable weight, heat transfer capacity and temperature ranges could be designed comparable with the other variable coupling approaches; however, the following points were considered serious disadvantages and no extra work was performed in this area:

- o The system would be complex; i.e., requires a motor, pump, valving, accumulator reservoir and line fittings
- o In avoidance of single point failure, almost each compartment loop must be redundant
- o The necessary instrumentation; i.e., flow or pressure transducers motor-pump speed, voltage and current, considered necessary for adequate test and mission support, is complex
- o The necessary pump power, estimated at 20 watts total is a significant thermal dissipation

#### 4.4.2.2 Heat Rejection Devices

The heat rejection device is the ultimate or final heat sink for disposing of the energy to the environment. They may be separated into two basic groups: 1) those which rely on radiation as the final heat transfer method and 2) those which do not.

Those approaches which do not rely on radiation to space have the unique advantage of not being vulnerable to the prevalent dust conditions. Water boilers and sublimators fall into this group. The typical heat rejection capacity of these devices are in the order of 1000 BTU per lb of liquid and at the DLRV levels of dissipation, is equivalent to about .95 lbs of water per hour of unmanned operation. Even in combination with radiators where sublimation would be used for peaking loads, the system weight would be excessive.

The only suitable approach appears to be a space radiator of a configuration, that is least affected by the dust environment. Selection of the proper radiator surface should be based on the following rationale:

- o To provide the smallest and lightest design, the radiator surface should have the lowest solar absorptivity with the highest emissivity presently achievable
- o To minimize weight, the required radiator structure should be adaptable to thin light weight design
- o Since it is expected that dust contamination cannot be avoided, the selected radiator surface should be of a type having low dust adhesion and good cleaning properties
- o Because of the long exposure to sunlight, the surface should have low susceptibility to UV degradation

#### 4.4.2.3 Dust

The concern for dust on the DLRV has been of major consequence because of its expected propagation by the vehicle wheels and detrimental affects on thermal surfaces. Figure 4.4-4 shows the expected heights vs wheel speed considering a free ballistic particle path. If we assume that colliding particles from adjacent wheels do not result in significant changes to the expected trajectory, we may deduce that the 2 km/hr wheel speed of the unmanned operation does not propagate dust any higher than 3.4 feet from the lunar surface. It would then follow that all power dissipation thermal surfaces located above this height are free of contamination during unmanned operations. This philosophy was applied to the Solar Array, the Steerable Antenna, the RF Hazard Detection Sensor, the Solar Aspect Sensor and the TV Camera. The added height of the



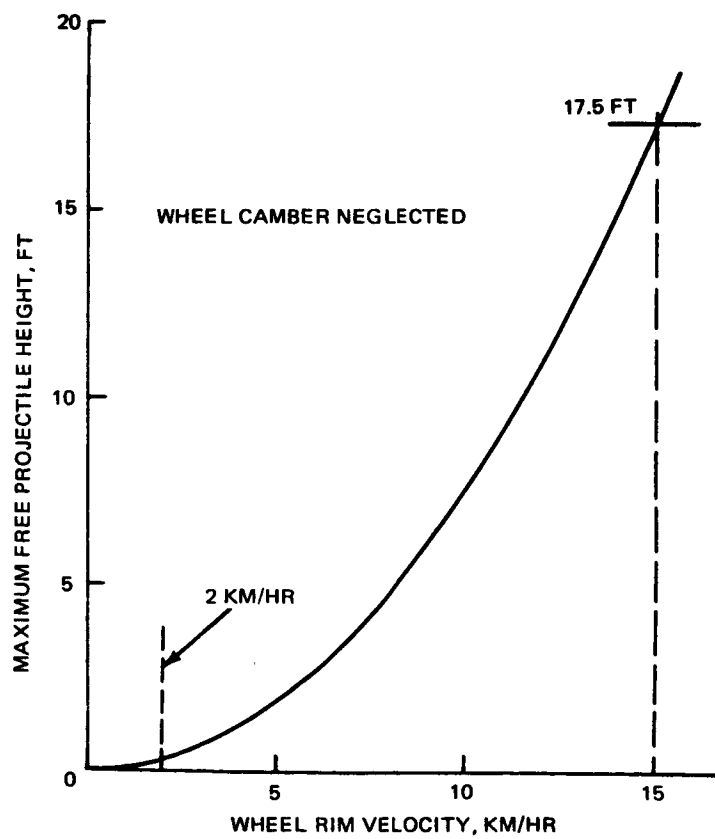
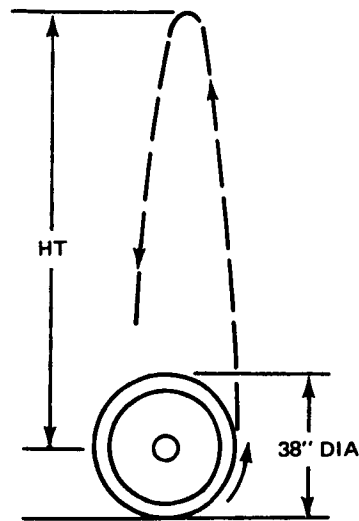


FIG. 4.4-4 MAXIMUM HEIGHT OF DUST

vehicle during remote operation and the 15° wheel camber is an additional advantage. The equipment compartment radiators are questionable during vehicle turns where particle collision could be excessive and are thus provided with dust abatement and removal devices.

The effect of dust on the thermal radiators are concluded to be as follows:

- o A thin layer of dust will radically increase the solar absorptivity of a low absorptance surface. Results of the Northrup/Huntsville dust investigation showed that a 10% dust coverage resulted in approximately a 90% increase in surface absorptivity. In the limits (100% coverage), this should cause surface degradation to an absorptivity of 0.9 this being the approximate absorptivity of the lunar soil. Figure 4.4-5 reflects this trend for a typical thermal surface.
- o As the dust build-up increases beyond this visible thin film, we must account for effective thermal resistance. Figure 4.4-6 is a plot of the effective thermal resistance versus thickness as determined from Annex C of the Statement of Work. This impedance to the flow of heat must then also be considered when analyzing the system. Since small dust thicknesses are both significant and unpredictable, a cleaning device together with a dust abatement shield for the radiators is deemed necessary.

The typical schematic of the dust device is shown in Fig. 4.4-7 and is to be provided for each of the three equipment compartments. This method of cleaning is at present, deemed the most workable. Test data provided by Report # TR-792-7-207A (Northrup/Huntsville Technical Report No. 321) on dust removal concepts shows a favorable appraisal of this approach.

We are at this time, limited in being able to predict the most suitable cleaning fluid, the required quantity per cleaning cycle, or the total quantity for one year operation. It is recommended that a thermal vacuum test program be initiated prior to a Phase C program and that recommended radiator surfaces be contaminated with lunar soil and cleaned by various methods in a vacuum.

Actual dust rate build-up information can most likely only be obtained from the interpolated results of earlier lunar vehicles or by other experience. In addition, information from Apollo 12 depicted a possibility of a natural dust fallout as evidenced by the light yellow dust coating found on Surveyor 3 and requires additional consideration.

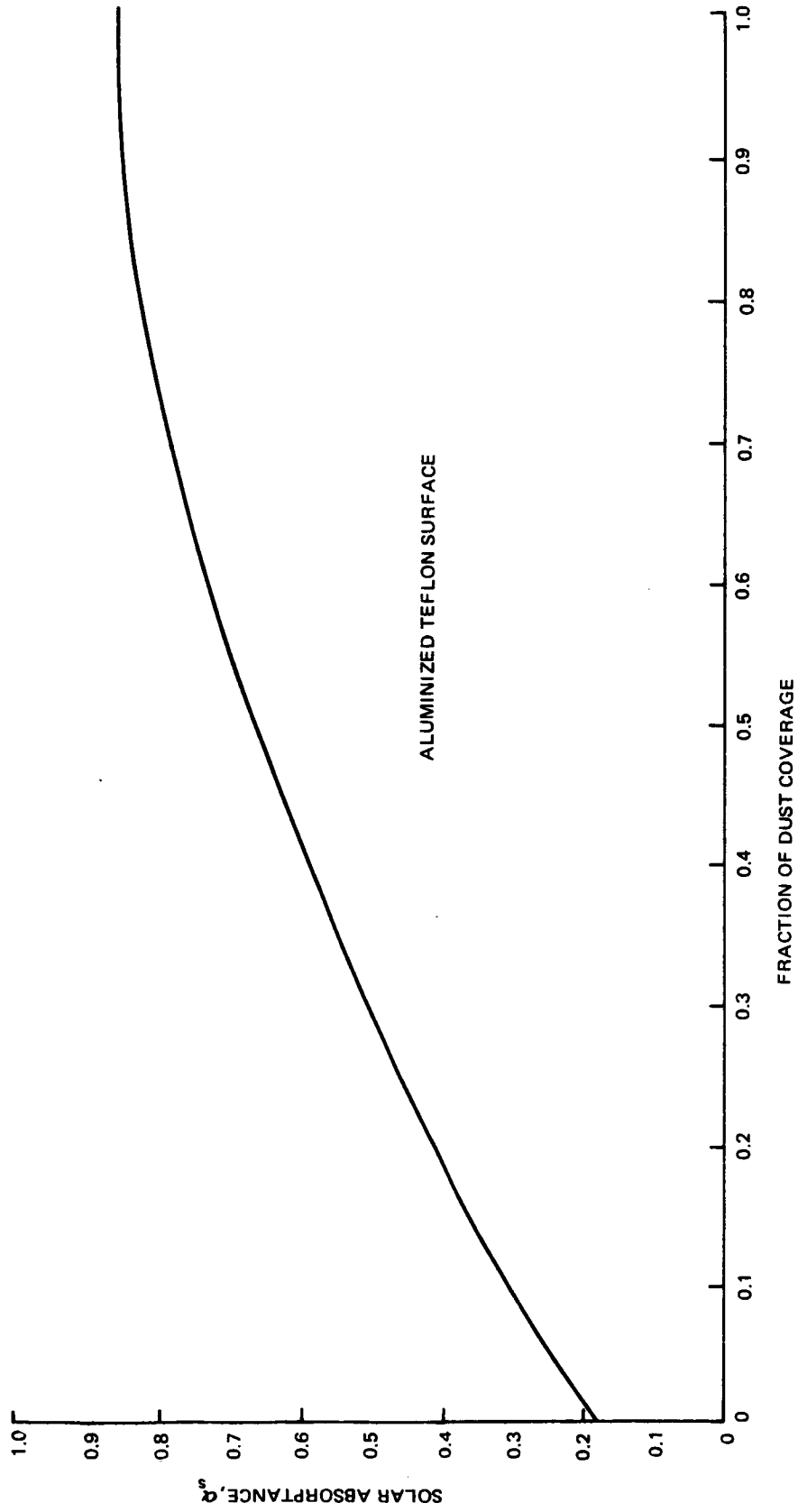


FIG. 4.4-5 VARIATION OF TOTAL SOLAR ABSORPTANCE WITH DUST COVERAGE (REF TR-792-207B)



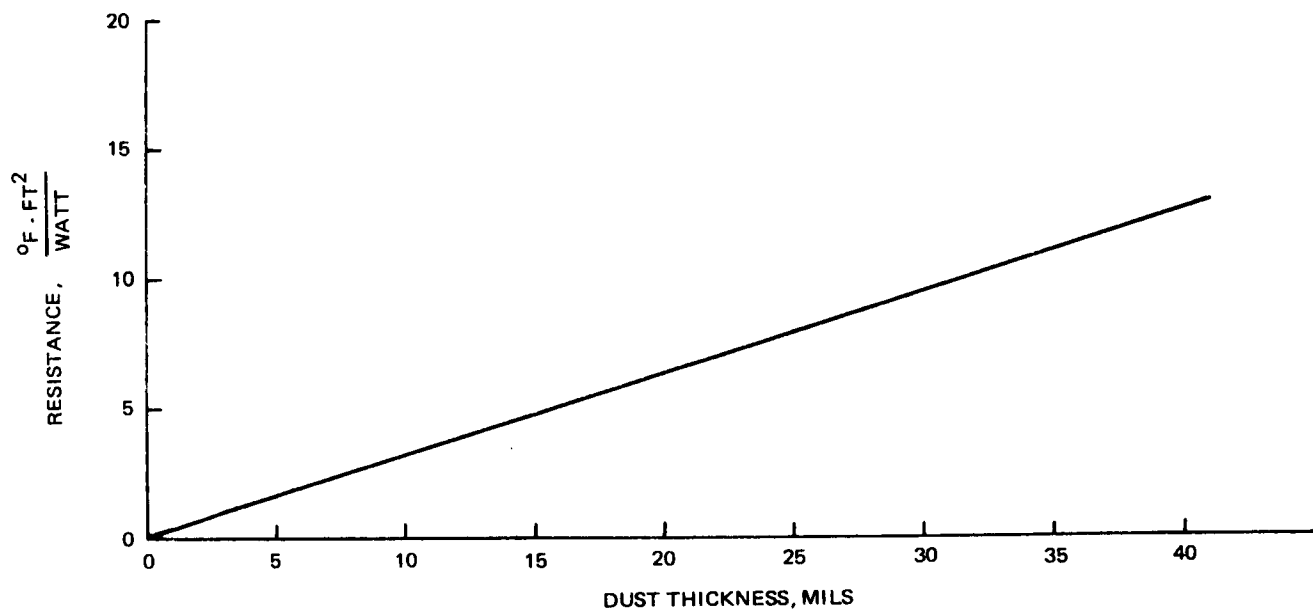


FIG. 4.46 LUNAR DUST THERMAL RESISTANCE

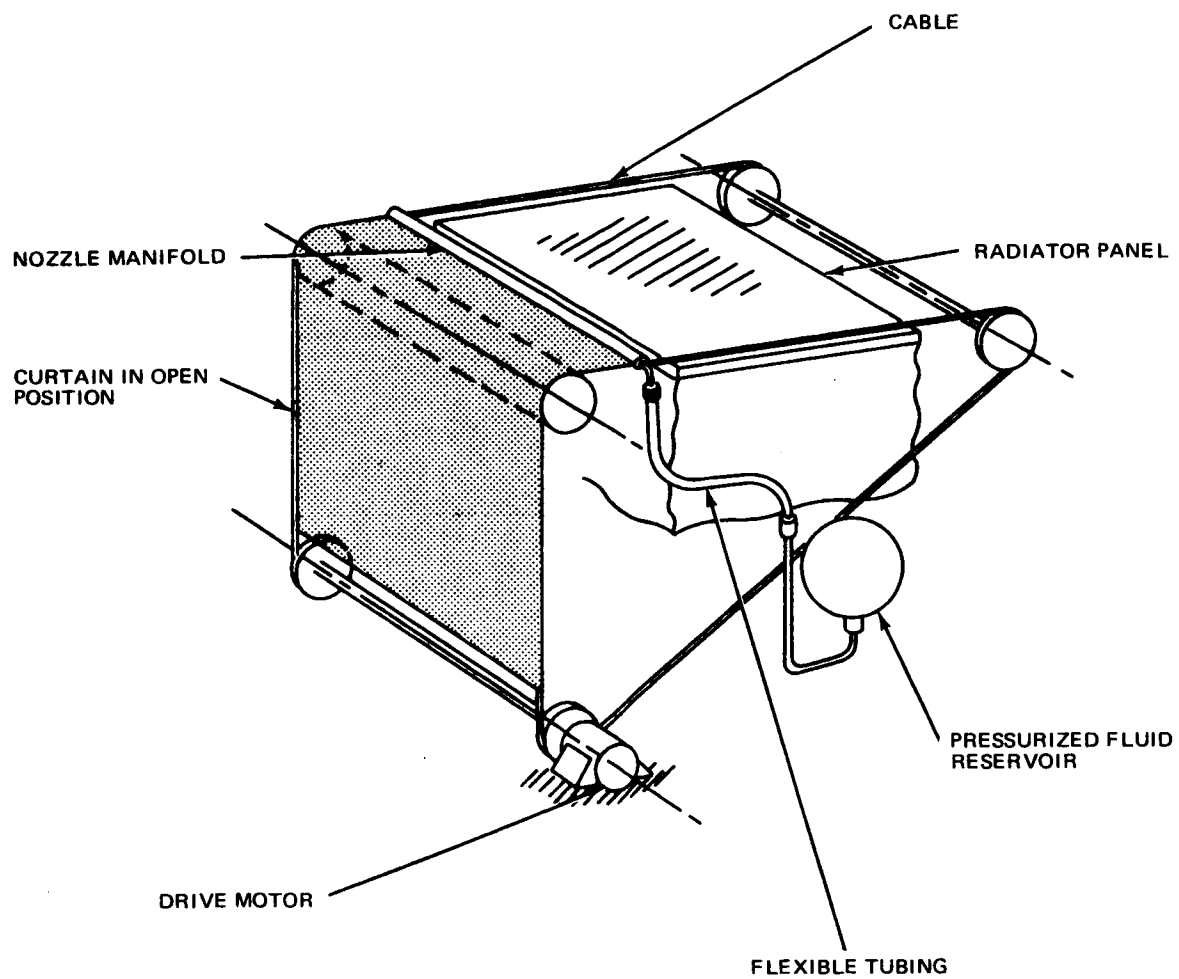
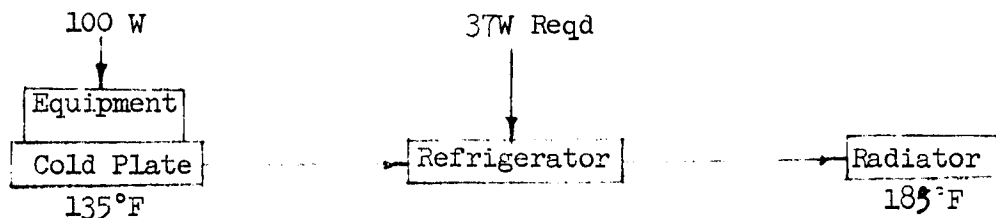


FIG. 4.4-7 DUST SHIELD AND CLEANING MECHANISM

In conclusion, it has been conservatively assumed that dust at low height on the DLRV will eventually permeate any intended shield and that eventual cleaning of some sort will be required. The DLRV's covered radiator approach is then a method of minimizing the contamination and thus, reducing the number of cleaning cycles required.

#### 4.4.2.4 Supplemental Cooling

Other devices such as refrigeration techniques could be applied between the equipment cold plates and the radiator permitting use of higher radiator temperatures or degraded radiator surfaces. Peltier and vapor cycle equipment are logical approach and would be applied for a typical case seen below.



The higher radiator temperature would permit use of a smaller radiator with the same solar absorptivity ( $\alpha_s = .11$ ) or the same size radiator with absorptivity degraded to .37.

A cursory examination of state-of-the-art hardware indicated a minimum of 10 lb. weight penalty for the refrigerator. Improvements appear impractical for such small (100 W) loads.

Realistic sizing for dust effects is impossible because of the uncertainty of this dust layer. If cleaning is provided, additional radiator surface area provides a better capacity per unit weight.

#### 4.4.3 System Concept

A thermally controlled equipment compartment is provided for each of the vehicle modules. Each compartment as located on Fig. 3.2-2 provides suitable thermal environments for the enclosed electrical and electronic equipment during all phases of both unmanned and manned missions. Thermal controls are achieved semi-passively and are considered suitable for a minimum life of one year while exposed to the lunar environments.

The thermal control system as depicted by the block diagram in Fig. 4.4-8 consists

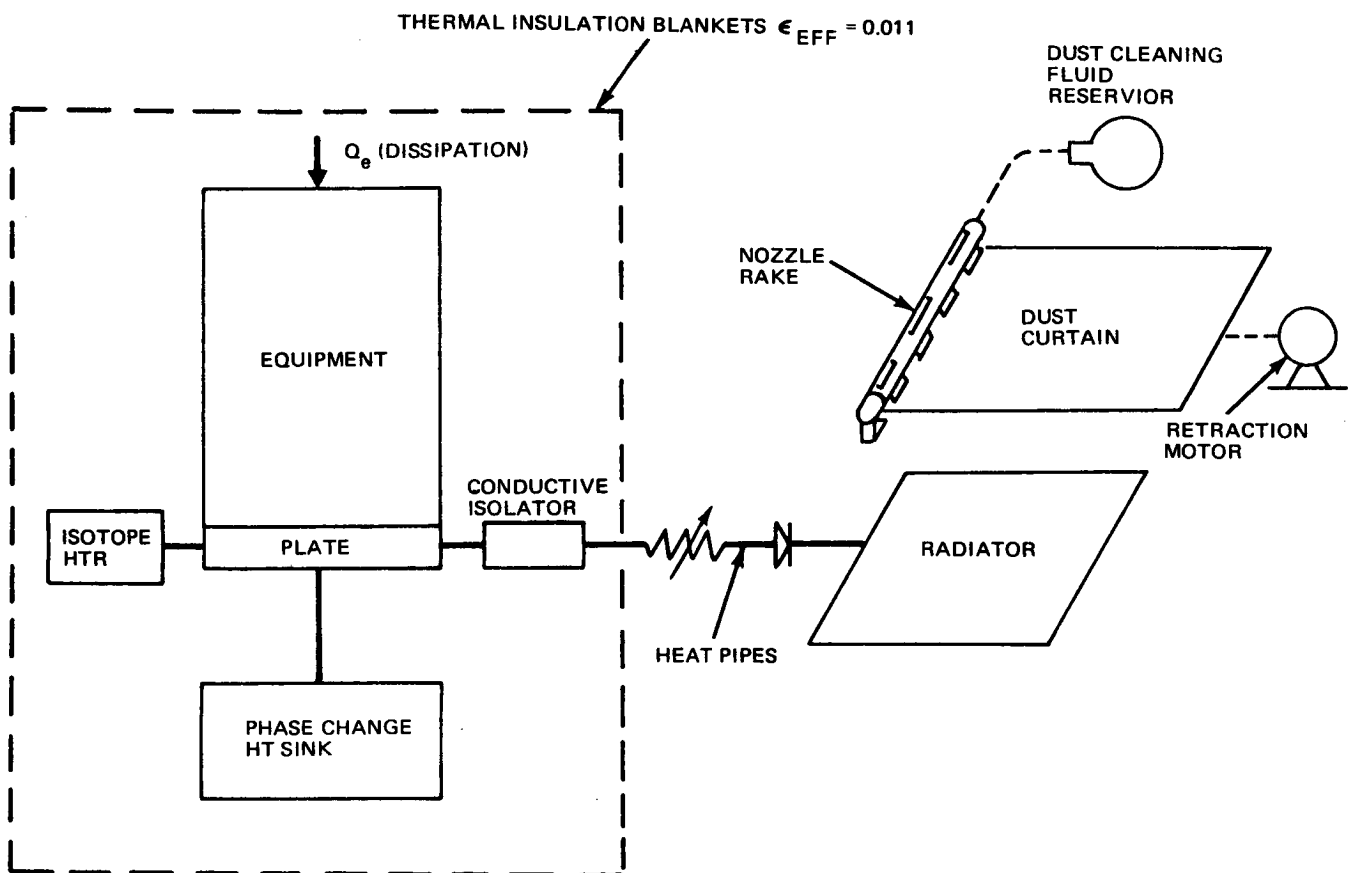


FIG. 4.48 THERMAL SYSTEM BLOCK DIAGRAM

of the following components:

- o Equipment Mounting Tray
- o Phase Change Heat Sinks
- o Variable Conductance Heat Pipes
- o Space Radiator
- o Insulation Blanket
- o Radio Isotope Heaters
- o Dust Control Device

#### 4.4.3.1 Equipment Mounting Tray

The equipment mounting tray provides a heat transfer mounting surface for the electrical components. The tray contains prescribed internal cavities which are filled with a change of phase heat storage material. In parallel to the heat storage material, the tray is attached to the thermal heat pipes.

#### 4.4.3.2 Phase Change Heat Sinks

Phase change heat storage material is provided in the system to permit high load operation of the DLRV with the radiators overloaded, ineffective or covered as may be required for dust conditions. The phase change temperature point of the substance is selected at the maximum allowable equipment heat sink temperatures, i.e., 136°F for the Control and Science Module compartments and 89°F for the Power Module compartment.

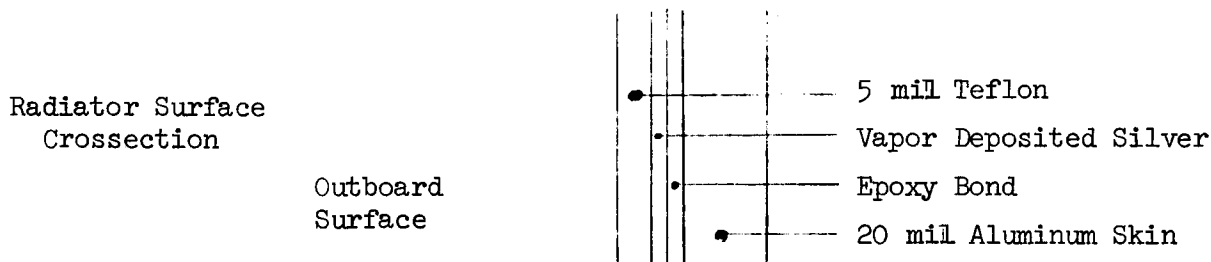
#### 4.4.3.3 Variable Conductance Heat Pipes

Variable conductance heat pipes are used to provide an adequate heat transport loop between the equipment mounting tray and the space radiator. These pipes are designed to transfer maximum thermal loads to the radiator at a minimum temperature differential. The variable conduction parameter shall be designed to provide a conductance turndown ratio in the range of 100:1 to minimize lunar night losses. The heat pipes should be capable of proper operation in the lunar gravity (1/6 earth) plus an acceleration of 20 in/sec<sup>2</sup> rms at a predominant frequency of 1 cps. The heat pipe is arranged to permit adequate operation at vehicle tilt angles of  $\pm 25^\circ$  in roll and pitch.



#### 4.4.3.4 Space Radiator

Space radiators provide the final heat sinks for internal equipment dissipation. The radiators are a light-weight thermo optical type as shown below.



This selection is considered suitable for one year exposure to UV radiation and has a hard non-adherence, non-porous type surface suitable for repeated cleaning. The configuration, and angle to the lunar surface was selected so that the radiator size required is within vehicle design envelope constraints.

#### 4.4.3.5 Insulation Blanket

Insulation blankets are used to provide thermal isolation of the enclosed equipments from the surrounding environment. The blanket serves to limit heat transfer into and out of the compartment to that governed by the heat pipes and radiators. The configuration selected is composed of 23 layers of crinkled 1/4 Mil. aluminized Mylar plus 2 layers of 1/2 Mil. aluminized Kapton (H-Film). The 2 H-Film layers are outside. The Kapton surface of the outermost blanket faces the space environment exposing a surface  $X_s/\epsilon$  ratio  $\leq 1.0$ .

#### 4.4.3.6 Radio Isotope Heaters

Radio isotope heaters are provided internal to each compartment. These devices located at the equipment mounting tray provide sufficient energy to maintain the mounting tray at the lowest permitted temperatures for lunar night mission requirements. These heaters are selected for the lowest dissipation possible since they cannot be turned off and must be included in the thermal load during lunar day. Plutonium 238 is considered to be a suitable material from a life and safety standpoint.

#### 4.4.3.7 Dust Control Device

Each equipment compartment radiator is provided with an integral dust curtain and dust cleaning device as represented by the schematic in Fig. 4.4-7. The curtain is made of a light weight flexible material such as multilayer H-Film and is to be remotely controlled. The leading edge of the curtain support is a hollow tube containing an array of multiple nozzles suitable for the uniform dispersion

of a cleaning fluid or gas on the radiator. A suitable linkage and motor drive provides for necessary actuation. The quantity of cleaning solution to be provided shall be determined from a laboratory evaluation. For purposes of this study 5 lbs has been allotted for this expendable.

#### 4.4.3.8 Self Induced Environments

In the interest of completeness, we should mention some of the self induced vehicle heat loads. The loads concerned are those imposed by vehicle structure and the powered, external equipments. With the exception of the RTG and the Solar Array panel, all equipment imposed loads are considered to be negligible because of either low surface temperature or small view factor.

The solar array is predicted to reach a maximum operating temperature of 230°F. Because of its large size, it can represent a substantial view to most of the Control Module external equipments and should be considered during their design phases. The size, location and operation of the array can be obtained from the Astrionics Volume of this report, the mounting location and geometry from the Mobility Section.

The RTG is supported on a thermally insulated mount to prevent excessive heat conductance to the vehicle chassis. It is located so that its outer thermal surfaces are not critically obstructed from their required view of space. The equipment compartment radiators do not have any view of the RTG. Most externally mounted equipments, however, do have a view of the RTG and must be considered during the detailed thermal analysis and design of these equipments. All close vehicle surfaces with a high view factor to the RTG shall be covered with aluminized H-Film or similar high temperature insulation. Table 4.4-2 shows expected incident IR radiation values.

TABLE 4.4-2 MAX. INCIDENT THERMAL RADIATION

Flux, BTU/Hr. Ft<sup>2</sup>

	S-Band Antenna	TV Camera	Hazard Sensor	Sample Storage Container	Solar Aspect Sensor	Steering Actuator
RTG SNAP 19 360°F source	20.8	20.9	19	137	11.2	175
Alternate, Multi-Hundred Watt RTG 600°F source	64	64	55	420	33.6	540

During the stacked prelaunch configuration, the total RTG waste heat is significant to other ELM and launch vehicle systems and must be adequately removed. For the SNAP 19 dissipating about 637 watts, the air cooling scheme presently available on LM should be adequate. For the Multi-Hundred Watt RTG dissipating about 3700 watts, some form of liquid cooling would be more desirable.

#### 4.4.4 Operations Concept

During the unmanned mission phases where vehicle velocities are less than 1 km/hr all the compartment radiator covers may be kept open because the expected max. height of the dust particles is lower than the radiator heights. For this condition, there should be no restrictions on drive time or solar elevation angles. For vehicle velocities between 1 and 2 km/hr, the Power and the Science compartment radiators are covered to prevent or minimize dust deposits. Since the Control compartment radiator is higher on the vehicle, it may remain open. When a compartment is covered, all equipment heat dissipation is absorbed in the equipment masses and the phase change heat sink. Heat flow from the outer environment is limited to a negligible influx through the insulated blankets and penetrations. Heat flux into the compartment from the covered radiator is also negligible since the cover is insulated and the heat pipes do not permit reverse heat flow. At each stop the radiator curtain would be retracted and the vehicle powered down for science. At the reduced power, the heat stored in the phase change material plus the existing electrical dissipation would be transferred to space by the radiator.

This cycle would be repeated during the entire unmanned mission. During early lunar dawn or dusk, the variable conductance heat pipes would prevent under-temperature operation. When the system temperature indicates a degradation of the radiator surfaces, a radiator cleaning cycle would be initiated with the retraction cycle of the radiator curtain.

During manned operation, both the expected dust deposits and equipment dissipation are greater due to higher wheel torque and speeds. On the other hand, the crew can better appraise the dust conditions and can execute cleaning cycles. In spite of this, it is considered advantageous to open all radiators at speeds greater than 1 km/hr, since the supply of cleaning expendable could be made ample.

#### 4.4.5 Thermal Loads

In order to determine the design loads for the three compartment radiators, heat pipes and phase change heat sinks a thermal load analysis was performed. Table 4.4-3 depicts the loads during various mission phases for all equipments mounted in the thermal compartments. Influx of environmental heat through the heat pipes, thermal insulation and structural mounts are limited by the design and are considered negligible.

##### 4.4.5.1 Open Radiators

The typical heat pipe and radiator sizing loads with radiators open were computed as follows. The sizing load  $\dot{Q}_{rs}$  is defined as

$$\dot{Q}_{rs} = \frac{\dot{Q}_D \times T_D + \dot{Q}_S \times T_S}{T_D + T_S}$$

where

$\dot{Q}_{rs}$  = Sizing load (watts)

$\dot{Q}_D$  = Driving phase dissipation (watts)

$\dot{Q}_S$  = Stop phase dissipation (watts)

$T_D$  = Drive time (hours)

$T_S$  = Stop time (hours)

TABLE 4.4-3 THERMAL DISSIPATION RATES - CONTROL MODULE COMPARTMENT

	4 WHEEL MANNED				6 WHEEL UNMANNED				
	16 KM/HR FLAT	2 HM/HR FLAT	10 KM/HR 6° SLOPE	EXPER STOP	CHARGE STOP	1 KM/HR FLAT	EXPER STOP	CHARGE STOP	NIGHT
o COMM. & INST.									
VERT. SENSOR	2.5	2.5	2.5	2.5	0	0	0	0	0
RF WIDE BD XMTR	0	0	0	33.5	0	33.5	33.5	4	0
RF NARROW BD XMTR	12	12	12	12.0	4	12	12	5	5
S-B RECEIVER	5	5	5	5.0	5	5	5	0	0
RF SW & TRIPLXR.	0	0	0	0	0	0	0	1	0
MSCL XDCRS	1	1	1	1	1	1	1	1	0
SIGNAL PROCESS.	5	5	5	5	0	5	5	1	0
o REMOTE CONTROL									
COMMAND DECODER	7.5	7.5	7.5	7.5	1.5	7.5	7.5	0.3	0.3
o CONTROL									
TRACTION DR ELEC.	120	49.2	66	0	0	73.5	0	0	0
STEER ELEC	15	10	15	0	0	10	0	0	0
o NAVIGATION									
SUN SENSOR	1	1	1	1	0	1	1	0	0
o ELEC POWER									
SOLAR ARRAY DR ELEC.	0	0	0	0	3	3	1	1	0
o THERMAL ISOTOPE HTRS	8.1	8.1	8.1	8.1	8.1	8.1	8.1	8.1	8.1
TOTAL DISSIPATION	177.1	101.3	122.1	75.6	22.6	159.6	74.1	20.4	13.4

TABLE 4.4-3, THERMAL DISSIPATION RATES - POWER MODULE COMPARTMENT

6 WHEEL UNMANNED									
4 WHEEL MANNED									
	16 KM/HR FLAT	2 KM/HR FLAT	10 KM/HR 60 SLOPE	EXPER STOP	CHARGE STOP	1 KM/HR FLAT	EXPER STOP	CHARGE STOP	NIGHT
o COMM. & INST. DATA HANDLING MSCL XDCRS	15 2	15 2	15 2	15 2	3 0	15 2	15 2	3 0	0 0
o REMOTE CONTROL COMM DIST ASSEM	10	10	10	10	2.0	10	10	0.5	0.5
o ELECTRICAL POWER BATTERIES AMP HOUR XDCR VOLT REG CONVERTER RTG BATT CHGR. CONTRL PWR SWITCH & PROT INVERTER	88 3 0 5.8 0 5.9 0	5 3 0 5.8 0 1.2 0	90 3 0 5.8 0 6 0	27 3 0 5.8 0 1.2 0	2.5 3 0 5.8 19 NEG 0	4.8 3 10 5.8 0 3.8 5	5 3 80/20 5.8 0 2.3 5	5 3 80/0 5.8 19.2 NEG 0	3 3 0 5.8 1 NEG 0
o THERMAL ISOTOPE HEATERS TOTAL DISSIPATION	4.5 129	4.5 46.5	4.5 136.3	4.5 64	4.5 35.3	4.5	4.5 132/72.6	4.5 121/41	4.5 17.8
* 80 W @ 5° SOLAR ELEVATION 28 W @ 40° SOLAR ELEVATION 20 W @ >75° SOLAR ELEVATION AND LOW BATT LOAD 0 W @ >75° SOLAR ELEVATION CHARGING									

\* 80 W @ 5° SOLAR ELEVATION  
28 W @ 40° SOLAR ELEVATION  
20 W @ >75° SOLAR ELEVATION AND LOW  
BATT LOAD  
0 W @ >75° SOLAR ELEVATION CHARGING

TABLE 4.4-3, THERMAL DISSIPATION RATES - SCIENCE MODULE COMPARTMENT

	4 WHEEL MANNED			6 WHEEL UNMANNED					
	16 KM/HR FLAT	2 KM/HR FLAT	10 KM/HR 60 SLOPE	EXPER STOP	CHARGE STOP	1 KM/HR FLAT	EXPER STOP	CHARGE STOP	NIGHT
○ NAVIGATION			NA			2.5	2.5	0	0
VERTICAL SENSOR						12	12	0	0
DIRECTIONAL GYRO									
○ HAZARD						3.5	3.5	0	0
HAZARD PROCESS.									
○ THERMAL						1.7	1.7	1.7	1.7
ISOTOPE HTRS									
TOTAL DISSIPATION						19.7	19.7	1.7	1.7

The drive cycle was evaluated for a total cycle time of one (1) hr (drive time plus stop time). One hour is based on a routine science stop time of 30 min plus an average unmanned drive time of 30 min as established in Section 2 for the Unmanned Reference Mission. The longest anticipated drive time is one hour, as mentioned in Design Missions, Section 2.3. It is not felt, however, that the system need be sized for the worst combination of all conditions. An example for the Control Module compartment at a 50% drive-to-stop cycle is presented.

$$\dot{Q}_{rs} = \frac{159.3 \text{ W} \times 0.5 \text{ hrs} + 74.1 \text{ W} \times 0.5 \text{ hrs}}{0.5 \text{ hrs} + 0.5 \text{ hrs}}$$

$$\dot{Q}_{rs} = 116.7 \text{ Watts}$$

This analysis was repeated for various drive cycles and is plotted on Fig. 4.4-9. It should be noted that the total drive cycle period was assumed to be after a number of repetitive cycles so that initial condition transients could be neglected.

#### 4.4.5.2 Covered Radiators

The sizing load  $\dot{Q}_{rs}$  for fully closed radiator operation is defined as:

$$\dot{Q}_{rs} = \frac{\dot{Q}_D \times T_D + \dot{Q}_S}{T_S}$$

An example for the Control Module is given below. Results are shown for all Modules in Fig. 4.4-9.

$$\dot{Q}_{rs} = \frac{53.9 \text{ W} \times 0.5 \text{ hrs} + 72.6 \text{ W}}{0.5 \text{ hrs}}$$

$$\dot{Q}_{rs} = 126.5 \text{ Watts}$$

A baseline cycle of 50% was selected for design sizing of radiators and heat pipes. This represents average unmanned driving speed operations. It is assumed that at infrequent overload conditions, radiators may be uncovered and cleaned more often if necessary.



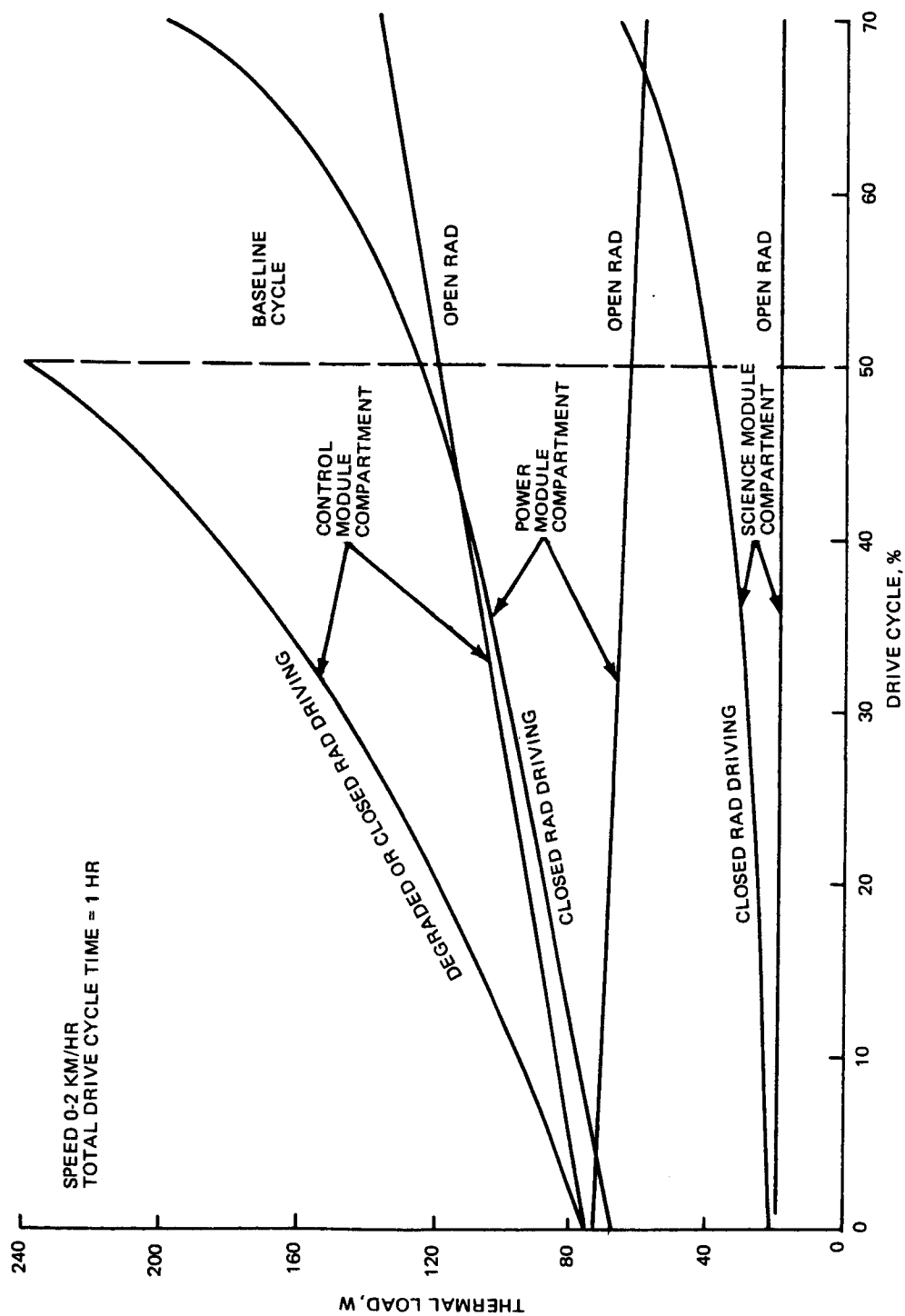


FIG. 4.4.9 SIZING LOAD VS DRIVE CYCLE

#### 4.4.5.3 Heat Storage and Discharge

The heat storage load requirement is derived from the need for closed radiator operation or for operational dissipations in excess of the radiator capacity. The conditions for heat storage operation have been selected for the manned and unmanned missions according to the rationale of the previous Sections. The conditions investigated are listed in Table 4.4-4.

The heat storage for the compartments is predicted as follows:

$$Q_a = \left( \dot{Q}_D - \dot{Q}_{RN} \right) T_D$$

where:  $Q_a$  = Heat storage requirement (watts-hrs)

$T_D$  = Drive time (hrs)

$\dot{Q}_D$  = Driving dissipation levels (watts)

$\dot{Q}_{RN}$  = Radiator capacity (watts), (0 when radiator is covered)

Using the drive dissipations from Table 4.4-3, and the radiator capacities selected in the subsequent subsection, the accumulated loads are given in Table 4.4-4. The Control Module with a radiator sized for 120W is critical unmanned while the other modules are critical manned.

After covered radiator operation, the accumulated load is discharged with open radiators while stopped. The minimum time should be less than the minimum science stop time of 30 min. (See Section 2., Mission Analysis). This recovery time  $T_r$ , is defined as:

$$T_r = \frac{Q_a}{\dot{Q}_{nr} - \dot{Q}_s}$$

Where:  $Q_a$  = Absorbed load

$\dot{Q}_{nr}$  = Net (subsolar) radiator capacity (W)

$\dot{Q}_s$  = Compartment dissipation during science stop

For the unmanned loads of Table 4.4-3 and the present radiator capacities they are:

.51 hr for the Power Module, 27 Whr/ (125-72.6) W

.49 hr for the Science Module, 9.9 Whr/(40-19.7) W

For the critical manned condition, a time of 2.3 hr is required.

#### 4.4.6 Thermal Performance

All thermal components are combined to provide the required performance. In addition to the requirements and concepts previously discussed, allowable temperatures for DLRV equipment were also established. These are given in Table 4.4-5.

This analysis was conducted using simplified heat flow model to provide preliminary performance predictions. Final performance predictions for these compartments will require evaluation by means of dynamic network analysis techniques.

##### 4.4.6.1 Basic Operations

The equipment mounted on the compartment trays at the designated loads and tray temperatures should not exceed internal temperatures defined in Grumman Report AED255-2, Part Derating Policy for the Apollo Applications Program, LM-A. It is presumed that the typical thermal resistance between the equipment and tray is less than 1.3°F/watt-in<sup>2</sup>. This is equivalent to less than a 2°F rise in the

TABLE 4.4-4 HEAT STORAGE REQUIRED

## OPEN RADIATORS (CLEAN)

Mode	Module	Speed km/hr	Slope Deg	Duration Hr	Dissipation W	Accumulated Load W-Hr
Unmanned	Control Module	1.0	0	0.5	160	20
		1.0	0	Unlim	154	0
Manned	Control	16	0	1.87	177	106
	Power	16	0	Unlim	129	0
	Power	16	6	1.5	136	17

## COVERED RADIATORS

Unmanned	Power	1.0	0	0.5	53.0	27.0
	Science	1.0	0	0.5	19.7	9.9
	Control*	-	-	-	-	-

\* The Control Modules radiators are not covered when  
unmanned

TABLE 4.4-5ALLOWABLE EQUIPMENT TEMPERATURES

	<u>Launch to Deploy.</u>	<u>Lunar Night</u>	<u>Lunar Day</u>
	<u>Deg.F</u>	<u>Deg.F</u>	<u>Deg.F</u>
Control Module Compartment Tray	30 to 130	0 Min	0 to 135
Power Module Compartment Tray	30 to 90	0 Min	0 to 90
Science Module Compartment Tray	30 to 130	-65 Min	-20 to 135
TV Camera	-20 to 130	-65 Min	-20 to 170
Crew Control Panel	0 to 130	-65 Min	-20 to 170
S-Band Directional Antenna Drives Elect.	20 to 130	-65 Min	-65 to 170 -20 to 170
Wheel Traction Drive Windings	20 to 130	-150 Min	-100 to 412
Oil	20 to 130	-60 Min	-50 to 250
Steer Actuator Assem Windings	20 to 130	-200 Min	-100 to 450
Oil	20 to 130	-60 Min	-50 to 250
Solar Array Drives	-20 to 130	-300 Min	-100 to 170
Cells	20 to 130	-300 Min	
Hazard Detector Sensor Drive	-20 to 130	-250 Min	-100 to 180
Elect	0 to 130	-65 Min	0 to 180
Solar Aspect Sensor	-20 to 130	-300 Min	-100 to 150

equipment temperature. Although not critical for cooling exterior surfaces of equipment should have an emittance of 0.85 or greater to provide more even temperature distribution.

Table 4.4-6 is a summary of the thermal system component characteristics for the designed compartments. These values have been computed on an independent component design basis to satisfy the necessary system performance.

The values shown are the result of various system level design iterations and are fully expected to be within achievable component design capability. In most cases, values have been correlated with Grumman experience in the LM and OAO space programs. The performance characteristics used for estimating the variable heat pipe designs were interpolated from data generated by the Grumman Heat Pipe Advanced Development Program.

The mounting tray temperatures can be verified from the parameters of the table. Using the sizing loads of the previous Subsection, the determined temperature rise for the heat pipes is:

15°F - Control Module

10°F - Power Module

10°F - Science Module

To provide the described equipment tray temperatures, the maximum radiator operating temperatures must be kept below:

120°F for Control Module

80°F for Power Module

125°F for Science Module

Knowing these design temperatures the required sizing loads and the selected radiator surface, we can solve for the radiator specific capacity and size. This is done for the three compartments at the subsolar condition.

The total net capacity ( $Q_N^o$ ) per ft<sup>2</sup> for each radiator can be defined by:

$$Q_N^o = (\text{total radiator emission at } T_o) - (\text{absorbed lunar incident radiation}) - (\text{absorbed solar incident radiation})$$

TABLE 4.4-6

## THERMAL COMPARTMENT CONTROL SYSTEM CHARACTERISTICS

ITEM	CONFIGURATION	QUANT.	SIZE	WEIGHT LB.	SIZING LOAD	THER. COND.	DEN. #/FT <sup>3</sup>
<u>Control Module</u>							
Heat Pipe	Figure 8	2 Loops	5/8 Dia Tube	2.6	120 Watts	4 W/Loop-°F	
Phase Chg Ht Sink	Integral to Tray		.028 Ft <sup>3</sup>	3.3	106 W-hrs		
Space Radiator	25°/Roof	2 Sections	4.4 Ft <sup>2</sup>	2.6(Incl. Support)	120 Watts		85
Insulation	Wrap Around Blanket	25 Layers	16.3 Ft <sup>2</sup>	.25			
Radio Isotope Heaters	Buttons	4	2.0 in <sup>3</sup> /ea	.8	8.1 Watts		
Mounting Tray	Aluminum Frame	1 Section	20" x 34.°	See Structure			
Dust Abatement and Control	H-Film Curtain	2 Sections	2.2 Ft <sup>3</sup> /ea	$\frac{1.2}{10.7}$			
<u>Power Module</u>							
Heat Pipe	Figure 8	8 Loops	$\frac{1}{2}$ Dia. Tube	2.8	130 Watts	1.6 W/Loop-°F	
Phase Change Heat Sink	Integral to Tray			1.7	64.5 W hrs		95
Space Radiator	Horizontal Roof		6.2 Ft <sup>2</sup>	3.1(Incl. Support)	124 Watts		
Insulation	Wrap Around Blanket	25 Layers	21.6 Ft <sup>2</sup>	.25			
Radio Isotope Heater	Buttons	2		.45	4.5 Watts		
Mounting Tray	Aluminum Frame	1 Section	35" x 27"	See Structure			
Dust Abatement & Control	H-Film Curtain	1 Section	6.5 Ft <sup>2</sup>	$\frac{1.0}{9.3}$			

TABLE 4.4-6 - Continued

ITEM	CONFIGURATION	QUANT.	SIZE	WEIGHT LB.	SIZING LOAD	THERM. COND.	DEN. #/FT <sup>3</sup>
<u>Science Module</u>							
Heat Pipe	Figure 8 Loop	1	1" Dia. Tube	.35	40 Watts	4.0 W/Loop°F	85
Phase Change Heat Sink	Integral to Tray	.003 Ft <sup>3</sup>		.30	9.8 W-Hrs		
Space Radiator	5° Roof	1	1.2 Ft <sup>2</sup>	.32	40 Watts		
Insulation	Wrap Around Blankets	25 Layers	8.3 Ft <sup>2</sup>	.15			
Radio Isotope Hours	Button	1	1.0 in <sup>3</sup>	.2	1.7		
Mounting Tray	Aluminum Frame	1	12" x 18"	See Structure			
Dust Abatement and Control	H-Film Curtain	1	13" x 20"	.6			
				<u>1.92</u>			

Expendables

System Total = 21.9 lbs.

Dust Cleaning Solution

(Est.) 5.0 lbs.

(Three Compartments)

Total Reported Sys Weight = 26.9 lbs.



TABLE 4.4-6 - Continued

ITEM	THERMAL CAPACITANCE	INFRA RED EMITTANCE ( $\epsilon$ )	SOLAR ABSORPTANCE ( $\alpha_s$ )	EFFECTIVE EMITTANCE ( $\epsilon_e$ )	TYPE	HEAT OF FUSION
<u>Contr. Module</u>						
Heat Pipe	Neg.	—	—	—	100:1 Variable Conduc- tance	—
Phase Chg Ht Sink	89.0 W-Hrs	—	—	—	136°F Melt.Point	32.3 W-Hrs/Lb
Space Radiator	Neg.	0.8 0.85	0.085 0.11	—	Silver-Teflon	—
Insulation	Neg.	0.8	0.8	0.011	23 Layer $\frac{1}{4}$ Mil Mylar 2 Layer $\frac{1}{2}$ Mil H-Film	—
Radio Isotope Heaters	Neg.	0.8	NA	—	Plutonium 238	—
Mounting Tray	Neg.	0.8	NA	—	—	—
Dust Abatement and Control	—	0.8	0.8	0.1 From Rad	Motor Pulley Linkage	—
<u>Power Module</u>						
Heat Pipe	Neg.	—	—	—	100:1 Variable Conduc- ting	—
Phase Change Heat Sink	64.5 W-hrs	—	—	—	89°F Melt Point	38. W-Hrs/Lb
Space Radiator	Neg.	0.8 0.85	1.085 0.11	—	Silver-Teflon	—
Insulation	Neg.	0.8	0.8	0.011	$\frac{1}{4}$ Mil Alum-Mylar 15 Mil H-Film	—
Radio Isotope Heaters	Neg.	0.8	NA	—	Plutonium 238	—
Mounting Tray	Neg.	0.8	NA	—	—	—
Dust Abatement and Control	—	0.8	0.8	0.1 From Rad	Motor Pulley	—

TABLE 4.4-6 - Continued

ITEM	THERMAL CAPACITANCE	INFRA RED EMISSIONANCE ( $\epsilon$ )	SOLAR ABSORPTANCE ( $\alpha_g$ )	EFFECTIVE EMISSIONANCE ( $\epsilon_e$ )	TYPE	HEAT OF FUSION
Science Module						
Heat Pipe	Neg	—	—	—	100:1 Variable Cond.	—
Phase Change Heat Sink	9.75 W-Hrs.	—	—	—	136°F Melt Pt	32.3 W-Hrs/Lb
Space Radiator	Neg	0.8 0.85	0.085 0.11	—	Silver-Teflon	—
Insulation	Neg	0.8	0.8	0.011	(23) $\frac{1}{4}$ Mil Mylar (2) .5 H-Film	—
Radio Isotope Heaters	Neg	0.8	NA	—	Plutonium 238	—
Mounting Tray	Neg	0.8	NA	—	—	—
Dust Abatement and Control	—	0.8	0.8	0.1 from Rad	Motor Pulley Linkage	—

where: radiator emission =  $\epsilon_R T_o^4$

$T_o$  = radiator temperature in  $^{\circ}R$

absorbed lunar incident rad =  $\epsilon_r F_{LR} \epsilon_L T_L^4$

absorbed solar incident rad =  $\alpha_s \cos \phi K_s$

and:  $T_L$  = Lunar temp at corresponding solar elevation,  $^{\circ}R$

$K_s$  = Solar Constant - 442 BTU/hr-ft<sup>2</sup>

$\phi$  = Angle of sun off the perpendicular to the receiving surface

$\alpha_s$  = Solar absorptance = 0.85 to 0.11 (silver Teflon radiator)

$F_{LR}$  = Configuration view factor, lunar surface to respective radiator surface

$\epsilon_R$  = IR radiator emittance = 0.80 (silver Teflon radiator)

$\epsilon_L$  = IR lunar surface emittance = 0.85

Figure 4.4-10 depicts the net radiator capacities per square foot at the worst case condition for each of the radiators.

Using the subsolar capacity and the sizing loads as defined in Section 4.4.5, the following radiator sizes are determined:

$$\text{Control Module} = \frac{120 \text{ Watts}}{27 \text{ Watts/ft}^2} = 4.4 \text{ ft}^2$$

$$\text{Power Module} = \frac{125 \text{ Watts}}{20 \text{ Watts/ft}^2} = 6.2 \text{ ft}^2$$

$$\text{Science Module} = \frac{40 \text{ Watts}}{33.2 \text{ Watts/ft}^2} = 1.2 \text{ ft}^2$$

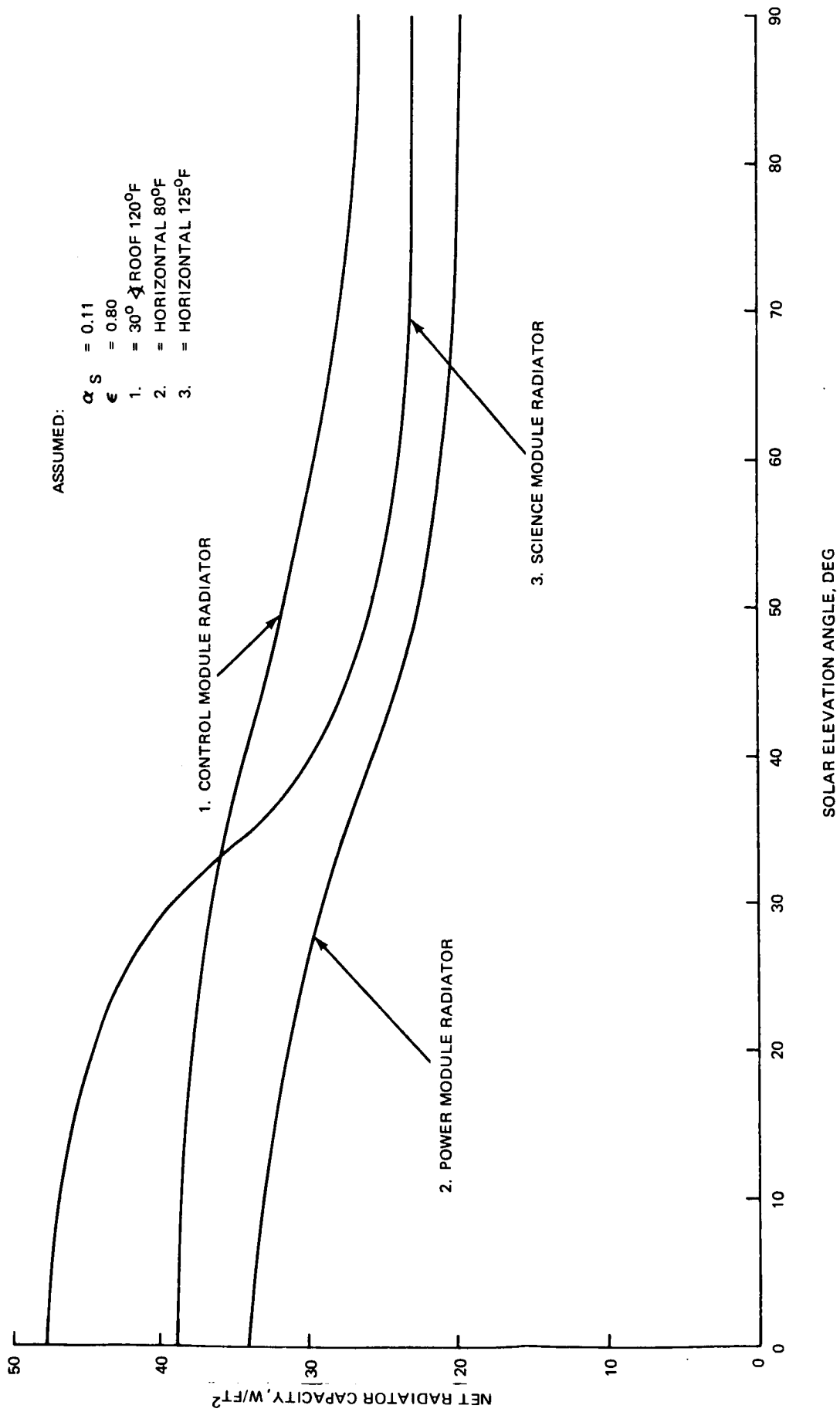


FIG. 4.4-10 RADIATOR CAPACITY

#### 4.4.6.2 Heat Storage

As related in Section 4.4.5.3, heat storage capability is required for some of the planned vehicle operations in order to stay within desired equipment temperature limits.

To provide adequate temperature regulation and rapid discharge capability, a constant temperature device was indicated and, hence, a phase change material (PCM) was selected. Assuming the PCM is adequately coupled to the equipment tray, suitable temperature control is only a function of quantity of material.

The design requirements for the PCM weight sizing were chosen as follows:

- Control Module Compartment - Manned 16 km/hr, 30 km  
Radiators Open  
Continuous Drive
- Power Module Compartment - Unmanned 1 km/hr, 0.5 km  
Drive with closed radiator  
Repeatative Cycles
- Science Module Compartment - Unmanned 1 km/hr, 0.5 km  
Drive with closed radiators  
Repeatiative cycles

Using the heats of fusion of the selected Transit Heat Binorganic salt solutions, weights were selected for each compartment. Table 4.4-6 reflects the PCM parameters and the allocated system weights. This particular material was chosen because of present availability, compatibility with aluminum structure and suitability for space instrument application. Present state-of-the-art depicts some PCM compounds with higher heats of fusion and further study in this area may improve the present weight allotments.

#### 4.4.6.3 Lunar Night

During lunar night, the vehicle is powered down to the level reflected in the dissipation summary, Table 4.4-3. The thermal system by virtue of the semi-passive variable conductance heat pipes automatically adjusts to a low conductance or minimum heat leak. To supplement heat pipe turn-down the radiator's curtains are also drawn. Since electrical power drain is very limited during the no-sunlight periods, it was important to minimize heat losses wherever possible and to employ non-electrical (isotope) heat sources for any additional energy.

Equipment compartment heat leaks or losses can be attributed to the following areas:

- o Insulation blankets
- o Heat pipe residual conductance
- o Cable penetrations
- o Conduction to structure

Table 4.4-7 is a summary of the predicted maximum heat leak rates for each of the compartments for the lunar night period. The heat flows were computed using the system parameters in Table 4.4-6 and applying the basic heat transfer equations. The residual heat pipe thermal conductance is obtained from the curves of predicted design performance in Fig. 4.4-11. The minimum compartment temperature limits allowable during night are those specified in Table 4.4-5.

TABLE 4.4-7 COMPARTMENT HEAT LEAK SUMMARY

	Cont'l Mod Comp't	Power Mod. Comp't	Sci. Mod. Comp't
Min. Temp., °F	0	0	-65
Insulation surface area Ft <sup>2</sup>	16.35	21.6	8.3
No. of heat pipes	2 figure, 8 loops	8 figure, 8 loops	1 figure, 8 loops
Cable penetrations	1	2	1
No. of structure tie points	4	5	3
Insulation effective emittance	.011	.011	.011
Lunar night radiator temp °F	-62	-65	-95
Lunar night equip. tray temp. °F	0	0	-65
$\dot{Q}_L$ Heat pipe losses, W	4.9	7.9	0.9
$\dot{Q}_L$ Blanket losses, W	4.0	5.3	2.0
$\dot{Q}_L$ Cable losses, W	3.5	3.8	0.5
$\dot{Q}_L$ Structure tie point losses, W	1.0	0.8	0.3
Total $\dot{Q}_L$ Losses, W	13.4	17.8	3.7

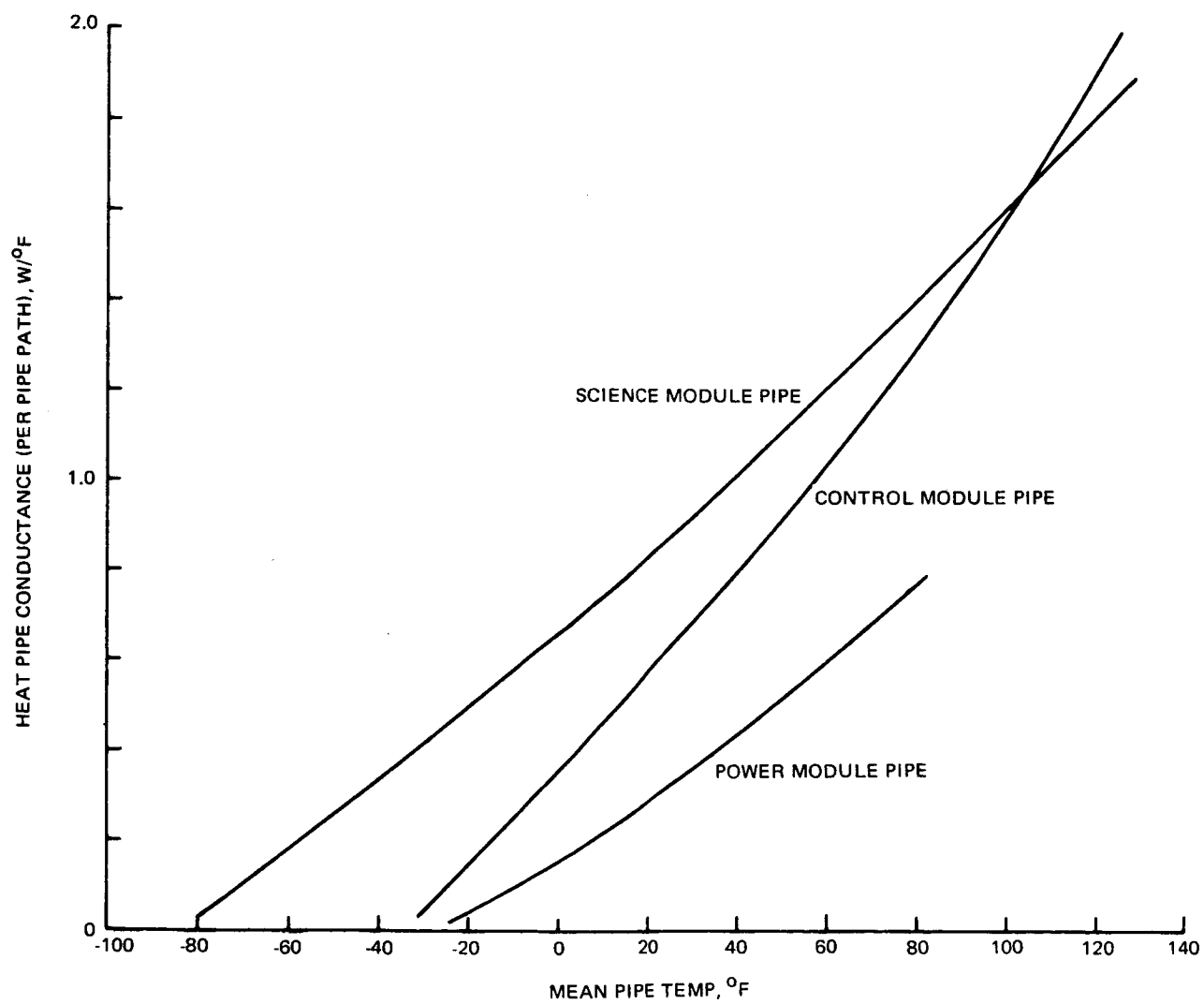


FIG. 4.4-11 VARIABLE HEAT PIPE DESIGN PERFORMANCE

These heat leaks were computed assuming  $-300^{\circ}\text{F}$  black body surroundings. The total losses less the expected lunar night electrical dissipation sets up the requirements for the additional heater power to maintain compartment lower limit temperature. It should be noted that careful consideration must be given to the detail design and manufacture of the equipment compartments to assure that their heat leak characteristics are acceptable. It is important to limit the total heat leak since the isotope heaters cannot be turned off and the thermal load must be carried by the system during daylight and subsolar operations.

#### 4.5 RELIABILITY

Reliability studies were conducted concurrent with selection of the preliminary design of the DLRV. These studies involved the following areas:

- o Failure Mode Effect and Criticality Analysis
- o Reliability Predictions and Establishment of Reliability Goals
- o Part Requirements
- o Hardware Test Requirements
- o Reliability Program Plan

This section contains the results of these studies. The Reliability Program Plan can be found in Volume VII Book I.

As a result of these studies, the following conclusions apply to the selected configuration:

- o No single point failure creates a safety hazard
- o Only four (4) failure modes result in the complete loss of mission capability for both the manned and unmanned mission
- o The configuration could be modified so that no failure mode would result in the complete loss of mission capability for a weight penalty of twenty four (24) pounds
- o The capability to operate in degraded modes is inherent
- o For the manned mission (five sorties) probabilities are:

	<u>Prediction</u>	<u>Goal</u>
Crew Safety	.999985	.99999
Full Mission Success	.996	.997
Degraded Mission Success	.9998	.9999



- o For the unmanned mission (one year)

	<u>Predicted</u>	<u>Goal</u>
Full Mission Success	.561	.640
Degraded Mission Success	.857	.900

- o The majority of the unreliability for full mission success is due to the failure of one of two batteries which would result in a degraded mission
- o AAP/LM Preferred Parts List is applicable to the DLRV program with the exception of certain radiation susceptible semi-conductor devices.

#### 4.5.1 Failure Mode Effect and Criticality Analysis

A Failure Mode Effect and Criticality Analysis (FME & CA) was conducted and is presented herein on the selected DLRV configuration. Throughout the entire Phase B study effort, a FME & CA was kept up-to-date in order to (1) systematically reduce the number of critically single point failures and (2) to provide a basis of comparison of the reliability for competing configurations. This effort has resulted in the selection of a DLRV configuration which contains no single point failures which would cause a safety hazard to the astronaut and contains only a bare minimum of single point failures which could result in complete loss of mission capability. This was accomplished within the weight limitation through the selection of equipments and subsystem configurations which inherently permit degraded modes of mission operation.

Table 4.5-1 contains a summary of all the critical failure modes as determined from the FME & CA effort. The FME & CA work sheets are contained in Table 4.5-2. Critical failure modes are defined as failures which would either cause a safety hazard or result in complete loss of mission capability. It should be noted that there are no failure modes which could create a safety hazard. Included in the table are recommendations to eliminate or alleviate the existing failure modes. These recommendations were not incorporated into the selected DLRV configuration during this study phase, due to weight limitations or insufficient design maturity to verify feasibility. In reviewing the results of this analysis, it can be concluded that the DLRV certainly has the inherent design potential to operate reliably for both the manned and unmanned mission.

TABLE 4.5-1  
SUMMARY OF CRITICAL EQUIPMENT FAILURE MODES

Subsystem	Equipment	Consequence	Recommendations
Electrical Power	None	-	-
Navigation	None	-	-
Mobility and Steering	Manual Drive Controller	During manned mission, if controller fails the astronaut must return the vehicle to the lander using the Emergency Controller. No further sorties should be taken since a failure of the Emergency Controller could jeopardize astronaut safety. Therefore, this failure would result in curtailment of all mission capability during manned missions.	Strongly recommend that an emergency mechanical brake be incorporated. Although no single point failure could be isolated which could prevent used of dynamic braking, it is advantageous to provide mechanical braking in the event of temporary loss of electrical power.
Communication and Instrumentation	Triplexer	Loss of all transmitted data causing complete loss of mission capability during both manned and unmanned missions.	None - Triplexer is a passive device and highly reliable.

TABLE 4.5-1 (Sheet 2 of 2)

Subsystem	Equipment	Consequence	Recommendations
Communication and Instrumentation	Data Handling Asbly. (pwr Sup, Osciltr., & Prog. Parts)	Loss of all transmitted data causing complete loss of mission capability during both manned and unmanned missions	During next study phase investigate feasibility of incorporating redundancy
Hazard Detection	Hazard Sensor & Hazard Processor	During unmanned mission, vehicle could only be driven at higher risk of encountering a hazard	Unless it can be proven that the TV camera can perform hazard detection functions at reduced vehicle speeds, all single point failures should be designed out of Hazard Sensor & Hazard Processor

In the paragraphs that follow, each subsystem will be discussed individually. The following basic assumptions were used in conducting the FME & CA:

- o Worst case conditions were used for both consequence and criticality classification of failure modes
- o Only one failure mode was considered at a time, i.e., multiple failure conditions are beyond the capability of this analysis
- o Due to lack of design detail (consistent with Phase B effort) in areas of wiring and fusing configuration, no shorting of power lines were considered. This is considered a design detail which will not effect results of the analysis
- o It was assumed that the manned mission would either be aborted or restricted if a failure occurred and a second failure would jeopardize astronaut safety
- o The following criticality definitions were used:
  - I - Exposure of the astronaut to safety hazards, e.g., astronaut walk-back, etc.
  - II A - Complete loss of mission capability
  - II B - Degraded mission capability
  - III - Full mission capability and crew safety

#### 4.5.1.1 Electrical Power Subsystem

Figure 4.5-1 shows the functional block diagram of the selected electrical power subsystem. The subsystem consists of two independent power supplies which are tied to two separate and isolatable busses. A crossfeed is provided to permit either power supply to feed both busses in the event of a failure in the other power supply. Each power supply consists of a half solar array with a shunt element and a battery with its own charger. The RTG provides power during the lunar night through two independent RTG No-Load Protectors and Converters, both capable of providing no-load protection and conversion at full load. Although only one RTG is utilized, high reliability is obtained in the inherent design which consists of series parallel strings of thermocouples and the failure of any one thermocouple will not significantly effect performance. The array drive contains redundant motors in both planes of motion.

The FME & CA of the electrical power subsystem is contained in Table 4.5-2. As indicated, no single failure will cause a hazard to the astronaut in the manned mission. In the event an equipment failure should occur (loss of a battery, battery charger, etc.) it is recommended that the vehicle be returned to walk-back range. Although full mission success would now be lost due to limited range,

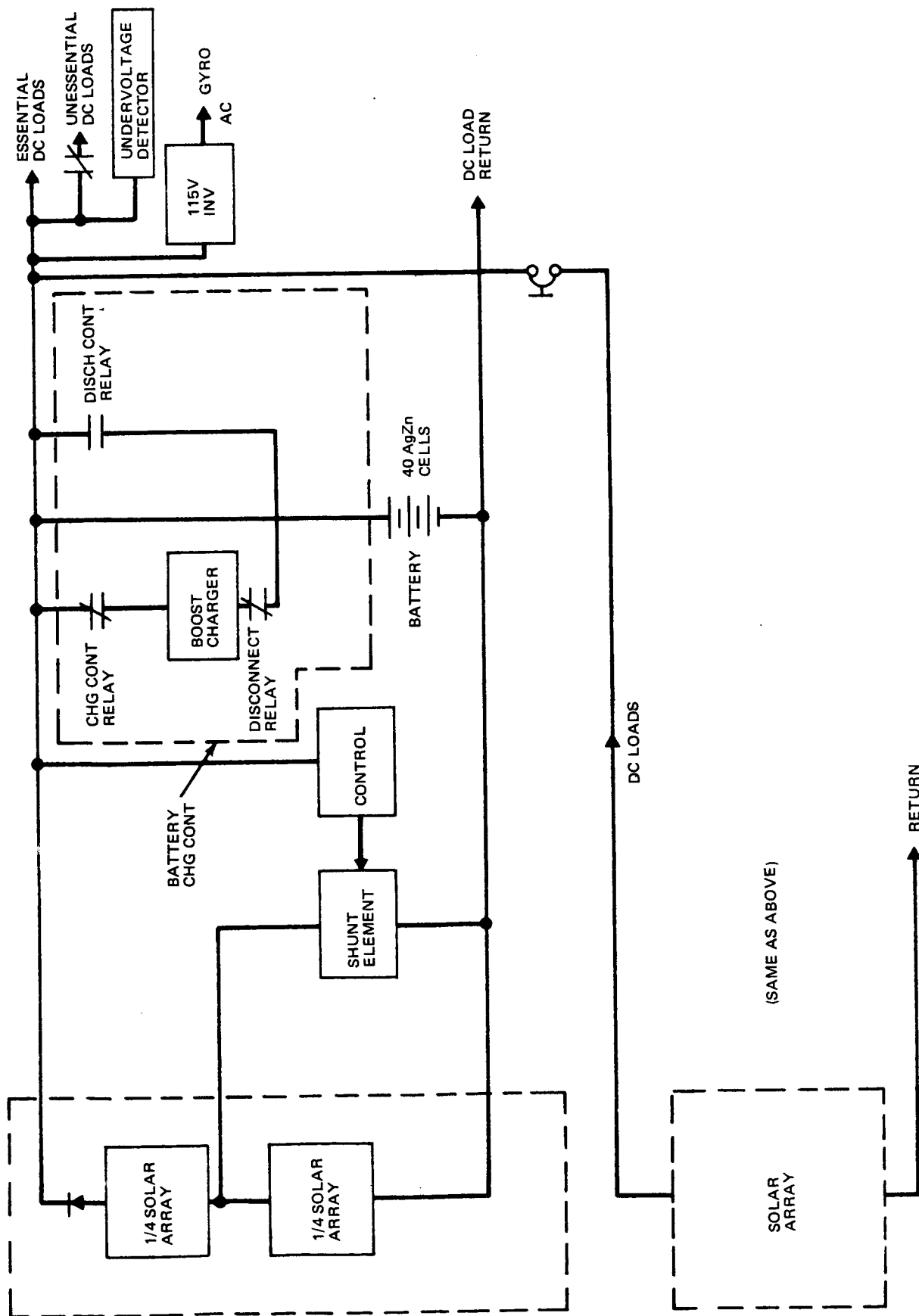


FIG. 4.5-1 ELECTRICAL POWER SUBSYSTEM BLOCK DIAGRAM

degraded mission capability remains. Since no failure mode exists which would cause a safety hazard or complete loss of mission capability, no recommendations for design change is warranted.

#### 4.5.1.2 Navigation Subsystem

Figures 4.5-2 and 4.5.3 show the functional block diagrams of the selected navigation subsystem for the manned and unmanned missions. In the manned mode, navigation capability is achieved through the use of a Solar Aspect Sensor (for direction) and wheel rotation transducers (for distance traveled). The navigation data is transmitted to the ground station for processing and transmitted to the vehicle for astronaut display. In the event of a navigation or communication equipment failure, a portable VHF Homing Receiver and a Sun Dial will assure the safe return of the astronaut to the lander. In the unmanned mode, continuous navigation is achieved using a directional gyro (Solar Aspect Sensor can be used as a back-up) and wheel rotation transducers. The TV camera is used to obtain landmark sightings and star pattern matchings for navigational update.

As can be seen by reviewing the FME & CA in Table 4.5-2, no single point failure exists which will create an astronaut hazard or cause complete loss of mission capability.

#### 4.5.1.3 Mobility and Steering Subsystem

Figure 4.5-4 shows the functional block diagram of the Mobility and Steering Subsystem. Mobility and steering is obtained through the use of motor driven wheels and an articulated steering joint. In the manned mode, the Manual Controller inputs the desired speed and direction into a Synchronizer (full circuit level redundancy) which resolves the commands into individual signals for the wheel motors and steering joint. An Emergency Controller is available as a back-up in the event that the Manual Controller should fail. In the unmanned mission, the Synchronizer is inputted via the normal uplink command link. Each motor can be decoupled in the event of a failure and mobility obtained on the remaining wheels. The Steering Joint Drive can also be decoupled and the vehicle driven in the "Differential Wheel Speed" mode. In this mode, vehicle steering is achieved by commanding different wheel velocities to adjacent wheels. Dynamic braking (all drive motors) is used to stop and slow down the vehicle.

The FME & CA of the mobility and steering subsystem is contained in Table 4.5-2. With the exception of a Manual Controller Failure, no signal point failure

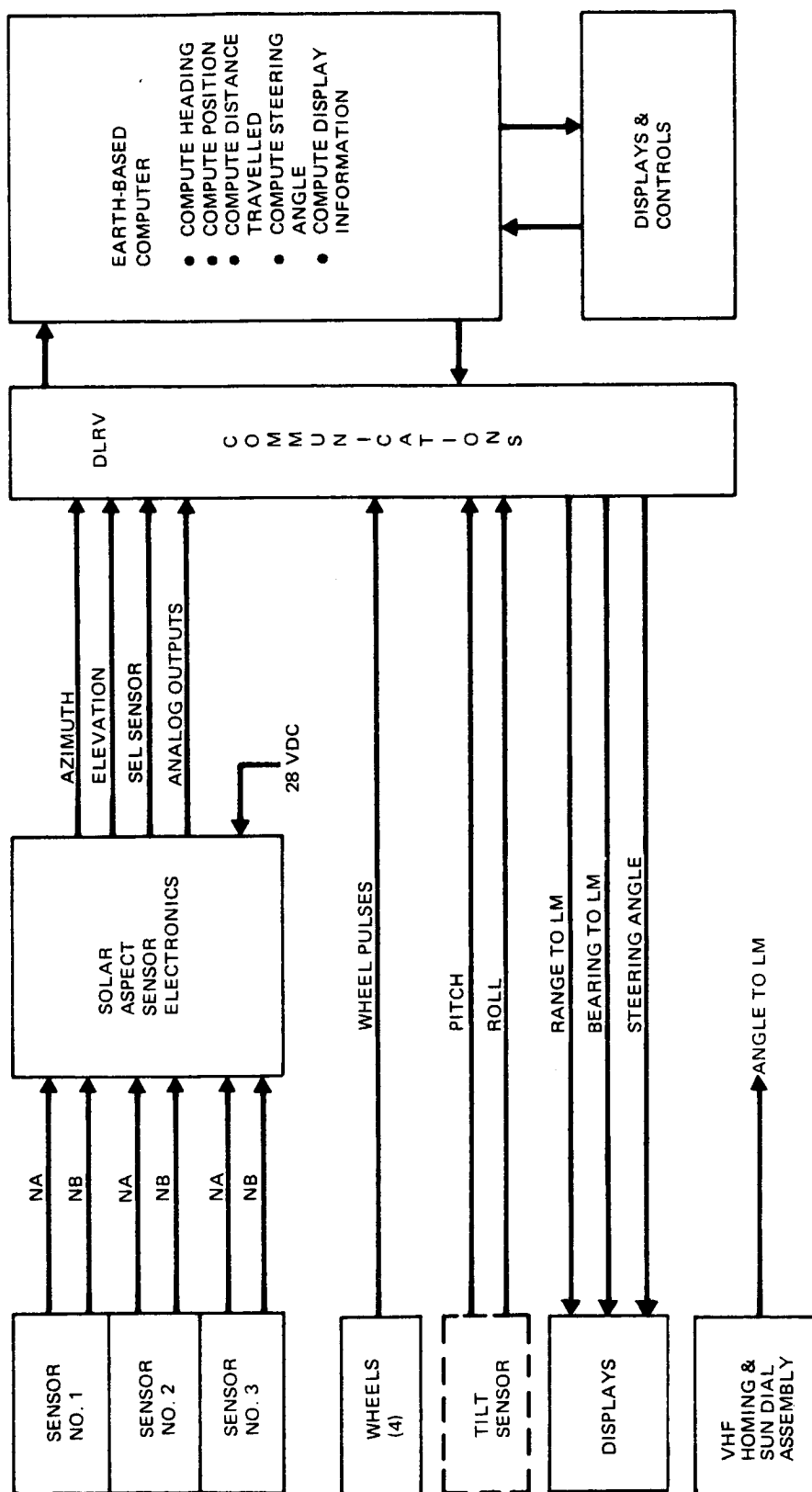


FIG. 4.5-2 NAVIGATION SUBSYSTEM - MANNED MODE

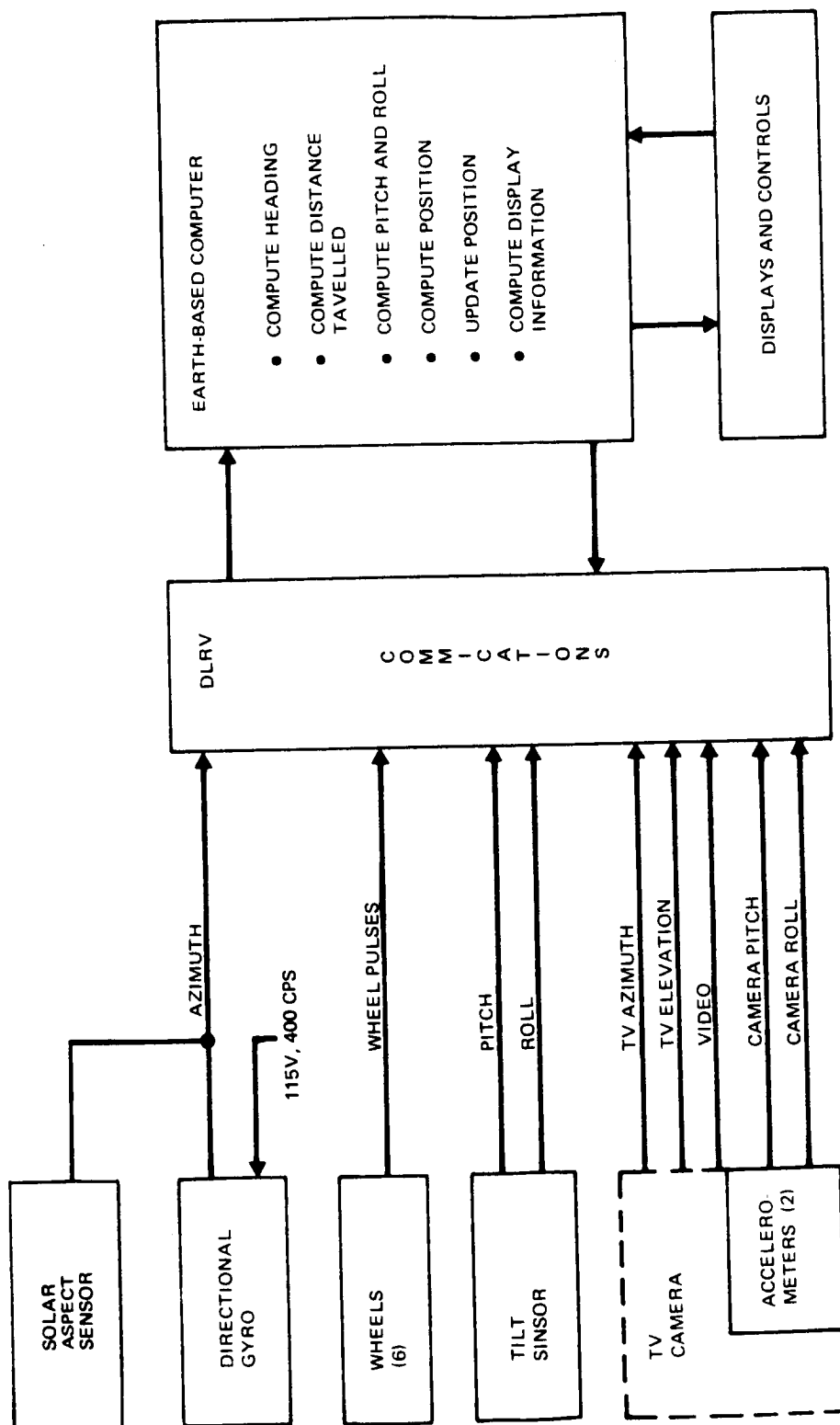


FIG. 4.5-3 NAVIGATION SUBSYSTEM - UNMANNED MODE



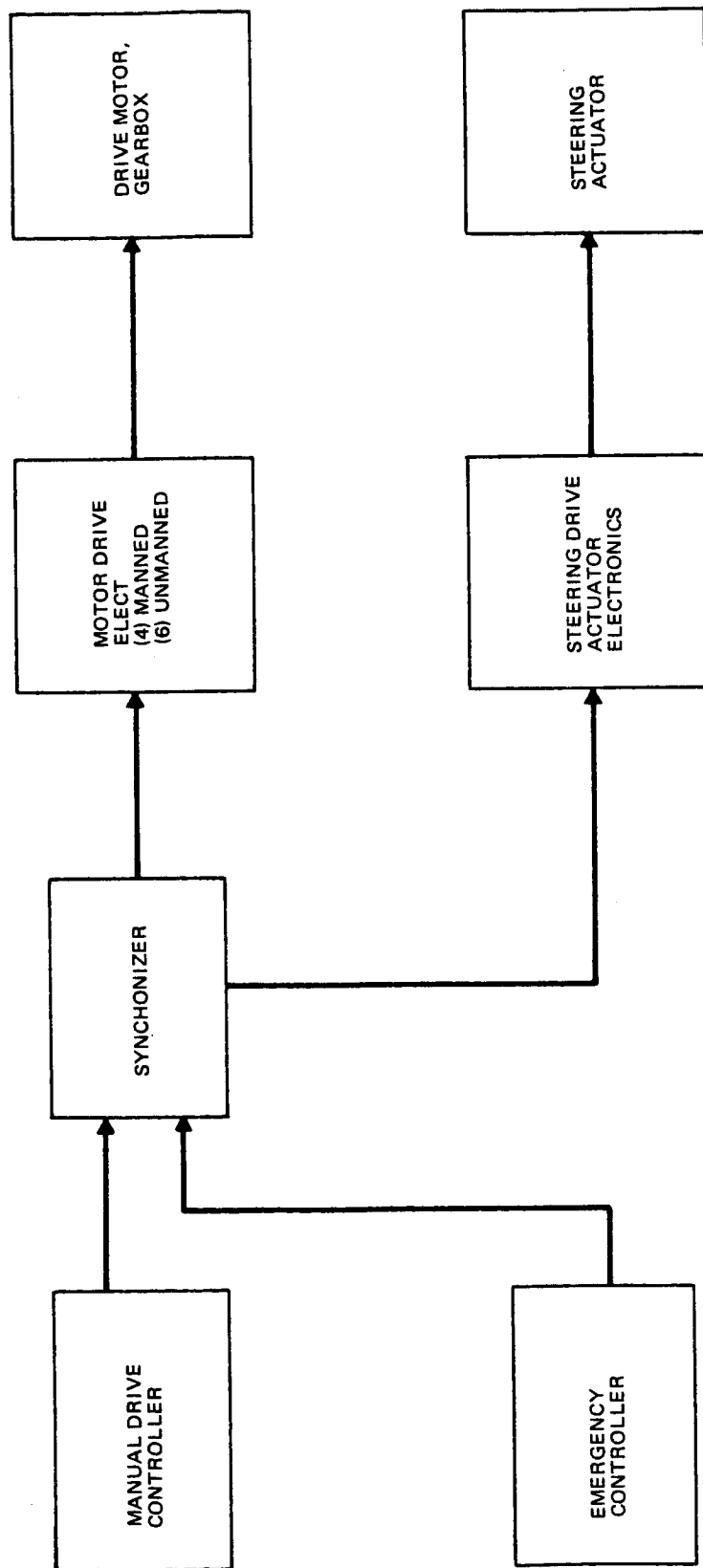


FIG. 4.5-4 MOBILITY AND STEERING BLOCK DIAGRAM

would cause a safety hazard or cause a complete loss of mission capability.

If the Manual Drive Controller should fail an abort would be initiated using the Emergency Controller. All future sorties should be cancelled since a second failure (to the Emergency Controller) would be a hazard to the astronaut. Sorties could be conducted within walk-back ranges if an emergency brake (mechanical) were incorporated into the design. This could eliminate the need for using a key type interlock. The emergency mechanical brake was considered during the study but was rejected because of weight considerations. It is highly recommended that mechanical brakes be further investigated to back-up the electrical braking system. Although no single point failure could presently cause loss of electrical braking capability, it would be good design practice to provide back-up braking which is independent of electrical power.

#### 4.5.1.4 Communication and Instrumentation Subsystems

Figure 4.5-5 contains a functional block diagram of the Communications and Instrumentation Subsystem. The vehicle can receive uplink commands via either the Omni or Steerable Antenna. Two receivers are continuously operating (one on Omni and one on Steerable) in conjunction with two paralleled Decoders which process uplink commands to the command distribution assembly for command execution. All critical commands will be made redundant in the Command Distribution Assembly. Downlink data is processed for transmission in the Data Handling Assembly. All critical data will be parallel channeled. The Narrow Band Transmitter contains two standby redundant transmitters for data transmission (except TV video). The Wide Band Transmitter also contains two standby redundant transmitters for TV video transmission and is capable of transmitting narrow band data in a contingency mode. Normal transmission is via the Steerable Antenna, however, degraded data transmission can be obtained using the Omni Antenna with TV video at a very low frame rate.

Table 4.5-2 contains the results of the FME and CA for the Communications and Instrumentation Subsystem. No single point failures exist which would cause a safety hazard. In both the manned and unmanned mission, the failure of the Triplexer would cause loss of all mission capability since science data will be lost. Since the Triplexer is essentially a passive device and extremely reliable, no recommendation for change is warranted. The power supply, oscillator, and pro-

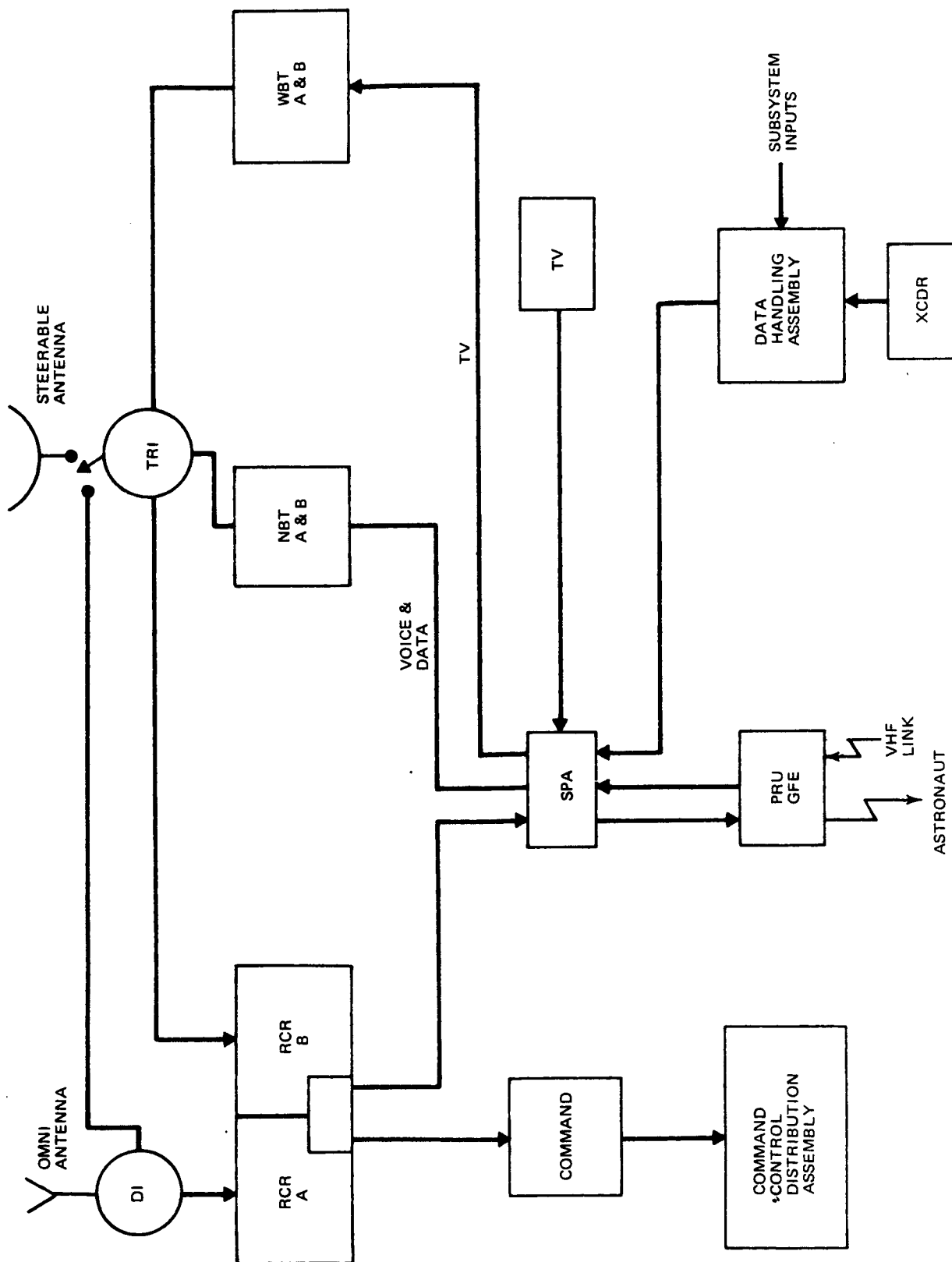


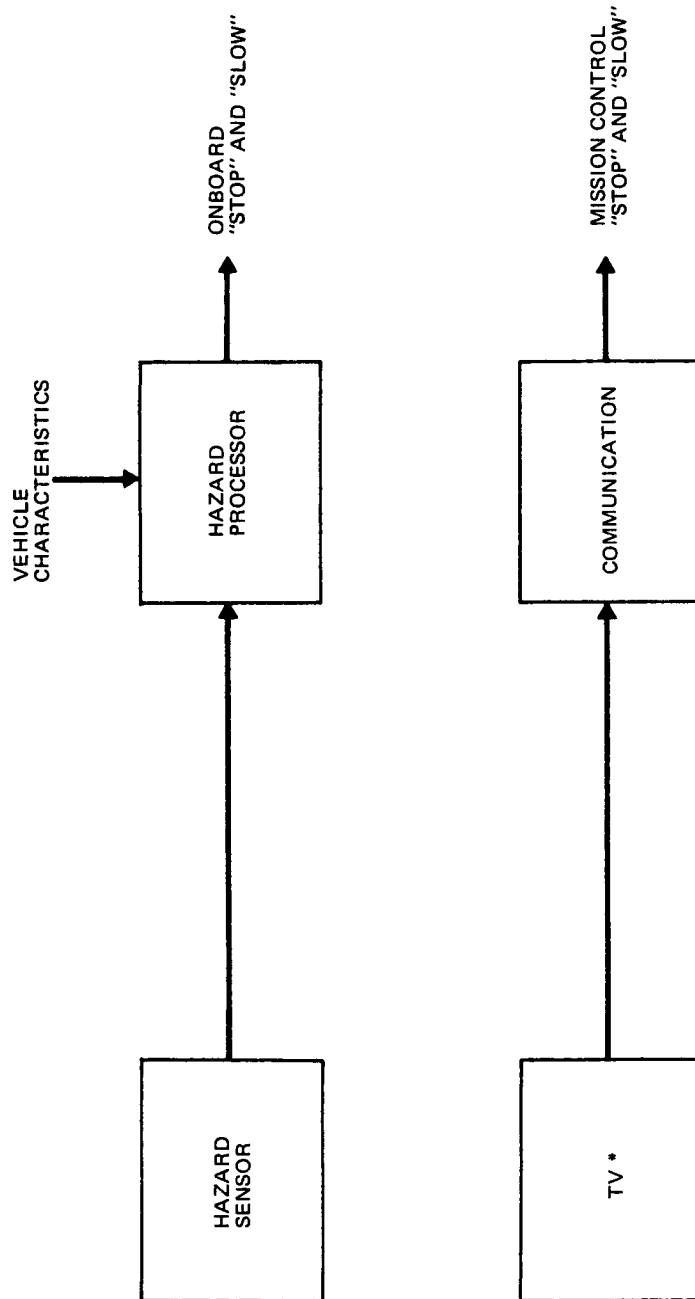
FIG. 4.5-5 COMMUNICATION/INSTRUMENTATION BLOCK DIAGRAM

grammer portions of the Data Handling Assembly are all single point mission success failures. These areas should be further investigated during the next study phase. It would appear feasible that redundancy could be incorporated without a great weight penalty.

#### 4.5.1.5 Hazard Detection Subsystem

Figure 4.5-6 contains a functional block diagram of the Hazard Detection Subsystem. Hazard detection is accomplished by scanning the area in front of the vehicle in search for a hazard using RF radar. These lunar terrain data items are input into the Hazard Processor along with other vehicle parameters such as: vehicle speed, vehicle attitude, etc. The processor then makes the decision (in real time) to either stop or slow down the vehicle. The TV camera will also scan the area in front of the vehicle for display and action at Mission Control.

The results of the FME and CA are shown in Table 4.5-2. There is a possibility that the vehicle could become immobilized causing complete loss of mission capability if a failure occurs in either the Hazard Sensor or Processor. The processor could be made completely redundant for only three (3) pounds. Presently, the Hazard Sensor has redundant receivers, redundancy in the output stage of the transmitter and a "spare" bi-level detector that can be utilized in the event of a detector failure. Unless it can be proven that the TV camera can perform the hazard detection function by itself (at reduced vehicle speeds), it is recommended that all single point failures be designed out of the Hazard Sensor and Processor.



\* NORMALLY NOT CONSIDERED PART OF HAZARD DETECTION SUBSYSTEM; INCLUDED HOWEVER, IN THIS ANALYSIS FUNCTION OF TV

FIG. 4.5-6 HAZARD DETECTION BLOCK DIAGRAM

DLRV FAILURE MODE & CRITICALITY ANALYSIS						
SUBSYSTEM: <u>A - POWER SUPPLY</u>						
EQUIPMENT	FAILURE MODE	CASE NO.	MANNED MISSION		UNMANNED MISSION	
			CONSEQUENCE OF FAILURE MODE	FAIL. CAT.	CONSEQUENCE OF FAILURE MODE	FAIL. CAT.
1. Solar Array	1. Short or open in solar array	A-1-1	Array consists of series - parallel arrangement of solar cells in strings. These strings are diode isolated from each other. Loss of a whole string will still permit full recharge of batteries between sorties.	III	Very slight degradation in array output, with no effect on mission success.	III
	2. Inability to orient array due to motor failure	A-1-2	Array is normally manually orientated, therefore no effect.	III	Redundant drive motors in both planes of motion are incorporated in design.	III
	3. Inability to orient array due to solar sensors failure	A-1-3	Same as Case A-1-2	III	Loss of array power during traverse. During recharge cycle array can be orientated via ground commands by observing shadow direction (from TV) and array output power (from telemetry).	IIB
2. Batteries	1. Loss of one battery	A-2-1	Failed battery can be switched off line and remaining battery will assure the safe return of the vehicle to the lander. Vehicle should be restricted to walk-back range for future sorties.	IIB	Failed battery can be switched off line and remaining battery will permit reduced operational capability.	II
3. Battery Charger(2)	1. Loss of one battery charger	A-3-1	Inability to properly charge one battery. Each battery has its own charger. Affected battery can be switched off line and vehicle should be restricted to walk-back range.	IIB	Inability to properly charge one battery. Each battery has its own charger. Affected battery can be switched off line and mission continued at reduced operational capability.	IIB
4. RTG	1. Loss of output	A-4-1	RTG contains series-parallel strings of thermocouples and the failure of any one thermocouple will not affect the vehicle.	III	RTG contains series-parallel strings of thermocouples. In addition the RTG outputs are parallel fed to redundant RTG converters separate busses. If only one thermocouple fails mission operation would not be affected.	III
5. RTG No-load Protection and Converter	1. Loss of no-load protection in one converter	A-5-1	RTG output is paralleled to two no-load protection circuits to assure protection of RTG in the event one circuit should fail.	III	Same as manned.	III

0312 7 00 00

GRUMMAN AIRCRAFT ENGINEERING CORPORATION

REPORT: File 4, J-2  
DATE  
CONF 76517 Sheet 1 of 3

FOLDOUT FRAME

FOLDOUT FRAME

II/I.4-131/132

DLRV FAILURE MODE & CRITICALITY ANALYSIS						
SUBSYSTEM: <u>A - POWER SUPPLY</u>						
EQUIPMENT	FAILURE MODE	CASE NO.	MANNED MISSION		UNMANNED MISSION	
			CONSEQUENCE OF FAILURE MODE	FAIL. CAT.	CONSEQUENCE OF FAILURE MODE	FAIL. CAT.
5. (continued)	2. Loss of output or inability to supply 28V due to failure in one converter	A-5-2	RTG output is paralleled to two converters, each capable of handling the full RTG load. Failed converter must be switched off-line.	III	Same as manned	III
6. Solar Array Regulator (2)	1. Loss of output or regulation due to one regulator failure.	A-6-1	Failure will result in loss of use of one battery and vehicle should be restricted to walk-back range.	IIB	Failure will result in the loss of use of one battery. Mission continued at reduced operational capability.	IIB
7. Busses	1. Short of one bus	A-7-1	Dual busses, which can be isolated, are incorporated in design. Vehicle should be restricted to walk-back range.	IIB	Dual busses which can be isolated, are incorporated in design. Loads are so arranged on each bus that a degraded mission can be conducted.	IIB
8. Inverter	1. Loss of output	A-8-1	Not required for manned mission.	III	Loss of gyro capability. Solar A spected Sensor can be used for direction during daylight.	IIB

0322 7 00 1A

REPORT: Table 4.5-2  
DATE  
CODE 76517 Sheet 2 of 9

GRUMMAN AIRCRAFT ENGINEERING CORPORATION

EOLDCUT FRAME

EOLDCUT FRAME

II/I.4-133/134

DLRV FAILURE MODE & CRITICALITY ANALYSIS						
SUBSYSTEM: <u>B - NAVIGATION</u>						
EQUIPMENT	FAILURE MODE	CASE NO.	MANNED MISSION		UNMANNED MISSION	
			CONSEQUENCE OF FAILURE MODE	FAIL. CAT.	CONSEQUENCE OF FAILURE MODE	FAIL. CAT.
1. Wheel Rotation Transducers (one per wheel)	1. Degradation or failure of one transducer	B-1-1	Degraded or failed transducer is discriminated (on ground), therefore neither range nor bearing is significantly effected.	III	Same as manned	III
	1. Loss of output	B-2-1	Loss of vehicle position capability. Use of Sun Dial and VHF homing will assure safe return to ELM. Vehicle should be restricted to LOS.	IIB	In the unmanned mode Solar Aspect Sensor is a back-up for the gyro.	III
	2. Wrong output	B-2-2	Periodic checks will be necessary to verify that Solar Aspect Sensor and VHF bearing to ELM agree. If they disagree the vehicle can be pointed to the sun and the ground can verify sensor performance by comparing the measured bearing angle with bearing angle as determined from vehicle position. If they don't agree the sensor is faulty and vehicle position capability is lost. Sun Dial and VHF homing will assure safe return to ELM. Vehicle should be restricted to LOS.	IIB	Same as Case B-2-1	III
3. VHF Homing Receiver	Loss of output	B-3-1	Periodic checks will verify that VHF receiver is inoperative. Vehicle should be restricted to LOS.	IIB	Not required for unmanned mission.	III
	2. Wrong output	B-3-2	Solar Aspect Sensor and VHF bearing to ELM will disagree. By pointing vehicle to sun and comparing measured bearing angle with the angle as determined by vehicle position, it will be determined that the VHF receiver is not operating properly. Vehicle should be restricted to LOS.	IIR	Not required for unmanned mission.	III
4. TV Camera (as related to nav. function only)	1. Loss of video or failure of camera gimbal drive	B-4-1	Not applicable to manned mission	III	Loss of vehicle position and heading update capability. Mission can continue with severe degradation in vehicle position.	IIB

0322 7 00 14

REP'D: Taole 4.5-2  
DATE  
CONF 7/85/7 Sheet 3 of 9

GRUMMAN AIRCRAFT ENGINEERING CORPORATION



DLRV FAILURE MODE & CRITICALITY ANALYSIS

SUBSYSTEM: B - NAVIGATION (CONTINUED)

EQUIPMENT	FAILURE MODE	CASE NO.	MANNED MISSION		UNMANNED MISSION	
			CONSEQUENCE OF FAILURE MODE	FAIL. CAT.	CONSEQUENCE OF FAILURE MODE	FAIL. CAT.
5. Accelerometers (2 on TV camera)	1. Loss of output	B-5-1	Not applicable to manned mission	III	Degradation of vehicle position and heading update. Vehicle deck mounted accelerometers can be used with the commanded camera gimbal angle to determine camera angle. Distortion of camera staff will cause slight error.	IIB
	2. Wrong output	B-5-2	Not applicable to manned mission	III	This failure would cause a significant difference in the gyro and TV update heading and position. A significant difference in camera position by using the camera mounted and deck mounted accelerometers will isolate the failure to the TV mounted accelerometers. Degraded vehicle position and heading updates can be achieved by using the deck mounted accelerometers.	IIB
6. Accelerometers (2 on vehicle deck)	1. Loss of output	B-6-1	Not applicable to manned mission	III	Degradation of continuous vehicle position and heading data. More frequent update using TV camera will be necessary.	III
	2. Wrong output	B-6-2	Not applicable to manned mission	III	During updated differences in position and heading will be significant. In addition, difference in data from TV accelerometer and deck accelerometer will be great. Accelerometer should be switched out and more frequent TV updates performed.	III
7. Sun Dial	1. No failure modes are anticipated	B-7-1	See failure mode	III	Not required for unmanned mission	III
8. Gyro	1. Loss of output	B-8-1	Not applicable to manned mission	III	Use of Solar Aspect Sensor and angle transducer between vehicle joints will permit continuous navigation, however vehicle will be restricted to daylight operation only.	III

0312 7 08 114

GRUMMAN AIRCRAFT ENGINEERING CORPORATION

REPORT Table 4.5-2  
DATE  
CODE 76517 Sheet 4 of 9

FOLDOUT FRAME

FOLDOUT FRAME

II/1.4-137/138

DLRV FAILURE MODE & CRITICALITY ANALYSIS

SUBSYSTEM: B - NAVIGATION (CONTINUED)

EQUIPMENT	FAILURE MODE	CASE NO.	MANNED MISSION		UNMANNED MISSION	
			CONSEQUENCE OF FAILURE MODE	FAIL. CAT.	CONSEQUENCE OF FAILURE MODE	FAIL. CAT.
8. Gyro (continued)	2. Wrong output	B-8-2	Not applicable to manned mission	III	This failure would cause a significant difference in the gyro and TV update heading and position. Use of Scalar Aspect Sensor and angle transducers between vehicle joints will permit continuous navigation however vehicle will be restricted to daylight operation only.	III

Q332 7 88 NM

GRUMMAN AIRCRAFT ENGINEERING CORPORATION

REPORT: Table 4.5-2  
DATE: Sheet 5 of 9  
CODE: NAS-7

FOLDOUT FRAME

FOLDOUT FRAME

II/I.4-139/140

DLRV FAILURE MODE & CRITICALITY ANALYSIS						
SUBSYSTEM: C - Mobility & Steering Subsystem						
EQUIPMENT	FAILURE MODE	CASE NO.	MANNED MISSION		UNMANNED MISSION	
			CONSEQUENCE OF FAILURE MODE	FAIL. CAT.	CONSEQUENCE OF FAILURE MODE	FAIL. CAT.
1. Manual Drive Controller	1-No output, wrong output, or stuck throttle	C-1-1	Astronaut can immediately brake vehicle by using Emergency Controller. This disables the Manual Drive Controller. Safe return can be accomplished using the Emergency Controller to drive the vehicle. No further sorties should be attempted.	II A	Not required for unmanned mission	III
2. Synchronizers	1-No output or wrong output	C-2-1	Complete internal redundancy is incorporated into the Synchronizer to preclude failure.	III	Same as manned	III
3. Motor Drive Electronics (one for each motor)	1-No output or wrong output to one motor	C-3-1	Affected motor will either cease to function or will be torqued improperly causing vehicle to veer. This can be compensated by moving the Manual Drive Controller in the opposite direction. The affected wheel can be disengaged and the vehicle driven at reduced speeds. Vehicle should be restricted to walkback range.	II B	Affected motor can be disengaged and the vehicle driven on remaining motors (5).	III
4. Drive Motor/gearbox (one for each wheel)	1-No output, wrong output to one wheel	C-4-1	Same as Case No. C-3-1	II B	Same as Case No. C-3-1	III
5. Steering Actuator Drive Electronics	1-No output or wrong output	C-5-1	The steering joint actuator can be disengaged and the Synchronizer put in the differential wheel speed mode. In this mode vehicle mobility is achieved without the need for a steering actuator. Vehicle should be restricted to walk-back range.	II B	Steering actuator can be disengaged and vehicle traversed in the differential wheel speed mode.	III
6. Steering Actuator	1-No output or binds	C-6-1	Same as Case No. C-5-1	II B	Same as Case No. C-5-1	III
7. Emergency Controller	1-Loss of output	C-7-1	No effect since it is only required to function in the event of another failure.	III	Not required for unmanned mode	III

0322 7 00 11

FOLDOUT FRAME

FOLDOUT FRAME 2

DLRV FAILURE MODE & CRITICALITY ANALYSIS						
SUBSYSTEM: D - COMMUNICATIONS & INSTRUMENTATION SUBSYSTEM						
EQUIPMENT	FAILURE MODE	CASE NO.	MANNED MISSION		UNMANNED MISSION	
			CONSEQUENCE OF FAILURE MODE	FAIL. CAT.	CONSEQUENCE OF FAILURE MODE	FAIL. CAT.
1. Steerable Antenna	1-Drive failure	D-1-1	Loss of normal data and voice transmission. All downlink data, except survey staff data can be transmitted via omni antenna. Steerable antenna can also be manually orientated to permit normal data transmission during science stop.	III	Loss of normal data and TV video transmission for visual display during remote driving. Degraded mission can be conducted by transmitting TV video at low frame rate via omni antenna while vehicle is stopped. Vehicle can then be traversed a short distance and the vehicle stopped again for TV video.	II B
	2-Loss of lock due to terrain interference	D-1-2	No effect - movement of vehicle will restore capability.	III	Uplink is continuously sensed and when lost, vehicle is automatically stopped. Omni antenna is on a 20 ft. staff to avoid terrain interference so that vehicle can retrace its path and then take an alternate course.	III
2. Omni Antenna and Diplexer	1-Structural failure	D-2-1	All data can be received and transmitted via steerable antenna.	III	Same as manned mission	III
3. Antenna Selection Switch	1-Inability to switch to steerable antenna	D-3-1	Loss of normal data, voice and TV transmission capability associated with science experiments. Low frame rate TV transmission is possible via omni antenna.	III	Same as Case No. D-1-1	II B
	2-Inability to switch to omni antenna	D-3-2	Same as Case No. D-2-1	III	All data can be transmitted via steerable antenna.	III
4. Triplexer	1-Loss of output	D-4-1	Loss of all data transmitted and received. Vehicle is reduced to mobility aid. Astronaut can return to lander using Sun Dial and VHF homing receiver.	II A	Loss of all data transmitted and received resulting in complete loss of mission	II A
5. Wire Band Transmitters (2)	1-Loss of one transmitter	D-5-1	No effect since redundant transmitter can be switched in.	III	Same as manned	III
6. Narrow Band Transmitters (2)	1-Loss of one transmitter	D-6-1	No effect since redundant transmitter can be switched in.	III	Same as manned	III
7. Signal Processor	1-Loss of output	D-7-1	No effect - contains part redundancy.	III	Same as manned	III

0312 7 44 44

GRUMMAN AIRCRAFT ENGINEERING CORPORATION

REPORT: Table 4.5-2  
DATE  
CODE 265 : Sheet 7 of 9

FOLDOUT FRAME

FOLDOUT FRAME 2

DLRV FAILURE MODE & CRITICALITY ANALYSIS						
SUBSYSTEM: D - COMMUNICATIONS & INSTRUMENTATION SUBSYSTEM						
EQUIPMENT	FAILURE MODE	CASE NO.	MANNED MISSION		UNMANNED MISSION	
			CONSEQUENCE OF FAILURE MODE	FAIL. CAT.	CONSEQUENCE OF FAILURE MODE	FAIL. CAT.
8. Receiver (2)	1-Loss of one	D-8-1	No effect since two independent receivers are available.	III	Same as manned.	III
	1-Loss of output of one decoder	D-9-1	No effect since two decoders are always paralleled which assures command decode function.	III	Same as manned	III
9. Command Decoder (2)	2-Inadvertant command output when not required	D-9-2	The decoder is designed so that the chance of inadvertant execution is one in $10^{-23}$ . If this condition does exist the effected decoder can be disabled.	III	Same as manned.	III
	1-Loss of output	D-10-1	All critical outputs will have to be made redundant (relay).	III	Same as manned.	III
10. Command Distribution Assembly	2-Inadvertant output	D-10-2	Two relay drivers must be commanded before a command can be executed.	III	Same as manned.	III
	1-Loss of power supply, oscillator, or programmer portion	D-11-1	Loss of all transmitted data (except TV). Vehicle is reduced to mobility aid. Astronaut can safely return to lander using VHF homeing and Sun Dial.	II A	Loss of all transmitted data (except TV). Complete loss of mission.	II A
11. Data Handling Assembly	2-Loss of a single channel	D-11-2	None - since all critical data are paralleled through different channels.	III	Same as manned.	III

0332 7 00 NW

REPORT: Table 4.5-2  
DATE:   
CODE: PAS-7 Sheet 8 of 9

GRUMMAN AIRCRAFT ENGINEERING CORPORATION

FOLDOUT FRAME

FOLDOUT FRAME 2

DLRV FAILURE MODE & CRITICALITY ANALYSIS						
SUBSYSTEM: E - HAZARD DETECTION						
EQUIPMENT	FAILURE MODE	CASE NO.	MANNED MISSION		UNMANNED MISSION	
			CONSEQUENCE OF FAILURE MODE	FAIL. CAT.	CONSEQUENCE OF FAILURE MODE	FAIL. CAT.
1. TV Camera (As related to remote driving only)	1-Loss of video	E-1-1	Not required for manned mission	III	Severe reduction in mission capability. As a contingency mode of operation facsimile camera (part of experiment package) can be used by stopping vehicle and taking a picture and then traversing. This iterative operation will reduce the average traverse velocity severely.	II B
2. Hazard Sensor	1-Any failure in sensor	E-2-1	Not required for manned mission	III	Severe reduction in mission capability with the possibility that the vehicle could be immobilized causing complete loss of mission. As a contingency mode of operation the Hazard Detection equipment can be disabled, the vehicle speed reduced, and the TV used to visually detect hazards. In so doing a risk is taken in that not all hazards can be determined, e.g. soft soil condition.	II A/ II B
3. Hazard Processor	1-Any failure	E-3-1	Not required for manned mission	III	Same as Case No. E-2-1	II A/ II B

0322 7 00 148

GRUMMAN AIRCRAFT ENGINEERING CORPORATION

REPORT: Table 4.3-2  
DATE  
CODE 74512  
Sheet 9 of 9

FOLDOUT FRAME

0

FOLDOUT FRAME

II/I.4-147/148

The results of the FME & CA were used as the basis for determining the reliability models for each subsystem. Predictions were calculated using the reliability math models and the associated equipment failure rates in Table 4.5-5. These subsystem predictions were then combined to obtain the overall estimates. In preparing the reliability models for mission success in the manned mode, consideration was given to the probable alternate mission operations that should be inacted to protect astronaut safety in the event a second failure could be critical. This has a tendency of reducing mission success probability, however it does resemble the real use situation. The assumptions that were used in classifying equipment failures as either full mission success, degraded mission capability, or complete loss of mission success; can best be evaluated by the reader by referring to the associated FME & CA worksheet. These classifications were based upon engineering judgement. Reliability predictions were calculated assuming that the failure rate remains constant for the duration of its useful life. It was also assumed that equipment failure rates are negligible when the equipment is non-operative and therefore was not considered in the analysis.

The manned mission consists of five EVA's separated by four recharge cycles. A typical EVA will consist of the following activities:

Ingress	10 min.
Checkout	10 min.
Traverse	2 hr.
Science Stops	1.73 hr.
Egress	10 min.

The battery recharge cycle is eight (8) hours in duration for the manned mission. Based upon the unmanned Reference Mission, 4730 hours is considered unusable time due to lunar nights and poor lighting conditions. Of the remaining 4030 hours, 1050 hours has been allocated to major sites, 1050 hours to traverse operations, 1263 hours to science stops during traverses, and 667 hours has been designated as surplus time suitable for battery recharging. The time at major sites are anticipated to be divided into 40% of the time for driving and 60% for science stops. Therefore the unmanned mission can be divided as follows:

Lunar Night (including poor lighting)	4730 hr.
Traverse (including driving at major sites)	1470
Science Stops (excluding driving)	1893
<u>Recharging (assumes all surplus time)</u>	<u>667</u>
Total Unmanned Mission (1 year)	8760

TABLE 4.5-4 - RELIABILITY GOALS

	ELECTRICAL POWER	NAVIGATION	MOBILITY AND STEERING	COMMUNICATIONS & INSTRUMENTATION	HAZARD DETECTION	DLRV SYSTEM
<u>MANNED MISSION</u>						
- Crew Safety	.999995	.999995	.999995	1.00	1.00	.99999
- Full Mission Success	.9985	.9999	.999	.9995	1.00	.997
- Degraded Mission Success	.999995	.999995	.999995	.99990	1.00	.9999
<u>UNMANNED MISSION</u>						
- Full Mission Success	.800	.955	.965	.900	.960	.640
- Degraded Mission Success	.980	.9998	.965	.975	.980	.900



TABLE 4.5-3 - RELIABILITY PREDICTIONS

	ELECTRICAL POWER	NAVIGATION	MOBILITY AND STEERING	COMMUNICATIONS & INSTRUMENTATION	HAZARD DETECTION	DLRV SYSTEM
<u>MANNED MISSION (5 SORTIES)</u>						
Crew Safety	.999995	.999995	.999995	1.000	1.000	.999985
Full Mission Success	.99856	.999885	.998200	.999500	1.000	.996145
Degraded Mission Success	.999995	.999995	.999995	.99980	1.000	.999785
<u>UNMANNED MISSION (ONE YEAR)</u>						
Full Mission Success	.748	.955	.965	.867	.940	.561
- Lunar Night ( $t_d$ )	.994	1.000	1.000	.996	1.000	.990
- Traverse ( $t_{tr}$ )	.905	.955	.965	.942	.940	.738
- Science Stop ( $t_{ss}$ )	.874	1.000	1.000	.925	1.000	.808
- Recharge ( $t_r$ )	.953	1.000	1.000	.999	1.000	.952
<u>DEGRADED MISSION SUCCESS</u>						
(TOTAL)	.975	.9998	.965	.951	.957	.857
- Lunar Night ( $t_d$ )	.994	1.000	1.000	.996	1.000	.990
- Traverse ( $t_{tr}$ )	.993	.9998	.965	.980	.957	.898
- Science Stop ( $t_{ss}$ )	.989	1.000	1.000	.975	1.000	.964
- Recharge ( $t_r$ )	.999	1.000	1.000	.999	1.000	.998

#### 4.5.2 Reliability Prediction

Reliability predictions have been generated for both the manned and unmanned missions. These predictions give a general indication of vehicle performance and also highlight specific areas of unreliability due primarily to lack of redundancy or acceptable back-up modes. As is the case with all such predictions they should be viewed on a relative basis and will not necessarily project actual vehicle performance.

Reliability math models have been developed to predict the following:

- o Probability of Astronaut Safety
- o Probability of Full Mission Success
- o Probability of Degraded Mission Capability

The results of the reliability predictions are shown in Table 4.5-3. Based upon these results it can be concluded that the manned mission (five sorties) represents no problem. The unmanned mission (one year) has a high probability of conducting at least a degraded mission (.857) and a probability of .561 for obtaining full mission success for one year. As stated previously full mission success implies no mission degradation. The major source of unreliability is the Electrical Power Subsystem (.748). This is primarily due to the effect of a failure of one of two batteries which would result in a degraded mission since the average traverse speeds would be reduced by about one-half. As an alternative, a third battery could be incorporated into the system which would increase full mission success probability to about .750. A weight penalty of 25 pounds would also have to be accepted if the third battery were incorporated. Because of weight constraints, the degraded mode of operation was accepted for the selected configuration. Based on the reliability predictions which were calculated during this study, reliability goals were established for both the subsystems and the DLRV system and are included in Table 4.5-4. These goals were approximately the same value as the predictions except in those areas where the results of the FME & CA (Table 4.5-1) indicated that recommendations for design change should be incorporated in order to eliminate or alleviate an undesirable failure mode. The system goals are included within the system specification and the subsystem goals can be apportioned down to the hardware level for eventual incorporation into equipment specifications.

FOLDOUT FRAME

TABLE 4.5-5 EQUIPMENT FAILURE RATES

CASE NO.	EQUIPMENT NAME	FAILURE MODE	FAILURE RATE (106 HOURS) PER EQUIPMENT
<u>ELECTRICAL POWER</u>			
A-1-1	Solar Array	Short/Open	0.0
A-1-2	Solar Array	Motor Failure	10.0
A-1-3	Solar Array	Failure of Solar Sensors	0.5
A-2-1	Battery (2)	Loss of One Battery	30.0
A-3-1	Battery Charger (2)	Loss of One Charger	5.0
A-4-1	RTG	No Output	0.2
A-5-1	RTG No-Load Protection	Loss of No-Load Protection in One Converter	2.0
A-5-2	RTG No-Load Protection	Loss 28V Converter	3.0
A-6-1	Solar Array Regulator	Loss of One Regulator	1.0
A-7-1	Busses	Short/Open	1.0
A-8-1	Inverter	No Output	2.0
<u>NAVIGATION</u>			
B-1-1	Wheel Rotation Xducer	Degradation/Failure	10.0
B-2-1	Solar Aspect Sensor	Loss of Sensor Output	3.0
B-2-2	Solar Aspect Sensor	Faulty Output	3.0
B-3-1	VHF Homing Receiver	Loss of Output	.01
B-3-2	VHF Homing Receiver	Faulty Output	.01
B-4-1	TV Camera	Loss of Video or Failure of Gimbal Drive	.12
B-5-1	Accelerometer (2/TV Camera)	Loss of Output	7.5
B-5-2	Accelerometer (2/TV Camera)	Faulty Output	7.5
B-6-1	Accelerometer (2/Vehicle Deck)	Loss of Output	7.5
B-6-2	Accelerometer (2/Vehicle Deck)	Faulty Output	7.5
B-7-1	Sun Dial	No Known Failure Modes	0.0
B-8-1	Gyro	Loss of Output	10.0
B-8-2	Gyro	Faulty Output	101.8
<u>MOBILITY &amp; STEERING</u>			
C-1-1	Manual Drive Controller	No Output/Faulty Output Jammed Throttle	5.0
C-2-1	Synchronizer	No Output/Faulty Output	15.0
C-3-1	Motor Drive Electronics (One per Wheel)	No Output/Faulty Output	5.0
C-5-1	Drive Motor/Gear Box	No Output/Faulty Output	12.0
C-5-1	Steering Actuator Drive Electronics	No Output/Faulty Output	3.0
C-6-1	Steering Actuator	No Output/Binds	1.0
C-7-1	Emergency Controller	Loss of Output	2.5
<u>COMMUNICATION &amp; INSTRUMENTATION</u>			
D-1-1	Steerable Antenna	Drive Failure	25.7
D-1-2	Steerable Antenna	Loss of Lock	25.7
D-2-1	Omni Antenna	Structural Failure	0.2
D-3-1	Antenna Selector Switch	Inability to Switch to Steerable	0.01
D-3-2	Antenna Selector Switch	Inability to Switch to Omni	0.01
D-4-1	Triplexer	Loss of Output	.04
D-5-1	Wide Band Transmitter (2)	Loss of One Transmitter	6.5 (1)
D-6-1	Narrow Band Transmitter (2)	Loss of One Transmitter	3.4 (1)
D-7-1	Signal Processor	Loss of Output	1.05
D-8-1	Receiver (2)	Loss of Receiver	3.96 (1)
D-9-1	Command Decoder (2)	Loss of Output of One Decoder	2.4
D-9-2	Command Decoder (2)	Inadvertant Command Output When Not Required	2.4
D-10-1	Command Distribution Assembly	Loss of Output	2.0
D-10-2	Command Distribution Assembly	Inadvertant Output	2.0
D-11-1	Data Handling Assembly	Loss of Power Supply/Oscillator/Programmer Portion	10.7
D-11-2	Data Handling Assembly	Loss of Single Channel	10.7
<u>HAZARD DETECTION</u>			
E-1-1	TV Camera	Loss of Video	12
E-2-1	Hazard Sensor	Any Failure in Sensor	15
E-3-1	Hazard Processor	Any Failure	15

FOLDOUT FRAME

II/I, 4-153/154

#### 4.5.2.1 Electrical Power Subsystem

##### 4.5.2.1.1 Manned Mission

A. Astronaut Safety - The probability of astronaut safety ( $P_{AS}$ ) is defined as the sum of the probability that an abort is not required plus the probability that an abort is required multiplied by the probability that the abort is successful.

$$P_{AS} = P_A(t_s) + [1 - P_A(t_s)] P(t'_s)$$

where  $t_s$  = total time of sortie

$t'_s$  = time required to safety abort

For the purpose of the reliability analysis, no astronaut walkback capability will be considered for mission aborts. This approach is used since the oxygen supply available from the PLSS is limited when considering the 4.23 hour EVA and the rather slow walking rate of an astronaut. For the electrical power subsystem  $t_s$  is 3.73 hours (2 hr. traverse plus 1.73 hr science stops. The time required to safely abort is .67 hours based upon the maximum vehicle speed of 15 Km/hr. and the maximum range from the lander of 10 Km.

For the electrical power subsystem a failure of any battery, battery charger, S/A regulator, or bus will require an abort to easy walkback range. Using the case numbers established in the FME & CA, the following equations evolve:

$$P_{AS} = P_A(t_s) + [1 - P_A(t_s)] P(t'_s)$$

$$P_{AS(m)} = P_{AS(s)}^5$$

where  $P_{AS}(s)$  = probability of astronaut safety for a single sortie

$P_{AS}(m)$  = probability of astronaut safety for the manned mission (5 sorties)

$$P_A(t_s) = P_{A-2-1}^2 P_{A-3-1}^2 P_{A-6-1}^2 P_{A-7-1}^2$$

$$P(t'_s) = P_{A-2-1} P_{A-3-1} P_{A-6-1} P_{A-7-1}$$

B. Full Mission Success - In order to realize full mission success in the manned mission an abort can not occur which would require returning and operating the vehicle within walkback range of the lander. Therefore,

$$P_{FMS}(t_{EVA}) = P(t_{EVA})$$

$$P_{FMS}(m) = P_{FMS}(t_{EVA})^5$$

where  $P_{FMS}(t_{EVA})$  = probability of full mission success for a single EVA

$P_{FMS}(m)$  = probability of full mission success for the manned mission (5 EVA's)

$$P(t_{EVA}) = P_{A-2-1}^2 P_{A-3-1}^2 P_{A-6-1}^2 P_{A-7-1}^2$$

$$P(t_{EVA}) = 3.90 \text{ hr. (10 min c/o, 2 hr. traverse, 1.73 hr science stops)}$$

C. Degraded Mission Capability - Degraded Mission Capability - Degraded mission capability will be realized as long as a sortie can be accomplished regardless of the range capability of the vehicle. Therefore degraded mission success will occur if a failure occurs during c/o which necessitates restricted range to assure astronaut safety or if an abort occurs during a sortie and the vehicle upon safe return is restricted in range. Therefore,

$$P_{DMC}(t_{EVA}) = [1 - P_A(t_{c/o})] P_{DMC}(t_s) + P_A(t_{c/o}) [P_A(t_s) + (1 - P_A(t_s)) P(t_s)]$$

$$P_{DMC}(t_{EVA}) = [1 - P_A(t_{c/o})] P_{DMC}(t_s) + P_A(t_{c/o}) P_{ASC}(t_s)$$

$$P_{DMC}(M) = P_{DMC}^S(t_{EVA})$$

where  $P_{DMC}(t_{EVA})$  = probability of degraded mission capability during an EVA

$P_{DMC}(M)$  = probability of degraded mission capability during manned mission

$$P_A(t_{c/o}) = P_{A-2-1}^2 P_{A-3-1}^2 P_{A-6-1}^2 P_{A-7-1}^2$$

$$P_{DMC}(t_s) = 2 P_{A-2-1} P_{A-3-1} P_{A-6-1} P_{A-7-1} - P_{A-2-1}^2 P_{A-3-1}^2 P_{A-6-1}^2 P_{A-7-1}^2$$

#### 4.5.2.1.2 Unmanned Mission

A. Full Mission success - Although the electrical power subsystem is completely redundant, in order to accomplish to 1000 Km science traverse within a year only a single failure of the RTG No Load Protection and Converter or solar array motor can be tolerated. Therefore,

$$P_{FMC}(t_{LR}) = P_{A-1-1} P_{A-1-3} P_{A-2-1}^2 P_{A-3-1}^2 P_{A-4-1} [2 P_{A-5-1} - P_{A-5-1}^2]$$

$$P_{FMS}(t_{SS}) = P_{A-1-1} P_{A-1-3} P_{A-4-1} [2 P_{A-5-1} - P_{A-5-1}^2] [2 P_{A-5-2} - P_{A-5-2}^2]$$

$$P_{FMS}(t_R) = P_{FMS}(t_{SS}) \text{ EXCEPT } t_{SS} = t_R$$

$$P_{FMS}(t_D) = P_{A-4-1} [2 P_{A-5-1} - P_{A-5-1}^2] [2 P_{A-5-2} - P_{A-5-2}^2] P_{A-7-1}^2$$

B. Degraded Mission Capability - Degraded contingency operation exists in

the event that a failure occurs that essentially knocks out one of the two busses, if the automatic array orientation device fails, inverter fails, or if the RTG No Load Protection and Converter fails. The consequence and resultant contingencies available are indicated in the FME & CA.

$$P_{DMC}(t_{LR}) = P_{A-1-1} P_{A-4-1} [2 P_{A-5-1} - P_{A-5-1}^2] [2 P_{A-5-2} - P_{A-5-2}^2]$$

$$[2 P_{A-2-1} P_{A-3-1} P_{A-6-1} P_{A-7-1} - (P_{A-2-1}^2 P_{A-3-1}^2 P_{A-6-1}^2 P_{A-7-1}^2)]$$

$$P_{DMC}(t_{SS}) = P_{DMC}(t_{LR}) \text{ EXCEPT } t = t_{SS}$$

$$P_{DMC}(t_R) = P_{DMC}(t_R) \text{ EXCEPT } t = t_R$$

$$P_{DMC}(t_D) = P_{A-4-1} [2 P_{A-5-1} - P_{A-5-1}^2] [2 P_{A-5-2} - P_{A-5-2}^2] P_{A-7-1}$$

#### 4.5.2.2 Navigation Subsystem

##### 4.5.2.2.1 Manned Mission

A. Astronaut Safety - Since in the manned mission the navigation computation is performed at the ground station and the vehicle communications subsystems is handled separately, only navigation sensors need be analyzed here.

$$P_{AS}(s) = P_A(t_s) + [1 - P_A(t_s)] P(t'_s)$$

$$P_{AS}(M) = P_{AS}^5(s)$$

$$P_A(t_s) = P_{B-2-1} P_{B-2-2} [P_{B-1-1}^4 + 4 P_{B-1-1}^3 (1 - P_{B-1-1})] P_{B-3-1} P_{B-3-2}$$

$$P(t'_s) = P_{B-3-1} P_{B-3-2} P_{B-7-1}$$

B. Full Mission Success = Full mission success can only be achieved if there is no necessity to abort the vehicle, i.e., full range is available.

Therefore,

$$P_{FMS}(s) = P_{B-2-1} P_{B-2-2} [P_{B-1-1}^4 + 4 P_{B-1-1}^3 (1 - P_{B-1-1})] P_{B-3-1} P_{B-3-2}$$

$$P_{FMS}(M) = P_{FMS}^5(s)$$

C. Degraded Mission Capability - It is assumed that degraded mission capability will exist even if no navigational data is attainable in the manned mode. Therefore degraded mission capability is limited only by the crew safety probability.

$$P_{DMC}(t_{EVA}) = [1 - P_A(t_{C/O})] P_{DMC}(t_s) + P_A(t_{C/O}) P_{AS}(s)$$

$$P_{DMC}(M) = P_{DMC}^5(t_{EVA})$$

$$P_{DMC}(t_s) = 1$$

$$P_A(t_{C/O}) = P_{B-2-1} P_{B-2-2} [P_{B-1-1}^4 + 4 P_{B-1-1}^3 (1 - P_{B-1-1})] P_{B-3-1} P_{B-3-2}$$

##### 4.5.2.2.2 Unmanned Mission

A. Full Mission Success - In order to obtain full mission success both continuous navigation (either through use of Gyro or Solar Aspect Sensor) and update will be required.

$$P_{FMS}(t_R) = P_{CONTINUOUS} P_{UPDATE}$$

$$P_{CONTINUOUS} = [P_{B-2-1} P_{B-2-2} + P_{B-6-1} P_{B-6-2} P_{B-8-1} - P_{B-2-1} P_{B-2-2} P_{B-6-1} P_{B-6-2} P_{B-8-1}] [P_{B-1-1}^6 + 6 P_{B-1-1}^5 (1 - P_{B-1-1})]$$

$$P_{UPDATE} = P_{B-4-1} P_{B-5-1} P_{B-5-2}$$

$$P_{FMS}(t_{SS}) = P_{DMS}(t_R) = P_{DMS}(t_D) = 1$$

B. Degraded Mission Success - A degraded mission can be conducted if either continuous navigation or update capability exists.

$$P_{DMC}(t_R) = [P_{CONTINUOUS} + P_{UPDATE} - P_{CONTINUOUS} P_{UPDATE}]$$

$$P_{DMC}(t_{SS}) = P_{DMC}(t_R) = P_{DMC}(t_D) = 1$$

#### 4.5.2.3 Mobility & Steering Subsystem

##### 4.5.2.3.1 Manned Mission

A. Astronaut Safety - In the manned mode, the DLRV derives its mobility from four (4) independently powered wheels and a powered articulated joint for steering. In the event of single wheel motor failures, the associated motor can be disabled and the wheel permitted to "free wheel". This permits the vehicle to be driven by the remaining wheel motors. In addition the differential wheel speed mode can be used to steer the vehicle in the event that a steering joint failure should occur.

$$P_{AS}(s) = P_A(t_S) + [1 - P_A(t_S)] P(t_S')$$

$$P_{AS}(M) = P_{AS}^5(s)$$

$$P_A(t_S) = P_{C-1-1} P_{C-2-1} P_{C-3-1}^4 P_{C-4-1}^4 P_{C-5-1} P_{C-6-1}$$

$$P(t_S') = P_{C-3-1}^3 P_{C-4-1}^3 P_{C-7-1}$$

B. Full Mission Success - Full mission success can only be achieved if the vehicle has the full range.

$$P_{FMS}(s) = P_A(t_{EVA}) = P_{C-1-1} P_{C-2-1} P_{C-3-1}^4 P_{C-4-1}^4 P_{C-5-1} P_{C-6-1}$$

$$P_{FMS}(M) = P_{FMS}^5(s)$$

C. Degraded Mission Capability - Degraded mission capability will exist if  
 (1) a failure occurs during checkout and the vehicle is restricted in range of  
 (2) a failure occurs during the sortie that requires an abort.

$$P_{DMC}(t_{EVA}) = [1 - P_A(t_{C/O})] P_{DMC}(t_S) + P_A(t_{C/O}) P_{AS}(s)$$

$$P_{DMC}(M) = P_{DMC}^5(t_{EVA})$$

$$P_A(t_{C/O}) = P_{C-1-1} P_{C-2-1} P_{C-3-1}^4 P_{C-4-1}^4 P_{C-5-1} P_{C-6-1}$$

$$P_{DMC}(t_S) = P_{C-3-1}^3 P_{C-4-1}^3 P_{C-7-1}$$

#### 4.2.3.2 Unmanned Mission

A. Full Mission Success - Full mission success can be achieved if a failure occurs which requires that one wheel (out of six) be disabled or if the steering actuator drive should fail requiring differential wheel speeds for turning.

$$P_{FMS}(t_{tr}) = P_{C-2-1} [P_{C-3-1}^6 P_{C-4-1}^6 + 6 P_{C-3-1}^5 P_{C-4-1}^5 (1 - P_{C-3-1} P_{C-4-1})]$$

$$P_{FMS}(t_{ss}) = P_{FMS}(t_R) = P_{FMS}(t_D) = 1$$

B. Degraded Mission Success - Degraded mission success for the Mobility & Steering Subsystem is equal to the full mission success probabilities.

$$P_{DMS}(t_{tr}) = P_{FMS}(t_{tr})$$

$$P_{DMS}(t_{ss}) = P_{DMS}(t_R) = P_{DMS}(t_D) = 1$$

#### 4.5.2.4 Communications & Instrumentation Subsystem

##### 4.5.2.4.1 Manned Mission

A. Astronaut Safety - The Communications & Instrumentations Subsystem can not fail by itself in any manner which would cause an astronaut hazard, i.e., loss of power, mobility, etc.

$$P_{AS}(s) = 1$$

$$P_{AS}(m) = 1$$

B. Full Mission Success - Full Mission Success can only be achieved if a sortie is not aborted or restricted in range. Although this subsystem by itself is not safety critical, sorties will be aborted or restricted if voice communication or subsystem performance data is lost. Therefore,

$$P_{FMS}(s) = P(t_{EVA})$$

$$P_{FMS}(m) = P_{FMS}(s)$$

$$P(t_{EVA}) = [2 P_{D-1-1} P_{D-2-1} P_{D-3-1} P_{D-3-2} - P_{D-1-1} P_{D-2-1} P_{D-3-1} P_{D-3-2}] \\ P_{D-4-1} [P_{D-5-1} (1 + \lambda_{D-5-1} t_{EVA})] [P_{D-6-1} (1 + \lambda_{D-6-1} t_{EVA})] \\ P_{D-7-1} [2 P_{D-8-1} - P_{D-8-1}^2] [2 P_{D-9-1} - P_{D-9-1}^2] \\ P_{D-10-1} P_{D-11-1}$$

C. Degraded Mission Success - A degraded mission can be conducted if uplink command capability is lost, as long as any one transmitter is operative and use of PPLS is available for voice communications.

$$P_{FMS}(s) = [2 P_{D-1-1} P_{D-2-1} P_{D-3-1} P_{D-3-2} - P_{D-1-1}^2 P_{D-2-1}^2 P_{D-3-1}^2 P_{D-3-2}^2] \\ [P_{D-5-1} (1 + \lambda_{D-5-1} t_{EVA}) + P_{D-6-1} (1 + \lambda_{D-6-1} t_{EVA}) - \\ P_{D-5-1} P_{D-6-1} (1 + \lambda_{D-5-1} t_{EVA}) (1 + \lambda_{D-6-1} t_{EVA})] \\ P_{D-4-1} P_{D-11-1} [2 P_{D-8-1} - P_{D-8-1}^2]$$



$$P_{DMS}(m) = P_{DMS}^5(s)$$

#### 4.5.2.4.2 Unmanned Mission

##### A. Full Mission Success -

$$P_{FMS}(t_{LR}) = P_{D-1-1} P_{D-2-1} P_{D-3-1} P_{D-4-1} [P_{D-5-1}(1 + \lambda_{D-5-1} t_{LR})] P_{D-10-1} P_{D-11-1} \\ [P_{D-6-1}(1 + \lambda_{D-6-1} t_{LR})] [2 P_{D-8-1} - P_{D-8-1}^2] [2 P_{D-9-1} - P_{D-9-1}^2]$$

$$P_{FMS}(t_{SS}) = P_{FMS}(t_{LR}) \text{ EXCEPT } t = t_{SS}$$

$$P_{FMS}(t_R) = P_{D-1-1} P_{D-2-1} P_{D-3-1} P_{D-4-1} [P_{D-6-1}(1 + \lambda_{D-6-1} t_X)] \\ [2 P_{D-8-1} - P_{D-8-1}^2] [2 P_{D-9-1} - P_{D-9-1}^2] P_{D-10-1} P_{D-11-1} \\ t_X = t_R/5, t = t_R$$

$$P_{FMS}(t_D) = P_{REC} P_{COMMAND} P_{XMIT}$$

$$P_{REC} = P_{D-2-1} P_{D-3-2} P_{D-4-1} \quad t = t_D$$

$$P_{COMMAND} = [2 P_{D-9-1} - P_{D-9-1}^2] P_{D-10-1} \quad t = t_D/10$$

$$P_{XMIT} = [P_{D-6-1}(1 + \lambda_{D-6-1} t) + P_{D-5-1}(1 + \lambda_{D-5-1} t) - \\ P_{D-6-1} P_{D-5-1}(1 + \lambda_{D-6-1} t)(1 + \lambda_{D-5-1} t)] P_{D-11-1} \\ t = t_D/10$$

##### B. Degraded Mission Success -

$$P_{DMS}(t_{LR}) = [2 P_{D-1-1} P_{D-2-1} P_{D-3-1} P_{D-3-2} - P_{D-1-1}^2 P_{D-2-1}^2 P_{D-3-1}^2 P_{D-3-2}^2] \\ P_{D-4-1} [P_{D-5-1}(1 + \lambda_{D-5-1} t_X) + P_{D-6-1}(1 + \lambda_{D-6-1} t_X) - \\ P_{D-5-1} P_{D-6-1}(1 + \lambda_{D-5-1} t_X)(1 + \lambda_{D-6-1} t_X)] \\ [2 P_{D-8-1} - P_{D-8-1}^2] [2 P_{D-9-1} - P_{D-9-1}^2] P_{D-10-1} P_{D-11-1} \\ t = t_R = t_X$$

$$P_{DMS}(t_{SS}) = P_{DMS}(t_{LR}) \quad t = t_{SS} = t_X$$

$$P_{DMS}(t_R) = P_{DMS}(t_{LR}) \quad t = t_R \quad t_X = t_R/5$$

$$P_{DMS}(t_D) = P_{FMS}(t_D)$$

#### 4.5.2.5 Hazard Detection Subsystem

##### 4.5.2.5.1 Manned Mission

This subsystem will not be required to operate during the manned mission.

##### 4.5.2.5.2 Unmanned Mission

A. Full Mission Success - Both the TV Camera and Hazard Sensor and Processor will be necessary for full success. Therefore,

$$P_{FMS}(t_{LR}) = P_{E-1-1} P_{E-2-1} P_{E-3-1}$$

and

$$P_{FMS}(t_{SS}) = P_{FMS}(t_R) = P_{FMS}(t_D) = 1$$

B. Degraded Mission Success - A degraded mission can be conducted if the TV Camera fails by using the experiment camera.

and

$$P_{DMS}(t_{tr}) = P_{E-2-1} P_{E-3-1}$$
$$P_{DMS}(t_{ss}) = P_{DMS}(t_r) = P_{DMS}(t_c) = 1$$

#### 4.5.3 Parts Environmental Requirements

A review was made of the environmental differences between the AAP/IM-A and the DLRV to determine the applicability of the AAP/IM-A Preferred Parts List (PPL) for the DLRV. This PPL was chosen as a reference point since it is an out-growth of the IM program and will assure compliance with MSFC Preferred Parts List 85M02716. Only common usage electronic parts such as resistors, capacitors, diodes, etc., were considered in this study. Temperature, pressure-time, and radiation are the significant environmental differences between the AAP/IM-A and DLRV missions, which might affect part acceptability. The affect of these environments on the AAP/IM-A PPL was investigated.

As a result of this study it was concluded that the AAP/IM-A PPL is applicable to the DLRV program with the exception of certain radiation susceptible semiconductor devices. Appropriate precautions will be required in the use of parts which might be affected by the one year operational period on the moon. Further studies are recommended for linear integrate circuits.

##### 4.5.3.1 Temperature

Since the DLRV is to be stored on the lunar surface during lunar nights and will be operational during lunar days, the possible temperature excursion could exceed part capabilities. A typical part on the AAP/IM-A Preferred Parts List is rated from  $-85^{\circ}\text{F}$  ( $-65^{\circ}\text{C}$ ) to  $+257^{\circ}\text{F}$  ( $125^{\circ}\text{C}$ ), with some parts rated to only  $+77^{\circ}\text{F}$  ( $25^{\circ}\text{C}$ ) at full power, e.g. RWR wirecound power resistor with derating at high ambient temperature. This apparent problem is resolved, however, since the DLRV will generate heat in its RTG and have passive cooling capability. The equipment temperature ranges are shown in the previous section, Thermal Control.

##### 4.5.3.2 Pressure-Time

The DLRV pressure-time environment will be more severe than that of the AAP/IM-A because of the longer duration without any atmosphere. Certain parts, such as composition resistors, wet electrolytic capacitors, and potentiometers might be affected. These may be used if protected by encapsulation, potting, or a hermetically sealed assembly. However, potentiometers should not be expected to

operate as moving devices i.e., manual controls, position sensors, etc., in a vacuum.

An important consideration is that the dielectric breakdown voltage of a gas has a minimum value. This minimum for a typical geometry occurs at a pressure equivalent to approximately 100,000 ft. altitude. Therefore, equipment with high voltages should be hermetically sealed or thoroughly potted if operated during and after the launch phase, or fully vented if not operated during launch.

#### 4.5.3.3 Radiation

Solar flare protons present the most serious natural radiation hazard for a moon based vehicle. This environment is highly indeterminate, varying from day to day as well as from year to year. It can be calculated only on the basis of probability of occurrence. The results of such a determination using the NASA Apollo solar flare model are presented in the Table 4.5.6 below.

TABLE 4.5-6

SOLAR FLARE PROTON ENVIRONMENT

Minimum Proton Energy $E_o$ (Mev)	$\phi(E > E_o)$ p/cm <sup>2</sup> -year x 10 <sup>-10</sup> For various probabilities of occurrence		
	p = 10%	p = 1.0%	p = 0.1%
10	1.37	8.0	34.3
20	0.58	3.40	14.6
30	0.300	1.75	7.5
40	0.21	1.2	5.1
50	1.15	0.9	3.7
75	0.07	0.4	1.8
100	0.04	0.2	1.0

} Removed by  
Inherent Shielding

↑

Potential  
Problem  
Exists

↓

SAFE

Radioisotope thermoelectric generators (RTG) can provide undesirable side effects, a radiation environment consisting of neutrons and gammas. The exposure level of these radiations are highly dependent on the type of RTG and the distance from the RTG. A power source of SNAP-19 type, that utilizes Plutonium-238 as the energy producing radioisotope, results in an environment, at a distance of one meter, equivalent to a fission neutron flux of  $6 \times 10^{10}$  neutrons per square centimeter per year and a 1 Mev gamma dose rate of 20-80 roentgen per year (R/year). Other RTG's, such as those using Curium-244, have much higher (by several orders of magnitude) neutron and gamma leakage fluxes.

The effect of damage produced by each radiation type in a mixed environment can be compared using radiation damage equivalents. The equivalences utilized in this study were:

A.  $10 \text{ n/cm}^2$  (fission spectrum neutrons) =  $1 \text{ p/cm}^2$  (solar flare protons) for producing displacement damage in silicon devices.

B.  $1 \text{ R}$  (1Mev equivalent gammas) =  $10^6 \text{ p/cm}^2$  (solar flare protons) for producing displacement damage in silicon devices.

To provide a more realistic assessment of radiation vulnerability it was assumed that all semiconductors have cases that shield against protons with energies below 10 Mev, but are transparent to gammas and neutrons. No shielding due to structure of "black boxes" was assumed.

#### 4.5.3.4 Radiation Vulnerability

Using the radiation equivalences indicated in the previous section it is clear that solar flare protons present the only radiation hazard to this mission. A literature search has been made to determine the levels at which radiation induced failure can occur in AED-255-1 parts, and the modes of failure. Table 4.5-13 lists this information for vulnerable parts with comments suggesting hardening approaches. A brief discussion of the hardening approaches follows:

1. Shielding - Because the dominant radiation hazard is solar flare protons, which require little shielding when compared to that required for neutrons and gammas, shielding is an attractive hardening technique. Nonvulnerable equipments such as batteries can provide most of the shielding.

2. Derating - When devices do not fail catastrophically it is possible to increase radiation tolerance by derating. One type of derating is to operate a device at less than rated power -- a technique which is suitable for power diodes. A second type of derating involves use of circuits which are insensitive to changes past performance affected by radiation. This approach is useful for transistors where the change in the emitter current gain,  $B$ , is the radiation sensitive parameter. Derating techniques cannot be used for SCR's and PNPN devices which may fail catastrophically in a radiation environment -- these parts must be shielded, and/or preselected.

3. Preselection - This hardening approach, the feasibility of which has been demonstrated by Grumman Research, offers great potential for hardening parts with wide ranges in fluence-to-failure and which fail catastrophically. This

TABLE 4.5-7  
PARTS VULNERABILITY ASSESSMENT

DEVICE	PROPERTY CHANGE	COMMENTS
Power Diodes UTR3320 IN3891 IN3911 379ID	Increase in $V_F$ $\phi_t = 10^{11}$ p/cm <sup>2</sup> due to displacement damage	This problem can be solved by derating which will prevent excessive power dissipation. <u>Not recommended for reference voltage use without radiation testing.</u>
Power Transistors MHT8303	Decrease in B $\phi_t = 10^{10}$ p/cm (displacement damage)	The problem can be solved by derating the device required for any circuit application (also the actual shielding may be greater than the assumed 10 mils of copper).
2N1774	As above, plus erratic increase in $I_{cbo}$ which may vary by $10^4$ for two devices from the same lot.	Do not use unless manufacture now offers a planar passivated device. (In that case see above.)
Controlled Rectifier Diode (2 terminal PNP) AAI 2N1776A	$V_F$ increase to point where device will not fire (catastrophic failures) $\phi_t = 10^{10} - 10^{11}$ p/cm <sup>2</sup>	Derating is <u>not feasible</u> and variation in fluence to failure of these devices makes use most dangerous without shielding. Shielding of 1-2.5 lbs/sq ft copper or equivalent will eliminate the proton hazard. Testing in radiation environments equivalent to mission fluence is recommended.
Low Power Signal Transistors 2N2484 2N2432 2N3965	Decrease in B and increase $I_{cbo}$ surface damage $\phi_t = 10^4$ R	This type of damage is strongly dependent on operating conditions. Derating will solve this problem if feasible; otherwise shielding or preselection is necessary.

TABLE 4.5-7  
PARTS VULNERABILITY ASSESSMENT  
CONTINUED

DEVICE	PROPERTY CHANGE	COMMENTS
<p>Monolithic Linear Integrated Circuits 702 709 710</p>	<p>No data available but may suffer the same type of damage as Low Power Signal Transistors.</p> <p><math>\phi_t</math> = threshold flux for producing damage in the specified device.</p>	<p>Test using protons or equivalent radiation environments. A radiation specification should be issued for these devices.</p>

technique is based on irradiating a population of parts of a given type from a given manufacturer with a fluence representative of the mission dose; selecting the most resistant parts; removing the radiation damage from the selected parts with high-temperature short-duration annealing, and using the selected parts in systems.

#### 4.5.4 Hardware Test Requirements

Contained within Volume VII - Sect 2 is the overall DLRV Test Plan which includes the development, qualification, and acceptance test requirements for all hardware, subsystems, and vehicles. This section will discuss the rationale which was used in establishing the test requirements for DLRV hardware as shown in Table 4.5-8.

##### 4.5.4.1 Development Tests

Development tests will be conducted on all hardware not previously qualified to environments compatible with those of the DLRV. The scope of these tests will vary depending upon the extent of modifications from existing designs. Development tests are divided into design feasibility tests (DFT) and design verification tests (DVT). DFT are conducted on preproduction hardware to substantiate component and part selection, material selection, investigate breadboard models under various environmental conditions, and to substantiate safety margins or other analytical assumptions. DVT are conducted on hardware which, as far as possible, reflects the intended production units. These tests will provide an early screen of possible design deficiencies. The test will verify effects of combined environments and out-of-tolerance conditions, and off-limit tests will determine failure mode/weak link characteristics and substantiate design margins.

An evaluation was performed using IM test program results to determine if a strict DVT program was effective. Figure 4.5-7 shows the difference in test results obtained when equipments had complete environmental DVT programs as compared to equipments having limited or no environmental DVT programs. The following conclusions become evident:

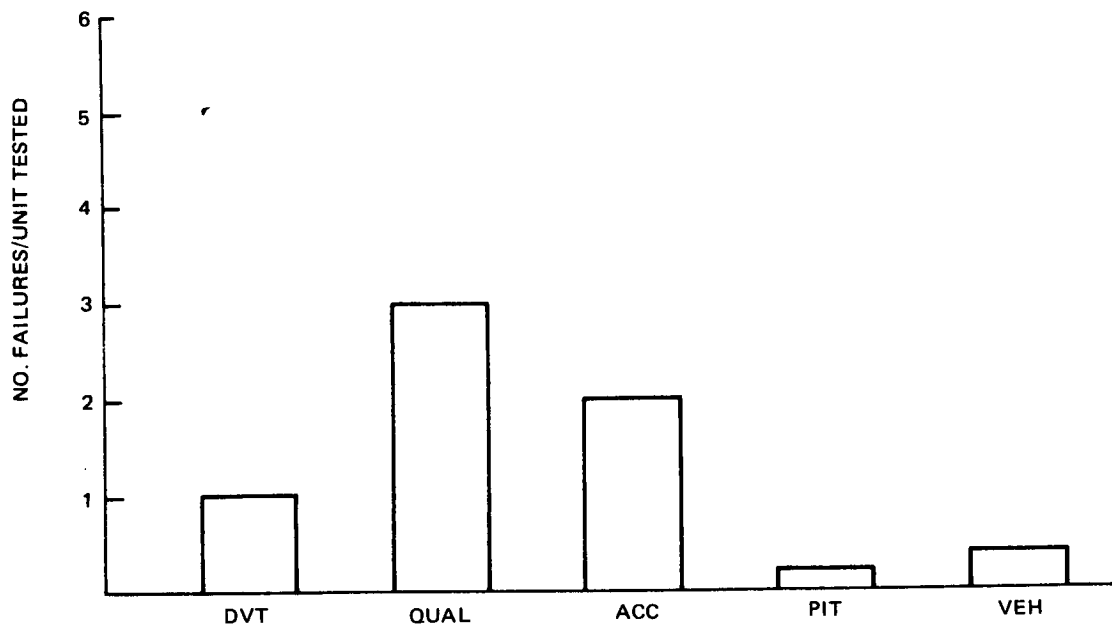
- o Strict DVT exposed four (4) times as many design deficiencies prior to qual.
- o Strict DVT reduced costly qual design deficiency failures by two-thirds.
- o The number of failures experienced during vehicle level tests were about the same.

TABLE 4.5-8

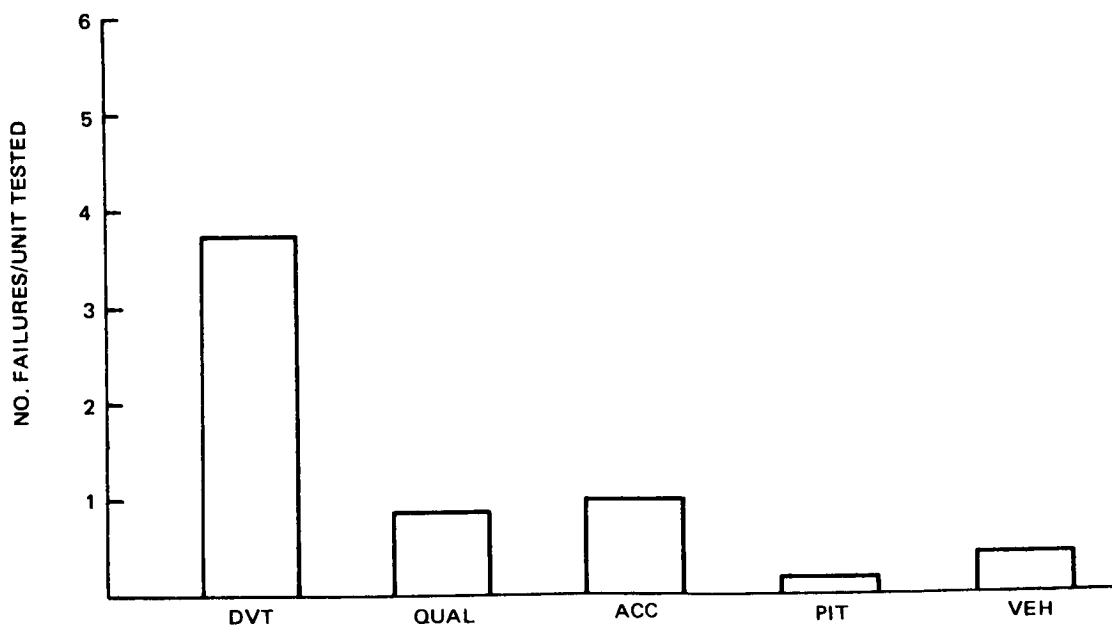
HARDWARE TEST ENVIRONMENTS SUMMARY

Test/Equipment	Environment																	
	Accept			Ground						Flight					Lunar			
	Burn in	Random Vib	Therm Vac/Therm Cycle	Integ & C/O	Temperature	Shock	Sea Air/Humid	Fungus	Vibration	Vib/Temp	Shock	Acceleration	Thermal/Vacuum	Thermal/Vacuum	Temp/Vib	Shock	Dust	EMI
DFT & DVT/Preprod				Mission Levels & Overstress As Required														
Qualification • Design Limit/ Production	1	2	1			3	3	4	2		3			1	1	1	1	1
• Endurance/ Production	1	2	1	1	3				2	3		3		1	1	1	1	
Environmental Acceptance/Production	1	2	1															
(1) Operating during Environ Exposure (2) Operating during Environ Exposure but need not be in Spec (Power-on Vib Quality Screen) (3) Non Operations during Environ Exposure (4) Test deleted if evidence of non-nutrient material submitted																		





A. LIMITED OR NO DEVELOPMENT PROGRAM



B. STRICT DEVELOPMENT PROGRAM

FIG. 4.5-7 EQUIPMENT FAILURES WITH/WITHOUT DVT PROGRAM

The major benefit to be derived by implementing a strict DVT program is that it will cull out deficiencies early in the program and thereby significantly reduce the need to retest and retrofit. The cost related to a failure requiring retest which happens during Qual/Accept are ten times higher as opposed to a failure that occurs during DVT. Since a strict DVT program was found to reduce the need to retest by 2:1, it can be seen that a strict DVT program is cost effective. In addition it can also be shown that it is also schedule effective. Therefore Grumman strongly recommends that the DVT program be a constraint to start of hardware qualification tests.

#### 4.5.4.2 Qualification Tests

Qualification tests will be performed to verify that production hardware meets the performance and design requirements under the anticipated operational environment. Qualification tests will be performed on two sets of production hardware in accordance with approved test procedures. One set of hardware will be subjected to design limit tests (DLT) and endurance tests will be performed on the other set of hardware. The DLT will subject the hardware to flight simulation tests of the operational cycle at design limit levels. Design limit stress levels are higher than the maximum mission levels. Therefore, successful test completion will demonstrate existence of safety factors for all critical modes under combined environments and combinations of tolerance and drift of design parameters. Endurance tests subject the unit to mission level environments using operating time, rather than stress level, as the critical parameter to affect an equipment's function. The duration of such an exposure is normally the equivalent of one complete operational cycle plus one additional flight, deployment and lunar operation cycle. An operational cycle is defined as ground operating time plus flight, deployment, and lunar operation time.

When one looks at the lunar operational time of 14 days in the manned mode and one year in the unmanned mode it becomes apparent that to test for this period of time would be both cost and schedule prohibitive. The manned and unmanned modes closely resemble the duration and mission of the LM and OAO spacecrafts respectively and therefore the test experience gained on these programs are applicable. Figure 4.5-8 indicates the three qualification endurance test alternatives that were considered. The first alternative suggests full mission duration tests for all hardware and would result in the highest degree of confidence for both safety and mission success. This alternative was rejected

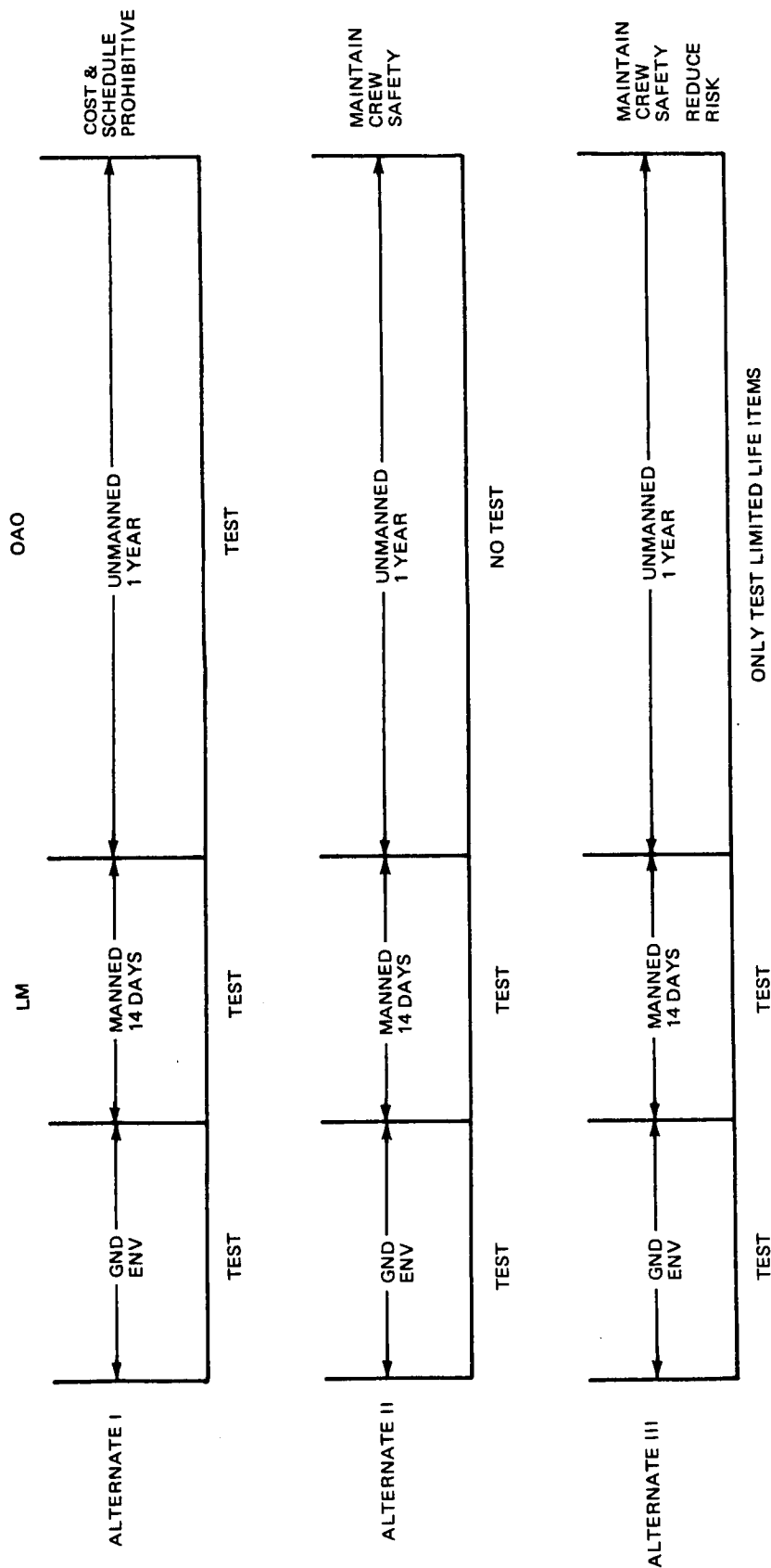


FIG. 4.5-8 QUALIFICATION ENDURANCE TEST ALTERNATIVES

because it is cost and schedule prohibitive. The second alternative considers endurance tests for the duration of the manned mode only. This would mean assuming an unduly high degree of risk of completing the one year unmanned mission. The third alternative combines the technology gained on the LM and OAO programs and is the recommended approach. Due to the risk of life, endurance tests will be performed on all hardware for the 14 day duration. For the unmanned mode, hardware will be reviewed for known limited life items such as: motor, gears, battery cells, etc. These items will be qualification tested for the equivalent duration of the unmanned mode with consideration given to duty cycle and possible accelerated testing. These tests will be performed at the lowest possible level of assembly, below the hardware level, in the interest of economy. This approach was successfully instituted on the OAO program. By conducting endurance tests on all hardware for the manned mode and performing endurance tests on known limited life items, safety confidence is maintained and also a good measure of mission success confidence in the unmanned mode will be obtained.

#### 4.5.4.3 Acceptance Tests

All production units will be subjected to an environmental acceptance tests to verify quality. Table 4.5-8 indicates the typical acceptance test cycle. High temperature burn-in will be used to weed out latent quality defects prior to environmental testing. The duration of burn-in will depend on the hardware and whether the unit has inherent limited life characteristics. For electronic hardware, a 50 to 100 hr. burn-in has proven very effective.

## SECTION 5

### MOBILITY SUBSYSTEM DESIGN

The components of the mobility subsystem are the chassis, suspension, wheels, wheel drive, and steering system. In this section preliminary designs for these components are presented, and the rationale leading to the selection of the specific approaches is given.

#### 5.1 CHASSIS

The DLRV chassis is a structural system comprised of three units connected by jointed structural members. This system is designed to serve a dual purpose. While being transported to the lunar surface in the delivery vehicle, it supports all vehicle-mounted components including wheels and suspensions. After deployment the chassis becomes an integral part of the mobility system, providing the structural continuity between the suspensions to support the crew and science equipment and the subsystem components. A high structural spring rate is required of the chassis when stowed in the delivery vehicle to minimize dynamic load magnification to the chassis-mounted equipment during launch.

An important guideline in the design of the chassis is the achievement of a minimum weight design through a maximum of structural efficiency. However, materials and construction methods must be chosen to be achievable within a realistic development schedule.

##### 5.1.1 Design Requirements

Since the DLRV is carried by the LM derivative lunar landing vehicle, it shares the same structural environment. This environment, described in section 4.3.1 and in Annex A of the Work Statement, specifies the levels of acceleration, vibration, and acoustic pressure expected. Failure of chassis structure or attachments to it during launch could be disastrous; therefore, the chassis must meet the same integrity requirements as the LM structure.

Structural requirements while operating on the lunar surface generally will not exceed the launch and landing conditions except in local areas. Vehicle operation design load conditions are applied with an ultimate load factor of 1.5 over limit load.

The chassis design must provide suitable attachment provisions for all equipment/science items. Also, hard points for GSE cradling as well as lift lugs for hoisting must be provided. All portions of the chassis structure which might come in contact with the suited astronaut must present a smooth surface to prevent suit damage.

#### 5.1.2 Chassis Preliminary Design

The DLRV chassis' structural arrangement is presented in four drawings. Figure 5.1-1 shows the control and power module chassis in the stowed condition and Figure 5.1-2 shows these elements as they appear deployed for operation. Figure 5.1-3 shows the science module chassis with its support structure as stowed and Figure 5.1-4 shows the unfolded condition. Presenting the conditions separately is done not only for clarity, but to show the different structural systems involved in the stowed and deployed conditions.

Each chassis is a riveted assembly of beam members utilizing efficient structural shapes between primary attachment fittings. Each is covered with a web on the upper surface to resist body shear loads during running and to provide shear continuity and torsional strength while stowed. Aluminum alloy 2024 is used for its good strength/weight ratio at the temperatures encountered, low cost, and well-developed fabrication techniques. Chem milling is employed to ensure efficient load distribution and minimum weight.

The riveted assembly method was chosen despite the overlap inefficiencies because the light gauges used are less than minimum required for welding and would require thickening at the joints. Additionally, considering the low number of units to be manufactured, the cost of automated welding would be prohibitive and possibly lead to further design inefficiencies to facilitate manufacture.

In the stowed configuration, the two chassis members are structurally tied together with shear pins to take advantage of the combined depth for beam loading. This combination is designed to efficiently distribute all applied loads to the three tie-down support points. Also, while in this folded position the combined elements comprise a torsionally stiff box. Where possible, load paths for stowed and running conditions have been made to coincide to minimize the number of structural members. The chassis inherently has adequate internal space for the deployment mechanisms and wiring harnesses.

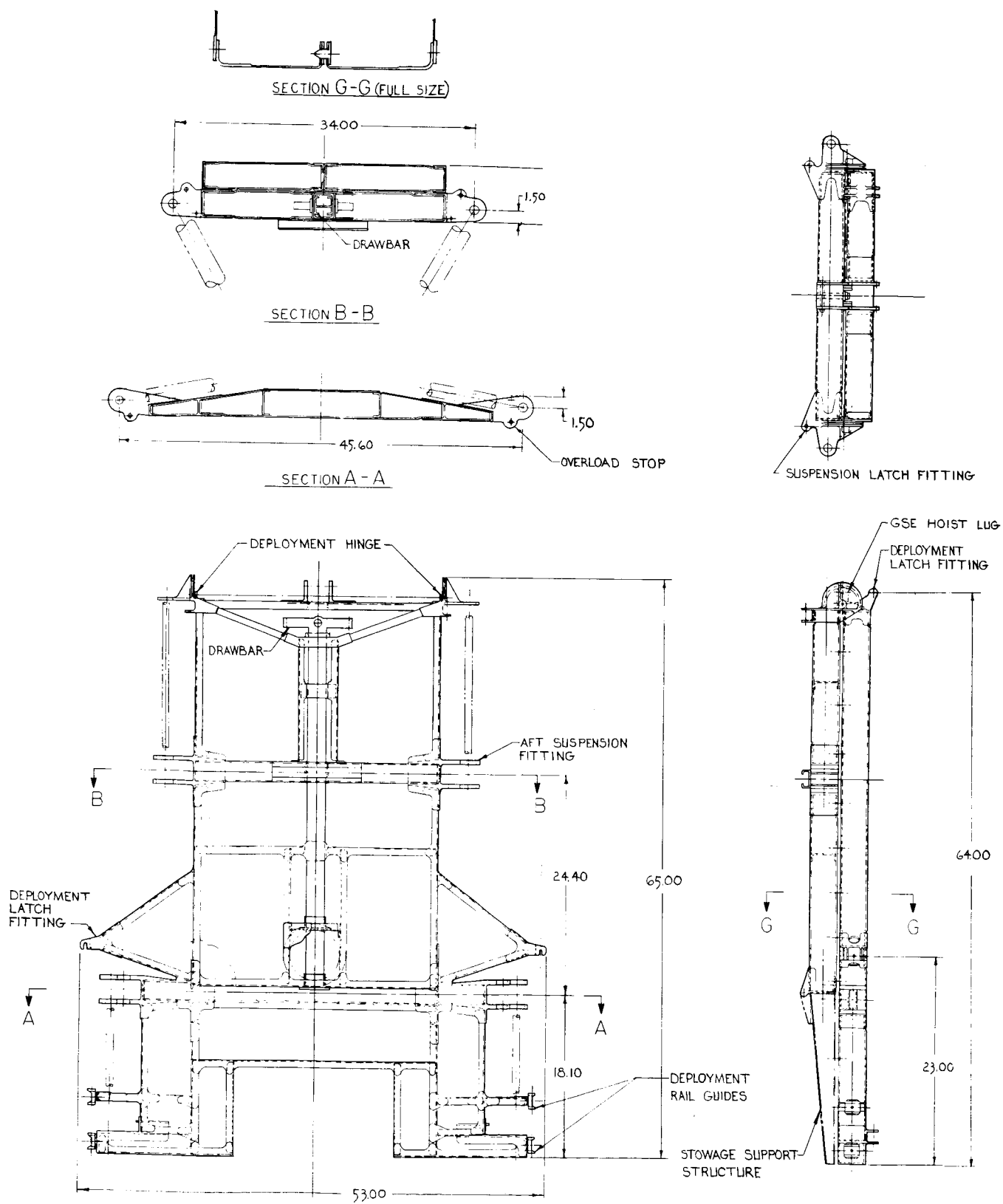
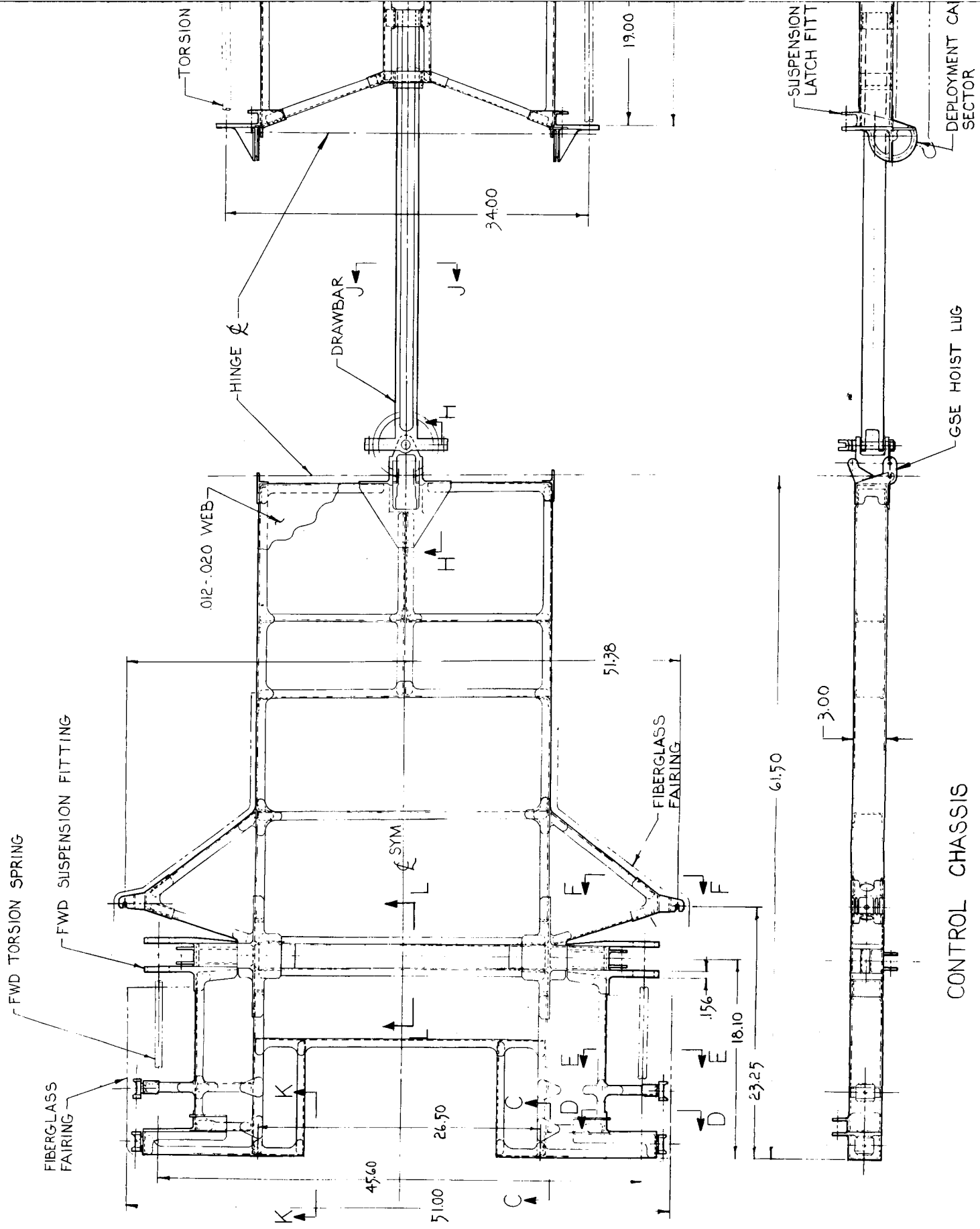
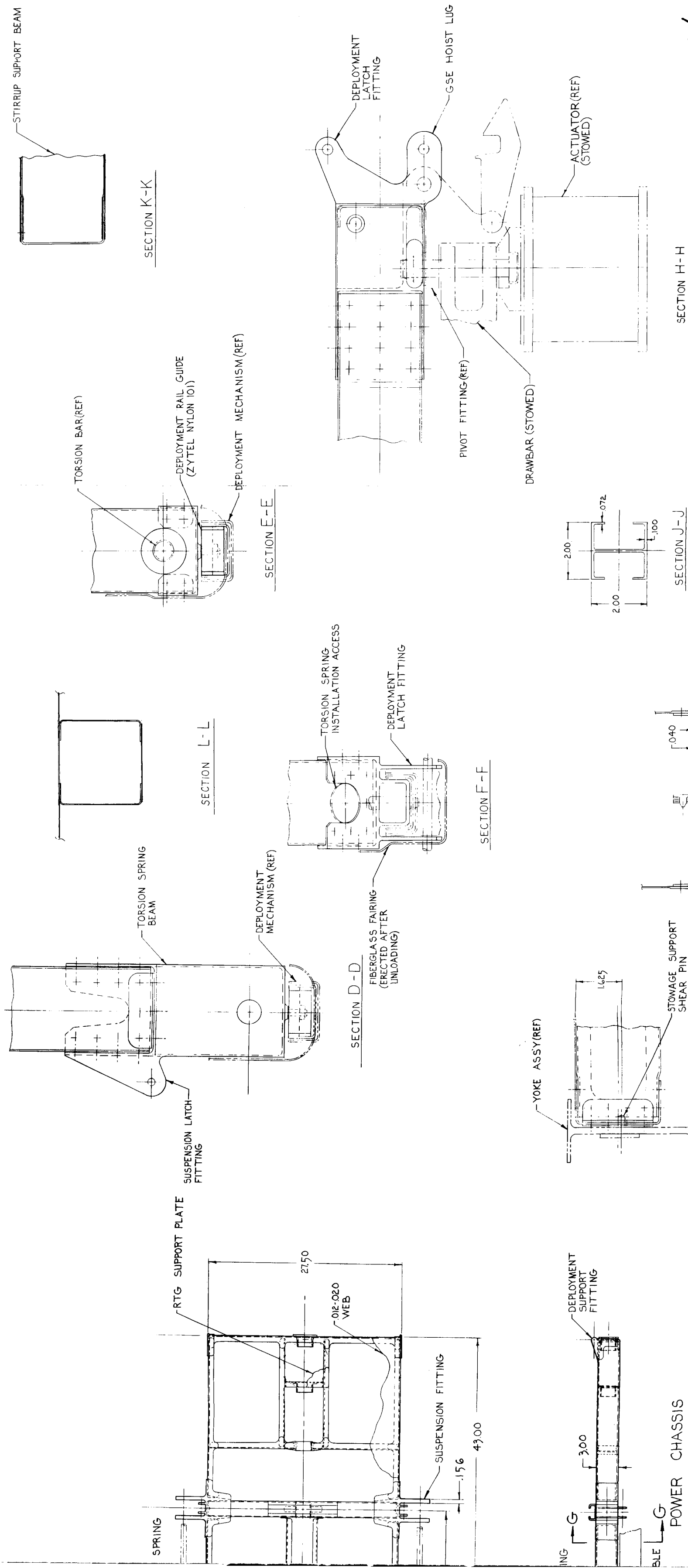


FIG. 5.1-1 STRUCTURAL ARRANGEMENT - CONTROL & POWER MODULE CHASSIS STOWED



FOLDOUT FRAME





NOTE: UNLESS OTHERWISE NOTED ALL MATERIAL IS 2024 AL ALLOY, SPEC QQ-A-250/4, FOR SHEET & PLATE AND SPEC GMPs 2007 FOR PREFORMED & ROLLED PLATE.

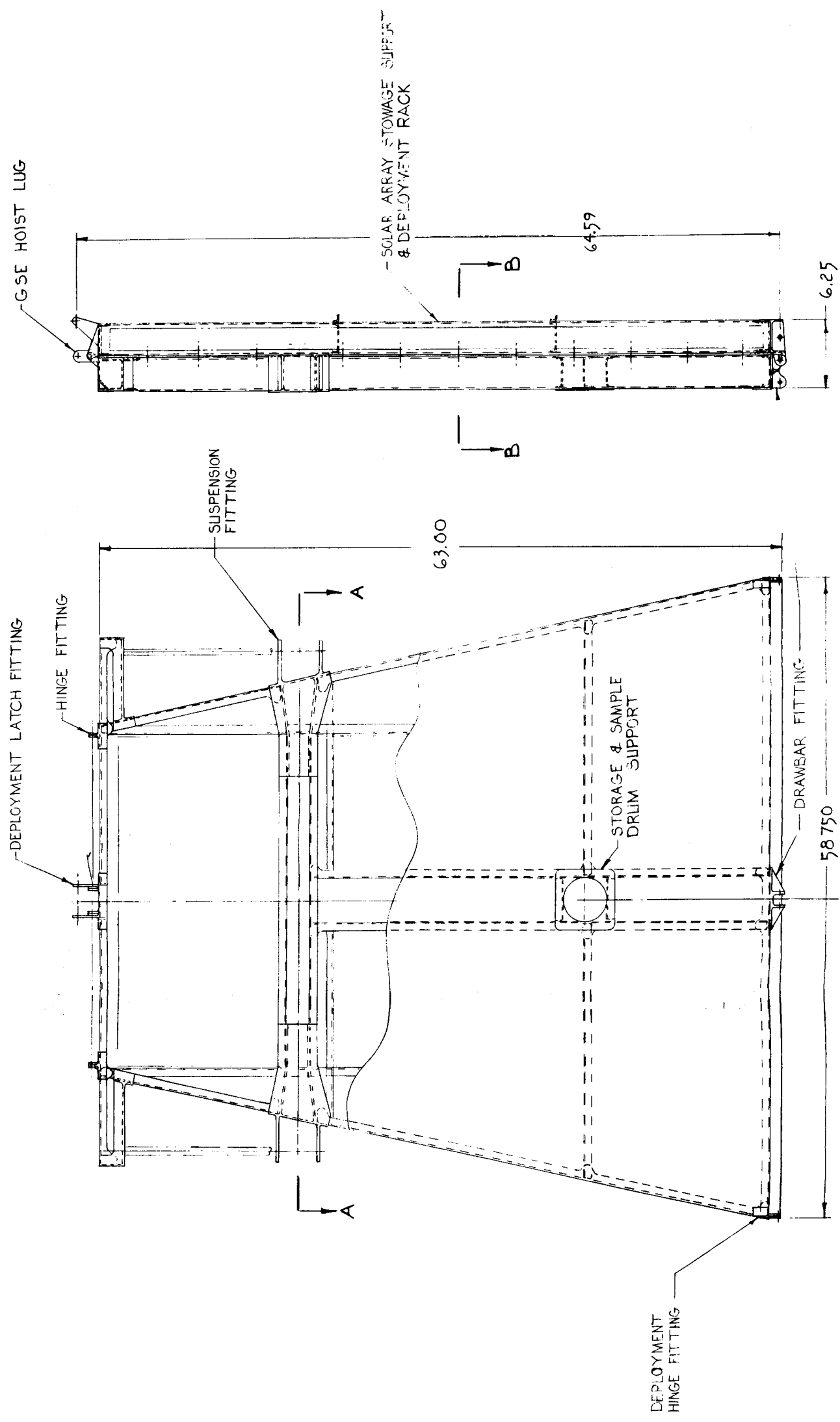
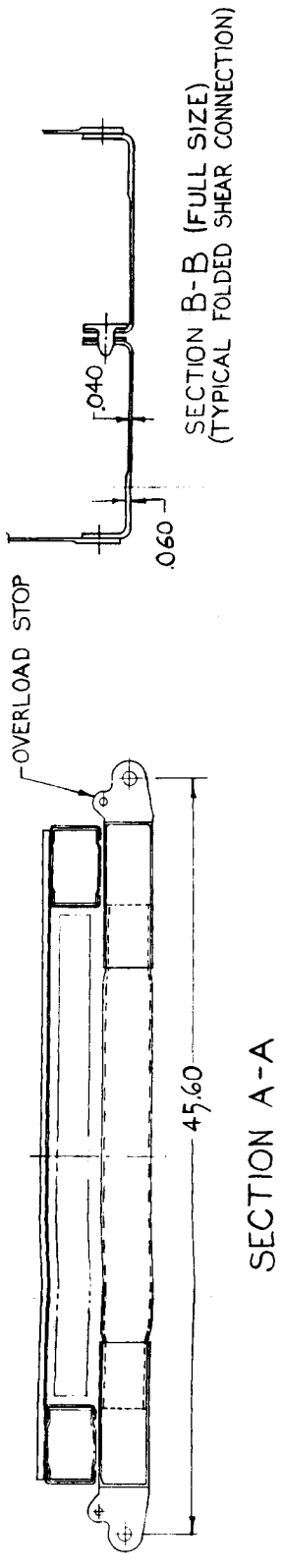
SECTION G-G (ROTATED 90°)  
TYPICAL FOLDED SHEAR CONNECTION

4  
FOLDOUT FRAME

FOLDOUT FRAME 3

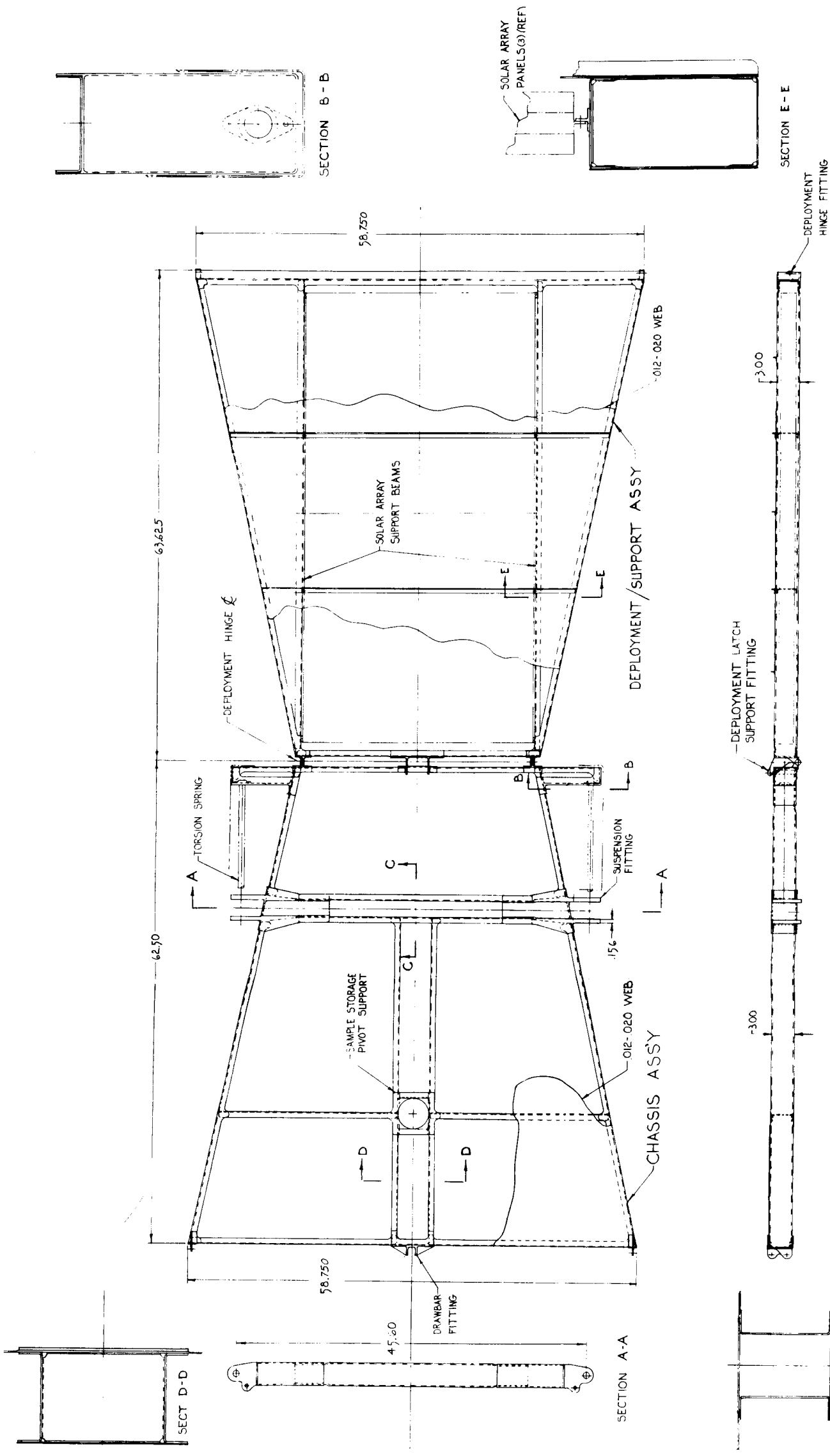
II/I.5-5/6

**FIG. 5.1-2 STRUCTURAL ARRANGEMENT - CHASSIS**



FOLDOUT FRAME

FOLDOUT FRAME 2 II/I.5-7/8



NOTE:

UNLESS OTHERWISE NOTED ALL MATERIAL IS 2024 AL ALLOY, SPEC 00-A-250/4 FOR SHEET & PLATE AND SPEC GMP5 2007 FOR PREFORGED & ROLLED PLATE.

FOLDOUT FRAME

FIG. 5.1 - 4 CHASSIS STRUCTURAL ARRANGEMENT, SCIENCE MODULE

2

While operating on the lunar surface, the chassis elements with the connecting drawbars provide the beam structure between suspension. The drawbars provide separation and clearance for articulated steering and include pitch and yaw pivot joints. They resist horizontal and vertical bending loads; however, the open section design provides intermodular torsional flexibility, eliminating the need for a rotating joint.

Attachment provisions have been made for crew support, science equipment, and vehicle subsystem components. Vehicle subsystem equipment is mounted to plate structures which can provide "tailored" thermal control and which can be easily changed for mission flexibility. These plates are attached to the DLRV chassis via fiberglass thermal isolators at a minimum of attachment points. Careful attention has been given to exposed surfaces and edges to eliminate protrusions which might cause suit snagging. In vulnerable areas, a plastic guard is provided to cover projecting structure.

During all earth checkout and test operations with the deployed vehicle, it must be supported at the chassis to prevent overloading the wheels and suspensions. Hard points for this purpose are located to coincide with points of application of operating loads. Also, a hoist lug is provided for use in the folded configuration for handling.

An important feature of the chassis design is its ability to accept a load increase due to mission growth without major redesign. A few thousands of additional material can be added in any critical area with no impact on the basic mobility system.

### 5.1.3 Thermal Considerations

The crew station and chassis thermal control requirements are governed largely by touch criteria, which specify that surfaces must be safe for the crew to touch, or be thermally shielded (Exhibit 5 of DLRV Work Statement).

Because of the severe dust environment anticipated, selective optical thermal coatings could not be relied on for long vehicle-operating periods without some provisions for cleaning. Since cleaning is impractical for the chassis structure, selective coatings were not considered.

Thermal analysis was done assuming the vehicle to consist essentially of gray surfaces having a solar absorptance and infra-red emittance of 0.85 or greater. The connections of the chassis structural elements are designed to provide adequate thermal conduction paths, so that solar heated surfaces are always in contact with cooler shadowed surfaces. For top-surface-to-side-surface ratios

greater than 2.5, maximum temperature due to environmental heating will be in the range of 180°F. Since lunar dust has absorptance and emittance values in the same 0.85 range used in the analysis, no change due to dust contamination is expected.

Additional heat loads will be imposed on the chassis due to dissipation from electrical wiring, which will run about 0.7 W per linear foot at maximum power locations. This additional thermal load should not raise temperatures above the allowable 250°F touch requirement, unless the insulation provided by dust deposits is unexpectedly high. (The resistive effect of dust accumulations is shown in Figure 4.4-6 of the Thermal Analysis Section.) It appears unlikely that dust will cover the chassis thoroughly enough to cause a thermal problem.

## 5.2 WHEELS

The mobility capabilities of the DLRV depend greatly on its wheel configuration. As a component, the wheel must satisfy the rigorous DLRV requirements of weak soil mobility, steep slope and obstacle negotiability, and applied vehicle loadings. Generally, the larger the footprint area, and the aspect ratio of this area, the better the mobility performance. Footprint area and its aspect ratio are functions of both the diameter and the flexibility of the basic shell of the wheel, hence, of the weight of the shell. Ideally, the search for the optimum wheel size and flexibility should be based on a trade-off analysis between wheel weight on the one hand, and a number of tangible and intangible factors such as power requirements, weight and dynamic characteristics of the wheel, and overall probability of mission success on the other hand. Considerations of these factors have been made; however, the trade-off analyses have been constrained by stowage volume. The vertical and lateral space allowed by stowage considerations has restricted the diameter and shape factor of the wheel. Coupled in with these functional requirements are the constraints of low component weight, high operational efficiency, and maximum mechanical reliability.

Four applicable wheel candidate designs were studied and evaluated. The conical wheel concept was selected from the evaluation since it best suited the combined wheel requirements for the DLRV.

### 5.2.1 Candidate Evaluation

A number of wheel designs was considered, but the choice was narrowed to four for final evaluation. These were conical, convoluted conical, multi-element, and wire frame concepts. The first two of these have been prototyped or modelled

at Grumman. The next two were analytically and graphically studied using prior LSSM designs established for the evaluation. Figure 5.2-1 shows the wheel candidates.

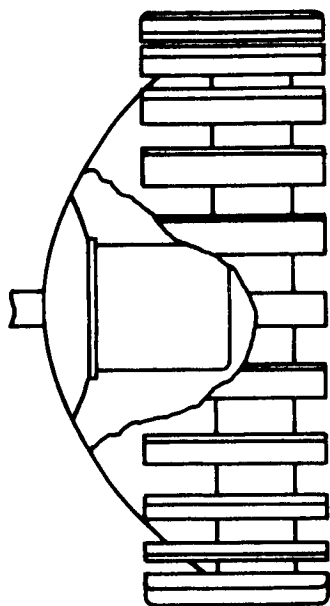
The results of the evaluation are summarized in Table 5.2-1 where a listing of nine evaluation criteria and their relative importance are shown. Weight and reliability received special emphasis; the former because of the tight weight budget on the DLRV and the fact that six wheels are involved, and the latter because of its importance in the successful completion of the prolonged mission.

The cone wheels' strongest points are its light weight, high reliability, and favorable structural characteristics. Its weight for the large diameter wheel was the lightest of those compared. Its reliability is enhanced by its self-cleaning tendency and its post-failure behavior. (Cracks at the rim propagate into lower stress areas where degradation proceeds slowly.) Gradual stiffening rather than hard bottoming, high torsional and side load capability, and low one-"g" stress loading (implying long fatigue life) are all desirable structural characteristics. On the negative side, the cone wheel requires more stowage volume. With the selected stowage arrangement, much of the volume taken by the wheel comes from the crew station, where it would not be usable for permanently mounted equipment in any event; however, there is a loss of about 15% in usable stowage volume with cone wheels. This disadvantage is reflected mainly in growth capability, since there is adequate volume to stow all required equipment and science with any of the wheel candidates.

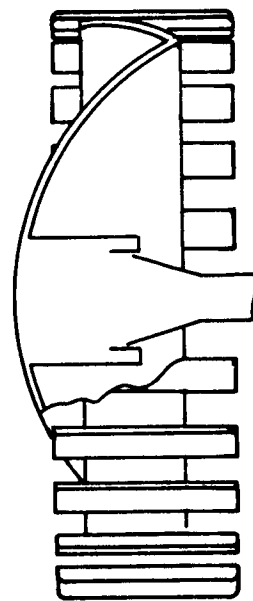
The conical convoluted wheel offers many of the advantages of the cone wheel but it takes less stowage volume. The folded geometry produces a moderate bottoming effect at about 2 g, and it allows for some debris entrapment.

Both the multi-element and wire-frame wheels are assembled units, limited in size because of their weight and low structural efficiency. Their weight is higher than that of the larger cone wheels. They have good locomotion performance (in terms of drawbar pull and efficiency) and a low stowage volume requirement. However, they are sensitive to debris entrapment and have undesirable structural characteristics (hard bottoming, high static stress, flexibility under torsional and side loads). The multi-element wheel is especially unsatisfactory in post-failure behavior, in that a single element failure propagates to adjoining elements producing a rapid disintegration.

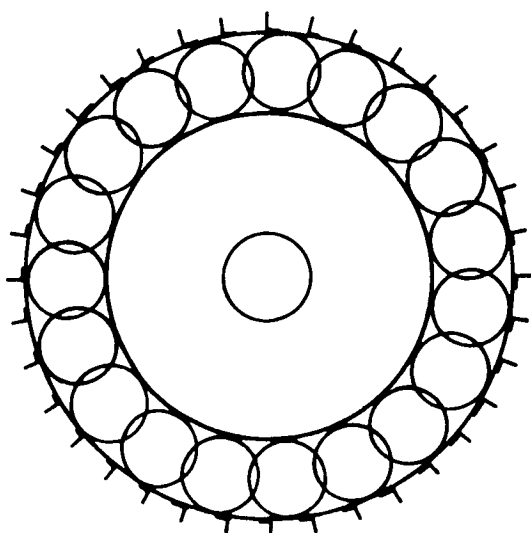
The evaluation given in Table 5.2-1 led to the conclusion that the cone wheel is



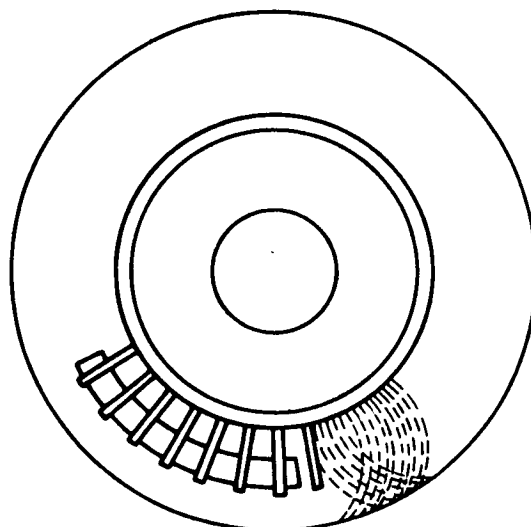
CONICAL WHEEL



CONVOLUTED CONICAL



MULTI ELEMENT



WIRE-FRAME

FIG. 5-2-1 CANDIDATE WHEELS

TABLE 5.2-1  
WHEEL EVALUATION STUDY

CRITERIA	VALUE FACTOR	CONICAL	SCORE	CONICAL CONVULATED	SCORE	MULTI-ELEMENT	SCORE	WIRE FRAME	SCORE
Reliability & Failure Mode	15	<ul style="list-style-type: none"> <li>Continuous Structure, No Fasteners</li> <li>Self Cleaning</li> <li>Good Test . Repeatability</li> <li>Potential for Repair</li> <li>Good Post Failure Life</li> </ul>	14	<ul style="list-style-type: none"> <li>Partial Debris</li> <li>Good Test Repeatability</li> <li>Potential for Repair</li> </ul>	13	<ul style="list-style-type: none"> <li>Rapidly Propagating Failure Mode</li> <li>Debris Entrapment</li> <li>Many Fasteners</li> <li>Poor Test Repeatability</li> </ul>	3	<ul style="list-style-type: none"> <li>Contacting Elements</li> <li>Debris Entrapment</li> <li>Good Post Failure</li> <li>Poor Test Repeatability</li> </ul>	10
Weight	15	<ul style="list-style-type: none"> <li>12.5 lbs.</li> <li>38" Diameter with 1" grouser</li> </ul>	15	<ul style="list-style-type: none"> <li>13 lbs. (Est)</li> <li>38" Diameter with 1" grouser</li> </ul>	14	<ul style="list-style-type: none"> <li>15.5 lbs.</li> <li>32" Diameter, 5" Width</li> </ul>	9	<ul style="list-style-type: none"> <li>18.0 lbs. (Est)</li> <li>32" Diameter, 8" Width</li> </ul>	7
Soft Soil Locomotion	12	<ul style="list-style-type: none"> <li>DP/W = .65 (Max.)</li> <li>Less Than 1 psi Loading</li> <li>Locomotive Efficiency = 55%</li> </ul>	7	<ul style="list-style-type: none"> <li>DP/W = .65 (Max)</li> <li>Less Than 1 psi Loading</li> <li>Locomotive Eff. = 55%</li> </ul>	6	<ul style="list-style-type: none"> <li>DP/W = .50 to 1.0</li> <li>0.5 psi Loading</li> <li>Locomotive Eff. = 70%</li> </ul>	10	<ul style="list-style-type: none"> <li>DP/W = .48</li> <li>0.75 to 1.0 psi Loading</li> <li>Locomotive Eff. = 65%</li> </ul>	9
Dynamic and Static Overload Behavior	12	<ul style="list-style-type: none"> <li>No Hard Bottoming</li> <li>1 G Stress 20% Ult</li> <li>Load Capability, Exceeds 5.5G</li> </ul>	11	<ul style="list-style-type: none"> <li>Moderate Bottoming 2G</li> <li>1 G Stress 20% Ult</li> <li>Frequent Bottoming at 16 KM/hr</li> </ul>	7	<ul style="list-style-type: none"> <li>Hard Bottoming 2G</li> <li>1 G Stress 40% Ult</li> <li>Frequent Bottoming at 16 KM/hr</li> <li>High Load Capability</li> </ul>	7	<ul style="list-style-type: none"> <li>Hard Bottoming 2G</li> <li>1 G Stress 60% Ult</li> <li>Frequent Bottoming at 16 km/hr</li> <li>High Load Capability</li> </ul>	6
Size Volumetrics	10	<ul style="list-style-type: none"> <li>Large Envelope-Dictates Vehicle Stowage</li> <li>Approx. 15% loss in Usable Vehicle Equipment Volume</li> </ul>	4	<ul style="list-style-type: none"> <li>Stowage Envelope 75% Conical</li> </ul>	7	<ul style="list-style-type: none"> <li>Stowage Envelope 45% Conical</li> </ul>	10	<ul style="list-style-type: none"> <li>Stowage Envelope 60% Conical</li> </ul>	9
Side Load & Torsional Flexibility	10	<ul style="list-style-type: none"> <li>Approx. 4-G Side Load capability (Designed for Scuff Damping)</li> </ul>	10	<ul style="list-style-type: none"> <li>Same as Conical</li> </ul>	9	<ul style="list-style-type: none"> <li>Poor Side Load Capability</li> <li>Very High Torsional Flexibility (3 Ft-lb/Deg Est)</li> </ul>	2	<ul style="list-style-type: none"> <li>Poor Obstacle Side Load Capability</li> <li>Good Normal Side Load Capability</li> <li>Low Torsional Flexibility</li> </ul>	8
Environmental Compatibility	10	<ul style="list-style-type: none"> <li>No Fraying Elements</li> <li>Self Cleaning</li> <li>Very Good Material Selection</li> </ul>	10	<ul style="list-style-type: none"> <li>Partial Self Cleaning</li> <li>Otherwise Same as Conical</li> </ul>	7	<ul style="list-style-type: none"> <li>Debris Entrapment</li> <li>Some Fraying Potential</li> </ul>	6	<ul style="list-style-type: none"> <li>Debris Vulnerability</li> <li>Fraying Elements</li> <li>Good Material Selection</li> </ul>	4
Operating Hysteresis	8	<ul style="list-style-type: none"> <li>Very Low Losses</li> </ul>	8	<ul style="list-style-type: none"> <li>Very Low Losses</li> </ul>	8	<ul style="list-style-type: none"> <li>Low Losses</li> </ul>	7	<ul style="list-style-type: none"> <li>Relatively High Operating Hysteresis</li> </ul>	5
Obstacle Mobility	8	<ul style="list-style-type: none"> <li>Cleats Provide Aid</li> </ul>	7	<ul style="list-style-type: none"> <li>Same as Conical</li> </ul>	7	<ul style="list-style-type: none"> <li>Good</li> </ul>	6	<ul style="list-style-type: none"> <li>Good</li> </ul>	6
TOTALS	100		86		78		60		54

FOLDOUT FRAME

FOLDOUT FRAME



the best choice for the DLRV mission. The convoluted cone has potential, but it requires considerable development. The wire frame and multi-element wheels appear much less attractive, with the wire frame being a slightly better choice.

#### 5.2.2 Material Selection

An outstanding feature of the conical wheel is that it permits fabrication from a wide selection of candidate materials. Table 5.2-2 lists these candidates and compares the resulting wheel designs on the basis of their weight and structural and mission capabilities. The table presents properties at the maximum wheel temperature of 300°F; lower or negative temperatures yield higher material allowables and are therefore less critical. The various wheel designs all have identical spring rates and the same general size and shape. In the critical weight comparison, the lightest wheel is found to be the aluminum one, with the fiberglass reinforced plastic (FRP) being a close second. The other materials are substantially heavier. Overload capability and fatigue life are also very important. The FRP and titanium wheels, with their low ratios of static stress to endurance limit, should have good fatigue characteristics. The greater the overload capability of a wheel, the more forgiving it will be to operational hazards, such as obstacle encounters. The FRP, titanium, and hybrid wheels (titanium/aluminum) are equally good in load capability; the aluminum wheel has the least capability. Based on these results, FRP was selected as the wheel material for DLRV.

Extensive studies of the permanence properties of fiberglass/epoxy show that in air or under vacuum this material degrades primarily as a result of UV radiation. If the surface is protected from UV, there is no degradation, as shown by aging tests equivalent to one year exposure. The protective surface selected for this application is a .002-inch pigmented tedlar film integrally molded onto the wheel. Trevarno F-161 impregnating resin has been thoroughly tested at Grumman under in-house programs and under a contract to PLASTEC Corp. to provide data for the new edition of MIL-HDBK-17. This is an excellent high-temperature resin and it retains much of its strength at temperatures as high as 400°F. Under low temperature, fiberglass becomes considerably stronger with little change in its modulus. "E" glass fabric may be used; however, "S" glass is a better choice since it provides at least 20% higher mechanical properties and in addition appears to have superior fatigue properties.

Since the wheel component is critical to the design and performance of the DLRV, it might be advisable to carry a backup design of titanium or the hybrid titanium/aluminum into the hardware program. In this way, should any unforeseen

TABLE 5.2-2 CONE WHEEL MATERIAL EVALUATION

CANDIDATE MATERIALS	NORMALIZED WHEEL WEIGHT	PROPERTIES AT +300°F			
		1G Stress (KSI)	Endur. Limit (KSI)	Ultimate Strength (KSI)	Mission Load Capability (G's)
FRP F-161/7581 181 Fabric Epoxy	1.0	10	21	59	5.5
AL Alloy 2024-T81	.98	22	22	64	3.5
TL 6AL 6V 2SN (ANN)	1.36	29	67	125	5.5
Steel 17-7 PH (TH1050)	1.72	51	78	171	4.5
Dual Material TL Rim - AL Hub	1.23	29	67	125	5.5

problem arise with the FRP design, a completely compatible alternative would be available. (Grumman is pursuing in-house fabrication technology for both hot spinning and cold forming titanium.) The hybrid wheel design, which uses an aluminum hub section and a titanium rim offers good thermal and structural performance at a relatively low weight.

### 5.2.3 Wheel Preliminary Design

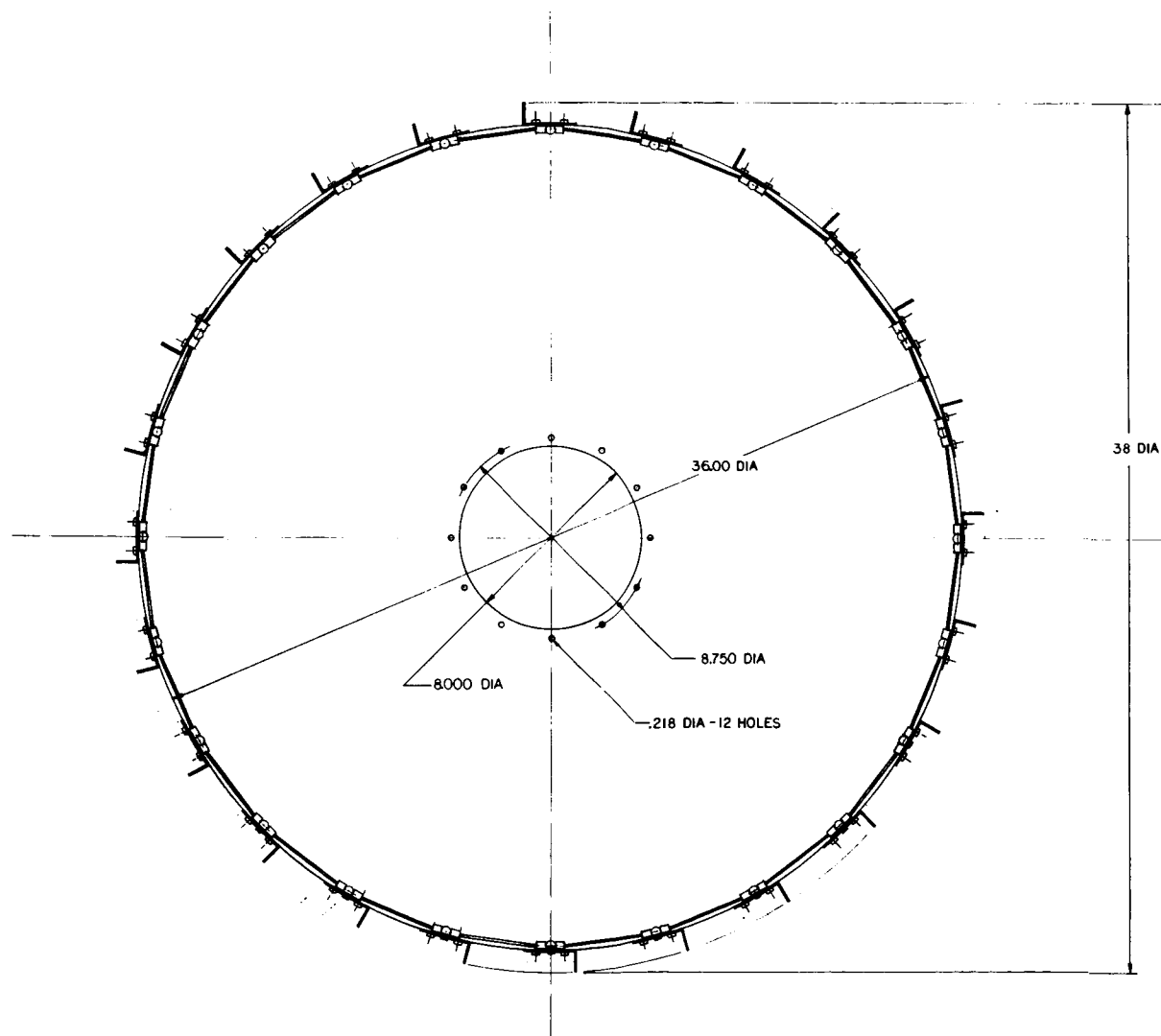
The design criteria for the wheel evolved from the configuration studies, and the mobility, dynamics and loads results discussed in Sections 3 and 4. These criteria are summarized in Table 5.2-3. Because of the large differences in static loads on the wheels during the mission, it was found advisable to design two wheel configurations, one for the heavily loaded control module, the other for the more lightly loaded power and science modules.

The preliminary design of the cone wheel is shown in Figure 5.2-2. It consists of three basic elements, a nominal .060-inch thick conical shell of revolution measuring 36 inches in diameter and 15 inches in depth, twenty four grouser cleats fastened in a space-link arrangement to the wheel rim section, and a .090-inch diameter cable assembly which interconnects the cleats aiding their support. The wheel assembly with cleats attached has a 38-inch diameter and a 17-inch depth.

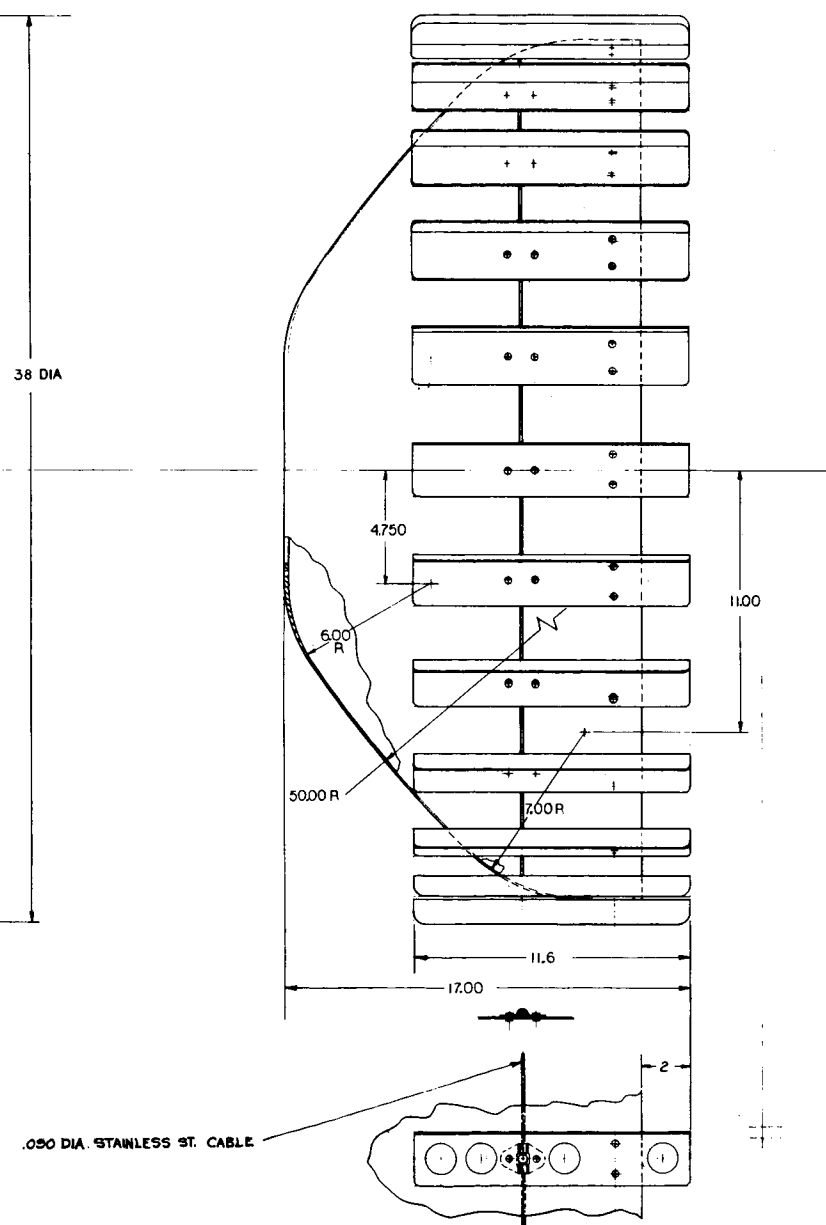
The conical shell element provides the wheel assembly with its necessary spring and structural characteristics. A combination of shape, thickness distribution and materials is used to achieve the desired cone wheel characteristics. The conical shell is fabricated from fiberglass reinforced plastic using style 778 fiberglass and Trevarno F-161 epoxy resin. A thin surface coating of Tedlar provides protection against ultraviolet radiation and improves wear resistance. The grouser-type cleat is used to enhance the wheel's traction and obstacle negotiation capability. Titanium alloy Ti-6AL-4V has been selected for the cleat material because of its superior resistance to abrasive wear and its thermal properties. The cleat has an open right-angle cross section allowing it to penetrate the lunar soil and perform its grouser thrusting action. The cleat spacing selected is based on consideration of assembly weight, cleat reliability, and soil-bridging effects (as reported in Section 4.1.1). Less priority has been placed on configuring the cleats for flotation since current mission data indicates that the lunar surface has sufficient strength to support the applicable wheel loads. A perforated open-angle titanium cleat, 11.6 inch long has been

TABLE 5.2-3 WHEEL DESIGN CRITERIA

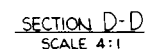
	CONFIG. "A"	CONFIG. "B"
Static Design Load	55	40
Wheel Dia. with Cleats ( lb )	38	38
Max. Radial Load ( lb )	300	220
Max. Lateral Load ( lb )	174	127
Max. Torque (lb-ft)	100	100
Effective Soil Pressure (psi)	1.0	1.0
Thermal Range (°F)	±300	±300
Life Cycles (Revs)	10 <sup>6</sup>	10 <sup>6</sup>
Max. Design Weight (lb )	12.4	11.4
Cleat Type	Grouser Space Link (Typ.)	
Cleat Length (in.)	12	12
Number of Cleats	24	24
Configuration "A" - Control Module Wheels		
Configuration "B" - Power and Science Module Wheels		



FOLDOUT FRAME



1. TERNARNO F-161 PREP FROM COAST MFG, DIVISION OF HEXCEL.  
USE 7781-350 GLASS FABRIC.
2. FABRICATE PER GRUMMAN STD. SPEC. 11102A AND MATERIAL  
PER GRUMMAN MATERIALS PROCUREMENT SPEC 4001
3. LAY UP TO BE ISOTOPICT WITH 1% MINIMUM.
4. CURE AND POSTCURE PER G.S.S. 1102A
5. STRUCTURAL FILLER MATERIAL TO BE EPOCAST 1310 OR  
EQUIVALENT.
6. OUTSIDE COATING TO BE EITHER TEDLAR FILM, .002" THICK,  
ONE SURFACE TREATED FOR ADHESION (DUPONT) OR A  
PIGMENTED EPOXY ENAMEL PER G.S.S. 4505.
7. ALL FAYING SURFACES TO HAVE A PEE PL.
8. .002" ALL OVER AND TFE FILLED POLYURETHANE  
COATING ON SURFACE INDICATED



II/I.5-21/22

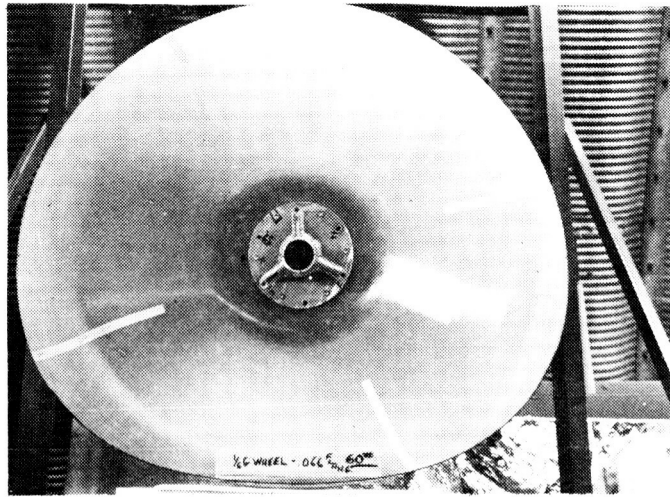
selected for the wheel. Tests have shown that a negligible increase in wheel rolling resistance is attributable to the cleat system. A feature of the grouser cleat system is the intercleat tensile attachment which acts to stabilize the cleat in active contact with the lunar surface and distributes the concentrated loads around the rim. This permits a lighter weight fiberglass cone to be used. A .090-inch diameter stainless steel flexible cable assembly is used for the intercleat member. The shape of the wheel is determined by load/deflection requirements and delivery vehicle stowage envelope constraints. The 38-inch diameter is the largest stowable wheel. The 17-inch depth and associated curved shape is designed to provide an initially soft spring rate to develop a large static deflection and footprint, followed by gently stiffening characteristics for overload. The hub area is flat and reinforced with a lightweight core filler to provide additional strength and to accommodate the wheel drive assembly.

#### 5.2.4 Structural Analysis and Test

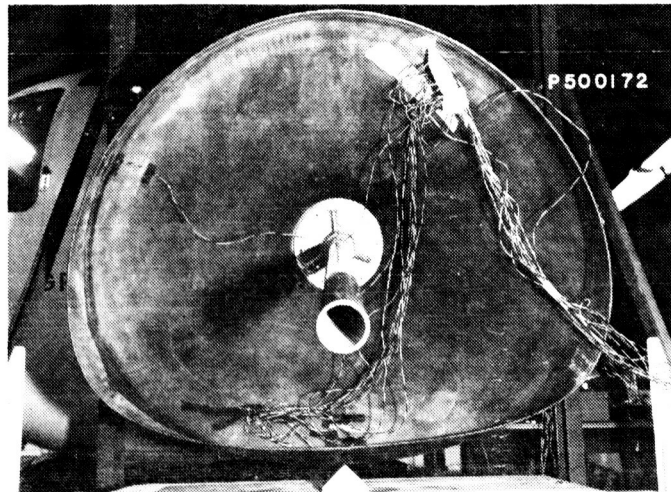
The cone wheel structure consists of a thin open shell of revolution. Deflections at the rim can be very large, making any analysis of the area quite difficult. Experimental test results have been used instead to form an empirical basis for the cone wheel design.

The area from the hub to a region near the rim is not subjected to such large deflections, and can be more readily analyzed. Grumman has a shell computer program (STARS II) that is capable of analyzing any structure that can be idealized as a combination of varying thin surfaces of revolution, including cylinder, ellipsoid, ogive, paraboloid and cone. The program obtains solutions to the equations of elasticity using assumptions of small displacement theory, and can handle symmetric and unsymmetric loadings. It has been used successfully at Grumman on a variety of shell structures including, among others, LM propulsion tanks, LM landing gear and foot pads. This program was used to size the cone wheel in the low deflection regions away from the rim.

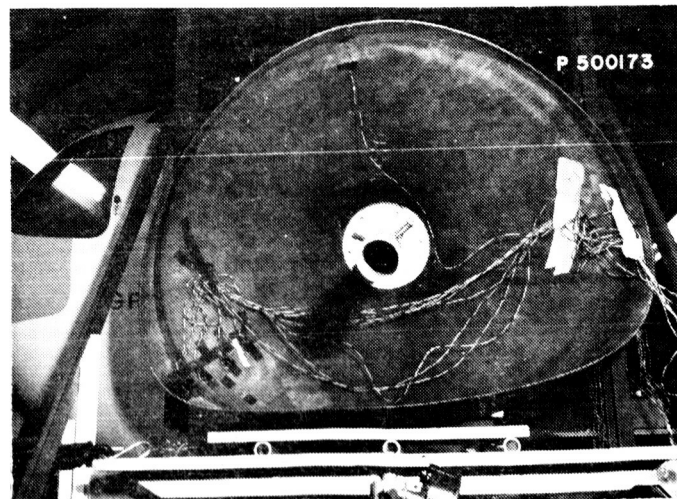
Extensive full scale testing on a 1/6-g FRP cone wheel has been used to augment the analysis. Figure 5.2-3 shows an instrumented wheel undergoing static testing. Normal loading on a flat surface, concentrated loading, and combined normal and drag loading conditions are shown. Note that the deformed shape under the concentrated load differs little from the flat surface load, indicating that there is no extreme stress build-up in the vicinity of a concentrated load with a cone wheel.



(A) TEST WHEEL AT STATIC LOAD



(B) STRAIN GAGED WHEEL WITH POINT LOAD



(C) STRAIN GAGED WHEEL WITH NORMAL AND DRAG LOADS APPLIED

FIG. 5.2-3 INSTRUMENTED DLRV WHEEL UNDERGOING TESTS



The load-deflection curves for a wheel with and without cleats are shown in Figure 5.2-4. The behavior is that of a nonlinear hardening system; the low initial stiffness allows the desired large footprint to develop under static loading, while the high stiffness in the upper load range provides favorable overload characteristics. The effect of the cleats is to provide reduced initial flexibility and increased overload stiffness, both desirable characteristics. Circumferential and meridional stress distributions are shown in Figs. 5.2-5 and 5.2-6. The most critically stressed area for both dynamic overload and repeated loading occurs at the rim edge of the wheel where stresses of the following magnitude were indicated:

- o 10,000 psi for nominal static load of 50 lb (1-g equivalent)
- o 18,000 psi for high combined loading: vertical 150 lb (3-g equivalent) and drag 110 lb
- o 24,000 psi for radial overload of 250 lb (5-g equivalent)

Although these tests have not yet been carried to failure, the results indicate that the typical failure mode will manifest itself as a meridional crack initiated by an overload at the rim edge. The decreasing stress field in the direction of crack propagation will retard its development, providing the wheel with inherent fail-safe properties.

The relatively low operating static stress level (less than 10,000 psi) compared to the allowable fiberglass flexural strength (about 59,000 psi) indicates ample fatigue life for the tested wheel. This is particularly so in view of the lack of stress concentrations inherent in the cone wheel design.

#### 5.2.5 Thermal Analysis

The thermal environment for the wheel is derived from a radiation interchange between the wheel traction drive, the lunar surface, the sun, and -460°F space. A detailed network computer analysis was performed to evaluate the design approach.

The thermal load from the traction drive results from inefficiencies in the motor and gear reduction unit. Table 5.2-4 shows these loads for various wheel drive load requirements.

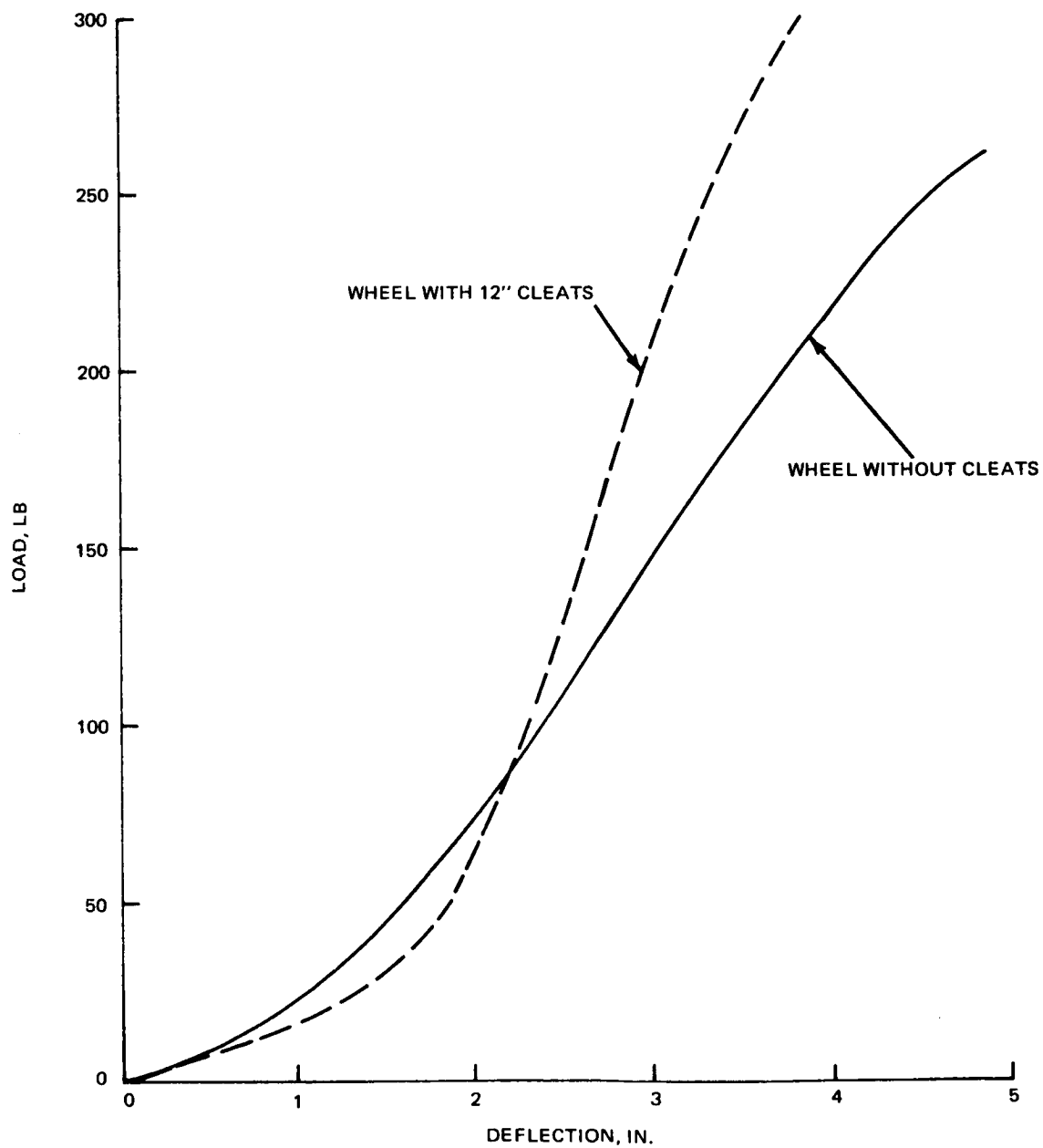


FIG. 5.24 LOAD DEFLECTION CURVE FOR CONE WHEEL

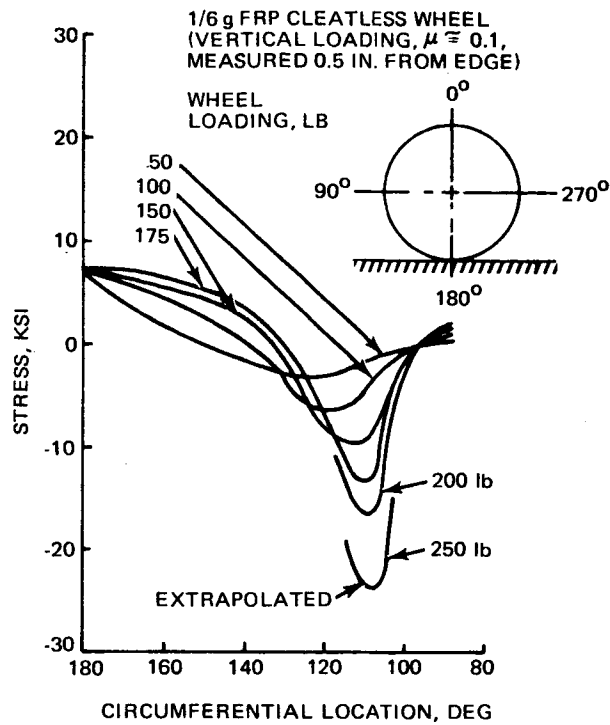


FIG. 5.2-5 CIRCUMFERENTIAL STRESS DISTRIBUTION

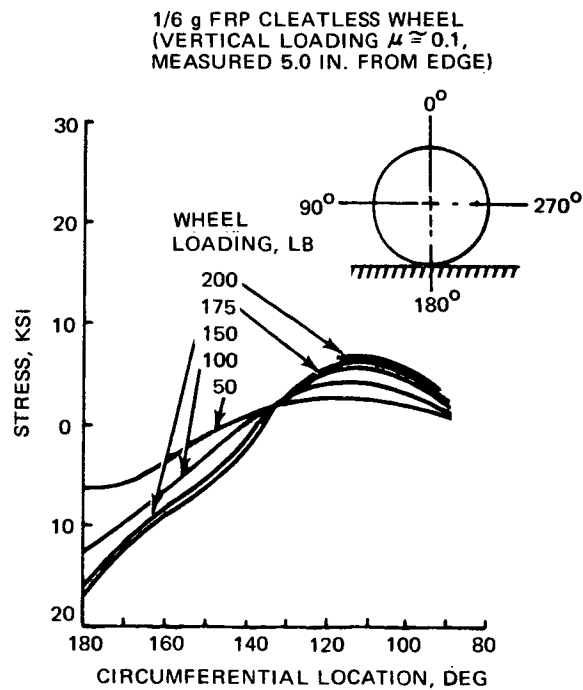


FIG. 5.2-6 MERIDIONAL STRESS DISTRIBUTION

TABLE 5.2-4 TRACTION DRIVE THERMAL LOAD

<u>Load and Speed</u>	<u>Motor</u>	<u>Gear Box</u>	<u>Total</u>
1 km/hr and 4 ft-lb	1.03	0.2	1.2
2 km/hr and 4 ft-lb	1.33	0.4	1.7
16 km/hr and 4 ft-lb	13.5	5.5	19.0
16 km/hr and 6 deg climb	44.0	6.0	50.0
1 km/hr and 2 deg climb	40.0	6.7	46.7
2 km/hr and 25 deg climb	60.5	7.2	67.5

A conservative dissipation of 50 watts was used in the analysis. Using the environmental data supplied by Annex C of the Statement of Work, lunar and solar incident radiation loads were computed. Figure 5.2-7 depicts these load levels and shows the worst-case solar elevation angle to be 75°.

The results of the analysis conducted are summarized in Figure 5.2-8. This analysis assumed that no selective thermal coatings were feasible because of the severe dust expected in this area. The thermal resistance due to dust was taken as that caused by a 0.002-inch build-up, a value considered achievable with mechanically wiped surface. (See Section 4.4.1 for the effects of dust on thermal resistance.) For the selected drive units, wiping of the inner wheel hub area was considered impractical; as an alternative an additional 1.2 ft.<sup>2</sup> of a conical radiator was added. This radiator design can be more easily wiped and will provide temperatures in approximately the same distribution shown in Figure 5.2-8. This design approach permits further growth if required by future operations.

WHEEL AND MOTOR SURFACE PROPERTIES:  $\alpha_s = \epsilon = 0.85$

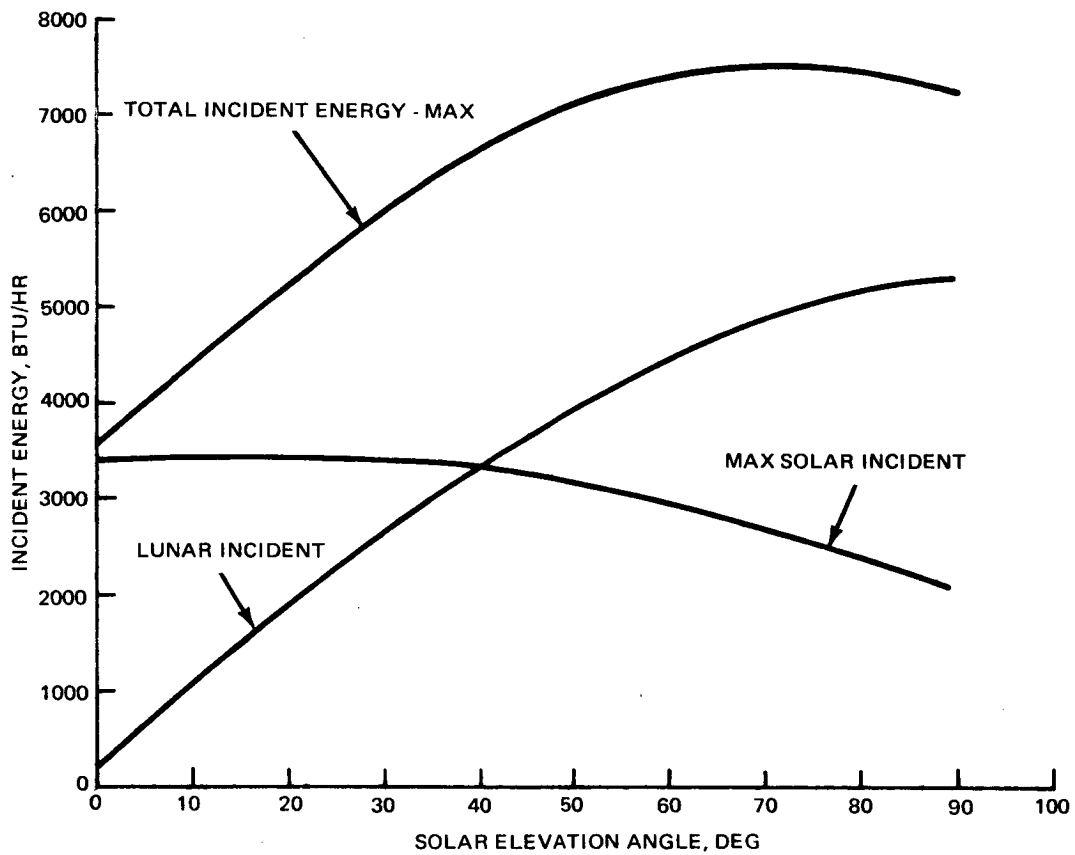
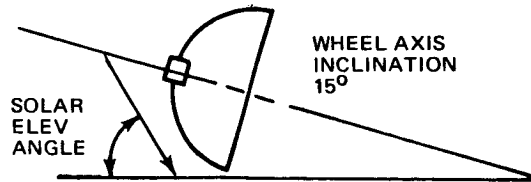


FIG. 5.2-7 WORST CASE TOTAL INCIDENT RADIATION

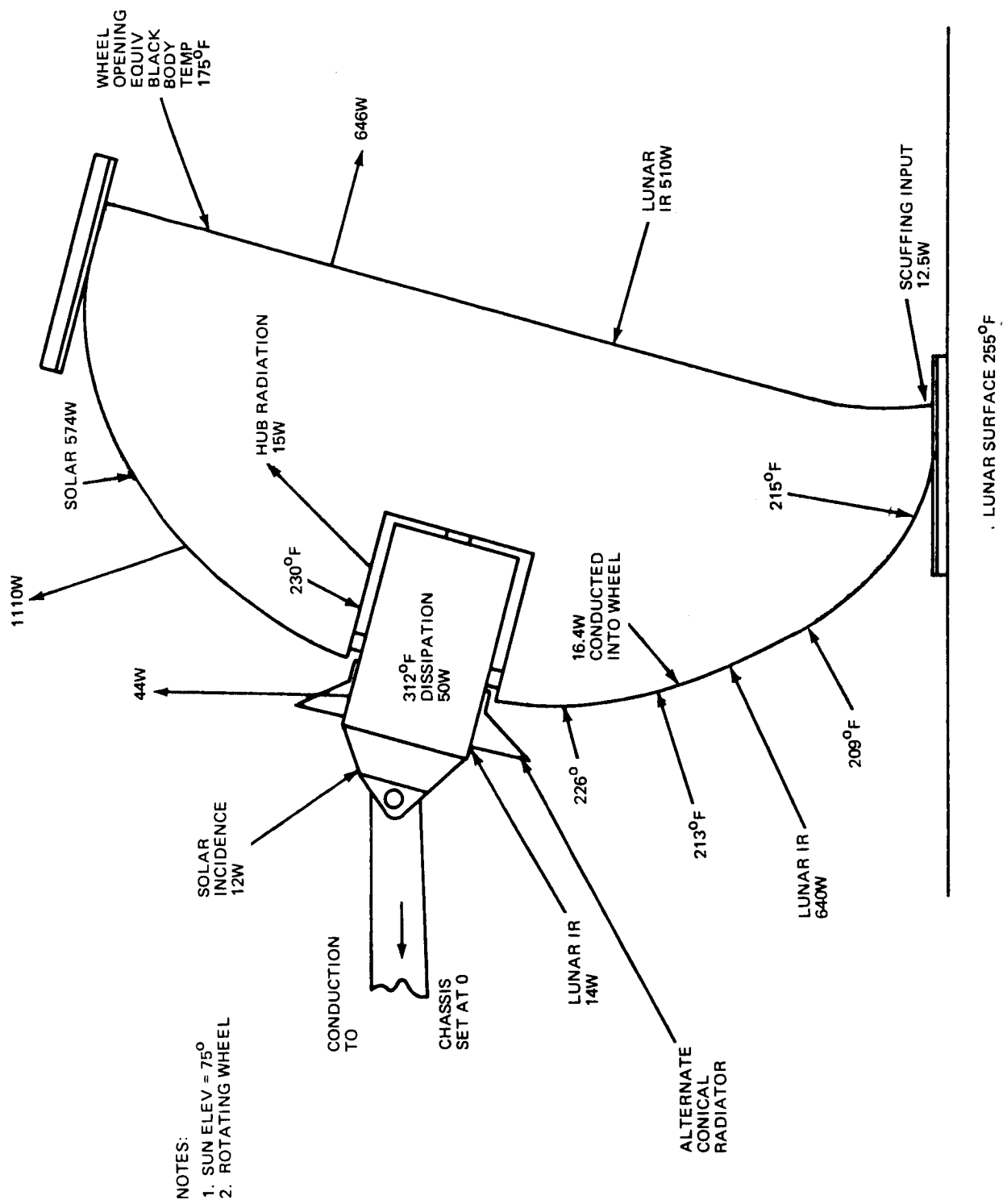


FIG. 5.2.8 WHEEL/DRIVE THERMAL DIAGRAM

### 5.3 SUSPENSION

The selection of the suspension system for the DLRV required consideration of a number of factors: stowage and deployment, steering system, weight allocation for the suspension system, and the wheel/suspension functional interface.

The DLRV stowage arrangement requires that the suspension assembly be both foldable and readily deployable with the structural integrity to take delivery and ground running loads. The selected chassis articulation steering design simplifies the suspension since it need not operate in conjunction with any steering mechanism such as an Ackerman system would require. Weight is a major constraining factor when deciding upon the type of system due to the number of DLRV wheels and their accompanying suspension assemblies. Finally, the suspension system must be integrated with the wheel and chassis components to provide the proper stroking geometry, load reaction, and flexibility.

#### 5.3.1 Candidate Evaluation

Three basic suspensions were considered and evaluated for this study. Inherent DLRV characteristics limited the selection of candidates to the trailing arm, swing arm, and the parallel arm suspension types. Figure 5.3-1 illustrates and describes the types of suspensions. Since the three-module concept is being used for the DLRV configuration, the suspension type selected will be typical for all three modules with minor design differences to accommodate stowage requirements.

The decision to configure the DLRV as a three-module assembly having two extendable intermodular drawbars cancelled the primary reason for using the trailing arm suspension design; namely, to acquire added wheelbase while maintaining a method for wheel stowage. Further, the methods applicable for stowing the multi-modular DLRV, while maintaining acceptable accessibility to critical equipments during spacecraft buildup and "on-pad" checkout eliminated this candidate approach. The study evaluation was then limited to the swing arm and parallel arm concepts.

Table 5.3-1 lists the individual criteria and value factors which were used to conduct the selection evaluation. The evaluation clearly pointed out the disadvantages of the parallel arm suspension for most criteria being considered. Briefly reviewed, the parallel arm system is a more complicated arrangement

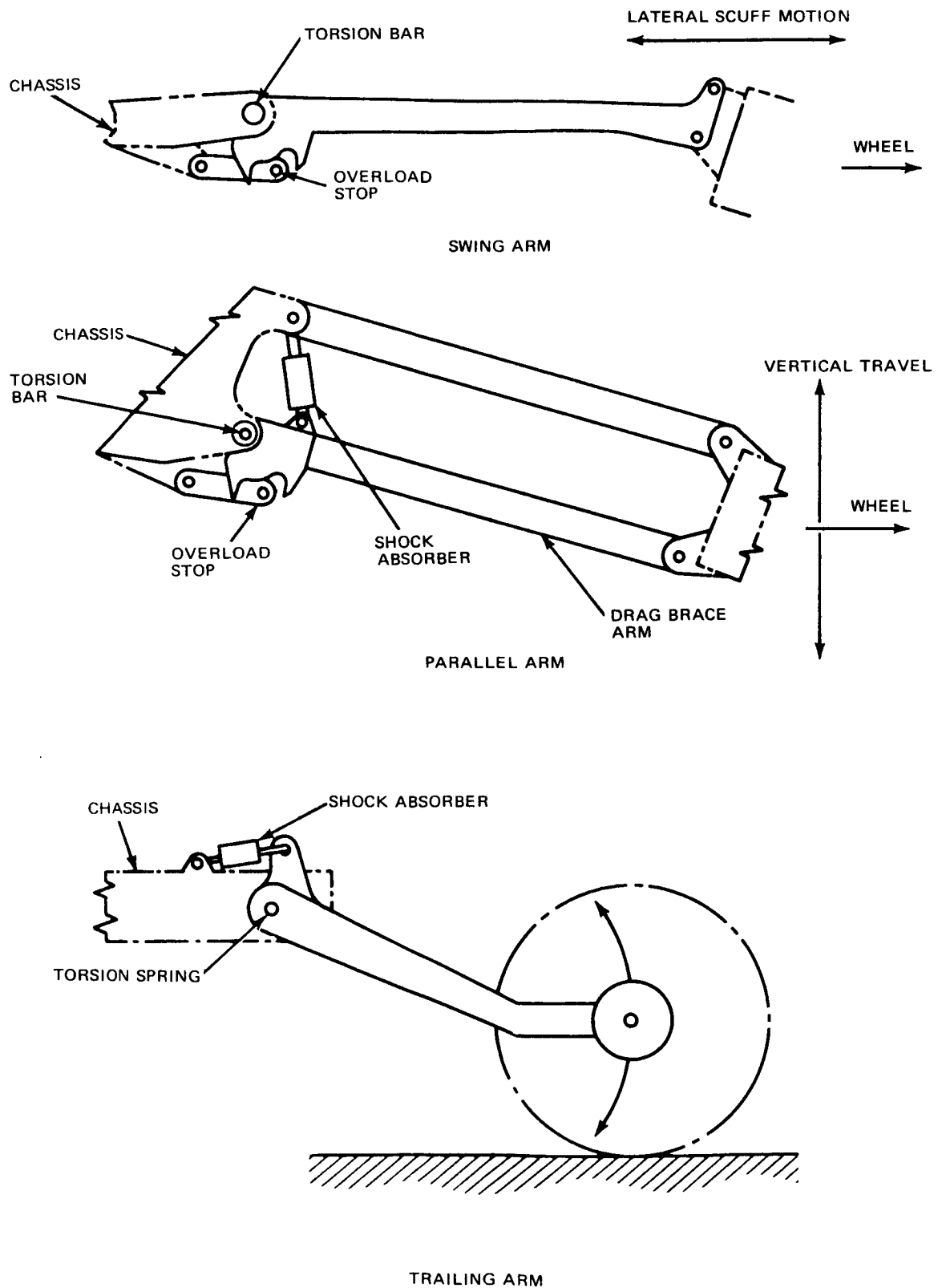


FIG. 5.3-1 CANDIDATE SUSPENSIONS



TABLE 5.3-1

## SUSPENSION SYSTEM EVALUATION

<u>CRITERIA AND REASON FOR LOWER SCORE</u>	<u>(VALUE FACTOR)</u>	<u>PARALLEL ARM</u>	<u>SWING ARM</u>
<u>MECHANICAL RELIABILITY/FAILURE MODE</u>	(15)	12	14
o 2 active link arms requiring 4 pivots vs. 1 strut and 1 pivot			
o shock absorber vs. wheel scuff damping			
<u>WEIGHT</u>	(15)	7	14
o shock absorbers (6) 10 lb			
o second arm + joints 9 lb			
<u>ENVIRONMENTAL COMPATIBILITY</u>	(10)	8	9
o shock absorber leakage			
o road damage			
<u>STOWAGE &amp; DEPLOYMENT</u>	(15)	10	12
o additional bulk & stowage complexity			
<u>GROWTH/OVERLOAD</u>	(10)	8	8
o no significant difference			

FIG. 5.3-1 (cont..)

<u>DYNAMIC PERFORMANCE/STABILITY</u>	(15)	14	9
o Less predictable damping performance due to nature of scuffing			
o Mechanical damper can be tailored to exact needs			
<u>DESIGN INTEGRATION</u>	(20)	14	16
o Additional chassis hard points required for struts and damper instal.			
TOTAL	<u>(100)</u>	<u>73</u>	<u>82</u>

requiring additional pivoting linkages and deployment locks. A velocity sensitive damper is needed for shock attenuation, whereas the swing arm concept uses wheel lateral motion for ground scuffing as an effective means of vehicle damping. Both analog computer runs investigating vehicle dynamics (Section 4.2) and Grumman's full scale lg rover simulator have verified the vehicle's satisfactory performance using wheel scuff damping.

The 6 x 6 weight penalty associated with the parallel arm concept is prohibitive; it is estimated to be a 19-lb increase over the swing arm. This weight and mechanical complexity are used to insure that the wheel follows a vertical path during suspension motion, a requirement which is not necessary when using the conical wheel. The vulnerability of the shock absorbers to the lunar environment is a further liability of the parallel concept.

Lastly, consideration must be given to the extent to which the DLRV suspension will be used. The unmanned mission, which is the major portion, does not require much more than ordinary wheel flexibility to maintain acceptable performance. Consequently, any penalty in weight and reliability to the DLRV above the minimum as needed by the swing arm suspension is not justifiable.

On the basis of the above results and the scores listed in Table 5.3-1, the swing arm suspension system was chosen for the DLRV.

### 5.3.2 Suspension Preliminary Design

The design requirements for the suspension system are derived mainly from the manned mission phase. This part of the mission produces 50% greater wheel loads on the control module and, as in the case of the wheel component, two designs are used - one for the control module and one for the power and science modules. Table 5.3-2 lists the design criteria for both suspensions, i.e., config. "A" control module, - config. "B" science and power module. These criteria were established through an iterative process of vehicle design changes and system parametric assumptions. The process continued until the DLRV configuration was decided upon and analog computer results indicated satisfactory dynamic performance.

The control and power module suspension system designs are shown in Figs. 5.3-2 and 5.3-3. The science module suspension details are similar, except for the two-position feature, which is not needed. The suspension combines a flexible

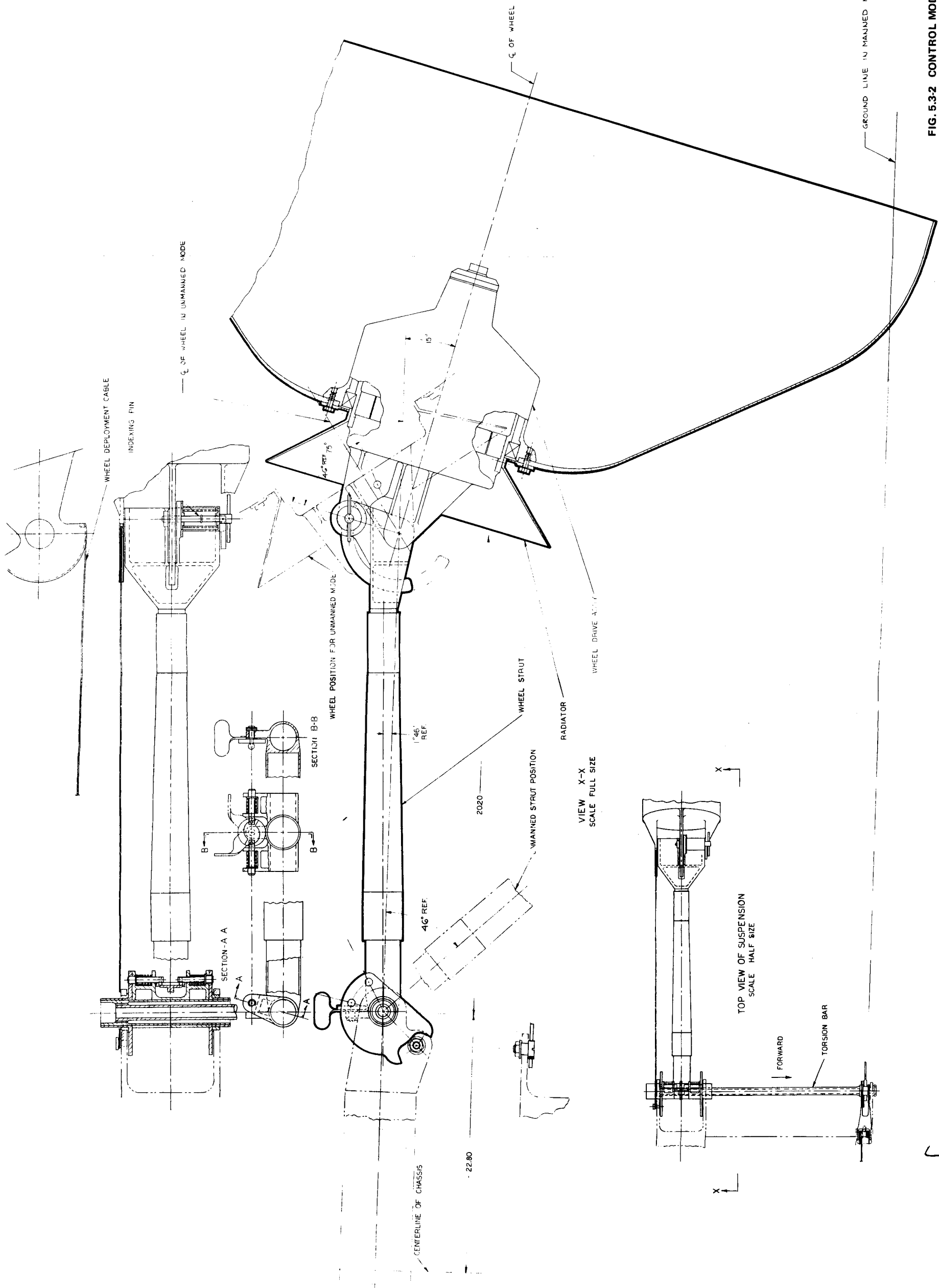
TABLE 5.3-2

Suspension Design Criteria

	<u>Config. "A"</u>	<u>Config. "B"</u>
Wheel Radial Load (Static) - lb.	55	40
Wheel Radial Load (Max) - lb.	300	220
Wheel Lateral Load (Max) - lb.	174	127
Wheel Torque (Max) - lb.-ft.	80	80
Wheel Tread - in.	114	114
Ground Clearance: - in.		
Manned	19.5	19.5
Unmanned	34	34
Max. Stroke - in.	16	16
Spring Rates: - lb./in.		
Suspension Spring	10.	7.5
Overload Spring	90	80
Life Cycle	10 <sup>6</sup> full travel	10 <sup>6</sup> full travel
Damping - lb.-sec.-ft. <sup>-1</sup>	10	10
Max. Weight - lb.	<5	<5
Thermal Range - (°F)	+350, -250	+350, -250
Torsional Rigidity - (in.-lb. <sup>-1</sup> ) degree	1000	500

Note: Config. A - Control Module

Config. B - Power & Science Modules

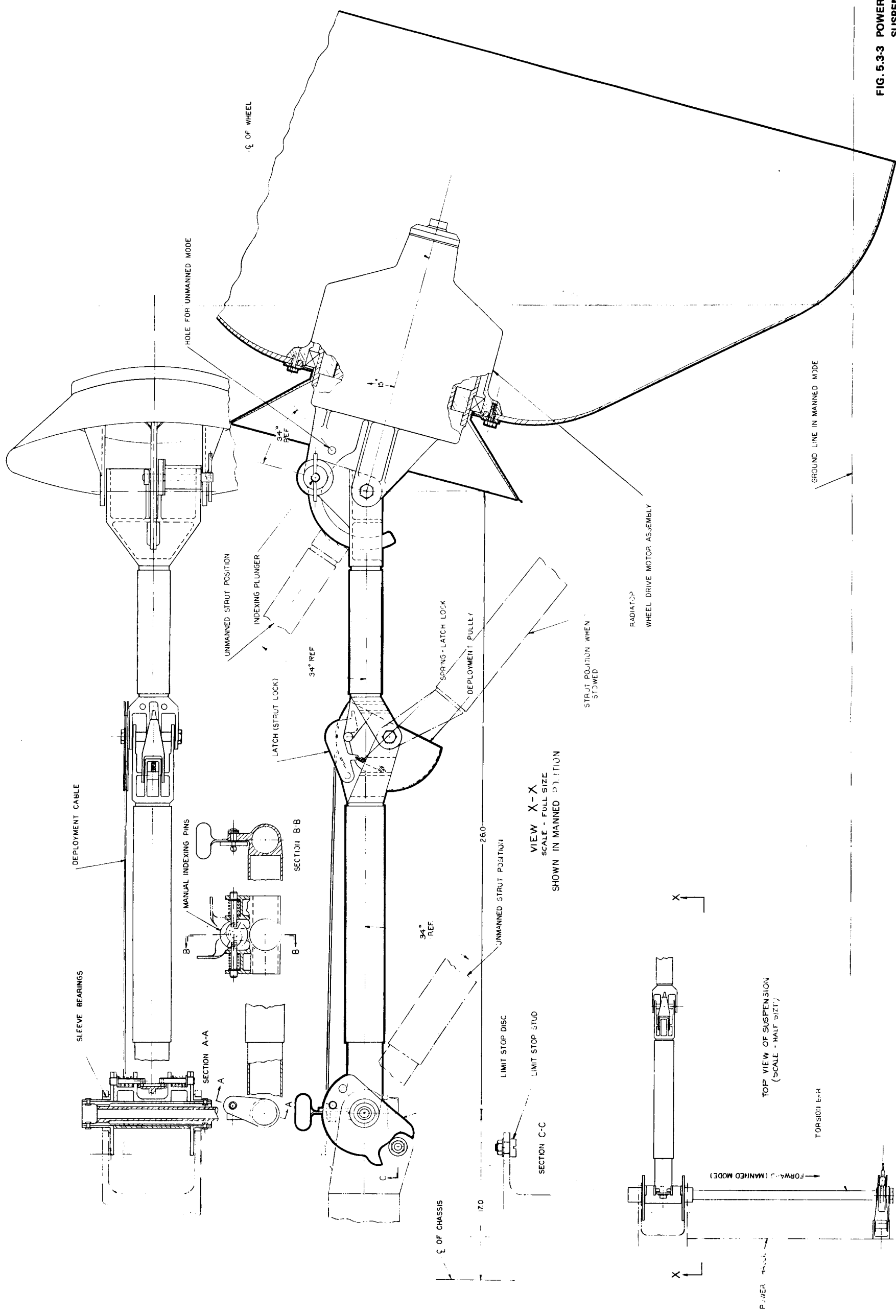


FOLDOUT FRAME

2

FIG. 5.3-2 CONTROL MODULE SUSPENSION

FOLDOUT FRAME



wheel, a semi-rigid wheel strut, and a torsion-bar spring attached to the chassis. Upward motion of the wheel is resisted by the support strut reacting against the chassis-grounded torsion bar.

Suspension damping is inherently provided by wheel-to-ground scuffing which is achieved by the change in tread that accompanies suspension deflection. The effective lateral coefficient of friction for a rolling wheel is a linearly increasing function of sideslip angle up to about 12 deg and is relatively constant for greater angles. Thus, the damping obtained is inversely proportional to vehicle forward velocity above the low speed range. The normal force between the wheel and ground is the variable wheel load which produces a nonlinear effective damping coefficient.

An advantage provided by scuff damping, in addition to the obvious one of eliminating the need for a mechanical damper, is the favorable way in which the energy is partially dissipated directly into the soil and the remainder is distributed over the outer rim of the wheel. This provides both a large radiating surface and time for cooling between wheel revolutions.

To stow the DLRV, the wheel struts are folded about the torsion bar axis. During deployment the struts swing down until spring loaded latches capture them and engage the torsion bars. Teflon-coated sleeve bearings are used at the suspension bearing points. This automatic locking method is extensively employed in aircraft landing gear downlock applications. It has also been used successfully on the IM landing gear downlock.

The latch used to lock the output end of the torsion bar sustains the normal operating loads up to nine inches of wheel hub deflection. When loads are greater, a latch riding in a slot at the torsion bar input end will bottom and transfer overloads directly to the chassis. Suspension flexibility is then due only to the wheel strut deflection. When the torsion bar, wheel strut, and wheel are all at their maximum deflection, the total stroke is 16 inches.

High-strength 4340 steel has been selected for the torsion bar spring material because it satisfies the fatigue life criteria of 1,000,000 cycles. This is equivalent to full travel at 1 cps for 600 hr operation. Shot preening and presetting are employed to develop full fatigue life.

Thin-walled tubular strut members are the lightest structure for supporting multi-directional and combined wheel loads. Wheel strut material is titanium Ti-6Al-4V. At its ultimate overload position the aft strut reaches a stress level of 106,000 psi. Stresses are lower on the forward strut. The allowable ultimate stress for Ti-6Al-4V at 250°F is 136,000 psi, giving safe margin for overloading.

The load deflection characteristics of the suspension are shown in Figure 5.3-4. The torsion bar spring rate of 7.5 lb/in govern the flexibility during normal operation. For the infrequent chassis loads which exceed 2.1 lunar g (9-in. deflection beyond static) the strut spring rate of 90 lb/in in series with wheel flexibility becomes the suspension stiffness.

In the unlikely event of a torsion bar failure, the suspension becomes harder, but safe. The overload latch engages and the DLRV continues to operate with a static chassis-ground clearance of 12 in. The spring rate in this case is that of the combined wheel and strut.

At the completion of the manned mission, the DLRV is reconfigured to the unmanned mission mode. The suspensions of the control and power modules are manually repositioned to gain greater chassis ground clearance and the required 35° break angle. This is accomplished by resetting the wheel and wheel strut lock pins after rotating the struts downward and reindexing the wheels relative to their support struts. This task is repeated at each wheel station of the 4 x 4. The science module suspension is fixed for the unmanned configuration and requires no further adjustment.



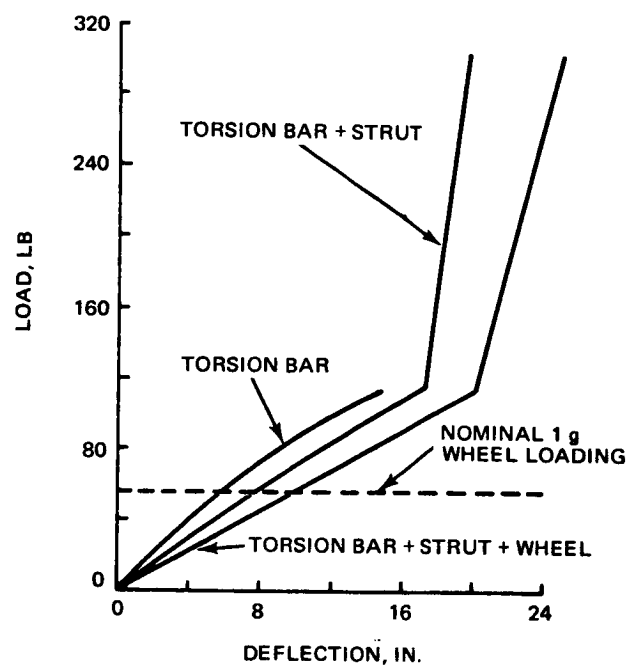


FIG. 5.34 SUSPENSION LOAD/DEFLECTION CHARACTERISTICS

## 5.4 STEERING MECHANISM

This section describes the study work leading to the selection and method of implementing the DLRV steering system. Both the Ackerman steering and full chassis articulation designs were evaluated, with the articulation concept being selected. The mechanical drive assembly which accomplishes the articulated steering and its performance requirements are also included as part of this section.

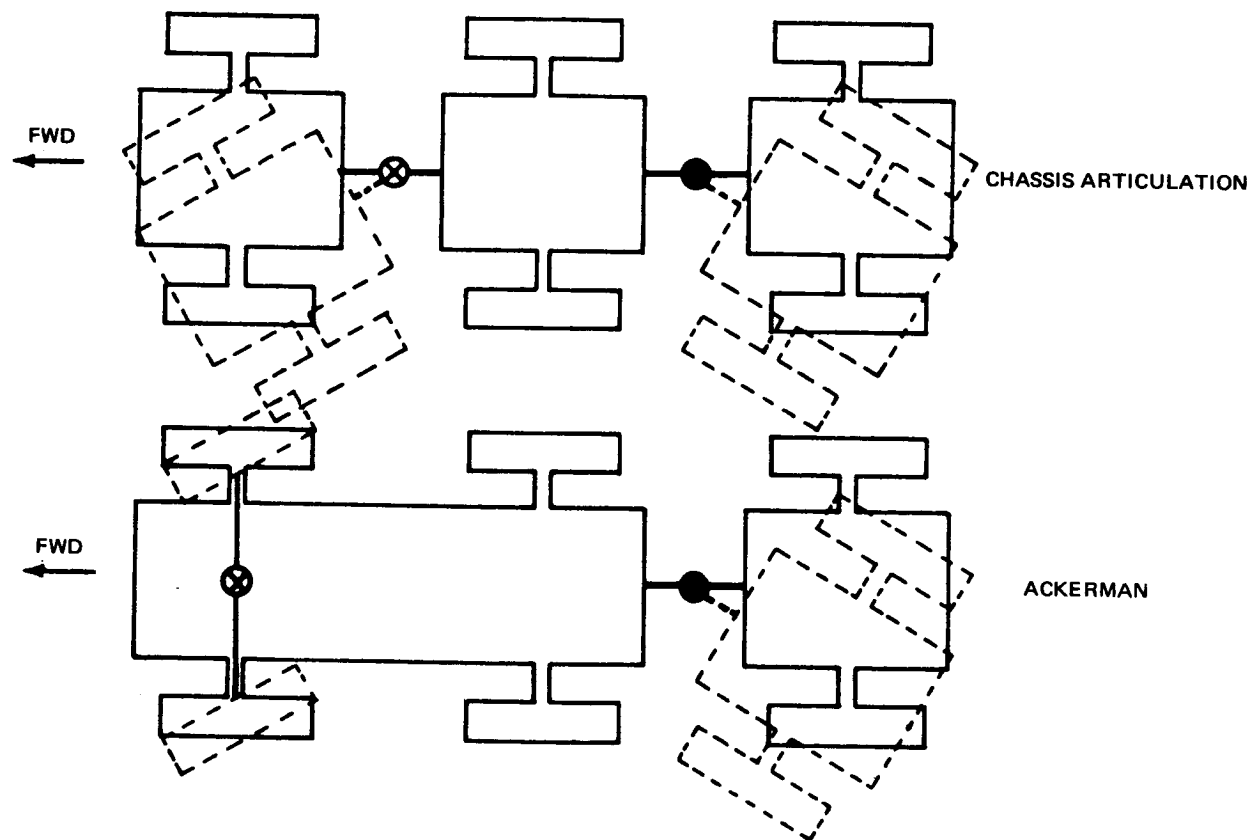
The problem of selecting one steering concept over another required an investigation into the vehicle's overall performance and mission capabilities. In general, the basic performance requirements can be satisfied by a number of steering methods, such as Ackerman, wagon, or articulation. However, there are sufficient differences between these concepts to permit a logical selection decision to be made. The steering system requirements are somewhat intangible, but the most important can be listed as follows:

- o The steering system should be capable of accepting the wheel folding requirement needed for DLRV stowage without undue complication
- o A high degree of primary system reliability is required backed up by a confident secondary system.
- o The steering system should allow the DLRV a turning radius equal to one vehicle length
- o The steering mechanism should be compatible with up to one year lunar environmental exposure

### 5.4.1 Candidate Evaluation

Two candidate steering systems were evaluated in detail for the DLRV: Ackerman and chassis articulation. Figure 5.4-1 illustrates the competing candidate concepts. The Ackerman arrangement required a rigid 4 x 4 chassis frame vehicle with the forward wheels being steered. The aft module is allowed to trail via a drawbar and is pivotable about a simple steer axis. Reliability is achieved by mechanically interconnecting the steered wheels with a tie rod system to a common activator. The activator uses two electric motors (one being redundant) driving through a reducer and outputting to the tie rods. Four fold-axis bellcranks are needed for vehicle stowage requirements.

The chassis articulation steering concept requires that steer signals energize an activator (either linear or rotary type) at the intermodular drawbar steer pivot, causing the modules to yaw relative to each other for steering. The aft



- ⊗ = POWERED ACTUATOR
- = FREE PIVOT

FIG. 5.4-1 CANDIDATE STEERING CONCEPTS (6 x 6)

module is again allowed to trail via its pivoting drawbar. The reliability of this system is achieved by providing differential speed control of the wheels, which serves as a back-up steering system should the actuator fail. To conserve power and provide maximum locomotion efficiency, it is necessary to design the DLRV with differential wheel speed control regardless of which steering concept is selected.

The results of the evaluation of the candidate steering concepts are presented in Table 5.4-1. The articulated system appears better than or equal to the Ackerman for every criterion considered. Brief comments to support the scores are given in the following paragraphs.

(a) Mobility - Table 5.4-2 shows the results of tests performed on the full-scale lg DLRV simulator comparing the work done for steering maneuvers with Ackerman and articulated steering. The test setup is shown in Fig. 5.4-2. For articulated steering only wheel rolling resistance and minimal wheel drive drag need be overcome; thus less work is required for static and obstacle steer maneuvers in relatively weak soil ( $k_A = 3$ ).

(b) Obstacle Negotiation and Maneuverability - No significant difference in step and crevasse crossing capability was noted between the candidates; however, articulation did offer an additional degree of emergency vehicle manipulation; i.e., the yawing or "crabbing" articulated action can be used to free an immobilized wheel or aid in negotiating obstacles. The ability to statically slew the DLRV via articulation also offers advantages in the following areas:

- o Science experimentation - enhancing the sample collector's view area of coverage
- o TV coverage - backup mode for panning TV camera should TV drive mechanism fail
- o The TV inherently pointed in the direction of travel, providing simpler MCC control. This advantage also applies to driving in reverse by presetting the vehicle heading prior to movement

Figure 5.4-3 shows the two candidate vehicles making turns with equal wall-to-wall turn radii. (Also ref. Fig. 3.1-3 for equal inside turn radii.) It is seen that the second and third modules do not track the first with Ackerman steering, resulting in higher locomotion energy during turns. Also, the swept area is greater for Ackerman steering because the inside radius is 23% less than the articulated; this results in reduced ability to maneuver between obstacles during

TABLE 5.4-1 STEERING SYSTEM EVALUATION CRITERIA, 6 X 6

<u>CRITERIA</u>	<u>VALUE FACTOR</u>	<u>RIGID FRAME</u>	<u>ARTICULATED FRAME</u>
- MOBILITY	15	7	8
- OBSTACLE NEGOTIATION	15	7	8
- MANEUVERABILITY	10	4.5	5.5
- STABILITY	15	7	8
- STOWAGE AND DEPLOYMENT	10	5	8
- RELIABILITY	15	7	8
- PAYLOAD COMPATIBILITY	10	5	5
- WEIGHT	10	4	6
	<u>100</u>	<u>46.5</u>	<u>53.5</u>

TABLE 5.4-2 STEERING ENERGY COMPARISON

(4X4 DLRV SIMULATOR - GROSS WT. = 1200 LBS.)

MODE	SOIL	WORK DONE (FT-LBS) FOR HEADING OF 15°	
		ACKERMAN	ARTICULATION
STATIC*STEER AT 2°/SEC	BEACH SAND $K_{\phi} \approx 3.0$	144	43
	ASPHALT OR CONCRETE SURFACE	72	43
OBSTACLE** STEER AT 2°/SEC	BEACH SAND $K_{\phi} \approx 3.0$	> 290	54
	ASPHALT OR CONCRETE SURFACE	> 250	50

\* VEHICLE FWD VELOCITY = 0

\*\* OBSTACLE = 4 X 4 INCH WOOD BEAM

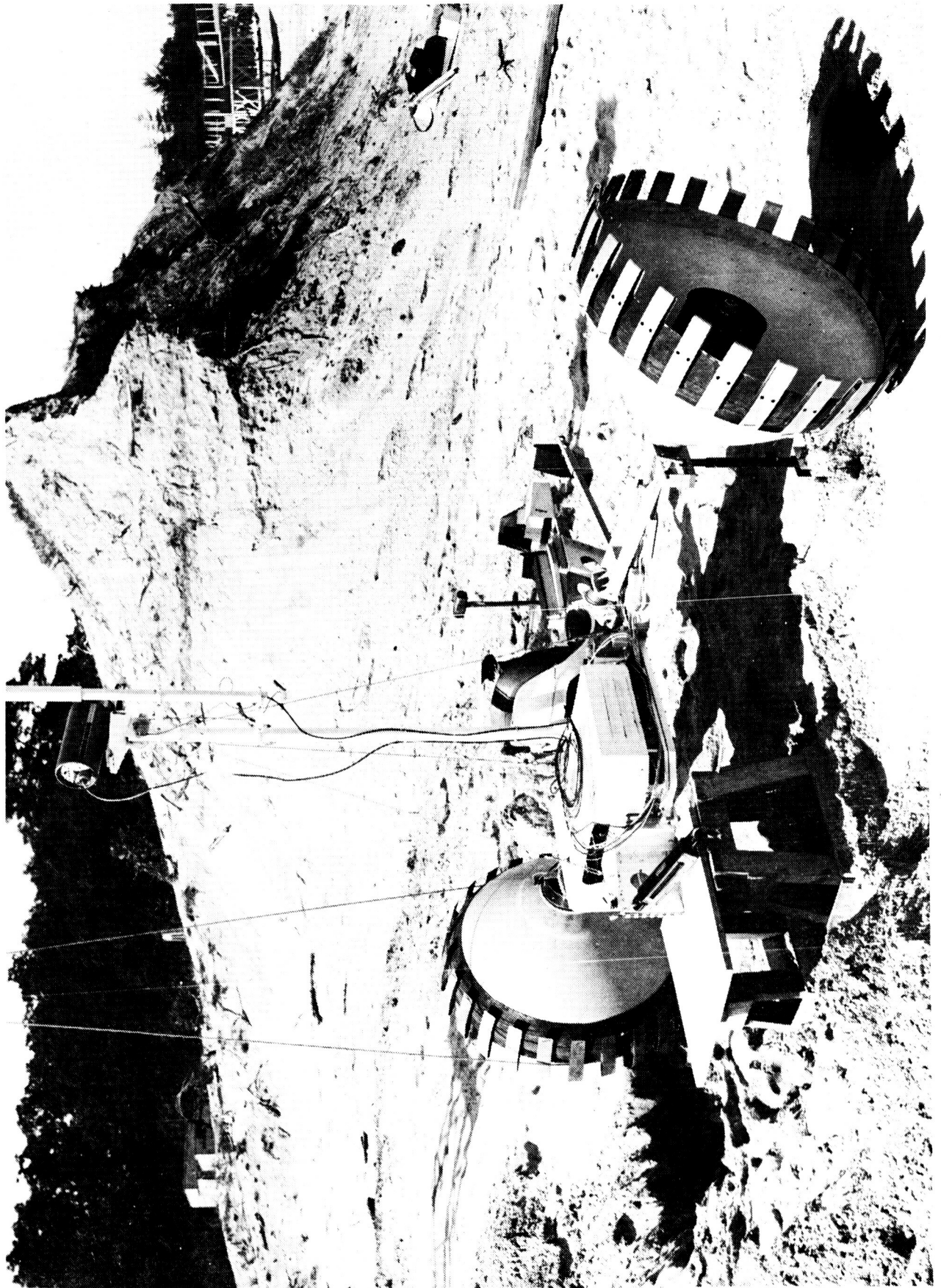


FIG. 5.4.2 MEASURING STEERING FORCES FOR CANDIDATE ACKERMAN SYSTEM

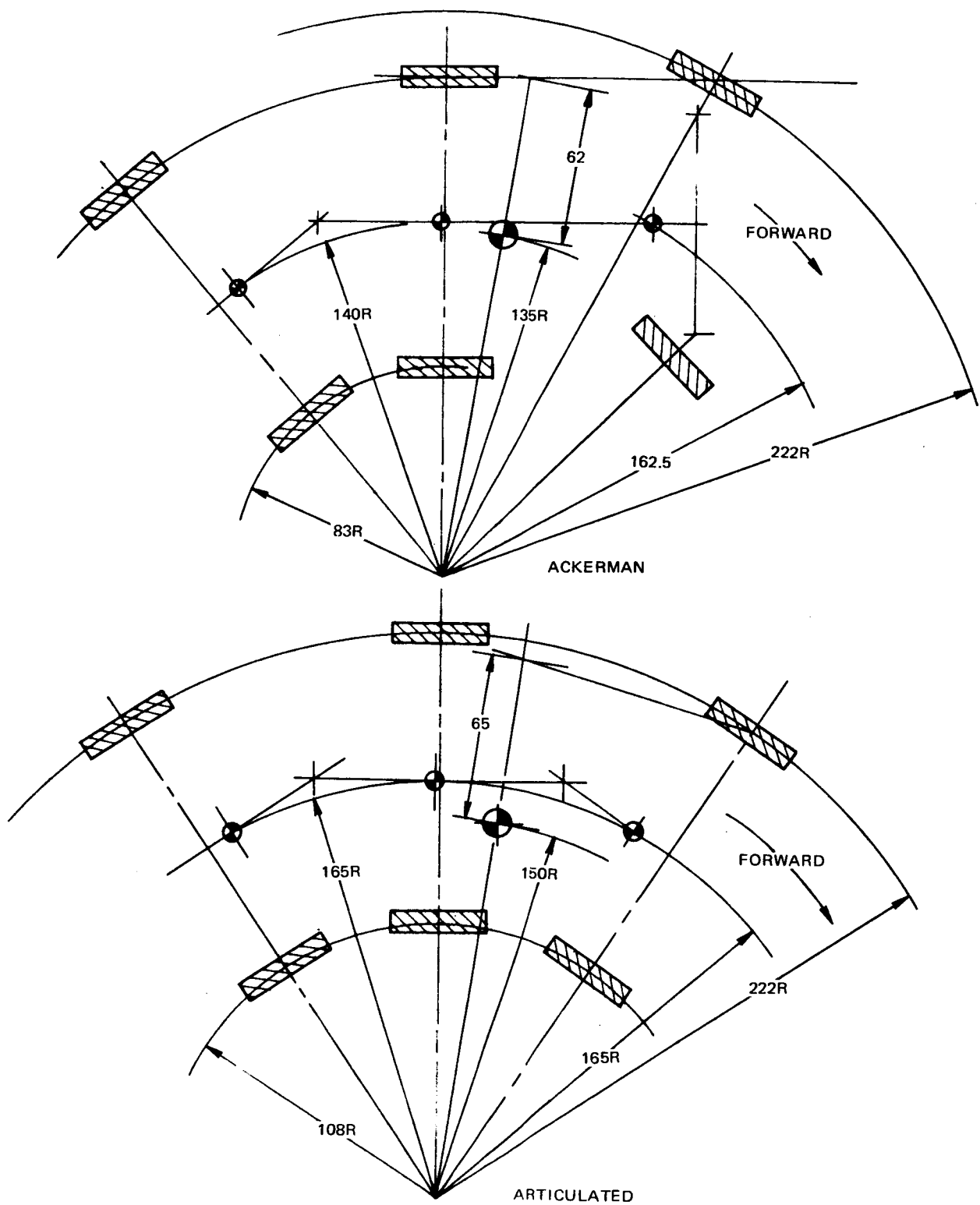


FIG. 5.4-3 STEERING COMPARISON

turns.

(c) Stability - The overturning stability for equal inside turning radii can also be compared using Figure 5.4-3. Centrifugal force varies inversely as turning radius. Therefore, for independent overturning of the modules, the articulated vehicle has the advantage for the last two modules, and the two vehicles are about equal for the first module. For dependent modules, the articulated again has the advantage since the radius to the overall vehicle c.g. is larger, and the stability arms are approximately equal.

(d) Reliability - The primary trade-off in reliability is associated with the differences between the mechanization of the steering methods. Loss of steering capability is a safety hazard. The failure modes to be considered are:

- o Binding in linkages, actuator and motor
- o Breaking of linkages
- o Electrical failure of motor

Acquired data has shown the ratio for electrical failures to be approximated one hundred times those of binding and breaking of linkage assemblies.

Assigning these failure modes and their frequency index values to the candidate systems allowed the reliability block diagrams shown in Fig. 5.4-4 to be drawn and analyzed. The conclusions were: (1) in both cases the most probable failure mode has back-up; (2) the failure modes with no back-up have greater hardware complexity with the Ackerman concept; (3) both systems are reliable; (4) articulation has fewer parts and is less vulnerable to debris entrapment or impact.

(e) Weight - The Ackerman system, using redundant motors in a single mechanical reducer, and the cross-over tie-rod system, weighs 16.5 pounds. The articulation weight, requiring the single actuator, is estimated at 9 pounds. A second approach for the Ackerman concept would be dual actuation; i. e., a synchronized motor at each wheel and no tie-rod system. The estimated weight for this system is 10.6 pounds; however, reliability suffers badly and additional weight penalties would be expected.



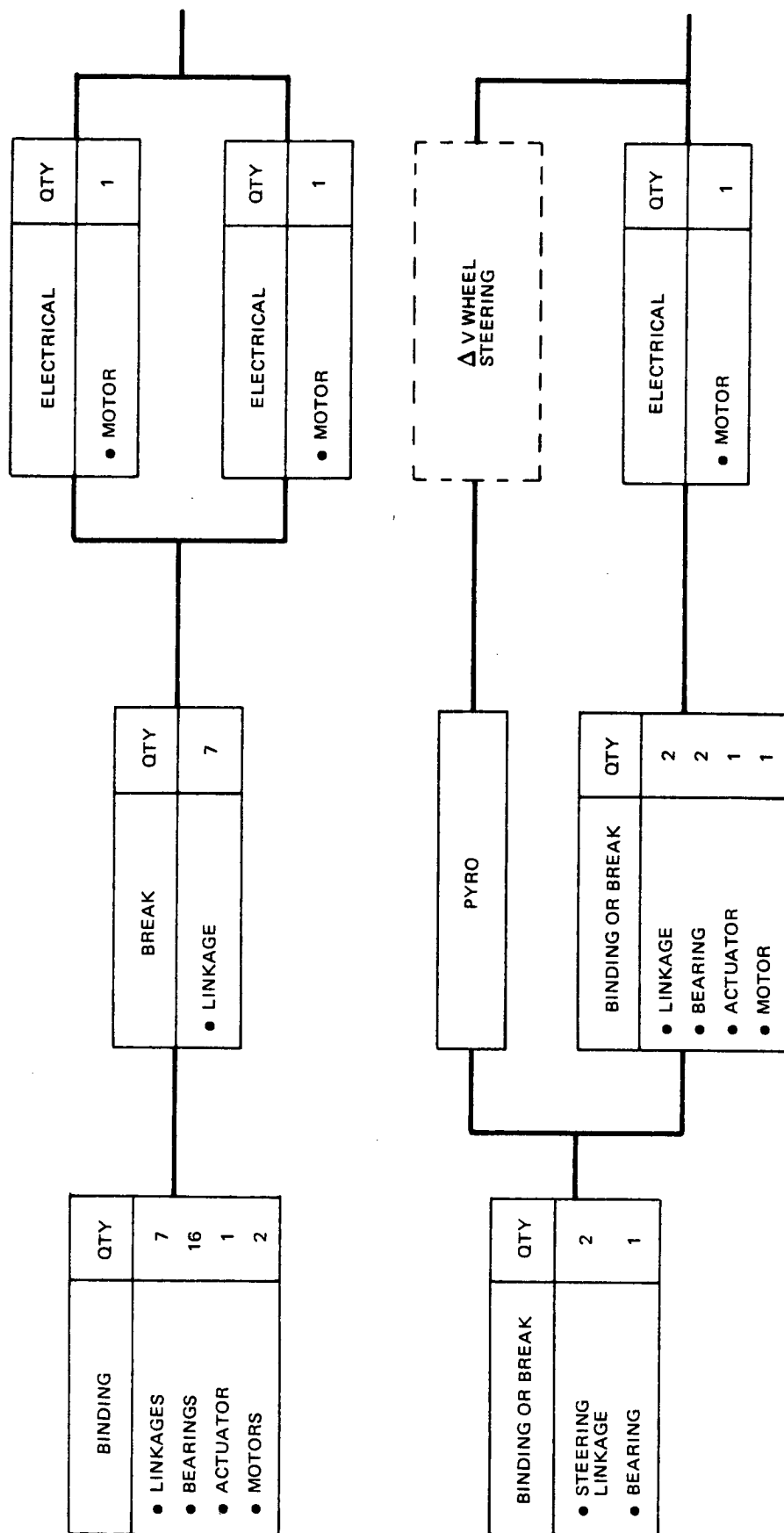


FIG. 5.4-4 STEERING RELIABILITY BLOCK DIAGRAMS

## 5.4.2 Steering Mechanism Preliminary Design

### 5.4.2.1 Design Criteria

For normal operations, the wheel speeds are matched to the articulated geometry established by the steer actuator. The resulting power required of the steer actuator in this synchronized mode is very small. To establish the duty cycle and the torque-speed character of the actuator it was necessary to investigate other conditions such as wheel drive failure modes. These conditions produce yawing torques at the steer pivot which must be reacted by the actuator. The following failure or off-nominal conditions for the 4 x 4 vehicle were used to size the system:

- o Condition 1 - All wheels actively driving; however, a mismatch of velocity profiles with the actuator setting exists. A level of drive power from the actuator is required depending on the degree of mismatch. Steer torques at the actuator could vary up to 250 ft.-lb. Analysis suggests using a value of 40 ft.-lb. at steer rate of 15°/sec. and consider this condition to be the continuous duty cycle.
- o Condition 2 - Two wheels active and two failed. Both failed wheel drives are diagonally opposed to each other, and the active wheel drives are performing at or near stall conditions. This condition creates the maximum steer torque requirement of 250 ft.-lb. for the actuator.
- o Condition 3 - DLRV forward wheel collides with an obstacle and experiences the maximum design load factor of 5.5 g's. The resulting structural loading at the actuator assuming no energy dissipation within the vehicle structure (very conservative) is 2000 ft.-lb. maximum.

Approximately a 50% weight savings can be realized in the steering subsystem by configuring the actuator such that it can be quickly disconnected from its manned intermodular position and positioned to its unmanned steer position. Since the double-ended DLRV is converted to the science module forward configuration for the unmanned mission phase, the actuator must be manually installed between the science and power modules, leaving the control module free to trail. Since the actuator constrains the science and power modules, the trailing control module is geometrically restricted from "fish tailing" unless it physically slides its wheels sideways. In view of the critical weight restriction on DLRV, the single actuator approach is recommended.

A summary of the design criteria for the steering system is given in Table 5.4-3.

TABLE 5.4-3  
STEERING DESIGN CRITERIA

- Operational Mode - Chassis articulation using differential wheel speed control and actuated steer joint.
- Actuator size based on 50% diagonal wheel failure on 4 x 4 manned vehicle.
- Performance - 40 ft.-lb. at 15°/sec (continuous duty)  
250 ft.-lb. at wheel stall  
2000 ft.-lb. max. structural loading
- Steer Angle  $\pm 40^\circ$
- Maximum Design Weight - 13 lb. including (2) steer pivot assemblies and one actuator assembly
- Power Supply - 56 VDC
- Steer Rate - controllable up to 15°/sec
- Failure Mode - Actuator disengagement mechanism requiring no power after command.
- Manual Disconnection - quick release design permitting placement of actuator from manned mission to unmanned mission pivot location

#### 5.4.2.2 Steer Actuator

Figure 5.4-5 illustrates the steering actuator and the steering pivot assembly preliminary designs. A number of candidate actuator designs were evaluated; namely, linear ball screw, rotary harmonic and the rotary planetary gearing type. The selected design, a hermetically sealed unit, which combines a brushless motor of the wheel traction type with a planetary gearhead, was considered to be the best arrangement. It provides:

- o Equal steering torques and rates for each chassis slew direction
- o Commonality of design with wheel drive assembly
- o Favorable envelope and location for DLRV/LM stowage configuration
- o Convenient configuration permitting quick manual disconnect
- o Best configuration to sustain prolonged lunar environment exposure

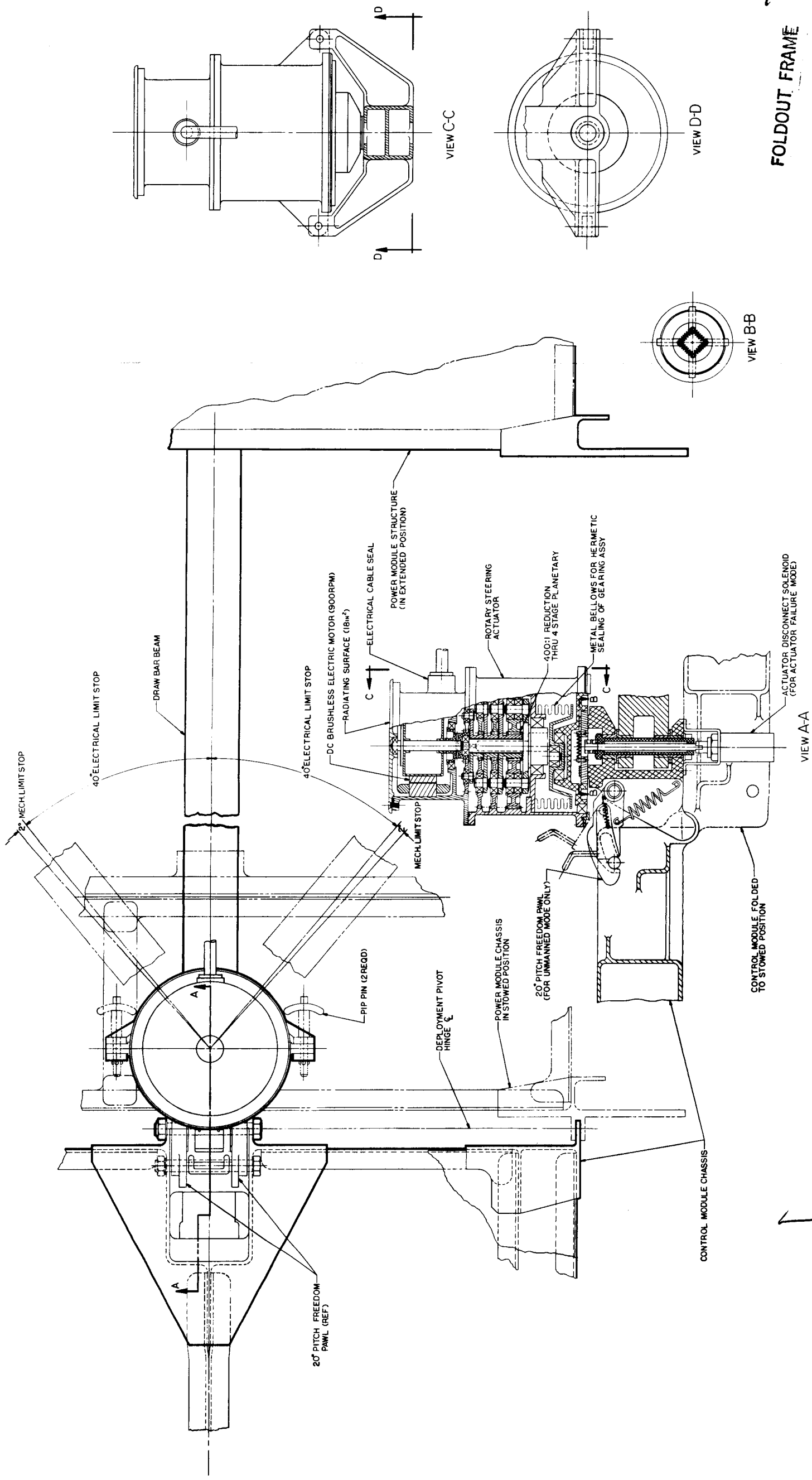
Shown as part of the actuator assembly is the dc PM brushless motor, a 360:1-ratio, four-stage planetary with fixed ring gears and a carrier eccentric output fitting, metallic bellows for hermetic sealing, a solenoid-actuated assembly for failure mode, disengagement and the manual quick release pins and mounting assembly required for the unmanned mission conversion.

A brief description of the components making up the Steer Actuator assembly follows:

(a) Motor/Gearhead - The motor is a two-phase brushless dc machine. The design is the Westinghouse concept, similar to the one used for the wheel drive, but differing by the deletion of the winding switching arrangement used to electronically shift between torque/speed ratios to the wheel. The full complement of motor windings is used to minimize  $I^2R$  losses and to operate at greater than 80% efficiency. The nominal continuous duty performance of the motor calls for the following:

Motor speed ( $15^\circ$ /sec. steer)	=	900-1000 RPM
Motor torque	=	13.5 inch-pounds
Motor power	=	21.8 watts *
Motor reversal rate	=	2 per second

\* This value includes motor efficiency of 80%, gearbox 82%, and 2% for other losses - overall actuator efficiency = 65%.



FOLDOUT FRAME

FOLDOUT FRAME

FIG. 5.45 DLRV STEERING ACTUATOR ASSEMBLY

The materials and components selected for the motor are listed under the Wheel Drive Assembly, Section 5.5.

The gear head is a conventional multi-stage involute-gearing planetary selected for its history of reliable performance and high operational efficiency. This speed reducer design was chosen from among the harmonic drive, nutator drive and other planetary and screw type designs. While the harmonic offers high reduction in a single stage with hermetic sealing, its drive efficiency is lower and its failure mode is very rapid. The harmonic is more sensitive to overload because of its highly stressed flex spline. Laboratory tests have shown that failures of this flex spline bind the mechanism, complicating the design of the backup free wheeling capability. The nutator design was not chosen because of its weight and lack of mechanical reliability. The conventional gear reducer in combination with a high efficiency hermetically sealed linear ball screw was seriously being considered. Three criteria eliminated this design in favor of the rotary planetary design: the desire to attain equal torques and rates in both steer directions, the complexity associated with manually disconnecting a linear actuator for re-installation to the unmanned mission position, and the structural penalty associated with the poor stowage arrangement required during DLRV tiedown.

The overall efficiency of the planetary is estimated to be 81% to 85% based on 22 gear meshes at 1.0% loss factor per mesh. The loss factor considers manufacturing and the wide thermal range. At this high mechanical efficiency, the unit would be reversible, making it possible to relieve structural loading caused by wheel collisions with large obstacles. Precision high-strength nitrided steel gears are to be used. The following data identifies the gearing system and its structural requirements (consider only the final stage of the planetary):

Output torque - continuous duty	40 ft.-lb.
- maximum	250 ft.-lb.
No. of gears	4 planets
Tooth load - continuous duty	44 lb.
- maximum	275 lb.
Diametral Pitch	16
Pressure Angle	20°

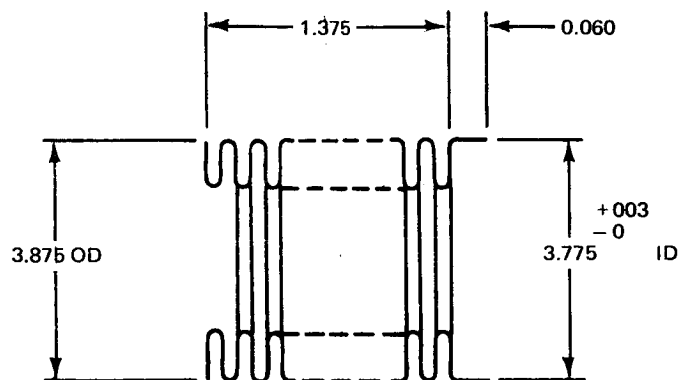
Tooth bending stress - continuous duty	14,000 psi
- maximum	88,000 psi
Tooth hertzian stress - continuous duty	27,300 psi
- maximum	170,000 psi

(b) Disengage Device - This mechanism is an integral part of the drawbar steer pivot assembly. Both intermodular steer pivots are equipped with the disengagement assembly. A pulse-energized pull solenoid is used to disconnect the drive output from the drawbar steering lugs. A center release rod is pulled downward by the solenoid permitting the spring-loaded drive fingers to retract thereby disconnecting the drawbar steer pivot assembly from the failed steering actuator. Should a finger not withdraw completely, steering action would cam the finger to its retracted position. Normally, the release rod is held in position by a compression spring. This mechanism is configured as a one-shot device used only when the actuator is no longer considered operational.

(c) Bellows - Since the output steer motion is limited to  $\pm 40^\circ$  angular motion, and the greater portion of DLRV driving occurs at considerably smaller steering angles, a convoluted metallic bellows is used to effect an hermetic seal for the critical mechanical and electrical components of the steering actuator. The bellows data is summarized in Fig. 5.4-6.

(d) Bearings - A combination of single and double row angular contact ball bearings are used to support the motor rotor shaft and the planetary gears and output fitting. Ball bearings are needed to maximize operational efficiency for vehicle power and thermal considerations. Bearing speeds are slow to low medium, varying from 900 RPM to 2.5 RPM. Most bearing loading throughout the actuator assembly is radial and accommodated by the single row bearing types. Due to the crank shaft design of the last stage carrier output, moments are also introduced and double row or moment carrying bearings have been indicated. The two bearings operating outside the hermetically sealed gear head are also ball types. These bearings experience very low speeds at moderate to low loads for their indicated sizes. They are both shielded and sealed to protect them from lunar dust contamination.

(e) Lubrication System - The problems of lubricating the steering actuator are somewhat less demanding than those associated with the DLRV wheel drive assemblies.



BELLOWS OD, IN.	= 3.875
BELLOWS ID, IN.	= 3.125
CONVOLUTION PITCH	= 0.249
AVERAGE WALL, IN.	= 0.005
EFFECTIVE AREA, IN. <sup>2</sup>	= 9.621
NO. GROOVES	= 6
CONVOLUTIONS ACTIVE:	
BEFORE ASSEMBLY	= 5.5
AFTER	= 5
ALLOWABLE AXIAL STROKE:	
COMPRESSION	= 0.500
EXTENSION	= 0.415
PRESSURE RATINGS: (PSI)	
MAX FOR 1/2 STROKE	= 57
PROOF	= 99
BURST	= 141
SPRING RATE, LB/IN.:	
BEFORE ASSEMBLY	= 38.5
AFTER	= 42.4
SPRING RATE TOLERANCE:	= +30%
LIFE EXPECTANCY	= 100,000 CYCLES
MAX OPERATING TEMP:	= 350°F
REGULAR NICKEL USED FOR SOLDERING	

FIG. 5.4-6 BELLOWS DESIGN



There are three contributing reasons for this: the actuator can be hermetically sealed; the duty cycle for normal usage requires low power; and the actuator is basically a slow speed unit. Nonetheless, it is still considered essential to provide a redundant lubrication system; i.e., using a combination of dry film  $\text{MoS}_2$  coatings on bearings and bearing surfaces and then applying synthetic oils and greases. Since the application requires operations at elevated temperature (i.e.,  $300^\circ\text{F}$  and above), and over wide temperature ranges ( $-65^\circ\text{F}$  to  $+400^\circ\text{F}$ ), the use of non-soap-thickened silicone grease is recommended. MIL-G-27549 (USAF) and MIL-G-25013(c) (Phenyl Methyl Polysiloxane with a dye thickener) are considered primary candidates based on their excellent performance as reported in References 1 and 2.

G.E. G-300 grease or a Dow Corning fluorosilicone grease should be considered for the application involved. Both of these greases utilize fluids containing halogens as part of the silicone molecule providing the chemical reactivity with metal surfaces required for effective lubrication. Both greases can be specially formulated for high-vacuum applications with vapor pressure at  $250^\circ\text{F}$  in the  $10^{-6}$  Torr range.

Ball bearings are to be equipped with phenolic retainers impregnated with these lubricants and shielded to provide added sealing to retain the lubricant.  $\text{MoS}_2$  films are applied before assembly of the bearing and only the races and retainers are treated, leaving the balls uncoated. Run-in periods are required for the bearing after the  $\text{MoS}_2$  has been applied. The gears are treated in the same manner;  $\text{MoS}_2$  is applied, followed by a run-in period, and then assembled and coated with the silicone grease lubricant. Successful lubrication performance within the steering actuator is predicated on numerous design factors inherent in the actuator: the slow speed operation, hermetic sealing of critical components, redundant lubrication, a vertical design with lunar gravity helping to supply the lubricant to the gears, and a feasible thermal system in which motor heat is conducted to strategic locations on the reducer, thereby, creating a balanced internal distribution of condensed lubricant vapors throughout the reducer. Low wattage isotope heaters may also serve this purpose. The exact lubricants can only be identified by extensive environmental and mission simulation tests. However, the design of the steering actuator does provide a logical mechanism from which to derive the final answer.

#### 5.4.2.3 Drawbar Steer Pivot

The pivot assembly provides structural continuity for loads in the vertical plane and twisting moments about the vehicle center line. In the yaw plane, it serves as the chassis articulation steering pivot. Steering moments are taken out by the couple produced by the actuator about the pivot assembly. The steer pivot assembly, having a hinge fitting perpendicular to the steer pivot, also acts as the hinge between the control and power chassis for stowage and deployment. Fittings in the pivot assembly are fabricated from 7075-T73 aluminum alloy. Nominal sizes are shown in Figure 5.4-5. The two intermodular drawbar assemblies are similar, differing only in design by the addition of the deployment hinge and latch assembly used on the control module unit. The science module drawbar locks out the science and power module in the pitch plane. Both pivots are equipped with the solenoid activated disengagement assembly used to declutch the steering actuator should it fail.

#### 5.4.2.4 Steering System Weight

The total calculated weight for the DLRV Steering Subsystem is 13 pounds. This weight estimate includes the actuator assembly, the control module steering pivot assembly and pitch control linkage, the power module pivot assembly, and both solenoid-operated disengagement units. The intermodular drawbars are considered vehicle structure and not charged to the steering system weight.

#### 5.4.3 Conversion from Manned to Unmanned Mode

Part of preparing the DLRV for its unmanned mission requires relocating the steering actuator to its science module pivot position. Removal of the actuator is accomplished manually by withdrawing two quick release pin pins connecting the actuator to the drawbar reaction support arms. Any locked-in steering torque is reacted by these arms and the mating actuator lugs, allowing the pins to be readily extracted. With all three modules aligned in an approximate straight line, the actuator is disconnected, removed, and reattached to the science module pivot. The control module pivot is then given a degree of pitch freedom by manually releasing the spring-loaded deployment latch, which allows the module to rotate  $20^{\circ}$  upward about the drawbar deployment hinge fitting. This degree of pitch freedom enhances the DLRV's obstacle negotiation capabilities and permits its wheels to maintain a good contact over an undulating terrain.

#### 5.4.4 Thermal Analysis

The steer actuator must dissipate about 8 watts at a total input level of 22 watts (100% duty cycle). Ninety percent of this dissipation is at the top or motor section. The top surface of the motor assembly is utilized as a radiator. Since a brush wiping scheme is provided for this surface, properties of  $\alpha_s = 0.85$  and  $\epsilon = 0.85$ , and a dust insulation buildup of less than 0.002 inches average were assumed. Limiting the top surface to 350°F to ensure internal windings at 450°F max was found to require about 18.0 square inches of area. More area than required is available. The analysis assumed a sub-solar condition and no heat lost to the vehicle or through other than the top surface. Since this assembly is hermetically sealed and contains some vapor at pressure there should be significant internal convective heat transfer and the 100°F winding self rise is considered very conservative. The top radiator surface can be easily extended to provide greater capability at a slight increase in weight if needed.

#### 5.4.5 References for Section 5.4

1. "Lubrication for Spacecraft Applications", W.C. Young, F.J. Clauss, Lubrication-Engineering, June 1966
2. "Grease Lubricants and their Potential in Aerospace Applications", H. Schwenker, Lubrication - Engineering, July 1964

## 5.5 WHEEL DRIVE MECHANISM

DLRV locomotion is accomplished by powering the wheel drive assemblies (WDA) located at each of the six wheel hubs. The WDA includes an electric drive motor and a mechanical reducer for torque/speed variations, wheel bearings for DLRV support, provisions for dynamic braking, a parking brake and a failure disengagement mechanism. This section discusses the mechanization requirements for the WDA and evaluates candidate types before selecting one concept. A preliminary design is then given which identifies the electrical and mechanical components of the WDA and their functional characteristics. Electrical characteristics of the wheel drive are only summarized herein. A detailed discussion of the motor and control system characteristics and trade-offs is given in Book IV of Volume III.

### 5.5.1 Design Requirements

The design requirements for the WDA were formulated from a combination of the DLRV mobility performance criteria and the demands created by the prolonged mission. Table 5.5-1 defines the WDA design criteria. These criteria reflect the wheel loading, traction demands, and drive system weight allocation associated with the chosen vehicle design. The less tangible requirements are related to the 1-year lunar operation criteria, including all the environmental and mission duration factors affecting the functional survivability of the WDA. Special emphasis was placed on these latter criteria during the evaluation since any number of motor/reducer types could satisfy the basic DLRV tractive performance requirements.

### 5.5.2 Candidate Evaluation

Three basic candidates were considered for the DLRV wheel drive assembly. These were classified according to their electric motor rated speeds; i.e., low-speed (900 rpm), mid-speed (2000 rpm), and high-speed (9000 rpm). All candidates, regardless of motor choice, were combined with a planetary gear system. The planetary speed reduction was conservatively selected because of its high operational efficiency and low weight supported with an extensive performance data bank. Other types such as the harmonic and nutator reducers are unjustified higher-risk candidates due to the fatigue failure considerations of the flex spline or the bellows seal assembly and the less predictable failure modes. The harmonic drive is considered unreliable when subjected to impact or stall-induced overloads due to its highly stressed flexspline; the failure mode is of a rapidly deteriorating type with no chance of recovery. A comparison of weight between the harmonic

TABLE 5.5-1

## WHEEL DRIVE ASSEMBLY DESIGN CRITERIA

Service Life	1 year lunar operations
Cycle Life	500,000 revolutions
Nominal Operating Efficiency (%)	60 (min.)
Power Supply (VDC)	56
Temperature Range ( $^{\circ}$ F)	-300 to +320 (housing)
WDA Weight (lb)	11.5 (max.)
System Weight (lb)	100 (includes six WDA and control electronics)
Performance:	
Continuous Duty	90 rpm at 5 ft.-lb (.085 HP)
Max. Operating Torque	65 ft.-lb.
Max. Holding Torque	80 ft.-lb.
Braking:	
Dynamic	108 lb-sec. Linear Momentum removal in 3 secs
Static	50 ft.-lb holding torque ( $35^{\circ}$ slope parking)
Loads Criteria	Wheel main bearings to be sized for loads indicated in Wheel Design Criteria
Failure Mode	Free wheeling operation post WDA failure requiring no power to be maintained.

and the nominal sized planetary showed them to be fairly close. The operational efficiency of the harmonic is 65% as compared to a planetary rating of over 90%.

An evaluation of the candidates, revealed that their weights and structural loading, were approximately equal and that only their internal mechanization provided means for comparison. The high-speed WDA design places more of the burden of reliable performance on the mechanical reducer. A three-stage planetary is used with a gear shift, permitting a 100:1 and 400:1 gear ratio selection. The accompanying lubrication concept uses a controlled leakage labyrinth seal and low vapor pressure silicone grease.

This design was compared with a mid-speed concept having a two-stage compound planetary with 14:1 and 200:1 reduction ratios. The lubrication system remained the same. The number of physical rotations in such mechanical elements as the bearings and gears was reduced by a factor of 4:1.

The low-speed WDA design represented a complete departure from the above designs. In contrast to the high-speed WDA, this design utilized a 10:1 fixed ratio planetary gearhead in combination with a multi-winding dc two-phase brushless motor. The required driving torque/speed relationships were accomplished by electronically switching motor windings between parallel and series settings, parallel windings, giving high output speeds and series giving high output torques. The use of a low-speed brushless motor and a simple single-stage planetary with no mechanical transmission is inherently more compatible with the environmental mission constraints than the mid- and high-speed designs using more complicated gearing. The electronics system which controls the motor winding switching (i.e., shifts "gears electronically") is more involved than the electronics of the other designs; however, it lies well within the present day state-of-the-art.

The conclusion reached from the evaluation was that the low-speed brushless motor using winding shifting is best suited for the DLRV vehicle. Details of the electrical trade-offs are given in Vol. III, Book IV. Some considerations are

summarized below.

Brush-type motors, both permanent-magnet and series, were considered, but the low-speed units tended to be heavy and have high losses. These losses occur in the rotating windings where radiant cooling to the outside housing is difficult, resulting in high temperature differentials across the rotating and stationary windings. These temperature extremes make it difficult to keep the commutator true and the armature insulation free of cracks. The permanent-magnet machines had higher efficiency and greater ease of incorporating dynamic braking. The controller for brush machines is inherently lighter than for brushless; however, "electrical gear shift" is not practical with the brush machine, and a mechanical gear shift adds weight and complexity. A comparison of a brushless d-c motor with an "electrical gear shift" and a brush machine with its controller shows little weight difference.

Inductive type motors were also considered and ruled out based on low efficiency due to air gap copper losses, sensitive voltage/frequency ratio control of air gap flux, and losses in the rotor causing hot running. The brushless PM motor has no rotor losses.

### 5.5.3 Wheel Drive Mechanism Preliminary Design

The selected DLRV wheel drive assembly, Figure 5.5-1 is a Westinghouse design consisting of a low-speed two-phase brushless d-c motor with a 10:1 fixed ratio planetary gear set. An infinitely variable output speed is possible, up to 90 rpm (16 km/hr), and a maximum torque of 65 pound-feet can be produced. (Maximum electrical holding torque is 80 pound-feet). A disconnect device allows the wheel to rotate freely independently of the drive motor and gearing, assuming a failure in either. The WDA provides dynamic braking for the DLRV and a parking brake which requires no power when in use. The WDA is passively cooled via a radiating disk, which is kept cleaned of dust and debris by a teflon brush assembly. Further discussion of the WDA components is given below.

#### o Motor/Gearhead

The motor/gearhead assembly provides the DLRV with the performance torque/speed relationships shown in Figure 5.5-2. The incremental power steps, created by the motor winding switching system, result in efficient operation over a wide power range. The brushless motor performance curves are given in Book IV of Vol. III, along with a further description of the selected motor and control system.

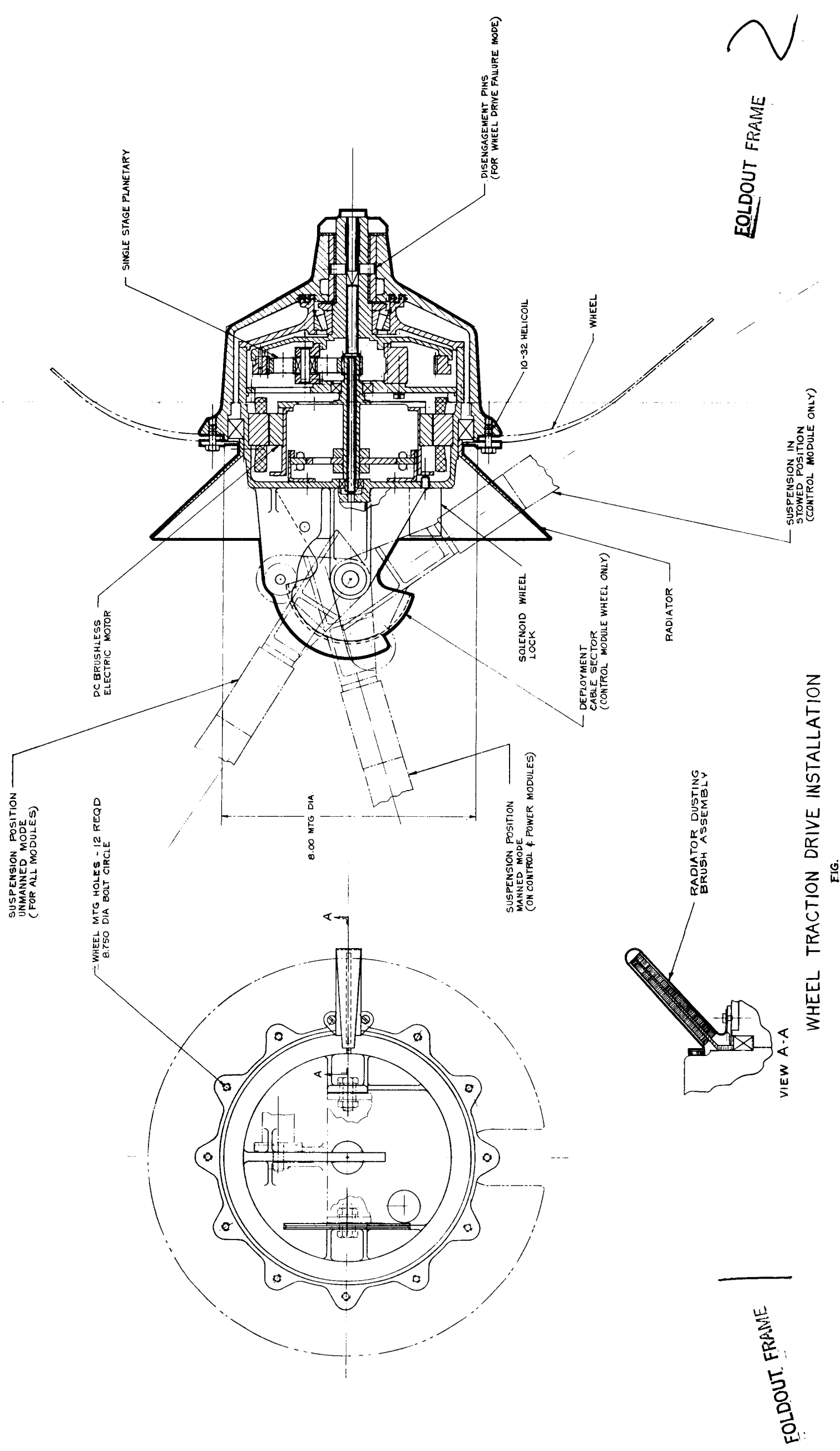


FIG. 5.5-1 DLRV WHEEL DRIVE ASSEMBLY



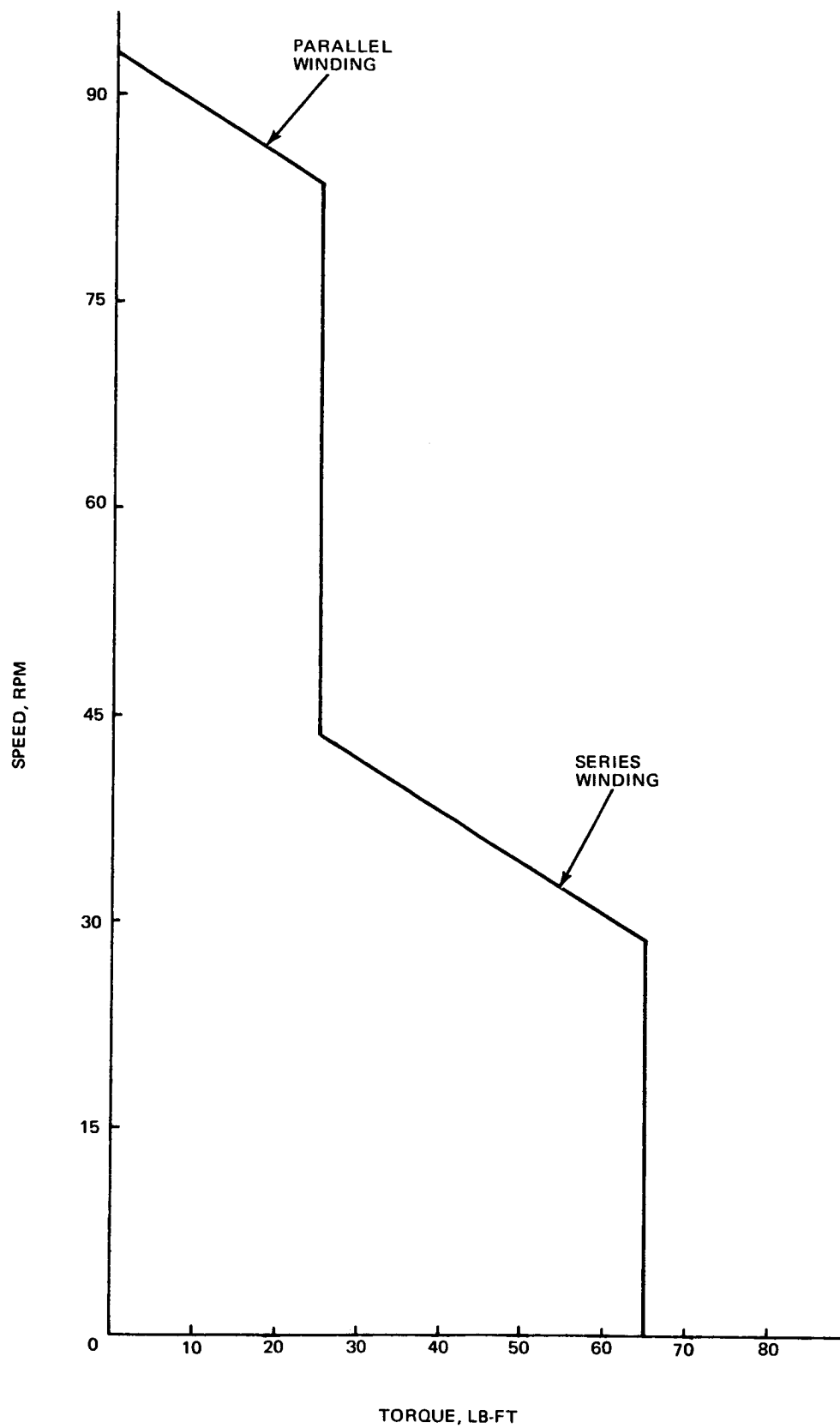


FIG. 5.5-2 WHEEL DRIVE ASSEMBLY PERFORMANCE CURVE

The gearhead is a conventional single stage 10:1 ratio planetary using involute profile gears. The ring gear acts as the output member while the planet carrier is held fixed. The overall efficiency of the planetary is estimated at over 94% based on six gear meshes at 1.0% loss factor per mesh. This loss factor considers manufacturing and the wide range thermal effects. At this high mechanical efficiency, the unit would be reversible, making it possible to manually maneuver the vehicle during preparations for the unmanned phase and also to provide some relief from structural loadings to the DLRV caused by wheel collisions with large obstacles. Precision high-strength nitrited steel gears are used. The following data defines the gearing system and its structural requirements:

Continuous duty	5 ft.-lb. @ 90 RPM
Intermittent duty	30 ft.-lb. @ 20 RPM
Maximum stall	65 ft.-lb.
Number of gears	3 planets
Tooth load	
- continuous duty	20 lb.
- maximum stall	260 lb.
Diametral pitch	16
pressure angle	20
Tooth bending stress	
- continuous duty	6,400 psi
- intermittent duty	38,000 psi
- maximum stall	83,000 psi
Tooth hertzian stress	
- continuous duty	12,700 psi
- intermittent duty	67,000 psi
- maximum stall	145,000 psi

#### o Disengage Device

The disengagement device can be seen in Figure 5.5-1. Upon actuation, the d-c solenoid axially repositions a rod in the motor shaft. The axially repositioned rod then activates a spring loaded trip that drives the taper ended pin from the output shaft. The taper ended pin is retained in the wheel assembly for further use. Actuation of the taper ended pin frees the two (or more) detents that are spring loaded to center themselves in the shaft permitting free rotation

of the wheel hub on the shaft. The free rotating wheel can be reconnected by inserting the taper ended pin to spread the detents (when the drive position aligns with the detents) and reapplying the spring loaded trip. There is no dynamic brake or parking brake action for the free rotating wheel in this degraded mode of operation; braking capability is adequately furnished by the remaining wheels.

- o Bearings

A tapered roller bearing of essentially standard automotive design carries the main thrust and radial load from the wheel. This bearing type has been selected to accommodate the impact loads anticipated for the DLRV. As in the case of all internal ball or roller bearings, porous retainers which have been impregnated with a grease lubricant are recommended.

The wheel hub is stabilized on the motor OD by employing a wire race ball bearing of loose internal fit and is provided with journal bearings and thrust washers that will enable rotation when the disengagement device is actuated. The wire race bearing was selected because of its excellent compliance to thermal changes created within the motor stator windings where it is located. In addition, it offers a capability for accepting higher loads for its size and weight as a bearing type. The externally mounted journal bearings and thrust washers are normally not under use since their service life commences only when the WDA has been disengaged. The bushing will be filled with teflon on a sintered bronze steel backing.

- o Lubrication System

A major consideration when selecting the type of WDA was the associated lubrication problem. The choice made resulted in a logical configuration, possessing good lubrication characteristics to maintain it for the prolonged lunar mission. The WDA is basically a high torque electric motor using a minimum of mechanical components. The single stage planetary with its 10:1 ratio has only six gear meshes and a maximum internal speed of 900 rpm, which is sufficiently low to minimize wear problems. The allowable gear and bearing loading (i.e., contact stress) of the lubricated components is largely dependent upon the strength of the basic material supporting the lubricant. The long life

requirement is, in effect, achieved by operating at low stress levels. The level of stress allowed in the design is dependent on the rpm of the component, which is a function of the overall gear ratio.

Maximum mechanical efficiency while still maintaining the highest possible degree of reliability for the WDA is achieved by the same redundant lubrication system recommended for the Steering Actuator Assembly (Section 5.4). The applications differ only by the method of sealing. The Steering Actuator is hermetically sealed whereas the WDA relies on a controlled leakage seal. A closely dimensioned labyrinth seal or a spring loaded face seal can be used for this application. A sufficient quantity of additional grease lubricant is loaded into the WDA to compensate for losses through the seal over the prolonged period.

The recommended lubricants which conform to MIL-G-25013, are compounded from methyphenylpolysiloxane oils and arylurea or silica thickeners. Under conditions of high vacuum, concern centers on the volatile constituent: methylphenylpolysiloxane. The polysiloxane most often used to formulate these greases is Dow Corning 510 Fluid, either 50 cs or 100 cs or combination of the two. The vapor pressure of 50 cs DC510 Fluid (representative of worst case in terms of volatility) at 250°F is 1 Torr. However, since the polysiloxanes are mixtures of polymers, this relatively high vapor pressure is misleading and is not representative of the actual vapor pressure after a very short time under conditions of high vacuum. After pumping at  $10^{-6}$  Torr for 24 hours, sufficient light ends of the polysiloxane are removed to drop the vapor pressure at 250°F to  $8 \times 10^{-4}$  Torr. Since the lubricant can be stripped prior to use or prior to formulating, the  $8 \times 10^{-4}$  Torr value can be used for calculating weight loss during vacuum storage. The other property required for calculating total weight loss is molecular weight. The average molecular weight for 50 cs DC510 Fluid is  $3.3 \times 10^{-3}$ . After stripping this value increases slightly, but for purposes of calculating weight loss is insignificant due to the rapid decrease in vapor pressure.

Lubricant leakage rate can be determined using the equation\*

\* "Leakage Sealing of Bearings for Fluid Lubrication in a Space Environment", H. I. Silversher, 3rd Aerospace Mechanisms Symposium, May 23 - 24, 1968

$$\text{Weight Loss (gm/sec)} = (.0583 P \left( \frac{M}{T} \right)^{\frac{1}{2}} A ) F$$

where

P = Vapor Pressure =  $8 \times 10^{-4}$  Torr

M = Molecular Wt. -  $3.3 \times 10^3$

T = 395°K

F = Seal Factor = 0.0025

A = Seal clearance area  $\text{CM}^2$ . = 0.12

The resulting weight loss rate is a low  $4 \times 10^{-8}$  gm/sec for vacuum stabilized polysiloxane portion of the lubricant (1.2 gm/yr.) The polysiloxane portion represents approximately 80 percent of the total weight.

The quantity of lubricant required for each WDA is approximately 60 gm., determined by gearbox size, surface coverage requirements, and, to a small extent, leakage.

As in the case of the steering actuator, a thermal balance system can be used to control the temperature gradients throughout the WDA thereby controlling the vapor depositing of lubricant grease. This concept is made possible by using the electric motor heat and conducting it to strategic locations within the WDA, or providing isotope heaters.

#### o Braking

The WDA is equipped with a mechanical parking brake and electrically induced dynamic braking. Dynamic braking is accomplished by reversing the applied voltage, causing the motor to electrically brake, generating a torque proportional to the magnitude of the voltage. A further discussion of the dynamic braking mode is given in Book IV of Vol. III.

The parking brake is a "key in the hole" type detent brake which is operated by pulse energizing a solenoid. The solenoid forces its plunger pin into a slotted hole fitting, locking out the motor rotor assembly. Multiple slotted holes are located on this fitting permitting a certainty of plunger engagement after minimum wheel rotation. Parking brakes are only located on two of the six wheels of the DLRV. The brakes are released by a second actuation of the pulse solenoid. Should the solenoid plunger hang up due to parking loads, steering or traction drive power would be applied to roll the wheels slightly, unloading the

plunger and permitting it to retract. It is not anticipated that parking brakes will be needed at many of the stops. Selective positioning of the vehicle, either by facing it sideways to the ground slope or by "crabbing" it via its articulated steering system will be adequate for most slope conditions.

o Weight

The total weight of the WDA is 11.5 lbs. The weight breakdown is as shown below.

Stator magnetic material (Hiperco 50)	1.63 lb
Stator electrical conductor (copper) insulation and leads	1.47
Resolver (brushless)	.45
Rotor (magnets and Armco iron)	1.6
Solenoids	0.32
Bearings	1.33
Gearing	2.06
Housing	<u>2.64</u>

Total 11.50

5.5.4 Thermal Analysis

The thermal environment for the Wheel Drive Assembly (WDA) is strongly related to its thermal interface with the wheel, lunar surface, and solar incident radiation. The analysis presented in Section 5.4.4 shows achievable motor and gear box case temperatures to be in the range of 320°F average. Considering the distribution of thermal load in the motor and gear box, it is expected that the motor end would operate about 30°F hotter and the gear box end about 50°F cooler.

The maximum operating winding temperature has been chosen as 450°F. This level permits a winding temperature rise of 100°F over the motor case temperature. This is considered by Grumman and the motor vendor to be achievable using present motor designs and thermal conductive and radiative transfer techniques.

The 25° slope climb condition is somewhat in excess of the 50 watt design load (see Table 5.2-4 of Section 5.2.5). A preliminary transient analysis shows this motor to have approximately a 21-minute time constant at the windings. The steady state winding temperature predicted at 67.5 watts dissipation (2 km/hr, 25° slope climb) is 490°F. Application of time constant theory predicts a winding temperature rise of about 25°F (to 475°F total) in 21 minutes. This temperature is considered acceptable for short-term operation and should not impair the reliability of this motor.

The winding temperature can be reduced by increasing the present radiation surface or by the addition of some mass to the windings to increase its time constant. For the lunar night condition, a minimum temperature limit of -60°F has been set to minimize lubricant degradation. This limit is achieved by the inclusion of 2.5 watts of isotope heater, located internal to the motor gear box at a point close to the lubricant. Radiation surfaces of the present design can be readily increased to compensate for this small additional load.

## SECTION 6

### CREW SYSTEM/HUMAN FACTORS

#### 6.1 RATIONALE FOR CREW STATION SELECTION

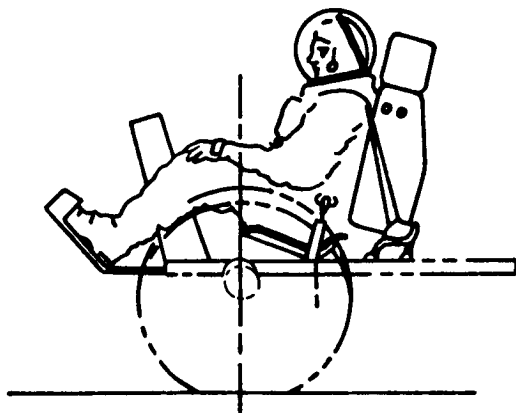
The crew station for the DLRV is designed primarily for a single astronaut with provisions for transporting a disabled astronaut in a rescue mission. All structural provisions, information displays, and controls are configured to accommodate the capabilities and limitations of the 5th through 95th percentile population of the U.S. Air Force personnel. Design requirements were based on human engineering criteria established by MFSC-STD-267A with due consideration for crew safety, comfort, mobility, ease of accessibility, and usage of CFE and GFE equipments.

Constraints imposed by the man-machine interface provide for ease of vehicle deployment by a single astronaut, minimum time and effort to assemble, install, and remove components, ease of ingress/egress, maximum forward visibility, and adequate crew protection from potential on-board hazards and/or ambient environmental conditions which tend to degrade operator performance.

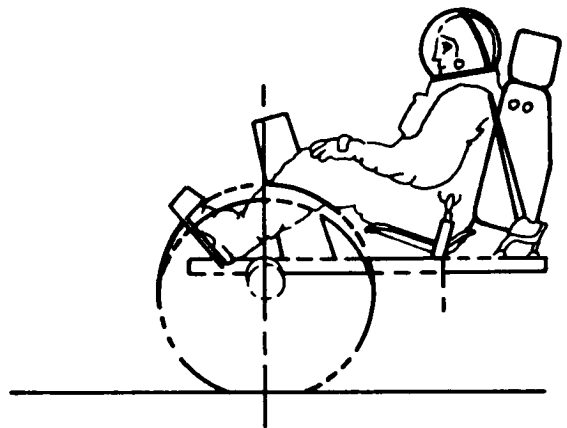
##### 6.1.1 Driver Station Studies

A trade-off study of four candidate driver positions was evaluated (See Fig. 6.1.-1); a seated position with legs protruding beyond the wheel radius; a seated position with the body moved further aft; an elevated seated position; and a standing position. The standing and elevated seated positions, although offering superior visibility of the forward terrain, were rejected because of difficulty of ingress/egress, decreased stability due to high man/vehicle CG, attendant increased head motions due to roll acceleration, and because, they represented the highest weight of the candidate positions and the greatest complexity for the arrangement of crew station stowage. The low aft seated position was similarly rejected because of its relatively greater complexity of ingress/egress, its greater seat weight and mechanical requirements for providing seat rotation, its increased complexity for crew station stowage, and, its adverse effect on the primary equipment stowage volume. The low forward seated position was selected as the best since it offered the simplest ingress/egress to a fixed, minimum weight seat, a low man/vehicle C.G. for optimum stability, a simple restraint system, a minimum impact on primary equipment stowage volume, and the least cost in the weight of supporting structure. Its disadvantage of the

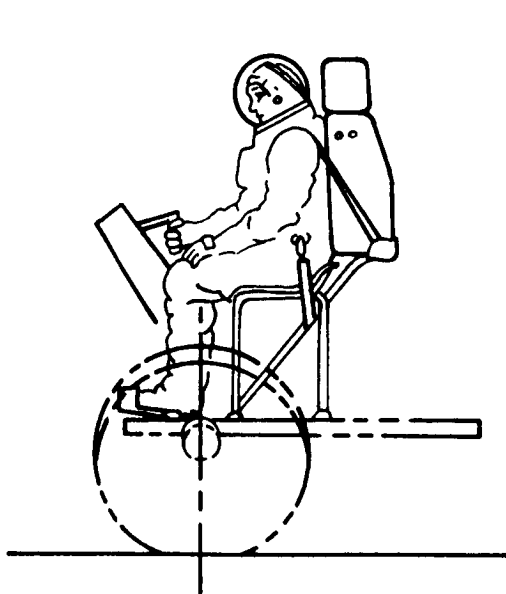




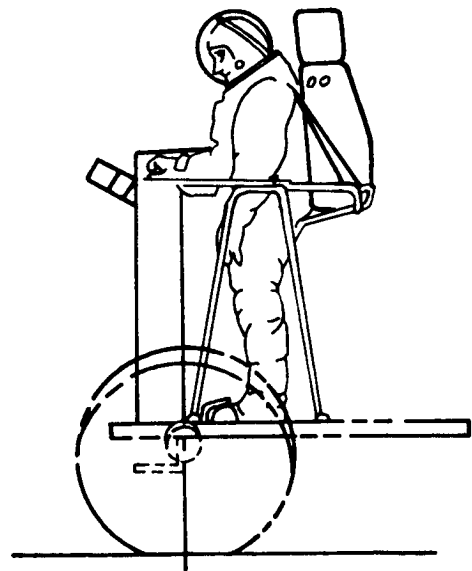
FORWARD SEATED



AFT SEATED



ELEVATED SEATED



STANDING

FIG. 6.1-1 CANDIDATE DRIVER POSITIONS

driver's feet protruding forward of the wheels was mitigated by designing sufficient strength in the foot supports to withstand potential impacts.

#### 6.1.2 Passenger Station Studies

Five alternate passenger positions were considered as candidate possibilities for the location of an emergency passenger in a rescue mission (see Figure 6.1-2). The evaluation of these positions is summarized in Table 6.1-1.

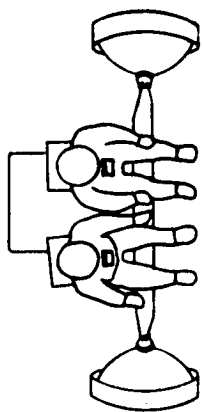
On the basis of the evaluation it was concluded that the center sling position, providing for adjustable lateral rotation enables the rescuer to lift, emplace, and harness a disabled astronaut with minimum effort while enabling the rescued astronaut to ride with maximum comfort and safety. Once emplaced in the sling, the sling arrangement is raised to its illustrated position and locked into place. The center sling position best meets the requirements for rescuing a disabled astronaut in the event of an emergency at minimum expense to alterations in the proposed configuration of the DLRV.

#### 6.1.3 Displays and Controls Studies

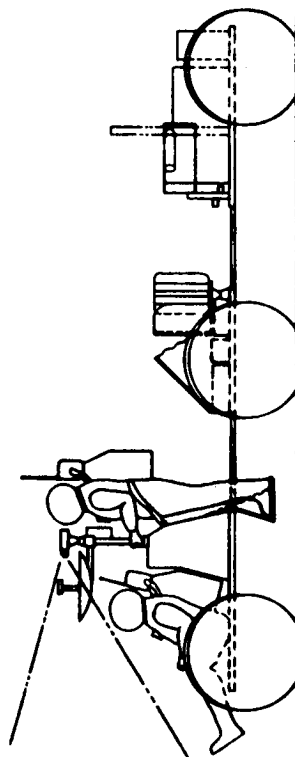
A trade-off study was performed to evaluate the number and complexity of the displays and controls to be provided in the manned mode of operation. Three possibilities were considered: a display/control console providing complete autonomy of vehicle control and evaluation of vehicle sub-system status information by the driver; a minimum version providing adequate vehicle control and manipulation including adequate navigation information to return to home-base in the event of a communications failure with the ground station. The intermediate version was selected for the following reasons:

- o Although the probability of a communications failure with the Earth station is relatively low, the remote possibility of its occurrence necessitates that the driver be provided with an indication of last bearing angle and range to home-base in order to return to sortie initial point.
- o At a minimum, driver control of vehicle mobility must include capability for full range of normal and emergency modes of operation.
- o Driver must be informed of danger or failure in the sub-system status by a master alarm. Detailed status information will be provided by uplink communication.
- o Driver requires, at a minimum, master power and communication on-off control and panel lighting control.

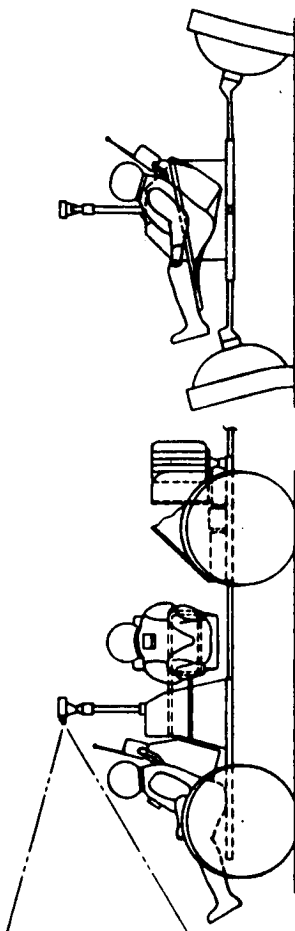
The evaluation indicated that the intermediate display/control console provided adequate control and information for normal and emergency modes of driving commensurate with weight and vehicle design limitations.



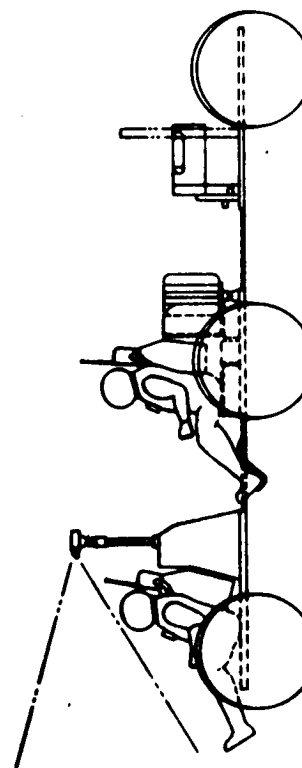
SIDE BY SIDE



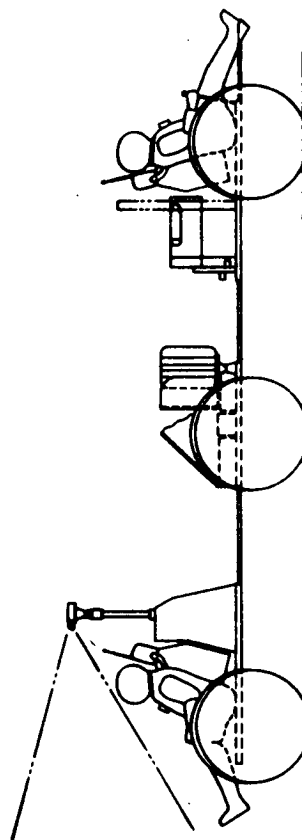
STANDING FWD



CENTER SLING



CENTER



AFT

FIG. 6.1.2 ALTERNATE PASSENGER POSITIONS

TABLE 6.1.1-1

Sheet 1 of 2

## PASSENGER STATION EVALUATION

<u>Standing Position</u>	<u>Advantages</u>	<u>Disadvantages</u>
Standing Fwd	<ul style="list-style-type: none"> <li>o Some forward visibility.</li> <li>o Desirable weight distribution</li> </ul>	<ul style="list-style-type: none"> <li>o Feet project below chassis.</li> <li>o Complex restraint/support system required, particularly if astronaut is unconscious.</li> <li>o Difficult ingress/egress and rescue/emplacement activity if astronaut is incapacitated.</li> </ul>
Center	<ul style="list-style-type: none"> <li>o More comfortable seated position.</li> </ul>	<ul style="list-style-type: none"> <li>o Feet susceptible to injury.</li> <li>o Difficult ingress/egress.</li> <li>o Undesirable weight distribution.</li> <li>o Complex structural arrangement.</li> <li>o Difficult rescue/emplacement procedures if astronaut is unconscious or incapacitated.</li> </ul>
Aft	<ul style="list-style-type: none"> <li>o Easy ingress/egress.</li> <li>o Light weight.</li> <li>o Easy rescue/emplacement procedures if astronaut is unconscious or incapacitated.</li> </ul>	<ul style="list-style-type: none"> <li>o 3rd module may not always be available.</li> <li>o Feet susceptible to injury when backing up.</li> <li>o No forward visibility.</li> <li>o Undesirable weight distribution.</li> <li>o Some science equipment must be jettisoned.</li> </ul>

TABLE 6.1.1-1

Sheet 2 of 2

Side by Side	<ul style="list-style-type: none"> <li>o Best forward visibility if astronaut is conscious.</li> <li>o Shared vehicle control if rescued astronaut is capable.</li> </ul>	<ul style="list-style-type: none"> <li>o Lateral unbalance of vehicle without passenger.</li> <li>o Difficult passenger station stowage problem in transport.</li> <li>o Difficult rescue/emplacement procedures if astronaut is unconscious or incapacitated.</li> </ul>
Center Sling	<ul style="list-style-type: none"> <li>o Easiest ingress/egress procedures for enabling rescuer to emplace rescued astronaut.</li> <li>o Most comfortable position for disabled astronaut.</li> <li>o Desirable weight distribution.</li> </ul>	<ul style="list-style-type: none"> <li>o Conscious astronaut has no forward visibility.</li> </ul>

#### 6.1.4 Areas Requiring Further Study

Future studies for the DLRV involve verification of design feasibility or the refinement of design by simulation testing to determine operation of the DLRV from a remote control Earth based station using variables of visibility, topography, time delay, and vehicle performance parameters. Present work going on under contract obligation NAS8-25117 entitled "Human Factors for Remote Control Vehicle" will investigate the influence of kinesthetic cues on remote driving performance and the effectivity of a predictor device. Future work will require greater levels of simulation, varying frame rate and time delay, integrating previous findings, and leading eventually to a full scale ground driver's station with the purpose of investigating the full interface of the DLRV and the ground station. Specific problems requiring further study are:

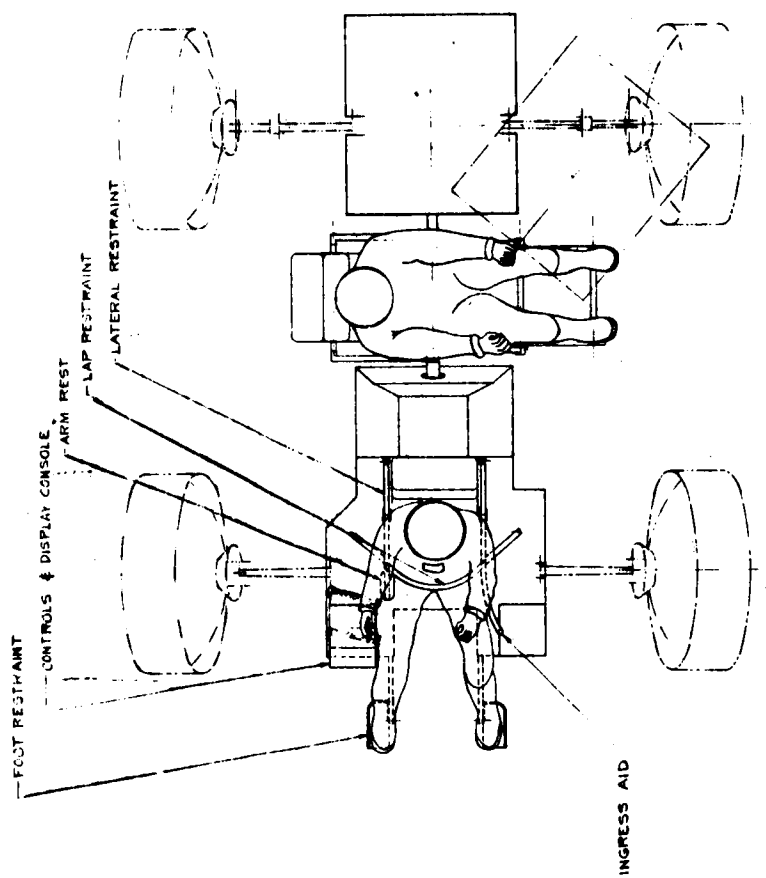
- o Ability to remotely drive the vehicle under lunar night visibility conditions.
- o The effect on driver performance, both in the manned and unmanned modes, of excessively high contrast ratios in lunar lighting conditions affecting judgements of size, distance and hazard avoidance.
- o The effect of adaptation time of the eye in going from very bright areas to very dark areas and vice versa, in the manned mode.
- o The size, quality, color and contrast ratio of information displays in the manned mode, particularly as they are affected by glare conditions.

#### 6.2 CREW STATION CONFIGURATION

The crew station includes all structure, equipment, and mechanical aids necessary for the crew to perform the mission functions. The general arrangement of the DLRV crew station is shown in Figure 6.2-1.

##### 6.2.1 Driver Station

The driver station, which is located in the forward portion of the control module, includes the console, controls and displays, driver's seat, restraint system, foot supports, driver stowage provisions, parking brake control, and driver aids for ingress/egress. The console rests on the platform of the control module chassis. The console provides support for the instrument panel, hand controller housing, isotope heater, safety switch, and the console deployment mechanism. The instrument panel mounted on the aft side of the console is tilted forward thirty degrees. The panel has approximately 125 square inches of surface. This surface is coated for thermal and glare reduction, as well as for environmental protection. Integral with the console is a circuit protection



II/I.6-8

LOADING POSITION

CARRYING POSITION

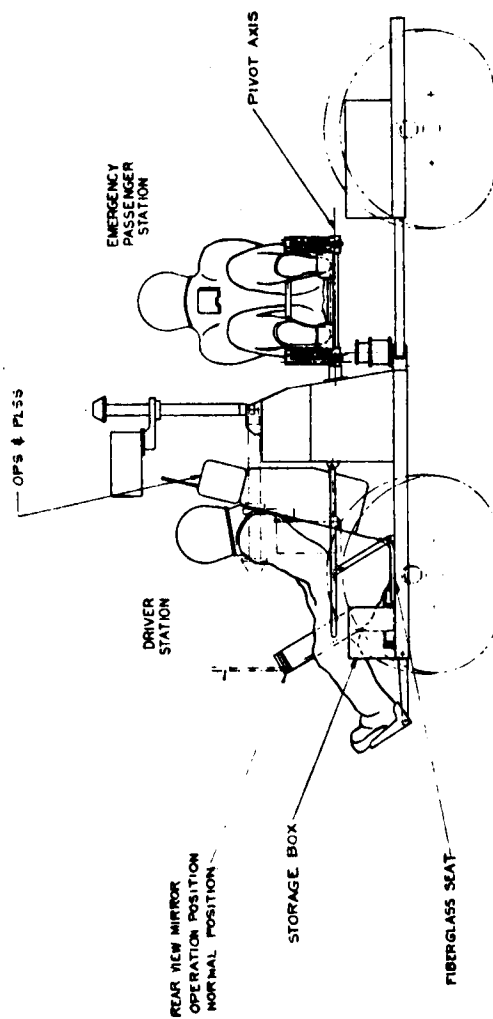


FIG. 6.2-1 DLRV CREW STATION ARRANGEMENT

panel which contains switches for activating relays that are in the circuit to protect selected electrical loads.

The driver seat includes the seat pan, a folding or stowing mechanism, an adjusting mechanism, and the structural attachments to the chassis.

The seat pan is a contoured fiberglass unit with pickup lugs on the lower side to attach to the support structure. The pan is fabricated with rolled over type edges to prevent pressure point pickup on the astronaut. The front edge is rolled down and the other three sides have rolled up sides approximately three inches high to support the man against lateral and rearward sliding.

The driver restraint system is made up of a lateral support railing both for the man and his life support system and a fold-in-front lock down bar. The railing is made of light gauge aluminum tubing or slightly heavier fiberglass tubing. The lock down bar pivots from a point in the console and swings down across the lap of the driver, securing him into the seat. The bar contains a positive locking feature in the down position. A safety switch installed in the console interrupts power to the wheel motors and steering actuator when the driver restraint system is in the up position. This safety feature prevents inadvertent actuation of the vehicle by driver error, system malfunction, or by the MCC while the astronaut is ingressing or egressing the vehicle or afoot in the vicinity of the DLRV.

The foot support is composed of two independent structures extending forward from the chassis, providing stirrups ahead of and on either side of the ingress/egress cutout in the chassis. The stirrups do not interfere with the ingress/egress operation of the driver. The structure is capable of withstanding impacts that may occur due to head-on collisions with rock formations.

A rear view mirror is provided for traveling in reverse, monitoring the disabled passenger, or for quick checks on the rear module. The mirror will telescope from the console and be adjustable angularly and relative to the driver. In the suited, pressurized and restrained position, astronaut head movement is limited to motions inside the helmet. The helmet, itself, is not rotatable. Consequently, to obtain maximum rear view vision, a wide range of adjustment must be provided.

Glare protection for the instrument panel is provided by a suitably placed translucent hood. Glare protection is required for two reasons: First, to permit the instruments to be read and the controls to be locatable. Secondly, since the instruments are environmentally protected by transparent sealed cases, they capture large quantities of heat due to solar radiation which jeopardize their



functioning. To provide for this contingency a translucent hood, transmitting sufficient diffuse light to read the instruments is provided.

Driver stowage provisions are provided on the left side of the control module, forward of the geological tool rack. It is anticipated that the items to be included in the stowage list will be primarily GFE. The list might include:

- o Lanyard/Life line
- o Aerosol dust remover
- o Operations manual
- o Charts
- o Photographs
- o Check lists
- o Film packs
- o Log
- o Drinking water container and water gun
- o Console Insulation Bag
- o Radiation Meter
- o US/NASA Flag markers

Ingress to the vehicle is accomplished by facing the driver's position, grasping the bell-mouthed restraint arm above the seat and rotating the body so that the astronaut is facing forward. In this position the arm is still visible to him. Lowering himself into the seat, the bell-mouthed arm permits the astronaut to fall automatically into a nested position with the torso inclined backwards at an angle of  $14^{\circ}$ . The driver then raises his legs into the foot supports which are gusseted on the outside ends to prevent foot slippage under motion. Both the seat and the foot supports are adjustable prior to stowage in the IM to accommodate the specific astronaut assigned as the driver. Ingress/egress has been validated by mock-up studies using pilots in a pressurized suit. The procedures were found to be easily learned and quickly performed. Additionally, body comfort, mobility, adequate visibility, and reachability of the displays and controls were confirmed. The restraint bar is easily lowered into position and can be quickly raised in the event of an emergency.

The stowage position for the driver station is shown in Figure 6.2-2. The seat restraint systems folds against the front of the control module equipment compartment, while the leg support struts fold under the chassis. Parallel dual tracks permit the console to slide inboard to the longitudinal centerline of the

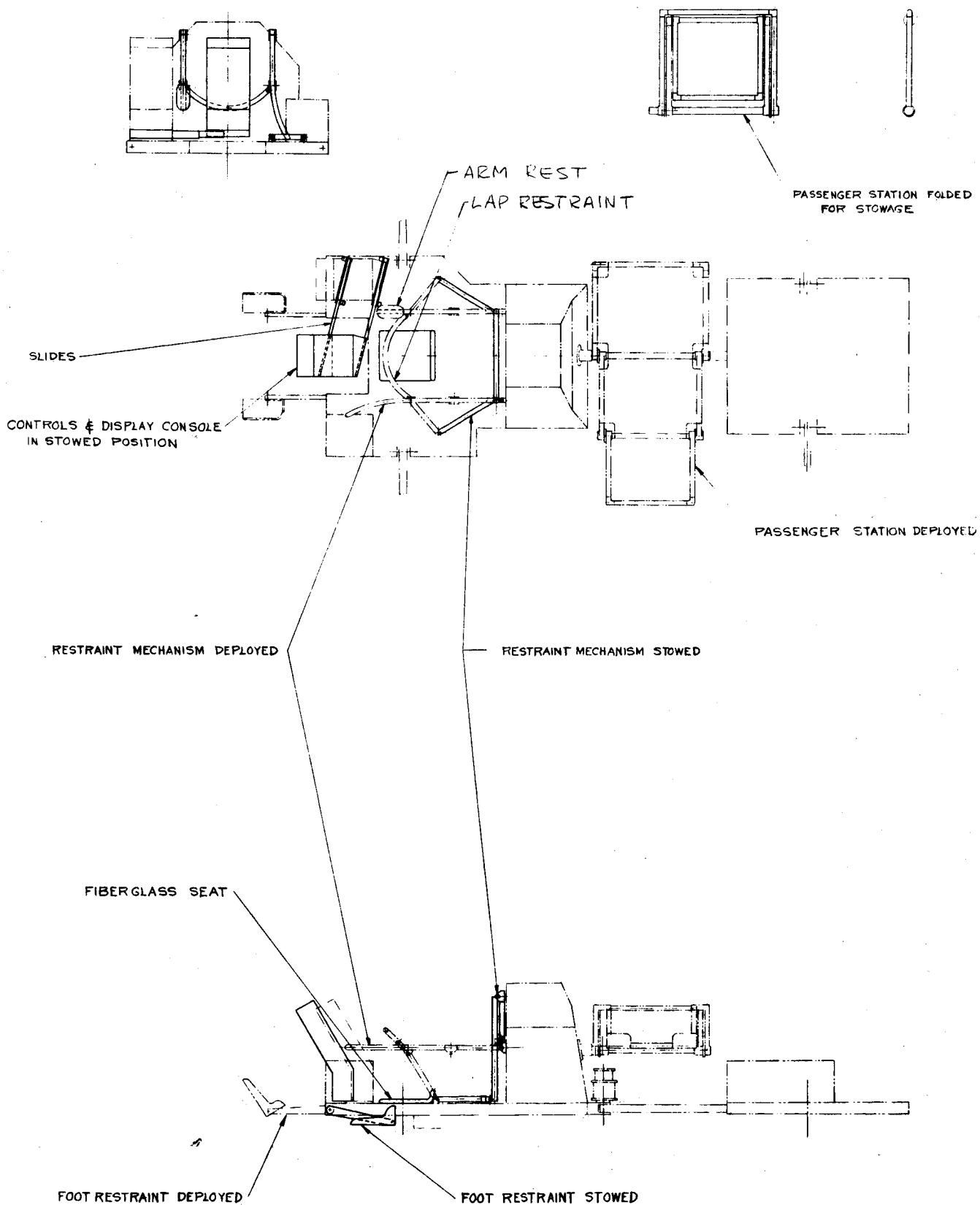


FIG. 6.2-2 CREW STATION STOWAGE

module, forward of the operational position. The mechanism provides for protection of the wire runs from the console and for a positive locking device when the console is in either extreme position. In the remote control mode of operation, the console is moved to the stowed position to avoid interference with the solar array. The stowage provisions box either collapses for stowage in its normal location, or is stowed intact on another part of the vehicle, depending on whether it is stocked before launch or after deployment.

An isotope heater provides thermal heating for the console instrumentation in the unmanned mode during the lunar night. The lower dormant temperature exposure limit of the instruments is approximately  $-60^{\circ}\text{F}$ . The heater produces 2.5 watts of thermal heat and weighs .25 pounds. Additionally, the console is wrapped in an insulation bag, composed of aluminized mylar and H-film in sufficient layers to provide adequate insulation to five sides of the console. The sixth or bottom side does not adversely affect the temperature equilibrium. The bag, which is reasonably form fitting (no tight fit is required), is attached close to the bottom of the console, effecting a modestly closed seal, with either velcro or attached spring clips. The combination of the heater and the insulation bag maintains the temperature of the instruments within the range of  $-60^{\circ}\text{F}$  to  $210^{\circ}\text{F}$  during their dormant period in the unmanned mission.

#### 6.2.2 Controls and Displays

The controls and displays complement consists of the panel arrangement and instruments of the instrument panel, the circuit protection panel, the hand controller grip and mechanism and the panel lighting.

The instrument panel configuration groups the controls and displays in accordance with subsystem function and in the order of operational importance to the driver. The arrangement is shown in Figure 6.2-3.

The mobility controls enable the driver to operate the DLRV in a normal operational mode or in an emergency mode. The operational controls are centered around the hand controllers. The hand controller, located in the lowerleft hand corner of the instrument panel projecting aft, provides incremental power to the mobility units to drive and brake the vehicle and for steering. Activation of the hand controllers is through a pistol grip shaped to accommodate the astronaut hand wearing an extravehicular glove. The grip handle pitches forward and back as well as rotates laterally both clockwise and counter-clockwise.

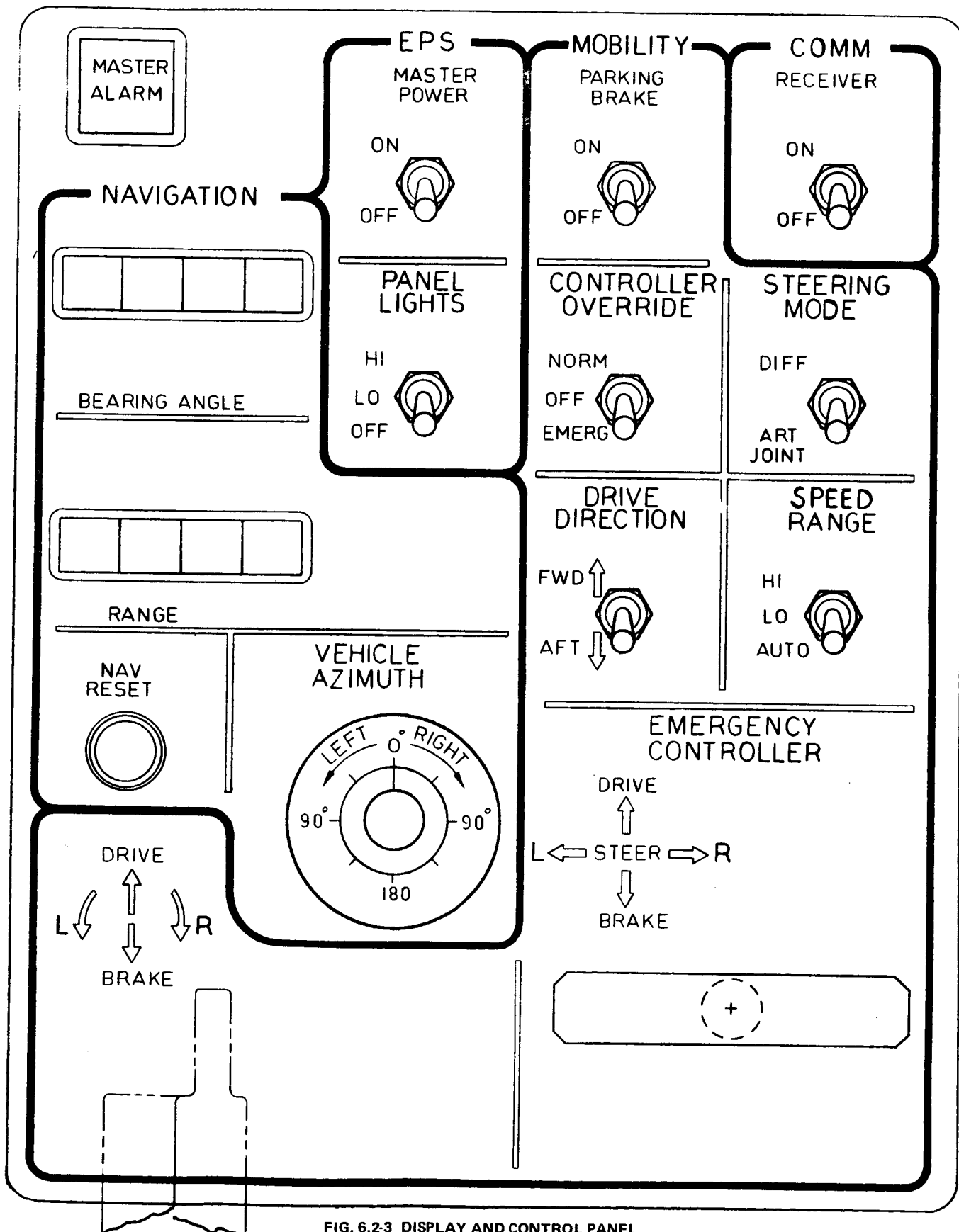


FIG. 6.2-3 DISPLAY AND CONTROL PANEL

The pivotal point for pitching movement is located between the ring finger and the index finger in the center of the grip to minimize the introduction of vehicle motion through the man into the controls. The rotational axis is located above the cleft for the thumb and forefinger. The forearm of the driver is braced by an armrest as a means of reducing lateral impulses in the controller. Functionally, the motions are translated as follows: pitching the upper portions aft produces incremental braking dependent upon grip setting; clockwise rotation of the pistol grip produces a steer right reaction, while counterclockwise rotation does the same to the left. A panel switch permits placing the vehicle in reverse drive, but all the controller functional motions remain the same.

Steering the vehicle can be accomplished in two ways: The normal approach is to power the steering actuator, which changes the angle between modules around the articulated joints. The back up approach is to vary the individual wheel driver motor speeds to product differential wheel speed steering. A switch on the panel permits selecting the steering mode.

The speed range available to the controller is a function of the motor winding setting. When high torque is required, it is obtained at the cost of a reduction in velocity through a change in the motor winding. A three position switch makes possible the choice of high or low speed setting, or an automatic mode. The low setting is used for velocities up to about 8 km/hr, while the high setting is for velocities above 8 km/hr. The automatic position provides an automatic selection of the appropriate setting.

An emergency controller can be substituted for the hand controller in the event of a malfunction. To do this a panel controller override switch is switched to emergency. This disconnects the hand controller signals from the system and substitutes the signals emanating from the emergency controller. The emergency controller has a tee handle grip that transmits the same functional signals through the same motions, except that it activates a simple four way switch, producing a bang-bang on/off control rather an an incremental one. The emergency controller is located on the instrument panel immediately outboard of the hand controller. The pivot for the tee handle is a universal joint at the panel surface.

The panel override switch has another position - "off". The purpose of this position is to disconnect both controllers. This capability permits the driver

to stop the DLRV, with no intention of alighting and to reconnoiter, photograph, study his map, perform scientific implementation or similar operations, and not expose himself to accidental actuation of the vehicle through jostling of a controller.

Electrical power control is represented by the master power switch and a panel light switch. The master power switch controls the power to all equipment except the communications receiver. This panel switch is an on/off switch which is used as a manual blanket shut down of power to units during translunar transport and between sorties. In an emergency, due to an unscheduled high power discharge on the vehicle, it offers a means of interrupting the discharge quickly.

Display panel lighting is provided in the form of integral lighting composed of redundant incandescent lamps. The panel lighting switch, in calling for a low level of illumination, uses one of the redundant lights. The high position uses all the lamps. The low position circuitry requires a blocking diode to prevent back powering the redundant lamp.

Navigational controls and displays are available in the form of two numerical readouts and one moving pointer over a circular marked display. One numerical readout presents the bearing angle, which is the angle between the vector from the LM landing site to the DLRV and the sun's rays. The other readout presents the range, which is the length of the vector from the LM to the DLRV. These two displays provide the driver with navigational data to locate himself on the lunar surface with respect to the LM. However, in covering a circuitous traverse the astronaut would have difficulty orienting the vehicle with respect to a vector, that is, selecting a specific direction. He can by noting range and bearing readings estimate the vehicle orientation, but this is not a very satisfactory driving mode. To improve this condition an azimuth angle display is included. The azimuth angle is the angle formed by the aforementioned vector to the DLRV and the longitudinal axis of the DLRV. Thus, driving away from the LM, the azimuth angle is  $180^{\circ}$ . When driving to the LM the driver tries to maintain this angle at  $0^{\circ}$ . All three displays maintain their last reading in the event of a power failure or a communications interruption. The latter is required because the computer integrating the sensor information for the displays is in the Mission Control Center.

At the end of each sortie or before commencing the next one the displays are brought back to the baseline. Theoretically, when the DLRV returns to the LM

site, the numerical readings should be zero and the azimuth angle represent the vehicle attitude but some increment of error can exist and should not be added to the next sortie. A reset button is therefore provided resetting the system. The button will be guarded to permit inadvertent actuation. However, should such action take place, the ground control can replace the erased data from the computer. Communications control on the instrument panel consists of a single communications receiver switch. This switch must of necessity be separated from the master power switch circuitry because without the capability to receive ground communications, MCC could not communicate in any fashion with the crew or the vehicle beyond the line of sight communication from the back pack through the IM. Separate control of communications allows all other systems to be shut down while a vehicle malfunction, such as excessive power consumption, is discussed with MCC. The caution and warning control and display is the master alarm combination light and switch in the upper left hand corner of the instrument panel. The light flashes on when a monitored malfunction occurs. The light continues to flash until the driver presses the alarm, which shuts off the light making it available to indicate any other malfunction. Verbally, the astronaut interrogates the MCC for specific details on the malfunction.

### 6.2.3 Passenger Station

The emergency passenger station is located aft of the equipment compartment, cantilevered off the rear of the control module, approximately on the longitudinal axis of the vehicle. (See Fig. 6.2-1). The passenger station is composed of a seat and support system, a restraint system, ingress/egress aids, and foldup mechanization.

The seat and support consists of a flexible material that conforms to the outline of the seated astronaut from behind his knees to his buttocks. The forces applied to the seat are transmitted to a tubular frame through the cloth under tension. The tubular frame acts as the main structural distribution member and supports directly the weight and position of the astronaut's backpack. This positioning of the incapacitated astronaut reduces the possibility of suffocation resulting from accumulations of his own vomitus.

The passenger restraint system must be capable of providing adequate security for an incapacitated astronaut even more than for a fully functioning passenger. The restraint system will be positive, simple and readily engaged/disengaged.

Also, the system will provide shielding for the astronaut from inadvertant harmful contact with portions of the vehicle moving relative to the passenger, if necessary.

Ingress/egress will be provided to assist the passenger in boarding and disembarking from the vehicle under his own power and initiative. Aids may also be needed to assist the driver in moving an incapacitated astronaut into and out of the vehicle.

A foldup mechanism is provided to fold the seat and support provisions into a transport stowage envelope during the translunar flight, as shown in Figure 6.2-2. The mechanism incorporates a positive lock and retention system in both the stowed and operational configuration.





SECTION 7  
SYSTEM TRADEOFFS AND ALTERNATIVES

In the course of the study various tradeoffs were made before the selection of the final system. Of these, three are reported herein. Two were requested by the Statement of Work and the third is of significant interest.

7.1 PENALTY FOR MANNED CAPABILITY

Crew Systems is the obvious candidate for deletion if the vehicle is never manned. The attendant weight reduction is 25 lb. In addition, many subsystem components could be eliminated or redesigned for more efficient performance. These are discussed for the affected subsystems.

- o Mobility - The chassis, suspension and wheels may be designed for lower dynamic loads since unmanned speeds are low. The complexity of the suspension system could be reduced, providing about a 4 lb weight saving. Manned science mountings (1 lb) could be eliminated. Structural redesign would allow a 13 lb savings.

The Traction Drive Assembly may be redesigned. The top velocity of 0-2 km/hr would allow a fixed gear ratio of about 80:1 to be substituted for the winding change circuitry. A consequent increase in reliability and reduction in weight would ensue. At least  $\frac{1}{2}$  lb. in the six circuits would be realized. The major change would be in the removal of four wires to each motor (two per phase) amounting to a  $\frac{1}{2}$  to  $\frac{3}{4}$  lb saving.

The power requirement of 1/8 HP could safely be cut at least 30%. This represents a power weight saving of at least 1 lb.

Note: Any reduction in weight from the 1500 lb max. would be a separate power item.

The total traction drive saving would be about 2 lb.

- o Electrical Power Supply - Batteries may be sized for peak unmanned power instead of manned sortie energy. The battery size is reduced from 1.68 KWH (50 lb.) to 0.7 KWH (36 lb.). The array is increased, however, from 270 W (25 lb.) to 310 W (29 lb.). Attendant weight saving is 10 lbs.
- o Navigation - The VHF Homing Assembly (3.2 lbs.) may be removed
- o Communications - The signal processor for voice and bio-med may be removed. Weight saving is 4 lbs.

- o Space Support Equipment - Assuming that deployment and activation are still manned, no changes are required. The provisions for unmanned deployment and activation would require an additional 50-100 lbs of weight.
- o Thermal Control - Thermal control is generally sized for unmanned operations but some weight reduction is possible by removal of approximately 2 lbs of phase change material from the Control Module.

A list of the total weight saved is as follows:

Crew System	25
Chassis and Suspension	18
Drive Assemblies	2
Batteries	6
VHF Homing	3
Signal Processor	4
Thermal Control	2
	<hr/> 60 lbs

## 7.2 NIGHT OPERATIONS

The present vehicle is designed for daylight operation and has limited night capability with the battery and RTG energy sources. Usable RTG power is 32 watts and fully charged batteries provide 588 watt-hr when discharged the design 35%. The normal daylight driving non-mobility load is 242 watts and the mobility power at 1 k/hr is 106 watts from Figure 4.1-17. About 2 hours of normal operation are possible, before the batteries require recharge. Alternately, the battery energy may be used only for intermittent science operations which would require an average power of 83.7 watts plus 120 watts for telemetry.

The most practical solution is the incorporation of multi-hundred watt RTG in the primary power supply. These RTG's are expected to be available in the DLRV time frame. A system with two 145 watt RTG plus batteries would be satisfactory but would increase vehicle weight by 64 lbs.

Another possibility is the integration of the RGM power supply with the vehicle power system. This would provide extra power prior to RGM deployment. The RGM power unit rating is estimated to be 50 watts. The present RTG maintains the vehicle during the quiescent period and, therefore, the RGM power would be available for battery recharge. This power would charge the batteries in about 17 hr (34 watt effective rate) thus allowing operations similar to those in daylight except that recharge time is increased from  $3\frac{1}{2}$  to  $17\frac{1}{3}$  hr.

There is a question about lighting for driving and sample inspection. The TV camera will operate under earthshine conditions but it is not known whether the picture would be adequate for driving, sampler arm operation or geological observations of subtle changes in photometric properties. The performance of the facsimile camera at low

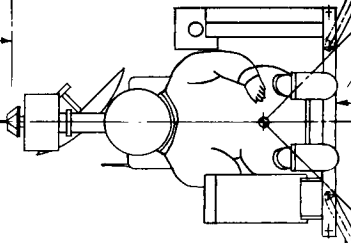
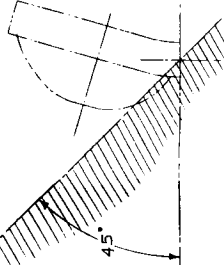
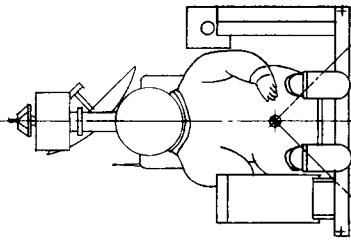
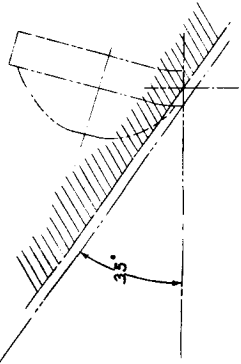
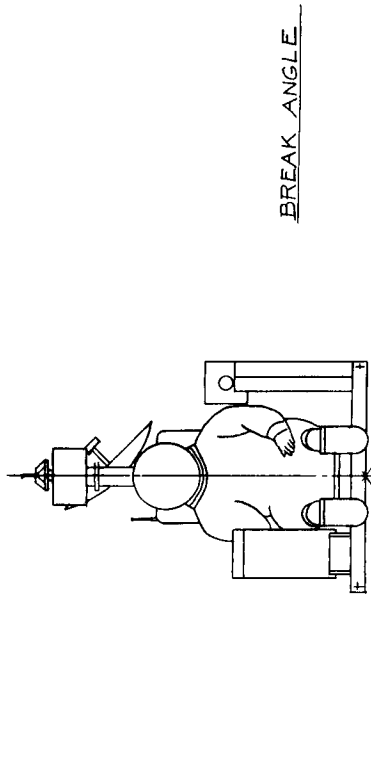
light levels is also unknown. Lighting for sample inspection and screening is considered necessary to provide a familiar frame of reference. Such a light would weigh 1 lb.

### 7.3 REDUCED SIZE VEHICLE

Lunar terrain mobility capability and safety considerations are closely related to vehicle sizing. Obstacle negotiation and weak soil mobility are enhanced by large tread, wheelbase, and wheel size. Additionally, a large planform contributes more to stability, and thus, to safety than any other characteristics of a vehicle designed to operate on the lunar terrain. The selected DLRV configuration has 38-in. diameter wheels, the largest that can be accommodated, and a 114-in. tread and 96-in. wheel base, obtained by utilizing extendable intermodular drawbars and a swing arm suspension. There is some weight penalty associated with the large vehicle, so studies were made to determine the characteristics and performance of the smallest vehicle that would meet the mobility requirements.

Figure 7.3-1 shows the derivation of the smallest planform vehicle that will meet the stability and break angle requirements. In order to satisfy the  $35^\circ$  break angle requirement, the wheel center of pressure must lie below the line shown in the upper left sketch. The  $45^\circ$  stability requirement can be satisfied only if the wheel center of pressure lies above the line shown in the left center diagram. Combining these two requirement results in the allowable range shown in the lower left diagram. The smallest allowable tread is then 82.6 in. If the wheels are made smaller, the suspension arms must be longer to reach the wheel hub, as shown in the lower left. The wheelbase for the small vehicle is 85-in., based on the break angle requirements shown in the lower right. The allowable range shown c.g. location will be most difficult to meet, in view of the weight variation during a mission; the c.g. on the selected design lies forward of this location.

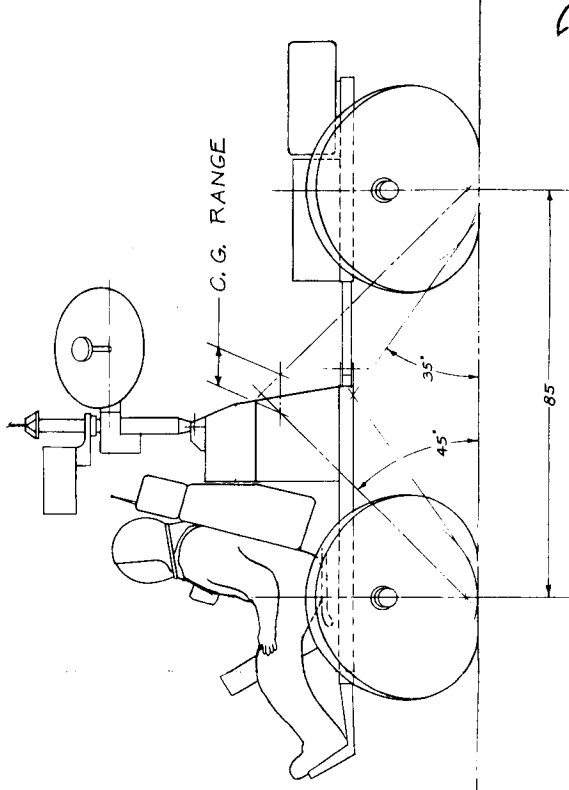
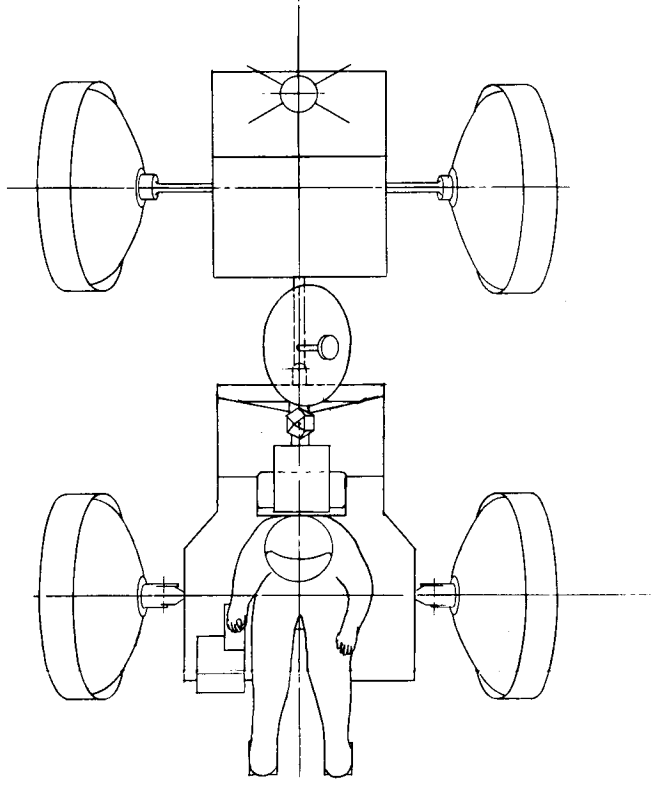
The plan views of the large and small vehicles are compared in Fig. 7.3-2. The planform areas must be the same due to equipment and science requirements. The differences lie simply in the length of the drawbar and the pivot location for the suspension arms (the lengths of the arms are nearly identical). The extra weight for the large planform is due only to the small drawbar extension and slightly larger cap areas required for the drawbar and chassis due to the longer spans.



ALLOWABLE WHEEL C.P. LOCATION

82.6

FOLDOUT FRAME



FOLDOUT FRAME 2

FIG. 7.3-1 MINIMUM PLANFORM DLRV

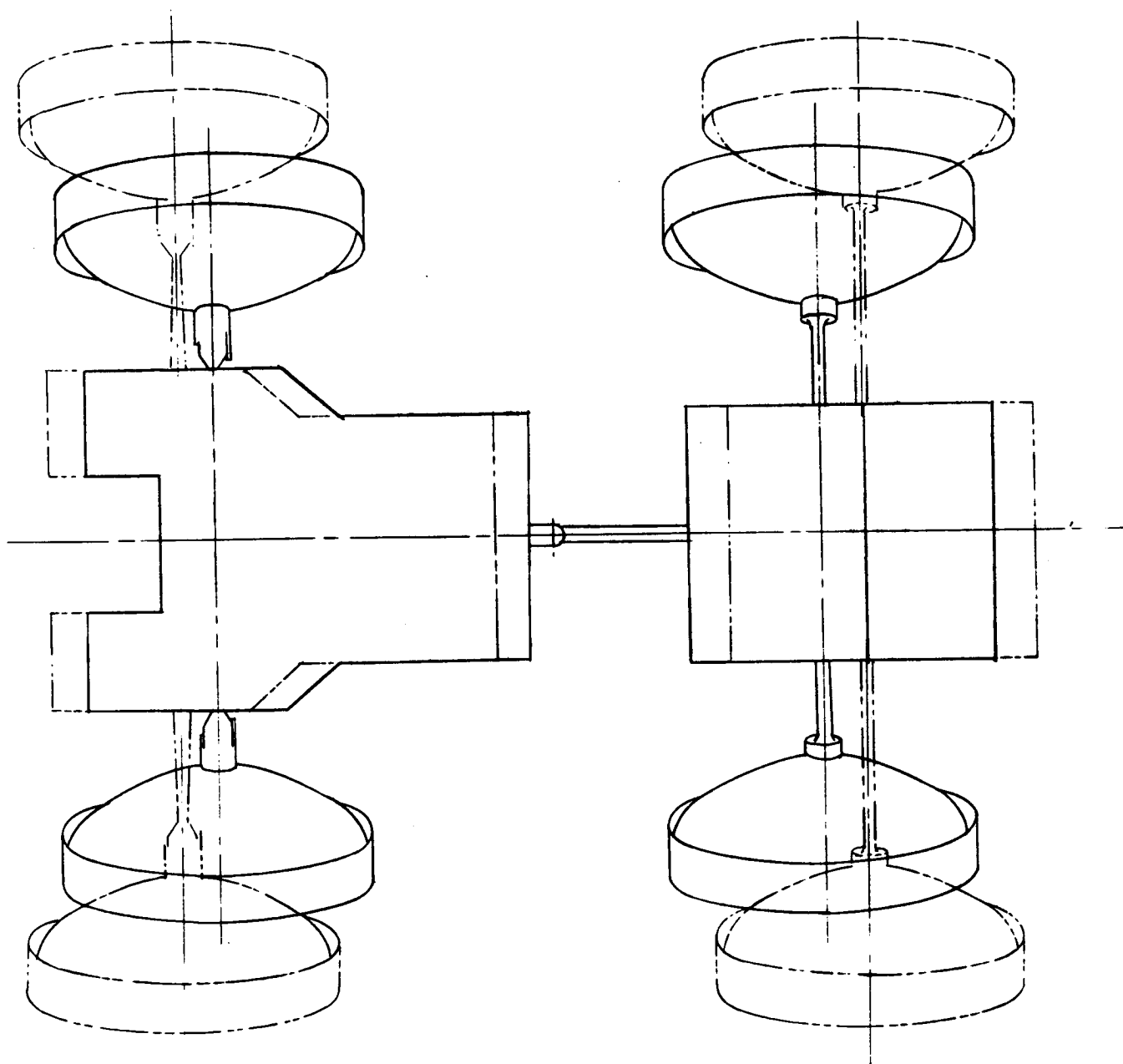


FIG. 7.3-2 MINIMUM SIZE VEHICLE VS SELECTED CONFIGURATION

The weight comparison for the two vehicles is shown in Table 7.3-1. The savings due to reducing the planform is only 7 lb. A structural weight savings of 13 lb. results from reducing wheel size; however, the associated increase in rolling resistance will require a partially offsetting weight increase in the power system.

A performance comparison of the small and large vehicles is shown in Table 7.3-2. The small vehicle has a smaller minimum turn radius which provides better maneuverability, but this turning capability must be used with caution because its stable turn radius at high speed is almost four times greater than the minimum, and it is 34% greater than that of the large vehicle. Roll acceleration, which is probably the most significant parameter from the ride comfort viewpoint, is must lower on the large vehicle. Another factor not shown in the table is the lower rolling resistance of the large vehicle in a turn, due to tracking of the wheels; the steering pivot for the small vehicle is not midway between the wheels, producing off-tracking in turns.

This study led to the conclusion that the large vehicle provided an increase in performance that justified the relatively small weight expenditure required to obtain it. Of course, if the weight penalty simply could not be afforded, the size would have to be reduced; however, in view of the importance of mobility performance to a lunar vehicle, reduction in size must be regarded as one of the least desirable approaches to weight reduction.

TABLE 7.3-1

## SIZE TRADEOFF

	<u>CURRENT</u>	<u>REDUCE WHEEL SIZE</u>	<u>REDUCE TREAD &amp; WHEELBASE</u>	<u>REDUCE TREAD, WHEELBASE &amp; WHEEL SIZE</u>
<u>Dimensions</u>				
Wheel Base (in.)	96	96	85	85
Tread (in.)	114	114	83	83
Wheel Dia. (in.)	38	32	38	32
Suspension Length (in.)	18	21	18	21
Footprint Length	1.0	.82	1.0	.82
<u>Weight</u>				
Wheel	75	59	75	59
Chassis	77	77	73	73
Wire	38	38	36	36
Suspension	30	33	30	33
Actuators	18	18	17	17
TOTAL CHANGE	238 (0)	225 (-13)	231 (-7)	218 (-20)

TABLE 7.3-2  
PERFORMANCE COMPARISON  
SMALL VS LARGE VEHICLE

	SMALL VEHICLE 83" x 85"	LARGE VEHICLE 114" x 96"
Roll Stability Angle	45°	57°
Pitch Stability Angle	42°	45°
Min. Turning Radius	108 in.	138 in.
Min. Stable Turn Radius at 16 km/hr	410 in.	300 in.
Roll Acceleration (Rough Mare @ 8 km/hr)	1.37 Rad/Sec <sup>2</sup>	1.13 Rad/Sec <sup>2</sup>
Obstacle Step Crossing (6 x 6 vehicle)	38"	46"
Ground Clearance	26 in.	34 in.



## CONTENTS

<u>Section</u>	<u>Page</u>
1 INTRODUCTION .....	1-1
2 TIEDOWN .....	2-1
2.1 REQUIREMENTS .....	2-1
2.2 STRUCTURAL ARRANGEMENTS .....	2-1
2.3 STRUCTURAL DESIGN .....	2-2
2.3.1 Strut Assembly .....	2-2
2.3.2 Yoke Assembly .....	2-2
2.3.3 Science Module Support Structure .....	2-5
3 UNLOADING .....	3-1
3.1 REQUIREMENTS .....	3-1
3.1.1 Automation .....	3-1
3.1.2 Landing Attitudes .....	3-1
3.1.3 Unloading Time .....	3-2
3.2 UNLOADING PRELIMINARY DESIGN .....	3-2
3.2.1 Control/Power Module Unloading .....	3-2
3.2.2 Science Module Unloading .....	3-5
3.2.3 Manual Override of Deployment .....	3-15
3.2.4 Mechanization .....	3-15
3.2.5 Safety Considerations .....	3-15
3.3 SET-UP TASKS .....	3-16
3.3.1 Manned Mission .....	3-16
3.3.2 Unmanned Mission .....	3-16

## CONTENTS (Continued)

<u>Section</u>	<u>Page</u>
4 CHECKOUT .....	4-1
4.1 INITIAL CHECKOUT - MANNED SORTIES .....	4-1
4.2 TYPICAL PRE-SORTIE CHECKOUT AND ACTIVATION .....	4-1
4.3 POST-SORTIE CHECK AND DEACTIVATION .....	4-3
4.4 UNMANNED CHECKOUT .....	4-3

## ILLUSTRATIONS

<u>Figure</u>	<u>Page</u>
2-1 STRUCTURAL ARRANGEMENT, TIEDOWN .....	2-3
2-2 TIE-DOWN DESIGN LOAD SUMMARY .....	2-6
2-3 CHASSIS STRUCTURAL ARRANGEMENT, SCIENCE MODULE .....	2-7
3-1 CRITICAL DEPLOYMENT GEOMETRY LM/SURFACE .....	3-3
3-2 DLRV OFFLOADING MECHANISM ASSEMBLY .....	3-7
3-3 UNLOADING SEQUENCE .....	3-9

TABLES

<u>Table</u>	<u>Page</u>
4-1 INITIAL CHECKOUT - MANNED SORTIES .....	4-2
4-2 UNMANNED CHECKOUT AFTER CONVERSION .....	4-4

PRECEDING PAGE BLANK NOT FILMED

## SECTION 1

### INTRODUCTION

The DLRV is to be carried to the lunar surface in two Quads of the ELM delivery vehicle. After touchdown it must be unloaded and readied for use. This book describes the tiedown, unloading, set-up, and checkout methods and procedures associated with the selected configuration.

Section 2.0 describes how the DLRV is supported in the ELM, and presents a preliminary design of the support structure.

Section 3.0 details the deployment operation, and presents a preliminary design of the off-loading mechanization. Also included is a description of the set-up operations required after unloading to make the vehicle ready for use.

Section 4.0 deals with the checkout procedures used by the astronauts and the ground control station to assure that the vehicle is operating properly.

The DLRV configurations, both stowed on the ELM and set-up for manned and unmanned operation, are discussed in Section 3.2 of Book I, Volume II.

## SECTION 2

### TIEDOWN

#### 2.1 REQUIREMENTS

The tiedown structure provides support for the DLRV during all mission phases from installation on the EIM up to and including deployment on the lunar surface. Additionally, it supports the DLRV in a manner that isolates it from EIM primary loads so that EIM structural load paths are not modified, and residual structural deformation after landing does not load the deployment joints.

The vibration and shock environment imposed by launch and landing makes it desirable that the support structure be as stiff as possible to raise the resonant frequency and minimize the dynamic accelerations applied to the DLRV.

The geometry of the support system must satisfy the load direction constraints applied to the EIM hard points and also facilitate unloading. Since the release of the DLRV work statement, development of the EIM has resulted in new payload hard point locations which are beneficial to both the EIM and the DLRV. These have been used in lieu of the points specified in Annex A of the work statement.

#### 2.2 STRUCTURAL ARRANGEMENTS

The structural arrangement of the DLRV tiedown is shown in Fig. 2-1. The drawing shows the support structure for the control and power modules carried in Quad I, but the geometry and method of support are identical for the science module in Quad IV.

The DLRV payload package is supported at three points, two lying in the plane of the lower shear deck of the descent stage and the third lying in the plane of the upper shear deck. The two lower points are trussed out from the descent stage box structure, and can resist loads in all directions. A line between these two points defines the hinge for initial deployment. Loads in a direction parallel to the hinge line are taken at only one support point to enable EIM structural deflection without loading the DLRV support structure.

The top of the DLRV package is stabilized by a horizontal strut to a support point at the inboard corner of the quad. This support point can resist loads only in a horizontal or Y-Z plane. By the use of this support method, a vertical displacement of the two outside corners of the quad relative to each other results in a rotation of the payload package and consequent translation of the upper portion without restraint. This eliminates binding at the deployment latch or hinge fittings caused

by deformation of the EIM design stage after landing.

The derivation of design loads for the stowed DLRV is discussed in Vol. II, Book II, Section 4.3.1. Using these criteria, preliminary design loads for the DLRV support were derived, and are summarized in Fig. 2-2.

### 2.3 STRUCTURAL DESIGN

The preliminary design of the support structure for the control and power modules in Quad I is shown in Fig. 2-1. The strut members are identical for the science module in Quad IV, but there is no yoke assembly. Instead there is a science module support structure as shown in Fig. 2-3.

#### 2.3.1 Strut Assembly

The strut assembly supporting the upper portion of the stowed DLRV is an axially loaded member about 36 inches long. The inboard end fitting provides the structural interface to the EIM while the outboard end incorporates the primary deployment latch. The remote control deployment actuator is mounted on this member. The strut clears the EIM upper diagonal member, but requires snubbing support to limit its deflection under vibration.

#### 2.3.2 Yoke Assembly

The yoke assembly provides the structural continuity between the control module chassis and the lower tiedown points. It also provides the means of rotation and translation during deployment.

The DLRV is supported in the vertical direction at the deployment translation latch located at the extremities of the yoke arms. The load is transferred by the arms to the hinge fittings. Loads normal to the chassis plane are sheared to the yoke beam and then to the hinge fittings. Horizontal loads are sheared to the yoke beam and then transferred axially to one of the hinge fittings.

The yoke arms incorporate the rail mechanism which supports the vehicle during the translation phase of deployment.

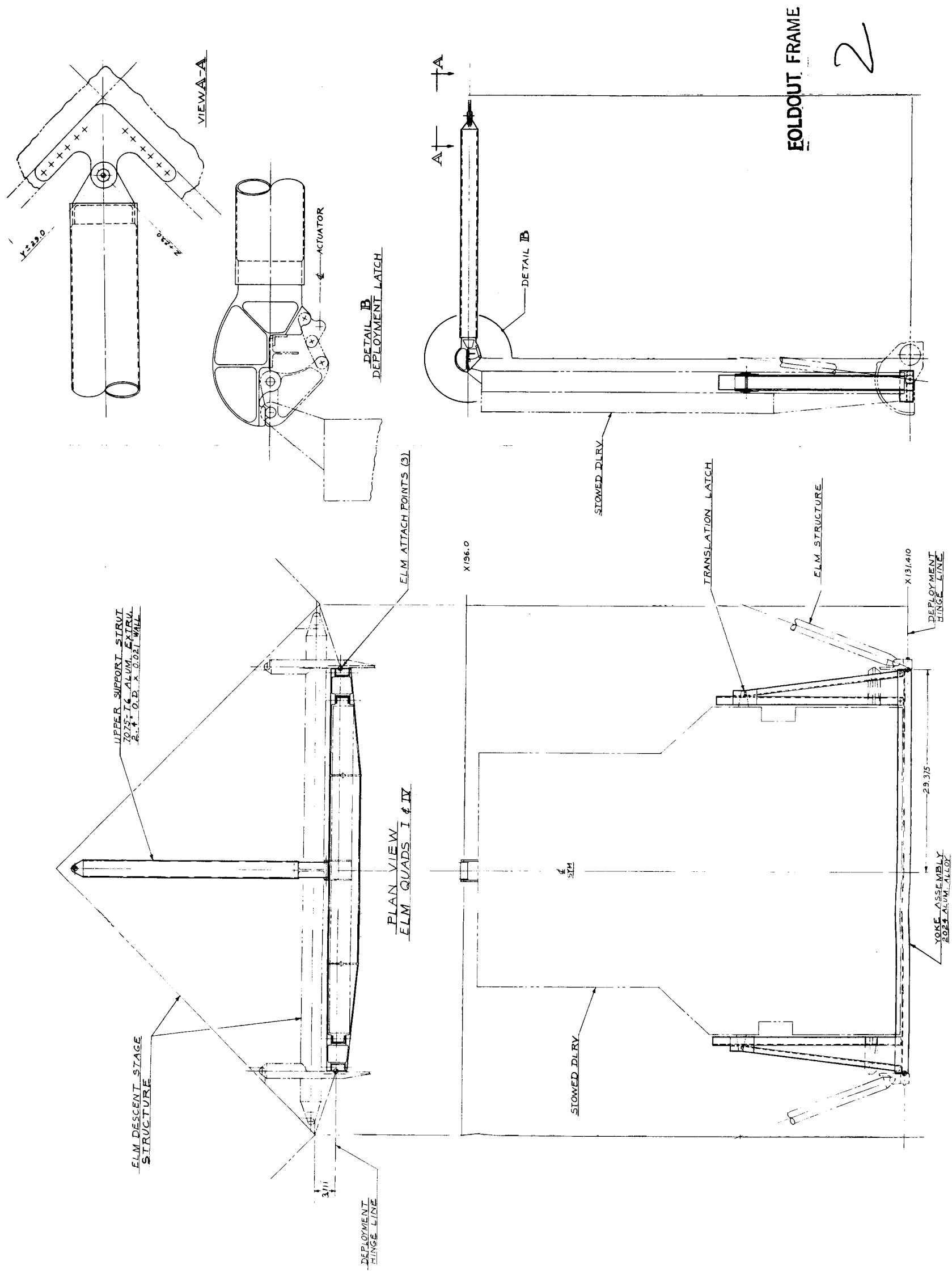


FIG. 2-1 STRUCTURAL ARRANGEMENT TIE-DOWN

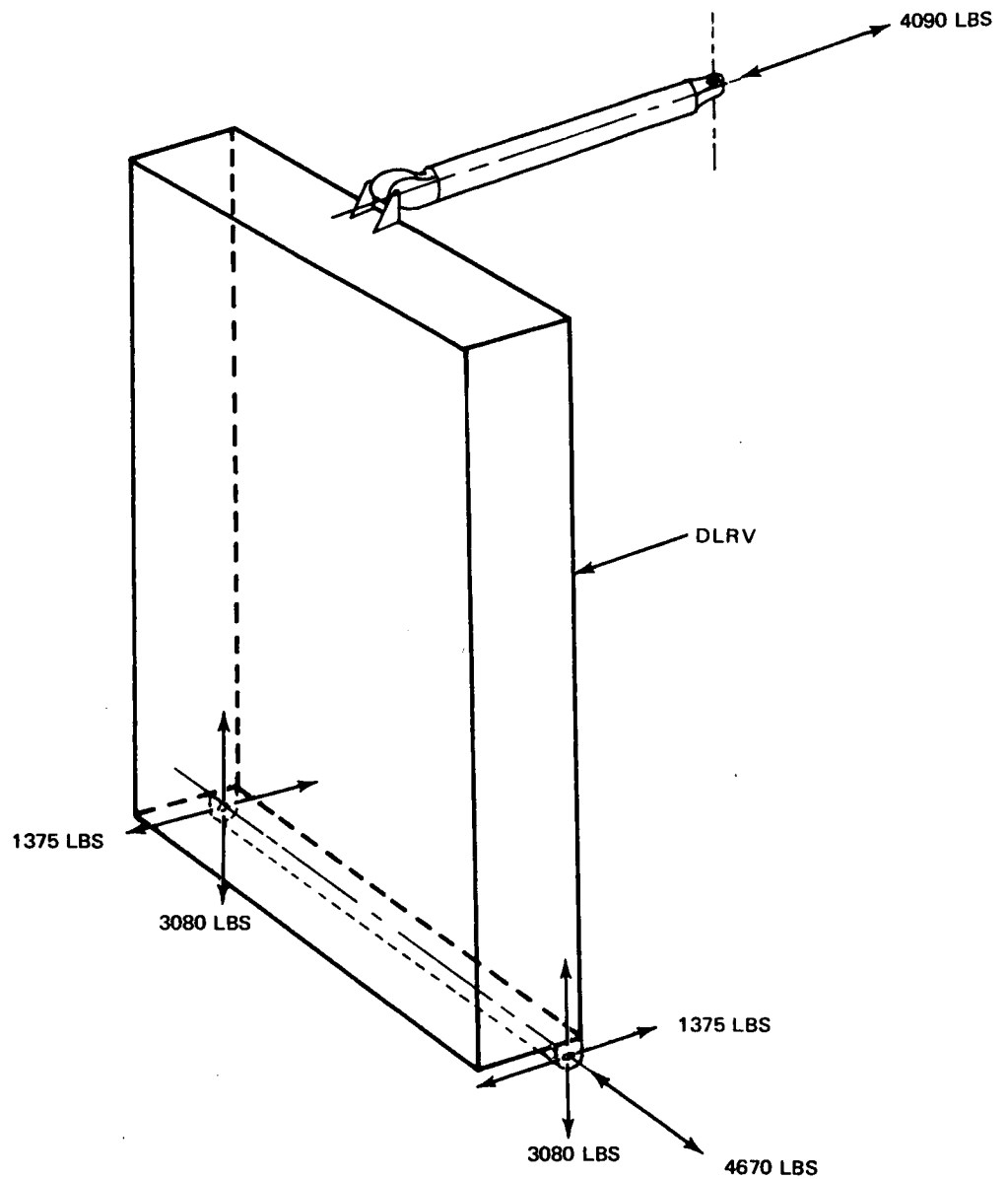
FOLDOUT FRAME

II/II.2-3/4



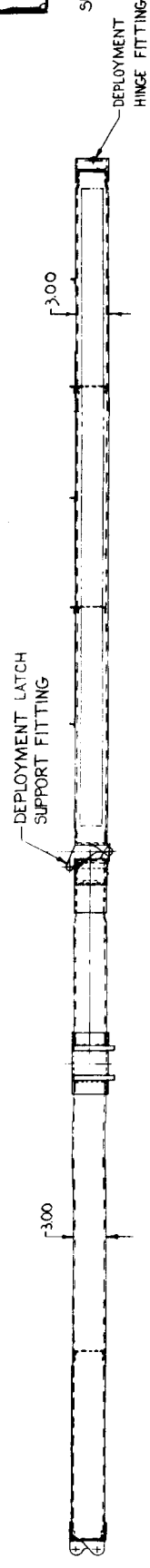
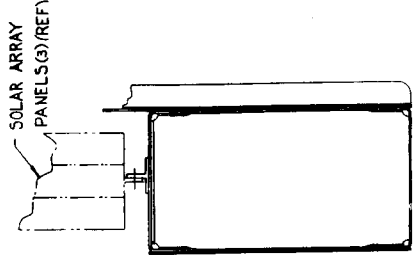
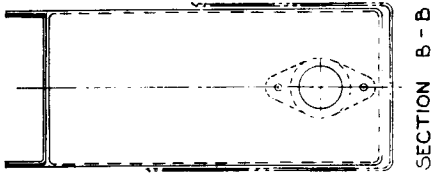
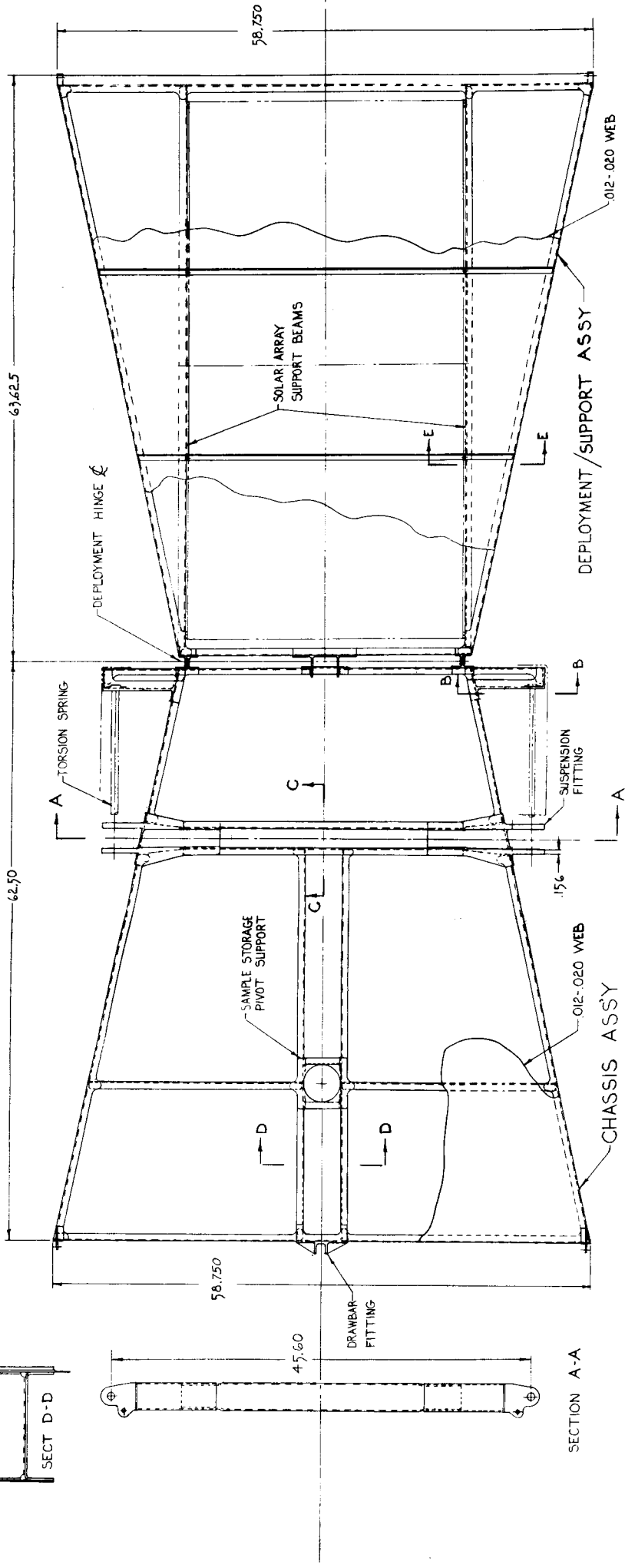
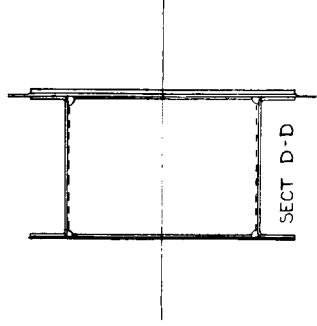
### 2.3.3 Science Module Support Structure

Fig. 2-3 shows the structural assembly which supports the science module during stowage by providing the structural continuity between the chassis and strut and deployment hinge fittings. Support is also provided for the module during and after deployment to the lunar surface until the module is separated by removal of the outer hinge pin. Additionally, this structure adds to chassis rigidity in the stowed configuration. (The science module chassis is also shown in the figure. See Section 5.1 of Book 1, Vol. II for a discussion of the chassis details). Included in science module support structure are stowage provisions for the solar array panels, tilt drive mechanism, and tripod support. Space is available for stowage of other items that may be required in the future.



ZERO MOMENT RESTRAINT AT EACH ATTACHMENT

FIG. 2-2 TIE-DOWN DESIGN LOAD SUMMARY



NOTE:

UNLESS OTHERWISE NOTED ALL MATERIAL IS 2024 AL ALLOY, SPEC 00-A-250/4 FOR SHEET & PLATE AND SPEC GMP5 2007 FOR PREFORMED & ROLLED PLATE.

FOLDOUT FRAME

FOLDOUT FRAME  
FIG. 2-3 CHASSIS STRUCTURAL ARRANGEMENT,  
SCIENCE MODULE

fy the maximum rotational motion required at the deployment hinge mechanism and the required length of the deployment support cable assembly. The last condition of maximum vehicle angular twist is created when the power module contacts the lunar surface and twists relative to the control module which is hinged and aligned to the ELM descent stage. These conditions result in an angle of twist of up to  $29^{\circ}$  which must be accommodated by the wheel suspensions and the intermodular drawbar assembly.

### 3.1.3 Unloading Time

The total time period needed to unload the DLRV is not considered vital to the mission profile assuming it is kept within reasonable limits. It can be reasoned that the shorter the time period, the less it impacts on the mission timeline, and the sooner a deployment failure can be uncovered and corrected. Less than a half a minute is estimated for unloading either the power and control modules or the science module. This time includes disconnecting the structural tiedown system, rotating downward, unfolding the vehicle, and displacing it clear of the delivery vehicle onto the lunar surface.

## 3.2 UNLOADING PRELIMINARY DESIGN

The total (6 x 6) assembly of the DLRV requires two separate unloadings. The control and power modules, which are stowed together in Quadrant I of the LM descent stage and kinematically function together during deployment, represent one unloading. The science module, which is mounted external to Quadrant IV, constitutes the other. The unloading kinematics for both are similar since the science module utilizes a structural tiedown support assembly which also kinematically functions with it during deployment.

The deployment of the DLRV is accomplished by a system of stored energy devices, gravitational forces, slave mechanisms, and locking devices which are mechanically sequenced. To save weight, all redundant mechanical systems have been eliminated by relying upon an astronaut to backup the primary automatic mode.

### 3.2.1 Control/Power Module Unloading

The control and power module unloading is done in two stages:

- o Unlatching from the LM and lowering of the power module wheels to the surface
- o Extension of the chassis and extraction from the ELM

### SECTION 3

#### UNLOADING

The method used for unloading the DLRV must consider the multiple interfaces and requirements created by the LM derivative delivery system and overall mission profile. The tiedown arrangement discussed in Section 2 forms the foundation for this unloading concept. The selected approach provides a highly automated deployment, requiring little astronaut participation, within the critical weight and reliability constraints.

#### 3.1 REQUIREMENTS

##### 3.1.1 Automation

It is considered desirable that the deployment of the DLRV be automated as far as possible to minimize astronaut participation, save EVA time, and allow ready growth to a fully remote mission. Deployment initiated by a signal from the ELM cabin has the advantage of enabling the astronauts to view the operation through the windows and confirm its success before the EVA. In the event of a problem with deployment, a recommended solution could be immediately worked out between the astronauts and MCC prior to the EVA, thus saving valuable EVA time.

##### 3.1.2 Landing Attitudes

An important design consideration of the unloading method and the kinematics of motion is the post-landing attitudes of the ELM and the probable lunar ground lines. Fig. 3-1 depicts the critical ELM landed positions and ground slopes which must be accommodated when DLRV deployment takes place. As is shown, the combination of ELM tilt ( $+ 14 \frac{1}{2}^{\circ}$ ) and ground slope ( $+ 6^{\circ}$ ) produce three critical landed conditions: minimum ground clearance, maximum ground clearance, and maximum angular twist of vehicle due to ground sloping. The indicated 14-inch minimum ground clearance condition defines the kinematic deployment geometry for the selected DLRV tiedown configuration. This condition points out the need for rotating the outboard power chassis upward and outward to clear the ground line, and to place the power chassis on the lunar surface with its payload upright. The power equipments (batteries, power conditioning unit and RTG) must be stowed facing outboard to allow for spacecraft checkout and servicing. The maximum ground clearance condition of 62 inches, although less critical in the kinematic sense, does identi-

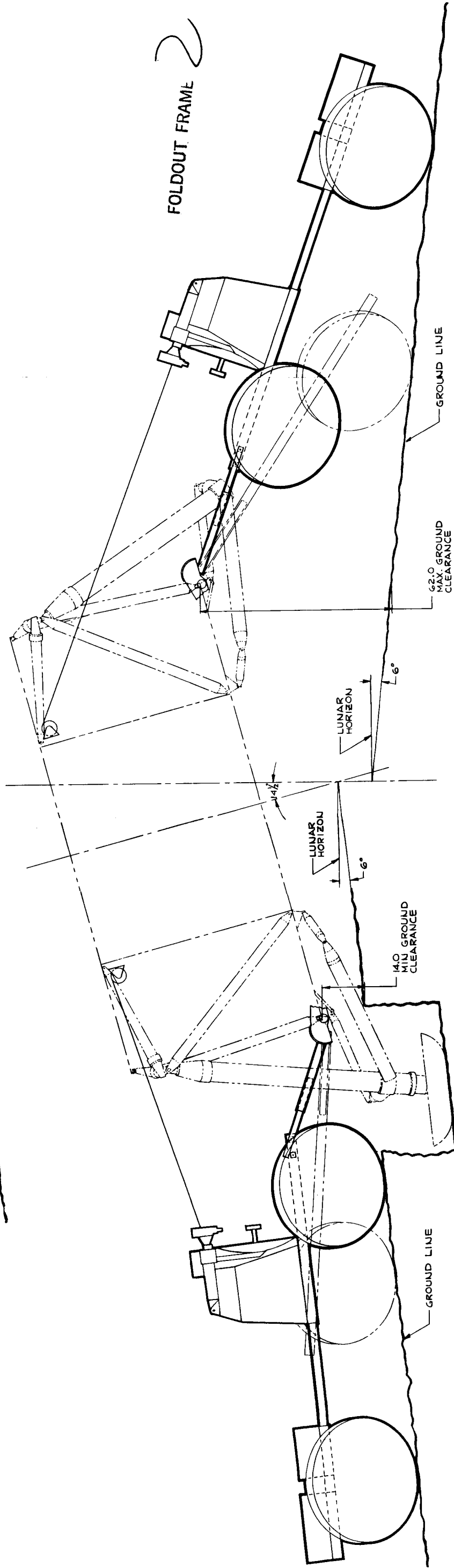
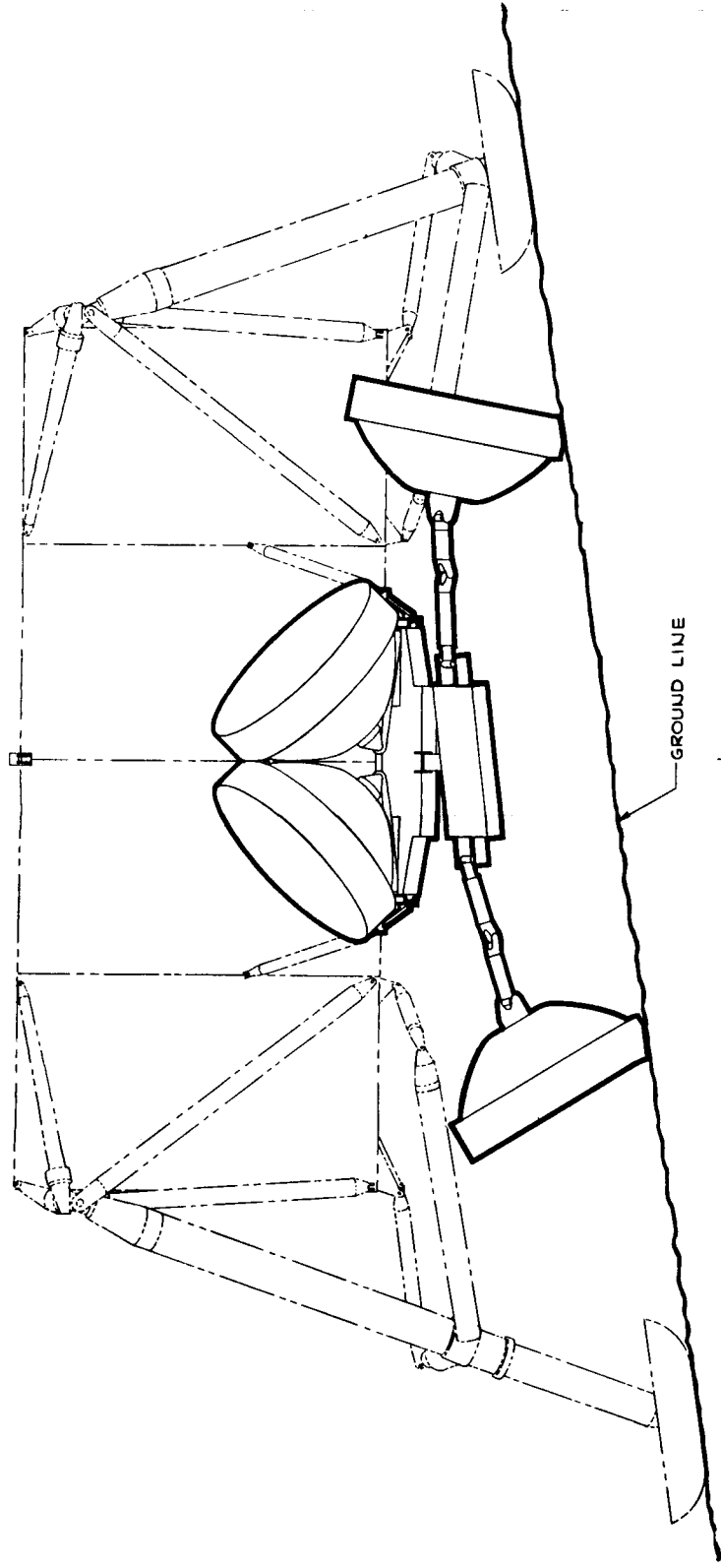


FIG. 3-1 CRITICAL DEPLOYMENT GEOMETRY  
LM/SURFACE

II/II.3-3/4

FOLDOUT FRAME

trol module combination. One difference is that no translation is required to clear the unfolding of a second pair of wheels. Once the science module wheels have contacted the lunar surface, the astronauts perform the remaining tasks of releasing and joining the modules together. The 4 x 4 vehicle is backed up within proximity of the off-loaded science module and its suspension repositioned to the unmanned vehicle mode. The science module deployment support cable is slackened allowing the astronaut to align the science chassis with the 4 x 4. The intermodular drawbar, which is stowed as a separate piece, is fastened to the science module. The science module is then detached from its support structure by pulling the hinge pin. It is then moved to the 4-wheeled vehicle. The drawbar is inserted into a bell-mounted receptacle on the power module where it latches. A visual inspection of the DLRV is performed noting all science module latches and locks. Verification of their assembled integrity is accomplished by observing a color-coded or otherwise clearly identified marking system.

Unlatching from the IM is initiated inside the ELM cabin by energizing two electrical solenoids which trip an over-center release latch at the upper support strut and allow a torsion spring to pivot the folded chassis out from Quad I. Figure 3-2 shows the mechanization for deployment, while Figure 3-3 shows the sequence. As the forward chassis module pivots about the hinge line, a synchronizing cable unfolds the aft module wheels to be deployed via a slave linkage, placing them in position to contact the surface. A cable restraint assembly lowers the chassis at a controlled rate until the aft wheels make contact with the surface.

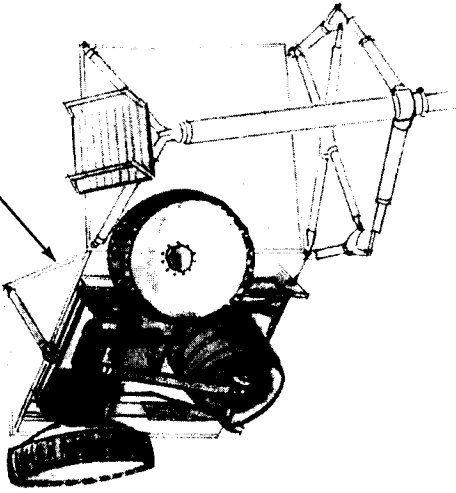
The second deployment stage requires that power be supplied to the power module wheels in order to operate them remotely. The unfolding motion of the chassis modules activates a switch in the power line of one DLRV battery to connect it to the electrical power bus. When the battery is connected, the aft wheel drive assemblies receive electrical power, and the aft wheels can be operated remotely. As the DLRV comes to rest on its rear wheels, a switch is operated by the astronaut in the ELM cabin to initiate the second part of the deployment sequence. With the aft chassis wheel drive preset for reverse operation, the switch circuit energizes the wheel motors causing the two chassis to telescope apart to the drawbar. When they are fully extended the drawbar is locked, the forward chassis is pulled free of the deployment yoke and the front wheels make surface contact. The parking brake is preset, (prior to launch) in the engaged position on the forward wheels to prevent any movement of the DLRV on the lunar surface. When the astronaut begins his checkout procedure he disconnects the two deployment cables and the electrical umbilical connected to the DLRV. The total estimated time required for unloading is less than 30 seconds.

### 3.2.2 Science Module Unloading

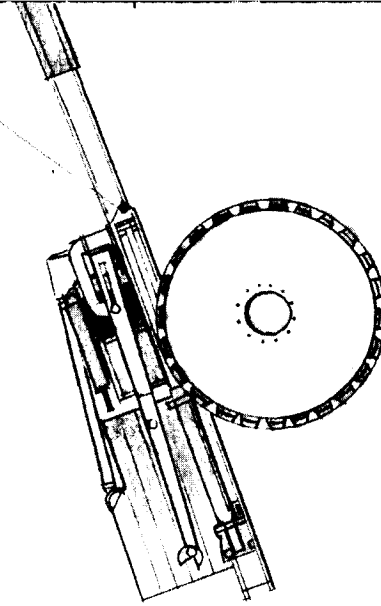
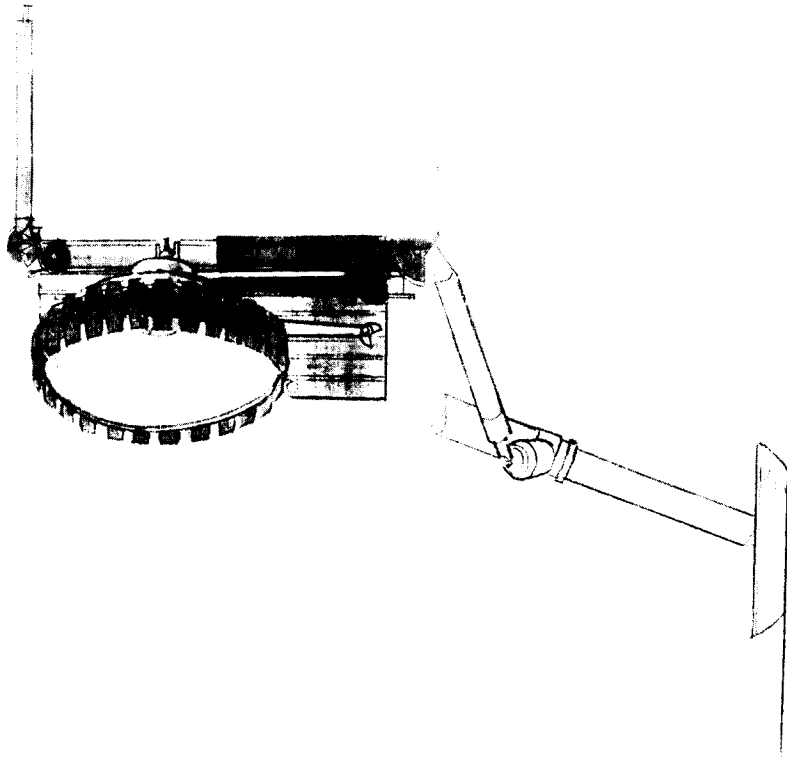
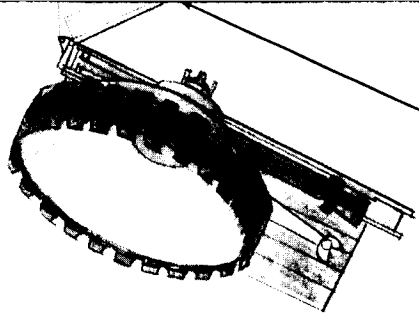
The unloading sequence shown in Figure 3-3 for the science module and its tiedown structural adaptor is the same as the sequence for the power and con-



QUADRANT IV



DEPLOYMENT/SUPPORT  
STRUCTURE

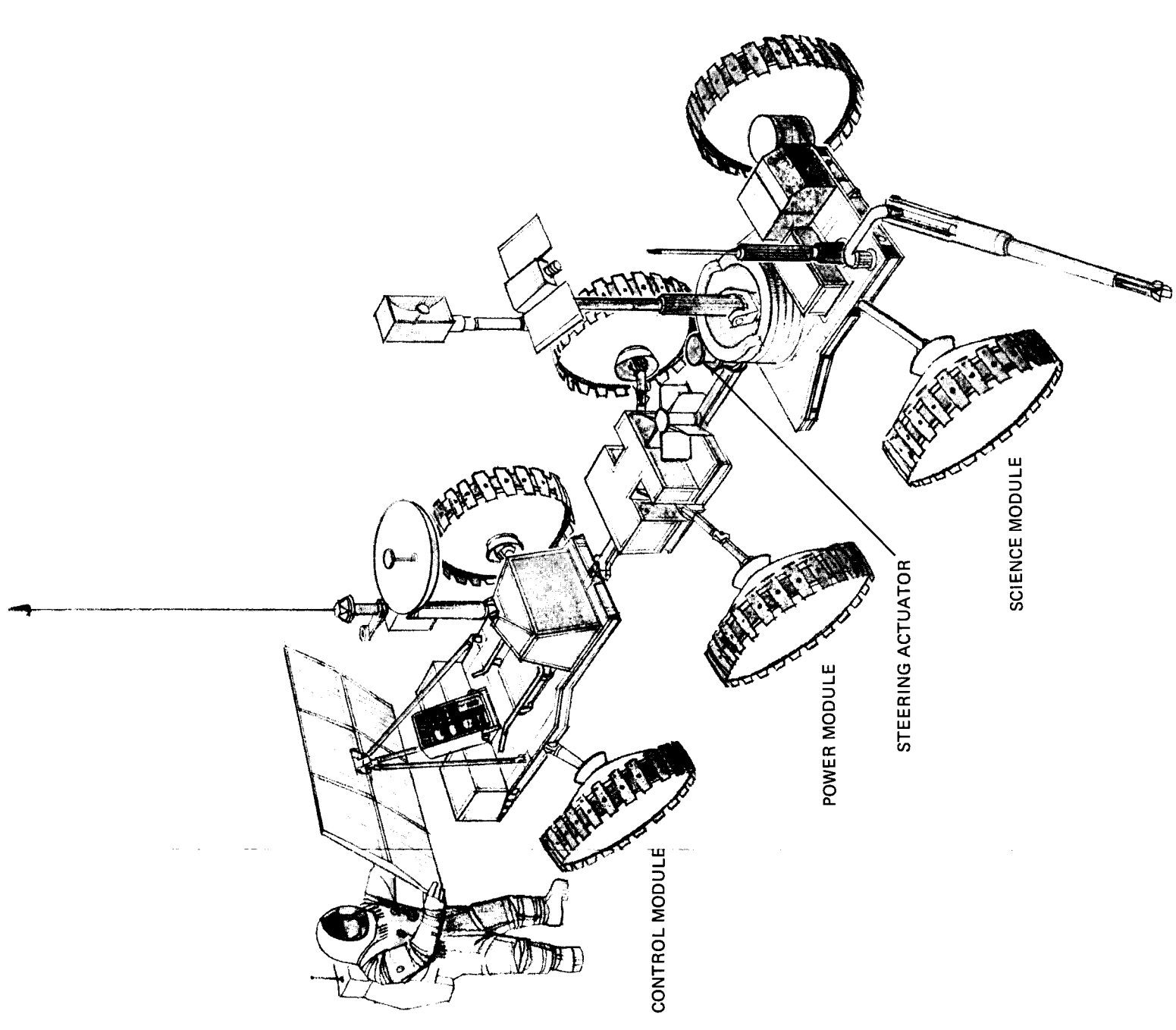


(H)  
SCIENCE MODULE TIEDOWN

(J)  
SCIENCE MODULE DEPLOY (HINGE TORSION BAR

FOLDOUT CASE

FOLDOUT CASE

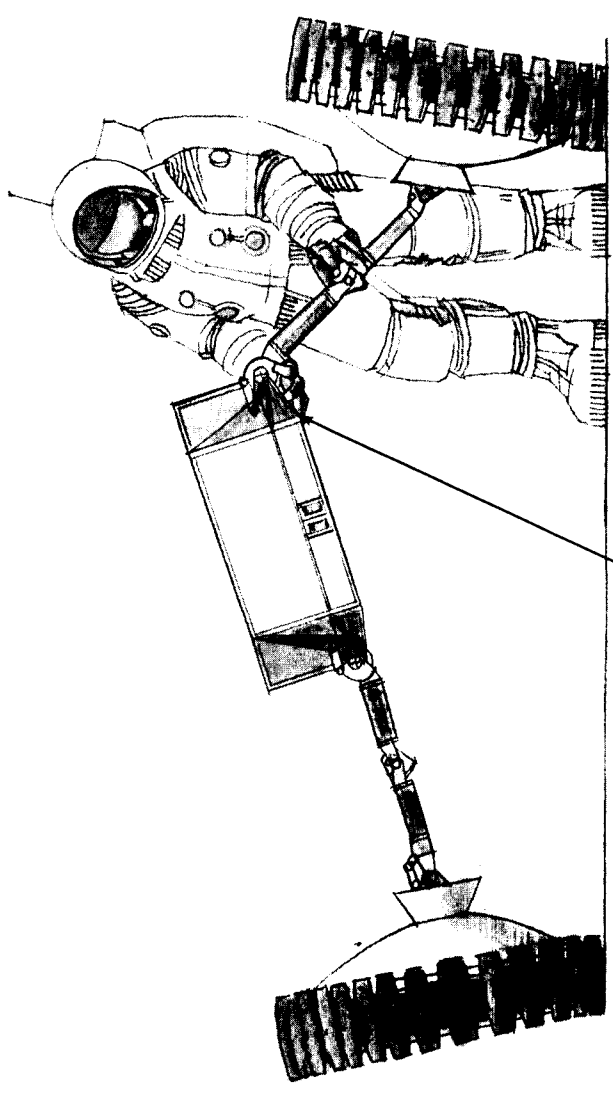


FOLDOUT FRAME 4

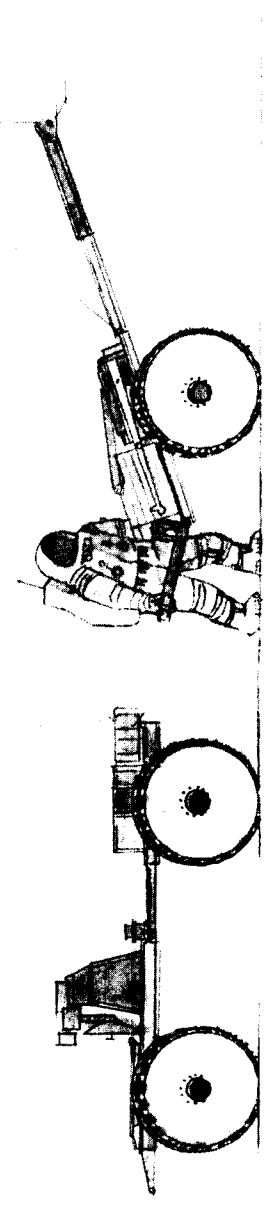
(L)  
UNMANNED (6 x 6) DLRV DEPLOYED

FIG. 3-3 UNLOADING SEQUENCE, SHEET 3 OF 3

II/II.3-13/14



SUSPENSION DETENT  
LOCKS



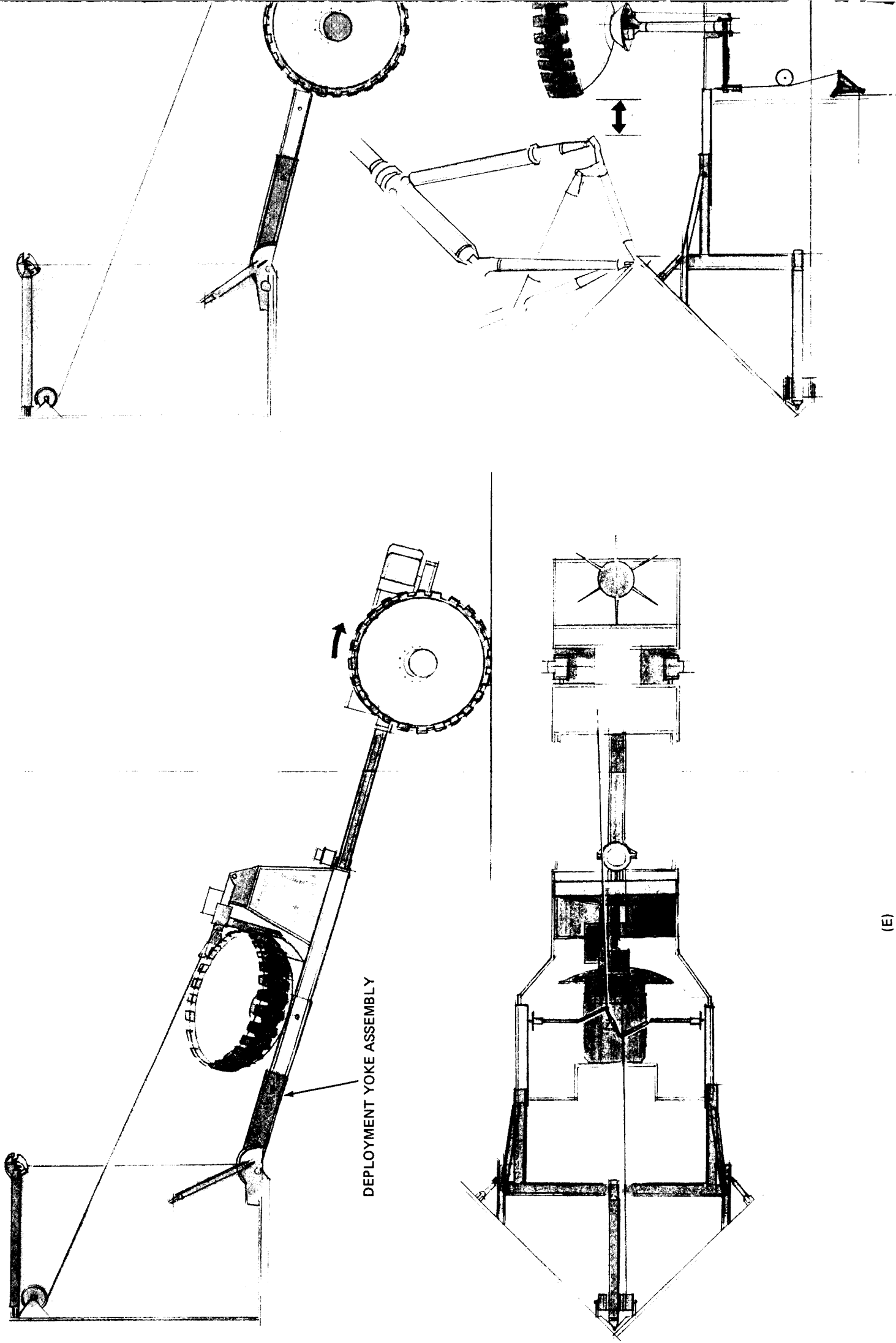
TORSION BAR

(K)  
4 x 4 CONFIGURED FOR UNMANNED MISSION

FOLDOUT FRAME 3

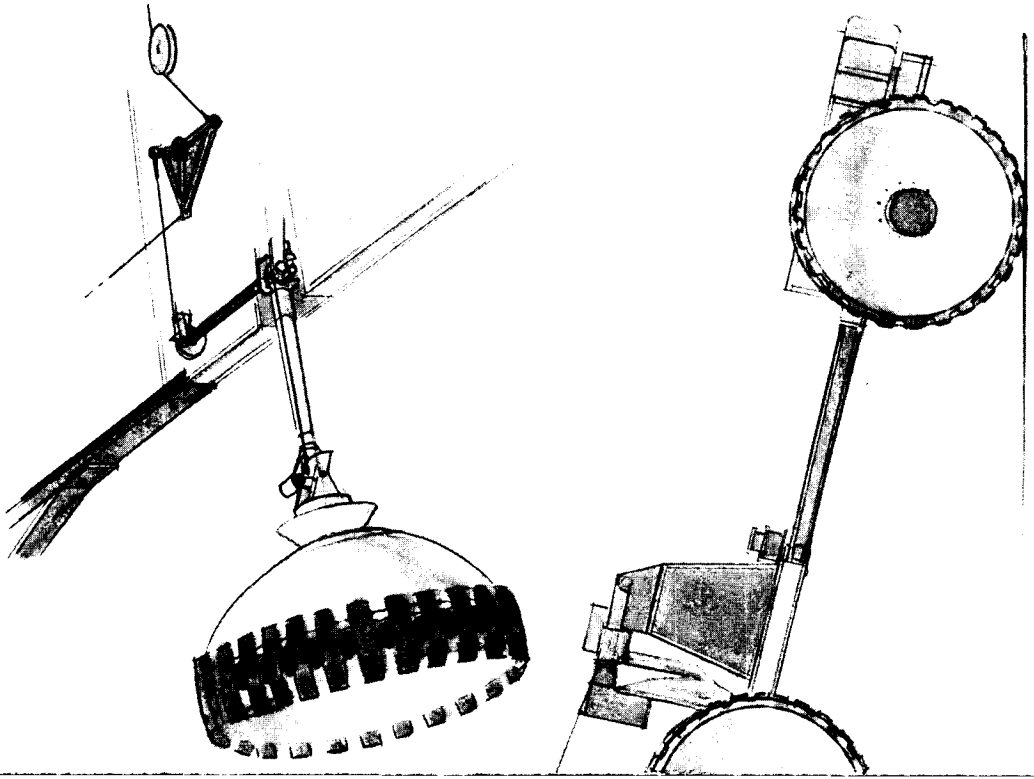
+ GRAVITY)

IT FRAME



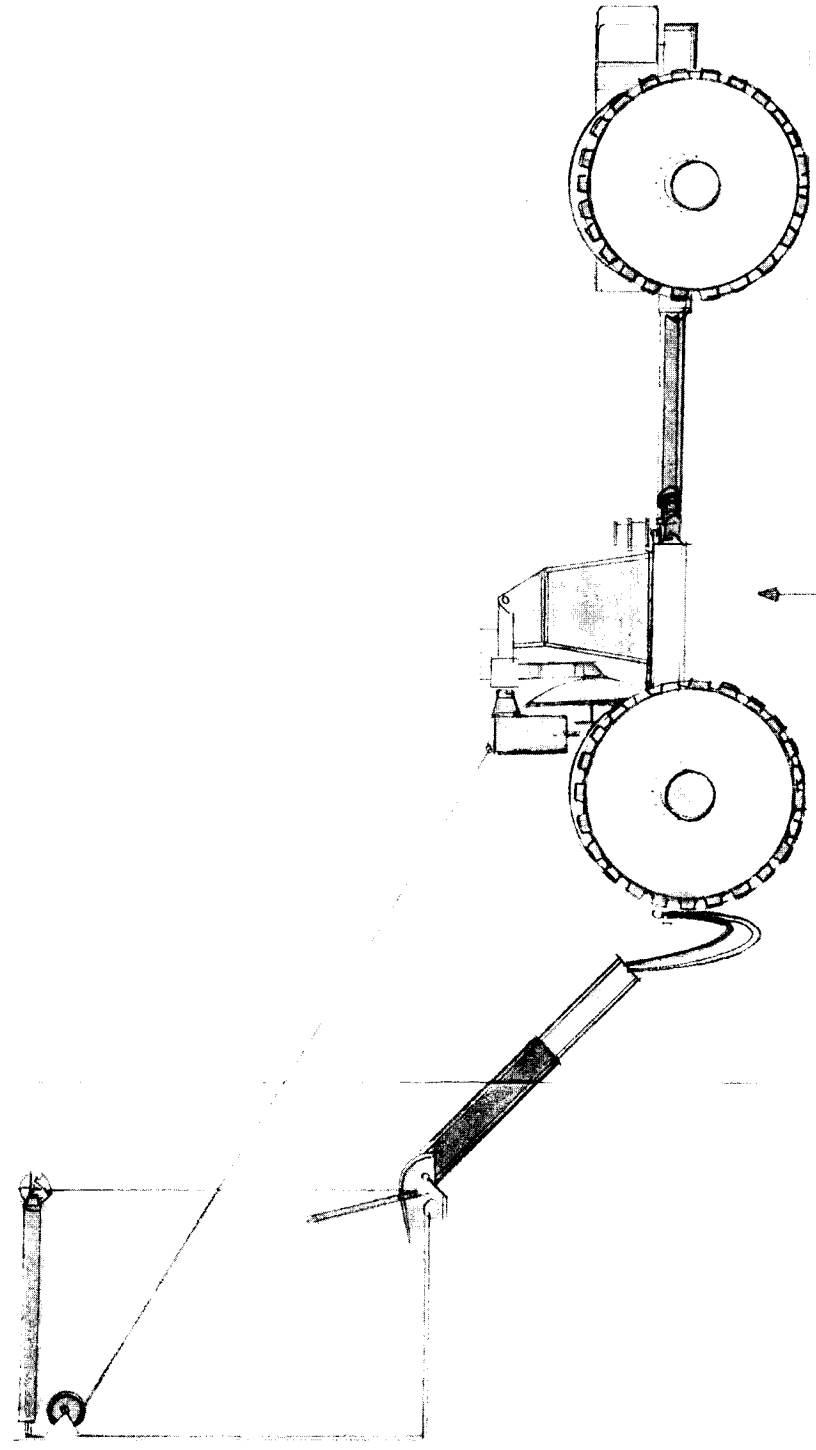
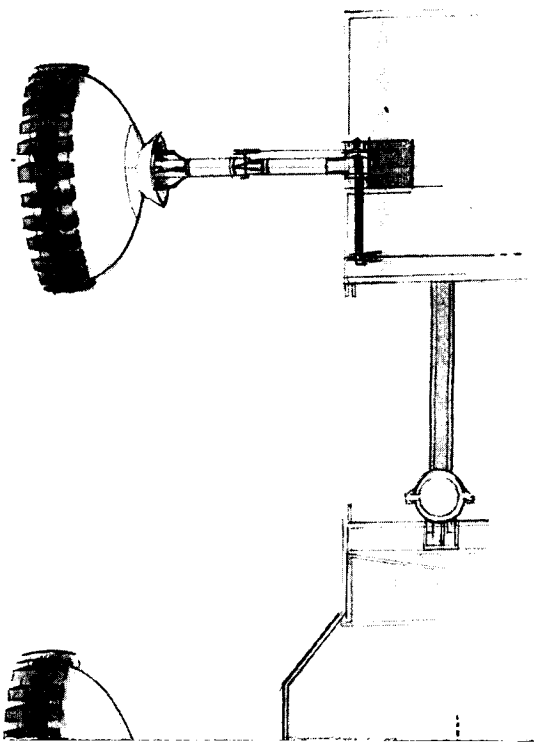
(E)  
VEHICLE TRANSLATION (AFT MODULE WHEELS POWERED)

FOLDOUT EXAMPLE

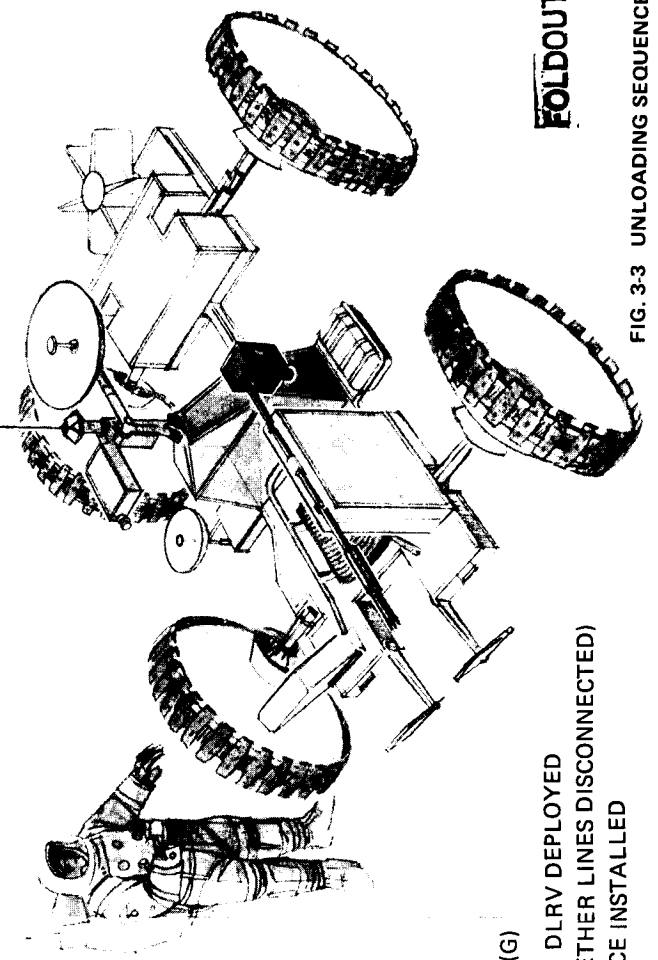


(F)  
WHEELS LOCKOUT

FOLDOUT FRAME



(G)  
MANNED (4 x 4) DLRV DEPLOYED  
(UMBILICAL AND TETHER LINES DISCONNECTED)  
AND SCIENCE INSTALLED

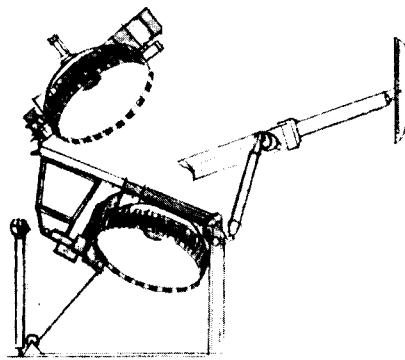
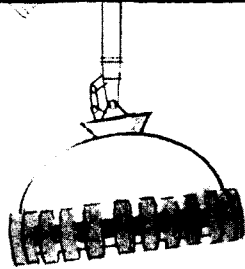
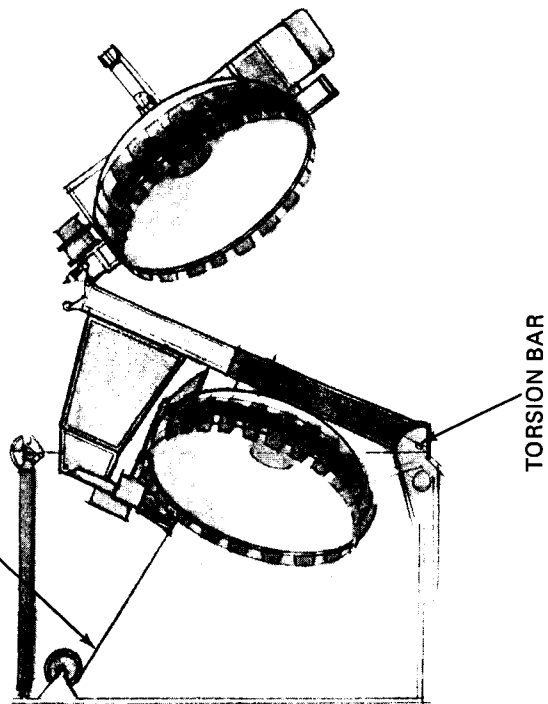


FOLDOUT FRAME

FIG. 3-3 UNLOADING SEQUENCE, SHEET 2 OF 3

II/II.3-11/12

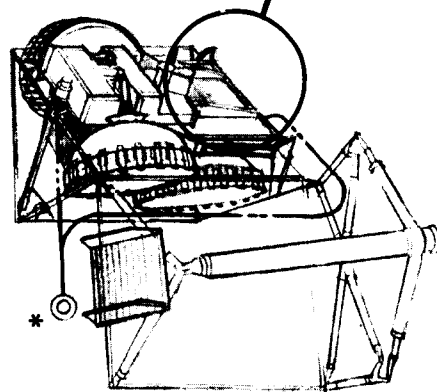
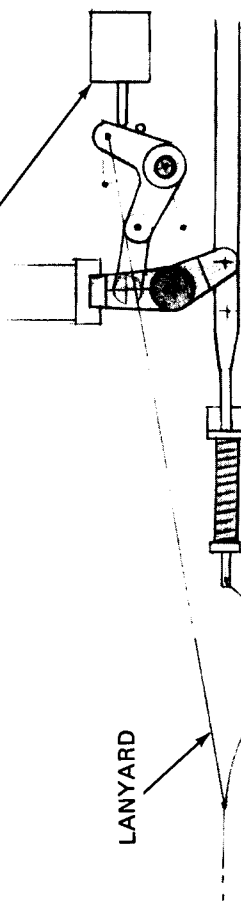
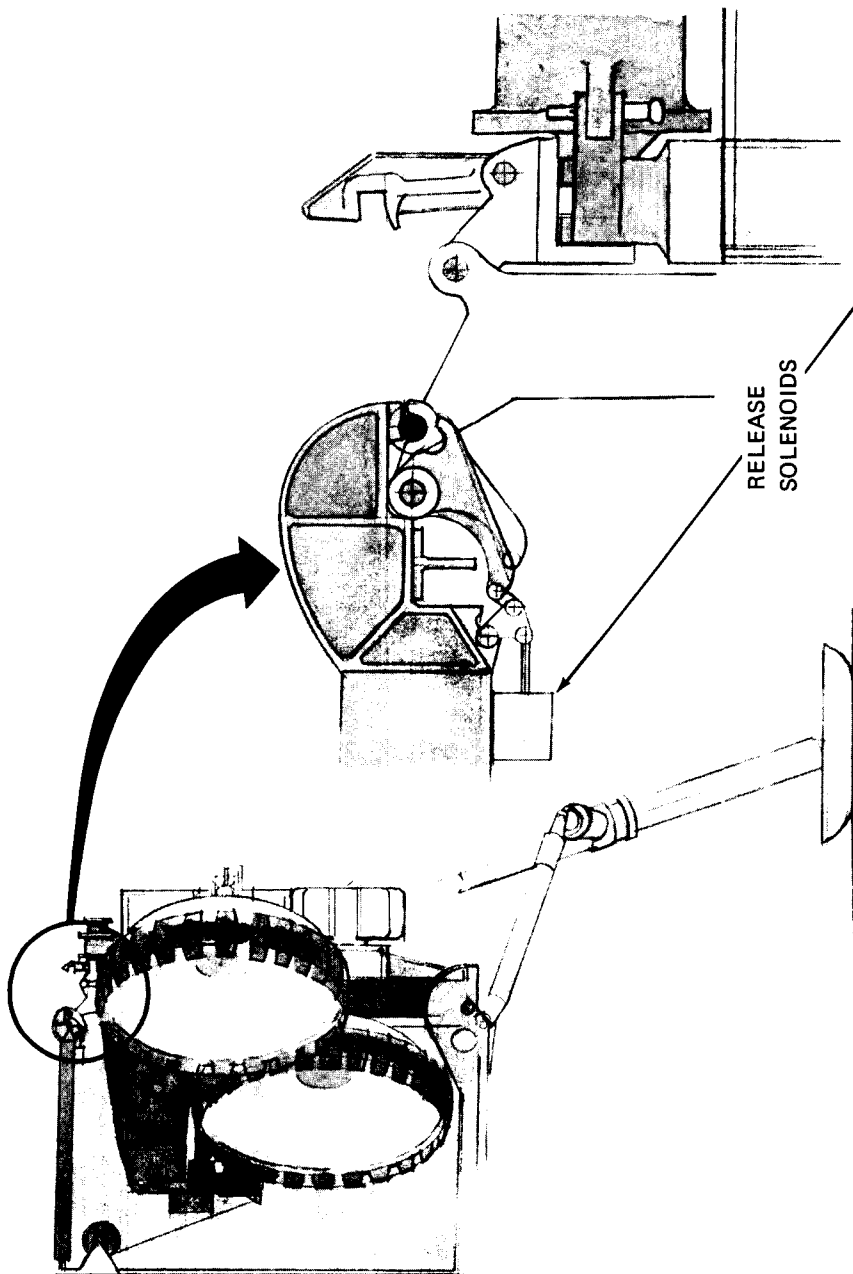
DEPLOYMENT CABLE/DRUM ASSEMBLY



(B)

MODULES DEPLOY (HINGE TORSION BAR ASSEMBLY)

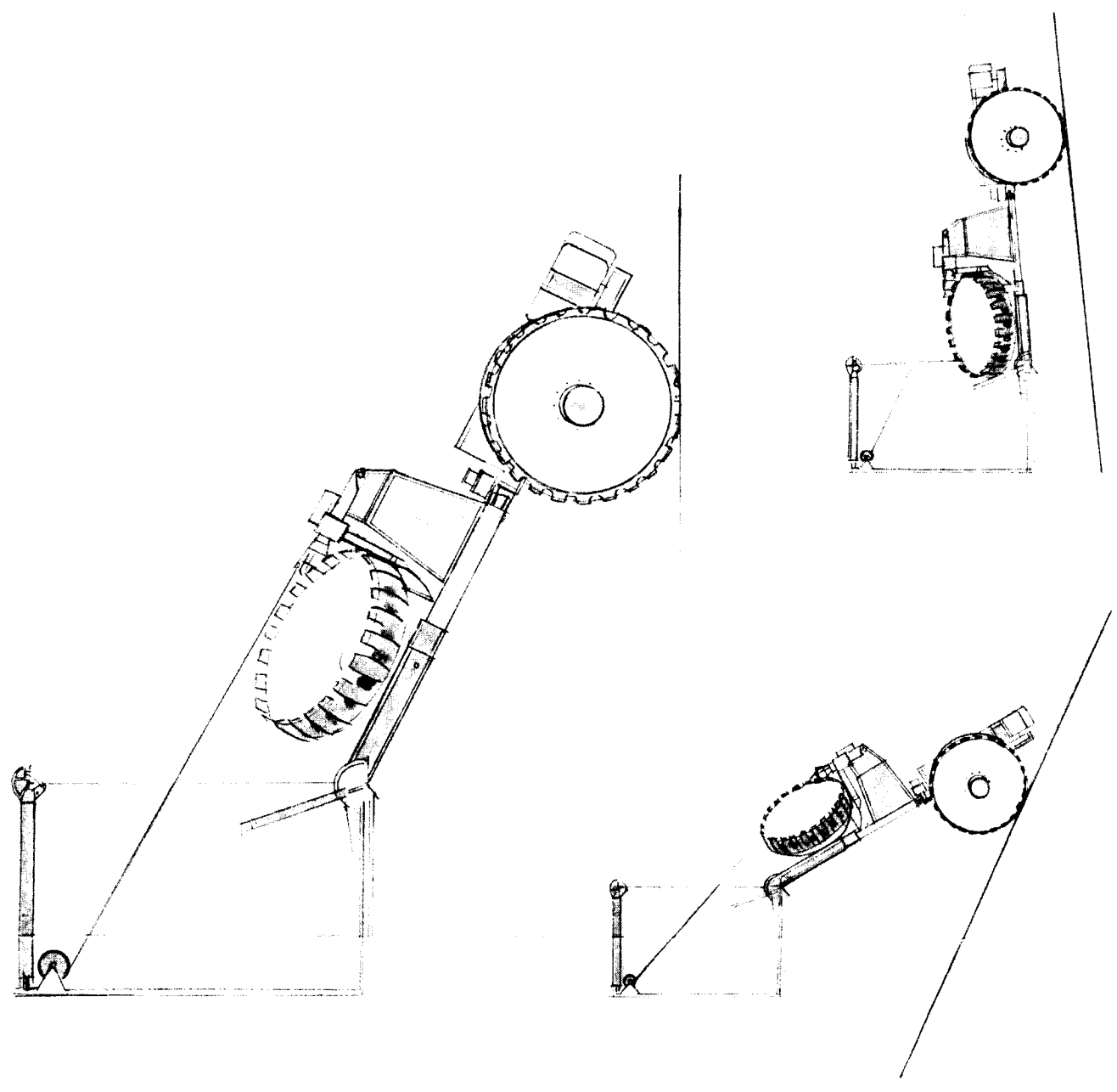
FOLDOUT FRONT



(A)  
TIE DOWN RELEASE

\*MANUAL BACKUP RELEASE

FOLDOUT FRONT



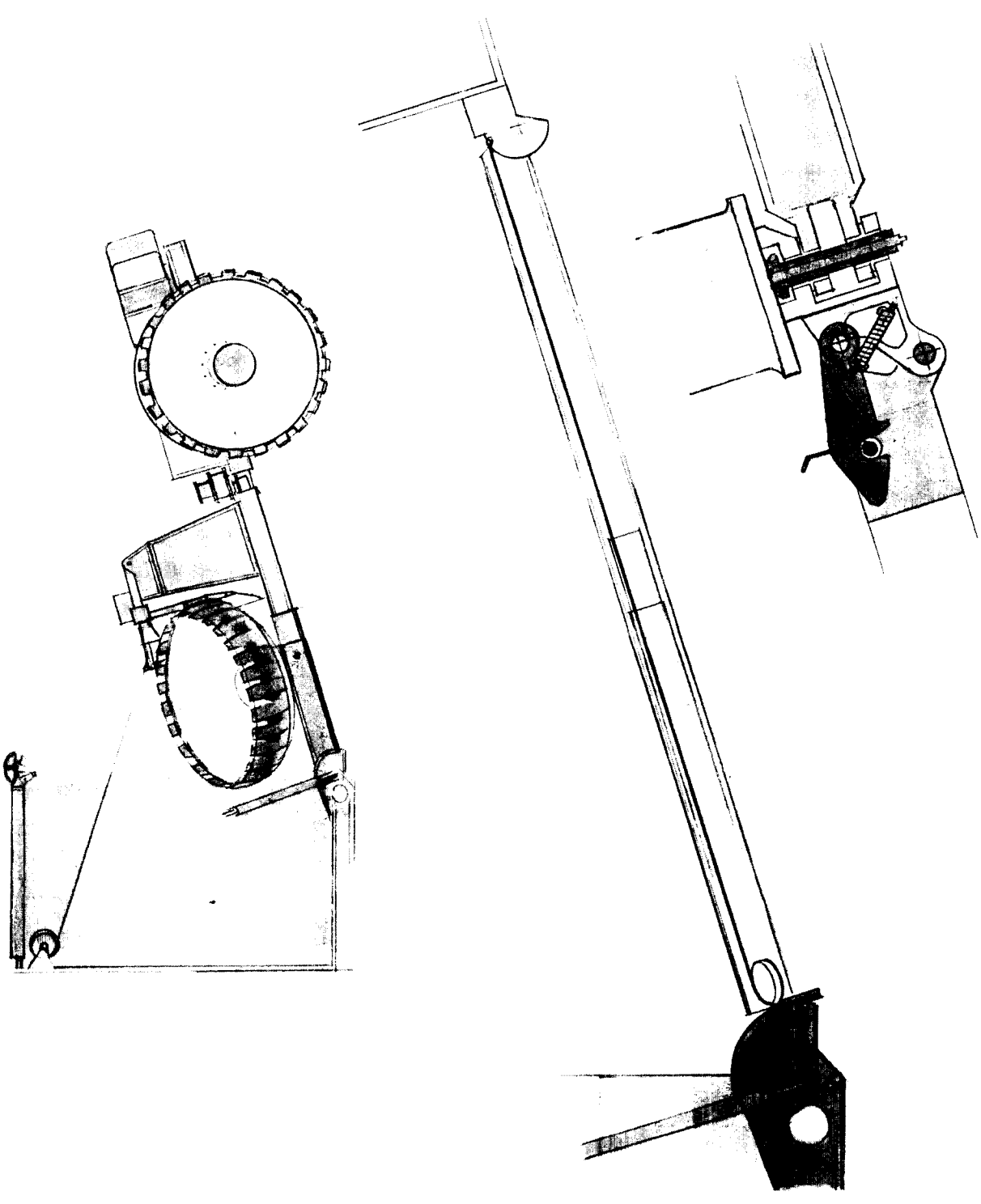
**FOLDOUT FRAME**

(D)

SURFACE CONTACT (GROUND LINE VARIATION)

4

FIG. 3-3 UNLOADING SEQUENCE, SHEET 1 OF 3

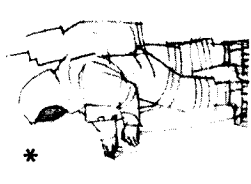
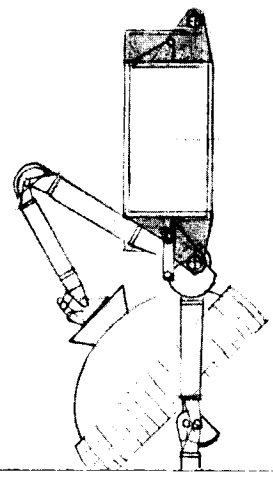


(C)

DRAWBAR AND AFT WHEEL LOCK OUT

**FOLDOUT FRAME,**

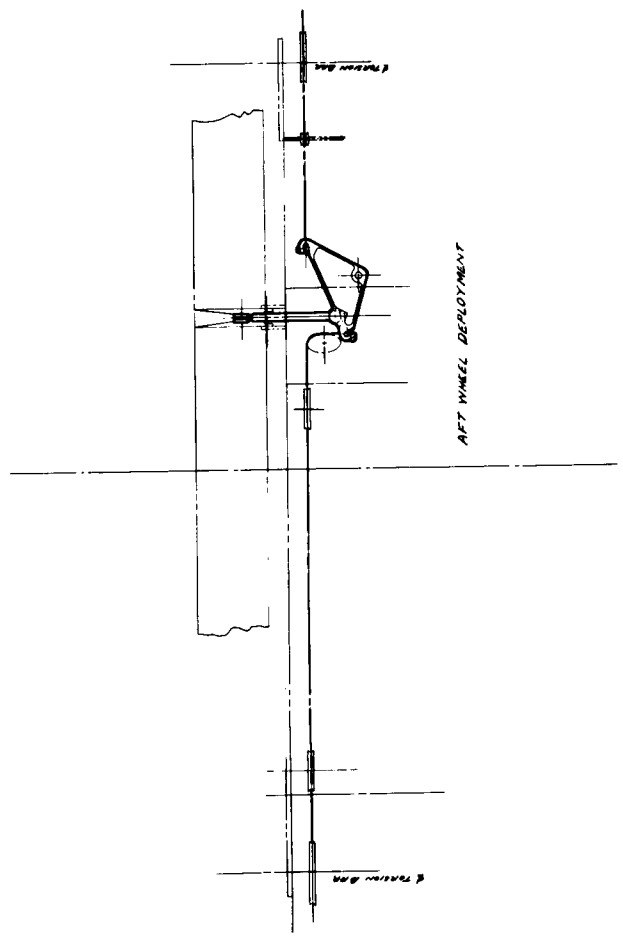
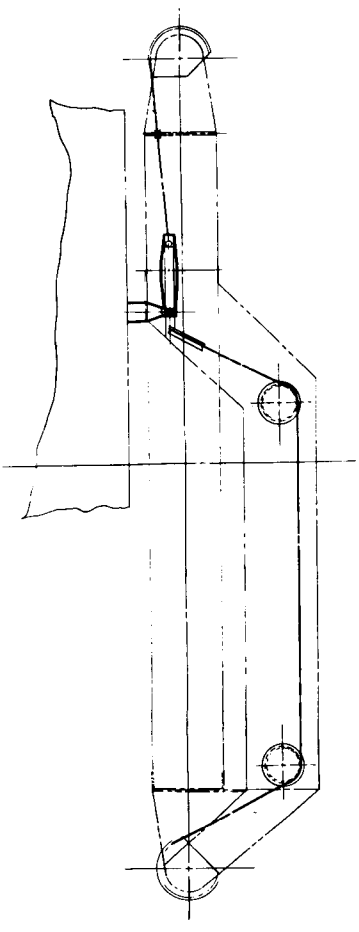
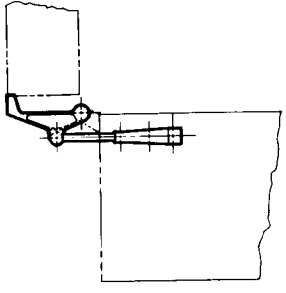
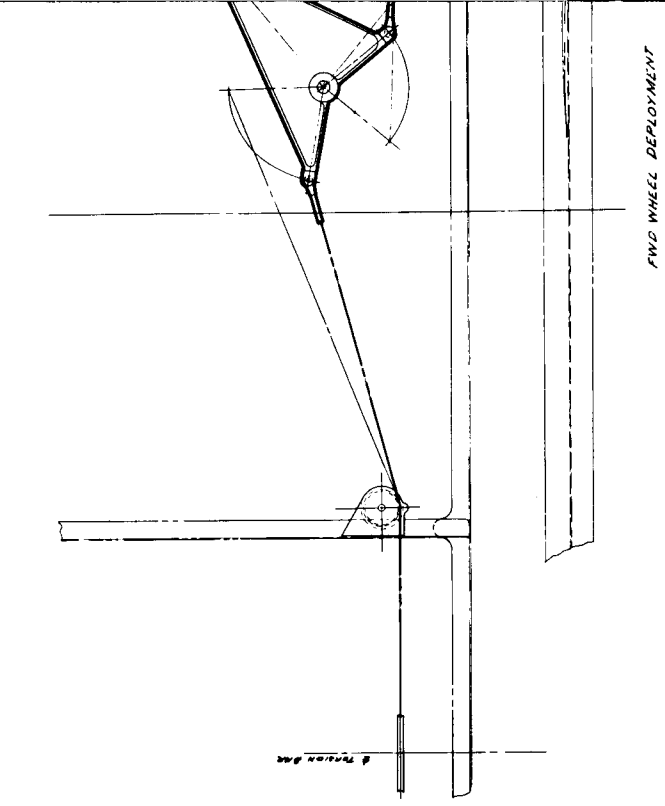
3



\*MANUAL BACKUP DEPLOYMENT

ND GRAVITY)

2



FOLDOUT FRAME

FOLDOUT FRAME





### 3.2.3 Manual Override of Deployment

In the event the DLRV unlatching solenoids fail to function, a lanyard accessible from the ELMegress platform is pulled by the astronaut to unlatch the DLRV and start the deployment sequence.

A second lanyard line attached to the power module is sufficiently long in length to permit the astronaut to remotely pull the vehicle causing it to free itself and continue the deployment sequence. Since all the unloading kinematics are accomplished by sequential operations, where each one is slaved to the preceding one, the simple chassis lanyard provides an excellent method for guaranteeing unloading.

### 3.2.4 Mechanization

The number of individual mechanical functions required for unloading demands that each be as reliable as possible consuming a minimum of mechanical energy. The recommended unloading design, shown in Fig. 3-2, relies mainly on mechanisms such as bellcranks and latches which require simple pivots for rotation. Sliding type mechanisms have also been used but only under lightly loaded conditions and then when backed up by redundant actuation. Mechanical springs, both torsion and compression/extension types, are used throughout the unloading mechanism to provide a passive actuation energy. Finally, the entire mechanical sequence is rate controlled via the deployment inertia cable drum assembly which allows substantial time for each event to take place.

### 3.2.5 Safety Considerations

Significant steps have been taken to insure a safe unloading procedure of the DLRV. Both the astronauts and the vehicle are safeguarded against any malfunctions of the deployment mechanisms. From the standpoint of the vehicle, an inertia cable/drum assembly supports the DLRV during unloading and controls its rate of deployment to the lunar surface. A system of electrical solenoids is used for initial actuation in lieu of pyrotechnic devices which could produce debris causing structural failures.

The safety precautions for the astronauts are derived mainly from the remote positioning of the astronauts relative to the areas of DLRV unloading. As already mentioned, normal operation occurs with the astronaut in the ELM cabin. The manual backup mode is accomplished using lanyards which again position the astronaut remotely from the unloading area. Once the vehicle has been unloaded and erected,

the astronaut can quickly determine the DLRV's structural integrity by visual inspection. All latches and locks necessary to assure the structural integrity of the vehicle are color coded or otherwise identified to permit a positive visual examination of their final structural positioning.

### 3.3 SET-UP TASKS

Some astronaut tasks are required to prepare the DLRV for both the manned and unmanned portions of the mission after it has been unloaded. These have been kept to a minimum, and the limitations of the suited astronaut and time constraints have been considered.

#### 3.3.1 Manned Mission

After the vehicle is off-loaded from the EIM, either automatically or by manual backup mode, and deposited on the lunar surface, it is in the condition shown in Fig. 3-3g. The vehicle is then prepared for operational readiness by performing the manual set-up tasks described below:

- o Walk-around inspection of the vehicle, removing wheel snubbing devices, plume shielding, and disconnecting the umbilical
- o 90° rotation of the antenna mast to the erect position. This action releases the omni antenna stem mast which self-erects
- o Set-up crew station by unfolding driver restraint structure, repositioning the console, extending the foot stirrups, and locating the storage box
- o Unload and erect solar array

The vehicle may now be driven for a short checkout, ending up at a location convenient for loading the manned science equipment. The total time for these tasks is estimate to be 10 min.

#### 3.3.2 Unmanned Mission

The science module is off-loaded automatically and rests on the lunar surface in the configuration shown in Fig. 3-3 (J). The tasks for remote mission set-up are as follows:

- o Remove manned science equipment
- o Cover console with thermal blanket
- o Reposition 4 suspensions
- o Unstow drawbar and attach to science module
- o Pull pin connecting science module to its support structure and attach module by inserting drawbar into socket in power module

- o Transfer steer actuator
- o Erect TV mast and attach hazard detector antenna
- o Erect solar array
- o Set up remote science by relocating gravimeter and magnetometer sensor assembly, and mounting RGM

The total time for these tasks is estimated to be 62 min. Refer to Section 2.2 of Book I, Vol. II, for a complete description of the DLRV timeline.

## SECTION 4

### CHECKOUT

Since essential measurements and telemetry are provided for unmanned operations (See Appendix A, Book II of Volume III for measurements list) the assessment of the vehicle integrity is done primarily by the ground during functional checks. The driver's panel does not provide any visual display of subsystem of status data. As long as the vehicle is not driven farther than convenient walk-back distance,  $\frac{1}{2}$  km, the functional checks and related ground monitoring may be integrated with the planned science operations.

#### 4.1 INITIAL CHECKOUT - MANNED SORTIES

The manned vehicle and science module are deployed by command from the ELM. The manned configuration is first checked and tested before continuing the initial sortie operations described in Vol II, Section 2.2 of Book I.

The recommended sequence of operational and estimated durations are listed in Table 4-1.

#### 4.2 TYPICAL PRE-SORTIE CHECKOUT AND ACTIVATION

Since the vehicle status is continuously monitored by the ground and the vehicle presumably was operating properly during the previous sortie, only a few operational checks are required before driving. These include the following procedures:

- o Inspect visually
- o Disconnect solar array
- o Turn on Power
- o Confirm ground communications
- o Initialize navigation

The total time is estimated to be 14 minutes.

TABLE 4-1

## INITIAL CHECKOUT - MANNED SORTIES

OPERATION	TIME	
	DURATION MIN	ELAPSED HR : MIN
1. Turn on electrical power which activates all subsystems. Confirm with ground via EIM voice link	5	0 : 0
2. Ground establishes communications. Steerable antenna is ground directed if necessary	5	0 : 05
3. Ground monitors subsystem status and confirms by vehicle voice link.	10	0 : 10
4. Ground checks all communication modes.	5	0 : 20
5. Ground checks all remote control commands except mobility commands	10	0 : 25
6. Test drive within $\frac{1}{2}$ km of EIM. Ground monitors. Check all modes throughout operating ranges: <ul style="list-style-type: none"> <li>• Forward and aft</li> <li>• Winding shift</li> <li>• Braking and parking brake</li> <li>• Articulated and differential steering</li> </ul>	15	0 : 35
7. Test mobility remote control by driving short distances with crewman monitoring	10	0 : 50
8. Initialize navigation computations	1	1 : 00
9. Check navigation subsystem by ground monitoring of test drive at $+90^\circ$ and $-90^\circ$ to sun. Check distance traveled with Survey Staff.	15	1 : 01
10. Begin other sortie operations		1 : 16

#### 4.3 POST-SORTIE CHECK AND DEACTIVATION

The post-sortie check is performed after each sortie and takes about 10 minutes.

Operations are:

- o Turn off power
- o Apply parking brake
- o Unload samples
- o Clean dust from sensitive areas
- o Connect solar array
- o Inspect visually

#### 4.4 UNMANNED CHECKOUT

After the conversion to the unmanned mode described in Section 2.2 of Book I, Vol II, the vehicle is checked by the ground and observed by the astronauts. This procedure permits assistance from the crew in the event of a malfunction. The science module has not been previously used. Related unused equipments are the hazard detection subsystem, all unmanned science, the directional gyro, tilt sensors, TV camera and the mobility components of the module. The solar array has been used but not when installed on the control module. The operations and estimated durations are listed in Table 4-2.

TABLE 4-2 UNMANNED CHECKOUT AFTER CONVERSION

OPERATION	TIME	
	DURATION MIN	ELAPSED HR : MIN
1 Turn on electrical power. Confirm with ground	5	0
2 Establish communications and check modes (except TV)	10	0 : 05
3 Check TV camera modes	10	0 : 15
4 Check remote control commands except mobility	15	0 : 25
5 Test drive by remote control within $\frac{1}{2}$ km of EIM. Check all modes. Monitor on ground. Concurrently test hazard detection system.	15	0 : 40
6 Remotely operate all science equipment in all modes	30	0 : 55
7 Initialize navigation computations	1	1 : 25
8 Check navigation during test drive at $+90^\circ$ and $-90^\circ$ to sun.	15	1 : 26
9 Begin unmanned mission		1 : 41

## TABLE OF CONTENTS

<u>Section</u>	<u>Page</u>
1 INTRODUCTION . . . . .	1-1
1.1 APPROACH . . . . .	1-1
1.1.1 Ground Rules and Assumptions . . . . .	1-1
1.1.2 Support Equipment Design . . . . .	1-1
1.1.3 Ground Systems Specification . . . . .	1-2
2 SUPPORT EQUIPMENT	2-1
2.1 MECHANICAL GSE . . . . .	2-1
2.1.1 Test Sets . . . . .	2-1
2.1.2 Servicing Equipment . . . . .	2-1
2.1.3 Checkout Equipment . . . . .	2-5
2.1.4 Handling and Shipping Equipment . . . . .	2-7
2.2 ELECTRICAL GSE . . . . .	2-9
2.2.1 Test Sets . . . . .	2-9
2.2.2 Servicing Equipment . . . . .	2-14
2.2.3 Checkout Equipment . . . . .	2-15
2.3 ADDITIONAL SUPPORT EQUIPMENT REQUIREMENTS . . . . .	2-16
3 GROUND OPERATING EQUIPMENT . . . . .	3-1
3.1 REMOTE CONTROL STATION . . . . .	3-1
3.2 MODIFICATION TO EXISTING MSFN/NASCOM EQUIPMENT . . . . .	3-1
3.3 NEW EQUIPMENT REQUIRED FOR THE MSFN FACILITY . . . . .	3-2
3.4 AREAS REQUIRING FURTHER DEFINITION . . . . .	3-2
4 LUNAR SUPPORT EQUIPMENT . . . . .	4-1
5 TRAINING EQUIPMENT . . . . .	5-1



TABLES

<u>Tables</u>		<u>Page</u>
2-1	Mechanical Support Equipment . . . . .	2-3
2-2	Electrical Support Equipment . . . . .	2-11

**PRECEDING PAGE BLANK NOT FILMED**

## SECTION 1

### INTRODUCTION

The support equipment (ground support, special test, lunar support, ground operating and training equipment) investigated and defined for the DLRV program are presented in this book of the final report. In general, the scope of the effort required in support of the DLRV during the development, manufacturing, testing pre-launch and mission operation phases of the program is composed of the following activities:

- o Support system engineering relative to equipment performance criteria, facility/support equipment design, and interface determination and control
- o Support equipment design, development, acquisition, manufacturing coordination and delivery
- o Support equipment test and evaluation
- o Site support
- o Scheduling of equipment for the DLRV program
- o Maintenance of support equipment
- o Material (spares, bulk, and modification kit material) support program to ensure hardware availability for the development, testing and operation of the DLRV and related support equipment
- o Training requirements
- o Transportation functions
- o Support manuals
- o Applicable product support documentation relative to the above (data for specifications, drawings, etc.)

#### 1.1 APPROACH

##### 1.1.1 Ground Rules and Assumptions

In the interest of economy and schedules, existing support equipment, spares, documentation and GFE will be utilized for the DLRV program. The equipment defined in this report does not include support equipment for ground checkout, servicing and handling of the scientific experiments or the DLRV Control Center.

##### 1.1.2 Support Equipment Design

The type, quantity and quality of support equipment were determined with regard to the following considerations:

- o Artificial stimuli will be provided to the vehicle only in situations where it is not feasible to provide normal intersubsystem inputs.
- o Malfunction detection and isolation capabilities will be provided for DLRV electronic replaceable assemblies (ERA's) or groups of several ERA's installed in the vehicle.
- o The majority of checkout operations performed on subsystems installed in the spacecraft will be performed by checkout equipment having remote semi-automatic capability. Some of the checkout operations will be performed by the equipment with manual-local control capability.
- o The absolute minimum weight penalty shall be imposed on flight equipment consistent with vehicle checkout requirements, even to the extent of increasing the complexity of the support equipment.
- o Electrical connections will be positively keyed to prevent incorrect connection with adjacent accessible connectors unless the mating connector(s) do not permit such keying.
- o Support equipment will be designed for fail-safe operations.
- o Checkout and servicing support equipment will be designed such that a failure of any specific support equipment will not cause a failure in the facility or in the flight equipment being serviced or checked.
- o Assure that the support equipment is designed to permit maximum possible ease of accessibility to equipment requiring replacement, servicing or adjustment of calibration.

### 1.1.3 Ground Systems Specification

A specification has been established for the specific types of support equipment required for support of the DLRV, flight equipment development tests, manufacturing assembly, transportation, acceptance and prelaunch checkout operations. The specification establishes the general performance, design, reliability, environmental requirements, maintainability, transportability, safety requirements, quality assurance provisions and shipping criteria of the DLRV support equipment.

This ground systems specification, published as Book II of Vol. VI, is generally applicable to the DLRV's control center consoles described in Vol. V, Mission Operations; however, specifications which apply to existing flight control consoles will be utilized.

## SECTION 2

### SUPPORT EQUIPMENT

#### 2.1 MECHANICAL GSE

Major articles of mechanical support equipment established by investigation of vehicle subsystems, systems, acceptance test procedures, factory buildup, site support and pre-launch operations are functionally identified in the following paragraphs. These items are listed in Table 2-1 and reflect the mechanical support equipment required for a specific vehicle configuration or site.

##### 2.1.1 Test Sets

###### 2.1.1.1 Installation and Test Fixture

This structural fixture supports the DLRV during final component installation and test operation. The fixture minimizes loads on the vehicle suspension and steering mechanism while allowing accessibility to all parts of the vehicle. For test purposes provisions are made for 1 - g operation and mounting of an integrated mobility checkout kit. Capability is provided for articulation and roll of the assembled DLRV. Configurations are provided for use in both ambient and thermal vacuum environments.

###### 2.1.1.2 Deployment Fixture

This fixture, when used in conjunction with the stow/transport fixture, demonstrates DLRV 1/6-g deployment capability in a 1 - g environment.

###### 2.1.1.3 Mobility Vehicle Test Set

This is a test set composed of the equipment necessary to support the DLRV mobility unit during simulated lunar site traverses. Included are tiedown bracketry for the support vehicle, a remote control station, and remote control cable support. Provisions are incorporated for cooling the flight electronics and measuring the steering joint angle.

##### 2.1.2 Servicing Equipment

###### 2.1.2.1 RTG Cooling (In SLA)

A cooling system is provided to dissipate excess heat from the activated RTG and prevent damage to critical ELM components near the stowed DLRV.

If a SNAP-19 RTG is used 675 W (2300 BTU/hr) of thermal output must be dissipated.

FOLDOUT FRAME

MECHANICAL SUPPORT EQUIPMENT

TABLE 2-1

SUPPORT EQUIPMENT NOMENCLATURE	STRUCT TEST	MOB UNIT	SYS INT	I-C TRAIN	QUAL UNIT	DLRV-1	DLRV-2	DLRV-3	DLRV-4	NEW GSE	GAC	WES	KSC	TOTAL UNITS	MAKE, BUY, OR GFE
INSTALLATION AND TEST FIXTURE			o	o	o	o	o	o	o	o	1		1	2	M
DEPLOYMENT FIXTURE	o		o	o	o	o	o	o	o	o	1		1	2	M
MOB. VEHICLE TEST SET		o								o	1	1		1	M
RTG COOLING (IN SIA)						o	o	o	o	o			1	1	M
DLRV/SIA PLATFORMS						o	o	o	o	o			1	1	GFE
BATTERY STORAGE TRACK TEMP CONT.			o		o	o	o	o	o	o	1		1	2	B
INSTALL. AND TEST KIT (THERM VAC. CHAMBER - BPA)					o	o	o	o	o	o	1			1	M
POWER DIST AND COND ASSY FIXTURE	o	o	o	o	o	o	o	o	o	o	1			1	M
INTEG MOB SYSTEM C/O KIT (MECH)		o	o		o	o	o	o	o	o	1		1	2	M
THERMAL RAD C/O KIT			o		o	o	o	o	o	o	1		1	2	M
TRACTION DRIVE C/O KIT	o	o	o	o	o	o	o	o	o	o	1			1	B
STEERING ACTUATOR C/O KIT	o	o	o	o	o	o	o	o	o	o	1			1	B
OPTICAL ALIGNMENT EQUIP. - C/O KIT	o	o	o	o	o	o	o	o	o	o	1			1	M
FIXTURE, CHASSIS ALIGNMENT	o	o	o	o	o	o	o	o	o	o	1		1	2	M
SOLAR ARRAY POSITION AND DEPLOY			o		o	o	o	o	o	o	1		1	2	M
STOW/TRANSPORT FIXTURE	o	o	o	o	o	o	o	o	o	o	2		1	3	M
INSTALLATION/EXTRACTION KIT	o		o		o	o	o	o	o	o	1		1	2	M
VEHICLE SLING	o	o	o	o	o	o	o	o	o	o	1		1	2	M
BATTERY SHIPPING CONTAINER			o		o	o	o	o	o	o	1		1	2	B
SOLAR ARRAY-INSTALL, REMOVAL AND PROTECTION			o		o	o	o	o	o	o	1		1	2	M
GSE CREW SEAT AND RESTRAINT	o		o		o	o	o	o	o	o	1		1	2	M
SEAT AND RESTRAINT INSTAL AND REMOVAL	o		o		o	o	o	o	o	o	1		1	2	M
CONTROLS AND DISPLAY INSTALL AND REMOVAL	o		o		o	o	o	o	o	o	1		1	2	M
NAVIGATION INSTALL. AND REMOVAL			o	o	o	o	o	o	o	o	1		1	2	M
PROTECTIVE COVERS/CONTAINERS	o		o		o	o	o	o	o	o	1		1	2	M
BATTERY SERVICING AND HANDLING EQUIP			o		o	o	o	o	o	o	1		1	2	M
SOLAR ARRAY SIMULATOR (MECH)	o		o	o	o	o	o	o	o	o	1		1	2	B
RTG SIMULATOR (MECH)	o		o		o	o	o	o	o	o	1		1	2	B
SPECIAL TOOLS	o	o	o	o	o	o	o	o	o	o	1		1	2	M

FOLDOUT FRAME

The existing cooling ring in the IU can provide this cooling. If additional capacity is required due to an increase in RTG size, the cooling will be provided by KSC facilities.

#### 2.1.2.2 DLRV/SLA Platforms

These provide access to the DLRV in the SLA for battery installation and monitoring. Modifications to these platforms will be accomplished through ICD's.

#### 2.1.2.3 Battery Storage Rack - Temperature Controlled

An environmentally controlled storage rack (temperature 35° - 45°F, relative humidity less than 50%) will be provided for long-term storage of batteries. It will be capable of accommodating two sets of vehicle batteries and providing ease of battery handling in and out of the storage rack.

#### 2.1.2.4 Installation and Test Kit - Thermal Vacuum Chamber - BPA

This set consists of equipment required to install and service the DLRV test configurations (control module and power module) or (power module and science module) in the thermal vacuum chamber in BPA. Equipment includes slings, work and access platforms and special installation/servicing tools.

#### 2.1.2.5 Power Distribution and Conditioning Assembly Fixture - Test and Servicing Equipment

A pre-installation fixture will be provided to support the power distribution and conditioning assembly during test and servicing. The fixture will be capable of maintaining a constant "Black Box" temperature during all test and service operations. The fixture consists of a regulated water cooler supplying 60°F water to cold rails for the transfer of heat from the electrical units under operation.

#### 2.1.3 Checkout Equipment

##### 2.1.3.1 Integrated Mobility System Checkout Kit (Mechanical)

This kit consists of the six assemblies required to check out the DLRV integrated mobility system. Each assembly, composed of loading cylinder, dynamometer, belt and load monitoring equipment is mounted to the installation and test fixture, and provides selected mission loads to the wheels, either individually or in any combination simulating lunar operational conditions. Two kit configurations will be provided, one for ambient tests, and the other for thermal-vacuum tests.

#### 2.1.3.2 Thermal Radiator Checkout Kit

This kit consists of the equipment necessary to verify the integrity of the DLRV thermal radiator and heat pipe system. The primary components are a halogen leak detector, freon purge and fill system, low wattage heaters and temperature transducers.

#### 2.1.3.3 Traction Drive Checkout Kit

The traction drive checkout kit will be used to verify the operational parameters of the wheel drive assembly (WDA) during test of the qualification test article and flight vehicles. The kit provides the capability to test the motor and gearbox, brake and declutch assemblies. The end item consists of force, velocity and displacement sensors, variable load units and associated controls and displays.

#### 2.1.3.4 Steering Actuator Checkout Kit

The steering actuator checkout kit will be used to verify the operational parameters of the steering actuator assembly (SAA) during test of the qualification test article and flight vehicles. The kit is composed for force, velocity and displacement sensors, variable load units and associated controls and displays.

#### 2.1.3.5 Optical Alignment Equipment Checkout Kit

This kit is used to optically verify the mechanical angular alignment of certain vehicle components with respect to the vehicle reference frame. Optical equipment includes vertical tooling bars with levelers, theodolites, and electronic levels. The kit is capable of checking the alignment of certain critical components, including the S-band directional antenna, S-band omni-antenna, solar sensor, video and facsimile cameras and solar array.

#### 2.1.3.6 Chassis alignment Fixture

Optical equipment (including theodolite and electronic levels) will be provided to optically check the alignment (bore sight) of critical components of the vehicle chassis with respect to a vehicle reference frame.

#### 2.1.3.7 Solar Array - Positioning and Deployment - Servicing and Checkout Equipment

This fixture supports the solar array to facilitate deployment and positioning under earth environment. The fixture will be capable of simulating a 1/6-g lunar environment during operation of the solar array, either on or off the vehicle.

## 2.2.4 Handling and Shipping Equipment

### 2.1.4.1 Stow/Transport Fixture

This dual-purpose fixture serves as a stowage fixture for the DLRV deployment fixture as well as a DLRV transportation fixture. In the former capacity it permits stowing the DLRV in its restraint mechanism while simulating the ELM interface mounting points, adjacent structure, and height. The fixture is used in conjunction with the deployment fixture. In the latter capacity, when fitted with a cover and wheels, it permits interplant and intersite transportation.

### 2.1.4.2 Installation/Extraction Kit

This kit of specially configured slings and guides is used to install (or remove) the DLRV and its restraint mechanism in the ELM descent stage. The design provides three-axis motion to permit alignment and prevent damage to the ELM/DLRV interface points.

### 2.1.4.3 Vehicle Sling

This item is used for handling any one or all three of the DLRV's modules, in both the deployed and stowed configurations. Adjustable straps allow pickup over the c.g. for the various hoisting modes. The inclusion of an adapter permits weight and balance determination of the DLRV in a stowed configuration.

### 2.1.4.4 Battery Shipping Container

A temperature-controlled atmosphere will be provided for storage and shipment of activated batteries prior to installation in the DLRV. This portable hermetically sealed container will maintain an environment which is impervious to atmospheric changes (35°F to 45°F, 50% maximum relative humidity for a minimum of 24 hours). The battery container is also shock resistant and comes equipped with a temperature and humidity indicator.

### 2.1.4.5 Solar Array Installation, Removal and Protection - Servicing Equipment

Handling equipment (tools, fixtures and covers) is required to facilitate installation, removal and protection of the solar array panel assemblies. Special handling equipment is required to insure the integrity of the solar array during all phases of handling including installation, removal, test, checkout, storage and moving.

### 2.2.4.6 GSE Crew Seat and Restraint

A crew seat and restraint system will be provided to simulate the vehicle seat. It will be capable of withstanding all loads (dynamic & static) during vehicle



test and checkout in earth environment.

2.1.4.7 Seat and Restraint - Installation and Removal Tools and Handling Fixtures

A handling fixture and special tools will be developed to permit efficient storage, installation, removal and handling for the vehicle seat and restraint.

2.1.4.8 Controls and Displays - Installation and Removal Tools and Handling Fixtures

A handling fixture and special tools will be developed to permit efficient storage, installation, removal and handling for the vehicle's controls and displays.

2.1.4.9 Navigation - Installation and Removal Tools and Handling Fixtures

A handling fixture and special tools will be developed to permit efficient storage, installation, removal and handling for the vehicle's navigation equipment.

2.1.4.10 Protective Covers/Containers

These consist of all the devices required to physically protect selected components and subassemblies during individual interplant shipment and after final component installation on the DLRV.

2.1.4.11 Battery Servicing and Handling Equipment

This set consists of all the equipment required for handling, shipping, servicing and installing the DLRV batteries.

2.1.4.12 Solar Array Simulator (Mechanical)

This unit, utilized as a mechanical integration mockup, has physical characteristics which duplicate earth weight, volume and cg of flight hardware.

2.1.4.13 RTG Simulator (Mechanical)

This unit, utilized as a mechanical integration mockup, physically duplicates the earth weight, volume and cg of the flight RTG.

2.1.4.14 Special Tools

The special tools are other than standard manufacturing tools required because of peculiar installation or adjustment features on selected components or subassemblies.

## 2.2 ELECTRICAL GSE

Major articles of electrical support equipment established by investigation of vehicle subsystems, systems, acceptance test procedures, factory buildup, site support and pre-launch operations are functionally identified in the following paragraphs. These items are identified in Table 2-2 and reflect the electrical support equipment required for a specific operation, activity and site location of the DLRV program.

### 2.2.1 Test Sets

#### 2.2.1.1 Power Subsystem Remote Control Station

This is a test station which provides switching signals simulating the remote mode of operation and monitors the resultant voltages, currents, signal conditioning and readout of the power subsystem's transducers.

#### 2.2.1.2 Inverter Test Station

This is a test station which furnishes simulated vehicle electrical loads and monitors the 26-V and 115-V single-phase and 115-V three-phase 400-Hz outputs of the power subsystem's inverter.

#### 2.2.1.3 Integrated Navigation Test Set

This test set furnishes power to the navigation subsystem's components and the solar aspect sensor simulator. The test set also provides interface signals and loads and monitors the navigation subsystem's outputs.

#### 2.2.1.4 Pulse Code Modulation Electronic Test Assembly (PCMTEA)

This test assembly provides power and input signals to the data handling assembly and monitors the non-return-to-zero serial data, timing, and format of the communications subsystem's data handling assembly.

#### 2.2.1.5 Transmitter and Receiver Test Station

This is a test set which provides power, audio inputs, RF dummy loads, and demodulation equipment to measure and demodulate the communications subsystem's S-band transmitters' outputs. The station also provides phase shift keyed (PSK) and voice-modulated RF inputs to the S-band receivers and selectable loads at the outputs of the receivers and the command decoder assembly.

#### 2.2.1.6 Hazard Detection Test Station

This station provides power and discrete, digital and analog signals which simulate subsystem interface signals. The station also provides a selected load between the radar transmitter/receiver and the hazard processor.

#### 2.2.1.7 Hazard Detection Interface Unit

This unit provides the capability for readout of the logic storage output registers of the hazard detection and avoidance subsystem's processor and couples the vehicle output interface with the input interface of the ground-based remote control station.

#### 2.2.1.8 Mobility (Steering) Remote Control Test Set

This test set simulates the commands (normally generated by the DLRV control center) which are needed for mobility subsystem integration testing. This set also provides the required interface loads and signals for the mobility subsystem and monitors critical mobility parameters.

#### 2.2.1.9 Hand Controller Test Set

This testset provides power to the vehicle hand controller and monitors the simulated vehicle interface load.

#### 2.2.1.10 Automatic Circuit Analyzer (ACA) Adaptor Cables

These cables provide the interface between the ACA equipment and the DLRV wiring harness. The ACA also automatically checks the DLRV harness for continuity, shorts and leakage paths.

#### 2.2.1.11 GFE Adaptor Cable Set

These cable sets provide the interface between the GFE (IM) test equipment and the DLRV subsystem.

#### 2.2.1.12 Thermal Vacuum Chamber Cable Set

This cable set provides the interface between the qualification vehicle and the thermal vacuum interface adaptors.

#### 2.2.1.13 Umbilical

This is a cable set which provides the interface between the vehicle-mounted wheel drive electronics (WDE) and the test vehicle wheel drive assembly (WDA) during mobility vehicle testing.

## 2.2.2 Servicing Equipment

### 2.2.2.1 RTG Simulator

This is a power supply with shaping circuits which provides the voltage/current characteristics of the RTG.

### 2.2.2.2 Solar Array Simulator

This power supply with shaping circuits simulates the voltage/current characteristics of the solar array.

### 2.2.2.3 Electrical Load Bank

Resistive and reactive loads which simulate the load characteristics of the vehicle and its subsystems.

### 2.2.2.4 Battery Maintenance Test Station

This console fills, activates, recharges and checks the DLRV batteries.

### 2.2.2.5 Vehicle Ground Power Supply

This equipment substitutes for flight batteries and supplies power to the DLRV during factory buildup and testing.

### 2.2.2.6 Batteries

These batteries supply power to the wheel drive electronics (WDE), wheel drive assembly (WDA) and GSE hand controller during mobility vehicle testing.

### 2.2.2.7 Interface Checkout Unit

This unit is the GSE power distribution assembly which provides the interface for the EPS components during integrated EPS subsystem testing.

### 2.2.2.8 Instrumentation Signal Generator Test Station

This test station generates simulated vehicle transducer inputs and monitors the Non Return to Zero (NRZ) PCM output and the vehicle caution and warning master alarm.

### 2.2.2.9 RF Signal Generator Test Station

This station provides phase shift keyed (PSK) and audio modulated RF power through GSE antenna hats to the DLRV Omni and steerable S Band antennas while monitoring the resultant outputs across selectable RF dummy loads. This station also simulates the 85 foot antenna site transmitter and antenna uplink signals during integrated DLRV Control Center/DLRV testing.

#### 2.2.2.10 Terrain Profile Simulator

This simulator is an antenna hat system with probes, delay lines, phase shifters, attenuators, and an electronic control assembly which simulate holes, obstacles, and nominal lunar terrain characteristics.

#### 2.2.2.11 GSE Hand Controller

An adjustable voltage source which provides the inputs to the wheel drive electronics of the mobility test vehicle during controlled test operation.

### 2.2.3 Checkout Equipment

#### 2.2.3.1 Solar Array Checkout Kit

This kit includes a high-intensity collimated light source to activate the solar array and an electrical load bank which is monitored to measure the voltage and current characteristics of the array. Sensors and readout equipment for measurement of solar array temperature are also provided.

#### 2.2.3.2 Solar Aspect Sensor Stimulator

This kit provides a high-intensity light source to stimulate the solar aspect sensor and its electronics during test.

#### 2.2.3.3 Digital Tape Recorder

This unit (single-track, 0-15 KHz, IBM-compatible) records the output of the data handling assembly during a test drive of the DLRV over a calibrated course. The taped data, reduced with the aid of the ground station's navigation computer subsequent to a vehicle test run, is used to verify the proper operation of the DLRV's navigation subsystem during developmental tests.

#### 2.2.3.4 Video Checkout Station

This station provides power and input signals to the DLRV's television equipment and monitors camera sensitivity, resolution, linearity, etc.

#### 2.2.3.5 Integrated Video Alignment Kit

This equipment, comprised of test pattern and TV Monitor, is used in conjunction with mechanical alignment equipment to provide camera boresighting and alignment with the vehicle planform.

#### 2.2.3.6 Integrated Mobility System Checkout Console

The integrated mobility subsystem checkout console will be used to monitor, record and control the integrated mobility subsystem checkout kit (mechanical). The monitoring equipment will be compatible with existing torque and force sensors and will measure the loading of the wheel drive assembly. A strip-chart recorder will be used to calibrate the transducers prior to testing and will also record the transducer outputs. Specialized manual controls will be provided to control the torque and loading applied by the integrated mobility subsystem checkout kit (mechanical) to the wheel drive assembly. The console will contain the recorder, gages, meters, manual controls and power supplies for these units.

#### 2.3 ADDITIONAL SUPPORT EQUIPMENT REQUIREMENTS

The equipment described in the preceding paragraphs was established from an investigation of the DLRV's subsystems and general configuration. However, additional mechanical and electrical support equipment may be required as further identification of vehicle, science, lunar support equipment and DLRV control center requirements become available. In this regard the following areas, particularly those which relate to the scientific community, require further definition:

- o Vehicle-mounted science (remote geophysical monitor, magnetometer, gravimeter, etc.) remote deployment systems
- o Scientific experiment support requirements
  - Conditioning
  - Handling
  - Test
  - Prelaunch checkout and monitoring
- o Lunar support equipment
- o DLRV control center support
  - Test
  - Checkout
  - Maintenance

Since the scientific experiment and DLRV control center support equipment areas have considerable impact on DLRV launch schedules, it is recommended that additional studies be conducted in these areas prior to award of a DLRV Phase C/D contract.

## SECTION 3

### GROUND OPERATING EQUIPMENT

The ground operating equipment (GOE) defined for the DLRV consists of the systems and equipments that provide or support the functions of control, navigation, hazard detection and avoidance, instrumentation, tracking, telemetry and communications as related to the vehicle and scientific experiments. These equipments are to be located in ground stations which interface with the MSFN/NASCOM facilities.

Vehicle checkout on a subsystem and higher level testing will be conducted using the DLRV ground operating equipment in lieu of the acceptance checkout equipment-spacecraft (ACE-S/C) presently utilized with the Apollo spacecraft. The rationale for not utilizing ACE is that the DLRV control center (DCC) effectively is a unique ACE station for the DLRV with the capability of stimulating all the vehicle systems and monitoring the resultant outputs. Thus it would be redundant to consider providing the signal conditioning required to interface the DLRV with existing ACE facilities since the DCC must be provided anyway. Additionally, it is desirable that the DLRV-DCC system be verified prior to vehicle shipment to KSC.

#### 3.1 REMOTE CONTROL STATION

The basic DLRV control center is described in Volume V Mission Operations. Presented there is the functional arrangement of the DCC together with the major interrelationships between vehicle operating, monitoring and scientific experiment stations. Typical displays and controls established for the major DCC stations are described and representative types of hardware available for the determined functions are indicated. A minimum of two DLRV control centers will be required for the DLRV program: one prototype station at Bethpage, New York which will serve as both a developmental station and a test station for use in integrated checkout of the vehicle prior to shipment to KSC; and one DLRV control center which will be the control center for lunar operation and pre-launch checkout at KSC.

#### 3.2 MODIFICATION TO EXISTING MSFN/NASCOM EQUIPMENT

A literature survey of NASA ground station documentation indicates that average pulse code modulation (PCM) downlink communication time delays of approximately eight seconds can be expected with the existing MSFN/NASCOM acquisition, transmission and processing equipment. Since the DLRV control and protective systems are inherently time dependent, a reduction in communication time would improve lunar

mission operation.

A recommended approach for reducing communication response time of the presently configured MSFN/NASCOM network is detailed in Volume V, Mission Operations (MSFN/NASCOM/DCC Section). The proposed modification takes advantage of the relatively simple processing and transmitting equipment used in existing NASCOM voice/data lines in lieu of the more sophisticated processing equipment used on the normal PCM channels.

### 3.3 NEW EQUIPMENT REQUIRED FOR THE MSFN FACILITY

Since the MSFN/NASCOM network interfaces with the DLRV control center, lunar based DLRV and KSC prelaunch DLRV, special conditioning and interface equipment will be required between the DCC and the DLRV at KSC since an integrated system checkout will be conducted prior to launch. No detailed analyses of these equipment requirements were performed during this phase of the program, however, it is realized that new computer hardware, software and conditioning equipment will be required for the DLRV program. Requirements for this type of equipment are discussed in the Mission Operations volume.

### 3.4 AREAS REQUIRING FURTHER DEFINITION

The DLRV control center equipment descriptions, control station interrelationships and operational procedures defined in the missions operations report (Volume V) were determined by assuming that no constraints were imposed by the interfaces of the DCC with the MSFN/NASCOM facilities. The required software and hardware associated with the existing MSFN/NASCOM facilities were presumed, for the purposes of this report, to be a NASA responsibility and were considered government-furnished equipment (GFE). Although this GFE has not been defined, it has been identified and is listed below for consideration in future DLRV/DCC requirement definition:

- o DLRV control center computer program requirements
  - Consoles and vehicle to GSFC/MSFN/DSN/NASCOM (interfaces)
  - Vehicle and science downlink data processing
  - Vehicle and science uplink command processing
- o DLRV control center computer hardware requirements associated with the above software
- o Remote control requirements of sampler arm and associated equipment
- o Remote control drive station/console



Preliminary determinations of ground-based processing for vehicle subsystems have been reported in the subsystem sections of this report and serve to form a basis for future detailed DCC studies.

## SECTION 4

### LUNAR SUPPORT EQUIPMENT

The requirements for equipment which may be used on the lunar surface in support of the DLRV and scientific experiments have been investigated and preliminary identification of possible lunar support equipment is presented below. Although the present configuration of the DLRV obviates the need for some of the lunar support equipment described, further interaction between vehicle design, astronaut preference, scientific community requirements and human factors study may result in the need for some of these items.

- o DLRV assembly tools - special equipment to aid the astronaut in the conversion of the manned four-wheeled vehicle into the unmanned six-wheeled configuration
- o Battery recharging kit - equipment required to support and interface the solar array with the DLRV batteries during post EVA battery recharge
- o Scientific equipment installation kit - equipment to aid the astronaut in the transfer of ELM-stowed experiments and equipment to the DLRV
- o Vehicle extraction kit - equipment provided to assist in the extrication of the vehicle in either the manned or remote configuration.

## SECTION 5

### TRAINING EQUIPMENT

Training equipment will be needed to train DLRV flight crews, backup flight crews, NASA ground support, command and training personnel, and vehicle support personnel. General training equipment design factors such as equipment growth capabilities, interchangeability, standardization and updating philosophy will have to be considered in the final training equipment study. Preliminary definition of the types of training equipment which will support the objectives of an extensive training program is provided in the paragraphs below. It should be noted that the baseline training equipment defined for this study is a 1-g training vehicle which provides the capability of conducting manned mission simulations in an earth environment.

- o DLRV mission trainer - trainer provided with the simulation required to reproduce the conditions necessary to train individuals or crews on an operational mission
- o DLRV system trainers - trainers utilized for familiarization and procedural instruction in DLRV subsystems
- o DLRV subsystem trainers - trainers which provide practice on one or more operator, maintenance, or control functions. These trainers permit selected aspects of a task or operation to be practiced independently of other aspects. They provide economical training on certain elements requiring special attention
- o Ground operating equipment mission trainers - trainers provided with the simulation required to reproduce the conditions necessary to train individuals or crews under operational mission conditions
- o Ground operating equipment system trainers - trainers utilized for familiarization and procedural instruction in the operation of the consoles associated with the DLRV and scientific equipment
- o Ground operating equipment subsystem trainers - trainers which provide practice on one or more operator, experimenter control, or maintenance functions. They permit selected aspects of a task or operation to be practiced independently of other aspects. They provide economical training on certain elements requiring special attention

## TABLE OF CONTENTS

<u>Section</u>		<u>Page</u>
1	INTRODUCTION AND SUMMARY . . . . .	1-1
2	HAZARD ANALYSIS TECHNICAL APPROACH . . . . .	2-1
	2.1 Introduction . . . . .	2-1
	2.2 Analysis Technique . . . . .	2-1
	2.2.1 Hazard Identification and Evaluation . . . . .	2-1
	2.2.2 Contributing Factors, Hazard Sources and Effects . . . . .	2-4
	2.2.3 Compensating Provisions . . . . .	2-6
	2.2.4 Safety Requirements . . . . .	2-6
	2.3 Application of System Safety Analysis to the DLRV . . . . .	2-6
	2.3.1 Scope . . . . .	2-6
	2.3.2 Data Development . . . . .	2-6
	2.3.3 Safety Assessment . . . . .	2-7
3	HAZARD IDENTIFICATION . . . . .	3-1
	3.1 Gross Hazard Categories . . . . .	3-1
	3.1.1 Environmental . . . . .	3-1
	3.1.2 Personnel Factors . . . . .	3-2
	3.1.3 Malfunctions and Deficiencies . . . . .	3-2
	3.2 Safety Mission Phases . . . . .	3-2
	3.3 Hazard Evaluation . . . . .	3-3
4	SAFETY REQUIREMENTS . . . . .	4-1
	4.1 Configuration . . . . .	4-1
	4.2 Crew Provisions Subsystem . . . . .	4-2
	4.3 Electrical Power . . . . .	4-4
	4.4 Mobility and Control Electronics . . . . .	4-5
	4.5 Navigation and Guidance . . . . .	4-6
	4.6 Thermal Control . . . . .	4-6
	4.7 Interface-Lander . . . . .	4-6
	4.8 Mission . . . . .	4-6
	4.9 Communication/Instrumentation . . . . .	4-7

## LIST OF ILLUSTRATIONS

<u>Figure</u>		<u>Page</u>
2-1	System Safety Hazard Analysis - Flow Chart. . . . .	2-2
2-2	Data Development . . . . .	2-3
2-3	Data Flow and Functional Group Interface. . . . .	2-5

## LIST OF TABLES

<u>No.</u>		
3-1	Hazard Evaluation, Environmental . . . . .	3-5
3-2	Hazard Evaluation - Personnel Factor (Error) . . . . .	3-7
3-3	Hazard Evaluation - Malfunctions and Deficiencies, Vehicle and Equipment . . . . .	3-10

**PRECEDING PAGE BLANK NOT FILMED**

## SECTION 1

### INTRODUCTION AND SUMMARY

#### 1. INTRODUCTION

The final report documents the effort during the Phase B Study. This effort has been directed toward the following:

- o Identification of design and operational hazards for the total system, each subsystem or critical crew activities
- o Establishment of safety design requirements to preclude, eliminate or minimize potential hazards. Establishment of operational guidelines and procedure requirements suitable for inclusion in operational handbooks

#### 2. SUMMARY

An analysis technique has been refined, documented, and utilized to determine the hazards and requirements as shown in this report. A total of 94 hazards have been identified and 40 safety requirements established. Only 2 of the 94 hazards remain "open", or unresolved. They are as follows:

- o Obstacle prevents deployment of DLRV. This will be risked and has no apparent solution
- o Tip-tilt information is not displayed to astronaut in real time. Ground will supply information to crew with a 6 second, minimum, delay

## SECTION 2

### HAZARD ANALYSIS TECHNICAL APPROACH

#### 2.1 INTRODUCTION

The hazard analysis takes into account all environmental factors, malfunctions and design deficiencies, and errors concerned with the design and operation of the vehicle and equipment. The analysis also includes all interfacing aspects of design and operations associated with the lander spacecraft, science packages, and crew activities.

The hazard analysis contains:

- o Identification and classification of hazards
- o Tabulation of factors that may contribute to hazards and the effects of the loss of the function (assuming loss)
- o Compensating provisions - preventive and remedial measures
- o Safety requirements established to minimize, eliminate, prevent or control hazards
- o Procedures for the incorporation of safety requirements and coordination of data flow
- o Safety assessment and residual hazards as results of the hazard analysis
- o Summary of safety assessments

#### 2.2 ANALYSIS TECHNIQUE

The major functions, support functions and tasks that are performed in the hazard analysis are shown in Figure 2-1. The analysis begins with a review of the mission, the identification of catastrophic situations and the identification of hazards that could possible lead to these situations. A gross hazards check list is tabulated under the primary categories as follows:

- o Environmental
- o Malfunctions and design deficiencies
- o Personnel factors (errors)

The development of data on a functional basis for the design and operation of vehicle and equipment is shown in Fig. 2-2.

##### 2.2.1 Hazard Identification and Evaluation

The gross hazards are further refined into specific hazards, then indexed, and their occurrence related to the mission timeline.

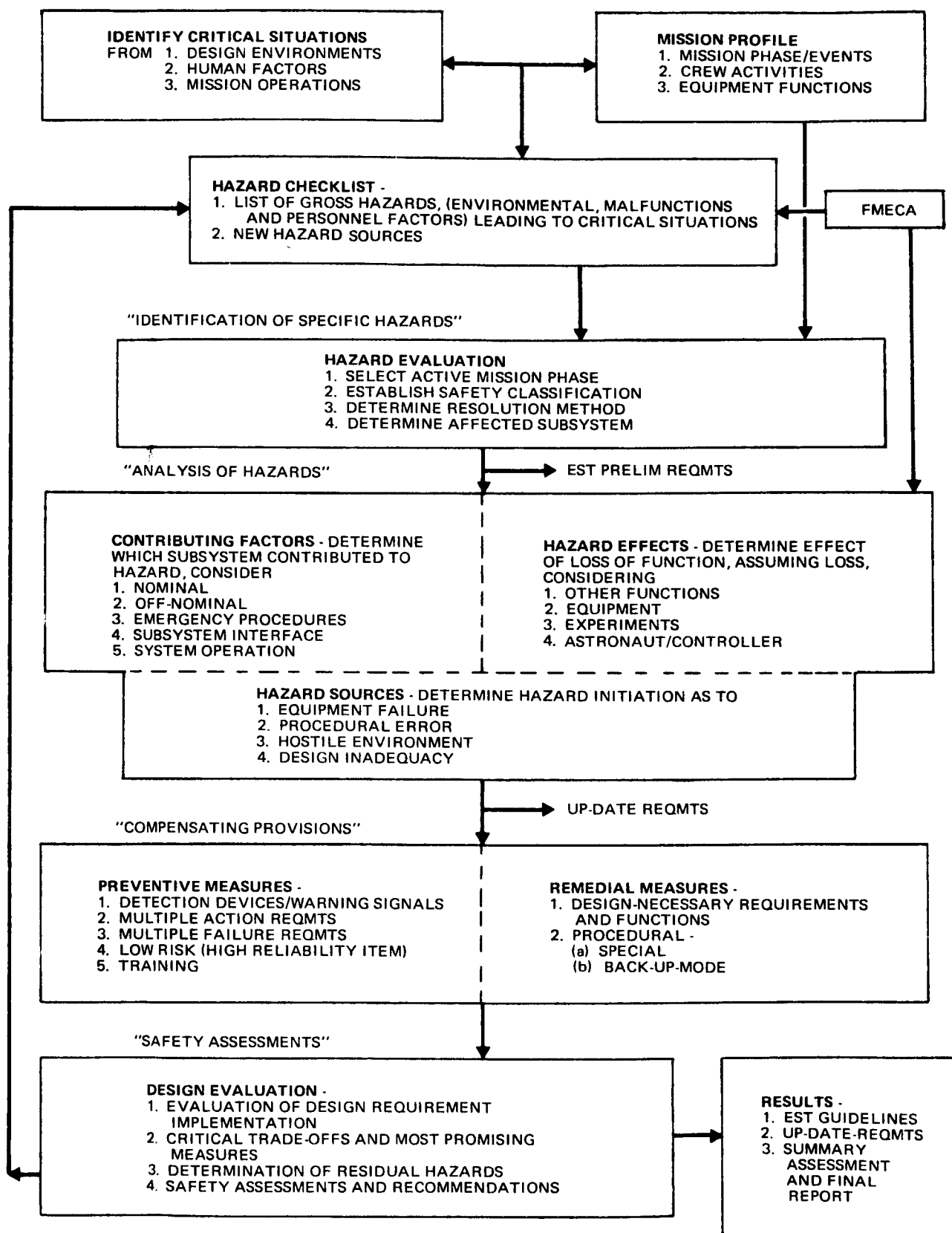


FIG. 2-1 SYSTEM SAFETY HAZARD ANALYSIS - FLOW CHART



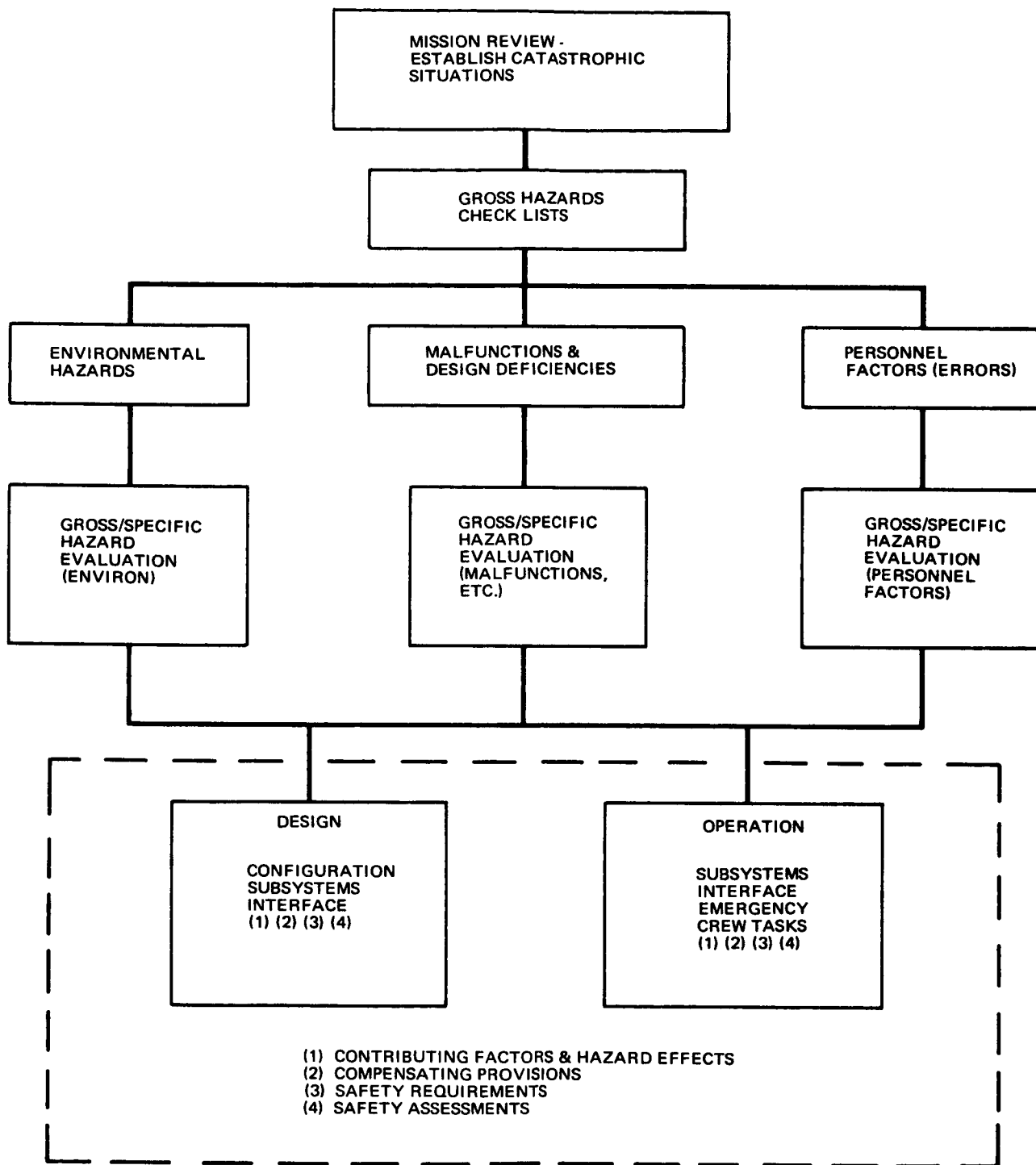


FIG. 2-2 DATA DEVELOPMENT

The hazards are also classified as they affect design or operations and configuration, subsystem or interface. Each specific hazard is assigned a safety criticality classification in accordance with the following Classification and Safety Program Directive No. 1 (SPD #1).<sup>\*</sup> The method of disposition to minimize hazards is also tabulated as to "eliminate, prevent, control or accept risk." The results of FMECA studies and any new sources of hazards that may develop through the reiteration process of the analysis are included as shown in Fig. 2-1.

The identified system hazardous conditions are classified as follows (Safety Classification SPD #1):

- o Safety Catastrophic - Condition(s) such that environment, personnel error, design characteristics, procedural deficiencies, or subsystem or component malfunction will severely degrade system performance and cause subsequent system loss, death, or multiple injuries to personnel
- o Safety Critical - Condition(s) such that environment, personnel error, design characteristics, procedural deficiencies, or subsystem or component malfunction will cause equipment damage or personnel injury, or will result in a hazard requiring immediate corrective action for personnel or system survival
- o Safety Marginal - Condition(s) such that environment, personnel error, design characteristics, procedural deficiencies, or subsystem failure or component malfunction will degrade system performance but which can be counteracted or controlled without major damage or any injury to personnel
- o Safety Negligible - Condition(s) such that personnel error, design characteristics, procedural deficiencies, or subsystem failure or component malfunction will not result in major system degradation, and will not produce system functional damage or personnel injury

\* NASA Document: "System Safety requirements for manned space flight." Safety Program Directive No. 1 dated January 1969. Prepared by Manned Space Flight Safety Office, National Aeronautics and Space Administration, Washington, D.C. 20546.

### 2.2.2 Contributing Factors, Hazard Sources and Effects

The specific hazards are tabulated and listed under the function affected (configuration, subsystem, interface, etc.). The applicable function is reviewed for details pertaining to hazard detection, contributing factors, the effect of the loss of the function (assuming loss), and possible event, source or initiation that may trigger off the hazard. These results are presented in tabular form and are the basis for the further definition of safety requirements.

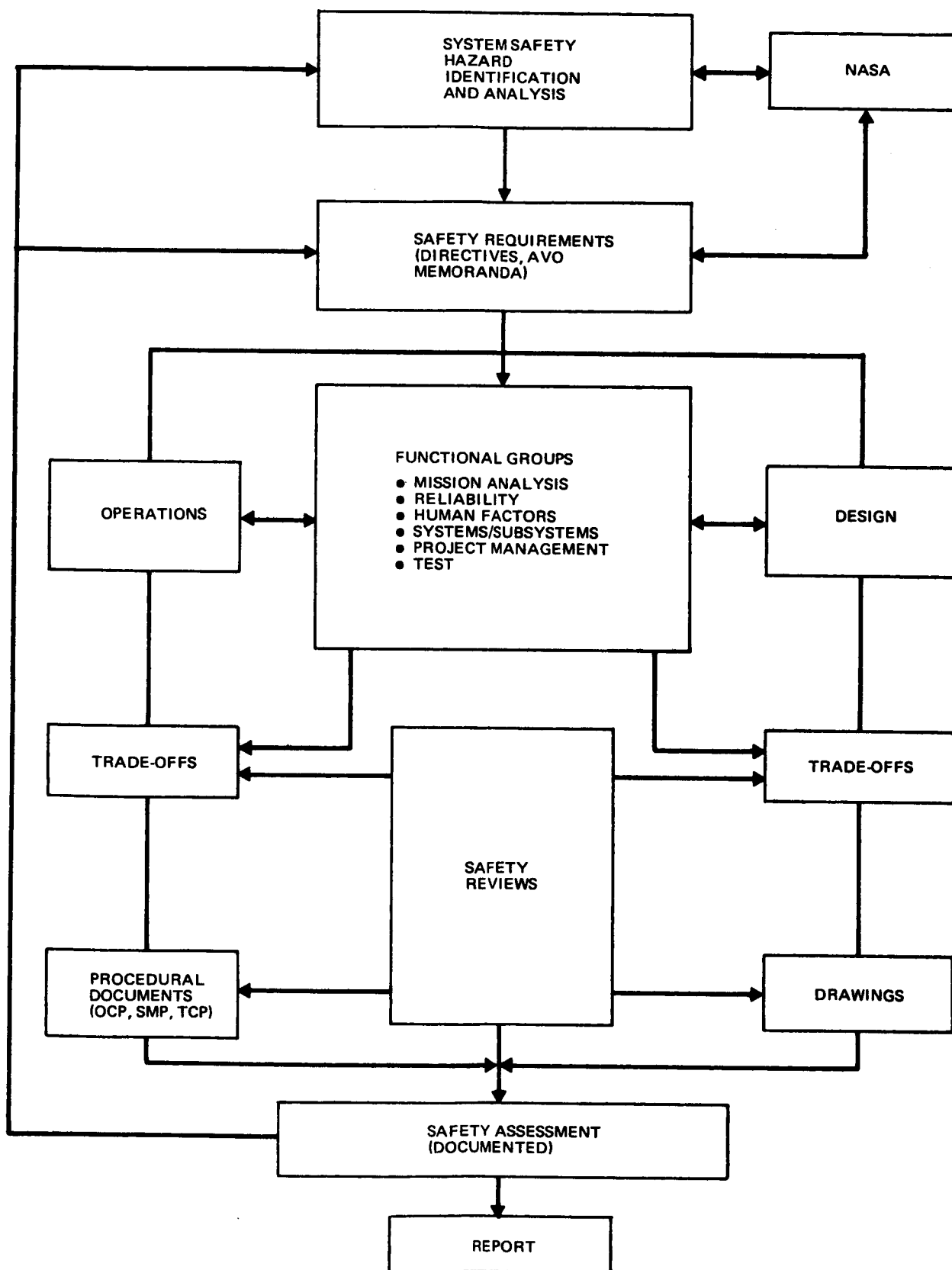


FIG. 2-3 DATA FLOW AND FUNCTIONAL GROUP INTERFACE

### 2.2.3 Compensating Provisions

The vehicle system/subsystems are further reviewed for preventive, or remedial measures available to minimize hazards. Detail considerations for preventive and remedial measures respectively are shown in Fig. 2-1. The results are presented with references to applicable safety requirements and safety assessments.

### 2.2.4 Safety Requirements

Preliminary and final safety requirements are documented for distribution to the program management and technical groups for incorporation into vehicle design and procedural documents. The coordination of data flow is shown in Fig. 2-3. The safety requirements are indexed and cross idicies of hazards and applicable safety requirements are provided for all hazards.

## 2.3 APPLICATION OF SYSTEM SAFETY HAZARD ANALYSIS TO THE DLRV

### 2.3.1 Scope

The analysis for the Phase B Study of the DLRV is of a preliminary nature in which all possible hazards that may lead to critical or catastrophic situations are fully considered. The analysis covers vehicle design and equipment, lunar surface mission/crew operations and interfaces as noted herein. It does not include pre-launch, in-flight, and delivery to the lunar surface mission phases. The hazard occurrence for the manned and unmanned configurations is shown by means of the mission time line.

### 2.3.2 Data Development

The development of data shown in Fig. 2-2 for the design and operation of the DLRV is further detailed as follows:

#### Design

Configuration  
Subsystems  
- Electrical Power  
- Crew Provisions  
- Controls  
- Navigation & Guidance  
- Mobility & Control Electronics  
- Mobility  
- Communications & Instrumentation  
- Hazard/Obstacle Detection & Avoidance  
- Life Support  
- Thermal

#### Operations

Subsystems  
- Electrical Power  
- Crew Provision  
- Controls  
- Navigation & Guidance  
- Mobility & Control Electronics  
- Mobility  
- Communications & Instrumentation  
- Hazard/Obstacle Detection & Avoidance  
- Life Support  
- Thermal

## Design

### Interface

- Spacecraft, Deployment
- Scientific Package

## Operations

### Interface

- Spacecraft, Deployment
- Checkout

### Emergency & Rescue

### Crew Tasks

### 2.3.3 Safety Assessment

Each specific hazard or risk identified is assessed for impact on crew safety or mission success. This provides a basis for establishment of final safety requirements, guidelines and development of contingency procedure requirements.

## SECTION 3

### HAZARD IDENTIFICATION

The scope of system safety effort for the DLRV Project is as follows:

- o The hazard analysis covers the DLRV activities occurring during the period of "lunar stay"
- o The prelaunch hazards due to earth environments, such as temperature, humidity, and salt-spray corrosion are the same as for the lander spacecraft and are not considered herein.
- o The in-flight hazards for the DLRV are considered the same as for the spacecraft. The exception is a possible ionizing radiation hazard due to additional RTG's
- o The ground support hazards of handling operations, loading, transporting and unloading the DLRV vehicle at BPA and KSC are well known; the analysis of any hazards identified in the course of these operations will be performed during Phase 'C' and 'D' of the program

The basic safety philosophy for the DLRV is to "provide for the crewman's safe return to the spacecraft at any time and from any location while he is on the lunar surface." Three critical situations identified are considered catastrophic to crew safety and mission success:

- o Loss of vehicle mobility
- o Inability to rendezvous due to loss of guidance
- o Loss of life support systems

The factors which can contribute to these situations as primary or secondary causes have been categorized into environmental, personnel factors, malfunctions and deficiencies, and are presented in the following gross hazard categories.

#### 3.1 GROSS HAZARD CATEGORIES

##### 3.1.1 Environmental

- o Lurain
- o Temperature
- o Vacuum
- o Radiation (solar flares, RTG)
- o Contamination (optics/solar arrays/display panels/visor)
- o Electromagnetic interference
- o Glare

- o Meteoroids and micro-meteoroids
- 3.1.2 Personnel Factors (Error)
  - o Inadvertent activation
  - o Path selection and obstacle avoidance
  - o Dexterity (ingress, egress, tasks)
  - o Direction selection
  - o Underestimating task time
  - o Incorrect deployment procedure
  - o Impact (collision)
  - o Overturning of DLRV
  - o Impact (astronaut/vehicle - obstructions)
  - o Scientific package, interface (handling, operations)
- 3.1.3 Malfunctions and Deficiencies -- Vehicle and Equipment
  - o Loss of power sources
  - o EPS distribution and control loss
  - o Loss of navigation and guidance functions
  - o Loss of life support
  - o Structural damage/failure (shock, vibration)
  - o Loss of communications (up-dating, bio-med, monitoring instrumentation)
  - o Sharp edges and corners
  - o Stress concentrations
  - o Loss of mobility (propulsion, steering, brakes)
  - o Loss of vehicle stability (pitch and roll excessive)
  - o Electrostatics
  - o Ionizing radiation (RTG)

### 3.2 SAFETY MISSION PHASES

The hazards identified are now considered as a function of mission phase.

The mission phases are

- o Deployment and checkout
- o Sorties - (manned)
  - Outbound
  - Science tasks/loitering
  - Egress-ingress lander/vehicle activation/de-activation/preparations for unmanned mode

- o Long range traverse (unmanned)
- o Rendezvous (unmanned)

### 3.3 HAZARD EVALUATION

Each of the specific hazards of risks identified must be assessed for impact on crew safety or mission success. Allocation of each hazard into its appropriate corrective action category considers this safety impact. All catastrophic and critical hazards must be prevented, eliminated or controlled by design, safety devices, or protective systems. Marginal and safety negligible hazards should be prevented or controlled by use of warning devices or special procedures.

Tables 3-1, 3-2, and 3-3 present the hazard data accumulated to date. The following material explains the table terminology:

Column (1) is a tabulation of specific hazards derived, as applicable, from the gross hazards listing.

Column (2) identifies the type of hazard: E = Environmental, P = Personal Error, M = Malfunction; The serial number (S/N) of the hazard; whether the hazard results from design (d) or operations (OP); and the applicable system/subsystem (S/S) in accordance with the following:

<u>Systems/Subsystems</u>	<u>S/S - D/Op</u>
Configuration, Vehicle Design Integration	VD (D or Op)
Mobility & Control Electronics	MC (etc.)
Thermal	TH
Crew Provisions	CP
Communications & Instrumentation	CI
Navigation & Guidance	NG
Electrical Power Systems	EP
Hazard Detection & Obstacle Avoidance	HD
Mobility	MB
Life Support System	LS
Interface, Deployment	ID
Interface, Lander	IL
Interface, Science Package	IS
Interface, Ground Station	IG
Rescue and Emergency	RE

Column (3) evaluates the hazards in accordance with the following method of disposition:

Prevent (Avoid)	--	P	
Eliminate	--	E	(see note below)
Control	--	C	
Risk	--	R	



Column (4) indicates the applicable or high risk mission phase in which the specific hazards may occur. (Ref. Definition of safety mission phases)

Column (5) assigns crew safety/mission success impact:

Catastrophic	--	CA
Critical	--	CR
Marginal	--	M
Negligible	--	N

NOTE:

- Prevent (Avoid) - (P) The hazard is present, but through vehicle design or operating procedures is prevented from happening.
- Eliminate - (E) The hazard is removed from the system/mission by a design change or operating constraint/procedures (e.g. solar flare activity - the mission is scheduled only in times of minimum solar flare activity).
- Control - (C) The hazard is present, but is controlled/minimized by design or operating procedures to the extent that it does not present a problem of crew safety/mission success.
- Risk - (R) The hazard is present, and the risk is acceptable as the probability of happening is remote (low risk), and testing has demonstrated satisfactory system performance.

TABLE 3-1 HAZARD EVALUATION, ENVIRONMENTAL, SHEET 1 OF 2

(1)	(2)	(3)	(4)			(5)	
GROSS/SPECIFIC HAZARDS	S/N-S/S-D/Op	HAZARD DISPOS 1.	MISSION PHASE			SAFETY CATEGORY	
			2.1	2.2	2.3		3.
<u>Terrain</u>							
o Lander attitude, DLRV gear damage on Deployment "drop"	E01-ID-Op	C	X	-	-	-	M
o Lander damage from DLRV deploy	E02-ID-Op	C	X	-	-	-	M
o Obstacle prevents mobility on deployment	E03-IL-Op	R	X	-	-	-	M
o Rough terrain induced vibration causes structural fatigue of vehicle, and equipment support	E04-VD-Op	C	-	X	-	X	CR
o Debris thrown by wheels impacts astronaut and LSS	E05-VD-Op	C	-	X	-	-	CR
o Debris thrown by wheels impacts equipment (solar array)	E06-VD-Op	C	-	X	-	-	M
o Astronaut, vehicle vibration & motion causes nausea & inadvertent loss of control	E07-CP-Op	C	-	X	-	-	M
o Vehicle shock, impact obstacles	(see Impact, Collision)						
o Vehicle overturn on slope	(see Overturning, DLRV)						
<u>Temperature, Solar, Lunar</u>							
o Thermal input to astronaut	E08-CP-D	C	X	X	X	-	M
o Thermal input to vehicle motors	E09-TH-Op	C	X	X	X	X	M
o Thermal input to equipment, (Comm., Nav & Guid)	E10-TH-Op	C	X	X	X	X	M
<u>Vacuum</u>							
o Astronaut environment - loss of suit integrity, (pressure)	E11-LS-Op	C	X	X	X	-	CA
o Vehicle operating components - lubricant outgassing/loss	E12-VD-Op	C	X	X	X	X	M
<u>Radiation (Solar Flares)</u>							
o Astronaut environment	E13-CP-Op	E	X	X	X	-	CA

TABLE 3-1 HAZARD EVALUATION, ENVIRONMENTAL, SHEET 2 OF 2

(1)	(2)	(3)	(4)			(5)
GROSS/SPECIFIC HAZARDS	S/N-S/S-D/Op	HAZARD DISPOS. 1.	MISSION PHASE			SAFETY CATEGORY
			2.1	2.2	2.3	4.
<u>Contamination, Dust</u>						
o Degrades optics	E14-CI - D	C	X	X	X	X
o Degrades solar arrays	E15-EP - D	C	X	X	X	X
o Degrades thermal radiating reflectors	E16-TH - D	C	X	X	X	X
o Degrades visibility of display panels	E17-CP - D	C	X	X	X	-
o Degrades visibility thru astronaut visor	E18-CP - D	C	X	X	X	-
o Lander contamination from astronaut suit	E19-IL - D	C	-	-	X	-
o Lander contamination from science pkg. container	E20-IL - D	C	-	-	X	-
<u>Electromagnetic Interference (Solar)</u>						
o Communications interference	E21-CI - Op	E	X	X	X	X
o Navigation & guidance interference	E22-NG - Op	E	X	X	X	X
o Hazard detection & obstacle avoidance interference	E23-ND - Op	E	X	X	X	X
<u>Glare</u>						
o Brightness of direct sun	E24-CP - Op	C	X	X	X	-
o Brightness of lunar surface reflections	E25-CP - Op	C	X	X	X	-
o Reflection off radiator surface	E26-CP - Op	C	X	X	X	-
<u>Meteoroids</u>						
o Astronaut environment suit puncture	E27-CP - D	C,R	X	X	X	-
o Vehicle damage	E28-TH - D	R	X	X	X	X
o Equipment damage	E29-TH - D	R	X	X	X	X
<u>Radioisotope Thermoelectric Generator(RTG)</u>						
o Injurious ionizing radiation	E30-VD - D	E	X	X	X	-
o Hot spots 250°F	E31-VD - D	E	X	X	X	-
<u>Miscellaneous</u>						
o Shadows prevent visibility of displays & controls	E32-CP - D	E	X	X	X	-

ELECTRICAL SUPPORT EQUIPMENT  
TABLE 2-2

SUPPORT EQUIPMENT NOMENCLATURE	STRUCT TEST	MOB UNIT	SYS INT	1-G TRAIN	QUAL UNIT	DIRV-1	DIRV-2	DIRV-3	DIRV-4	EXIST. GSE UNMOD.	ADAP GSE	NEW GSE	GAC	WES	KSC	TOTAL UNITS	MAKE, BUY OR GFE	REMARKS
STATION, POWER SUBSYSTEM REMOTE CONTROL			o	o	o	o	o	o	o			o	o			1	M	
STATION, TEST, INVERTER			o	o	o	o	o	o	o			o	o			1	M	
SET, TEST, INTEGRATED NAVIGATION			o	o	o	o	o	o	o			o	o			1	M	
PCMTEA			o	o	o	o	o	o	o		o		o			1	M	GFE LDW410-7500(LM)
STATION, TEST, TRANSMITTER AND RECEIVER			o	o	o	o	o	o	o		o		o			1	M	GFE LDW410-32280
STATION, TEST, HAZARD DETECTION			o	o	o	o	o	o	o			o	o			1	B	
SET, TEST, MOBILITY REMOTE, CONTROL	o		o	o	o	o	o	o	o			o	o			1	M	
SET, TEST, HAND CONTROLLER		o	o	o	o	o	o	o	o			o	o			1	M	
ACA ADAPTOR CABLES	o	o	o	o	o	o	o	o	o		o		o			1	M	
GFE ADAPTOR CABLE SET	o		o	o	o	o	o	o	o			o	o			1	M	
CABLE, T/V CHAMBER					o							o	o			1	M	
UMBILICAL		o										o	o	o		1	M	
SIMULATOR, RTG			o		o	o	o	o	o			o	o			2	B	
SIMULATOR, SOLAR ARRAY			o		o	o	o	o	o			o	o			1	M	
LOAD BANK, ELECTRICAL	o	o	o	o	o	o	o	o	o	o			o			1	G	GFE LDW410-8800(LM)
STATION, TEST, BATTERY, MAIN	o		o	o	o	o	o	o	o			o	o		o	2	B	
GROUND POWER SUPPLY, VEHICLE	o	o	o	o	o	o	o	o	o		o		o			1	M	GFE LDW410-82140(LM)
BATTERIES		o										o	o	o		1	B	
UNIT, CHECKOUT, INTERFACE	o	o	o	o	o	o	o	o	o	o			o			1	G	GFE LDW410-81060(LM)
STATION, TEST, ISG			o	o	o	o	o	o	o		o		o			1	M	GFE LDW 410-7900(LM)
STATION, TEST, RF SIG. GEN.			o	o	o	o	o	o	o			o	o		o	2		
SIMULATOR, TERRAIN PROFILE			o	o	o	o	o	o	o			o	o		o	2	M	1-KSC 1 BPA T/V 1 BPA Feat
GSE HAND CONTROLLER		o									o		o	o		1	M	
KIT, CHECKOUT, SOLAR ARRAY			o		o	o	o	o	o			o	o			1	M	
STIMULATOR, SOLAR ASPECT SENSOR			o	o	o	o	o	o	o			o	o		o	2	B	
RECORDER, DIGITAL TAPE		o										o	o			1	B	
STATION, CHECKOUT, VIDEO			o	o	o	o	o	o	o			o	o		o	2	M	
KIT, INTEGRATED VIDEO ALIGNMENT			o	o	o	o	o	o	o			o	o		o	2	B	
CONSOLE, INTEGRATED MOBILITY SYS C/O	o	o	o	o	o	o	o	o	o			o	o		o	2	M	

FOLDOUT FRAME

FOLDOUT FRAME

TABLE 3-2 HAZARD EVALUATION - PERSONNEL FACTOR (ERROR), SHEET 1 OF 3

(1) GROSS/SPECIFIC HAZARDS	(2) S/N-S/S-D/Op	(3) HAZARD DISPOS.	(4) MISSION PHASE				(5) SAFETY CATEGORY		
			1.	2.1	2.2	2.3		3.	4.
<u>Inadvertent Activation</u>									
o Vehicle - movement by astronaut	P01-CM - Op	P	X	X	X	X	-	CR	
o - movement by controller	P02-IG - Op	P	X	X	X	X	X	CR	
o Life support system - Controls	P03-IS - Op	P	X	X	X	X	-	CR	
o Vehicle - movement from terrain slope angle	P04-MC - Op	P	X	X	X	X	X	CR	
o Vehicle - deployment	P05-ID - Op	P	X	-	-	-	-	CR	
<u>Path Selection &amp; Obstacle Avoidance</u>									
o Impact, turning radius/obstacle recognition distance	P06-CP - Op	C	X	X	X	X	-	CR	
o Incorrect path selection may require driving in reverse - rear view visibility limited	P07-CP - Op	C	-	X	X	X	-	CR	
<u>Dexterity</u>									
o Ingress, Egress, DLRV vehicle/SC (Suit impact corners & edges, head clearance)	P08-CP - Op	C	X	-	X	X	-	M	
o Driving in reverse	P10-CP - Op	C	X	X	-	-	X	M	

TABLE 3-2 HAZARD EVALUATION - PERSONNEL FACTOR (ERROR), SHEET 2 OF 3

(1) GROSS/SPECIFIC HAZARDS	(2) S/N-S/S-D/Op	(3) HAZARD DISPOS. 1	(4) MISSION PHASE				(5) SAFETY CATEGORY
			2.1 2.2 2.3				
			2.1	2.2	2.3	4.	
<u>Direction Selection Incorrect</u>							
o Navigation Error	P11-CP - Op	C	-	X	-	-	CR
o Arbitrary Selection	P12-CP - Op	R	-	X	-	-	M
<u>Underestimating Task Time</u>							
o Inbound drive requires more time in comparison to outbound drive.	P13-NG - Op	C	-	X	-	-	CA
o Science Tasks	P14-IS - Op	C	-	-	X	-	M
o Navigation Problem	P15-NG - Op	C	-	X	X	-	M
<u>Impact, Collision</u>							
o Shock, Impact on slope, speed/braking, slipping	P16-VD - Op	C	-	X	-	X	CR

TABLE 3-2 HAZARD EVALUATION - PERSONNEL FACTOR (ERROR), SHEET 3 OF 3

(1)	(2)	(3)	(4)	(5)
<u>GROSS/SPECIFIC HAZARDS</u>	<u>S/N-S/S-D/Op</u>	<u>HAZARD</u>	<u>MISSION PHASE</u>	<u>SAFETY</u>
<u>Overturning DLRV</u>		<u>DISPOS. 1.</u>	<u>2.1 2.2 2.3</u>	<u>3. 4. 5.</u>

- o Vehicle impacts protrusion/depression while on slope causing overturning.

P17-VD - Op C - - - X X X CR

TABLE 3-3 HAZARD EVALUATION - MALFUNCTIONS AND DEFICIENCIES, VEHICLE AND EQUIPMENT, SHEET 1 OF 6

(1)	(2)	(3)	(4)			(5)	
<u>GROSS/SPECIFIC HAZARDS</u>	<u>S/N-S/S-D/Op</u>	<u>HAZARD DISPOS.</u>	<u>MISSION PHASE</u>			SAFETY CATEGORY	
			1.	2.1	2.2		2.3
Loss of Power Sources/EPS Distribution and Control Loss:							
a) Open/short circuits							
b) Switch failures "on/off"							
c) Short to ground							
d) Component failures - per subsystem							
o Mobility and control electronics	M01-MC - D	C	X	X	X	X	CR, M
o Navigation & guidance	M02-NG - D	C	-	X	X	-	CR, M
o Communications & instrumentation	M03-CI - D	C	X	X	X	X	M
o Thermal control	M04-TH - D	C	X	X	X	X	M
o Hazard detection & obstacle avoidance sys.	M05-HD - D	C	X	X	-	-	CR, M



TABLE 3-3 HAZARD EVALUATION - MALFUNCTIONS AND DEFICIENCIES, VEHICLE AND EQUIPMENT, SHEET 2 OF 6

(1) GROSS/SPECIFIC HAZARDS	(2) S/N-S/S-D/Op	(3) HAZARD DISPOS. 1	(4) MISSION PHASE				(5) SAFETY CATEGORY
			2.1	2.2	2.3	3	
<u>Loss of Navigation &amp; Guidance Functions:</u>							
o Loss of heading	M12-NG-D	C	X	X	X	X	CR
o Loss of capability to determine vertical	M13-NG-D	C	X	X	X	X	M
o Loss of ability to determine distance traveled	M14-NG-D	C	X	X	X	X	CR
o Loss of position up-date capability	M15-NG-D	C	X	X	X	X	M
<u>Loss of Life Support</u>							
o Oxygen supply, (a) leak, (b) early depletion	M16-IS-D	C	X	X	X	-	CA
o Loss of Suit Integrity, (a) puncture (sharp corners), (b) RTG heat damage	M17-IS-D	P	X	X	X	-	CA
<u>Structural Damage/Failure of -</u>							
o Vehicle frame, (a) axle, (b) equipment supports, (c) seat	M18-VD-D	C	X	X	X	X	CR
o Overhead component supports in vicinity of crew station	M19-VD-D	C	X	X	X	-	M
o Steering mechanism	M20-MB-D	C	X	X	X	X	CR
o Wheel and brake assembly	M21-MB-D	C	X	X	X	X	CR
o Vehicle gear on deployment	M22-ID-Op	C	X	-	-	-	M
o Vehicle during traverse due to vibration/fatigue	M23-VD-D	C	X	X	-	X	CR
o Vehicle impacting obstacles	M24-VD-Op	R	X	X	-	X	CR

TABLE 3-3 HAZARD EVALUATION - MALFUNCTIONS AND DEFICIENCIES, VEHICLE &amp; EQUIPMENT, SHEET 3 OF 6

(1)	(2)	(3)	(4)				(5)
<u>GROSS/SPECIFIC HAZARDS</u>	<u>S/N-S/S-D/Op</u>	<u>HAZARD DISPOS. 1</u>	<u>MISSION PHASE</u>				<u>SAFETY CATEGORY</u>
			<u>2.1</u>	<u>2.2</u>	<u>2.3</u>	<u>3</u>	
<u>Loss of Communication Functions:</u>							
o Range of PLSS (emergency cond.)	M25-CI - Op	R	-	X	X	-	M
o Up-dating navigation & guidance			(See Loss of N & G)				
o Bio-medical monitoring of the astronauts' condition	M26-CI - D	C	X	X	X	-	M
o Monitoring instrumentation/condition of the vehicle	M27-CI - D	C	X	X	X	X	M
<u>Sharp Edges &amp; Corners damaging Astronaut's Suit, on:</u>							
o Vehicle Frame	M28-VD - D	C	X	X	X	-	CR
o Seat & Crew Station	M29-VD - D	C	X	X	X	-	CR
o Vehicle Equipment	M30-VD - D	C	X	X	X	-	CR
o Scientific Packages	M31-VD - D	C	X	X	X	-	CR

TABLE 3-3 HAZARD EVALUATION - MALFUNCTIONS AND DEFICIENCIES, VEHICLE AND EQUIPMENT, SHEET 4 OF 6

(1) GROSS/SPECIFIC HAZARDS	(2) S/N-S/S-D/Op.	(3) HAZARD DISPOS. 1	(4) MISSION PHASE				(5) SAFETY CATEGORY
			2.1	2.2	2.3	3	
			4				
<u>Stress Concentrations, Failure due to</u>							
o Fastener patterns, bolt & rivet holes	M32-VD - D	P	X	X	X	X	M
o Weldments, heat effected zones	M33-VD - D	C	X	X	X	X	M
o Improper clearances, & shimming by design and manufacturing	M34-VD - D	P	X	X	X	X	M
o Concentrated load effects	M35-VD - D	C	X	X	X	X	M
<u>Loss of Mobility and Control Electronics:</u>							
o Propulsion, (a) wheel motors, (b) propulsion controls	M36-MC - D	C	X	X	X	X	CR
o Steering, (a) actuator, (b) steering controls	M37-MC - D	C	X	X	X	X	CR
o Brakes, (a) actuator, (b) controls	M38-MC - D	C	X	X	X	X	CR
<u>Design Deficiency</u>							
o Battery explosion	M39-EP - D	P	X	X	X	X	CR
o Battery over temperature	M40-EP - D	R	-	X	X	X	M
o Arcing of connectors during mating/demating	M41-EP - D	E	X	X	X	-	M

TABLE 3-3 HAZARD EVALUATION - MALFUNCTIONS AND DEFICIENCIES, VEHICLE AND EQUIPMENT, SHEET 5 OF 6

(1) GROSS/SPECIFIC HAZARDS	(2) S/N-S/S-D/Op	(3) HAZARD DISPOS. 1.	(4) MISSION PHASE				(5) SAFETY CATEGORY
			1.	2.1	2.2	2.3	
			3	4			
<u>Loss of Vehicle Stability Causing -</u>							
o Overturning, due to excessive roll and pitch	M42-VD - D	C -	X	-	-	X	CR
o Astronaut motion sickness	M43-CP - D	R	X	X	X		CR
<u>Electrostatics from Wheel Operations Causing-</u>							
(see Contamination, Dust)							
<u>Radiation</u>							
o Radioisotope thermoelectric generator (RTG) mechanical failure causing ionization radiation hazard to (a) astronaut, (b) equipment	M44-VD - D M45-VD - D	C C	X X	X X	X X	X -	CR M
o Laser-tracker, eye damage to astronaut	M46-CP - D	C	X	X	-	-	CR
o Ionizing radiation from isotope heaters	M47-TH - D	C	X	X	X	-	M, N
<u>Inadequate Clearances</u>							
o Insufficient clearance to reach and operate PLSS controls	M48-CP - D	E	X	X	X	-	M

TABLE 3-3 HAZARD EVALUATION - MALFUNCTIONS AND DEFICIENCIES, VEHICLE AND EQUIPMENT, SHEET 6 OF 6

(1) <u>GROSS/SPECIFIC HAZARDS</u>	(2) <u>S/N-S/S-D/Op</u>	(3) <u>HAZARD DISPOS. 1.</u>	(4) <u>MISSION PHASE</u>			(5) <u>SAFETY CATEGORY</u>
			<u>2.1</u>	<u>2.2</u>	<u>2.3</u>	
<u>General</u>						
o Injured or incapacitated astronaut	G01-CP - Op	C	X	X	-	M
o Static discharge when astronaut dismounts from vehicle	G02-CP - Op	C	X	X	-	M
o Generation of spurious commands	G03-CI - Op	C	-	-	X	CR

# SECTION 4

## SAFETY REQUIREMENTS

### 4.1 CONFIGURATION (VD)

S/N	Requirement	Hazard S/N	Hazard	Rationale
R 01	Provide roll bar or equivalent	P 17 M 42	Vehicle over turns	Protect astronaut from injury and provide crawl-out space
R 02	Provide leg/foot protection for astronaut in the event of collision	P 16	Collision with terrain/obstacle	Astronauts' feet are forward of wheels and require protection
R 03	Provide protection for astronaut and equipment from material thrown by wheels, particularly in reverse	E 05 E 06 E 11 E 17 E 18 M 16 M 17	Loss of visibility of displays due to dust. Loss of suit integrity. Damage to equipment. Dust on radiators	Vehicle geometry has been designed in an attempt to preclude this hazard, i.e. wheels canted outboard
R 04	Eliminate all sharp edges and corners on crew accessible hardware	E 11 M 17 M 28 M 29 M 30 M 31 P 08	Loss of suit integrity	Catastrophic failure could result
R 05	Static/dynamic tests are required to prove factors of safety for primary and secondary structure	E 01 E 02 E 04 M 18 M 19 M 20 M 21 M 22 M 23 M 24 M 32 M 33 M 34 M 35	Vibration and/or shock load causes structural damage	Any structural failure could curtail mission, may cause abort

S/N	Requirement	Hazard S/N	Hazard	Rationale
R 06	Proper material selection is imperative to be compatible with environmental conditions	E 12	Loss of lubricant due to outgassing	Lubricant loss may cause binding
R 07	Provide shielding for injurious ionizing radiation	E 30 M 44 M 45 M 47	Exposure of astronaut or equipment to excessive radiation	Max whole body dose = 8 MREMS/HR. Shield sensitive equipment
R 08	Provide shield or screen for RTG high temperature areas	E 31	Burn astronaut or lose suit integrity	Temperatures 250°F are beyond capability
R 09	Provide micro-meteoroid protection for sensitive equipments	E 28 E 29	Vehicle and/or equipment damage due to meteoroid/micrometeoroid impact	Mission success
4.2	CREW PROVISIONS SUBSYSTEM (CP)			
R 10	Provide switch(es) or circuit breakers to remove power in all cables prior to connecting/disconnecting	M 41	Arcing of "hot" connectors when mating/demating	Arcing may cause build-up on sockets or pins
R 11	Provide seat restraints in the driving position	E 01	Vehicle motion causes inadvertent loss of control and/or astronaut sickness	Restraining astronaut in seat assures maintenance of control
R 12	Provide a rescue/passenger crew station complete with restraint system to load and restrain and incapacitated astronaut	G 01	Injured or incapacitated astronaut	Crew safety
R 13	Provide adequate clearance to operate PLSS controls and to prevent inadvertent actuation	P 03 M 48	Insufficient clearance to reach PLSS controls and inadvertent actuation	Controls must be reachable for change of heat load or emergency communications.

S/N	Requirement	Hazard S/N	Hazard	Rationale
R 14	Provide personal radiation dosimeter for each astronaut	E 13 E 30	Excessive total radiation	Dosage must not exceed allowable. Protection is reqd. on a total dosage basis (RTG, solar etc)
R 15	Provide thermal and micrometeoroid protection for each astronaut	E 08 E 27	High heat loads or suit puncture could be catastrophic	GFE suits incorporate some micrometeorite protection, good for Temperatures 250°F
R 16	Provide for rear viewing	P 07 P 10	Limited visibility when driving in reverse	Provide visibility for reverse driving
R 17	Provide glare shields and intensity controls	E 24 E 25 E 26 E 32	Difficult to read displays in sunlight or shadow	Visibility of displays required at all times when manned.
R 18	Provide the capability for "dusting-off"/cleaning or protection of control/display panel, radiator, visor and other visual aids, solar array	E 14 E 15 E 16 E 17 E 18	Degradation of equipment as a result of dust	Visibility of displays required at all times when manned. Function may be impaired by dust
R 19	Provide crews with sufficient training via simulation, 1" g" vehicles, 1/6 "g" training flights etc. to aid in their dexterity and proficiency to perform required tasks	P 06 P 10 P 11 P 12 P 14 P 15	Obstacle recognition, ingress/egress, navigation error, etc.	Training will help preclude personal errors (note: This is a combined Crew Provisions/Crew Systems task).
R 41	Provide some type of electrical grounding to eliminate static charge in vehicle	G 02	Static discharge when dismounting	Discomfort and possible injury to crew



#### 4.3 ELECTRICAL POWER (EP)

S/N	Requirement	Hazard S/N	Hazard	Rationale
R 20	The electrical power information for on-board display (d) shall include a Master Alarm Light and Tone, Caution and Warning Lights (C&W) and status indicating meters for the following, with telemetry (T) data only as noted:	M 01 M 02 M 03 M 04 M 05	Inadequate warning of EPS malfunctions such as loss of primary power affecting all subsystem unless timely warning is given	Provides astronaut with information that may be acted upon to prevent total loss of EPS, in turn affecting crew safety and mission success. Tone is required if sun prevents seeing lights/displays. Displays are required to prevent a second failure from being catastrophic e.g. communication failure prevents ground from warning of an EPS malfunction or failure

Batteries - Voltage, current temperature, and state of charge: (D, C&W)

RTG - Voltage, current, Temp: (T)

Solar Array - Voltage, Temp, current, position and motor temp: (T)

Battery Charger - Output voltage, input voltage, current and temp: (T)

Shunt Regulator - Output voltage, temp: (C&W)  
(T)

Busses - DC voltage  
(T)

S/N	Requirement	Hazard S/N	Hazard	Rationale
	A vent shall be provided for each cell and each battery	M 39	Pressure build-up during recharge may cause battery explosion	Crew safety/mission success
R 24	Provide an automatic cutoff of battery recharge at the max allowable temperature	M 40	Excessive temperature may result in loss or degradation of battery	Could jeopardize mission success
4.4	MOBILITY AND CONTROL ELECTRONIC (MC)			
R 25	Provide redundant reversing capability	M 01	Reversing switch fails when vehicle is at an unnegotiable object	Single failure must cause mission abort
R 26	Provide temperature sensor and warning display for wheel motor and brake assembly	E 09	Loss of drive motor	To provide astronaut with warning of high temp in time for corrective action
R 27	Provide braking capability which will hold full-up vehicle on maximum negotiable slope	P 04 P 16	Failure of normal brakes. Inadvertent vehicle movement	Need for emergency braking
R 28	Provide constant "tip-tilt" information to both astronaut and ground for manned and unmanned sorties	P 18 P 13	Vehicle overturns when negotiating slopes	Prevent injury to astronaut and loss of mission. Cue to non-negotiable slope.
R 29	Prevent inadvertent vehicle movement in manned mode. e.g. switch guards or lock-out switches	P 01 P 02	Astronaut injury from inadvertent vehicle motion	Crew safety
R 30	Prevent inadvertent deployment initiation from lander e.g. switch guards or sequencing	P 05	Inadvertent deployment	Crew safety/mission success

#### 4.5 NAVIGATION AND GUIDANCE (NG)

S/N	Requirement	Hazard S/N	Hazard	Rationale
R 31	Provide sufficient guidance to enable the astronaut to walk-back, under emergency conditions, at any time, during a sortie. (e.g. portable VHF direction finder - or equivalent) or ride back with complete or partial NAV/GUIDE failure	P 11 P 15 M 12 M 13 M 14 M 15	Inability to rendezvous with lander	Crew safety

#### 4.6 THERMAL CONTROL (TH)

R 32	Provide thermal insulation for sensitive areas and equipments	E 09 E 10	Temperature Limits of Equipment exceeded	Mission success
------	---	--------------	--	-----------------

#### 4.7 INTERFACE - LANDER

R 33	Provide for "Dusting-off"/cleaning/removal of suit contamination and cleaning of lunar sample containers prior to cabin entry	E 19 E 20	Lander contamination	Possible degradation of lander. (This has not been recognized as a hazard by Apollo, but may be for ELM. Will probably be GFE or LM supplied if required)
------	---	--------------	----------------------	---

#### 4.8 MISSION

R 34	The walk-back distance must determine the operational radius on the early DLRV missions. (Walk-back distance is limited by expendables remaining in PLSS and man's ability to walk on lunar surface).	M 01 M 25 M 36 M 37 M 38	Loss of vehicle mobility	Crew safety
------	---	--------------------------------------	--------------------------	-------------

S/N	Requirement	Hazard S/N	Hazard	Rationale
R 35	The vehicle shall not descend/ascend any slope beyond the capability of the astronaut to ascent/descend on foot	M 01 M 25 M 36 M 37 M 38	Loss of vehicle mobility	Crew safety
R 36	Mission shall be scheduled in periods of minimum solar flare activity	E 13 E 21 E 22 E 23	Solar radiation	Crew safety and mission success
R 37	Return legs of sorties shall not be made over previously unexplored terrain.	P 13 M 16	Exceeding life support capability	Direct return may not be possible due to unforeseen terrain features between rover and lander.
R 38	Provide protection for the astronaut's eyes, either operationally or mechanically to prevent the laser from contacting the eyes.	M 46	Eye damage from laser	Crew safety
4.9	COMMUNICATION/INSTRUMENTATION			
R 39	Communications (voice, bio-med) required at all times. Hard-line between astronaut and vehicle not acceptable	E 11 G 02	Torn suit or broken wire causing leak or loss of communications, respectively	Crew safety
R 40	Any communication failure is cause for mission abort	M 25 M 26 M 27	Electrical malfunction resulting in loss of communications (voice, bio-med), and/or vehicle instrumentation.	If manned mode, restrict sortie to line-of-sight (for PLSS communication via lander)
R 42	Identify safety critical commands (e.g. wheel disengagement) and add redundant relays for those commands	G 03	Generation of spurious commands	Mission success